USGS
science for a changing world

Baseline and Projected Future Carbon Storage and Greenhouse-Gas Fluxes in Ecosystems of the Western United States

Professional Paper 1797

U.S. Department of the Interior
U.S. Geological Survey

Front of cover: A stand of mixed conifer trees in Glacier National Park, northwestern Montana. The mesic, closed-canopy forests are typically distributed on mountain slopes with high moisture gradients and include western hemlock, western redcedar, Douglas-fir, lodgepole pine, as well as spruce and fir species. These types of forests are affected by natural disturbances such as wildland fires with relatively long fire-return intervals. The major land-management activities affecting forests include fire suppression, timber harvesting, and recreation. (Photograph by Zhiliang Zhu.)

Inside of cover: An open-canopy scrub landscape under late-afternoon sun in Petrified Forest National Park, northeastern Arizona. The desert ecosystem is composed primarily of creosote bush, saltbush, winterfat, and Mormon tea. (Photograph by Zhiliang Zhu.)

Back of cover: A riparian grassland on Antelope Flats in Grand Teton National Park near Jackson, Wyoming. In the fall, the grassland provides a strong contrast with the Teton Range and its forest-covered foothills in the background. (Photograph by Benjamin M. Sleeter.)

Baseline and Projected Future Carbon Storage and Greenhouse-Gas Fluxes in Ecosystems of the Western United States

By Zhiliang Zhu and Bradley C. Reed, Editors

Professional Paper 1797

U.S. Department of the Interior
U.S. Geological Survey

U.S. Department of the Interior
KEN SALAZAR, Secretary

U.S. Geological Survey
Marcia K. McNutt, Director

U.S. Geological Survey, Reston, Virginia: 2012

Suggested citation:
Zhu, Zhiliang, and Reed, B.C., eds., 2012, Baseline and projected future carbon storage and greenhouse-gas fluxes in ecosystems of the Western United States: U.S. Geological Survey Professional Paper 1797, 192 p.
(Also available at http://pubs.usgs.gov/pp/1797/.)

Acknowledgments

Many people helped with the development of the methods and the models, the preparation and analysis of data, and the preparation of this report. The development of soil and wetland data was provided by Norman Bliss of Arctic Slope Regional Corporation Research and Technology Solutions and Kristin Byrd of the U.S. Geological Survey (USGS). Guidance on the use of the U.S. Department of Agriculture (USDA) Forest Service's forest inventory and assessment data was provided by Samuel Lambert, Elizabeth LaPoint, Patrick Miles, Ronald Piva, Jeffery Turner, and Brad Smith of the USDA Forest Service's Forest Inventory and Analysis Program. Software, data, and computation support was provided by Brian Davis, Layth Grangaard, Ronald Kanengieter, and Rob Quenzer of Stinger Ghaffarian Technologies, Inc. Guidance on the wildland-fire-model codes and computation was provided by Mark Finney, Matt Jolly, and Robert Keane of the USDA Forest Service's Missoula Fire Sciences Laboratory; Elizabeth Reinhardt of the USDA Forest Service's Office of the Climate Change Advisor; and Jodi Riegle of the USGS. Ashwan Reddy (USGS) and Feng Zhao (University of Maryland) provided literature review and data-processing support. Christopher Torbert of the USGS provided management support for the project.

Special thanks go to 10 anonymous peer reviewers of this report.

This page intentionally left blank.

Contents

Conversion Factors

Multiply	By	To obtain
	Length	
centimeter (cm)	0.3937	inch (in.)
millimeter (mm)	0.03937	inch (in.)
meter (m)	3.281	foot (ft)
kilometer (km)	0.6214	mile (mi)
meter (m)	1.094	yard (yd)
	Area	
square meter (m^2)	0.0002471	acre
hectare (ha)	2.471	acre
square kilometer (km^2)	247.1	acre
square meter (m^2)	10.76	square foot (ft^2)
hectare (ha)	0.003861	square mile (mi^2)
square kilometer (km^2)	0.3861	square mile (mi^2)
acre	4,047	square meter (m^2)
acre	0.4047	hectare (ha)
acre	0.4047	square hectometer (hm^2)
acre	0.004047	square kilometer (km^2)
	Flow rate	
cubic meter per second (m^3/s)	70.07	acre-foot per day (acre-ft/d)
meter per second (m/s)	3.281	foot per second (ft/s)
meter per day (m/d)	3.281	foot per day (ft/d)
cubic meter per second (m^3/s)	35.31	cubic foot per second (ft^3/s)
cubic meter per second (m^3/s)	22.83	million gallons per day (Mgal/d)
millimeter per year (mm/yr)	0.03937	inch per year (in/yr)
	Hydraulic conductivity	
meter per day (m/d)	3.281	foot per day (ft/d)
	Application rate	
kilograms per hectare per year [(kg/ha)/yr]	0.8921	pounds per acre per year [(lb/acre)/yr]

Temperature in degrees Celsius (°C) may be converted to degrees Fahrenheit (°F) as follows:

$$°F=(1.8×°C)+32$$

The resolution of pixels in spatial datasets follows the conventions used in the spatial data and modeling communities. The format is "*n*-meter resolution," where *n* is a numerical value for the length. The usage translates into a pixel with a length of *n* on all sides that covers an area of *n* meters × *n* meters.

How Megagrams, Gigagrams, Teragrams, and Petagrams Relate to Metric Tons

1 megagram (Mg)	=	1 million grams (10^6 g)	=	1 metric ton (t)
1 gigagram (Gg)	=	1 billion grams (10^9 g)	=	1,000 metric tons
1 teragram (Tg)	=	1 trillion grams (10^{12} g)	=	1 million metric tons (Mt)
1 petagram (Pg)	=	1 quadrillion grams (10^{15} g)	=	1 billion metric tons (Gt)

Abbreviations, Acronyms, and Chemical Symbols

µatm	microatmospheres
µeq/L	microequivalents per liter
AMLE	Adjusted Maximum Likelihood Estimation
ANC	acid neutralizing capacity
ARMS	Agricultural Resource Management Survey
AUC	area under the curve
AUM	animal unit month
BGC	biogeochemical
°C	Celsius
C	carbon
C_3	cool-season grasses
C_4	warm-season grasses
C_{burial}	carbon in buried sediment
C_{CONC}	carbon concentration in sediments
CCCma CGCM3.1	The Third Generation Coupled Global Climate Model of the Canadian Centre for Climate Modelling and Analysis
CENTURY	a biogeochemical model
CFS	Canadian Forest Service
CH_4	methane
CMIP3	Coupled Model Intercomparison Project phase 3
CO	carbon monoxide
CO_2	carbon dioxide
$CO_{2\text{-air}}$	concentration of CO_2 in the atmosphere
$CO_{2\text{-eq}}$	carbon dioxide equivalent
$CO_{2\text{-eq}}$/yr	carbon dioxide equivalent per year
$CO_{2\text{-water}}$	dissolved CO_2 concentrations
CO_3^{2-}	carbonate
CONUS	conterminous United States
CRM	crop residue management
Cs	cesium
CSIRO–Mk3.0	Australia's Commonwealth Scientific and Industrial Research Organisation Mark 3.0
CTIC	Conservation Technology Information Center
DB 0.33 bar H_2O	the oven-dry weight of the less than 2 mm soil material per unit volume of soil at a water tension of 1/3 bar (as used in the SSURGO database)
DIC	dissolved inorganic carbon
DOC	dissolved organic carbon
ECHAM5	European Centre for Medium-Range Weather Forecasts—Hamburg 5
EDCM	Erosion-Deposition-Carbon Model
EISA	Energy Independence and Security Act
EPA	Environmental Protection Agency
ERC	energy release component
ETM+	Enhanced Thematic Mapper Plus
FCCS	Fuel Characterization Classification System
FIA	U.S. Forest Service Forest Inventory and Analysis Program
FIPS	Federal Information Processing Standard
FLM	fuel loading model
FOFEM	First Order Fire Effects Model

Abbreviations, Acronyms, and Chemical Symbols—Continued

FORE–SCE	"forecasting scenarios of land-cover change" model
FS	U.S. Forest Service
g	gram
gC	grams of carbon
gC/m^2	grams of carbon per square meter
$gC/m^2/d$	grams of carbon per square meter per day
$gC/m^2/yr$	grams of carbon per square meter per year
GCM	general circulation model
$gCO_{2\text{-}eq}$	grams of carbon dioxide equivalent
$gCO_{2\text{-}eq}/m^2$	grams of carbon dioxide equivalent per square meter
$gCO_{2\text{-}eq}/m^2/d$	grams of carbon dioxide equivalent per square meter per day
$gCO_{2\text{-}eq}\ m^2/yr$	grams of carbon dioxide equivalent per square meter per year
GEMS	General Ensemble Modeling System
GFDL	Geophysical Fluid Dynamics Laboratory
GFED	Global Fire Emissions Database
Gg	gigagrams
Gg/yr	gigagrams per year
GgC/yr	gigagrams of carbon per year
GHG	greenhouse gas
GIS	geographic information system
GISS	Goddard Institute for Space Studies
GLM	general linear model
GPP	gross primary productivity
GWP	global warming potential
H_2CO_3	carbonic acid
HadCM2	Hadley Centre Coupled Model 2
HadCM3	Hadley Centre Coupled Model 3
HCO_3^-	bicarbonate
HR	heterotrophic respiration
HUC	hydrologic unit code
IAM	integrated assessment model
IMAGE	The Netherlands Environmental Assessment Agency's Integrated Model to Assess the Global Environment
IPCC	Intergovernmental Panel on Climate Change
k	gas transfer velocity
kCO_2	kilograms of carbon dioxide
K factor	soil erodibility factor
kg	kilogram
kg/d	kilograms per day
kg/yr	kilograms per year
kgC	kilograms of carbon
kgC/m^2	kilograms of carbon per square meter
$kgCO_{2\text{-}eq}/m^2/yr$	kilograms of carbon dioxide equivalent per square meter per year
km^2	square kilometers
km^2/yr	square kilometers per year
L	liter
LANDFIRE	Landscape Fire and Resource Management Planning Tools Project
Landsat	USGS and NASA Satellite Program

Abbreviations, Acronyms, and Chemical Symbols—Continued

LOADEST	USGS Load Estimator program
LPDAAC	Land Processes Distributed Active Archive Center
LULC	land use and land cover
CH_4	methane
Mha	megahectares
MIrAD–US	MODIS-derived national irrigated agricultural dataset
MIROC 3.2–medres	Model for Interdisciplinary Research on Climate version 3.2, medium resolution
MLR	multiple linear regression
MODIS	Moderate Resolution Imaging Spectroradiometer
moles/L	moles per liter
MSS	Multispectral Scanner
MTBS	Monitoring Trends in Burn Severity project
MT–CLIM	Mountain Climate Simulator
MTT	minimum travel time
N	nitrogen
NA	not applicable
NASS	National Agricultural Statistics Service
NBCD	National Biomass Carbon Dataset
NECB	net ecosystem carbon balance
NED	National Elevation Dataset
NEE	net ecosystem exchange
NEP	net ecosystem production
NFDRS	National Fire Danger Rating System
NHD	National Hydrography Dataset
NID	National Inventory of Dams
N_2O	nitrous oxide
NLA	National Lakes Assessment
NLCD	National Land Cover Database
NO_3	nitrate
NOAA	National Oceanic and Atmospheric Administration
NPP	net primary productivity
NRCS	National Resources Conservation Service
NTSG	Numerical Terradynamic Simulation Group
NWIS	National Water Information Service
Pb	lead
PCM	Parallel Climate Model
pCO_2	partial pressure of carbon dioxide
PDSI	Palmer Drought Severity Index
Pg	petagram
PgC	petagrams of carbon
PgC/yr	petagrams of carbon per year
PHREEQC	USGS computer program that simulates chemical reactions and transport processes in natural or polluted water
PRDX	potential maximum production parameter
PRISM	parameter-elevation regressions on independent slopes model
PRMS	Precipitation-Runoff Modeling System
R^2	coefficient of determination

Abbreviations, Acronyms, and Chemical Symbols—Continued

RESSED	Reservoir Sedimentation Database
RMSE	root mean square error
RPA	U.S. Forest Service Forest and Rangeland Renewable Resources Planning Act of 1974
R–FME	Flexible Modeling Environment using R software
SCE	Shuffled Complex Evolution
SOC	soil organic carbon
SPARROW	"spatially referenced regression on watershed attributes " water-quality model
SRES	IPCC's Special Report on Emissions Scenarios
SSURGO	Soil Survey Geographic database (NRCS)
Tg	teragram
TgC	teragrams of carbon
TgC/yr	teragrams of carbon per year
$TgCO_2/yr$	teragrams of carbon dioxide per year
$TgCO_{2\text{-}eq}$	teragrams of carbon dioxide equivalent
$TgCO_{2\text{-}eq}/yr$	teragrams of carbon dioxide equivalent per year
Tg/yr	teragrams per year
TM	Landsat's Thematic Mapper
TN	total nitrogen
TOC	total organic carbon
TPO	timber product output
TSS	total suspended sediment
USDA	U.S. Department of Agriculture
U.S. EPA	U.S. Environmental Protection Agency
USFS	U.S. Forest Service
USGS	U.S. Geological Survey
VCT	vegetation change tracker
WCRP	World Climate Research Programme

Executive Summary—Baseline and Projected Future Carbon Storage and Greenhouse-Gas Fluxes in Ecosystems of the Western United States

By Zhiliang Zhu[1], Brian A. Bergamaschi[2], David Butman[3], David W. Clow[4], Todd J. Hawbaker[4], Jinxun Liu[5], Shuguang Liu[6], Cory P. McDonald[7], Benjamin M. Sleeter[8], Richard A. Smith[1], Terry L. Sohl[6], Sarah M. Stackpoole[4], Anne Wein[8], and Yiping Wu[9]

This is the second in a series of reports produced by the U.S. Geological Survey (USGS) to fulfill the requirements of section 712 of the Energy Independence and Security Act (EISA) of 2007 and to conduct a comprehensive national assessment of carbon (C) storage and flux (flow) and the fluxes of other greenhouse gases (GHGs, including carbon dioxide (CO_2), methane (CH_4), and nitrous oxide (N_2O)). These carbon and GHG variables were examined in the Western United States for major terrestrial ecosystems (forests, grasslands/shrublands, agricultural lands, and wetlands) and aquatic ecosystems (rivers, streams, lakes, estuaries, and coastal waters) in two time periods: baseline (the first half of the 2000s) and future (projections from baseline to 2050).

The major questions that this assessment attempted to answer included the following: (1) How much carbon was stored in ecosystems of the Western United States? (2) How much carbon could be stored in future years? (3) How were the carbon storage and fluxes in the Western United States influenced by both natural and anthropogenic processes such as land use, wildland fire, and climate change? (4) How might carbon storage, carbon flux, and the natural and anthropogenic processes that influence carbon cycling in western ecosystems vary both geographically and temporally?

The assessment covered 2.66 million square kilometers (km^2) in the Western United States, which is divided into in five level II ecoregions (as defined by the Environmental Protection Agency (EPA)): Western Cordillera, Marine West Coast Forest, Cold Deserts, Warm Deserts, and Mediterranean California. The assessment was based on measured and remotely sensed data collected by the USGS and many other agencies and organizations combined with statistical methods and simulation models. The major findings and discussion follow below.

Baseline and Projected Future Land-Use and Land-Cover Change

- In 2005, the total area of the Western United States (2.66 million km^2) was distributed over these ecosystems: grasslands/shrublands (58.9 percent), forests (28.1 percent), agricultural lands (6.1 percent), water (1.5 percent), wetlands (0.38 percent), and other land types (5.2 percent). Between 1992 and 2005, changes in land use (such as croplands) and land cover (such as wetlands) in the Western United States affected 2.9 percent of that land area and were driven by demands for forest products, urban development, and agriculture. The change in land use and land cover (LULC) from 2006 to 2050 for all ecosystems in the Western United States was projected to be between 5.8 and 7.8 percent. The most active ecoregions of projected land use and cover (LULC) change were the Marine West Coast Forest, Western Cordillera, and Mediterranean California.

[1]U.S. Geological Survey, Reston, Va.

[2]U.S. Geological Survey, Sacramento, Calif.

[3]Yale University, New Haven, Conn.

[4]U.S. Geological Survey, Denver, Colo.

[5]Stinger Ghaffarian Technologies, Inc., Sioux Falls, S.D.

[6]U.S. Geological Survey, Sioux Falls, S.D.

[7]U.S. Geological Survey, Boulder, Colo.

[8]U.S. Geological Survey, Menlo Park, Calif.

[9]Arctic Slope Regional Corporation Research and Technology Solutions, Sioux Falls, S.D.

- The projected changes (to 2050) in both LULC and climate were used in this assessment to support the projection of future potential carbon storage and fluxes in relation to both ecological and economic processes. The resulting projections were highly variable across regions as were the assumptions that were made. Between the regions and the assumptions, the overall rates of projected LULC change varied from 1.3 percent to 45 percent. The models of projected climate change (using general circulation model data) indicated (1) a projected general increase in both the mean temperature and in extreme temperatures throughout the Western United States, and (2) a projected high variability in precipitation change that depended on the ecoregion, seasonality, downscaling, and interannual variability.

Baseline Carbon Storage and Flux

- The estimated average total carbon storage in the ecosystems of the Western United States in 2005 was approximately 13,920 (12,418–15,460) teragrams of carbon (TgC), which was distributed in forests (69 percent), grasslands/shrublands (25 percent), agricultural lands (4.3 percent), wetlands (0.46 percent), and other lands (0.63 percent). Geographically, the estimated total and per-unit-of-area carbon stocks ranged from 700.2 TgC (the Cold Deserts) to 8,162.8 TgC (the Western Cordillera) and from 1.5 kilograms of carbon per square meter (kgC/m^2) (the Cold Deserts) to 16.1 kgC/m^2 (the Marine West Coast Forest), respectively. On average, the forests in the Western United States maintained the largest stock of carbon per unit of area among all of the ecosystems at 13.0 kgC/m^2, followed by wetlands (6.3 kgC/m^2), agricultural lands (3.7 kgC/m^2), grasslands/shrublands (2.2 kgC/m^2), and other land types (0.5 kgC/m^2). Overall, live biomass and soil organic carbon (assessed in the top 20-cm-thick layer) accounted for 38 and 39 percent of the total carbon stock, respectively, and woody debris and other surface carbon pools represented the remaining 23 percent.

- The net carbon flux was calculated as the change of carbon stock between two points in time. A negative number indicates carbon uptake, carbon sequestration, or a carbon sink; a positive number indicates a carbon emission or a carbon source. From 2001 to 2005, an average annual net flux of −86.6 (−162.9 to −13.6) TgC/yr was estimated for all of the terrestrial ecosystems in the Western United States. In lakes and reservoirs throughout the Western United States, an additional −2.4 (−3.7 to −1.2) TgC/yr was estimated to be buried and sequestered in sediments. The flux in the Pacific coastal waters was approximately −2.0 TgC/yr. Thus, the combined estimates resulted in a total annual carbon-sequestration rate of −91 TgC/yr across all of the major ecosystems in the Western United States; this rate is equivalent to 4.9 percent of the nation's net fossil-fuel emissions in 2010 as reported by the U.S. Environmental Protection Agency (EPA, 2010). Most of the net carbon flux was in forests (62.2 percent, −72.1 grams of carbon per square meter per year, or $gC/m^2/yr$), followed by grasslands/shrublands (29.6 percent, −16.4 $gC/m^2/yr$), agricultural lands (7.1 percent, −38.3 $gC/m^2/yr$), and wetlands (0.96 percent, −82.1 $gC/m^2/yr$). For comparison, a recent study found that the net carbon fluxes in forests were approximately −93 $gC/m^2/yr$ for the United States as a whole and −103 $gC/m^2/yr$ for the world's temperate forests (Pan, Birdsey, and others, 2011). Of the total carbon sink, live biomass accounted for 32 percent, soil organic matter accounted for 45 percent, and dead biomass accounted for 23 percent.

Projected Future Potential Carbon Storage and Flux

In order to project the future potential carbon storage amounts and flux rates, combinations of LULC scenarios and climate projections, developed on an annual basis between 2006 and 2050, were used along with multiple biogeochemical models for the assessment. The results of these combinations led to a range of estimates for both carbon storage and flux under a range of projected future conditions. The results of projected future potential carbon stock and flux were highly variable among multiple model runs, ecoregions, and ecosystems

- The total amount of carbon that potentially could be stored in the ecosystems of the Western United States in 2050 was projected to range from 13,743 to 19,407 TgC, which is an increase of 1,325 to 3,947 TgC (or 10.7 to 25.5 percent) from baseline conditions of 2005. Among the five ecoregions, the Western Cordillera potentially could store the most carbon, accounting for 60 percent of the projected future total carbon storage for the Western United States, followed by the Cold Deserts (18 percent of the total), Marine West Coast Forest (10 percent), Mediterranean California (8 percent), and Warm Deserts (4 percent). Among the different ecosystems, the forests potentially could store the most carbon, accounting for 70 percent of the total potential carbon storage in the Western United States, followed by grasslands/shrublands (23 percent of the total), and agricultural lands (6 percent).

- The potential mean annual net carbon flux between 2006 and 2050 was projected to range from −113.9 TgC/yr to 2.9 TgC/yr. When compared to the baseline net carbon flux estimates (−162.9 to −13.6 TgC/yr), the projected future carbon-sequestration rates in the Western United States represented a potential decline by 16.5 to 49 TgC/yr. The projected decline came largely from ecosystems of grasslands/shrublands and forests and was distributed mostly in the Western Cordillera ecoregion.

Baseline and Projected Future Potential Wildland Fire Combustion Emissions

Wildland fire is a major ecosystem disturbance in the Western United States that is influenced by changes in both climate and land use and leads to a considerable interannual and regional variability in GHG emissions.

- Between 2001 and 2008 in the Western United States, the burned areas and their GHG emissions from combustion ranged from 3,345 to 25,206 square kilometers per year (km^2/yr), and from 6.8 to 75.3 teragrams of carbon dioxide equivalents per year ($TgCO_{2\text{-}eq}$/yr) (1.9 to 20.6 TgC/yr), respectively, mostly in the Western Cordillera and Cold Deserts ecoregions. The annual average GHG emission from the fires was 36.7 $TgCO_{2\text{-}eq}$/yr (10.0 TgC/yr), which was equivalent to 11.6 percent of the estimated average rate of carbon sequestration by terrestrial ecosystems in the Western United States.

- Under future projections of climate change, the area burned by wildland fires was projected to increase by 31 to 66 percent and the GHG combustion emissions from wildland fires were projected to increase by 28 to 56 percent, relative to baseline conditions. These projections, combined with the projected decline in future terrestrial carbon sequestration, could lead to wildland fire combustion emissions equivalent to 27 to 43 percent of carbon sequestration by terrestrial ecosystems in the Western United States. Under extreme climate conditions, wildland fire emissions were projected to increase 73 to 150 percent relative to baseline conditions. Carbon stored in the arid and semiarid parts of the Western United States is especially vulnerable to wildland-fire emissions.

Carbon Cycling in Aquatic Ecosystems of the Western United States

Carbon cycling in and out of the aquatic ecosystems was studied separately from the terrestrial ecosystems in the Western United States. Carbon fluxes and rates of burial within sediments in inland water bodies and coastal waters were estimated using separate methods. The derived results are as follows.

- Using data collected between the 1970s and the present, rivers and streams throughout the Western United States were estimated to transport between 5.5 and 8.9 (average 7.2) TgC/yr (or an average of 3.4 gC/m^2/yr in yield per unit of area) of dissolved inorganic and total organic carbon annually from upstream sources to estuaries and the coastal oceans, where most was returned to the atmosphere. The emissions of carbon dioxide to the atmosphere from inland waters of the Western United States ranged from 16.8 to 48.7 (average 28.2) TgC/yr (or an average of 14.8 gC/m^2/yr in yield per unit of area); 93 percent of the total emissions were from rivers and streams and 7 percent were from lakes and reservoirs.

- The rate of carbon burial (sequestration) in the sediments in the lakes and reservoirs was estimated to range from −1.2 to −3.7 (average 2.4) TgC/yr (or an average of −1.2 gC/m^2/yr in yield per unit of area), whereas in coastal waters the average burial rate was approximately 2.0 TgC/yr. The estimates of carbon fluxes in aquatic ecosystems were highly variable because of differences in precipitation, topography, lithology, and other controlling processes.

Baseline and Projected Future Greenhouse-Gas Fluxes

- In addition to the baseline net carbon flux estimates (−162.9 to −13.6 TgC/yr, or −597.7 to −50.0 $TgCO_{2\text{-}eq}$/yr), the baseline methane (CH_4) and nitrous oxide (N_2O) flux rates were also estimated and were relatively low and highly variable among ecosystems and ecoregions. Overall, the estimated flux rate of methane during the baseline years ranged from −3.1 to −2.9 $TgCO_{2\text{-}eq}$/yr. The estimated flux rate of nitrous oxide remained stable over the baseline years and averaged 1.7 $TgCO_{2\text{-}eq}$/yr. The balance between the three GHGs was projected to continue to 2050, with a large but weakened sink for CO_2 and a weak sink or source for CH_4 and N_2O, depending on the variability of the projected results.

Limitations of the Assessment Report

The known limitations of the assessment report include the following: (1) Forest thinning and rangeland grazing were not considered in estimating the carbon stocks and fluxes. (2) The effects of conservation and recreation management were not specifically analyzed in this report. (3) Wildland-fire combustion emissions were estimated, but the long-term effects of wildland fires on the production of carbon in ecosystems were not analyzed separately in this report. (4) Methane and nitrous oxide fluxes were projected to future years based on a set of LULC scenarios without considering the effects of climate change projections. (5) The baseline carbon fluxes were estimated for the first time for aquatic ecosystems, but the existing carbon storage in the sediments of the aquatic ecosystems was not estimated. (6) Uncertainties from model runs of different components of the assessment were quantified using simple statistical methods to account for the spread of the estimates. Other sources of uncertainties were described in the report but were not quantified. As a result, the total uncertainty of the assessment is unknown. In addition, there were limitations resulting from the methodology used for the assessment; specifically, (a) the changes in vegetation types or structures as the result of plant succession or climate change were not addressed, and (b) the mapping and modeling of major components (such as LULC and wildland fires) of the assessment were not coupled in a completely integrative modeling system.

Chapter 1. An Assessment of Carbon Sequestration in Ecosystems of the Western United States—Scope, Methodology, and Geography

By Zhiliang Zhu[1], Benjamin M. Sleeter[2], Glenn E. Griffith[2], Sarah M. Stackpoole[3], Todd J. Hawbaker[3], and Brian A. Bergamaschi[4]

1.1. Scope and General Methodology of the Assessment

This is the second in a series of reports produced by the USGS for a national assessment of carbon sequestration and greenhouse-gas (GHG) fluxes in ecosystems. The first report (Zhu and others, 2011) covered ecosystems of the Great Plains region of the United States. This report covers ecosystems in the Western United States, which extends from the Rocky Mountains in the east to the Pacific coastal waters in the west. The area of coverage is approximately 2.66 million square kilometers (fig. 1.1).

The carbon sequestration and GHG flux assessment was mandated by the Energy Independence and Security Act of 2007 (EISA; U.S. Congress, 2007), which directed the U.S. Department of the Interior to produce a methodology and conduct a national assessment to quantify (1) the amount of carbon stored in ecosystems, (2) the capacity of ecosystems to sequester carbon, and (3) the rate of GHG fluxes in and out of the ecosystems. This regional assessment has two major objectives: (1) implement the EISA mandate to conduct a national assessment of carbon sequestration and GHG fluxes, and (2) improve the understanding of the regional carbon cycling by focusing on changes in carbon stocks and fluxes in all the major ecosystems, and on the major natural and anthropogenic processes that control carbon cycling (such as climate change, land use, and wildland fires). The GHGs considered in this assessment were carbon dioxide (CO_2), carbon monoxide (CO, from wildland fires only), dissolved inorganic carbon (DIC), methane (CH_4), and nitrous oxide (N_2O).

The major ecosystems evaluated in this study are both terrestrial (forests, wetlands, grasslands/shrublands, and agricultural lands) and aquatic (rivers, lakes, estuaries, and coastal waters). The thematic definitions of the ecosystems and their spatial boundaries are outlined in table 2.1 of chapter 2 of this report and in Zhu and others (2010). The definitions are largely based on the National Land Cover Database (NLCD; Vogelmann and others, 2001; Homer and others, 2007), which was the primary source of initial land-use and land-cover (LULC) data for this assessment. The LULC data derived from remote sensing datasets were used to define the spatial boundaries of the ecosystems that were assessed in this study; because the remote-sensing data allowed for wall-to-wall coverage of the Western United States, the resulting spatially and temporally explicit data products and estimates are considered to be comprehensive.

Within the NLCD database, both land use (for example, agricultural lands) and land cover (for example, forests) are mapped using using data acquired from Landsat satellites. Within the LULC classes, land-management activities were defined as those actions that were aligned with the LULC classes and modified the way land was used, but did not change the LULC classes; for instance, cropland irrigation or fertilization was a land-management activity that did not change the LULC class of the land. Ecosystem disturbances were defined as those natural disturbances that altered the production of carbon or other functions in an ecosystem. For this assessment, wildland fire was the only natural disturbance that was considered.

[1]U.S. Geological Survey, Reston, Va.

[2]U.S. Geological Survey, Menlo Park, Calif.

[3]U.S. Geological Survey, Denver, Colo.

[4]U.S. Geological Survey, Sacramento, Calif.


120°
110°
45°
40°
35°
30°
CANADA
MONTANA
NORTH DAKOTA
SOUTH DAKOTA
NEBRASKA
COLORADO
KANSAS
OKLAHOMA
TEXAS
NEW MEXICO
WYOMING
WASHINGTON
OREGON
IDAHO
NEVADA
UTAH
CALIFORNIA
ARIZONA
MEXICO
PACIFIC OCEAN
NC
PL
CP
CR
BM
NR
MR
WV
C
ECSF
KM
NBR
SRP
WB
WUM
CBR
SNM
CCV
SCCCOW
SCM
MBR
ANP
ANM
SBR
MA
CD
SR
0 100 200 300 MILES
0 100 200 300 KILOMETERS
Base from 2001 National Land Cover Database
(Homer and others, 2007)

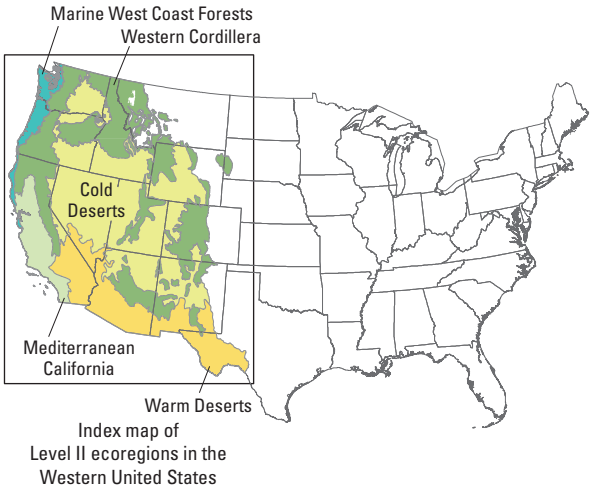

Index map of Level II ecoregions in the Western United States

EXPLANATION

Land cover

- Water
- Developed
- Mechanically disturbed (national forest)
- Mechanically disturbed (other public protected)
- Mechanically disturbed (private land)
- Mining
- Barren
- Deciduous forest
- Evergreen forest
- Mixed forest
- Grassland
- Shrubland
- Agriculture
- Hay/pasture
- Herbaceous wetland
- Woody wetland
- Ice/snow

Ecoregion boundary

- Level III
- Level II

Western Cordillera

C	Cascades
NC	North Cascades
ECSF	East Cascades—Slopes and Foothills
KM	Klamath Mountains
BM	Blue Mountains
SNM	Sierra Nevada Mountains
NR	Northern Rockies
CR	Canadian Rockies
WUM	Wasatch-Uinta Mountains
MR	Middle Rockies
SR	Southern Rockies
ANM	Arizona-New Mexico Mountains

Marine West Coast Forest

CR	Coast Range
PL	Puget Lowland
WV	Willamette Valley

Cold Deserts

CP	Columbia Plateau
SRP	Snake River Plain
NBR	Northern Basin and Range
CBR	Central Basin and Range
WB	Wyoming Basin
CP	Colorado Plateaus
ANP	Arizona-New Mexico Plateau

Warm Deserts

MBR	Mojave Basin and Range
SBR	Sonoran Basin and Range
MA	Madrean Archipelago
CD	Chihuahuan Deserts

Mediterranean California

CCV	Central California Valley
SCM	Southern California Mountains
SCCCOW	Southern and Central California Chaparral and Oak Woodlands

Figure 1.1 (see facing page). Map showing the spatial extent of this assessment. The Western United States region consists of five level II ecoregions (modified from U.S. Environmental Protection Agency, 1999); they are the Marine West Coast Forest, Western Cordillera, Cold Deserts, Warm Deserts, and Mediterranean California. The level III ecoregions also are shown. The total area of the Western United States is approximately 2.66 million square kilometers. The land-use and land-cover classes shown on the map represent conditions that existed around 2005.

The assessment was conducted using a methodology framework that (1) linked land use, land management, and climate data with statistical and process-based methods and models to generate spatially and temporally explicit carbon storage and GHG flux estimates; (2) used remote sensing input data, existing resource and soil inventories, climate histories, and measurements made by a national network of streamgages; and (3) applied a set of future land- and climate-change scenarios to the assessment to estimate a range of carbon stocks and sequestration rates in ecosystems. The major components of the assessment methodology and their connections are shown in figure 1.2, with corresponding chapters of this report marked in the boxes and methodological details described in the chapters.

The methodology framework shown in figure 1.2 is both spatially and temporally explicit. The spatial foundation of the assessment is the LULC modeling component (chapter 2), in which the ecosystems were mapped seamlessly, and all pixels were partitioned into LULC and LULC-change classes. The temporal foundation of the assessment was twofold and included baseline data (currently available data for various controlling variables) and future projected data (generated by the use of scenarios; chapter 6). Both the baseline and future projected data (from contemporary time to 2050) were collected in a manner consistent with the Intergovernmental Panel on Climate Change (IPCC) Special Report on Emission Scenarios (Nakicenovic and others, 2000). The area burned by, severity of, and emissions from wildland fires during both the baseline and future projection periods were estimated by integrating remote sensing data with statistical and landscape modeling (chapters 3 and 8). The baseline and future projected terrestrial ecosystems' carbon stocks and fluxes were estimated by using process-based models, which took into account various biomass and soil-carbon input data as well as the the results of LULC and wildland-fire modeling (chapters 5 and 9). Estimates of baseline carbon flux and sequestration in both inland and coastal aquatic ecosystems were calculated separately and were based on a series of studies detailed in chapters 10 and 11. General circulation models of future climate-change projections (described in chapter 7) were

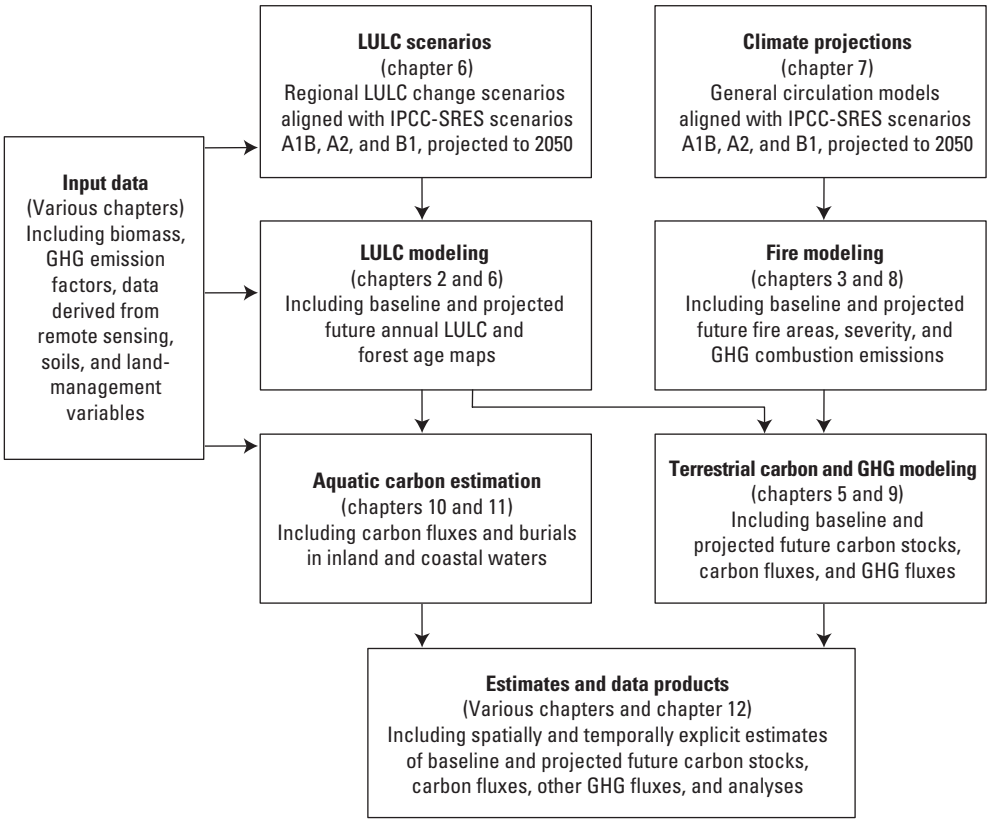

Figure 1.2. Flow diagram showing the general methodology framework. The heading in each box represents a major component of the assessment. The chapter numbers indicate where in this report those components are discussed. Arrows show relations between components. GHG, greenhouse gas; IPCC-SRES, Intergovernmental Panel of Climate Change Special Report on Emissions Scenarios (Nakicenovic and others, 2000); LULC, land use and land cover.

incorporated into the assessment to allow for an analysis of the effects of future climate change. The relation between the estimates of carbon sequestration and flux and natural and anthropogenic processes is briefly presented in chapter 12.

Both current and projected future changes in carbon storage and GHG fluxes were estimated in the assessment in order to establish a baseline and provide a range of potential carbon-sequestration capacities, which is a requirement of the EISA. The term "baseline" is defined as the average contemporary annual conditions to be assessed. Different components of the assessment have different ranges of baseline years because they are limited by the years for which data were available, as follows: LULC (1992–2005), wildland fires (2001–2008), terrestrial carbon and GHG fluxes (2001–2005), and aquatic carbon fluxes (1920s to present). The input datasets used for the assessment include those developed by the USGS and other agencies and organizations. The output datasets are in the form of either annual digital maps or annual statistics. The digital maps have a nominal spatial resolution of 250 by 250 meters. Because the assessment was conducted at both national and broad regional scales, the resulting information and data products should be applied only at the regional scale or broader.

The methodology was developed to meet the above-noted objectives, particularly to analyze the carbon dynamics in relation to land use, land management, and climate changes. This assessment did not include a GHG life-cycle analysis or an economic feasibility modeling of land use changes. In addition, vegetation dynamics from succession or climate change were not modeled for the assessment, and the major components of the assessment were not coupled in a completely integrative modeling system (such a modeling system is not yet available for such a comprehensive assessment). The justification of the methodology, design rationales, and technical specifications are detailed in Zhu and others (2010) and are therefore not repeated in this report.

This assessment is organized by five level II ecological regions (ecoregions), which were adapted from the U.S. Environmental Protection Agency ecoregion map (EPA, 1999): (1) Western Cordillera, (2) Marine West Coast Forest, (3) Cold Deserts, (4) Warm Deserts, and (5) Mediterranean California (fig. 1.1). All of the assessment models were parameterized and the results were calibrated and validated on the basis of these ecoregions. In this report, the term "region" is often used in a general sense, depending on the context, whereas the term "ecoregion" refers to the EPA ecoregion hierarchy (EPA, 1999). The major terrestrial and aquatic ecosystems are analyzed within these ecoregions. The use of the ecoregions and the NLCD's LULC classes chosen for the ecosystems in this assessment suggests that the reported results are meaningful within the defined ecoregion and ecosystem boundaries and may not be directly comparable with other national-level or regional estimates because of the different boundary definitions. Further discussion of the ecoregions and ecosystems may be found in Zhu and others (2010).

The term "flux" refers both to emissions of GHG (such as carbon) to the atmosphere and to uptake by ecosystems. In presenting the results of terrestrial carbon flux assessment, the terms "net flux" and "net ecosystem carbon balance" (NECB) are also used interchangeably in the report to refer to the net rate of the change in carbon storage in ecosystems. The terms used in calculating NECB and (or) net flux include "net ecosystem production" (NEP, which is the difference between the net primary production and the heterotrophic respiration), "long-term fire emissions," and "biomass harvesting." When reporting losses or gains in carbon storage, a negative number indicates carbon uptake, carbon sequestration, or a carbon sink; a positive number indicates a carbon emission or a carbon source. These conventions are used throughout the report unless noted. The usages follow standard conventions found in the literature on this topic (such as Chapin and others, 2006; EPA, 2012) and are consistent with the terms used in the assessment report for the Great Plains region (Zhu and others, 2011).

In addition to assessing carbon storage and fluxes in ecosystems, the fluxes or emissions of other GHGs (such as CO_2, CH_4, CO, DIC, and N_2O) were also assessed. Fluxes or emissions of the other GHGs are reported as carbon dioxide equivalent ($CO_{2\text{-eq}}$) values and flux estimates were calculated on the basis of their respective global warming potential factors.

The units of measurement used in this report also follow previous usages. The total amount of carbon for a given region is reported in teragrams of carbon (TgC). When reporting carbon stock per unit of area, the values are given in kilograms of carbon (kgC). When reporting the carbon flux per unit of area, the values are given in grams of carbon (gC).

Whenever possible, the estimates are provided as a range of values in order to represent the spread of variability in assessment results. The ranges of values were derived on the following basis: (1) the range of baseline values was derived from the minimum and maximum of averages of model runs over the years 2001 to 2005, and (2) the range of projected future values was derived from the means of the unique LULC scenarios, climate-change projections, and biogeochemical models over projection years (2006–2050). The same calculations were applied to the baseline and future potential components of the wildland-fire assessment (chapters 3 and 8). For the aquatic ecosystem assessment (chapter 10), the range of values was derived from the 5th and 95th confidence intervals of Monte Carlo simulations.

1.2. Regional Geography

The five level II ecoregions covered by this assessment include the Western Cordillera, the Marine West Coast Forest, the Cold Deserts, the Warm Deserts, and Mediterranean California. The five ecoregions can be grouped into two large areas: (1) the Western Cordillera and Marine West Coast Forest, and (2) the Cold Deserts, Warm Deserts, and Mediterranean California. The following sections summarize the climate, physiography, hydrology, vegetation, and land use in these groupings of ecoregions. This geographic characterization provides a foundation for understanding the differences in carbon sequestration and fluxes between ecoregions in the Western United States.

1.2.1. The Western Cordillera and Marine West Coast Forest

The maritime and inland mountains and forests of the Western United States generally coincide with the Western Cordillera and Marine West Coast Forest (fig. 1.2). The mountainous areas of the Pacific Coast States include the Coast Range, the Cascades (including the North Cascades and the East Cascades—Slopes and Foothills), the Klamath Mountains, and the Sierra Nevada Mountains. Inland, the mountainous areas include the Rocky Mountains (Canadian Rockies, Northern Rockies, Middle Rockies (including the Black Hills), and Southern Rockies), Blue Mountains, Wasatch-Uinta Mountains, and the Arizona-New Mexico Mountains. These ecoregions contain some of the country's wettest climates (coastal temperate rain forests) and extremely cold climates (high alpine peaks), as well as semiarid and arid areas at low elevations, especially in the southern portions of the area. Although this area is mostly forested in comparison to the surrounding ecoregions, grasslands/shrublands also cover some parts of it. Forestry, mining, livestock grazing, wildlife habitat, tourism, and recreation are major land uses, along with some cropland and pasture in the larger valleys.

The Western United States is generally more arid than the rest of the country. Because of the topographic effect of the mountains, however, precipitation and runoff amounts in these two ecoregions are higher than in the adjacent ecoregions in the Great Plains, Basin and Range, and deserts. As much as 80 percent of the runoff is snowmelt (Stewart and others, 2004) and runoff distinctly increases with elevation, contributing to the headwaters of major rivers such as the Columbia and Colorado Rivers. A large portion of runoff originates in a relatively small fraction of the area compared to the Eastern United States, where runoff is relatively and spatially more uniform (Lettenmaier and others, 2008). Another distinct hydrologic feature is the Great Basin, a large endorheic (closed) basin that is disconnected from any coastal outlet. Therefore, any water that falls as rain or snow into this region does not escape out of it; surface water either evaporates or percolates instead of flowing toward the ocean (Orme, 2002).

The Western Cordillera ecoregion is a region of high, rugged, mostly forested mountains with a few open valleys. Plants, animals, and land use vary greatly with elevation. The lower elevations are commonly covered by grasslands/shrublands, the middle elevations are mostly forested, and most of the higher alpine areas above the timberline are covered with snow and ice for much of the year. Coniferous forests vary by latitude, elevation, and proximity to maritime influence but are primarily dominated by species such as Douglas-fir (*Pseudotsuga menziesii*), western hemlock (*Tsuga heterophylla*), western red cedar (*Thuja plicata*), subalpine fir (*Abies lasiocarpa*), grand fir (*A. grandis*), Engelmann spruce (*Picea engelmannii*), whitebark pine (*Pinus albicaulis*), lodgepole pine (*P. contorta*), ponderosa pine (*P. ponderosa*), and quaking aspen (*Populus tremuloides*).

Numerous small- to medium-sized streams and rivers and many small, naturally formed mountain lakes are found at high elevations (Melack and others, 1997; EPA, 2009). Caldera lakes, such as Crater Lake in Oregon and Yellowstone Lake in Wyoming, are located in the ecoregion (EPA, 2009). Several large rivers, such as the Columbia, Snake, Missouri, and Colorado River, have their headwaters in this region; downstream, these rivers are totally or partially regulated (Benke and Cushing, 2005). Grazing, which is the leading land use in the valleys and lower elevations of the Western Cordillera, has had a major impact on the quality of lands and streams. Timber harvesting is an important land use in the more heavily forested lower and middle elevations. Mining activities cover relatively small but numerous areas. Wildland fires are common and can burn extensive areas during drought years, especially when preceded by moist years with high vegetation productivity (Swetnam and Betancourt, 1990; Westerling and others, 2006; Littell and others, 2009). Large areas of the region are Federally managed public lands.

The Marine West Coast Forest ecoregion is characterized by a cool, moist climate with dry summers and wet, generally snowless winters. The low mountains of the Coast Range are covered by highly productive, rain-drenched needleleaf evergreen forests. The high levels of precipitation contribute to the magnitude of the streamflow found in many of the large rivers of the ecoregion, particularly the Columbia River. The Columbia, Umpqua, Rogue, Klamath, and Sacramento Rivers have their headwaters in the Western Cordillera and run through the maritime forests before draining to the Pacific Ocean. Sitka spruce (*Picea sitchensis*) forests originally dominated the fog-shrouded coast, and a mosaic of western red cedar, western hemlock, and seral Douglas-fir blanketed the inland areas. Wildland fires are rare, largely because of the moisture regime of this ecoregion; however, wildland fires

can be severe and extensive when they do occur (Agee, 1993; Littell and others, 2009). Today, Douglas-fir plantations are prevalent on the intensively logged and managed landscape and play a major role in producing forest carbon stocks. In California, redwood (*Sequoia sempervirens*) forests, which represent one of the largest carbon stocks in the country, are a dominant component of the region, along with some hardwoods such as tanoak (*Lithocarpus densiflorus*), Pacific madrone (*Arbutus menziessi*), bigleaf maple (*Acer macrophyllum*), and red alder (*Alnus rubra*). This ecoregion includes the drier, flatter, and more populated Willamette Valley and Puget Lowland, which are in the rain shadow of the Coast Range and Olympic Mountains. The fertile soil and temperate climate make the Willamette Valley an extremely productive agricultural area.

1.2.2. Cold Deserts, Warm Deserts, and Mediterranean California

The Cold Deserts, Warm Deserts, and Mediterranean California ecoregions stretch from Canada to Mexico and from the Pacific to the Great Plains, covering portions of 11 Western States. They are distinguished from the adjacent Western Cordillera and Marine West Coast Forest ecoregions by their aridity; mostly shrub, grass, and desert scrub vegetation; and generally lower relief and elevations. The dominant landforms include plains with hills and low mountains, plateaus and high-relief tablelands, some high mountains, and intermountain basins and valleys. The climate of the deserts is generally dry and Mediterranean California has a milder Mediterranean (hot summer and mild, wet winter) climate. Because of the climate, the hydrology of the ecoregions is different than that of the Western Cordillera and Marine West Coast Forest ecoregions. The annual precipitation in these ecoregions is highly variable and extreme droughts are not uncommon. Most streams and small rivers in these ecoregions are ephemeral, and the few perennial rivers originate in the adjacent forested mountainous ecoregions. A high proportion of the region is Federally managed public land, and the hydrology of many of the larger rivers has been greatly modified by dams, irrigation projects, and groundwater and surface-water extraction. The dry conditions and water withdrawals have caused some internal drainages to end in saline lakes (such as Utah's Great Salt Lake) or desert basins without reaching the ocean.

The Cold Deserts ecoregion is arid and includes a variety of physiographic features, such as basin-and-range terrain (a series of alternating linear valleys and mountain ranges), broad plateaus, and other mountains ranges and valleys. The ecoregion includes the Columbia Plateau and Snake River Plain (both of volcanic origin), the northern and central Great Basin, the Wyoming Basin, and the Colorado Plateau. The ecoregion is almost completely surrounded by the wetter, higher, more rugged, and forested mountain ranges of the Western Cordillera ecoregion. These wetter regions feed some of the headwaters and upper reaches of smaller rivers such as the Humboldt, Bear, Truckee, and Sevier Rivers. Vegetation is sparse and typically dominated by cold-temperate species such as sagebrush (*Artemisia* spp.), various bunchgrasses, and saltbush (*Atriplex spp*.); in the southern part of the ecoregion, there is more blackbrush (*Coleogyne ramosissima*), winterfat (*Krascheninnikovia lanata*), and greasewood (*Sarcobatus vermiculatus*). Juniper (*Juniperus spp.)*, pinyon pine (*Pinus edulis*), and singleleaf pinyon (*P. monophylla*) grow in the mountains, along with other conifers at higher elevations. Some areas are barren. Wildland fires are common and their occurrence is strongly related to climate, vegetation productivity, and the presence of invasive species such as cheatgrass (*Bromus tectorum*) (D'Antonio and Vitousek, 1992; Brooks and others, 2004; Mensing and others, 2006). Most of the ecoregion is used as rangeland. There are agricultural lands where irrigation is possible, either by groundwater or by diverting water from the Snake and Columbia Rivers, which flow through the region. Lakes formed by mainstem impoundments are common, including Lake Powell (the reservoir formed by Glen Canyon Dam on the Colorado River) and Franklin D. Roosevelt Lake (formed by the Grand Coulee Dam on the Columbia River).

The Warm Deserts ecoregion includes the Mojave, Sonoran, and Chihuahuan Deserts of the southwestern United States. Most of the ecoregion consists of basin-and-range terrain, where typically north-to-south-trending mountains are separated by broad basins and valleys bordered by sloping alluvial fans. As the name implies, this ecoregion is warmer than the Cold Deserts to the north, and large parts of the ecoregion are drier and at lower elevations. Winter snow is rare. Compared to the Cold Deserts, a larger percentage of the annual precipitation in this more subtropical desert ecoregion falls during the summer months and contributes to the rich diversity of plants and animals. This ecoregion encompasses the middle and lower sections of the Colorado and Rio Grande Rivers, which drain southward to the Gulf of California and the Gulf of Mexico, respectively. In many areas of the Mojave and western and central Sonoran Deserts, desert scrub commonly consists of creosote bush (*Larrea tridentata*) and white bursage (*Ambrosia dumosa*). In the eastern Sonoran Desert, the palo verde (*Cercidium spp.*)-cacti-mixed scrub vegetation includes the saguaro (*Carnegia gigantea*). Farther to the east, the high Chihuahuan Desert includes some desert grassland and large areas of arid shrubland dominated by creosote bush. The higher mountains in the ecoregion are forested by oak (*Quercus* spp.), juniper, and pinyon woodlands. Historically, wildland fires have been rare in the Warm Deserts, but the presence of invasive species has lead to an increase in wildland-fire occurrence (D'Antonio and Vitousek, 1992; Brooks and others, 2004; Brooks and

Chambers, 2011). Large parts of the Warm Deserts ecoregion are Federally owned, and many large lakes in the southwestern canyon regions are the products of large dam construction projects (EPA, 2009). The largest reservoir in the United States, Lake Mead (which was formed by the construction of the Hoover Dam), is located in this ecoregion. Water levels in reservoirs throughout this ecoregion can vary greatly because of drought and large-scale water removal for municipal and agricultural uses.

The Mediterranean California ecoregion is distinguished by a warm, mild Mediterranean climate, shrubland vegetation consisting of chaparral mixed with areas of grassland and oak savanna, agriculturally productive valleys, and a high population (over 30 million people) in extensive urban agglomerations. The vegetation on the chaparral-covered hills includes ceanothus (*Ceanothus* spp.), California buckeye (*Aesculus californica*), manzanita (*Arctostaphylos* spp.), scrub oak (*Quercus* spp.), and mountain-mahogany (*Cercocarpus* spp.). Coast live oak (*Quercus agrifolia*), canyon live oak (*Q. chrysolepis*), Pacific poison oak (*Toxicodendron diversilobum*), and California black walnut (*Juglans californica*) also grow in this ecoregion. The coastal sage scrub consists of chamise (*Adenostoma fasciculatum*), red shank (*A. sparsifolium*), white sage (*Salvia apiana*), black sage (*Salvia mellifera*), buckwheat (*Eriogonum fasciculatum)*, golden-yarrow (*Eriophyllum confertifolium*), and coastal cholla (*Cylindropuntia prolifera*). Wildland fires occur frequently in Mediterranean California. Although wildland fires are driven by climate in the arid parts of the Western United States, human influences, invasive species, and extreme winds are particularly important drivers in the Mediterranean California ecoregion (Keeley, 2006; Syphard and others, 2007; Moritz and others, 2010). Most of the larger perennial streams in the ecoregion originate in the bordering higher, wetter, mountainous ecoregions. Although the ecoregion is centered on the broad San Joaquin and Sacramento Valleys, it also contains several low coastal mountain ranges and, in the south, some higher mountain ranges, all of which are of sufficient elevation to contain perennial streams. The bigger rivers in the area—the Sacramento, San Joaquin, and Salinas Rivers—all drain to the Pacific Ocean. The widespread and diversified agriculture with many high-value crops and supporting hydrological engineering have greatly altered the ecosystems that occupy this ecoregion. Urban, suburban, and industrial land uses are significant drivers of land-cover change in some parts of the ecoregion. The central foothills and some of the coastal ranges are livestock grazing areas.

The river discharge into the Pacific coastal waters is dominated by small mountainous rivers. These small mountainous rivers tend to be short, drain watershed areas with high relief, and typically have river mouths discharging near the coast rather than into an estuary (Milliman and Syvitski, 1992; Wheatcroft and others, 2010). The result is that the Pacific coastal waters receive disproportionately large sediment loads compared to the other regions, which bury carbon directly or help transport it into the deep ocean (Hedges and Keil, 1995). The two largest rivers in the west, the Columbia and Sacramento Rivers, both drain areas of intensive agriculture and carry elevated nutrient loads to coastal waters, leading to an elevated carbon uptake by phytoplankton. Another important physiographic attribute is the shape of the Pacific Ocean basin, which allows the California Current to supply nutrients very close to the coast, which also contributes to phytoplankton production and—because of the high influx of sediment—the sequestration of carbon in coastal waters (Cotrim Da Cunha and others, 2007; Aufdenkampe and others, 2011). Finally, the presence of a narrow continental shelf results in the transport of a large proportion of sediment- and phytoplankton-derived carbon into the deep ocean, where it is effectively sequestered from the atmosphere (Hedges and Keil, 1995).

1.3. National and Regional Studies of Carbon Stock and Greenhouse-Gas Fluxes in Ecosystems

Existing estimates of carbon storage, sequestration, and GHG fluxes varied widely by ecosystem and by region in the Western United States. Forests occupy significant land areas and are the most important carbon sink. The forest inventories that were conducted by the U.S. Department of Agriculture (USDA) Forest Service indicated that in 2005, the forests in the Pacific Coast and Rocky Mountain regions (Forest Service regions 1 through 6), regardless of ownership, had a combined carbon stock of 15,095 teragrams of carbon (TgC) (15.7 kilograms of carbon per square meter, or kgC/m^2); the carbon stock in forests managed by the Forest Service was 8,278 TgC (18.0 kgC/m^2) (J.E. Smith and Heath, 2008; Heath and others, 2011).

Among the major forest carbon pools in the Western United States, live biomass represented approximately 50 percent of the total carbon stock, with the remaining carbon stock approximately evenly divided between soil organic carbon and dead woody debris (Donnegan and others, 2008; USDA, 2011). Furthermore, forests in the region sequestered carbon at an approximate rate of 87 teragrams of carbon per year (TgC/yr,) or 90.85 grams of carbon per square meter per year ($gC/m^2/yr$) (excluding the soil organic carbon pool) (J.E. Smith and Heath, 2008). In a separate analysis of recent forest inventories, the carbon stock in western forests was calculated for the five ecoregions used for this assessment (Brad Smith, USDA Forest Service, unpub. data, 2010; USDA Forest Service, 2012b). The results of the analysis showed that, among the five ecoregions and for all the major carbon pools, the Western Cordillera ecoregion contained the most stored carbon in forests and the Marine West Coast Forest had the largest carbon stock per unit of area in forests (table 1.1).

Table 1.1. Total and per-unit-of-area carbon stock from all of the major pools in the forest ecosystems in the five ecoregions of the Western United States.

[Data were derived from recent USDA Forest Service inventories and provided by Brad Smith (USDA Forest Service, unpub. data, 2010). Ecoregions are modified from EPA (1999). EPA, Environmental Protection Agency; kgC/m^2, kilograms of carbon per square meter; TgC, teragrams of carbon]

Modified level II EPA ecoregion	Carbon stock (TgC)	Carbon stock per unit of area (kgC/m^2)
Western Cordillera	9,878.0	15.9
Marine West Coast Forest	1,809.5	29.6
Cold Deserts	1,248.8	7.0
Warm Deserts	291.5	6.7
Mediterranean California	351.4	11.4
Western United States (total)	13,579.2	14.5

The most recent national GHG inventory report covering the conterminous United States suggested a net flux of −293.1 TgC in 2010 by forests, grasslands, agricultural lands, and settled areas, which represented an offset of approximately 15.4 percent of the total carbon dioxide emissions in the United States (EPA, 2012). Although the national inventory did not differentiate between regions, the net carbon flux per unit of area may be derived for three main categories that were similar to the ecosystem categories used for this assessment: forestlands remaining as forestlands, croplands (which include both row crops and hay and pasture and are similar to the agricultural lands ecosystem of this assessment) remaining as croplands, and grasslands (which include both shrublands and grasslands and are similar to the grasslands/shrublands ecosystem of this assessment) remaining as grasslands. From 2005 to 2010 for the conterminous United States, the derived mean net carbon flux rate per unit of area was −96.75, −3.42, and −0.97 gC/m^2/yr, respectively, for the above three categories. Using similar input data, Hayes and others (2012) separately determined that from 2000 to 2006, the average annual net fluxes for forests and croplands in the United States were −244.4 and −264.3 TgC/yr, respectively.

Using forest inventory data collected from 2000 to 2008 and covering the six USDA Forest Service regions (regions 1 through 6) in the Western United States (from the Pacific Coast to the Rocky Mountains), Heath and others (2011) estimated that net annual average carbon flux from forested land ranged from 24.9 to −111.2 TgC/yr (mean value of −43.1 TgC/yr, or −93.8 gC/m^2/yr). The annual carbon sink in the Western United States' forested land was from publicly owned forests; privately owned forests were a minor source (Heath and others, 2011). In a separate study for the State of Oregon, where climate and other biophysical conditions are favorable for carbon sequestration (particularly in the Marine West Coast Forest part of the State), D.P. Turner, Gockede, and others (2011) used forest-inventory data, land-use maps, and a process-based model to obtain estimates of per-unit-of-area net ecosystem production (NEP) for 2007 (a year with near-average climate conditions). The estimates were −101, −143, −88, 18, and −7 gC/m^2/yr, respectively, for forests, agricultural lands, woodlands, grasslands, and shrublands ecosystems.

Carbon sequestration is a function of the biogeochemical exchange between plants and the atmosphere, and it is strongly influenced by key controlling processes such as land use, land-management activities, ecosystem disturbances, and climate (Bachelet and others, 2003; Law and others, 2004; Running, 2008). Because water availability is the most limiting factor in the Western United States, carbon production in ecosystems tends to follow a precipitation gradient from west to east (Derner and Schuman, 2007). As a result, there is a high degree of year-to-year variation driven by the availability of moisture and the frequency or severity of related ecosystem disturbances, such as wildland fires. In a study comparing a year with normal average precipitation with a drought year, it was found that drought can reduce the NEP in forests of the Pacific Northwest by as much as 81 percent (D.P. Turner, Gockede, and others, 2011). On the other hand, simulation studies (such as Hudiburg and others, 2009; Smithwick and others, 2009) indicated that, under future climate-change scenarios with more precipitation and higher temperatures, increases in both carbon storage and the rate of sequestration may be expected.

Recent studies have documented an increase in wildland-fire activity in the Western United States as a result of climate change (Swetnam and Betancourt, 1990; Gedalof and others, 2005; Westerling and others, 2006; Littell and others, 2009). The impact of wildland fires on carbon sequestration in ecosystems included both (1) the immediate release of GHGs from combustion emissions and (2) the long-term combined effects of decomposing biomass, which releases carbon into the atmosphere, and regenerating vegetation, which increased the uptake of carbon (Law and others, 2004; Hurteau and Brooks, 2011; D.P. Turner, Ritts, and others, 2011). Although the short-term combustion emissions may be estimated relatively accurately by using remote-sensing data and emission models (van der Werf and others, 2010; French and others, 2011; chapter 3 of this report), other studies have shown that emissions from decomposition over the long term (years and decades) can be higher but more uncertain because burned landscapes may require years or decades for their NEP to return to pre-fire levels (Kashian and others, 2006; Cleary and others, 2010; Hurteau and Brooks, 2011; Kashian and others, in press). If the increases in fire frequency since 2000 in the Western United States continue into the future, the effects on carbon sequestration in ecosystems can be profound and need to be properly accounted for.

Various land-use policies and land-management actions in the Western United States have been implemented over the last 30 years to adapt to the changing climate and to the societal needs for ecosystem services. For example, since the 1980s in the Pacific Northwest, a decline in forest clearcutting, which was the result of changes in forest-management policies, has led to an increased per-unit-of area net flux of carbon: from 48 $gC/m^2/yr$ (a source) in the 1980s to −141 and −136 $gC/m^2/yr$ (sinks) in the 1990s and 2000s, respectively (D.P. Turner, Ritts, and others, 2011). A similar trend with an overall smaller magnitude of change was also observed for private forests in the above study. In the forested landscapes of the Northern Rockies, forest thinning, prescribed burning, and mechanical fuel treatment are frequently applied forest-management practices. Such practices have been studied for both the positive and negative effects on restoring the fire regime and reducing fire emissions to the atmosphere; the results were mixed across landscape types in the Western United States. The mechanical fuel treatments were generally found to reduce fire severity, fire risks, and immediate combustion emissions (Stephens and others, 2009; Wiedinmyer and Hurteau, 2010; North and Hurteau, 2011); however, their long-term effects on carbon sequestration in ecosystems were mixed. The use of mechanical fuel treatments and forest thinning as a means to reduce emissions and increase carbon sequestration were found to be ineffective or counterproductive in the Pacific Northwest (Hudiburg and others, 2011; Mitchelle and others, 2009) and the Northern Rockies (Reinhardt and Holsinger, 2010), but beneficial in the Sierra Nevada in California (North and Hurteau, 2011).

Grasslands/shrublands are the most prevalent ecosystem types in the Western United States, occupying almost 60 percent of the total land area. They are distributed primarily in the semiarid Great Basin and Colorado Plateau, as well as along the slopes of the major mountain systems. As with the forest ecosystems, carbon storage and sequestration in grasslands/shrublands ecosystems were highly correlated to the moisture gradient and influenced by land-management activities, particularly grazing-intensity management (Lal, 2004; Derner and Schuman, 2007). Heavy grazing during extended seasons may cause changes in species composition (including C_4 grasses replacing C_3 grasses and the dominance of cheatgrass (*Bromus tectorum*) in sagebrush communities), which may lead to a reduced amount of aboveground biomass, accelerated soil decomposition, and a loss of soil organic carbon stock to the atmosphere (Bradley and others, 2006; Derner and Schuman, 2007; Schuman and others, 2009). Reducing (but not necessarily excluding) grazing intensity usually helps improve soil-carbon preservation and sequestration because there is more decomposed vegetation contributing to the soils (Schuman and others, 2009). Although the net flux of carbon per unit of area in arid lands tends to be small or negligible, grasslands/shrublands cover vast areas; as a result, land use and management still exerts profound effects on the overall carbon balance of the ecosystem (Follett, 2001).

Most of the agricultural lands covered by this assessment are concentrated in the Mediterranean California ecoregion (where mainly orchards and annual vegetable crops are grown) and the Columbia River Basin and Snake River Plain in the Cold Deserts ecoregion (where irrigated row crops, hay, and pastures are dominant). In a study to quantify the effect of agriculture on California's carbon balance, Kroodsma and Field (2006) modeled changes in biomass and soil carbon in all of the agricultural lands in the State. Between 1980 and 2000, the study estimated the average annual net carbon flux for orchards (−26 $gC/m^2/yr$), vineyards (−26 $gC/m^2/yr$), annual vegetable crops (−14 $gC/m^2/yr$), and annual silages (about 0 $gC/m^2/yr$), with a mean value of −19 $gC/m^2/yr$ for all agricultural lands in California. The per-unit-of-area estimate for California was higher than the current-year (2010) EPA estimate (EPA, 2012) for all agricultural lands in the conterminous United States (CONUS), but was much lower than the estimate of −143 $gC/m^2/yr$ for the State of Oregon (D.P. Turner, Gockede, and others, 2011). In comparison, the assessment conducted for the Great Plains region (Zhu and others, 2011) produced an estimate of −18.8 $gC/m^2/yr$ for potential carbon sequestration by agricultural lands.

Bridgham and others (2006), who synthesized data from the literature, estimated that wetlands represented 11 percent of the total area of the United States (7 percent in Alaska, 4 percent in the CONUS). Most of the CONUS wetlands are distributed in the Atlantic and Gulf Coast Coastal Plains, the Great Lakes States, and the Great Plains. In the five western ecoregions of this assessment, wetlands represented less than half of one percent of the total area, as mapped using the 1992 NLCD (Vogelmann and others, 2001). Although they noted that uncertainties were very high, Bridgham and others (2006) put the carbon stock and sequestration rates in the wetlands of the CONUS at 19,600 TgC and 17.3 TgC/yr, respectively, which translated to 45.5 kgC/m^2 for the per-unit-of-area of carbon stock and 40.1 $gC/m^2/yr$ for the per-unit-of-area sequestration rate in the CONUS. The sequestration rate of wetlands in the CONUS was considered to be evenly distributed between peatlands, freshwater mineral soils, and tidal marshes (estuaries). Sequestration in estuaries is mostly accomplished as the result of sedimentation (Bridgham and others, 2006). Brevik and Homburg (2004) found that the net carbon flux in an estuary in southern California averaged −33 $gC/m^2/yr$ on the basis of an analysis of sediment samples spanning 5,000 years. Chmura and others (2003), however, estimated that sequestration in coastal salt marshes occurs at a much higher rate, ranging from 136.5 $gC/m^2/yr$ on the East Coast, to 206.3 $gC/m^2/yr$ in an estuary in southern California, to 296.6 $gC/m^2/yr$ on the Gulf Coast. Methane

emissions from ecosystems in the CONUS were estimated at approximately 50.4 $TgCO_{2\text{-}eq}$/yr (Bridgham and others, 2006) and were mostly emitted from freshwater, mineral-rich soil in wetlands because of its low salinity content (Poffenbarger and others, 2011).

The emission, transport, and sequestration of carbon by aquatic ecosystems should be considered when estimating carbon balances in ecosystems (Chapin and others, 2006; Cole and others, 2007; Tranvik and others, 2009; Aufdenkampe and others, 2011). The existing national-scale studies suggested that lateral transport of carbon fixed within the CONUS and exported to coastal areas can represent between about 10 percent of the total carbon sequestered in forests (trees and soils), croplands, and shrublands (Pacala and others, 2001). Nearly all of the 3.9 to 5.2 $gC/m^2/yr$ consisted of inorganic carbon. Also, human-made reservoirs can also be sinks for carbon and can sequester between 1.3 and 5.2 $gC/m^2/yr$ (Pacala and others, 2001). Although the role of aquatic ecosystems in transporting and sequestering carbon may be well documented for the CONUS, recent global studies have indicated that inland waters can also be sources of carbon emitted into the atmosphere (Cole and others, 2007; Tranvik and others, 2009; Aufkenkampe and others, 2011). The effect of carbon dioxide emissions from lakes and rivers and their roles in regional carbon budgets has yet to be determined for the Western United States.

The above-referenced studies produced a range of net carbon flux estimates that were spatially and temporally variable; however, these estimates also provided a set of reference points against which this assessment may be compared. Table 1.2 provides a summary of the net carbon fluxes per unit of area from a sample of the referenced works for the four major terrestrial ecosystems covered in this assessment. Uncertainties and caveats reported in these studies were not reproduced for the table.

Table 1.2. Estimates of the mean net carbon flux per unit of area from a selected sample of studies.

[Three sample estimates are included for each of the four major terrestrial ecosystems: forests, agricultural lands, grasslands/shrublands, and wetlands. CONUS, conterminous United States; EPA, Environmental Protection Agency; gCm^2/yr, grams of carbon per square meter per year]

Geography	Mean net carbon flux ($gC/m^2/yr$)	Source	Timeframe of the sourced work
		Forests	
Western States	−90.85	J.E. Smith and Heath (2008)	Early 2000s.
CONUS	−96.75	EPA (2012)	2010.
Oregon	−136	D.P. Turner, Gockede, and others (2011)	Early 2000s.
		Agricultural lands	
CONUS	−3.42	EPA (2012)	2010.
Oregon	−143	D.P. Turner, Ritts, and others (2011)	2007.
California	−19	Kroodsma and Field (2006)	1980–2000.
		Grasslands/shrublands	
CONUS	−0.97	EPA (2012)	2010.
Oregon[1]	18	D.P. Turner, Ritts, and others (2011)	2007.
Oregon[2]	−7	D.P. Turner, Ritts, and others (2011)	2007.
		Wetlands	
CONUS	−40.1	Bridgham and others (2006)	Various, previous decades.
Southern California[3]	−33	Brevik and Homburg (2004)	Over 5,000 years.
Southern California[3]	−206.3	Chmura and others (2003)	1990s.
		Aquatic ecosystems	
CONUS[4]	3.9 to 5.2	Pacala and others (2001)	Various, previous decades.
CONUS[5]	−1.3 to 5.2	Pacala and others (2001)	Various, previous decades.

[1]Grasslands only.

[2]Shrublands only.

[3]Specifically, coastal salt marsh.

[4]Inland to coastal carbon export.

[5]Carbon burial in reservoirs.

This page intentionally left blank.

Chapter 2. Baseline Land-Use and Land-Cover Changes in the Western United States Between 1992 and 2005

By Terry L. Sohl[1], Benjamin M. Sleeter[2], Tamara S. Wilson[2], Michelle A. Bouchard[3], Rachel R. Sleeter[2], Kristi L. Sayler[1], Ryan R. Reker[3], Christopher E. Soulard[2], and Stacie L. Bennett[4]

2.1. Highlights

- Annual, 250-m resolution land-use and land-cover (LULC) maps were produced for the baseline period of 1992 to 2005.
- Observed data derived from remotely sensed sources were used when possible for the baseline map products.
- When annual, observed data were not available, a spatial LULC model based on input data derived from LULC studies was used to produce the annual LULC maps.
- The baseline LULC change was relatively low but variable between ecoregions; some ecoregions experienced significant amounts of change and some ecoregions experienced very little change.
- LULC change associated with forestry was the most common form of LULC change, followed by urban development.

2.2. Introduction

As indicated in figure 1.2 (a graphic representation of the overall methodology for this assessment) of chapter 1 of this report, the mapping and modeling of LULC described in this chapter are some of the spatial foundations of this regional assessment and help define the boundaries and compositions of the assessed ecosystems. The results of the LULC mapping and modeling component feed into other components of the assessment, particularly chapter 5 (baseline terrestrial carbon storage and greenhouse-gas fluxes) and chapter 6 (development of future LULC scenarios).

The LULC in the Western United States is diverse; vast forests, shrublands, and grasslands are interspersed with human agricultural activities, mining, and some of the largest urban areas in the United States. Topography, soils, climate, and water availability interact to determine the landscape potential and anthropogenic land use, producing a mosaic of different LULC types across the West. Silviculture, agriculture, urban development, mining, and natural disturbances such as wildland fires have dramatically altered portions of the Western United States, but the LULC change is fragmented; some areas have experienced little change over the last century and others have experienced rapid and frequent changes.

The annual LULC maps for the Western United States serve as the spatial and temporal foundation for assessing the baseline carbon storage and fluxes for terrestrial ecosystems (chapter 5). The classification scheme (as discussed below) is a combination of land-use and land-cover classes that closely follows the classes used by the 1992 National Land Cover Database (NLCD) (Vogelmann and others, 2001). The disturbance of ecosystems by wildland fires is discussed separately (chapter 3). Land-management activities (for example, crop tillage, crop rotation, and fertilization) are also discussed separately (chapter 4). In order to provide a partitioned spatial framework for the Western United States, the region was divided into five level II ecoregions (modified from U.S. Department of Environmental Protection (EPA), 1999): Western Cordillera, Marine West Coast Forest, Cold Deserts, Warm Deserts, and Mediterranean California. The five ecoregions were mapped and modeled to create annual LULC maps for the baseline period of 1992 to 2005. The following sections discuss the data sources and methodologies used to map and model annual LULC change and the baseline LULC results.

[1]U.S. Geological Survey, Sioux Falls, S.D.

[2]U.S. Geological Survey, Menlo Park, Calif.

[3]Arctic Slope Regional Corporation Research and Technology Solutions, Sioux Falls, S.D.

[4]U.S. Geological Survey, Sacramento, Calif.

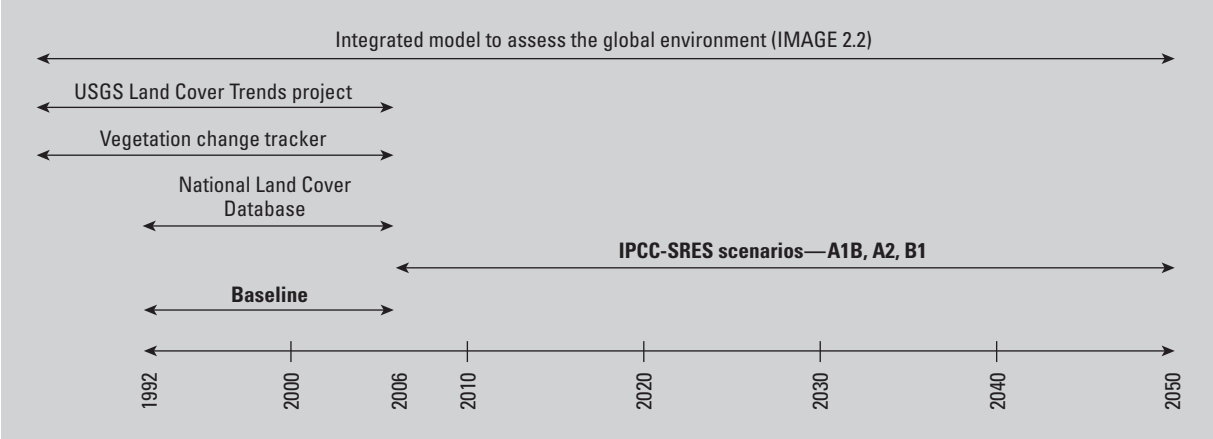

Figure 2.1. Timeline for LULC change mapping and modeling for both the baseline and scenario-based projections. The baseline period runs from 1992 to 2005; the modeled scenarios (from the Intergovernmental Panel on Climate Change's Special Report on Emissions Scenarios (IPCC–SRES; Nakicenovic and others, 2000) were run from 2006 to 2050. The data sources at the top of the graphic were used to support the analysis of baseline, scenarios, or both. USGS, U.S. Geological Survey.

2.3. Input Data and Methods

The baseline period for this assessment was defined as the period from 1992 to 2005. The baseline period allowed for an examination of recent LULC change and for the calibration of both the LULC and biogeochemical modeling frameworks before beginning the simulations of future LULC. The year 1992 was chosen as the start of the baseline period because it marked the earliest year for which consistent, nationwide, high-spatial-resolution LULC data were available. A modified version of the 1992 National Land Cover Dataset (NLCD) (Vogelmann and others, 2001) served as the initial LULC data for this work; the NLCD data had been extensively assessed for accuracy (Stehman and others, 2003; Wickham and others, 2004). The year 2005 was chosen as the endpoint for the baseline period. The choice of the baseline years 1992 to 2005 thus maximized the use of consistent, spatially explicit, nationwide, observed LULC data available when work on the assessment began. Scenario-based projections of potential future land-cover change were created to cover 2006 through 2050 (see chapter 6 of this report) (fig. 2.1).

The NLCD thematic classification system provides a level of thematic detail that allows for an examination of the effects of LULC change on fluxes of carbon and greenhouse gases, but the classification system can also be directly collapsed to the primary ecosystem types that were analyzed for this assessment (table 2.1). The original resolution of the 1992 NLCD was 30 meters, but the data were resampled to 250 meters for this assessment to reduce the volume of data and hold the modeling requirements to a more manageable level. Several adjustments were made to the thematic classes in order to facilitate this assessment, including the collapsing of the four urban classes from the 1992 NLCD into one "urban/developed" class. Similarly, three agricultural classes from the 1992 NLCD (row crop, small grains, and fallow) were collapsed into one "agriculture" class that represented cultivated crops.

The 1992 NLCD dataset was also augmented by incorporating information from LANDFIRE's vegetation change tracker (VCT) data (Chengquan Huang and others, 2010) (fig. 2.2). The VCT data mapped natural and anthropogenic disturbances by analyzing historical layers of Landsat Thematic Mapper (TM) data. Polygons of clearcut forest derived from VCT data were used to populate "mechanically disturbed" classes 3, 4, and 5 (table 2.1) for 1992. The three mechanically disturbed classes represented clearcuts that occurred on land owned by three different entities: (1) national forest, (2) other public land, and (3) private land. Given that each of these ownership types have varying management strategies, the Protected Area Database of the United States (PAD–US Partnership, 2009) was used to spatially distinguish ownership for the three disturbance classes. The PAD–US database includes Federal, State, and local protected lands, as well as information from national nonprofit organizations. The database does not cover all protected lands (such as conservation easements), but it is the most comprehensive and accurate protected lands database available for the United States. Thematically distinguishing clearcutting by these three different classes of ownership resulted in an improved ability to map and model LULC change related to forestry and thus improved the ability to examine the effects of forestry on carbon and greenhouse-gas fluxes.

Table 2.1. Thematic land-use and land-cover classes used in this assessment, the corresponding ecosystems defined for this assessment, percent area (from 1992) of the Western United States, and the source of the input data.

[LANDFIRE, Landscape Fire and Resource Management Planning Tools Project (Rollins, 2009); NLCD, National Land Cover Dataset (Vogelmann and others (2001); VCT, vegetation change tracker (a product of LANDFIRE; Chengquan Huang and others, 2010)]

Land-use and land-cover (LULC) class	Ecosystem	Area (percent)	Source
Open water	Aquatic ecosystems	1.5	NLCD—Open water.
Urban/developed	Other lands	1.0	NLCD—Low-intensity residential. NLCD—High-intensity residential. NLCD—Commercial/industry/transportation. NLCD—Urban/recreational grasses.
Mechanically disturbed—National forest	Forests	0.4	LANDFIRE VCT.
Mechanically disturbed—Other public land	Forests	0.1	LANDFIRE VCT.
Mechanically disturbed—Private land	Forests	0.1	LANDFIRE VCT.
Mining	Other lands	0.1	NLCD—Quarries/strip mines/gravel pits.
Barren	Other lands	3.8	NLCD—Bare rock/sand/clay.
Deciduous forest	Forests	2.0	NLCD—Deciduous forest.
Evergreen forest	Forests	23.9	NLCD—Evergreen forest.
Mixed forest	Forests	1.4	NLCD—Mixed forest.
Grassland	Grasslands/shrublands	13.9	NLCD—Grassland/herbaceous.
Shrubland	Grasslands/shrublands	45.1	NLCD—Shrubland.
Cultivated crop	Agricultural lands	3.6	NLCD—Row crops. NLCD—Small grains. NLCD—Fallow.
Hay/pasture	Agricultural lands	2.5	NLCD—Pasture/hay.
Herbaceous wetland	Wetlands	0.1	NLCD—Emergent herbaceous wetlands.
Woody wetland	Wetlands	0.3	NLCD—Woody wetlands.
Ice/snow	Other lands	0.1	NLCD—Perennial ice/snow.

The modified 1992 NLCD data served as the initial land cover dataset for the assessment. Annual LULC maps for the baseline period were required to adequately portray gross changes between LULC classes that could be missed by a wider temporal interval and thus could affect carbon and GHG calculations; however, there were no annual, nationally consistent, spatially explicit LULC data available for the entire baseline period of 1992 to 2005. NLCD data were available for 1992, 2001, and 2006 (Vogelmann and others, 2001; Homer and others, 2007; Xian and others, 2009), but different classification systems and different mapping methodologies between NLCD versions precluded the use of NLCD alone for providing LULC data for the 1992 to 2005 period. The VCT data were available on an annual basis, but only provided information on areas of disturbance such as forest clearcuts and fires (Chengquan Huang and others, 2010). The USGS Land Cover Trends project (Loveland and others, 2002) provided historical LULC data, but only sample-based data were available for 1992 and 2000. Even though the individual datasets could not provide the consistent, annual, wall-to-wall LULC maps needed for the assessment, they could be used to directly inform a spatial modeling framework to produce annual LULC maps from 1992 to 2005.

The spatial modeling framework, "forecasting scenarios of land-cover change" (FORE–SCE), was used to produce annual LULC maps from 1992 to 2005. FORE–SCE was successfully used to model annual LULC maps for large geographic regions (Sohl and Sayler, 2008; Sohl, Sleeter, Zhu, and others, 2012; Sohl, Sleeter, Sayler, and others, 2012). The FORE–SCE model used separate but linked "Demand" and "Spatial Allocation" components to produce spatially explicit, annual LULC maps. The "Demand" component provided aggregate-level quantities of LULC change for a region, or a "prescription" for the overall regional LULC proportions. The "Spatial Allocation" component ingested "Demand" and produced spatially explicit LULC maps using a patch-based allocation procedure.

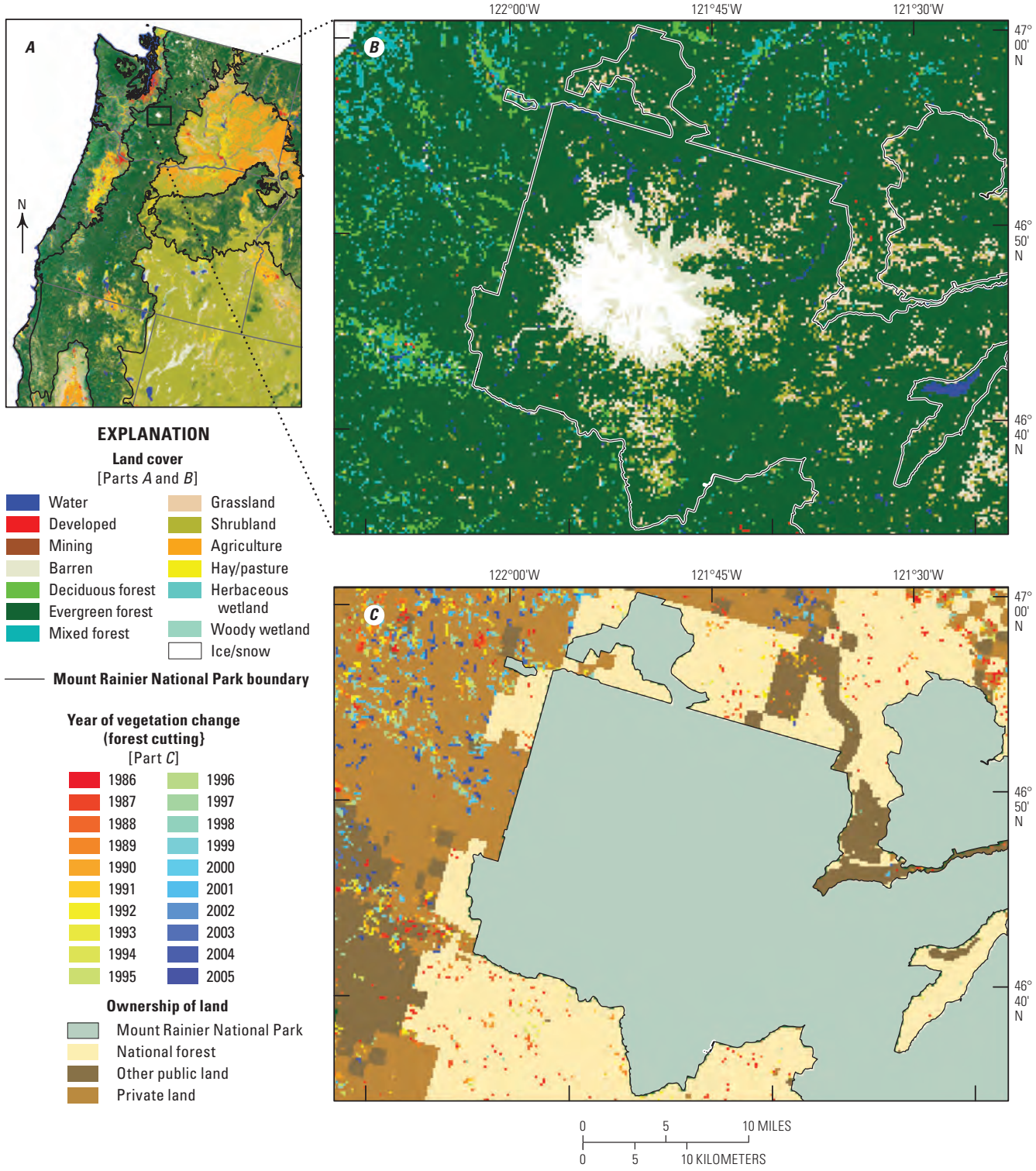

Figure 2.2. Map showing how data from LANDFIRE's vegetation change tracker (VCT) provided information on ecosystem disturbances. In this assessment, the VCT data were used to identify polygons that represented forest clearcuts for the baseline period (1992–2005). *A,* Land-use and land-cover map of a portion of the Western United States. *B,* Inset map showing land use and land cover of Mount Ranier National Park and the surrounding national forest, other public land, and private land. *C,* Inset map showing vegetation changes in the same area as part *B*. The small colored polygons outside of the national park boundary (national forest, other public land, and private land) represent forest clearcuts, color-coded by the year in which the clearcutting occurred. LANDFIRE, Landscape Fire and Resource Management Planning Tools Project.

The "Demand" for the baseline LULC change was split into two time periods to take advantage of temporally specific historical data. Demand from 1992 to 2000 was provided by USGS Land Cover Trends data (U.S. Geological Survey, 2012a). The USGS Land Cover Trends project used a sampling approach and the historical archive of Landsat Multispectral Scanner (MSS), Thematic Mapper (TM), and Enhanced Thematic Mapper Plus (ETM+) data to produce estimates of LULC change for each of the 84 level III ecoregions (modified from EPA, 1999) in the conterminous United States (Loveland and others, 2002). Although the coarser-scale level II ecoregion framework was used for the overall assessment in the Western United States, the finer-scale level III ecoregion framework served as the primary framework for all FORE–SCE-based LULC modeling, thus improving the representation of spatial LULC change patterns in the very heterogeneous Western United States. As a result, the "Demand" information from the USGS Land Cover Trends project was provided separately for each level III ecoregion, and the "Spatial Allocation" component of FORE–SCE was parameterized individually for each level III ecoregion. For the 1992 to 2000 period, USGS Land Cover Trends data provided baseline regional proportions of LULC change ("Demand") for each level III ecoregion; however, these data were thematically less detailed than the LULC classes used for this assessment (table 2.1). For example, USGS Land Cover Trends only estimated one aggregate "forest" class, while this assessment differentiated between deciduous, evergreen, and mixed forest types. To obtain the three forest types and their transitions from the USGS Land Cover Trends data for 1992 to 2000, proportions of the three forest types from the 1992 NLCD were used to disaggregate the USGS Land Cover Trends single forest class for each level III ecoregion. A similar disaggregation of USGS Land Cover Trends classes using the 1992 NLCD was performed to split the class "grass/shrub" into the "grassland" and "shrubland" classes, split "wetland" into the "herbaceous wetland" and "woody wetland" classes, and split "agriculture" into "hay/pasture" and "cultivated crop." Finally, the 1992 to 2000 estimates by ecoregion were annualized to produce annual rates of change that served as annual "Demand" for the FORE–SCE model.

A similar methodology was used to populate the "Demand" component of the model for 2001 to 2005. The "Demand" for this period was provided by the 2001 to 2006 NLCD change-product data (Xian and others, 2009). The 2001 and 2006 NLCD data provided a LULC change product that provided consistent, wall-to-wall LULC data for the United States. The level of thematic detail was compatible with this assessment, and, unlike the USGS Land Cover Trends data for 1992 to 2000, no disaggregation to a finer thematic scale was necessary. The 2001 to 2006 NLCD change data were annualized to produce rates of change that served as yearly "Demand" for 2001 to 2005 for the FORE–SCE model.

The 1992 to 2005 annual "Demand" for LULC served as input to the spatial modeling component of FORE–SCE. FORE–SCE used logistic regression to quantify empirical relationships between LULC and spatially explicit biophysical and socioeconomic variables. Suitability surfaces were produced for each unique LULC class that was modeled (table 2.1) for each level III ecoregion. The suitability surfaces were used to guide the placement of individual patches of LULC change; the characteristics of the patches were parameterized using historical LULC data from the USGS Land Cover Trends project. The US–PAD data were used to restrict the placement of specific forms of LULC change on certain types of protected lands (for example, restricting urban development in national park lands). Individual patches of LULC were placed on the landscape for a given annual model run until "Demand" was met for that year. The processing then continued to the next year until the baseline period of 1992 to 2005 was complete. Additional details on the FORE–SCE model structure may be found in Sohl and Sayler (2008); Sohl, Sleeter, Zhu, and others (2012); and Sohl, Sleeter, Sayler, and others (2012).

The age of forest stands was also tracked spatially and temporally and was estimated in the modeling environment. Data about forest-stand ages were used to ensure realistic clearcutting cycles (based on the typical age when a forest stand is ready for harvesting) for a given geographic area, and provided information on forest structure that could be used for biogeochemical or climate modeling. An initial map of forest-stand ages was generated for the region using a combination of data from LANDFIRE's VCT and the U.S. Forest Service's (USFS's) Forest Inventory and Analysis (FIA; USDA Forest Service, 2012b). Where the LANDFIRE VCT measured a disturbance, the forest-stand age was directly calculated for the initial year of 1992. In areas where no disturbance was measured by the LANDFIRE VCT, the FIA data points were used to create an interpolated, continuous surface of forest-stand age. The FORE–SCE model tracked forest-stand age for each yearly model iteration and reset the stand age to "0" whenever a new forest area was generated or whenever a forest was clearcut; however, to ensure the use of as much observed spatial data as possible for the baseline period, the clearcutting of forests (classes 3, 4, and 5) in table 2.1 was not modeled using the procedures outlined above; instead, the models were extracted from the LANDFIRE VCT data. All areas of forest that the VCT had identified as clearcut between 1992 and 2005 were "burned in" to the appropriately dated LULC maps produced from the FORE–SCE model (for example, all 1994 clearcut areas identified by the VCT were burned in to the 1994 LULC map produced from the FORE–SCE model). The forest-stand age was appropriately updated throughout the baseline period, mimicking measured dates of forest clearcuts from the VCT.

The result of the mapping and modeling efforts for 1992 to 2005 LULC were annual, 250-meter-resolution LULC maps depicting the LULC classes (shown in table 2.1) and annual, 250-meter-resolution data on forest-stand age. Given the limitations of available, spatially and thematically consistent LULC data for 1992 to 2005, the combined mapping and modeling technique ensured that the overall proportions of the 1992 to 2005 LULC maps were as representative as possible of the real, measured LULC change distributions that were provided by the USGS Land Cover Trends, NLCD, and LANDFIRE VCT projects. The location of LULC change after the initial 1992 year was a mix of actual mapped change and modeled change. The VCT provided the actual locations of clearcut forest patches between 1992 and 2005, a welcome dataset given that forest clearcutting represented the largest LULC change in the Western United States per unit of area (Benjamin M. Sleeter, USGS, unpub. data, 2012). For other LULC types, the "Spatial Allocation" component for LULC change was modeled using the FORE–SCE model.

The validation of the baseline 1992 to 2005 LULC maps was accomplished through a combination of qualitative and quantitative assessment. A quantitative assessment of the model's performance was obviously preferred. The quantitative validation of LULC model output could be performed by examining measures of quantity disagreement and allocation disagreement that reflected the model's capability to map the correct quantity and location of LULC change, respectively (Pontius and Millones, 2012). An examination of quantity disagreement was unnecessary for this assessment, however. The quantity of LULC change was dictated by the USGS Land Cover Trends project for 1992 to 2000 and by the NLCD 2001 to 2006 change product for 2001 to 2005. The FORE–SCE model was designed to precisely match prescribed proportions of LULC change as dictated by the "Demand" component of the model. Given the design of the FORE–SCE model, quantity disagreement was, therefore, not an issue because the model matched the annual, prescribed LULC "Demand" for 1992 to 2005 on a regional basis.

Given that all level III ecoregions were parameterized and modeled independently, the allocation disagreement was already partially mitigated because the proportions of change were spatially distributed to the ecoregion level. The allocation disagreement was only an issue within a level III ecoregion. The allocation disagreement (where LULC change was mapped) was not an issue for the clearcutting of forests (the most prevalent form of LULC change in the Western United States) because the 1992 to 2005 polygons of forest change were mapped by the LANDFIRE VCT, not modeled by FORE–SCE. All of the other types of LULC change, however, were modeled by FORE–SCE and were thus subject to allocation disagreement. There were difficulties in performing an assessment of allocation disagreement, however, given the inability to directly compare USGS Land Cover Trends, the 1992 NLCD, and the 2001 and 2006 NLCD data. The 2001 and 2006 NLCD data were produced using a consistent methodology and could theoretically be used to evaluate the allocation disagreement of the modeled LULC change for that period; however, outside of the dominant LULC change in the Western United States (forest clearcutting and associated forest regeneration, mapped by VCT and not modeled), other LULC change was very minor as only 0.76 percent of the region changed between 2001 and 2006. An assessment of the model's performance by examining small amounts of LULC change over very short temporal intervals is of questionable value (Sohl, Sleeter, Zhu, and others, 2012). Allocation disagreement for classes other than forest clearcutting was thus evaluated through qualitative assessment. During the modeling process, the performance of the model from 1992 to 2005 was evaluated independently for each level III ecoregion using a visual assessment of the LULC-change distribution. An unacceptable distribution of LULC change resulted in a re-parameterization of the FORE–SCE model and a subsequent new model was run until the model performance was deemed acceptable.

2.4. Results and Discussion

2.4.1. Baseline LULC Mapping and Modeling—Results for the Western United States

At the beginning of the simulation period in 1992, the Western United States as a whole was dominated by shrubland (45.1 percent), evergreen forest (23.9 percent), and grassland (13.9 percent)—three LULC classes that covered nearly 83 percent of the Western United States. The less common but significant LULC classes included cultivated crop (3.8 percent), barren (3.8 percent), hay/pasture (2.5 percent), and developed (1.0 percent). The three mechanically disturbed classes, derived from the LANDFIRE VCT data and representing clearcut forest, covered nearly 1.0 percent of the region.

Between 1992 and 2005, 2.9 percent of the land area in the Western United States changed its LULC class at least once. Most LULC classes experienced relatively small net changes during the study period (table 2.2). The three largest LULC classes—shrubland, evergreen forest, and grassland—changed by −2,854 km^2, +5,201 km^2, and −1,426 km^2, respectively. Although the areal change may seem large for the three major classes, the amount of net change was less than 1 percent of the total area for each LULC class during the time period.

The most dynamic changes to LULC classes in the Western United States, both in terms of absolute net change and in terms of relative change for a given LULC class, were changes related to (1) forest clearcutting and (2) urban development. The area covered by the three mechanically

Table 2.2. Mapped and modeled land-use and land-cover (LULC) change (in square kilometers) indicating trends in mapped and modeled LULC classes for the Western United States for the baseline period (1992–2005).

[km^2, square kilometers; LULC, land use and land cover]

LULC class	1992 (km^2)	2005 (km^2)	Change (km^2)	Percent change
Water	39,289	39,744	455	1.2
Urban/developed	27,430	32,486	5,056	18.4
Mechanically disturbed—National forest	9,227	3,888	−5,339	−57.9
Mechanically disturbed—Other public	2,544	1,909	−635	−25.0
Mechanically disturbed—Private	11,580	8,103	−3,476	−30.0
Mining	1,329	2,032	703	52.9
Barren	100,658	100,783	125	0.1
Deciduous forest	52,088	53,791	1,704	3.3
Evergreen forest	636,190	641,391	5,201	0.8
Mixed forest	36,286	37,289	1,003	2.8
Grassland	369,279	367,853	−1,426	−0.4
Shrubland	1,199,764	1,196,910	−2,854	−0.2
Cropland	95,943	95,893	−50	−0.1
Hay/pasture	65,573	64,820	−753	−1.2
Herbaceous wetland	6,913	6,890	−22	−0.3
Woody wetland	2,913	3,223	310	10.7
Ice/snow	1,521	1,521	0	0

disturbed classes of forest clearcutting experienced a total net decline of nearly 9,500 km^2 by 2005, which was a reduction of over 40 percent in areal extent since 1992 (fig. 2.3). The 5,201 km^2 increase in evergreen forest during the same time period was strongly tied to the reduction in overall clearcutting rates. Although clearcutting declined in all classes of mechanically disturbed lands, the sharpest decline in clearcutting was on national forest lands, which declined by 58 percent between 1992 and 2005. Clearcutting on privately held forested land also declined sharply (by 30 percent), but at a much lower rate than the clearcutting on National Forest land.

A number of factors drove the lower rates of forest clearcutting in the Western United States during the baseline time period of 1992 to 2005. Federal environmental policy strongly affected clearcutting practices in the Pacific Northwest. On June 23, 1990, the Northern Spotted Owl (*Strix occidentalis caurina*) was listed as "threatened" under the Endangered Species Act. On May 21, 1991, a U.S. District Court blocked further clearcutting on national forest lands in the region. Those restrictions held until the passing of the Northwest Forest Plan in 1993, an agreement which limited the clearcutting of forested public lands to 1 billion board feet annually, which was roughly one-fourth of the clearcutting rates during the 1980s. Those timber harvesting constraints rippled through the global timber export markets; the higher prices lead Asian importers to look for cheaper timber from New Zealand, Chile, Russia, and elsewhere (Daniels, 2005).

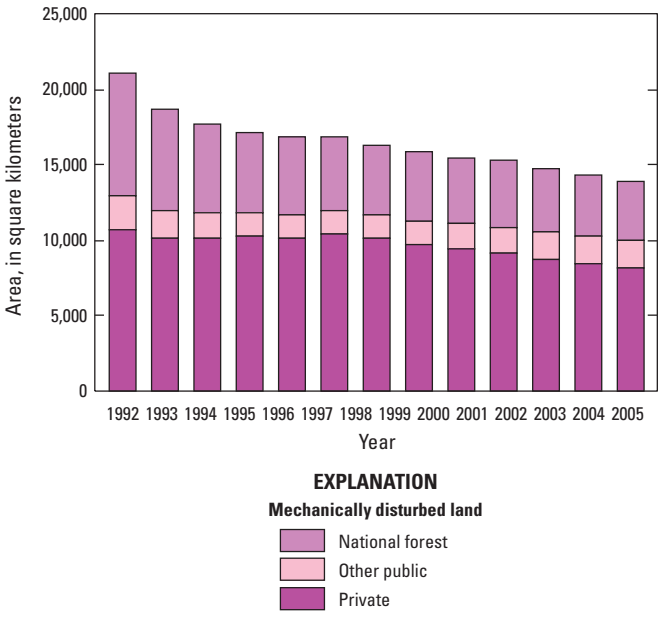

Figure 2.3. Chart showing the declining trend of forest clearcutting in the Western United States between 1992 and 2005. The areal extent of mechanically disturbed (clearcut) land declined significantly over the baseline study period of 1992 to 2005. The strongest declines were noted on national forest lands.

The Asian demand for timber products from the Western United States declined even further in response to the Asian economic crisis in 1997 (Daniels, 2005). Predictions of the decline in forest clearcutting rates in the Western United States, however, had been made far in advance of the passage of the Northwest Forest Plan or the Asian economic crisis in the 1990s, as studies noted that the rates of forest clearcutting in parts of the Western United States before the 1990s were unsustainable (Beuter and others, 1976). The decline in clearcutting noted in this assessment was preceded by additional declines before 1992. Timber harvests in the Pacific Northwest declined by 87 percent from 1988 to 1996 (Warren, 1999; Daniels, 2005).

Urban development was the other most active LULC class in terms of absolute net change relative to initial 1992 LULC conditions. Urban development in the Western United States increased by over 5,000 km^2 from 1992 to 2005, which was an 18.4 percent increase in area (fig. 2.4). Although the rate of increase in development was realistic, the initial extent of urban development in the 1992 LULC data was likely an underestimation of the actual urban extent because it was difficult to identify and map low-density residential areas using Landsat data (Claggett and others, 2004; McCauley and Goetz, 2004). In addition, the 2001 NLCD data had significantly more urban land mapped than the 1992 NLCD, which was likely due to improved source data and methodologies just as much as actual urban expansion. Although urban development was likely underestimated in the initial 1992 map, urban lands still represented only a small portion of the Western United States landscape, and the "story" of urban growth was represented through the measured rates of urban development between 1992 and 2005.

The net change of other LULC types in table 2.2 was relatively minor. The evergreen forest class increased by over 5,200 km^2 (0.8 percent) from 1992 to 2005, as did deciduous forest (+1,704 km^2, or 3.3 percent) and mixed forest (+1,003 km^2, or 2.8 percent). As noted above, the increase in area of the three forest classes was primarily related to the reduction in the rates of forest clearcutting, which resulted in more area categorized as forest in 2005 because of the regeneration of forest in formerly clearcut areas. Other notable LULC changes included an increase of 700 km^2 of mining by 2005, which was a 60 percent increase from 1992. The two agricultural classes, cultivated crop and hay/pasture, each declined with a negligible decline for cultivated crop and a decrease of 1.1 percent in hay/pasture from 1992 to 2005. Grassland and shrubland both declined, with grassland losing 1,426 km^2 and shrubland losing 2,854 km^2. Given the vast expanses of grassland and shrubland in the Western United States, however, this only represented a net loss of −0.39 percent and −0.24 percent, respectively, from the initial 1992 extents of grassland and shrubland.

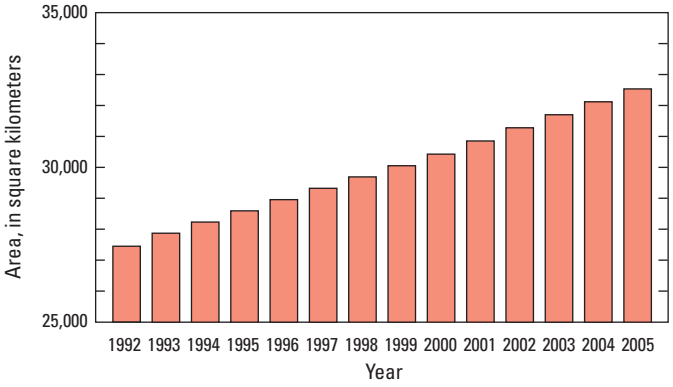

Figure 2.4. Chart showing the increasing trend in the areal extent of urban development in the Western United States between 1992 and 2005. The data were derived from the USGS Land Cover Trends project for the 1992 to 2000 period and from the National Land Cover Dataset (NLCD) 2001 to 2006 change product for the 2001 to 2005 period. A consistent annual rate of change was modeled between 1992 and 2000, and again for 2001 to 2005, on the basis of the USGS Land Cover Trends and NLCD data, respectively. The measured rate of urban development for those two periods was nearly constant.

2.4.2. Regional Results

Although table 2.2 indicates overall net changes in the primary LULC types for the Western United States from 1992 to 2005, regional variability resulted in a heterogeneous pattern of LULC change during the study period. Within the level III ecoregions where significant amounts of forest clearcutting had occurred, 20 percent or more of the land area changed its LULC class at some point between 1992 and 2005, whereas within the ecoregions covered primarily by desert, 1 percent or less of the area changed its LULC class (fig. 2.5). The total spatial change closely mimicked the spatial variability of forest clearcutting, which was the most prevalent form of LULC conversion in the Western United States (fig. 2.6). Forest clearcutting was only one part of the story, however. Each ecoregion had greater internal homogeneity than the Western United States' landscape as a whole, and each had a unique "story" about its baseline land-cover change from 1992 to 2005. The following sections describe the basic characteristics of each level II ecoregion and discuss the primary LULC changes from 1992 to 2005, including a brief discussion of the major driving forces of the changes.

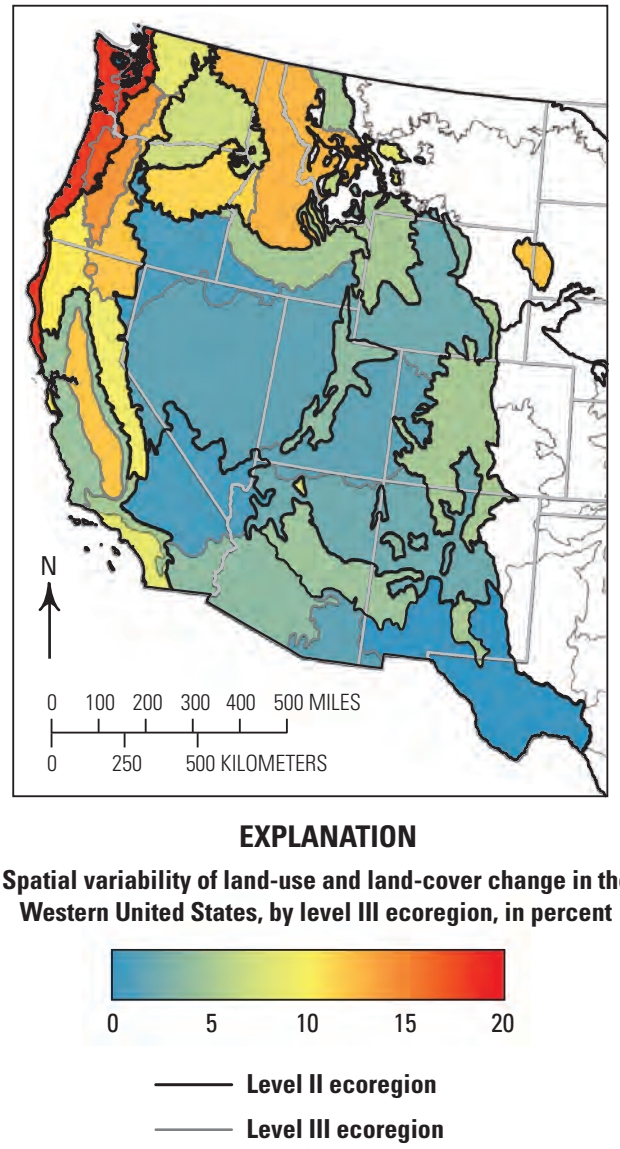

Figure 2.5. Map showing the spatial variability of land-use and land-cover change in the Western United States between 1992 and 2005. The spatial change (the percent of area that changed at least once from 1992 to 2005) varied greatly between the ecoregions. See figure 1.1 in chapter 1 for ecoregion names.

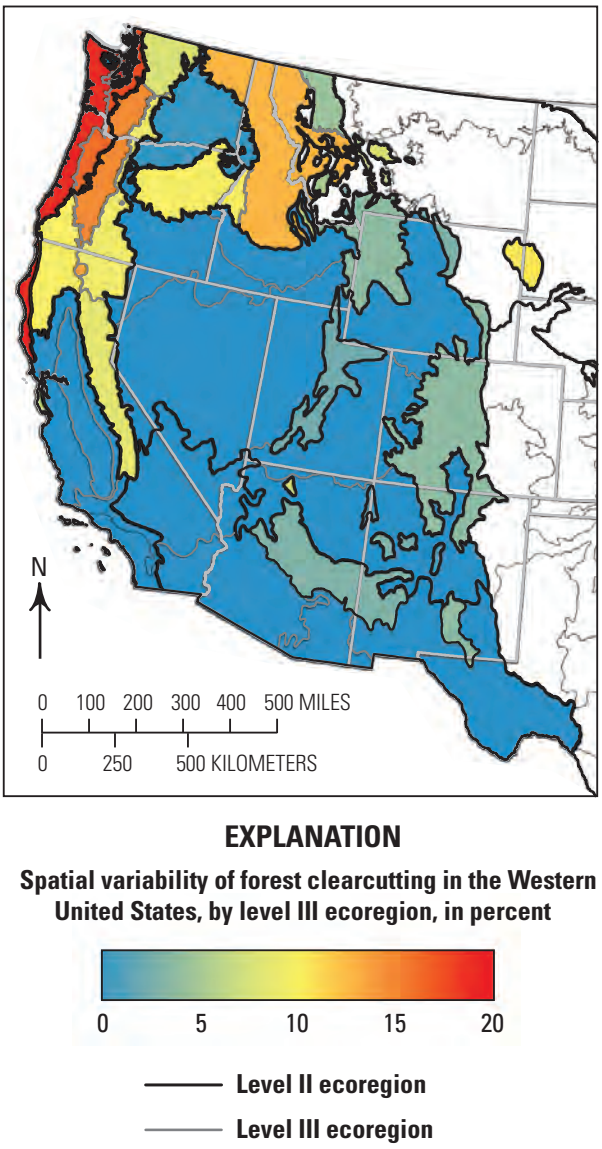

Figure 2.6. Map showing the spatial variability of forest clearcutting in the Western United States from 1992 to 2005. Given that forestry activity was the primary driver of measured land-use and land-cover (LULC) change in the region, the distribution of clearcutting by ecoregion was very similar to the overall pattern of LULC change of Western United States. See figure 1.1 in chapter 1 for ecoregion names.

2.4.2.1. Western Cordillera

The Western Cordillera ecoregion covers most of the forested lands in the interior of the Western United States and consists of a number of geographically disparate regions stretching from the Canadian border in Washington to the "sky islands" of New Mexico and Arizona. The Western Cordillera is characterized by generally rugged topography (including mountain ranges that have the highest elevations in the Western United States) and predominantly natural landscapes. In 1992, forest cover (evergreen, mixed, and deciduous forest) alone covered 60.8 percent of the ecoregion. The "natural" land-cover classes (forested classes, grassland, shrubland, wetland classes, and water) covered over 95.9 percent of the ecoregion whereas anthropogenic land uses (urban development, forest cutting, mining, and agriculture) covered only 4.1 percent of the ecoregion (fig. 2.7).

Approximately 4.4 percent (38,447 km^2) of the ecoregion experienced LULC change at least once during the baseline period (1992–2005). Although a relatively small proportion of the ecoregion changed, this was the second most active level II ecoregion in the Western United States for this period. Between 1992 and 2005, the vast majority of LULC change was associated with forestry activity; 87.8 percent (33,739 km^2) of the changed pixels were associated with either clearcutting for timber or the regeneration of the clearcut areas. As with the Western United States as a whole, the net changes in LULC classes were small, and the largest changes by absolute area and by percentage loss or gain were associated with the timber industry (fig. 2.7). Between 1992 and 2005, clearcutting activity declined sharply in all three mechanically disturbed classes (national forests, other public forests, and private forests). The cutting rates on national forest land experienced both the largest absolute change (−5,130 km^2) and relative change (−57.7 percent) from 1992 to 2005. Forested lands (evergreen, deciduous, and mixed forest) increased by 1.4 percent (7,335 km^2), which was primarily due to the declines in clearcutting rates. The developed lands experienced a modest increase of 367 km^2, or an increase of 16.2 percent, between 1992 and 2005.

2.4.2.2. Marine West Coast Forest

The Marine West Coast Forest ecoregion covers the maritime forests along the West Coast of the United States. This ecoregion was the most heavily forested of the five level II ecoregions in the Western United States with approximately 70 percent of the land area covered by one of the three forest classes in 1992. This ecoregion was similar to the Western Cordillera ecoregion in that the "natural" land-cover classes covered the majority of the ecoregion, and a smaller percentage (24.8 percent) of the land area of this ecoregion was categorized by anthropogenic land uses in 1992. In 1992, the terrestrial portion of the Marine West Coast Forest had higher proportions of clearcut land (7.9 percent), a higher proportion of developed lands (4.5 percent, mostly around the Puget Sound and around the Willamette Valley), and significantly more agricultural land (12.4 percent, the majority of which was hay/pasture) than the Western Cordillera (fig. 2.7).

The spatial footprint of LULC change between 1992 and 2005 was much higher in this ecoregion than in any other level II ecoregion in the Western United States. Approximately 19.7 percent (16,850 km^2) of the landscape changed LULC classes at least once between 1992 and 2005 with the vast majority of the change related to forestry activity (a spatial footprint of 15,061 km^2). As with the Western Cordillera ecoregion, forest clearcutting declined from 1992 to 2005, although not as sharply with a total decline of 24.9 percent (1,671 km^2). Forest clearcutting on National Forest land dropped by nearly 70 percent; however, most of the forested land in this ecoregion was privately held, and the more modest declines in clearcutting rates on private land mitigated the decline in the ecoregion's overall rate of clearcutting. Despite the overall decline in clearcutting rates, the amount of land in the three forest classes only increased slightly—by 0.5 percent (520 km^2)—between 1992 and 2005. The increase in forested land was less than that in the Western Cordillera largely because the decreases in forest clearcutting were partially offset by clearing forested land for urban development. Even though the Marine West Coast Forest ecoregion is smaller in area than the Western Cordillera ecoregion, it had 1,563 km^2 more developed land in 1992 and more new urban development between 1992 and 2005 (893 km^2 in the Marine West Coast Forest compared to 367 km^2 in the Western Cordillera). The net change within the other LULC classes was minor; no land area categorized by those classes changed by more than 200 km^2 between 1992 and 2005.

2.4.2.3. Cold Deserts

The Cold Deserts ecoregion encompasses the temperate and cooler arid lands of the interior Western United States. Grassland and shrubland were the most common land-cover types in the ecoregion; in 1992, they covered 61.9 percent and 14.5 percent of the ecoregion, respectively. In 1992, forests (evergreen, deciduous, and mixed) covered 9.2 percent of the ecoregion and were found throughout the ecoregion in scattered pockets of land with suitable soils, moisture, and climate. In 1992, agricultural lands (cultivated crop and hay/pasture) covered 7.7 percent of the ecoregion; the majority was irrigated agricultural land located in the Columbia Plateau and the Snake River Plain level III ecoregions. The Cold Deserts ecoregion had a low population density with only a few large urban areas, including Salt Lake City, Utah, and Albuquerque, New Mexico. Urban development covered 5,085 km^2 of the ecoregion at the beginning of the baseline period in 1992.

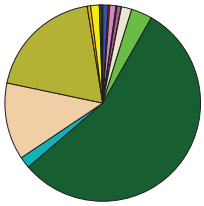

Land-use or land-cover class	Open water	Developed	Mechanically disturbed (national forest)	Mechanically disturbed (other public)	Mechanically disturbed (private)	Mining	Barren	Deciduous forest	Evergreen forest	Mixed forest	Grassland	Shrubland	Agriculture	Hay/pasture	Woody wetland	Herbaceous wetland	Ice/snow
Western Cordillera ecoregion																	
1992 (area, in km²)	7,827	2,260	8,896	1,557	5,987	266	14,916	30,213	483,704	16,541	110,982	166,953	4,977	12,289	2,229	1,176	1,507
2005 (area, in km²)	7,939	2,627	3,767	1,113	3,889	393	15,004	31,104	489,702	16,987	110,983	166,892	4,778	11,944	2,303	1,353	1,507
Net change in area (in km²)	111	367	–5,130	–444	–2,099	127	88	891	5,998	446	1	–61	–200	–346	74	177	0
Change in area (in percent)	1.4	16.2	–57.7	–28.5	–35.1	48.0	0.6	2.9	1.2	2.7	0.0	0.0	–4.0	–2.8	3.3	15.0	0.0

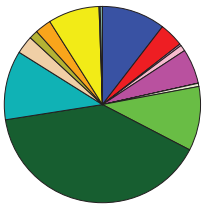

Marine West Coast Forest ecoregion																	
1992 (area, in km²)	9,964	3,823	290	953	5,471	32	505	10,082	38,077	10,880	2,846	1,367	2,561	8,042	182	347	0
2005 (area, in km²)	10,004	4,715	89	783	4,170	52	499	10,888	37,345	11,326	3,037	1,507	2,516	7,902	223	364	0
Net change in area (in km²)	40	892	–201	–170	–1,301	20	–6	806	–732	446	191	140	–45	–140	41	17	0
Change in area (in percent)	0.4	23.3	–69.3	–17.8	–23.8	62.5	–1.2	8.0	–1.9	4.1	6.7	10.2	–1.8	–1.7	22.5	4.9	0.0

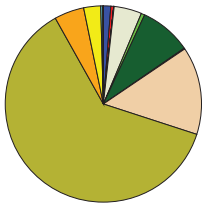

Cold Deserts ecoregion																	
1992 (area, in km²)	12,804	5,085	11	20	61	645	48,201	6,089	89,580	1,499	152,950	653,289	51,675	29,562	3,538	1,037	10
2005 (area, in km²)	12,924	6,237	2	4	11	937	48,284	6,098	89,552	1,513	152,684	651,974	51,865	29,325	3,458	1,177	10
Net change in area (in km²)	121	1,153	–9	–16	–50	291	84	9	–28	14	–267	–1,315	190	–237	–80	139	0
Change in area (in percent)	0.9	22.7	–80.0	–81.0	–81.8	45.2	0.2	0.2	0.0	1.0	–0.2	–0.2	0.4	–0.8	–2.3	13.4	0.0

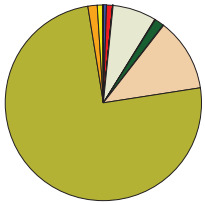

Warm Deserts ecoregion																	
1992 (area, in km²)	2,424	4,618	16	7	19	322	33,539	497	7,120	466	55,915	348,558	7,168	4,286	129	205	0
2005 (area, in km²)	2,446	5,747	12	3	3	507	33,450	499	7,100	466	55,806	347,586	7,097	4,240	135	191	0
Net change in area (in km²)	21	1,129	–3	–4	–16	185	–89	2	–20	0	–109	–972	–71	–46	6	–14	0
Change in area (in percent)	0.9	24.4	–21.9	–52.3	–83.4	57.6	–0.3	0.4	–0.3	0.0	–0.2	–0.3	–1.0	–1.1	4.8	–6.8	0.0

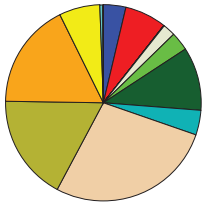

Mediterranean California ecoregion																	
1992 (area, in km²)	6,270	11,645	14	7	42	64	3,498	5,207	17,709	6,901	46,586	29,598	29,562	11,393	835	149	3
2005 (area, in km²)	6,431	13,160	18	6	31	144	3,547	5,202	17,692	6,997	45,343	28,951	29,638	11,409	772	139	3
Net change in area (in km²)	162	1,515	4	–1	–11	80	49	–5	–17	96	–1,243	–646	76	16	–64	–10	–0
Change in area (in percent)	2.6	13.0	25.9	–16.5	–26.5	123.5	1.4	–0.1	–0.1	1.4	–2.7	–2.2	0.3	0.1	–7.6	–6.4	–4.0

EXPLANATION

[Pie charts represent data for 2005]

Land-use or land-cover class

- Open water
- Developed
- Mechanically disturbed (national forest)
- Mechanically disturbed (other public land)
- Mechanically disturbed (private land)
- Mining
- Barren
- Deciduous forest
- Evergreen forest
- Mixed forest
- Grassland
- Shrubland
- Agriculture
- Hay/pasture
- Woody wetland
- Herbaceous wetland
- Ice/snow

Figure 2.7. Charts showing the proportions of land use and land cover (LULC) at the end of the baseline period (pie charts for 2005) and the net change in the mapped and modeled LULC classes between 1992 and 2005, by level II ecoregion.

The spatial footprint of LULC change between 1992 and 2005 was only 1.1 percent of the ecoregion area. Commercial forestry activity and other forest clearcutting, which were major sources of LULC change in the Western Cordillera and Marine West Coast Forest ecoregions, were negligible in the Cold Deserts ecoregion because of the absence of suitable forest resources. Urban development was responsible for the largest net changes in LULC types, as shown in figure 2.7. An estimated 1,153 km^2 of new urban lands were developed by 2005, which was a net increase of 22.7 percent over the 1992 urban extent. The largest absolute net change by class was a 1,315 km^2 loss of shrubland, which was primarily due to the conversion of shrubland to urban development and irrigated agriculture; however, given the prevalence of shrubland in this ecoregion, the areal extent of shrubland declined by only 0.2 percent from 1992 to 2005. The absolute net changes in all other LULC classes were minor. No land area categorized by those classes changed by more than 300 km^2 from 1992 to 2005. Mining lands, however, increased by 291 km^2 from 1992 to 2005, an increase of 45.2 percent.

2.4.2.4. Warm Deserts

The Warm Deserts ecoregion covers the warmer deserts and arid regions of the interior Southwestern United States. Three LULC classes alone covered 94.1 percent of the ecoregion in 1992: shrubland, 74.9 percent; grassland, 12.0 percent; and barren land, 7.2 percent. Forests and agricultural lands were only found in a few scattered locations in the ecoregion. The forested lands (evergreen, deciduous, and mixed) were primarily found in a few areas of higher elevation and near water sources and together covered 1.7 percent of the ecoregion in 1992. The agricultural lands (cultivated crop and hay/pasture) were primarily found in areas where irrigation sources were available, such as near the Salton Sea in California and near Phoenix, Arizona; in 1992, they covered 2.5 percent of the ecoregion. Urban development only covered 1.0 percent of the ecoregion in 1992, yet several large urban centers are located in this ecoregion, including Phoenix and Tucson in Arizona, and Las Vegas, Nevada.

The spatial footprint of LULC change between 1992 and 2005 was only 0.8 percent of the Warm Deserts ecoregion, making it the ecoregion with the least amount of LULC change in the Western United States. Urban development increased by 1,129 km^2, a 24 percent increase from 1992. Shrubland declined by 972 km^2, a decline of 0.3 percent, with most of the loss attributed to the conversion of shrubland to urban development. Other LULC changes in the ecoregion were minor. Commercial forestry was negligible in the ecoregion. Mining lands expanded by 185 km^2, an increase of 57.6 percent from 1992.

2.4.2.5. Mediterranean California

The LULC of the Mediterranean California ecoregion is more heterogeneous than the other ecoregions in the Western United States. This ecoregion is the only one where forests (evergreen, mixed, and deciduous) or shrubland alone did not cover a majority (>50 percent) of the ecoregion area. Grassland (27.5 percent), agricultural classes (24.2 percent for the two classes), forest (17.6 percent for the three classes), shrubland (17.5 percent), and urban development (6.9 percent) each represented the dominant LULC class for specific portions of the ecoregion in 1992. Grassland was scattered throughout the ecoregion but there was a high concentration around the periphery of the Central California Valley level III ecoregion. Agricultural land was concentrated in the Central California Valley, although there were smaller, scattered patches in western and southern California. Forested lands were concentrated in the Southern California Mountains level III ecoregion and along the edges of the Southern and Central California Chaparral and Oak Woodlands level III ecoregion. The vast majority of shrubland was found in the far southern third of the ecoregion, and areas of dense urban development were found throughout the ecoregion.

The spatial footprint of LULC change between 1992 and 2005 was 3.5 percent of the ecoregion area. The greatest amount of change by area was associated with the gross change between the cultivated crop and hay/pasture classes. The net change in those two classes was very small, with cultivated crop increasing by 76 km^2 (0.3 percent) and hay/pasture increasing by 16 km^2 (0.1 percent). Underlying the small amount of net change, however, were large amounts of gross change with near balances of cultivated crop converting to hay/pasture and vice versa. The highest net changes in LULC classes were associated with urban development. Over 1,500 km^2 of new urban development occurred between 1992 and 2005, which was a 13.0 percent increase over the 1992 extent. Grassland declined by 1,243 km^2 (2.7 percent) and shrubland declined by 646 km^2 (2.2 percent), with the majority of the declines caused by conversion to urban development. Other LULC changes in the ecoregion were minor.

Chapter 3. Baseline Wildland Fires and Emissions for the Western United States

By Todd J. Hawbaker[1] and Zhiliang Zhu[2]

3.1. Highlights

- Wildland fires burned an annual average of 13,173 km^2 between 2001 and 2008 in the Western United States.
- The interannual variability in the area that was burned between 2001 and 2008 was high; as few as 3,345 km^2 burned in 2004 and as much as 25,206 km^2 burned in 2007.
- The annual average emissions from wildland fires from 2001 to 2008 were 36.7 $TgCO_{2\text{-}eq}$/yr (10.0 TgC/yr), with a median value of 41.0 $TgCO_{2\text{-}eq}$/yr (11.2 TgC/yr), and a range from 6.8 $TgCO_{2\text{-}eq}$ (1.9 TgC/yr) in 2004 to 75.3 $TgCO_{2\text{-}eq}$ (20.6 TgC/yr) in 2007.
- The minimum, average, and maximum emissions from wildland fires in the Western United States from 2001 to 2008 were equivalent to 7.9 percent, 11.6 percent, and 87.0 percent, respectively, of the mean terrestrial carbon sequestration estimated for the Western United States in this study.
- The minimum, average, and maximum emissions from annual wildland fires in the Western United States from 2001 to 2008 were equivalent to 0.1 percent, 0.7 percent, and 1.3 percent, respectively, of the 2010 fossil-fuel emissions for the entire United States.
- The Western Cordillera ecoregion produced 77 percent of all emissions in the Western United States during the baseline period.

3.2. Introduction

The methodology for this assessment explicitly addressed ecosystem disturbances, including human- and naturally caused wildland fires, as required by the EISA legislation (U.S. Congress, 2007; Zhu and others, 2010). As indicated by figure 1.2 in chapter 1 of this report, the estimates for the baseline biomass combustion emissions from wildland fires are presented in this chapter. The projected future potential wildland fire emissions are described in chapter 8. The baseline burned areas and the projected future potential burned areas for wildland fires and their severity, described in the two chapters, were used as input into the assessment of baseline and projected future potential terrestrial carbon and greenhouse-gas fluxes (chapters 5 and 9 of this report, respectively).

Wildland fires are a critical component of the global carbon cycle because they produce an immediate release of greenhouse gases—carbon monoxide (CO), carbon dioxide (CO_2), and methane (CH_4)—when biomass is consumed through combustion (Seiler and Crutzen, 1980). Wildland fires also have long-term effects on ecosystem carbon cycling by influencing the rate of carbon sequestration after combustion, both through the decomposition of dead vegetation and through photosynthesis, which helps establish new vegetation; because of those effects, years to decades can pass before carbon stocks return to pre-fire conditions (M.G. Turner and others, 1998; Cleary and others, 2010; Hurteau and Brooks, 2011; Kashian and others, in press). If fire regimes are stable, the long-term effects of wildland fires on carbon

[1]U.S. Geological Survey, Denver, Colo.

[2]U.S. Geological Survey, Reston, Va.

cycling are typically negligible because carbon sequestration through vegetation growth and carbon loss through wildland fire emissions cancel out each other over long time periods (Balshi, McGuire, Duffy, Flanigan, Kicklighter, and Melillo, 2009; Flannigan and others, 2009). If a fire regime changes, however, the vulnerability for carbon storage is high because the amount of carbon stored in the ecosystem can be altered or lost through emissions. Substantial evidence is available to document that fire regimes are not static. For example, the frequency of wildland fires has been greatly reduced since settlement of the United States began, mainly due to land-use changes and the success of fire suppression in the last century (Cleland and others, 2004); however, the frequency of wildland fires has been increasing since the 1990s because of an increasingly earlier snowmelt (Westerling and others, 2006). Therefore, any credible assessment of carbon storage and fluxes in ecosystems through time must account for the potential changes in wildland-fire occurrence and emissions.

In the conterminous United States (CONUS), the net carbon flux in ecosystems reported by the Environmental Protection Agency (EPA) was 1,075 $TgCO_{2\text{-}eq}$/yr (293 TgC/yr) in 2010, the majority of which was sequestered within forests (EPA, 2012). The estimates of emissions from wildland fires in the United States were highly variable; after converting the reported emissions to carbon dioxide equivalent, they were as follows: (1) from 15 to 73 $TgCO_{2\text{-}eq}$/yr, (2001–2008; Global Fire Emissions Database (GFED), Oak Ridge National Laboratory Distributed Active Archive Center, 2012; see also Giglio and others, 2010; van der Werf and others, 2010); (2) from 29 to 199 $TgCO_{2\text{-}eq}$/yr (2001–2008; French and others, 2011; Michigan Tech Research Institute, 2012), and (3) from 157 to 283 $TgCO_{2\text{-}eq}$/yr (2002–2006; Wiedinmyer and Neff, 2007). When compared with the 2010 net carbon flux of ecosystems in the CONUS (EPA, 2012), the annual emissions from wildland fires were equivalent to 1 to 26 percent of the ecosystem's total annual flux. In contrast, from 2001 to 2008, the combustion of fossil fuels produced 5,642 $TgCO_{2\text{-}eq}$/yr (EPA, 2012) and flux increased at a rate of 1 percent per year (Pacala and others, 2007). Based on these rates, the annual emissions from wildland fires were equivalent to 0.3 to 5.1 percent of the emissions from fossil-fuel consumption.

The differences among the accuracy and quality of these data, their spatial and temporal resolution, and assumptions about variations in combustion efficiency were the primary sources of uncertainties in wildland-fire emissions estimates (Larkin and others, 2009; French and others, 2011). The assumptions about the proportion of aboveground biomass consumed by wildland fire, especially aboveground woody biomass in forests, can have a substantial influence on emission estimates (Campbell and others, 2007; Meigs and others, 2009). The methods used for calculating emissions relied on estimates of the area that was burned, fuel loads (available live and dead biomass for burning), combustion efficiency, and emission factors (Seiler and Crutzen, 1980; Albini and others, 1995; Wiedinmyer and Neff, 2007; Ottmar and others, 2008). For instance, the GFED (Giglio and others, 2010; van der Werf and others, 2010) estimates biomass consumption and emission at fire locations detected by MODIS (Roy and others, 2002; Giglio and others, 2003) on the basis of land-cover types, combustion completeness, soil moisture, and land-cover specific emission factors. GFED also incorporates changes in fuel loads using the Carnegie Ames Stanford Approach to characterize biomass production (Potter and others, 1993, 2012). Wiedinmyer and Neff (2007) also used active wildland fire observations from NASA's MODIS (Giglio and others, 2003), but calculated the emissions based on static land-cover types, percent land cover, and biomass at 1-km resolution. French and others (2011) used the CONSUME model (Ottmar and others, 2008), which calculated fuel consumption and emission using fuel loads derived from the Fuel Characterization Classification System (FCCS; Ottmar and others, 2007) and fuel moistures derived from weather-station data.

These existing studies provided an estimate of the effects of wildland fires on a national scale but lacked the regional detail required by this assessment. Furthermore, there were few projections of future potential wildland-fire emissions that were consistent with the existing baseline emission estimates. Therefore, a set of baseline emissions (this chapter) and projected future potential emissions (chapter 8) was developed to ensure consistency throughout this and other regional assessments. This chapter focuses on the baseline estimates of wildland-fire occurrence and emissions for the Western United States and strives to answer two primary questions: (1) What were the patterns of wildland-fire occurrence and emissions in the Western United States?, and (2) How did wildland fires vary temporally and spatially among the ecoregions of the Western United States? The results from this chapter were also used in the assessment of baseline carbon storage, sequestration, and greenhouse-gas fluxes of terrestrial ecosystems (chapter 5).

3.3. Input Data and Methods

The baseline estimates for the number of wildfires, the area burned, and emissions were derived from the Monitoring Trends in Burn Severity (MTBS) database (Eidenshink and others, 2007) and the First Order Fire Effects Model (FOFEM; Reinhardt and others, 1997) for the major GHGs: carbon dioxide (CO_2), carbon monoxide (CO), and methane (CH_4). This method was applied to each wildland fire in the region that was in the MTBS database to produce estimates of CO_2, CO, and CH_4 emissions (converted to CO_2 equivalent). The results were aggregated to produce an estimate of emissions for the Western United States as a whole and for each level II ecoregion within it.

The locations of wildland-fire scars were taken from the MTBS database, which includes information about wildland fires in the Western United States that occurred between 1984 and 2008 and that were greater than 404 ha (1,000 acres). The MTBS data were selected because of the high degree of confidence in the data (fire size and severity were derived manually). Other data sources were considered but ultimately not used, including the various versions of Federal wildland-fire databases, because of the spatial inaccuracies and duplicate records that would have introduced uncertainties (T.J. Brown and others, 2002). The MODIS active fire (Giglio and others, 2003) and burned area (Roy and others, 2002) products were also considered but not used because they contained no information about the causes of the wildland fires and had a coarse spatial resolution that complicated the calculations of emissions and the modeling of future trends.

Wildland-fire emissions were calculated for each burned pixel in the MTBS database using the FOFEM, which used fuel loads along with fuel moistures to estimate the amount of forest litter and downed deadwood that was consumed (Albini and others, 1995; Albini and Reinhardt, 1995, 1997). The consumption of duff (decaying forest litter), trees, plants, and shrubs was estimated as a function of the region, season, fuel moistures, and fuel loads. Canopy fuel consumption was estimated as a function of the burn severity provided by the MTBS data. The emissions of CO_2, CO, and CH_4 were then calculated on the basis of the amount of fuel consumed, the organic-matter content of the fuel, and how efficiently it burned. The required input data for the FOFEM included fuel loads, burn severity, and dead and live fuel moistures (fig. 3.1).

Fuel-load data provided an estimate of the amount of biomass that was available for consumption and were derived from the LANDFIRE project's Fuel Loading Models data layer (FLM; Lutes and others, 2009). These fuel-load data were categorized by 1-, 10-, 100-, and 1,000-hour fuel classes (Lutes and others, 2009) for dead biomass, decaying biomass (duff and forest litter), and live biomass (grass, shrubs, and tree canopy). In the FOFEM, the amount of tree canopy that was consumed was a direct function of burn-severity values from the MTBS data. The amount of canopy foliage that was consumed in the high, moderate, and low burn-severity categories was assumed to be 100, 60, and 20 percent, respectively. Similarly, the consumption of the canopy's branch wood was set at 50, 30, and 10 percent for the high, moderate, and low burn-severity categories, respectively. These values were based on previously published estimates (Spracklen and others, 2009; Zhu and others, 2010) and on a comparison of the FOFEM emissions with previously published results for selected wildland fires. Prior to processing with the FOFEM, the LANDFIRE FLM and MTBS raster data were aggregated to 250 m resolution using a nearest-neighbor method to match the resolution of other raster data being used in this assessment. The emissions were calculated for wildland fires occurring between 2001 and 2008, which is the baseline time period for this component of the assessment. Wildland fires before 2001 were excluded because the LANDFIRE fuels data were derived from circa 2001 Landsat imagery. The year-to-year variability in the amount of burned area was high. Therefore, data on all wildland fires that occurred after 2001 were included to help reduce the influence of extreme wildland fire years (either high or low occurrence) on the baseline statistics.

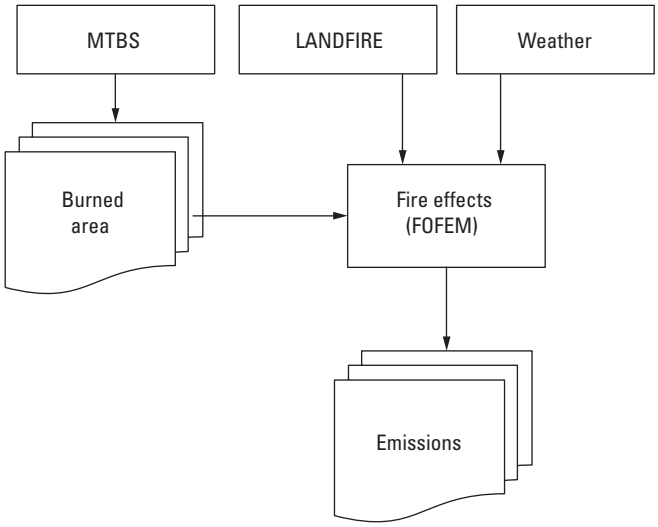

Figure 3.1. Flowchart showing the process for calculating baseline estimates of greenhouse-gas emissions from wildland fires.

Fuel moistures were estimated by applying the National Fire Danger Rating System (NFDRS; Bradshaw and others, 1983) algorithms to a 1/8° gridded daily weather dataset that spanned the conterminous United States (Maurer and others, 2002). These data spanned 1950 to 2010 and included the minimum and maximum daily temperature and daily precipitation. The Mountain Climate Simulator (MT–CLIM) algorithms (Glassy and Running, 1994) were used to calculate relative humidity based on minimum and afternoon daily temperatures (Kimball and others, 1997). Dead and live fuel moistures were calculated by using the NFDRS (Deeming and others, 1977; Bradshaw and others, 1983; Burgan, 1988). The NFDRS algorithms required information about the beginning of both spring ("green-up") and fall ("brown-down") to estimate live fuel moistures. To generate the green-up and brown-down dates, a technique was implemented that determined the dates of seasonal changes in live fuel on the basis of the daily amount of exposure to light, minimum temperature, and the vapor-pressure deficit (Jolly and others, 2005).

3.4. Results

In the five ecoregions of this assessment, the number of wildland fires between 2001 and 2008 averaged 303 per year, but was as high as 467 in 2006 and as low as 131 in 2004 (table 3.1 and fig. 3.2). The area burned by wildland fires averaged 13,173 km^2/yr or 0.49 percent of the Western United States, which has a total area of approximately 2.66 million km^2. The area burned ranged from 3,345 km^2 (0.13 percent of total area) in 2004 to 25,206 km^2 (0.94 percent of total area) in 2007. The emissions from wildland fires and their interannual variability followed the patterns of the burned area and averaged 36.7 $TgCO_{2\text{-}eq}$/yr, ranging from 6.8 $TgCO_{2\text{-}eq}$ in 2004 to 75.3 $TgCO_{2\text{-}eq}$ in 2007. When normalized for the area burned, the annual emissions averaged 2.9 $kgCO_{2\text{-}eq}/m^2$/yr, but ranged from 1.7 to 3.9 $kgCO_{2\text{-}eq}/m^2$/yr (or 0.8 kgC/m^2/yr, ranging from 0.4 to 1.1 kgC/m^2/yr).

The Western Cordillera ecoregion had the most wildland fires and the highest emissions among all the Western United States ecoregions (table 3.1 and fig. 3.3*A*). The number of wildland fires between 2001 and 2008 averaged 123/yr and ranged from 61 in 2004 to 173 in 2003. The burned area and the emissions averaged 5,708 km^2/yr and 28.2 $TgCO_{2\text{-}eq}$/yr, respectively. The interannual variability was high and the area burned and the emissions ranged between 1,856 km^2 and 4.7 $TgCO_{2\text{-}eq}$ in 2004 and 10,449 km^2 and 64.1 $TgCO_{2\text{-}eq}$ in 2007, respectively. The Western Cordillera covers approximately 872,000 km^2. After normalizing the area burned and the emissions for the ecoregion's area, the annual area burned ranged between 0.21 and 1.20 percent and the annual emissions ranged between 2.6 and 6.2 $kgCO_{2\text{-}eq}/m^2$/yr for the entire Western Cordillera.

Table 3.1. Summary statistics for the number of wildland fires, area burned, and emissions, by EPA level II ecoregion and for the entire Western United States region between 2001 and 2008.

[km^2, square kilometers; $TgCO_{2\text{-}eq}$, teragrams of carbon dioxide equivalent]

	Western Cordillera	Marine West Coast Forest	Cold Deserts	Warm Deserts	Mediterranean California	Western United States
Number of wildfires per year						
Mean	123	5	121	25	31	303
Standard deviation	34.1	5.5	72.4	20.0	7.8	97.1
Minimum	61	1	36	7	15	131
Median	117	3	115	19	32	290
95th quantile	168	12	225	57	39	434
Maximum	173	13	245	66	39	467
Area burned per year (km^2)						
Mean	5,708	79	5,056	785	1,585	13,173
Standard deviation	2,966	87	4,212	702	1,198	6,736
Minimum	1,856	9	583	198	301	3,345
Median	5,371	58	3,962	544	1,220	12,136
95th quantile	9,926	178	10,926	1,920	3,292	23,261
Maximum	10,449	191	11,237	2,217	3,304	25,206
Emissions per year ($TgCO_{2\text{-}eq}$)						
Mean	28.2	0.3	4.1	2.4	1.8	36.7
Standard deviation	18.9	0.3	2.6	2.2	1.4	21.3
Minimum	4.7	0.0	0.8	0.5	0.3	6.8
Median	28.8	0.2	4.0	2.1	1.3	41.0
95th quantile	54.7	0.6	7.1	6.0	3.6	65.0
Maximum	64.1	0.7	7.1	7.4	3.7	75.3

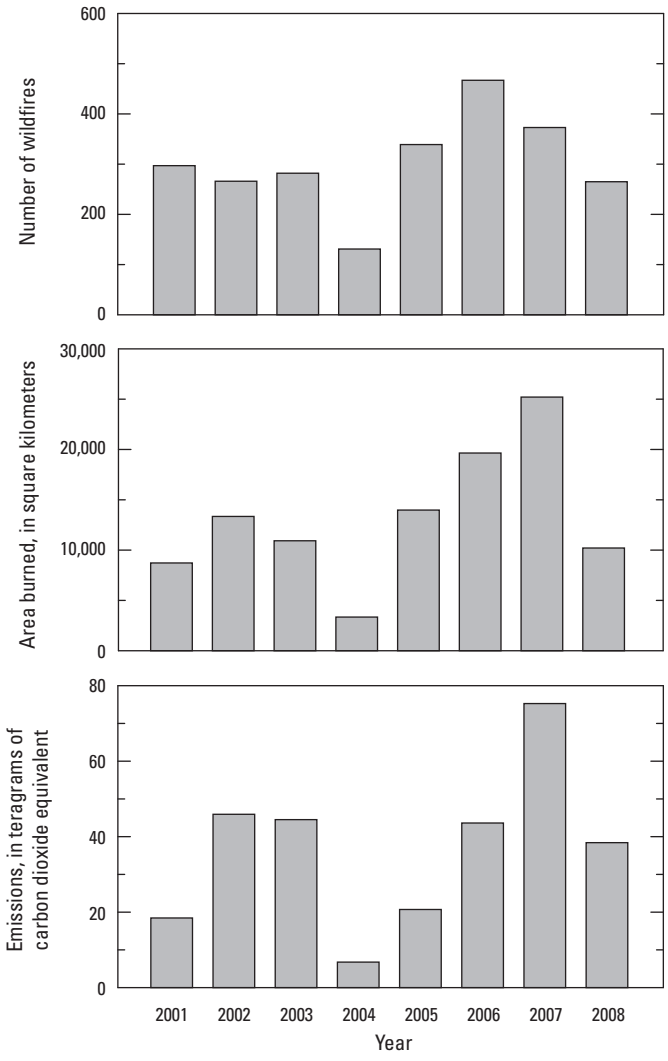

Figure 3.2. Graphs showing the annual number of wildland fires, area burned, and emissions for the baseline time period (2001–2008) in the Western United States.

Of all the ecoregions in the Western United States, the Marine West Coast Forest ecoregion had the fewest wildland fires, the smallest area burned, and the lowest emissions (table 3.1 and fig. 3.3*B*). The number of wildland fires averaged 5/yr and ranged from 1 to 13. The area burned ranged from 9 to 200 km^2 and averaged 79 km^2/yr. The emissions from the Marine West Coast Forest ranged from 0 to 0.7 $TgCO_{2\text{-}eq}$ /yr and averaged 0.3 $TgCO_{2\text{-}eq}$/yr. The area of the Marine West Coast Forest ecoregion is approximately 98,000 km^2. After normalizing the wildland-fire-occurrence statistics for area, from 0.01 to 0.13 percent of the ecoregion burned each year and emissions ranged from 2.6 to 4.8 $kgCO_{2\text{-}eq}/m^2$/yr.

The Cold Deserts ecoregion is the largest ecoregion in the Western United States at 1 million km^2 and had nearly as much wildland-fire activity as the Western Cordillera (table 3.1 and fig. 3.3*C*). On average, there were 121 wildland fires per year, but the interannual variability was high; as few as 36 wildland fires were observed in 2004 and as many as 245 were observed in 2006. The amount of area burned each year in the Cold Deserts ecoregion was similar to that of the Western Cordillera and averaged 5,056 km^2/yr, ranging from 583 km^2 in 2004 to 11,237 km^2 in 2007. This range is equivalent to 0.06 to 1.07 percent of the area of entire ecoregion; however, because the vegetation in the Cold Deserts is predominantly grass and shrubs, emissions were lower, averaging only 4.1 $TgCO_{2\text{-}eq}$/yr and ranging from 0.8 to 7.1 $TgCO_{2\text{-}eq}$ in 2004 and 2007, respectively.

In the Warm Deserts ecoregion, wildland fires were infrequent with an average of 25 wildfires per year, but as many as 66 in 2005 and as few as 7 in 2004 (table 3.1 and fig. 3.3*D*). The amount of area burned was also small and ranged from 198 km^2 in 2004 to 2,217 km^2 in 2005 with an average of 785 km^2/yr. This range equated to 0.16 to 0.46 percent of the ecoregion area, which was 478,000 km^2. The emissions were generally low, with an average of 2.4 $TgCO_{2\text{-}eq}$/yr; the variability in emissions was high, however, and varied from 0.5 $TgCO_{2\text{-}eq}$ in 2004 to 7.4 $TgCO_{2\text{-}eq}$ in 2008. When normalized for the area burned, the emissions ranged from 1.0 to 3.5 $kgCO_{2\text{-}eq}/m^2$/yr.

The Mediterranean California ecoregion is the smallest in the Western United States (173,000 km^2) but still had a substantial amount of wildland-fire activity. On average, there were 31 wildland fires per year with a range from 15 to 39 (table 3.1 and fig. 3.3*E*). The area burned averaged 1,585 km^2/yr and had a range of 301 to 3,304 km^2 in 2001 and 2003, respectively. The emissions averaged 1.8 $TgCO_{2\text{-}eq}$/yr but ranged from 0.3 to 3.7 $TgCO_{2\text{-}eq}$ in 2005 and 2008, respectively. The amount of area burned and emissions were large relative to the total area of the ecoregion. The area burned ranged from 0.17 to 1.91 percent of the entire ecoregion (the highest percent area in the Western United States), and the emissions ranged from 0.6 to 1.2 $kgCO_{2\text{-}eq}/m^2$/yr.

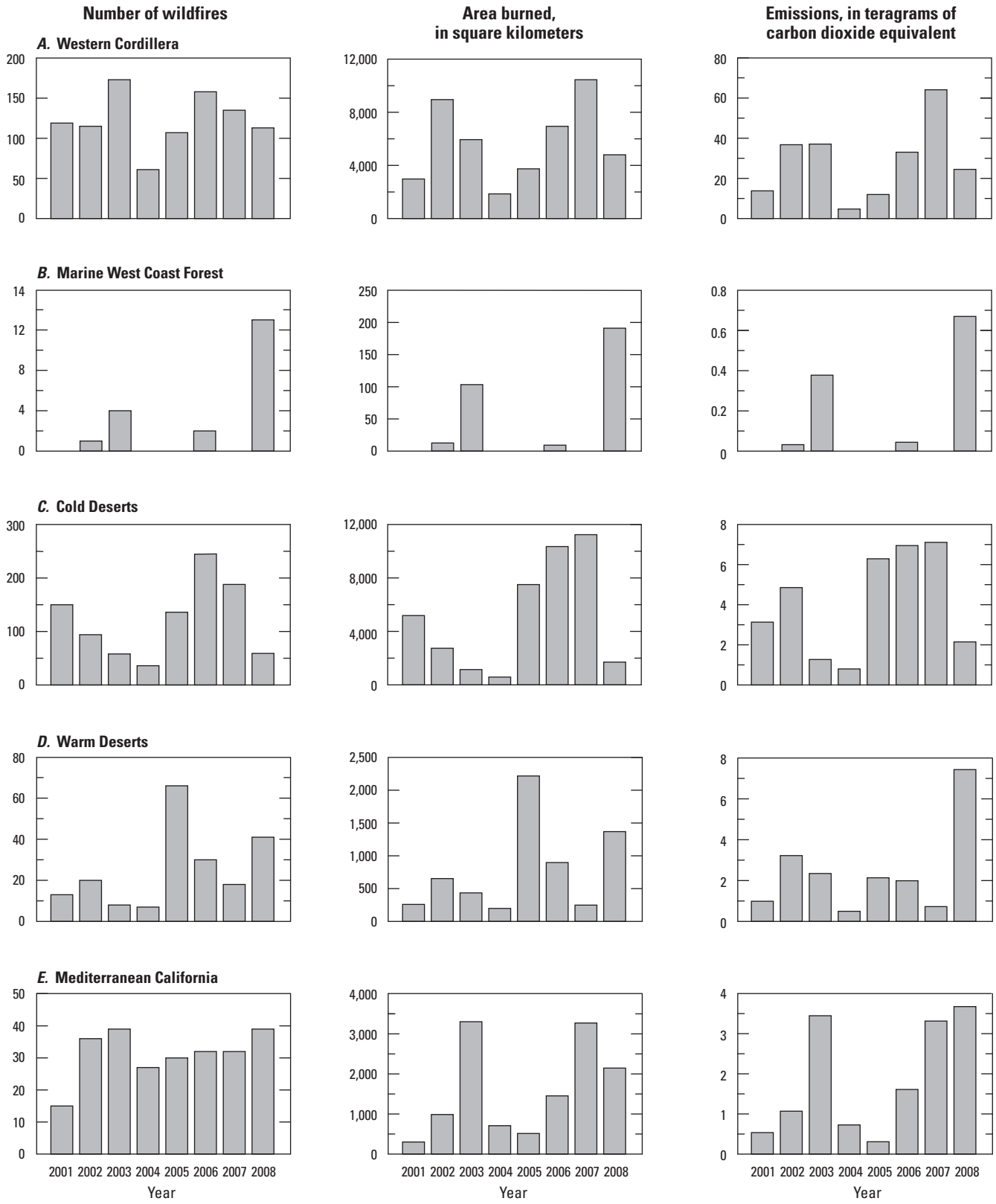

Figure 3.3. Graphs showing the annual number of wildland fires, area burned, and emissions for the baseline time period (2001–2008) for level II ecoregions in the Western United States (EPA, 1999). The vertical scales are not constant among ecoregions.

3.5. Discussion

From 2001 to 2008, wildland-fire activity in the Western United States was substantial; large wildland fires numbered between 131 and 467 per year and burned from 3,345 to 25,206 km^2 each year. These western wildland fires represented 58 percent of all the wildland fires that occurred nationwide from 2001 to 2008 and are mapped in the MTBS database, and accounted for 75 percent of the all area burned. The annual emissions averaged 36.7 $TgCO_{2\text{-}eq}$/yr, which was equivalent to 0.7 percent of the nationwide fossil-fuel emissions in 2010 (5,594 $TgCO_{2\text{-}eq}$/yr; EPA, 2012). The interannual variability in emissions was high and ranged from 6.8 to 75.3 $TgCO_{2\text{-}eq}$ in the Western United States, which was equivalent to 0.1 to 1.3 percent of the nationwide fossil-fuel emissions, respectively. Thus, the relative contribution of wildland fires of the Western United States to nationwide greenhouse-gas emissions was small when compared to the contribution of anthropogenically generated emissions.

There was a large amount of year-to-year variability in wildland-fire occurrences, area burned, and emissions among the five ecoregions in the Western United States (table 3.1 and fig. 3.3), which was related to differences in vegetation and fire regimes. The Marine West Coast Forest and Western Cordillera ecoregions are dominated by coniferous forests, but have quite different fire regimes. Precipitation is high in the Marine West Coasts Forest, which results in highly productive vegetation, but the infrequent wildland fires can be severe (Agee, 1993). The forests in the Western Cordillera tend to exist in a drier climate with more frequent wildland fires, but the severity is mixed and depends on drought and vegetation conditions (Schoennagel and others, 2004). In both the Marine West Coast Forest and Western Cordillera ecoregions, wildland-fire emissions can be high under severe conditions because large amounts of canopy fuels can be consumed by a crown fire. The Marine West Coast Forest did not produce a substantial amount of emissions in this analysis, but that may be in part because the wildland-fire frequency was low in this ecoregion and the 25-year span covered by the MTBS did not include a sizeable amount of fire activity there. The results of this assessment, however, do highlight the importance of wildland-fire emissions in the Western Cordillera at both a regional and national scale because this ecoregion produced 77 percent of all emissions in the Western United States during the baseline period.

In contrast to the Marine West Coast Forest and the Western Cordillera, the Cold Deserts, Warm Deserts, and Mediterranean California ecoregions are dominated by the grasslands/shrublands ecosystem and other ecosystems (primarily deserts). Wildland fires were frequent in all three ecoregions but were more common in the Cold Deserts and Mediterranean California than in the Warm Deserts. The fire regimes in the desert ecoregions were related to vegetation productivity and climate (Mensing and others, 2006; Brooks and Chambers, 2011). These same drivers influenced wildland fires in the Mediterranean California ecoregion, but human influences and extreme winds also played a large role (Syphard and others, 2007; Moritz and others, 2010). Invasive species were also present in all three ecoregions, often displacing native vegetation and thus increasing wildland-fire frequency (D'Antonio and Vitousek, 1992; Brooks and others, 2004; Keeley, 2006). These results suggest that an extensive amount of area can burn in these regions, but the emissions are generally lower than those of the forested ecoregions simply because of the difference in the amount of available fuel.

3.6. Limitations and Uncertainties

The MTBS data used in this assessment did not include small wildland fires, but they still captured the majority of the area burned because they included the largest wildland fires which contributed most to the amount of area burned (Strauss and others, 1989; Stocks and others, 2002). A comparison of the MTBS data with the Federal wildland-fire-occurrence database (U.S Department of the Interior, 2012) showed that the MTBS listed only 2 percent of all wildland fires but that 2 percent accounted for 80 percent of the area burned in the five ecoregions covered by this assessment. Therefore, the results of this assessment captured the general patterns and trends of western wildland fires, but provided a slight underestimate of wildland-fire emissions.

In this assessment, the estimates of area burned and of emissions also did not include the influence of prescribed and agricultural fires (for example, burning crop residues); however, the emissions produced by those types of fires were suspected to be low relative to the wildland-fire emissions. The influence of prescribed fires on emissions was difficult to assess because the data characterizing prescribed fires were generally poor based on inconsistent reporting about them across the country. The existing estimates of emissions from prescribed fires suggested that they produced only 10 percent of the emissions from wildland fires (Y. Liu, 2004), in part because prescribed fires usually burn under less extreme meteorological conditions than wildland fires. The influence of agricultural fires was also estimated to be about 10 percent of the wildland-fire emissions in the GFED database. In the Western United States, the relative amount of emissions produced by prescribed and agricultural fires was likely to be even lower, because agricultural fires were more common in the Great Plains and the Eastern United States (Korontzi and others, 2006; Tulbure and others, 2011) and prescribed fires in the Western United States only accounted for 22 percent of the area burned by prescribed fires nationwide (National Interagency Fire Center, 2012).

The emissions results generated for this assessment differed and were generally lower than past estimates of emissions for the Western United States. The highest emissions estimates were from Wiedinmyer and Neff (2007), who used the active wildland fire data from the MODIS from 2002 to 2006 and estimated the mean and standard deviation of annual emissions at 105.0 and 42.0 $TgCO_{2\text{-}eq}$, respectively, for the following States: Arizona, California, Colorado, Idaho, Montana, New Mexico, Nevada, Oregon, Utah, Washington, and Wyoming; the five ecoregions in this assessment do not cover the exact same area. French and others (2011) calculated emissions using the MTBS data and CONSUME model (Ottmar and others, 2008) for wildland fires occurring from 2001 to 2008; their results are available online as ecoregion-level summaries (Michigan Tech Research Institute, 2012). When their results were summarized across the Western United States, the average and standard deviation of annual emissions was 78.4 and 43.3 $TgCO_{2\text{-}eq}$, respectively, which is nearly twice the amount of the emissions estimated in this assessment. The emission estimates from both of these analyses were substantially greater than the estimates generated for this assessment. The differences are most likely due to differences in methods, data, and the resolution of the data used. Wiedinmyer and Neff (2007) relied on 1-km resolution, active-wildland-fire data from MODIS and fuels data from the Fuels Characterization Classification System (FCCS; USDA Forest Service, 2012d). They also assumed that all of the available biomass could potentially burn, and that is often not the case, especially for woody fuels (Campbell and others 2007; Meigs and others, 2009). French and others (2011) also used the 1-km-resolution FCCS fuels data and aggregated 1-km-resolution MTBS data. The fuels data in their report differed from the data layer used in this assessment both in terms of information and resolution. The methods used in this assessment made use of fuel moistures, which are based on gridded daily weather data. The methods used by French and others (2011) also made use of fuel moistures, but recommended 10 percent levels for 1,000-hour availability and duff moistures, which are very favorable conditions for combustion. The full effects of the differences in fuel maps and moisture levels on this assessment were difficult to assess, but these comparisons suggest that the results in this assessment are more conservative than previously published estimates of wildland-fire emissions.

3.7. Implications for Management and Mitigation

For this assessment, the effects of different strategies for wildland-fire management and mitigation on fire emmissions were not explicitly addressed, but there is a growing body of literature from which to draw some conclusions. Increasing the effectiveness of fire suppression (which includes firefighting, prevention, and education) is a popular first choice but unlikely to work to reduce fire emmissions given that fire suppression over the past 100 years has had mixed success (Rollins and others, 2001; Keane and others, 2002; Stephens and Ruth, 2005). In some ecoregions, reducing the area that could potentially be burned may be possible and critical to maintain ecosystem health, especially in areas where wildland-fire frequency is suspected to be unnaturally high because of the increase in human influence due to arson, accidental ignitions, or the accidental or deliberate introduction of invasive species, such as in Southern California (Keeley and others, 1999) and in the grasslands, shrublands, and deserts of the Southwestern United States where fire-adapted invasive species are altering wildland-fire cycles (D'Antonio and Vitousek, 1992; Brooks and others, 2004; Keeley, 2006).

A more effective way to reduce wildland-fire emissions from forests may be to implement management strategies designed to reduce wildland-fire severity, which is directly related to the amount of biomass consumed. In many parts of the Western United States, fire suppression has resulted in unnaturally high fuel loads producing wildland fires that are of uncharacteristically high severity (Stephens, 1998; Keane and others, 2002; Agee, 2003; Stephens and Ruth, 2005). Fuel treatments, including mechanical forest thinning and prescribed fires, are designed to reduce fuel loads so that wildland fires are less intense and easier to manage if they do occur (Agee and Skinner, 2005; Reinhardt and others, 2008). Most of the evidence suggests that fuel treatments can reduce carbon loss through wildland-fire emissions over the long term even though there is a short-term loss in carbon storage due to biomass removal (Stephens and others, 2009; Reinhardt and Holsinger, 2010; Wiedinmyer and Hurteau, 2010; North and Hurteau, 2011). Such treatments are most effective in forests where fuel loads are uncharacteristically high and may

not be ecologically appropriate in other forest and vegetation types (Sibold and others, 2006; Mitchell and others, 2009). To produce a noticeable effect at a regional scale, between 20 and 40 percent of the Western United States' forests need to be treated (Finney, 2001, 2007). The potency of fuel treatments can be short-lived, on the order of 10 to 20 years (Collins and others, 2011); therefore, 1 to 4 percent of the forested landscape would need to be treated annually (Finney and others, 2007). Given that wildland fires are rare events, the proportion of the landscape that must be treated is much larger than the proportion of the landscape that burns and because of that relation, the amount of carbon removed from biomass pools in fuel treatments may be greater than the amount of carbon protected from fire (Campbell and others, 2012).

In some nonforested ecosystems in the Western United States (especially southern California, the Great Basin, and the Sonoran and Mojave Deserts), the frequencies of wildland fires are uncharacteristically high and are driven by human ignition of some fires and by invasive species which provide extra fuel (D'Antonio and Vitousek, 1992; Keeley and others, 1999; Brooks and others, 2004; Keeley, 2006). Wildland-fire emissions in these nonforested ecosystems are likely to be greater and carbon stocks lower than in historic time because native woody vegetation has been replaced by invasive grasses (Bradley and others, 2006). Even though wildland-fire emissions from these nonforested ecosystems are low relative to those from forested ecosystems, reducing the wildland-fire frequency to the historical range of variability may result in only slightly reduced overall wildland-fire emissions. In other nonforested ecosystems in the Western United States (such as grasslands/shrublands), the opposite has happened. Grazing pressure has reduced the grass cover and the frequency of wildland fires, thus allowing woody vegetation to expand its range and increase in cover (Van Auken, 2000). The expansion of woody vegetation usually results in an increase in carbon stocks (Asner and others, 2003); however, it is uncertain if the increased carbon stocks will persist over long time periods given changes in climate and fire regimes (Barger and others, 2011).

Much uncertainty remains about the short- and long-term effects of wildland-fire management on carbon budgets in many ecosystems in the Western United States. Any carbon-management strategy focused on increasing ecological carbon stocks or sequestration rates should carefully consider the benefits and risks of wildland-fire management over both short and long time periods, as well as the effects on other ecosystem characteristics and services (Jackson and others, 2005; McKinley and others, 2011; Olander and others, 2012).

This page intentionally left blank.

Chapter 4. Major Land-Management Activities and Natural Disturbances Considered in This Assessment

By Shuguang Liu[1], Jennifer Oeding[2], Zhengxi Tan[3], Gail L. Schmidt[2], and Devendra Dahal[2]

4.1. Introduction

Carbon stocks and fluxes of ecosystems are strongly influenced by, among other factors, land-management activities and natural disturbances. The U.S. Forest Service (USFS) estimated that approximately 4.05 million hectares (or 1.3 percent) of forested land is harvested each year (W.B. Smith and Darr, 2004), which may significantly affect the carbon cycle at local to national levels (Cohen and others, 1996; Pan, Birdsey, and others, 2011). Although the effects of natural disturbances and land management on carbon dynamics are significant, few datasets exist that adequately describe the spatial and temporal characteristics of various land-management activities. This chapter provides a brief review of major natural disturbances and land-management activities in the Western United States in relation to carbon sequestration, describes the status of data availability for the activities, and introduces those activities that were included in the assessment and their data-processing steps. Wildland fires are the most significant natural disturbances in the Western United States. Chapters 3 and 8 of this report provide extensive treatment of wildland fires; therefore, the primary focus of this chapter is on the land-management activities that were considered in the modeling process for this assessment.

4.2. Review of Major Land-Management Activities and Natural Disturbances

Major land-management activities and natural disturbances, their impacts on carbon dynamics, and the status of the geospatial data layers characterizing their spatial and temporal changes in the Western United States are briefly reviewed below.

4.2.1. Forest Harvesting

There are many examples of forest harvesting data at a local scale, but they are rarely available at a national or regional scale in a spatial format. The USFS Forest Inventory and Analysis (FIA) Program (USDA Forest Service, 2012b) provides nationwide information on the extent, condition, volume, growth, and removal of trees. The FIA is the best available resource for information on forest-management activities and its database was extensively used in support of this assessment. On the other hand, the FIA is a site-specific characterization of forest conditions, which was both an advantage and a limitation. The lack of wall-to-wall geospatial information from the FIA often made it difficult to identify the real clearcutting patterns for modeling efforts over a large area. Current approaches that merge remotely sensed land-cover-change information with FIA inventories have shown promising results (for example, Hicke and others, 2007; Goward and others, 2008; Cho-ying Huang and others, 2010; D.P. Turner, Gockede, and others, 2011; Williams and others, 2012).

4.2.2. Wildland Fires

Wildland-fire combustion releases carbon into the atmosphere and resets the pathways for carbon-sequestration across the landscape (Running, 2008). For this assessment, the treatment of both the baseline and the projected future potential fire emissions is covered in chapters 3 and 8; the fire-extent and fire-severity data layers were used to support the biogeochemical modeling (see chapters 5 and 9).

[1]U.S. Geological Survey, Sioux Falls, S.D.

[2]Stinger Ghaffarian Technologies, Inc., Sioux Falls, S.D.

[3]Arctic Slope Regional Corporation Research and Technology Solutions, Sioux Falls, S.D.

4.2.3. Insects and Disease

Insects and disease, such as the western pine bark beetle, cause extensive defoliation, mortality, and reduced carbon stocks in forests across the Western United States (Fellin and Dewey, 1992; Man, 2010; Pfeifer and others, 2011). The carbon-cycle processes that are affected by insects or disease depend on the type of disturbance and whether it causes defoliation or tree mortality (S. Liu and others, 2011). The USFS FIA database (USDA Forest Service, 2012b) contained information related to the types and severity of insects and disease and related information on defoliation and mortalities; however, the database was limited by a lack of repeated inventories, which limited the analysis for insects and disease.

4.2.4. Grazing on Grasslands and Shrublands

Grazing on grasslands and shrublands in the Western United States, particularly in the Great Basin and the Colorado Plateau, is a leading land-use activity and has had a major effect on the carbon cycle and other qualities of the landscape (Wagner, 1978; Crumpacker, 1984; Fleischner, 1994). Many studies have documented the effects of grazing on carbon cycles (for example, Lal, 2004; Derner and Schuman, 2007; Schuman and others, 2009), but often at the local scale. The USGS carbon-sequestration assessment for the Great Plains (Zhu and others, 2011) relied on assumed relationships between the animal unit month (AUM, the amount of forage required by an animal unit for one month; Ruyle and Ogden, 1993) and carbon removal, but the uncertainty was very high. Ultimately, any regional or national assessment of the effects of grazing is limited by the absence of synthesized data or a georeferenced database.

4.2.5. Crop Rotation and Tillage

Tillage is one of the major land-management activites that could substantially affect carbon storage in and GHG fluxes from the soil (Ogle and others, 2005; Alluvione and others 2009). Crop rotation, residue management, and tillage practices are exercised in all agricultural areas of the Western United States. In practice, both residue management and tillage practices (either no tillage, conventional tillage, or reduced tillage) are commonly coupled to form a cropping system. The data by acreage for both practices are usually reported as county-based statistics by the Conservation Technology Information Center (CTIC, 2012). For this assessment, although the CTIC data were not georeferenced, they were allocated to each crop type using a method by Schmidt and others (2011).

4.2.6. Irrigation and Drainage

The Snake River Plain and Columbia River Basin support agriculture production (row crops, hay and pasture) with large-scale irrigation projects. Irrigation can increase soil moisture, improve crop yields, and potentially enhance carbon sequestration in soil (Lal and others, 1998). The drainage of wet soils may increase crop and animal productivity and reduce methane emissions, but it may also lead to a loss of soil organic carbon (SOC) stock by increasing the decomposition of soil organic matter and the leaching of dissolved organic carbon (Watson and others, 2000); however, data about irrigation are limited (Wu and others, 2008). A nationwide MODIS-derived dataset about irrigated agriculture (MIrAD-US) was developed by the USGS for 2002 (USGS, 2010) and 2007 (Pervez and Brown, 2010) at both 1,000-m and 250-m resolution. They are available at USGS (2010).

4.2.7. Manure Application

Manure is widely used in agricultural fields to supply nutrients because of the high price of fertilizers (Lentz and Lehrsch, 2010). According to MacDonald and others (2009), about 15.8 million acres of cropland, equivalent to about 5 percent of all cropland in the United States, are fertilized with livestock manure. Data on manure production and application are usually estimated through the USDA's Agricultural Resource Management Survey (ARMS; USDA Economic Research Service, 2011a). The EPA estimated the annual manure-related GHG emissions at both State and national levels on the basis of annual yields of animal products and determined that manure application was one of the major contributors to the total GHG emissions from agricultural lands, amounting to up to 19.88 $TgCO_{2\text{-}eq}$ in 2010 over the Western United States, of which California made the greatest contribution (52 percent), followed by Idaho (about 20 percent) (EPA, 2012).

4.3. Data Processing for Major Land-Management Activities and Natural Disturbances Included in the Assessment

As with the Great Plains assessment conducted by the USGS (Zhu and others, 2011), this assessment relied on nationwide geospatial data layers in order to characterize the spatial and temporal dynamics of land-management activities and natural disturbances (Schmidt and others, 2011). Table 4.1 lists the data layers used for major land-management activities and natural disturbances for this assessment and figure 4.1 depicts the spatial patterns of some data layers for 2005.

The spatial resolution of some of the data layers in table 4.1, especially those derived from censuses and inventories, was at the county, State, or FIA-unit level. These data layers were further downscaled to pixels to generate spatially explicit map layers using a Monte Carlo procedure, land cover, and other information (Schmidt and others, 2011). The most common pixel resolution among all the map layers was 250 meters. The data covered the time period from 1992 to 2050 on an annual basis. Annual maps showing areas of forest clearcutting were produced as part of the LULC-change modeling detailed in chapter 2 of this report. Annual maps of wildland-fire disturbances were modeled using an approach described in chapter 3 of this report.

Table 4.1. Summary of data for the major land-management activities and natural disturbances that were considered as part of this assessment.

[CFS, Canadian Forest Service; CTIC, Conservation Technology Information Center; m, meter; NA, not applicable; PRISM, parameter-elevation regressions on independent slopes model; USDA, U.S. Department of Agriculture; USDA ERS, USDA Economic Research Service; USDA FIA RPA, USDA Forest Inventory Analysis Resource Planning Act; TPO, timber product output; USGS, U.S. Geological Survey]

Type	Source	Spatial resolution	Time period	Reference
Crop management				
Crop yield	USDA crop yield table	County	1992–2050	USDA National Agricultural Statistics Service (2011).
Fertilization	USDA ERS fertilization table	County	1992–2050	USDA Economic Research Service (2011b).
Manure	USDA manure table	County	1996–2050	USDA Economic Research Service (2011a).
Tillage	CTIC tillage table	County	1992–2050	CTIC (2011); USDA Economic Research Service (2011a).
Irrigation	USGS	250 m	NA	USGS (2010).
Derived crop management				
Derived crop type, manure, tillage, and fertilizer	Derived grids for this assessment	250 m	1992–2050	Schmidt and others (2011).
Fire				
Extent, severity, frequency	This assessment	250 m	1992–2050	Chapters 3 and 8 of this report.
Forest clearcuts				
Forest-stand age	USGS Land Cover Trends Project	250 m	1992–2050	USGS (2012a).
Timber product output	TPO from USDA FIA RPA	State	2002	USDA Forest Service (2011)
Drought				
Precipitation	PRISM and CFS	250 m	1992–2050	Canadian Forest Service (2012); PRISM Climate Group (2012).

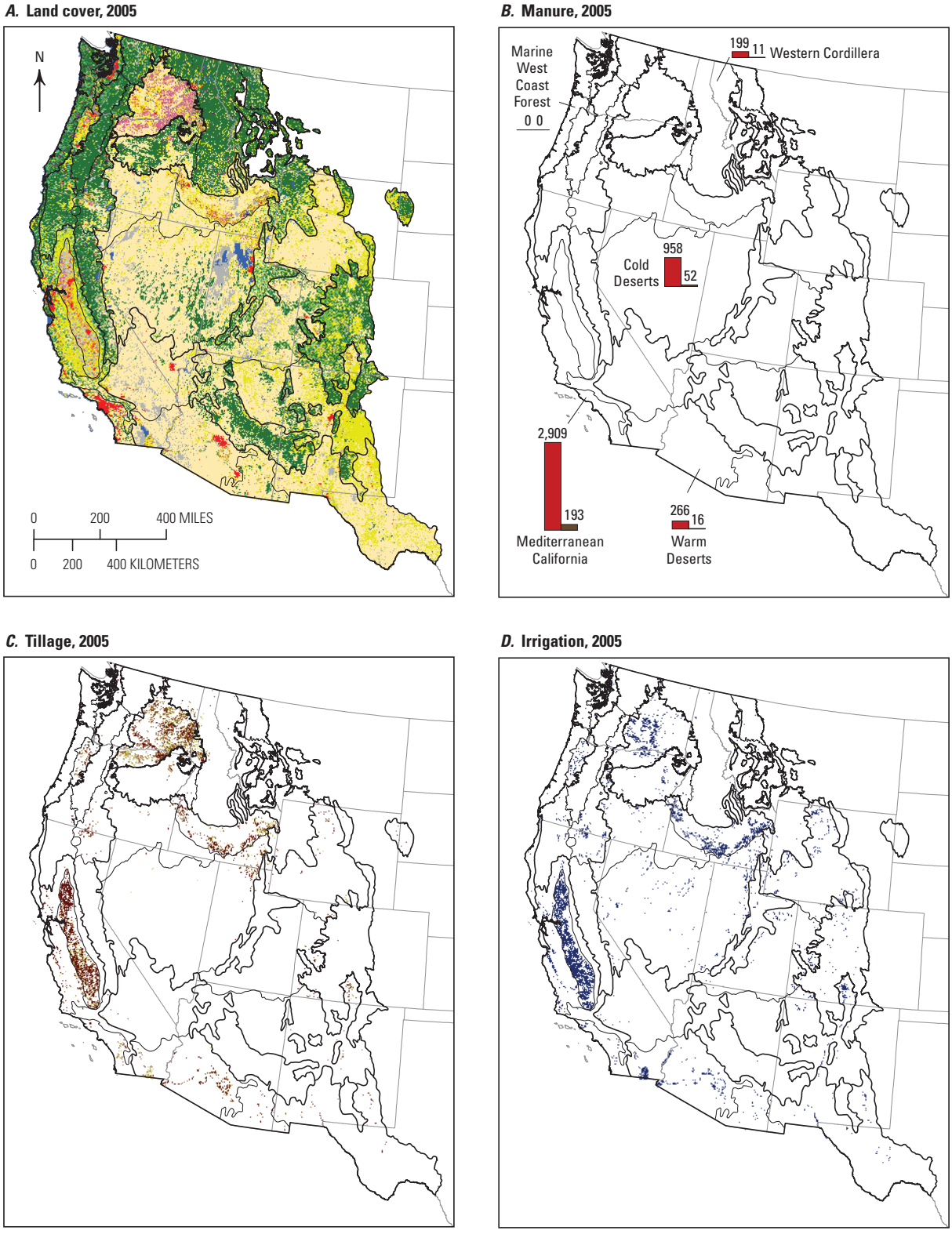

Figure 4.1. Maps showing examples of the data layers for land-management activities and natural disturbances in the Western United States for 2005. *A*, Land cover. *B*, Manure. *C*, Tillage. *D*, Irrigation. *E*, Fire severity. *F*, Stand age. See figure 1.1 in chapter 1 for ecoregion names.

E. **Fire severity, 2005**

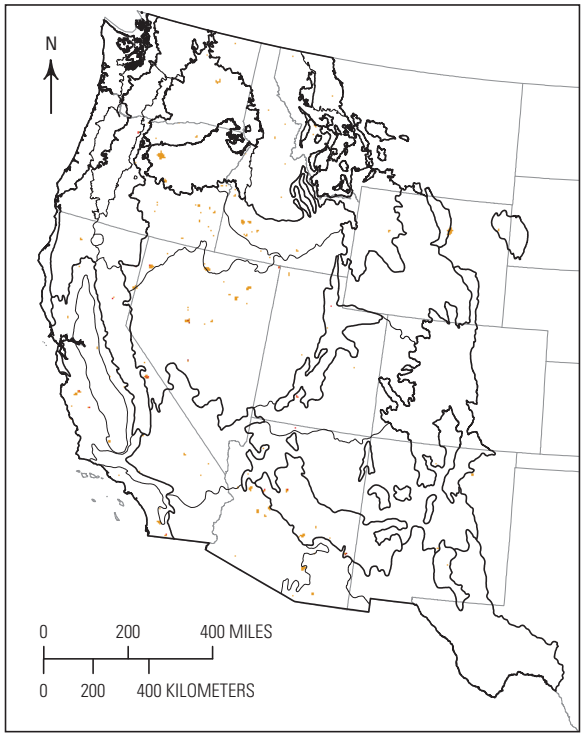

F. **Stand age, 2005**

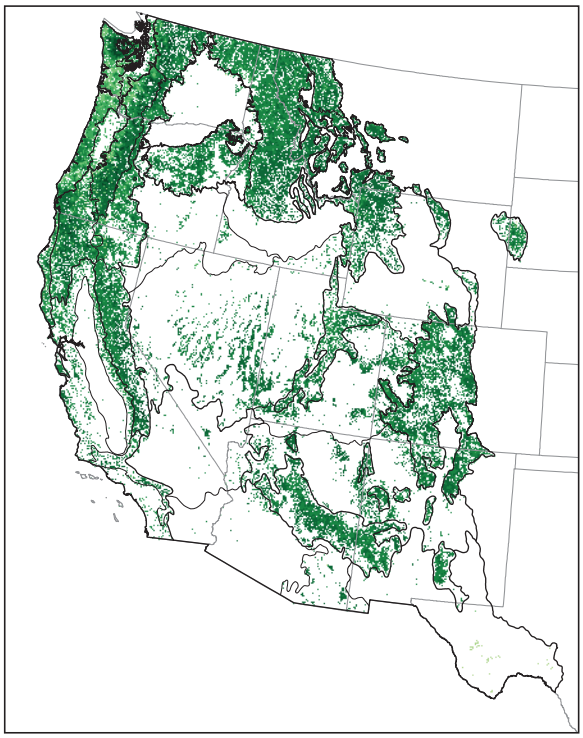

EXPLANATION

Land use and land cover

- Water
- Developed
- Mechanically disturbed national forest
- Mechanically disturbed other public land
- Mechanically disturbed private land
- Mining
- Barren
- Deciduous forest
- Evergreen forest
- Mixed forest
- Grassland
- Shrubland
- Hay/pasture
- Woody wetlands
- Herbaceous wetlands
- Perennial ice/snow
- Barley
- Beans
- Corn grain
- Corn silage
- Cotton
- Flaxseed
- Lentils
- Sorghum silage
- Oats
- Peanuts
- Peas
- Potatoes
- Rice
- Rye
- Safflower
- Sorghum
- Soybeans
- Sugarbeets
- Sunflowers
- Tomatoes
- Wheat durum
- Wheat spring
- Wheat winter

Total manure application per level II ecoregion— In kilograms

1,500 750 Carbon Nitrogen

Tillage

- None
- Ridge
- Mulch
- Reduced
- Conventional

Irrigation

- Non-irrigated
- Irrigated

Fire severity

- Low
- Moderate
- High

Stand age— In years

- 0
- 1 to 5
- 6 to 10
- 11 to 15
- 16 to 30
- 31 to 50
- 51 to 100
- 101 to 250
- >250

Ecoregion boundary

- Level III
- Level II

Figure 4.1.—Continued

The crop-management information used in this assessment includes crop type, crop rotation, fertilization, manure addition, tillage practices, irrigation, and harvesting practices. All of the crop-management activities were specific to various crops and locations. All of the pixels representing agricultural lands in the land-cover data layers, generated in the LULC mapping and modeling process described in chapter 2 of this report, were downscaled (using a probability-based Monte Carlo approach) to crop types according to the crop-composition information derived from the USDA agricultural census data (USDA National Agricultural Statistics Service, 2011). All of the crop-management data layers (except irrigation) were subsequently generated from these land-cover data layers and more than 20 major crops were presented consistently for the United States (Schmidt and others, 2011). The tabular data about manure application were derived from the USDA census (USDA, Economic Research Service, 2011a), which included, for each crop type in each State, the following information: the State Federal Information Processing Standard (FIPS) code, the year, the total planted area, the percentage of the planted area that was treated with manure, the amount of manure that was applied, the rate at which the manure was applied, the rate at which the nitrogen in the manure was applied, and rate at which the carbon in the manure was applied. A gridded manure dataset for all agricultural lands in the region was generated from this tabular data along with the land-cover maps using a Monte Carlo procedure.

The information about tillage practices was acquired from the CTIC in tabular format. The tabular data include the following information: the State FIPS code, the year, the total planted area that was tilled, the total percentage of residue on all tilled areas, the planted area for each tillage type, and the percentage of residue for each tillage type by crop type within the State. The tillage practices included in the database included conventional, mulch, no-till, reduced, and ridge tillage. A gridded dataset showing the spatial and temporal changes of tillage practices for all agricultural lands was generated from this tabular data along with the land-cover maps using a Monte Carlo procedure. Figure 4.1 shows the spatial distribution of tillage practices in the Western United States in 2005. An irrigation map derived from the MODIS for the United States (USGS, 2010) was used to characterize the locations of irrigated land. Because of the lack of data showing the temporal changes in irrigation across the Western United States, this assessment assumed that the locations of irrigated land did not change over time during the assessment period.

Only nitrogen fertilization was considered in this assessment. A nationally consistent procedure was put in place to generate crop- and location-specific nitrogen-fertilization data for all croplands (see Schmidt and others, 2011). The tabular dataset included the State FIPS code, year, the total planted area where nitrogen fertilizer was applied, the percentage of total area that was fertilized with nitrogen, the rate of application for nitrogen fertilizer, and the total amount of nitrogen fertilizer applied for each crop type within each State. Because several States in the Western United States did not report this information, this assessment assumed that croplands were automatically fertilized every year in order to satisfy growth requirements.

4.4. Land-Management Activities or Natural Disturbances Not Included in the Assessment

Because of the lack of input data and constraints on resources, this assessment did not explicitly consider the following activities:

- Selective or partial forest cutting. One of major factors driving carbon dynamics in forest ecosystems is selective or partial forest cutting, which should have been considered for the modeling steps in this assessment. Unfortunately, there were no spatial datasets available that characterized the spatial and temporal changes of selective or partial forest cutting in the Western United States.
- Insects and diseases. Various studies and inventories of natural disturbances by insects and diseases have been conducted at a broad regional scale. For example, Raffa and others (2008) provided an estimate of forest mortality caused by bark beetle eruptions in western North American forests. These types of data were not included in this assessment because their spatial and temporal extents and resolution were usually limited.
- Grazing. Grazing on grasslands and shrublands is extensive and varies in both time and space; however, there are no geospatial datasets available that characterize grazing in the Western United States.

Chapter 5. Baseline Carbon Storage, Carbon Sequestration, and Greenhouse-Gas Fluxes in Terrestrial Ecosystems of the Western United States

By Shuguang Liu[1], Jinxun Liu[2], Claudia J. Young[3], Jeremy M. Werner[1], Yiping Wu[4], Zhengpeng Li[5], Devendra Dahal[2], Jennifer Oeding[2], Gail L. Schmidt[2], Terry L. Sohl[1], Todd J. Hawbaker[6], and Benjamin M. Sleeter[7]

5.1. Highlights

- From 2001 to 2005 in the Western United States, the average annual total carbon stored in vegetation and soils (up to 20 cm in depth) was estimated to be 13,920 TgC, ranging from 12,418 to 15,461 TgC.
  - The Western Cordillera ecoregion stored the most carbon (59 percent of the total), followed by the Cold Deserts (19 percent), Marine West Coast Forest (11 percent), Mediterranean California (6 percent), and Warm Deserts (5 percent) ecoregions.
  - Forests, grasslands/shrublands, and agricultural lands stored 69 percent, 25 percent, and 4.3 percent of the total carbon in ecosystems of the Western United States, respectively.
  - Live biomass, soil organic carbon (SOC) in the top 20 cm of the soil layer, and dead biomass (forest litter and dead woody debris) accounted for 38 percent, 39 percent, and 23 percent, respectively, of the total carbon stored in the Western United States.
- The average annual net carbon flux in the terrestrial ecosystems of the Western United States was estimated to be −86.5 TgC/yr, ranging from −162.9 to −13.6 TgC/yr from 2001 to 2005. (Negative values denote a carbon sink.)
  - Forests were the largest carbon sink (62 percent of the average), followed by grasslands/shrublands (30 percent), and agricultural lands (7 percent).
  - The live biomass pool provided about one-third of the carbon sink; the rest was provided by the dead biomass and the SOC pools.
- The ecosystems of the Western United States served as a greenhouse-gas (GHG) sink for three gases: carbon dioxide (CO_2), nitrous oxide (N_2O), and methane (CH_4). These GHGs accumulated at an estimated −599.1 to −51.3 $TgCO_{2\text{-eq}}$/yr. Overall, the carbon dioxide sink provided by the ecosystems was responsible for about 99 percent of the total GHG flux. The fluxes of nitrous oxide (for which the Western United States was a source) and methane (for which the Western United States was a sink) were relatively very small.

5.2. Introduction

This chapter describes the modeling and analysis of the baseline carbon storage and GHG flux in ecosystems of the Western United States. As indicated by the methodology diagram (figure 1.2 of chapter 1 of this assessment), this component of the assessment uses land-use and land-cover (LULC) mapping and modeling results (chapter 2) and wildland-fire modeling results (chapter 3) as the primary input data in addition to other input data described later in this chapter. The definitions of the ecosystems and the descriptions of the ecoregions are provided in chapters 1 and 2 of this report. See table 2.1 of chapter 2 of this report for definitions of the ecosystems covered in this chapter. The tables in this

[1]U.S. Geological Survey, Sioux Falls, S.D.

[2]Stinger Ghaffarian Technologies, Inc., Sioux Falls, S.D.

[3]ERT, Inc., Sioux Falls, S.D.

[4]Arctic Slope Regional Corporation Research and Technology Solutions, Sioux Falls, S.D.

[5]University of Maryland, College Park, Md.

[6]U.S. Geological Survey, Denver, Colo.

[7]U.S. Geological Survey, Menlo Park, Calif.

chapter present the results of carbon stock, carbon flux, and GHG fluxes in terms of the following pools: live biomass (both aboveground and belowground), soil organic carbon (SOC; measured in the top 20 cm of the soil layer), and dead biomass (forest litter and dead, woody debris).

Land-use and land-cover change, natural disturbances, and climate change directly alter carbon fluxes and carbon stocks in ecosystems. Although these influences on the carbon cycle have been observed from local to global scales, there is increasing scientific and political interest in regional patterns and causes of terrestrial carbon sources and sinks (Intergovernmental Panel on Climate Change, 2007; Piao and others, 2009; Pan, Birdsey, and others, 2011). Many studies have evaluated the carbon stocks and fluxes in diverse ecosystems and addressed their complicated interactions with climate change, LULC change, and natural disturbances. The U.S. Environmental Protection Agency (EPA) has reported annual carbon fluxes for the United States since 1997 and estimated that U.S. forests sequestered approximately −256 TgC/yr (EPA, 2012). The U.S. Forest Service (USFS) estimated a combined stock of 15,095 TgC in all of the major pools of the Pacific Coast and Rocky Mountain regions for 2005 and that, on average between 2000 and 2008, the forest ecosystems sequestered approximately −43.1 TgC/yr in those two regions (Heath and others, 2011). Hudiburg and others (2011) estimated that the net biome production (NBP) of the forests in the Pacific coastal regions of Washington, Oregon and California averaged −95 $TgCO_{2\text{-}eq}$/yr (−25.9 TgC/yr) between 2001 to 2006. In California, the annual carbon flux for all forests in 2010 was estimated to be −30 $TgCO_{2\text{-}eq}$/yr on the basis of USFS permanent-plot data, forest-growth models, wildland-fire emission estimates, and timber harvest data (California Department of Forestry and Fire Protection, 2010; Robards, 2010). A separate study found that forests and rangelands in California in the 1990s were responsible for a net removal of –7.55 $TgCO_{2\text{-}eq}$ per year from the atmosphere and that agricultural lands were responsible for a net emission of 0.35 $TgCO_{2\text{-}eq}$/yr (S. Brown, Pearson, Dushku, and others, 2004). Citing wildland-fire disturbances and human-induced land-cover changes as two key factors that drive carbon balance in ecosystems of California, J. Liu and others (2011) estimated that California's natural ecosystems were generally carbon neutral from 1951 to 2000 (with an average NBP of −0.3 TgC/yr), even when the balancing effects of carbon dioxide fertilization and climate-induced increases in the length of the growing season were considered. In Oregon and the rest of the Pacific Northwest, the net ecosystem production (NEP) for forests, agricultural lands, woodlands, grasslands, and shrublands was estimated using forest-inventory data, land-use maps, and a process-based model (D.P. Turner, Ritts, and others, 2011). The study concluded that a decline in forest clearcutting (the result of changes in forest-management policies since the 1990s) has had a profound effect on carbon storage and sequestration, resulting in a switch from a carbon source to a carbon sink around 1990. Some recent regional studies of carbon stocks and fluxes are listed in tables 1.1 and 1.2 of chapter 1 of this report.

As noted in chapter 1, conventional carbon and GHG terminology (such as Chapin and others, 2006) was followed in the assessment. Two concepts are most relevant here. The first is the net ecosystem carbon balance (NECB), which is defined as the net rate of carbon-storage change in ecosystems. The second is the NEP, which is defined as the imbalance between the gross primary production and ecosystem respiration, or the difference between the net primary production and heterotrophic respiration. For this assessment, the NECB was calculated as the carbon storage change of an ecosystem over a period of time. For example, the NECB for year t was calculated as the carbon storage in year t-1 minus the carbon storage in year t. Therefore, a negative value for the NECB indicates a carbon accumulation or sequestration in an ecosystem and a positive value indicates a loss of carbon from the ecosystem, which is the opposite suggested by Chapin and others (2006). The negative value indicates a carbon loss in the atmosphere because of carbon sequestration in ecosystems. This convention is consistent with the Great Plains assessment report (Zhu and others, 2011).

5.3. Input Data and Methods

5.3.1. Input Data for Baseline Simulation Modeling

A variety of input data were needed to model the biogeochemical processes related to carbon stocks, carbon fluxes, and GHG fluxes in the Western United States, including data about climate, LULC, soils, elevation, forest types, biomass, land and forest management, and natural disturbances. The treatment of land-management activities and natural disturbances in ecosystems is discussed in detail in chapter 4 of this report. Table 5.1 lists the input data layers that were used to provide the baseline information for the assessment.

Each of the input datasets was obtained from the indicated data source in table 5.1 and converted to standard spatial and temporal resolutions, projection, and data format. Some examples of input data layers (maps) are provided in figure 5.1.

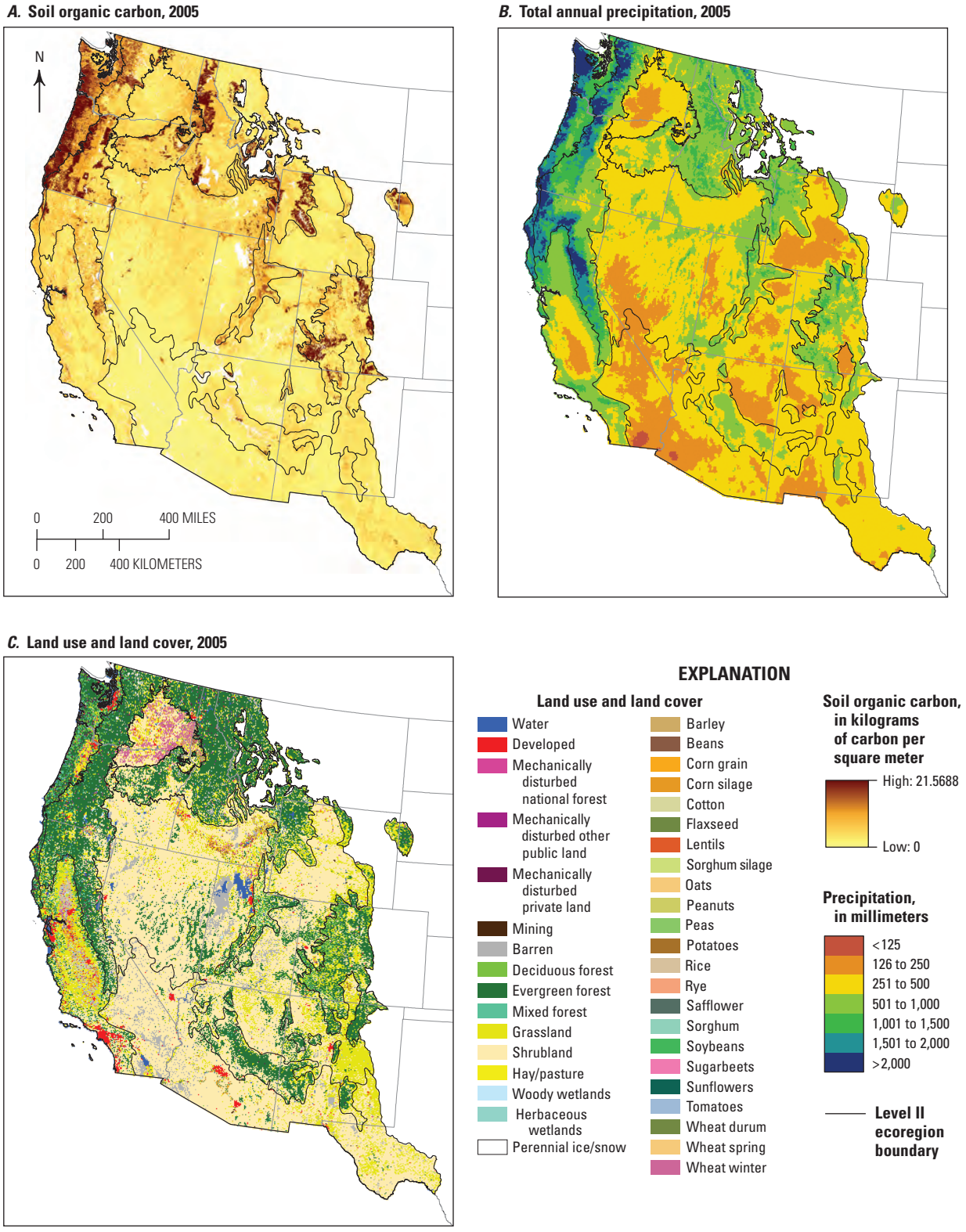

Figure 5.1. Examples of maps showing input data for the Western United States. *A*, Soil organic carbon (SOC) for the top 0 to 5 centimeters of the soil layer; the data were derived from the Soil Survey Geographic (SSURGO) Database (USDA Natural Resources Conservation Service, 2009). *B*, Total annual precipitation in 2005 (PRISM Climate Group, 2012). *C*, Land cover in 2005 from chapter 2 of this report with the agricultural land class downscaled to the crop types (chapter 4 of this report). See figure 1.1 in chapter 1 for ecoregion names.

Table 5.1. Input data used in the baseline-data model runs for the assessment.

[Most of the input data have a 250-m spatial resolution and variable temporal characteristics, although most data cover the first decade of the 21st century. Db 0.33 bar H_2O, the oven-dry weight of the less than 2 mm soil material per unit volume of soil at a water tension of 1/3 bar (as used in the SSURGO database). EDCM, Erosion-Deposition-Carbon Model; FIA, USDA Forest Service's Forest Inventory & Analysis; FIPS, Federal Information Processing Standard; K factor, an erodibility factor that quantifies the susceptibility of soil particles to detachment by water; LP DAAC, Land Processes Active Archive Center; LULC, land use and land cover; mm, millimeter; MODIS, Moderate Resolution Imaging Spectrometer on board NASA's Terra satellite; NASA, National Aeronautics and Space Administration; NPP, net primary productivity; NRCS, USDA's Natural Resources Conservation Service; NTSG, Numerical Terradynamic Simulation Group; PRISM, parameter-elevation regressions on independent slopes model; RPA, U.S. Forest Service Forest and Rangeland Renewable Resources Planning Act of 1974; SSURGO, Soil Survey Geographic Database (NRCS); TPO, timber product output; USDA, U.S. Department of Agriculture]

Data category	Data type	Data source	Model		
			Spreadsheet	EDCM	CENTURY
LULC	LULC classes	Chapter 2 of this report	X	X	
Climate	Monthly minimum and maximum temperature, monthly total precipitation	PRISM Climate Group (2012)		X	X
Soils	Total sand	SSURGO (USDA NRCS, 2009)		X	X
	Total clay			X	X
	Total silt			X	X
	Soil thickness			X	
	Soil organic carbon		X	X	X
	Available water capacity			X	
	Db 0.33 bar H_2O			X	
	K factor				
Forests	Biomass	Geodata (USDA Forest Service, 2012c)	X		
	Stand age	Chapter 2 of this report	X	X	X
	FIA species growth curves, height, diameter, and biomass measurements	USDA FIA (USDA Forest Service, 2012b)	X		
	Timber product output	USDA FIA RPA (USDA Forest Service, 2012b); USDA RPA TPO (USDA Forest Service, 2011)	X		
Crops	Derived crop type	Schmidt and others (2011); Chapter 4 of this report	X	X	X
	USDA crop yield table	USDA National Agricultural Statistics Service (2011)		X	X
	USDA fertilization table	USDA Economic Research Service (2011b)			
	USDA manure table	USDA Economic Research Service (2011a)			
	CTIC tillage table	Conservation Technology Information Center (2011); USDA Economic Research Service (2011a)			
Management	Derived manure	Schmidt and others (2011); Chapter 4 of this report	X	X	X
	Derived tillage	Schmidt and others (2011); Chapter 4 of this report	X	X	X
	Derived fertilizer	Schmidt and others (2011); Chapter 4 of this report	X	X	X
	Irrigation	USGS (2010)	X	X	X

Table 5.1. Input data used in the baseline-data model runs for the assessment.—Continued

[Most of the input data have a 250-m spatial resolution and variable temporal characteristics, although most data cover the first decade of the 21st century. Db 0.33 bar H_2O, the oven-dry weight of the less than 2 mm soil material per unit volume of soil at a water tension of 1/3 bar (as used in the SSURGO database). EDCM, Erosion-Deposition-Carbon Model; FIA, USDA Forest Service's Forest Inventory & Analysis; FIPS, Federal Information Processing Standard; K factor, an erodibility factor that quantifies the susceptibility of soil particles to detachment by water; LP DAAC, Land Processes Active Archive Center; LULC, land use and land cover; mm, millimeter; MODIS, Moderate Resolution Imaging Spectrometer on board NASA's Terra satellite; NASA, National Aeronautics and Space Administration; NPP, net primary productivity; NRCS, USDA's Natural Resources Conservation Service; NTSG, Numerical Terradynamic Simulation Group; PRISM, parameter-elevation regressions on independent slopes model; RPA, U.S. Forest Service Forest and Rangeland Renewable Resources Planning Act of 1974; SSURGO, Soil Survey Geographic Database (NRCS); TPO, timber product output; USDA, U.S. Department of Agriculture]

Data category	Data type	Data source	Model		
			Spreadsheet	EDCM	CENTURY
Elevation	Elevation	USGS (2012b)			
Remote sensing	NPP	M. Zhao and others (2005)		X	X
Wildland fires	Fire size, severity, combustion emissions	Eidenshink and others (2007); Chapter 3 of this report		X	X
Reference information	State and county FIPS codes	U.S. Census Bureau (2012)	X	X	X
Initial conditions	Forest litter biomass	Chapter 5 of this report		X	X
	Aboveground live biomass	Chapter 5 of this report		X	X
	Belowground live biomass	Chapter 5 of this report		X	X
	Deadwood biomass	Chapter 5 of this report		X	X
	Standing wood biomass	Chapter 5 of this report		X	X

5.3.2. The General Ensemble Biogeochemical Modeling System

The General Ensemble Biogeochemical Modeling System (GEMS) (S. Liu and others, 2012) was developed to integrate the well-established biogeochemical models for ecosystems with various spatial databases in order to simulate biogeochemical cycles over large areas. Figure 5.2 shows the overall structure of the GEMS. Some of the key features of the GEMS are described below.

5.3.3. Using the Biogeochemical Model Ensemble to Address Model Biases

All models are imperfect and have simulation biases and errors. As an example, comparison studies by the North American Carbon Program of major biogeochemical models yielded variable estimates of carbon stocks and fluxes (Schwalm and others, 2010; Huntzinger and others, 2012). To minimize biases and errors in the individual models and to quantify the uncertainty of the model outputs, multiple site scale biogeochemical models were encapsulated into the GEMS and used simultaneously to simulate ecosystem dynamics over time and space.

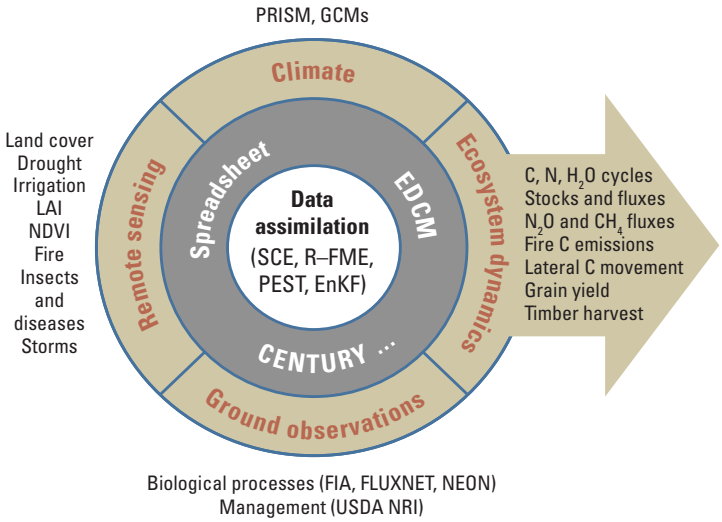

Figure 5.2. Diagram of the General Ensemble Modeling System (GEMS) showing (1) the inputs (climate, remote sensing, and ground observations) and outputs (ecosystem dynamics), (2) the underlying biogeochemical models (spreadsheet, EDCM, and CENTURY), and (3) the data assimilation procedures. Abbreviations are as follows: C, carbon; CH_4, methane; EDCM, Erosion-Deposition-Carbon Model; EnKF, Ensemble Kalman Filter; FIA, U.S. Forest Service's Forest Inventory & Analysis Program; FLUXNET, flux network; GCM, General Circulation Model; H_2O, water; LAI, leaf area index; N, nitrogen; N_2O, nitrous oxide; NDVI, Normalized Difference Vegetation Index; NEON, National Ecological Observatory Network; NRI, Natural Resource Conservation Service's National Resources Inventory; PEST, model independent parameter estimation application; PRISM, parameter-elevation regressions on independent slopes model; R–FME, R Flexible Modeling Environment; SCE, Shuffled Complex Evolution; USDA, U.S. Department of Agriculture.

For this assessment, the CENTURY model (Parton and others, 1987; Parton and others, 1994), the Erosion-Deposition-Carbon Model (EDCM, S. Liu and others, 2003), and a spreadsheet model were incorporated into the GEMS to simulate dynamics of carbon stocks, carbon fluxes, and fluxes of the GHG. These three models were already linked to the GEMS for the assessment of the Great Plains (Zhu and others, 2011).

Two modifications were made to the CENTURY model for the assessment. First, the model's data input and output interface was modified and linked to the GEMS system by using a static FORTRAN library with shared memory to increase the efficiency of the computations. The change did not affect the format of the input and output data for the model. Second, the regional-level NPP and grain-yield calibration process (see section entitled "Calibration of the Model," below) were modified.

Improved modeling of water availability is critical for the predictions of ecosystem productivity and soil organic matter decay because both processes are strongly controlled by soil moisture. The EDCM, which was modified from the CENTURY model, used up to 10 soil layers in a soil profile, compared to the CENTURY model, which used one layer for SOC simulations. In the EDCM, the thickness of the surface soil layer was fixed at the plowing depth of either 20 or 30 cm, whereas the thicknesses of other layers were flexible. The thickness and SOC dynamics of each of the layers were then simulated by modeling the interactions of erosion or deposition, forest-litter input, decomposition, and leaching (Liu and others, 2000; S. Liu and others, 2003). The five SOC pools (metabolic, structural, fast, slow, and passive) in each soil layer were used in the EDCM to characterize the quantity and quality of the SOC, which was similar to the structure for the surface soil depth in the CENTURY model (Parton and others, 1987; Metherell and others, 1993; Parton and others, 1993).

The spreadsheet model (described in Zhu and others, 2010) was developed for this assessment and is based on a simple accounting approach. For SOC, 10 soil layers from the Soil Survey Geographic Database (SSURGO; USDA Natural Resources Conservation Service, 2009) (Sundquist and others, 2009) were used to represent the SOC at each location or pixel. Simplicity in the spreadsheet model was maintained by keeping the SOC unchanged after the model was initialized. For biomass carbon, the grassland/shrubland and agricultural biomass pools were held as constants, whereas the forests biomass pools (including aboveground and belowground live biomass, standing wood, deadwood, forest litter, and other carbon pools) were assigned as a function of forest types (evergreen, broadleaf, and mixed forest) and forest age (both from the LULC modeling described in chapter 2 of this report), as well as the forest age-carbon stock relation. The forest age-carbon stock relation is a set of growth curves specific for forest types (such as softwood, hardwood, and mixed) and FIA units. Derived from FIA inventory data, the relation describes quantitatively the amount of biomass carbon as a function of average forest age. Each forest type has a distinct forest age-carbon stock relation unless the number of FIA plots was not large enough to derive such a relation. In this case, a representative regional forest age-carbon stock relation was used.

On the basis of the forest age-carbon stock relation (growth curve) discussed above and the LULC maps, the effects of either forest aging or clearcutting were quantified in the spreadsheet model. The spreadsheet model, however, was not intended to quantify the effects of climate variability and change or of carbon-dioxide fertilization on carbon. The algorithms for estimating wildland-fire emissions were not implemented in the spreadsheet model for this assessment. Following a recommendation by the Intergovernmental Panel on Climate Change, the spreadsheet model estimated methane and nitrous-oxide fluxes for different LULC classes using emission factors that were compiled from an extensive review of the literature (Mosier and others, 1997; Kessavalou and others, 1998; Gleason and others, 2007; Sainju, 2008; Liebig and others, 2010). Emission factors were compiled and synthesized by ecosystem type and ecoregion for this assessment.

Although the biogeochemical models in the GEMS have different output variables, their common output variables include gross and net primary productivity (GPP, NPP), autotrophic and heterotrophic respiration, grain production, and carbon stock estimates over time in vegetation and soil pools for terrestrial ecosystems.

5.3.4. Model Initializations

The following soil properties were initialized on the basis of data from the SSURGO database (USDA Natural Resources Conservation Service, 2009): soil thickness, organic carbon storage, texture (fractions of sand, silt, and clay), bulk density, and drainage. Forest biomass carbon pools (aboveground and belowground live biomass, or dead biomass consisting of forest litter and dead, woody debris) were initialized using the initial forest-age map (derived from FIA data; USDA Forest Service, 2012b), forest type (evergreen, broadleaf, and mixed), and the forest age-carbon stock relation. For consistency and to avoid potential errors, the initialization of the SOC and biomass was done using the spreadsheet model, and its outputs for 1992 (the first year of the model simulations) were then read directly by the CENTURY model and the EDCM as their initial conditions. The years from 1992 to 2000 were used as a period of calibrations to achieve relative stabilization (that is, model spin-up) for the EDCM and CENTURY simulations.

5.3.5. Model Calibration

Models usually contain parameters that (1) cannot be determined by using local field measurements or (2) can be measured locally but cannot be used regionally because of the effects of the scale of the measurements. Models are calibrated by adjusting such model parameters to optimize the agreement between observation and simulation. The observed data available for calibrating carbon-flux model runs from 2001 to 2005 included (1) county-based grain-yield-survey data by crop type, published by the USDA (USDA, National Agricultural Statistics Service, 2011); and (2) 250-m resolution NPP data from the MODIS for other LULC types such as forests and grasslands (Zhao and others, 2005). The MODIS NPP was found to lack consistent performance for calibrating crop production on agricultural lands and, therefore, crop yields from the USDA were used. An automated calibration was implemented for the EDCM using the Shuffled Complex Evolution (SCE) (Duan and others, 1992) and an R software package, Flexible Modeling Environment (R–FME) (Soetaert and Petzoldt, 2010; Wu and Liu, 2012). On the other hand, manual calibration was used for the CENTURY model. The potential maximum production parameter (PRDX) was adjusted by comparing the modeled grain yield and the forest NPP with the USDA's county-level statistics of grain yield and county-level, MODIS-derived NPP from 2001 to 2005.

5.3.6. Model Validation

Maps, binned scatterplots, and correlation plots were generated for different ecosystems in each ecoregion of the Western United States in order to compare the simulated results of the three models run within the GEMS with observational data (for example, the USDA FIA biomass estimate, an estimate from the National Biomass and Carbon Dataset 2000 (Kellndorfer and others, 2004), the MODIS-derived NPP (Zhao and others, 2005), and the USDA grain yield (USDA, National Agricultural Statistics Service, 2011) for 2006, 2008, and 2010. Simple linear-regression modeling, the coefficient of determination, and the root mean square error (RMSE) between the observed and modeled data were calculated to evaluate the performance of the models. Some of the results of the validation are shown in figure 5.3 and table 5.2.

5.3.7. Model Run Setup

The simulation models were run for every year from 1992 to 2050, with the years 1992 to 2000 used as model spin-up, 2001 to 2005 used as the baseline period (this chapter), and 2006 to 2050 as the projection period (chapter 9). A total of three GEMS simulations (by the spreadsheet model, CENTURY model, and the EDCM) were used to support the assessment of carbon dynamics during the baseline period. As noted previously, the purpose of using multiple models was to minimize the potential biases and errors that were inherent in the models and to provide an opportunity to quantify structure-related uncertainties in the models.

Before the full-resolution or wall-to-wall simulations were run to produce spatial data products for this assessment, a systematic sampling approach was used first to improve the performance of the model simulations. Both the EDCM and the CENTURY model were run with a 10×10 systematic subsample factor to ensure adequate time for processing, generating statistics, and calibrating the estimates. Therefore, for these two models, the results reported here were based on a systematic sample of 1 percent of the total pixels. A comparison of the sampling results with the full-resolution simulations indicated that the sampling approach provided the same regional statistics as the full-resolution simulation.

Table 5.2. Comparison of the three different biogeochemical models in the General Ensemble Modeling System (GEMS) based on aggregated results at the county level, for 2006.

[MODIS NPP, net primary productivity derived from the Moderate Resolution Imaging Spectroradiometer; NBCD, National Biomass and Carbon Dataset (Kellndorfer and others, 2004); USDA FS, U.S. Forest Service; R^2, coefficient of determination; RMSE, root mean squared error; USDA U.S. Department of Agriculture].

Observation	Model	Land use or land cover	RMSE	R^2
NBCD live biomass	Spreadsheet	Forests	7.312	0.61
USDA FS live biomass	Spreadsheet	Forests	4.376	0.90
MODIS NPP	CENTURY	Forests	0.216	0.95
MODIS NPP	EDCM	Forests	0.167	0.98
MODIS NPP	CENTURY	Grasslands/shrublands	0.100	0.74
MODIS NPP	EDCM	Grasslands/shrublands	0.038	0.96
USDA grain yield	CENTURY	Winter wheat	0.003	0.97
USDA grain yield	EDCM	Winter wheat	0.005	0.94

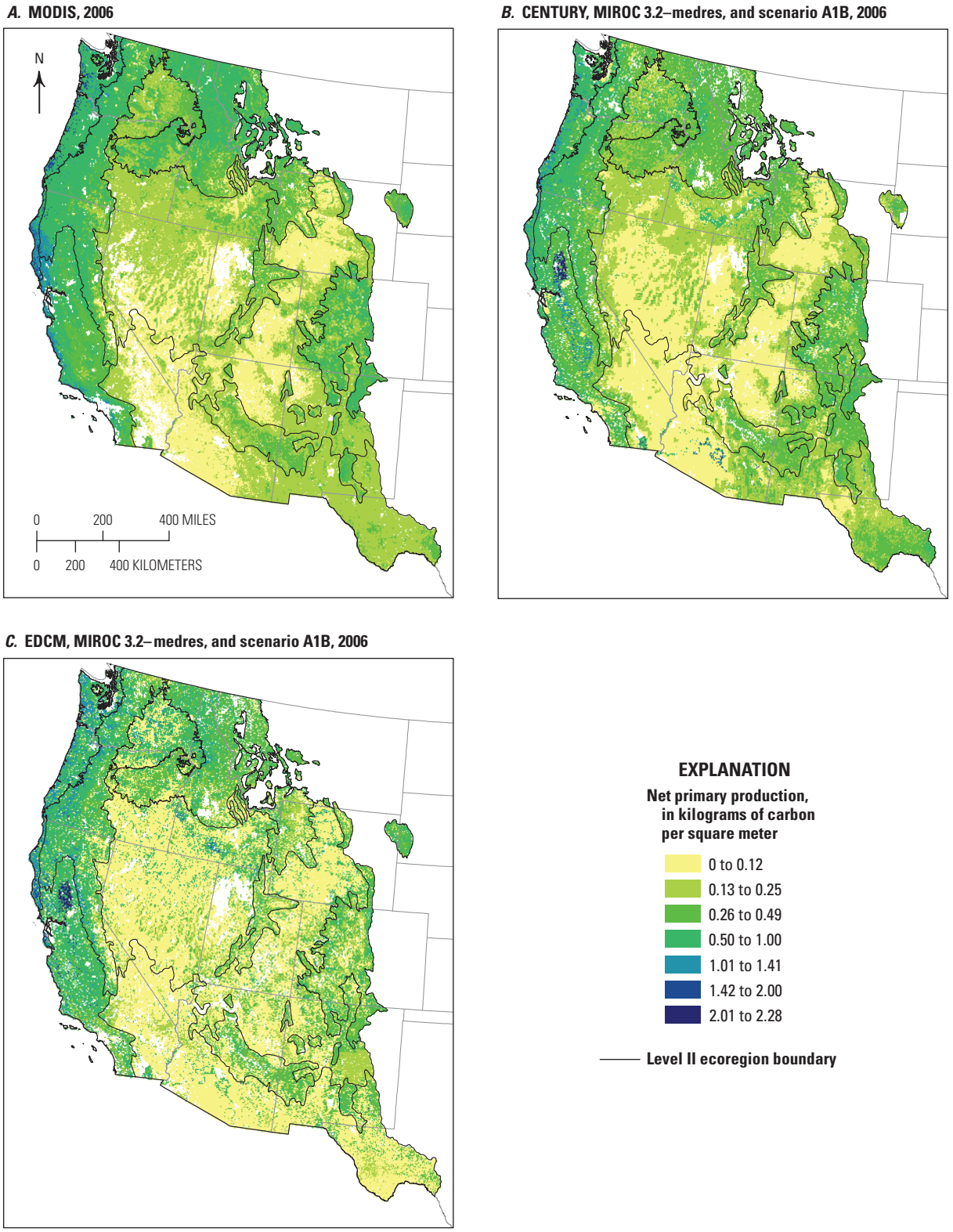

Figure 5.3. Maps showing a comparison of net primary productivity (NPP) in the Western United States for 2006 estimated by three different methods and tools . *A*, Data from the Moderate Resolution Imaging Spectroradiometer (MODIS). *B*, The CENTURY model run under IPCC–SRES scenario A1B and using the MIROC 3.2-medres general circulation model. *C*, The Erosion-Deposition-Carbon Model (EDCM) run under IPCC–SRES scenario A1B and using the MIROC 3.2-medres general circulation model. IPCC–SRES, Intergovernmental Panel on Climate Change Special Report on Emissions Scenarios (Nakicenovic and others, 2000). MIROC 3.2-medres, Model for Interdisciplinary Research on Climate version 3.2, medium resolution. See figure 1.1 in chapter 1 for ecoregion names.

5.4. Results and Discussion

5.4.1. Carbon Stocks in 2005

The magnitude and spatial pattern of the carbon stock estimated from 2001 to 2005 remained relatively stable, therefore the estimates for 2005 are presented here. The map in figure 5.4*A* shows the spatial distribution of the mean amount of carbon stored (based on the average of three carbon-stock maps from the three models) in all of the ecosystems of the Western United States in 2005, and the standard deviation of the results, which indicates a measure of uncertainty. The total carbon stored included carbon in live biomass, SOC in the top 20 cm of the soil layer, and dead biomass. The map indicates that forests in the Marine West Coast Forest and Western Cordillera ecoregions stored the most carbon, whereas there was relatively less carbon stored in the grasslands/shrublands-dominated Cold Deserts and Warm Deserts ecoregions and in the mixed agricultural lands, grasslands/shrublands, and forests of the Mediterranean California ecoregion. The standard deviation of the estimates of the three models was generally higher in the coastal forests and in the Cascades, which is likely the result of the high biomass levels and logging rates. The uncertainties in the carbon stock were lower in the interior forests, where the biomass levels and logging rates were lower. The uncertainties were also lower in landscapes dominated by grasslands/shrublands.

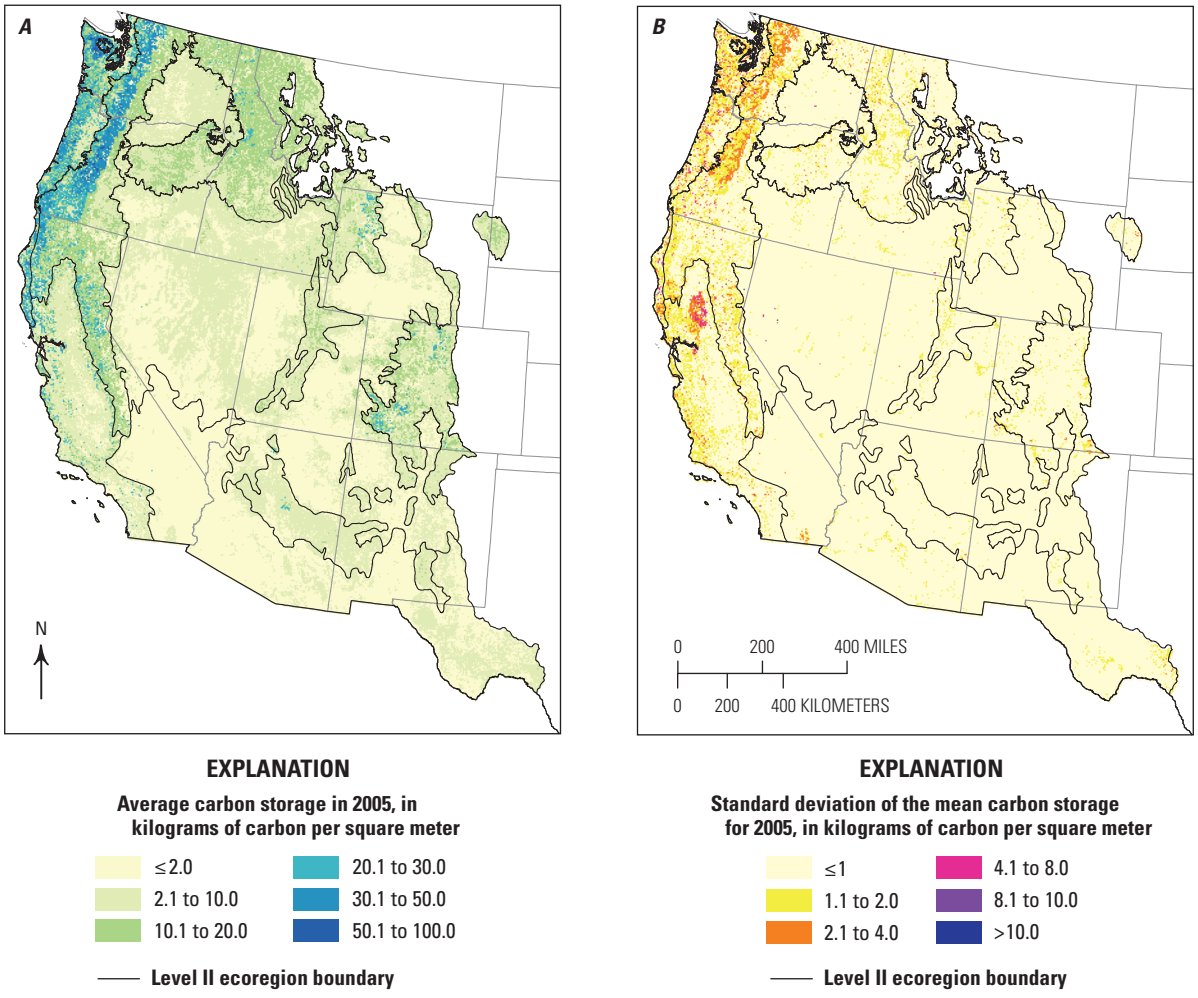

Figure 5.4. Maps showing the mean amount of carbon stored and the standard deviation for 2005. *A*, The estimated mean amount of carbon stored in 2005, which was derived by averaging the results from the three General Ensemble Modeling System (GEMS) models (spreadsheet, CENTURY, and EDCM). *B*, The standard deviation of the three modeling results around the mean. EDCM, Erosion-Deposition-Carbon Model. See figure 1.1 in chapter 1 for ecoregion names.

Annual maps of estimated carbon stocks by the terrestrial ecosystems and ecoregions from 2001 to 2005 were produced using the three models, as previously described. At the regional scale, temporal variability remained relatively small between the years. Table 5.3 gives the range (minimum to maximum) of the estimated amounts of carbon stored as simulated by the three models (spreadsheet, EDCM, and CENTURY) for 2005, the last year of the baseline conditions. During 2005, the average total amount of carbon stored in the entire Western United States was estimated to be 13,920 TgC (ranging from 12,418 to 15,461 TgC). The estimates for the Western United States are about 8 percent lower than a previously published estimate of 15,095 TgC for all major carbon pools in the Pacific Coast and Rocky Mountain regions in 2005 (J.E. Smith and Heath, 2008). Among all the ecoregions, the Western Cordillera stored the most carbon at over 8,162 TgC (59 percent), followed by the Cold Deserts (19 percent), the Marine West Coast Forest (11 percent), Mediterranean California (6 percent), and the Warm Deserts (5 percent). Live biomass, SOC, and dead biomass accounted for 39.0 percent, 38.3 percent, and 22.7 percent, respectively, of the total carbon stored in the Western United States. In terms of ecosystems, forests, grasslands/shrublands, and agricultural lands stored 69 percent, 25 percent, and 4.3 percent, respectively, of the total carbon. Among the different ecosystems, forests stored the most carbon in the Western Cordillera, Marine West Coast Forest, and Mediterranean California ecoregions; grasslands/shrublands stored the most carbon in the Cold Deserts and Warm Deserts ecoregions.

Using table 5.3, the carbon density (that is, the amount of carbon stored per unit of area) could be derived by ecosystem and ecoregion. Forests stored the most carbon in the Marine West Coast Forest (21.9 kgC/m^2), followed by Mediterranean California (14.9 kgC/m^2), the Western Cordillera (13.0 kgC/m^2), the Cold Deserts (6.7 kgC/m^2), and the Warm Deserts (5.2 kgC/m^2). The ecoregions that had highest and lowest carbon densities in grasslands/shrublands were the Marine West Coast Forest at 6.6 kgC/m^2 and the Warm Deserts at 1.5 kgC/m^2, respectively. Although agricultural lands covered only a small percentage of the Western United States, most of this ecosystem stored more carbon than grasslands/shrublands. For example, in the Western Cordillera ecoregion, the carbon density in the top 20 cm of soil for forests, grasslands/shrublands, and agricultural lands was 3.3, 2.4, and 3.9 kgC/m^2, respectively. Further results for each ecoregion are provided below.

5.4.1.1. Western Cordillera

The Western Cordillera is the second largest ecoregion in the Western United States. In 2005, the average total amount of carbon stored in this ecoregion was estimated to be 8,163 TgC (ranging from 7,488 to 8,793 TgC), of which an average of 43 percent was in live biomass, 32 percent in soil, and 25 percent in dead biomass. Among the different ecosystems, forests occupied 63 percent of the total land area and stored an average of 87 percent of the total carbon stock (7,123 TgC or 13.0 kgC/m^2). Grasslands/shrublands occupied 32 percent of the total land area but only stored an average of 11 percent of the total carbon stock (923 TgC, or 3.3 kgC/m^2). Agricultural lands occupied a small area of the ecoregion (2 percent) and stored only an average of 1 percent of the total carbon stock (72 TgC, or 4.3 kgC/m^2).

5.4.1.2. Marine West Coast Forest

In 2005, the average total amount of carbon stored in the Marine West Coast Forest was estimated to be 1,534 TgC (ranging from 1,447 to 1,646 TgC), of which an average of 48 percent was in live biomass, 33 percent in soil, and 19 percent in dead biomass. Forests stored the most carbon in the ecoregion (an average of 1,415 TgC, 92 percent of the total), followed by agricultural lands (an average of 67 TgC, 4 percent of the total) and grasslands/shrublands (an average of 30 TgC, 2 percent of the total). This small coastal ecoregion had the highest percentage of its total land area covered by forests (68 percent) and those forests had the highest average carbon density (21.9 kgC/m^2) of any forests in the five ecoregions. The carbon densities in grasslands/shrublands (6.6 kgC/m^2) and agricultural lands (6.4 kgC/m^2) were also higher than the carbon densities in the same ecosystems in the other ecoregions.

5.4.1.3. Cold Deserts

The Cold Deserts ecoregion is the largest in the Western United States and was dominated by the grasslands/shrublands ecosystem (76 percent of the total land area). In 2005, the average total amount of carbon stored in this ecoregion was estimated to be 2,651 TgC (ranging from 2,267 to 3,124 TgC), of which an average of 23 percent was in live biomass, 58 percent in soil, and 18 percent in dead biomass. The grasslands/shrublands stored the most carbon in the ecoregion (an average of 1,672 TgC, 63 percent of the total), followed by forests (an average of 647 TgC, 23 percent of the total) and agricultural lands (an average of 282 TgC, 18 percent of the total). The average total carbon density in this ecoregion was 2.5 kgC/m^2, which was lower than that of the Western Cordillera (9.4 kgC/m^2) and the Marine West Coast Forest (16.1 kgC/m^2).

5.4.1.4. Warm Deserts

The vegetation in the extremely arid Warm Deserts ecoregion was also dominated by the grasslands/shrublands ecosystem (87 percent of total land area). In 2005, the average total carbon stored in this ecoregion was estimated to be only 700 TgC (ranging from 525 to 921 TgC), of which 26 percent

Table 5.3. Minimum and maximum estimates of carbon stored in the Western United States in 2005, by carbon pool for each ecoregion and ecosystem.

[Only soil organic carbon (SOC) in the top 20 cm of the soil layer was calculated. km^2, square kilometers; max, maximum; min, minimum; TgC, teragrams of carbon or 10^{12} grams of carbon].

Ecoregion	Ecosystem	Area (km^2)	Live biomass (TgC)		Soil (TgC)		Dead biomass (TgC)		Total (TgC)	
			Min	Max	Min	Max	Min	Max	Min	Max
Western Cordillera	Forests	546,533	3,304.6	3,689.4	1,599.5	1,887.7	1,398.0	2,348.2	6,648.2	7,557.6
	Grasslands/shrublands	277,874	71.5	148.6	629.1	718.9	0.0	222.5	745.8	1,090.0
	Agricultural lands	16,722	0.1	2.4	64.4	65.3	0.0	8.1	67.7	72.6
	Wetlands	3,656	4.7	5.2	13.8	18.4	2.4	5.7	23.2	28.8
	Other lands	27,469	0.2	0.4	1.9	43.9	0.0	0.7	2.9	44.1
	Total	872,253	3,381.1	3,846.0	2,308.7	2,734.2	1,400.4	2,585.2	7,487.7	8,793.1
Marine West Coast Forest	Forests	64,601	696.0	829.8	398.7	416.4	235.8	336.2	1,347.6	1,510.5
	Grasslands/shrublands	4,542	1.7	4.0	19.1	23.4	0.0	6.0	20.7	32.7
	Agricultural lands	10,418	0.1	1.5	61.1	64.6	0.0	6.0	65.9	67.2
	Wetlands	588	2.3	2.8	3.0	3.8	0.4	1.0	5.6	7.1
	Other lands	15,262	0.0	1.0	4.0	28.4	0.0	2.2	7.0	28.4
	Total	95,411	700.1	839.0	485.8	536.6	236.2	351.5	1,446.9	1,645.9
Cold Deserts	Forests	97,180	269.4	293.6	179.6	213.5	131.7	222.2	638.8	685.1
	Grasslands/shrublands	804,658	275.1	371.8	960.1	1,191.0	0.0	519.6	1,370.9	2,066.1
	Agricultural lands	81,191	0.1	12.9	222.0	254.3	0.0	41.9	234.9	296.3
	Wetlands	4,635	2.6	3.7	14.9	20.0	1.9	5.3	21.0	27.9
	Other lands	68,392	0.0	0.3	2.7	49.0	0.0	0.3	3.0	49.0
	Total	1,056,055	547.2	682.4	1,379.3	1,727.9	133.6	789.4	2,268.6	3,124.4
Warm Deserts	Forests	8,084	20.1	22.7	7.3	10.4	8.7	19.8	39.9	49.8
	Grasslands/shrublands	403,390	120.4	193.5	300.3	418.1	0.0	204.1	470.7	815.7
	Agricultural lands	11,334	0.0	2.0	10.7	25.4	0.0	8.6	12.6	35.5
	Wetlands	326	0.2	0.3	0.3	0.5	0.0	0.6	0.5	1.1
	Other lands	42,150	0.0	0.2	0.8	18.4	0.0	0.2	0.9	18.9
	Total	465,285	140.6	218.6	319.4	472.8	8.8	233.3	524.6	921.0
Mediterranean California	Forests	29,945	250.9	296.0	56.9	85.7	88.3	119.0	424.9	469.8
	Grasslands/shrublands	74,294	28.1	37.2	125.9	179.9	0.0	62.9	154.0	279.8
	Agricultural lands	41,046	0.0	7.4	94.2	146.6	0	35.1	101.6	188.4
	Wetlands	910	0.5	0.9	4.4	5.0	0.4	1.5	5.8	7.0
	Other lands	23,259	0.0	0.4	3.9	31.2	0.0	0.3	4.3	31.2
	Total	169,455	279.5	341.8	285.3	448.4	88.7	218.8	690.5	976.3
Western United States (total)	Forests	746,343	4,541.0	5,131.4	2,242.0	2,613.8	1,862.6	3,045.5	9,099.4	10,272.8
	Grasslands/shrublands	1,564,759	496.7	755.0	2,034.4	2,531.2	0.0	1,015.1	2,762.0	4,284.2
	Agricultural lands	160,711	0.3	26.1	452.4	556.2	0.0	99.7	482.7	660.0
	Wetlands	10,114	10.2	12.8	36.3	47.7	5.1	14.1	56.1	71.9
	Other lands	176,532	0.2	2.4	13.4	171.0	0.0	3.8	18.1	171.7
	Total	2,658,459	5,048.5	5,927.8	4,778.5	5,919.9	1,867.7	4,178.2	12,418.3	15,460.6

was in live biomass, 56 percent in soil, and 18 percent in dead biomass. The grasslands/shrublands stored the most carbon in the ecoregion (623 TgC, an average of 89 percent of total), followed by forests (42 TgC, an average of 6 percent of total) and agricultural lands (24 TgC, an average of 3 percent of total). The carbon densities were the lowest among all of the ecoregions (5.1, 1.5, and 2.1 kgC/m^2 for forests, grasslands/shrublands, and agricultural lands, respectively).

5.4.1.5. Mediterranean California

In 2005, the Mediterranean California ecoregion stored an estimated average total carbon stock of 873 TgC (ranging from 691 to 976 TgC), of which 34 percent was in live biomass, 45 percent was in soil, and 20 percent was in dead biomass. Forests stored half of the total carbon stock (448 TgC, an average of 51 percent of total), followed by grasslands/shrublands (246 TgC, an average of 28 percent of total) and agricultural lands (157 TgC, an average of 18 percent of total). The percentage of agricultural land in this ecoregion was high compared to the other ecoregions in the Western United States. The estimated carbon densities were approximately 15.0, 3.3, and 3.8 kgC/m^2 for forests, grasslands/shrublands, and agricultural lands, respectively).

5.4.1.6. Discussion of Baseline Carbon Storage

For the five western ecoregions in 2005, the estimated average amount of carbon stored in 74.6 megahectares (Mha) of forest ecosystems, as mapped and modeled using the assessment methodology, was approximately 9,675 TgC (ranging from 9,099 to 10,273 TgC), distributed in live biomass (4,674 TgC, ranging from 4,541 to 5,131 TgC), the top 20 cm of the soil (SOC; 2,503 TgC, ranging from 2,242 to 2,614 TgC), and dead biomass (2,498 TgC, ranging from 1,863 to 3,046 TgC). The average per-unit-of-area forest carbon stock density estimates were derived from the total forest carbon stock and total forest area estimates and ranged from 12.2 to 13.8 kgC/m^2 with a mean of 13.0 kgC/m^2. As a comparison, a separate analysis using the USFS FIA carbon stock and forest area estimates (Brad Smith, USDA Forest Service, unpub. data, 2010) suggested a total carbon stock of 13,579 TgC in 93.6 Mha of forested area (or an average of 14.5 kgC/m^2) in the same five ecoregions. The differences in estimates of the total carbon stock and stock density between the two studies may be primarily attributed to (1) the different amount of area that was categorized as forest, which was derived on the basis of different forest definitions and mapping or modeling approaches (Nelson and Vissage, 2005; chapter 2 of this report) and (2) the fact that only carbon in the top 20 cm of the soil layer was modeled as SOC in this assessment, compared to the FIA SOC estimate, which was based on the top 1 m of the soil layer.

5.4.2. Baseline Carbon Flux from 2001 to 2005

The magnitude and spatial distribution of the mean net carbon fluxes across the Western United States are shown in figure 5.5, which indicates that the forested regions of the Pacific Coast gained the most carbon. The standard deviations were generally positively correlated with carbon gains, as expected.

Table 5.4 gives the range (minimum and maximum) of the net carbon flux in the Western United States from 2001 to 2005 by ecoregion, ecosystem, and carbon pool (live biomass, soil, and dead biomass). The estimated overall carbon-sequestration rate ranged from −162.9 to −13.6 TgC/yr with an average of −86.6 TgC/yr, of which −27.6 TgC/yr may be attributed to live biomass accumulation and −58.9 TgC/yr to the dead biomass and soil carbon pools. The forest ecosystem was the largest carbon sink (62 percent of the total), followed by grasslands/shrublands (30 percent) and agricultural lands (7 percent). In forests, the major portion of sequestered carbon was allocated to live biomass. In grasslands/shrublands and agricultural lands, carbon accumulated mainly in soil and dead biomass.

On a per-unit-of-area basis, the estimated average carbon net flux by forests, grasslands/shrublands, and agricultural lands was −72, −16, and −38 gC/m^2/yr, respectively, from all carbon pools. Of these estimates, the soil carbon pool was responsible for –23, –10, and –26 gC/m^2/yr, respectively for the ecosystems. The gain by soil in agricultural lands was higher than the gain by soil in grasslands/shrublands. Two possible reasons for the higher gain by soil in agricultural lands are increased biomass productivity due to genetically improved seeds and improved management practices including fertilizer and (or) irrigation, which may have lead to the overall higher yield of biomass than in the grasslands/shrublands. Although both the Western Cordillera and the Cold Deserts ecoregions were considered to be carbon sinks from 2001 to 2005, the grasslands/shrublands in these two ecoregions were estimated to have lost carbon in the live biomass at an average estimated rate of 0.23 and 3.82 TgC/yr, respectively. Further descriptions of the net carbon fluxes for each ecoregion are provided below.

5.4.2.1. Western Cordillera

From 2001 to 2005, the average estimated net carbon flux in the Western Cordillera was −50 TgC/yr (ranging from −86.1 to −19.1 TgC/yr), of which 48 percent was allocated to live biomass, 37 percent to soil, and 15 percent to dead biomass. Among the different ecosystems, forests sequestered an estimated average of −43 TgC/yr (85 percent of total), grasslands/shrublands sequestered an estimated average of −7 TgC/yr (14 percent of total), and agricultural lands sequestered an estimated average of –0.22 TgC/yr (less than 1 percent of total).

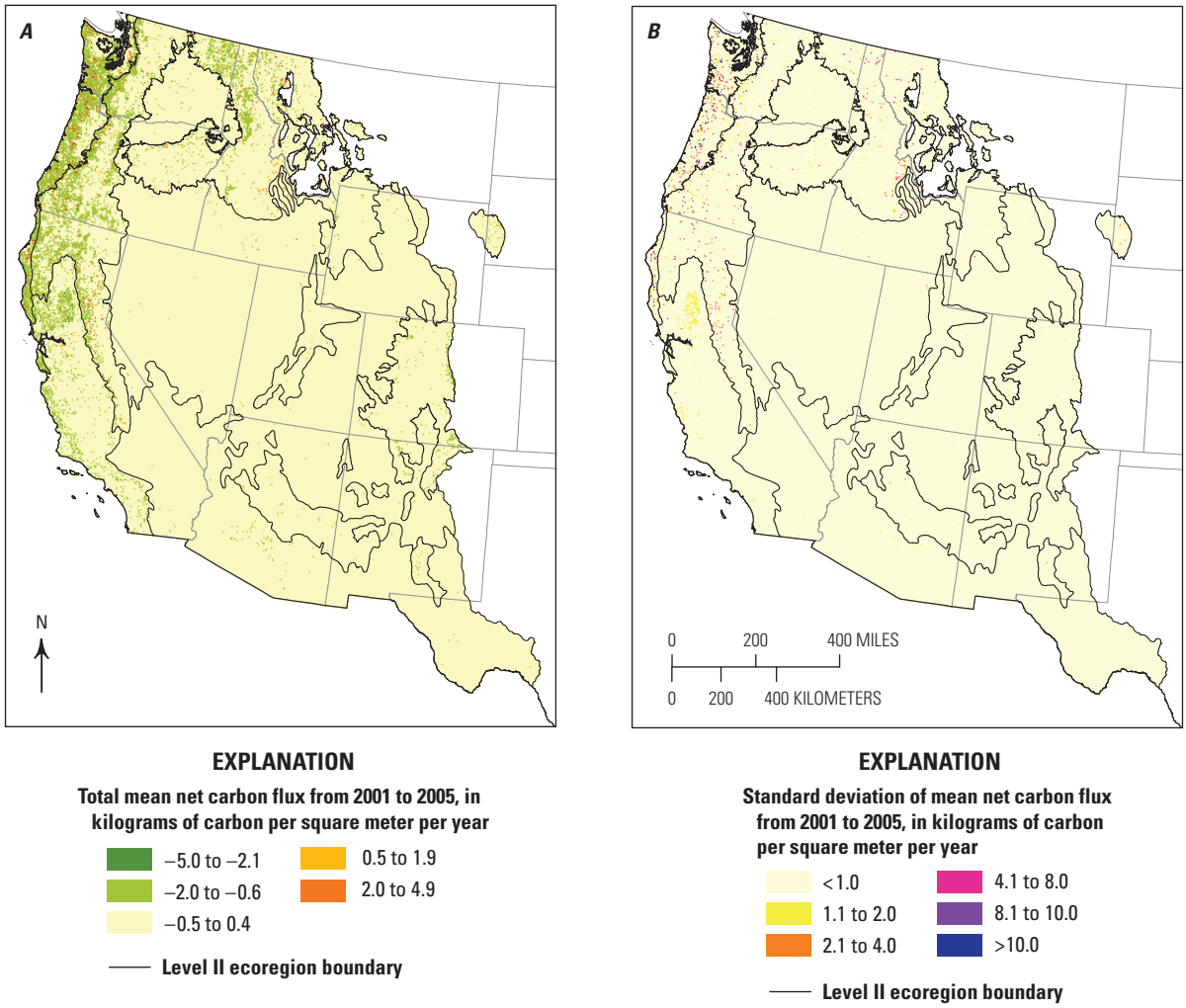

Figure 5.5. Maps showing carbon flux in ecosystems of the Western United States. *A*, The mean net carbon flux derived from each of the three models (spreadsheet, CENTURY, and EDCM) and averaged for the baseline years, 2001 to 2005. *B*, The standard deviation of the three models for the baseline years. Negative values indicate net carbon gains and positive values indicate net carbon losses. EDCM, Erosion-Deposition-Carbon Model. See figure 1.1 in chapter 1 for ecoregion names.

5.4.2.2. Marine West Coast Forest

From 2001 to 2005, the estimated average net carbon flux in the Marine West Coast Forest was −3.8 TgC/yr (ranging from −6.9 to −1.0 TgC/yr). Forests sequestered an estimated average of −3.4 TgC/yr, followed by grasslands/shrublands at an estimated average of −0.5 TgC/yr. Agricultural lands lost carbon to the atmosphere at a low estimated average rate of 0.04 TgC/yr, mostly from soil organic matter.

5.4.2.3. Cold Deserts

From 2001 to 2005, the estimated average net carbon flux in the Cold Deserts ecoregion was −12.3 TgC/yr (ranging from −32.6 to 5.7 TgC/yr). In forests, live biomass and soil sequestered carbon (estimated average rate of −3.72 TgC/yr) but dead biomass lost carbon (estimated average rate of 0.77 TgC/yr). Conversely, live biomass in grasslands/shrublands lost carbon (estimated average rate of 3.82 TgC/yr) but soil and dead biomass sequestered carbon (estimated average rate of −11.1 TgC/yr). Agricultural lands sequestered carbon at an estimated average rate of −1.82 TgC/yr.

5.4.2.4. Warm Deserts

The Warm Deserts ecoregion was dominated by grasslands/shrublands (87 percent of total land area). From 2001 to 2005, the estimated average net carbon flux was −6.8 TgC/yr (ranging from −18.6 to 2.9 TgC/yr); carbon sequestration occurred mainly in the grasslands/shrublands ecosystem. Agricultural lands also sequestered an estimated average of −0.84 TgC/yr while forests only gained carbon at −0.18 TgC/yr.

Table 5.4. Minimum and maximum estimates of net carbon flux in the Western United States from 2001 to 2005, by carbon pool for each ecoregion and ecosystem.

[Negative numbers indicate carbon sequestration; positive numbers indicate a loss of carbon to the atmosphere. Only soil organic carbon (SOC) in the top 20 cm of the soil layer was calculated. km^2, square kilometers; max, maximum; min, minimum; TgC/yr, teragrams of carbon per year, or 10^{12} grams of carbon per year]

Ecoregion	Ecosystem	Area (km^2)	Net carbon flux (TgC/yr)							
			Live biomass		Soil		Dead biomass		Total	
			Min	Max	Min	Max	Min	Max	Min	Max
Western Cordillera	Forests	546,533	−29.7	−16.5	−21.7	0	−18.9	9.4	−70.3	−19.6
	Grasslands/shrublands	277,874	−0.5	1.1	−7.7	0.2	−6.4	0	−14.6	0.2
	Agricultural lands	16,722	0	0	−0.1	0.1	−0.2	0	−0.4	0
	Wetlands	3,656	−0.1	0	−0.5	−0.1	−0.1	0	−0.7	−0.1
	Other lands	27,469	0	0	−0.2	0.4	0	0	−0.2	0.4
	Total	872,253	−30.3	−15.4	−30.2	0.6	−25.6	9.4	−86.1	−19.1
Marine West Coast Forest	Forests	64,601	−2.4	−0.4	−2.8	0.2	−1.7	0.3	−6	−1.3
	Grasslands/shrublands	4,542	−0.2	0	−0.4	0	−0.1	0	−0.7	0
	Agricultural lands	10,418	0	0	0.1	0.2	−0.1	0	0	0.1
	Wetlands	588	0	0.1	−0.1	0	0	0	0	0
	Other lands	15,262	0	0	−0.2	0.2	0	0.1	−0.2	0.2
	Total	95,411	−2.6	−0.3	−3.4	0.5	−1.9	0.4	−6.9	−1
Cold Deserts	Forests	97,180	−4.6	−1.5	−1.6	0.3	−1.6	3.5	−7.8	1.5
	Grasslands/shrublands	804,658	0	5.5	−13.4	0.1	−10.9	0	−20.9	3.8
	Agriculture	81,191	−0.2	0	−2.1	0.2	−1	0	−3	0
	Wetlands	4,635	0	0	−0.5	0	−0.1	0	−0.6	0
	Other lands	68,392	0	0	−0.3	0.4	0	0	−0.3	0.4
	Total	1,056,055	−4.8	4.1	−17.8	1	−13.6	3.5	−32.6	5.7
Warm Deserts	Forests	8,084	−0.3	−0.1	−0.1	0	−0.2	0.4	−0.6	0.2
	Grasslands/shrublands	403,390	−3	2.8	−5.4	0.1	−7.7	0.7	−16.1	2.7
	Agricultural lands	11,334	0	0	−1.1	0	−0.7	0	−1.8	0
	Wetlands	326	0	0	0	0	0	0	0	0
	Other lands	42,150	0	0	−0.1	0.1	0	0	−0.1	0
	Total	465,285	−3.3	2.7	−6.7	0.2	−8.6	1.1	−18.6	2.9
Mediterranean California	Forests	29,945	−2.9	−2.3	−2.1	0	−1.8	−0.1	−6.1	−2.6
	Grasslands/shrublands	74,294	−0.6	0.1	−5	0.2	−2.2	0	−6.4	0.3
	Agricultural lands	41,046	0	0.1	−4.3	0.1	−1.3	0	−5.6	0.2
	Wetlands	910	0	0	−0.1	0.1	0	0	−0.1	0.1
	Other lands	23,259	0	0	−0.4	−0.1	0	0	−0.4	−0.1
	Total	169,455	−3.6	−2.1	−11.9	0.2	−5.4	0	−18.7	−2.2
Western United States (total)	Forests	746,343	−39.8	−20.8	−28.3	0.6	−24.1	13.4	−90.7	−21.8
	Grasslands/shrublands	1,564,759	−4.3	9.5	−31.9	0.6	−27.3	0.7	−58.7	7
	Agricultural lands	160,711	−0.3	0.1	−7.5	0.5	−3.3	0	−10.8	0.3
	Wetlands	10,114	−0.1	0.2	−1.2	−0.1	−0.3	0	−1.5	0
	Other lands	176,532	−0.1	0	−1.1	0.9	−0.1	0.1	−1.2	0.9
	Total	2,658,459	−44.6	−11.1	−70	2.5	−55	14.2	−162.9	−13.6

5.4.2.5. Mediterranean California

From 2001 to 2005, the estimated average net carbon flux in the Mediterranean California ecoregion was −13.7 TgC/yr (ranging from −18.7 to −2.2 TgC/yr). The total rate of carbon sequestration was attributed to forests (−4.8 TgC/yr), grasslands/shrublands (−5.3 TgC/yr), and agricultural lands (−3.3 TgC/yr).

5.4.2.6. Discussion of Baseline Net Carbon Flux

In the Western United States, the evergreen forest of the Pacific Coast was the most productive ecosystem and sequestered a significant amount of carbon. D.P. Turner, Gockede, and others (2011) estimated that the per-unit-of-area NEP of Oregon's coastal forests (an average of private and public forest) during 2007 was around −75 gC/m^2/yr. In this assessment, the average estimated net carbon flux for the Marine West Coast Forest ecoregion in the baseline period was −52 gC/m^2/yr on a per-unit-of-area basis, about 30 percent lower. For the five western ecoregions, the estimated average net carbon flux in forests was −54 TgC/yr (ranging from −90.7 to −21.8 TgC/yr), which is comparable to an estimate by Heath and others (2011) of −43.1 TgC/yr (ranging from 24.9 to −111.2 TgC/yr) for the years 2000 to 2008. The average annual net carbon flux estimates from the two studies may be expressed as per-unit-of-area carbon flux: −72.4 gC/m^2/yr from this assessment and −93.8 gC/m^2/yr from Heath and others (2011).

Estimates of net carbon flux in California's agricultural lands were variable. Kroodsma and Field (2006) estimated that California's agricultural lands sequestered an average of −19 gC/m^2/yr between 1980 and 2000. For this assessment, however, the Mediterranean California ecoregion (not the entire state of California) was estimated to have sequestered an average of −81 gC/m^2/yr (−3.3 TgC/yr over 41,046 km^2) during the baseline period. The large gap between the results of this assessment and those of the earlier studies can be attributed to several observations. First, Kroodsma and Field (2006) estimated that the conversion of annual crops to vineyards or orchards generated a carbon sink of −68 to −85 gC/m^2/yr, which was very close to the estimate in this assessment. Second, they also indicated that rice fields sequestered −55 gC/m^2/yr due to a reduction of field burning. This assessment did not include field burning of crop residue, and therefore the estimated carbon sink in this assessment should be high.

As noted previously (see section entitled "Model Run Setup"), the purpose of using multiple models on the GEMS platform was to provide an opportunity to quantify uncertainties related to model structures and inherent biases and errors. Table 5.5 shows the average estimates of carbon stocks and carbon fluxes derived by each of the three models for each of the five ecoregions. A variability value (in percent) was also calculated by dividing the range of the minimum and maximum estimates of the subset by their mean, and multiplying by 100.

5.4.3. Greenhouse-Gas Fluxes in Baseline Years

Methane and nitrous oxide (CH_4 and N_2O) fluxes in and out of the terrestrial ecosystems were included in the assessment and were modeled using the spreadsheet model. The fluxes of the two gases were converted to carbon dioxide equivalent (denoted as $CO_{2\text{-eq}}$) by using the respective global warming potential (GWP) factors—21 for methane and 310 for nitrous oxide (EPA, 2003). The carbon flux estimates reported in the previous section were converted to carbon dioxide equivalent using a conversion factor of 3.664 and a GWP factor of 1 (EPA, 2003). The average estimated fluxes of the three gases during the baseline years are presented in table 5.6. Note that these flux estimates do not include the aquatic fluxes presented in chapter 10 of this report. The combined flux estimates in a regional carbon budget are presented and discussed in chapter 12 of this report.

Table 5.5. Comparison of estimated average carbon stocks and fluxes in the five ecoregions of the Western United States, by the three simulation models.

[Negative numbers indicate carbon sequestration; positive numbers indicate loss of carbon to the atmosphere. EDCM, Erosion-Deposition-Carbon Model; TgC, teragrams of carbon; TgC/yr, teragrams of carbon per year]

	Models	Ecoregions					
		Western Cordillera	Marine West Coast Forest	Cold Deserts	Warm Deserts	Mediterranean California	Western United States
Carbon stock (TgC)	CENTURY	7,867.7	1,474.9	3,055.1	910.3	920.6	14,228.7
	EDCM	8,365.9	1,560.7	2,342.8	529.2	861.3	13,659.8
	Spreadsheet	8,439.0	1,632.7	2,362.6	582.7	762.3	13,779.2
	Model variability (percent)	7	10	28	57	19	4
Carbon flux (TgC/yr)	CENTURY	−85.3	−6.2	−30.1	−18.4	−18.0	−158.0
	EDCM	−24.6	−2.0	1.9	2.7	−13.2	−35.2
	Spreadsheet	−19.7	−2.1	−1.9	−0.2	−2.4	−26.3
	Model variability (percent)	152	121	320	398	139	180

Table 5.6. Minimum and maximum estimated averages of annual carbon dioxide, methane, and nitrous oxide fluxes and their total global warming potential from 2001 to 2005 in the Western United States, by greenhouse-gas type for each ecosystem in each ecoregion.

[Estimates of methane (CH_4) and nitrous oxide (N_2O) were generated by the spreadsheet model. The carbon-dioxide (CO_2) estimate is the average of the EDCM and CENTURY model simulations. Global warming potential is the sum of carbon dioxide, methane, and nitrous oxide; $TgCO_{2\text{-eq}}$/yr, teragrams of carbon dioxide equivalent per year]

Ecoregion	Ecosystem	Carbon dioxide ($TgCO_{2\text{-eq}}$/yr)		Methane ($TgCO_{2\text{-eq}}$/yr)		Nitrous oxide ($TgCO_{2\text{-eq}}$/yr)		Global warming potential ($TgCO_{2\text{-eq}}$/yr)	
		Min	Max	Min	Max	Min	Max	Min	Max
Western Cordillera	Forests	−257.9	−72.0	−0.9	−0.9	0.3	0.3	−258.5	−72.6
	Grasslands/shrublands	−53.6	0.8	−0.8	−0.8	0.2	0.2	−54.2	0.2
	Agricultural lands	−1.4	0.1	0.0	0.0	0.0	0.0	−1.4	0.1
	Wetlands	−2.7	−0.4	0.4	0.4	0.0	0.0	−2.3	0.0
	Other lands	−0.6	1.6	0.0	0.0	0.0	0.0	−0.6	1.6
	Total	−316.1	−69.9	−1.3	−1.3	0.6	0.6	−316.8	−70.6
Marine West Coast Forest	Forests	−21.9	−4.9	−0.2	−0.2	0.0	0.0	−22.1	−5.1
	Grasslands/shrublands	−2.5	−0.2	0.0	0.0	0.0	0.0	−2.5	−0.2
	Agricultural lands	0.0	0.4	0.0	0.0	0.0	0.0	0.0	0.4
	Wetlands	−0.1	0.1	0.1	0.1	0.0	0.0	0.0	0.2
	Other lands	−0.9	0.9	0.4	0.4	0.0	0.0	−0.5	1.3
	Total	−25.3	−3.7	0.3	0.3	0.1	0.1	−24.9	−3.3
Cold Deserts	Forests	−28.6	5.7	−0.4	−0.4	0.1	0.1	−29.0	5.3
	Grasslands/shrublands	−76.6	13.9	−2.8	−2.8	0.2	0.2	−79.2	11.3
	Agricultural lands	−11.2	0.0	−0.1	−0.1	0.1	0.1	−11.1	0.1
	Wetlands	−2.2	0.1	0.8	0.8	0.0	0.0	−1.4	0.9
	Other lands	−0.9	1.3	0.4	0.4	0.0	0.0	−0.5	1.7
	Total	−119.6	21.0	−2.1	−2.0	0.4	0.4	−121.3	19.4
Warm Deserts	Forests	−2.1	0.8	0.0	0.0	0.0	0.0	−2.1	0.8
	Grasslands/shrublands	−59.0	10.0	−1.0	−1.0	0.4	0.4	−59.7	9.4
	Agricultural lands	−6.6	−0.2	0.0	0.0	0.0	0.0	−6.6	−0.2
	Wetlands	−0.1	0.0	0.1	0.1	0.0	0.0	0.0	0.1
	Other lands	−0.4	0.1	0.1	0.1	0.0	0.0	−0.3	0.2
	Total	−68.2	10.8	−0.9	−0.9	0.4	0.4	−68.7	10.3
Mediterranean California	Forests	−22.5	−9.6	−0.1	−0.1	0.0	0.0	−22.6	−9.7
	Grasslands/shrublands	−23.6	1.0	−0.2	−0.2	0.1	0.1	−23.7	0.9
	Agricultural lands	−20.5	0.7	0.8	0.9	0.1	0.1	−19.6	1.7
	Wetlands	−0.5	0.3	0.2	0.2	0.0	0.0	−0.4	0.5
	Other lands	−1.5	−0.5	0.2	0.2	0.0	0.0	−1.3	−0.3
	Total	−68.6	−8.2	0.9	1.0	0.2	0.2	−67.5	−7.0
Western United States (total)	Forests	−333.0	−80.1	−1.7	−1.7	0.4	0.4	−334.2	−81.3
	Grasslands/shrublands	−215.3	25.5	−4.8	−4.8	0.9	0.9	−219.2	21.6
	Agricultural lands	−39.7	0.9	0.7	0.8	0.3	0.3	−38.8	2.0
	Wetlands	−5.5	0.2	1.6	1.6	0.0	0.0	−4.0	1.8
	Other lands	−4.3	3.4	1.1	1.2	0.1	0.1	−3.1	4.6
	Total	−597.7	−50.0	−3.1	−2.9	1.7	1.7	−599.1	−51.3

The data in table 5.6 indicate that the fluxes of methane and nitrous oxide in the ecoregions of the Western United States were generally low. As a whole, the Western United States served as a GHG sink, sequestering GHGs at an estimated average rate of −232.51 $TgCO_{2\text{-}eq}$/yr (ranging from −599.1 to −51.3 $TgCO_{2\text{-}eq}$/yr). The CO_2 sink dominated the contribution (about 99 percent) to the total GWP of the GHGs. The overall GHG sink in the terrestrial ecosystems of the Western United States is equivalent to 4.9 percent of the Nation's total greenhouse gas emissions in 2010, as reported by the EPA's 2012 national greenhouse gas inventory report (EPA, 2012). The average annual nitrous oxide emission rate for the entire Western United States was 1.65 $TgCO_{2\text{-}eq}$/yr, of which the Western Cordillera and Warm Deserts ecoregions contributed 61 percent even though they cover only 50 percent of the land area. The Marine West Coast Forest and Mediterranean California ecoregions acted as methane sources at 0.3 and 0.9 $TgCO_{2\text{-}eq}$/yr, respectively, for the baseline years, whereas other ecoregions acted as methane sinks. The Mediterranean California ecoregion is only 1.8 times larger in area than the Marine West Coast Forest but its methane emissions were 3 times greater because Mediterranean California had more wetlands and agricultural lands, which had higher methane emission rates than other ecosystems (fig. 5.6). Whether an ecoregion was a sink or source of methane was largely associated with the land-cover composition, especially its proportion of wetlands and agricultural lands. Agricultural lands and wetlands tended to emit methane, whereas forests and grasslands/shrublands tended to sequester methane.

On average, all of the ecosystems in the Western United States were carbon dioxide sinks and nitrous-oxide sources; for the baseline years, both forests and grasslands/shrublands were methane sinks, and wetlands were methane sources. The methane budget varied regionally; Mediterranean California was a source (estimated average of 0.82 $TgCO_{2\text{-}eq}$/yr) and the other ecoregions were sinks. The grasslands/shrublands ecosystem in the Cold Deserts and the Western Cordillera consumed methane at −5.9 and −9.4 $gCO_{2\text{-}eq}/m^2$/yr, respectively (fig. 5.6*B*). The wetlands ecosystem for the Western United States emitted the largest amount of methane at an average rate of 105 $gCO_{2\text{-}eq}/m^2$/yr (fig. 5.6*B*). Agricultural lands emitted nitrous oxide at a rate of 97.9 $gCO_{2\text{-}eq}/m^2$/yr in some parts of Mediterranean California, higher than for any of the other ecosystems (fig. 5.6*C*). The spatial distribution of the GWP for each GHG generally coincided with the spatial distribution of the ecosystems (fig. 5.6). A higher carbon dioxide uptake was associated with forested areas (green color in figure 5.6*A*), but higher carbon dioxide emissions were associated with agricultural lands and clearcut areas of forests (red color in figure 5.6*A*). Overall, forests covered 28 percent of the land area of the Western United States (746,343 km^2) but accounted for 64 percent of the GHG flux. On the other hand, grasslands/shrublands covered 59 percent of the area but accounted for only 32 percent of the GHG flux. Agricultural lands covered only 6 percent of the area but emitted 15 percent of nitrous oxide, whereas wetlands covered only 0.4 percent of the area and emitted roughly the same amount of methane (1.6 $TgCO_{2\text{-}eq}$/yr) as all other emitters combined.

5.5. Summary

The total carbon stocks and fluxes in terrestrial ecosystems were estimated using three biogeochemical models on the GEMS platform. The modeling was constrained by the USDA FIA forest inventory data, the USDA NASS grain-yield statistics, and the MODIS NPP product. For carbon stocks in the ecosystems of the entire Western United States in 2005, the biomass and the top 20 cm of the soil layer contained an estimated average of 13,920 TgC (ranging from 12,418 to 15,460 TgC). The Western Cordillera stored the most carbon (59 percent of the total), followed by the Cold Deserts (19 percent), the Marine West Coast Forest (11 percent), the Mediterranean California (6 percent), and the Warm Deserts (5 percent). Forests, grasslands/shrublands, and agricultural lands stored 69 percent, 25 percent, and 4 percent of the total carbon, respectively. As a comparison, the total forest area, the average total forest carbon stock, and the average forest stock density estimated by this assessment for 2005 in the five ecoregions were 74.6 Mha, 9,675 TgC, and 13.0 kgC/m^2, respectively. A separate analysis (Brad Smith, USDA Forest Service, unpub. data, 2010) using the USFS FIA forest area and forest carbon stock estimation methods (Nelson and Vissage, 2005; J.E. Smith and Heath, 2008) suggested a total of 93.6 Mha of forested area, a total forest carbon stock of 13,579 TgC, and an average forest carbon stock density of 14.5 kgC/m^2 for the same five ecoregions. The differences between the two studies may be attributed to two factors: (1) the total forest area used by the two studies was different, and (2) only carbon in the top 20 cm of the soil layer was modeled as SOC in this assessment, compared to the FIA SOC estimate, which used the top 1 m of the soil layer.

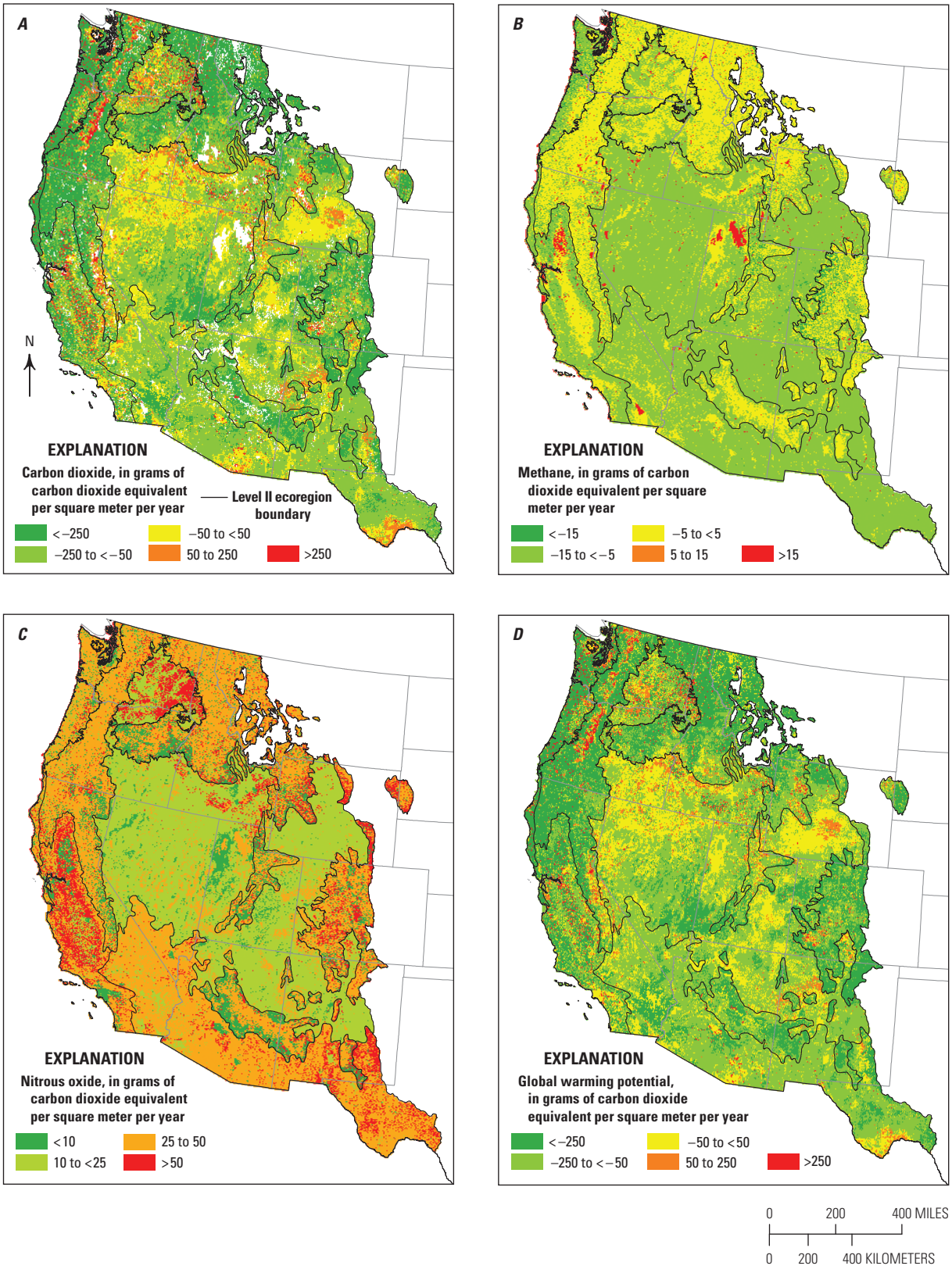
A
N
EXPLANATION
Carbon dioxide, in grams of carbon dioxide equivalent per square meter per year
Level II ecoregion boundary
<–250
–250 to <–50
–50 to <50
50 to 250
>250
B
EXPLANATION
Methane, in grams of carbon dioxide equivalent per square meter per year
<–15
–15 to <–5
–5 to <5
5 to 15
>15
C
EXPLANATION
Nitrous oxide, in grams of carbon dioxide equivalent per square meter per year
<10
10 to <25
25 to 50
>50
D
EXPLANATION
Global warming potential, in grams of carbon dioxide equivalent per square meter per year
<–250
–250 to <–50
–50 to <50
50 to 250
>250
0 200 400 MILES
0 200 400 KILOMETERS

The overall average annual net carbon flux in terrestrial ecosystems of the Western United States was estimated to be −86.5 TgC/yr (ranging from −162.9 to −13.6 TgC/yr) from 2001 to 2005. Forests were the largest carbon sink (62 percent of the total), followed by grasslands/shrublands (30 percent) and agricultural lands (7 percent). Of the total carbon sequestered on an annual basis, about one-third was accumulated in live biomass and the rest was allocated to the dead biomass (forest litter and dead, woody debris) and soil carbon pools. For the baseline years of 2001 to 2005, the estimated average annual net carbon flux in forests estimated in this assessment (−54 TgC/yr, ranging from −90.7 to −21.8 TgC/yr) was comparable to an estimate by Heath and others (2011) of −43.1 TgC/yr (ranging from 24.9 to −111.2 TgC/yr) for the years 2000 to 2008. The average annual net carbon flux estimates from the two studies may be expressed as per-unit-of-area carbon flux: −72.4 $gC/m^2/yr$ from this assessment and −93.8 $gC/m^2/yr$ from Heath and others (2011).

A comparison of carbon stock and flux indicates that there are still profound differences and uncertainties within carbon estimation methods, models, and data sources. Further comparisons between models may help to reveal the major causes of those differences, such as model structure, parameter sensitivity, and data assimilation.

Figure 5.6. (see facing page). Maps showing the spatial distribution of the average annual carbon dioxide, methane, and nitrous oxide fluxes and their total global warming potential from 2001 to 2005 in the Western United States. The flux of carbon dioxide is an average of estimates derived from the spreadsheet model, CENTURY model, and the EDCM in the General Ensemble Modeling System (GEMS). The fluxes of methane and nitrous oxide were derived from the spreadsheet model alone in the GEMS. *A*, Carbon dioxide. *B*, Methane. *C*, Nitrous oxide. *D*, Global warming potential. EDCM, Erosion-Deposition-Carbon Model. See figure 1.1 in chapter 1 for ecoregion names.

This page intentionally left blank.

Chapter 6. Projected Land-Use and Land-Cover Change in the Western United States

By Benjamin M. Sleeter[1], Terry L. Sohl[1], Tamara S. Wilson[1], Rachel R. Sleeter[1], Christopher E. Soulard[1], Michelle A. Bouchard[1], Kristi L. Sayler[2], Ryan R. Reker[3], and Glenn E. Griffith[1]

6.1. Highlights

- The projected changes in land use and land cover are highly variable across ecoregions and scenarios. The overall rates of projected change varied from 1.3 percent in the Warm Deserts ecoregion under the A2 scenario to 44.9 percent in the Marine West Coast Forest ecoregion under the A1B scenario.
- Land-use and land-cover change was generally projected to be greatest under the economically oriented scenarios and smaller in the environment-oriented scenarios.
- Forest harvesting and regrowth accounted for the greatest amount of projected land-use and land-cover change under all of the scenarios; however, the projected rates of change were highly variable across the level III ecoregions and were driven by the regions' enabling environmental characteristics and resource potential.
- Urbanization was a key component of projected land-use and land-cover change in all of the scenarios and was most pronounced in the Mediterranean California and Marine West Coast Forest ecoregions.
- Forests were projected to decline in the economically oriented scenarios, resulting primarily from the projected high demand for urban land uses and, to a lesser extent, the expansion of agricultural land.

6.2. Introduction and Review of Methods

The current and projected changes in land use and land cover (LULC) are key components for this assessment of carbon and greenhouse-gas (GHG) stocks and fluxes (Zhu and others, 2010). As noted in chapter 1 of this report, mapping of the baseline (1992–2005) LULC conditions, discussed in detail in chapter 2 of this report, provided a spatial foundation for the wall-to-wall assessment of carbon stocks and GHG fluxes in various ecosystems. The development of a range of future potential LULC projections, together with corresponding climate-change projections, allowed for an evaluation of future potential carbon sequestration capacities and vulnerabilities as influenced by these projected drivers. This chapter provides an overview of the methods used to develop alternative future scenarios of LULC and presents the spatially explicit LULC modeling results for each level II ecoregion in the Western United States. The relation between the future LULC scenarios described in this chapter and other components of the assessment is depicted in figure 1.2 of chapter 1. The level II and level III ecoregion names and boundaries are modified from the Commission for Environmental Cooperation (2006) and U.S Environmental Protection Agency (EPA, 1999).

[1]U.S. Geological Survey, Menlo Park, Calif.

[2]U.S. Geological Survey, Sioux Falls, S.D.

[3]Arctic Slope Regional Corporation Research and Technology Solutions, Sioux Falls, S.D.

6.2.1. Scenario Framework

In 2001, the Intergovernmental Panel on Climate Change (IPCC) published the Special Report on Emission Scenarios (SRES) (Nakicenovic and others, 2000). The IPCC–SRES documented the development of a global set of greenhouse-gas-emissions scenarios, which were based on an underlying set of socioeconomic conditions that were consistent with the current (at the time) scenario literature. The IPCC–SRES scenarios were designed to assess the impacts of alternative GHG-emission pathways on coupled human and environmental systems and evaluate future vulnerabilities on those systems under various combinations of projected change. The IPCC–SRES scenarios consist of four basic narrative storylines, each of which describe alternative developments in the major drivers of GHG emissions, such as population growth, economic growth, technological change, energy use, globalization, and environmental protection. The four storylines are oriented along two axes with either economic growth (A) or environmental protection (B) aligned along one axis and either global development (1) or regional development (2) aligned along the other; for example, the B1 scenario assumes strong environmental protection and global cooperation.

In order to explore sensitivities in the energy sector, the A1 storyline was subdivided into three subscenarios that focused on fossil-fuel use (A1FI), renewable technologies (A1T), and a balanced energy sector that did not rely on any particular energy source (A1B). Six modeling teams characterized the various storylines, ultimately producing 40 quantified scenarios. No probability of occurrence was assigned to any one of the IPCC–SRES scenarios and all should be considered equally plausible with none considered more or less preferable. Furthermore, no integrated climate-change policies, such as the emissions targets of the Kyoto Protocol (United Nations Framework Convention on Climate Change, 1997), are incorporated into any of the scenarios; therefore, the scenarios serve as reference conditions to evaluate the effects of potential mitigation actions and strategies. Since the inception of the IPCC–SRES scenarios, a suite of future climate-change projections (known as the general circulation model (GCM) data) have also become available and correspond to the major storylines. At the early stage of this assessment, GCM data corresponding to the B2 storyline were not available. Because this assessment required the use of both the LULC scenarios and climate-change projection scenarios, only the A1B, A2, and B1 scenarios were used in the assessment. See table 6.1 for assumptions about the major driving forces associated with each scenario.

Table 6.1. Assumptions about the primary driving forces affecting land-use and land-cover change.

[These assumptions were used to downscale the A1B, A2, and B1 scenarios of the Intergovernmental Panel for Climate Change's Special Report on Emission Scenarios (Nakicenovic and others, 2000). Population and per-capita income projections are from Strengers and others (2004)]

Driving forces	A1B	A2	B1
Population growth (global and United States)	Medium. Globally, 8.7 billion by 2050, then declining; in the United States, 385 million by 2050	High. Globally, 15.1 billion by 2100; in the United States, 417 million by 2050	Medium. Globally, 8.7 billion by 2050, then declining; in the United States, 385 million by 2050.
Economic growth	Very high. U.S. per-capita income $72,531 by 2050	Medium. U.S. per-capita income $47,766 by 2050	High. U.S. per-capita income $59,880 by 2050.
Regional or global orientation	Global	Regional	Global.
Technological innovation	Rapid	Slow	Rapid.
Energy sector	Balanced use	Adaptation to local resources	Smooth transition to renewable.
Environmental protection	Active management	Local and regional focus	Protection of biodiversity.

6.2.2. Scenario Downscaling

In order to use the global scenarios, a scenario downscaling process was needed to translate the coarse-scale scenario data to finer geographic scales while maintaining consistency with the original dataset and local data (van Vuuren and others, 2007, 2010). Land-change scenarios were developed using a modular modeling approach. A global integrated assessment model (IAM) was used to supply future projections of land use at the national scale. An accounting model was developed to refine the national-scale IAM projections and to downscale to hierarchically nested ecoregions. The ecoregion-based projections were then converted into annual maps of LULC using a spatially explicit LULC change model. The approach used for this assessment follows the methods described in Zhu and others (2010) and more recently in Sohl, Sleeter, Zhu, and others (2012) and Sleeter, Sohl, Bouchard, and others (2012). A brief review of each of the major components is found below.

Initial quantities of projected LULC changes (scenario "demand") were formulated by implementing a land-use-scenario downscaling accounting model (described in detail in Sleeter, Sohl, Bouchard, and others, 2012). National-scale LULC projections were based on national-scale projections from the Integrated Model to Assess the Global Environment (IMAGE, version 2.2), land-use histories, and expert knowledge. IMAGE was used to simulate future environmental change, including GHG emissions and land-use changes, for the three SRES marker scenarios (A1B, A2, B1) (Strengers and others, 2004). IMAGE used a series of linked modules to project environmental consequences resulting from anthropogenic activity (Alcamo and others, 1998; IMAGE Team, 2001). Environmental changes were projected for 17 world regions (the United States was treated as a single region) with some data (land use and land cover) available in a 30′ × 30′ grid. IMAGE produced projections of demand for agriculture and forest harvest, which were incorporated directly into the scenario downscaling model described in Sleeter, Sohl, Bouchard, and others (2012). Future projections of development and mining were developed through the use of proxy data (population and coal usage, respectively) from the IMAGE. Land-use histories were then used to expand the scenario projections of net change in major land-use classes into comprehensive projections of gross changes between all major LULC types.

Land-use histories described the recent historical LULC changes occurring in ecoregions of the United States. These data came primarily from the USGS Land Cover Trends project, which provided ecoregion-based estimates on the rates, extent, and types of LULC change for multiple dates between 1973 and 2000 (Loveland and others, 2002; Sleeter, Wilson, and Acevedo, 2012). USGS Land Cover Trends data were incorporated into the scenarios' construction and downscaling in two primary ways. First, the data were used to expand projections of net change in development, mining, and agriculture into gross conversions between all primary LULC classes at the national scale. Second, the data were used to proportionally downscale these LULC conversions to ecoregions of the conterminous United States. Throughout the downscaling process, regional and sectoral experts were consulted in a series of workshops and ad-hoc consultations. The data served as a default parameter for downscaling, and experts were able to modify certain variables in order to produce regionally specific scenarios that retained consistency with the IPCC–SRES storylines. A complete description of the downscaling process can be found in Sleeter, Sohl, Bouchard, and others (2012).

Regional LULC scenarios, developed in the process as described above, were used as input to the "forecasting scenarios of land-use change" (FORE–SCE) model (Sohl and Sayler, 2008; Sohl, Sleeter, Sayler, and others, 2012). The FORE–SCE model produced annual, spatially explicit LULC maps from 2006 to 2050 that were consistent with the scenario assumptions and LULC proportions from the scenario downscaling process. The initial LULC map for the start of the simulation period was the 2005 LULC map produced from the baseline LULC modeling described in chapter 2 of this report. The suitability-of-occurrence surfaces that were used for the modeling of the baseline LULC change guided the placement of patches of change for the 2006 to 2050 scenarios. The Protected Area Database (PAD–US) used in the modeling of baseline LULC was also used for the scenario modeling. Different decision rules were used for each scenario, with more land protected from significant LULC change in the environment-oriented B1 scenario and more lands available for development in the economically oriented A1 and A2 scenarios. Each level III ecoregion was individually parameterized and modeled by applying the FORE–SCE model for each of the three IPCC–SRES scenarios. The 2006 to 2050 models of LULC provide spatial representations of plausible outcomes that are based on the IPCC–SRES scenarios. When combined with the mapped and modeled baseline (1992 to 2005) LULC maps described in chapter 2, the baseline and modeled scenarios resulted in a continuous, consistent LULC map database from 1992 to 2050.

6.3. Results

6.3.1. Scenario Downscaling Results for the Western United States

The projected changes in LULC were variable across ecoregions and scenarios. The LULC-change footprint was the area of the Western United States that changed at least once over the projection period. Under the three scenarios used for this assessment, the projected LULC change ranged from a low of 5.8 percent in the B1 scenario to a high of 7.8 percent in the A1B scenario; in the A2 scenario, the LULC change was 6.4 percent. The scenarios that indicated the greatest (A1B) and smallest (B1) amounts of projected LULC change shared the same assumptions about population growth; however, the greatest change indicated by the A1B scenario resulted from high demand for forest products, agricultural intensification, and high rates of urbanization. The B1 scenario was characterized by strengthening environmental protections, which limited the anthropogenic conversion of natural land covers to either agricultural land or urbanized land. The demand for forest products and agricultural commodities was reduced in scenario B1 compared to A1B, and the environmental emphasis associated with scenario B1 resulted in a more compact pattern of urbanization. The variability was even greater between the level II ecoregions in the Western United States (table 6.2). The greatest projected LULC change of any of the ecoregion regions was in the Marine West Coast Forest, followed by the Western Cordillera and Mediterranean California. The projected LULC change of the Cold Deserts and Warm Deserts ecoregions was below 3 percent (table 6.2 and fig. 6.1).

Forest ecosystems accounted for 746,370 km^2 of the Western United States in 2005 and were projected to decline by 5,630 km^2 in the A1B scenario and by 5,350 km^2 in the A2 scenario by 2050 (fig. 6.2) with the harvesting of evergreen forests accounting for more than 80 percent of the loss. In the B1 scenario, forests were projected to remain relatively stable, declining by 630 km^2 by 2050 (fig. 6.3). The projected net forest loss was driven primarily by the demand for urbanization and new agricultural lands. New developed areas were projected to increase by 62 percent in the B1 scenario, 69 percent in the A2 scenario, and 90 percent in the A1B scenario, whereas agriculture was projected to increase by 12 percent in the A1B scenario and 4 percent in the A2 scenario, and decline by 1 percent in the B1 scenario (fig. 6.2).

The projected changes in urban and built-up areas for each ecoregion and scenario can be found in figure 6.4. Forest harvesting was also a major driver of forest change in the west. The rate of forest harvesting was projected to increase in both the A1B and A2 scenarios but decline in the B1 scenario. By 2050, clearcut logging was projected to affect 21 percent of Western United States' forests in the A1B scenario, 19 percent in the A2 scenario, and 17 percent in the B1 scenario. The grasslands/shrublands ecosystem was projected to experience the greatest areal changes of any ecosystem in the Western United States, declining in all scenarios. Figure 6.2 shows the projected net change in major ecosystem types between 2005 and 2050 for each of the three scenarios, and figure 6.3 shows the projected trends in ecosystem composition over time. Below is a brief overview of the major projected LULC changes in each of the five level II ecoregions in the Western United States for each of the three IPCC–SRES scenarios.

Table 6.2. The projected land-use- and land-cover-change footprint in the level II ecoregions of the Western United States.

[Values given in the A1B, A2, and B1 column are the percent of each level II ecoregion that experienced a change in land use or land cover at least once between 2005 and 2050]

Ecoregion	Area (square kilometers)	A1B (percent change)	A2 (percent change)	B1 (percent change)
Western Cordillera	872,023	12.7	11.1	9.6
Marine West Coast Forest	85,324	44.9	41.6	34.9
Cold Deserts	1,056,072	2.7	1.8	1.8
Warm Deserts	464,312	2.0	1.3	1.5
Mediterranean California	164,481	12.1	7.9	8.5
Western United States (total)	2,642,212	7.8	6.4	5.8

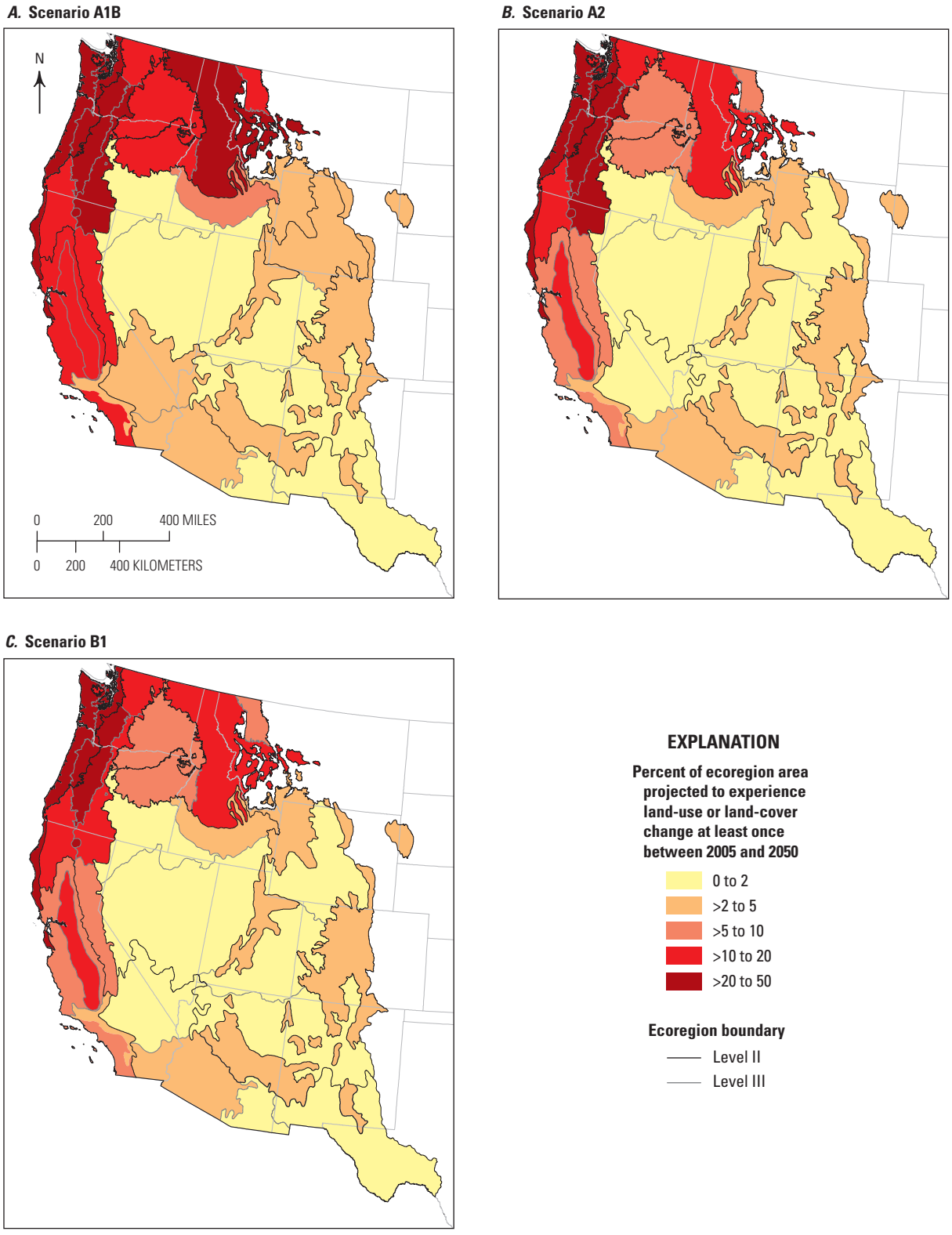

Figure 6.1. Maps showing the projected land-use- and land-cover-change footprint for each of the level III ecoregions in the Western United States. The footprint represents the percent of the ecoregion that changed at least once between 2005 and 2050. *A*, Scenario A1B. *B*, Scenario A2. *C*, Scenario B1.

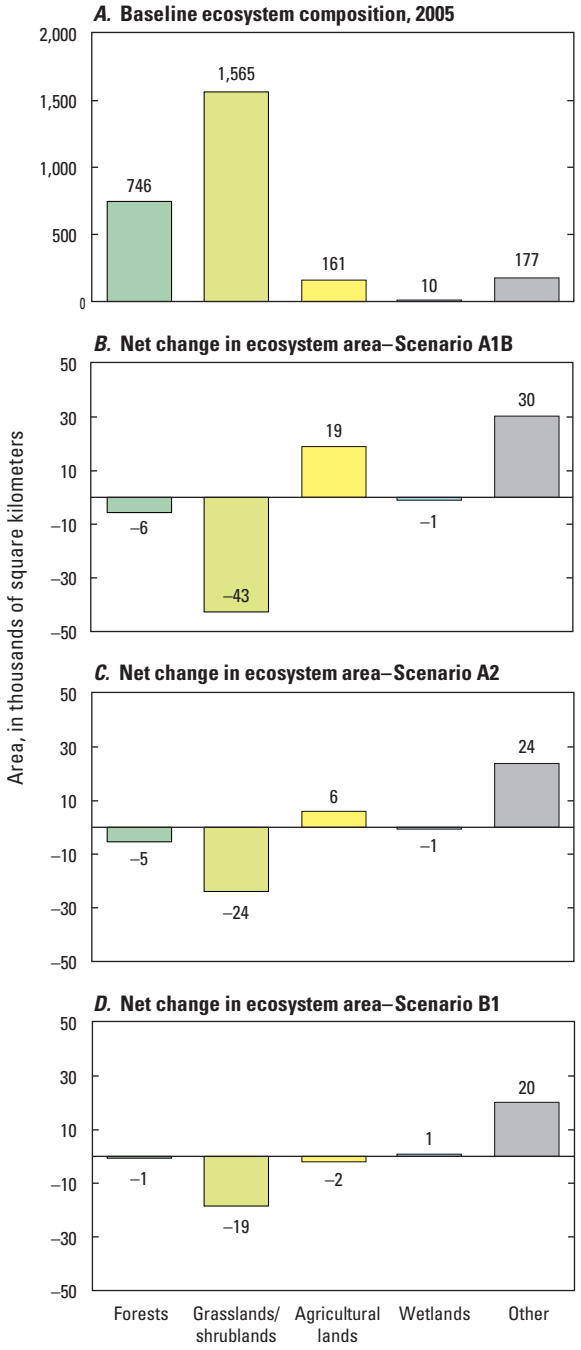

Figure 6.2. Chart showing the baseline composition of and projected net change in major ecosystems between 2005 and 2050 in the Western United States, for the end of the baseline period and for each scenario. *A*, The percent of land area assigned to each of the major ecosystems at the end of the baseline period (2005). *B*, The projected net land-use- and land-cover-change, in percent, between 2005 and 2050 for scenario A1B. *C*, The projected net land-use- and land-cover-change, in percent, between 2005 and 2050 for scenario A2. *D*, The projected net land-use- and land-cover-change, in percent, between 2005 and 2050 for scenario B1. Forests that had been harvested (logged) were included within the forest ecosystem totals. The "other" ecosystem includes developed land, mined land, barren land, and water.

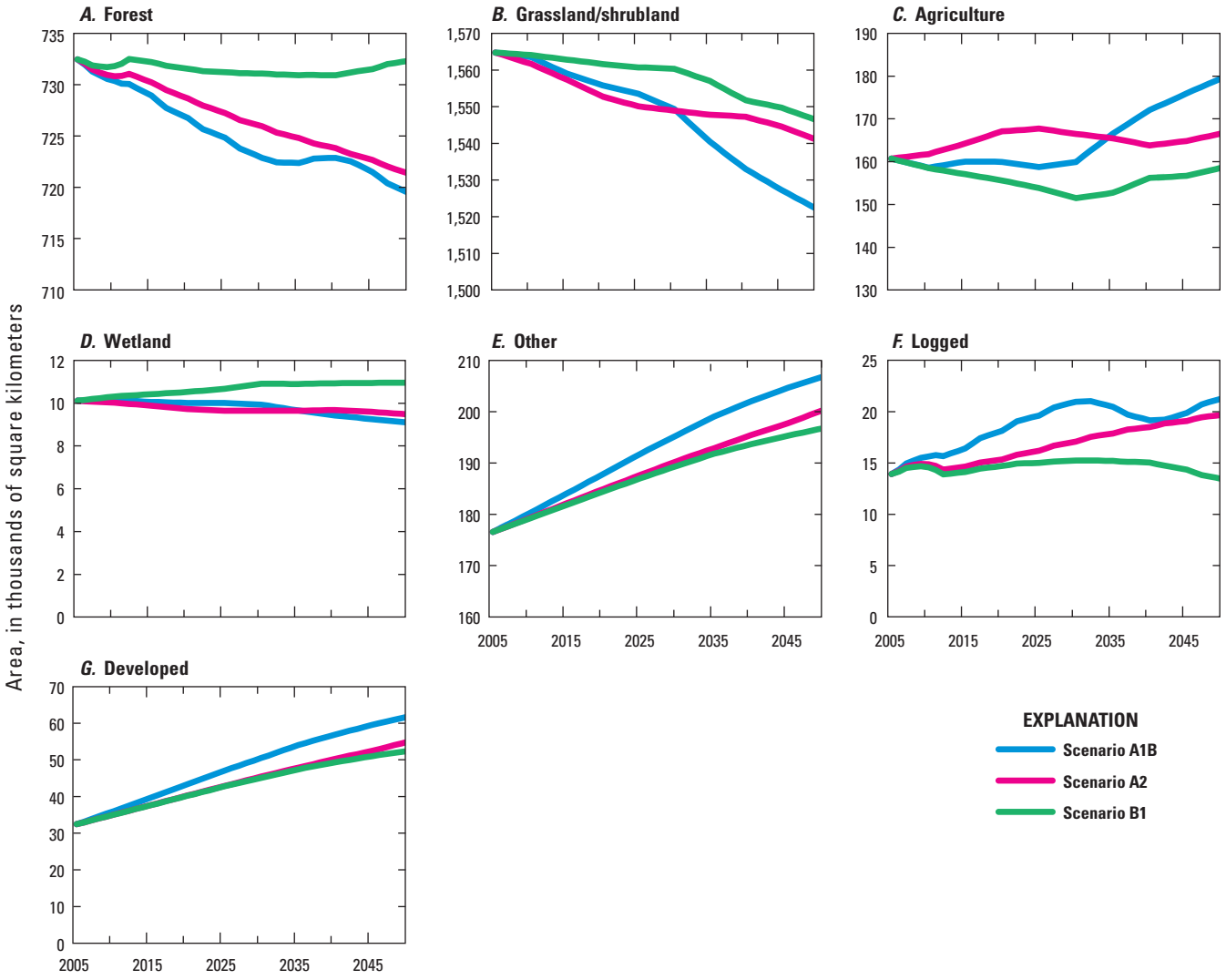

Figure 6.3. Graphs showing trends in the projected composition of the major land-use and land-cover classes over the projection period (2005 to 2050) for the Western United States, by scenario. *A*, Forest. *B*, Grassland/shrubland. *C*, Agriculture. *D*, Wetland. *E*, Other (includes developed land, mined land, barren land, and snow/ice). *F*, Logged (shown separately from other forests because it is a major driver of forest change). *G*, Developed.

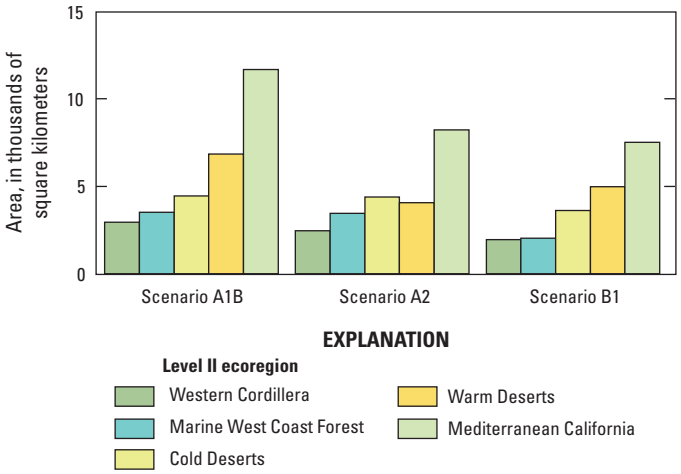

Figure 6.4. Chart showing projected change in area of developed land by level II ecoregion for the A1B, A2, and B1 scenarios for the period 2005 to 2050.

6.3.2. Regional Results

6.3.2.1. Western Cordillera

The Western Cordillera level II ecoregion includes 12 level III ecoregions: Cascades, North Cascades, Eastern Cascades—Slopes and Foothills, Klamath Mountains, Blue Mountains, Sierra Nevada Mountains, Northern Rockies, Canadian Rockies, Wasatch-Uinta Mountains, Middle Rockies, Southern Rockies, and Arizona-New Mexico Mountains. The ecoregion includes the high mountains of the interior Western United States and highly variable climate, vegetation, and land use because of its rugged topography and extensive ranges in elevation. A large proportion of this ecoregion is publicly owned, which affects land-use and land-management practices. Landscapes range from grass- and shrub-covered lowlands, forested middle elevations, and alpine areas of rock, snow, and ice. Livestock grazing is common in valleys and the lower to middle elevations, and logging is typical in forested areas. Recreation, wildlife, and land-management issues related to watersheds or water supply also influence the LULC. Forestry activity over recent historical times has accounted for as much as two-thirds of all of the regional LULC change; however, forestry activities were highly variable across the level III ecoregions. Data from the USGS Land Cover Trends project (Sleeter, Soulard, and others, 2012) indicated that 74 percent of all logging activity in the past three decades occurred in four level III ecoregions: Cascades, Northern Rockies, Eastern Cascades—Slopes and Foothills, and Klamath Mountains. Furthermore, the overall amount of LULC change was geographically highly variable and ranged from 1 percent in the Southern Rockies to 25 percent in the Cascades. Approximately three-fourths of the Western Cordillera is Federally managed public land, and within it, 22 percent is designated as either highly protected wilderness or a national park, which spatially limits timber harvesting and other anthropogenic activities. Population growth is sparse and scattered in this ecoregion due to the rugged terrain, lack of infrastructure, and proximity to goods and services, which limits the growth of urban and developed land. Agriculture is also limited and is generally confined to lower elevations, where livestock grazing is common.

In all of the scenarios, the projected LULC change in the Western Cordillera ecoregion centered on forestry activities. Approximately three-fourths of all logging was projected to occur in the Cascades, Eastern Cascades—Slopes and Foothills, Northern Rockies, and Klamath Mountains level III ecoregions.

In the A1B scenario, 92,990 km^2 of forested land was projected to be harvested between 2005 and 2050. Most of the projected harvest was conifer forest, with 58 percent occurring in national forests and 32 percent in privately owned forests (table 6.3). The overall extent of forested land was projected to decline from 546,560 km^2 in 2005 to 545,010 km^2 by 2050 (fig. 6.5). Agricultural lands were projected to expand by 3,500 km^2 (from 16,720 km^2 in 2005); the Blue Mountains ecoregion was projected to have the largest increase in agricultural land (1,220 km^2), with most of the increase due to the conversion of grasslands/shrublands (880 km^2). The primary type of agricultural land was hay/pasture land. Between 2005 and 2050, developed land was projected to more than double, expanding by 2,940 km^2 (from 2,630 km^2 in 2005); 44 percent of this growth was projected to occur near Spokane, Washington, and Coeur d'Alene, Idaho, within the Northern Rockies ecoregion.

In the A2 scenario, 82,730 km^2 of forested land was projected to be harvested between 2005 and 2050 (table 6.3). As in the A1B scenario, national forests were projected to account for the majority of forest harvesting. The overall forested area was projected to decline from 546,560 km^2 in 2005 to 545,170 km^2 in 2050, while agricultural land was projected to increase by 1,400 km^2 (from 16,720 km^2 in 2005) (fig. 6.5). Most of the agricultural expansion was projected to occur because of the conversion of grasslands/shrublands to hay/pasture lands to support livestock. Developed land was projected to double in area, increasing from 2,630 km^2 in 2005 to 5,090 km^2 in 2050 (fig. 6.4). The projected expansion of agricultural and developed land resulted in a projected decline in the grasslands/shrublands ecosystem of 1 percent, from 277,880 km^2 in 2005 to 275,110 km^2 in 2050 (fig. 6.5).

Table 6.3. Projected extent of forest logging (driven by demand for forest products) in national, other publicly owned, and privately owned forests in the Western United States and two ecoregions, by ecoregion and ownership category, for the A1B, A2, and B1 scenarios.

[For each set of data, the area is the projected sum of all logged area between 2006 and 2050 and the percentages are the allocation of logged area across the three ownership categories. Data for other three ecoregions covered in this assessment were not included because timber harvesting is not a major economic activity in these regions]

		A1B	A2	B1
Western United States (includes all ecoregions)	Total cut area (km^2)	124,288	110,576	93,485
	National forests (percent)	43.9	44.0	43.2
	Other publicly owned forests (percent)	11.9	12.2	11.4
	Private forests (percent)	44.2	43.7	45.4
Western Cordillera ecoregion	Total cut area (km^2)	92,986	82,728	69,944
	National forests (percent)	57.9	57.6	57.3
	Other publicly owned forest (percent)	10.2	10.2	10.3
	Private forests (percent)	31.8	32.2	32.4
Marine West Coast Forest ecoregion	Total cut area (km^2)	30,991	27,576	23,307
	National forests (percent)	1.9	3.5	0.8
	Other publicly owned forests (percent)	17.0	18.2	14.7
	Private forests (percent)	81.1	78.2	84.5

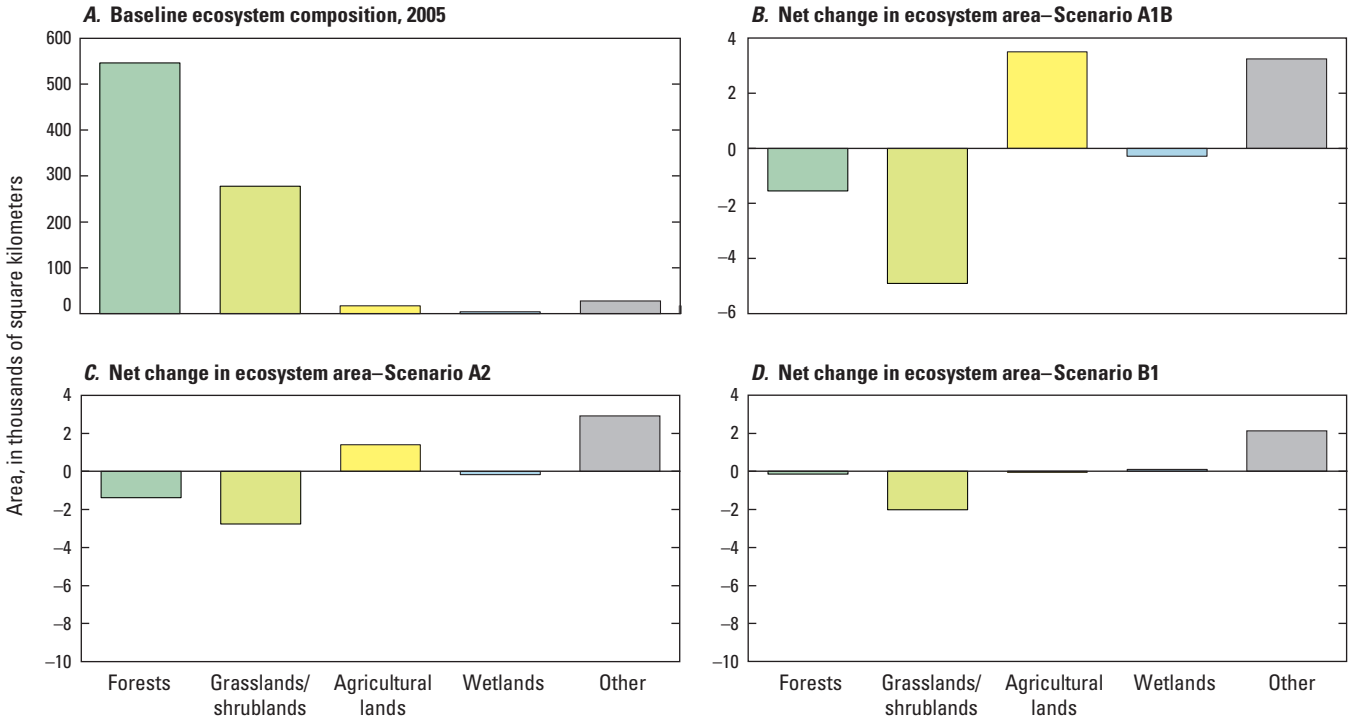

Figure 6.5. Charts showing the baseline composition of and projected net change in major ecosystems between 2005 and 2050 in the Western Cordillera ecoregion, for the final year of the baseline period and for each scenario. *A*, The percent of land area assigned to each of the major ecosystems at the end of the baseline period (2005). *B*, The projected net land-use- and land-cover-change, in percent, between 2005 and 2050 for scenario A1B. *C*, The projected net land-use- and land-cover-change, in percent, between 2005 and 2050 for scenario A2. *D*, The projected net land-use- and land-cover-change, in percent, between 2005 and 2050 for scenario B1. Forests that had been harvested (logged) were included within the forest ecosystem totals. The "other" ecosystem includes developed land, mined land, barren land, and water. The large projected net changes in the "other" class were primarily attributed to the projected increases in developed land.

In the B1 scenario, the demand for wood products was projected to be lower than in the other scenarios, resulting from a large focus on conservation and protection of biodiversity. Forest harvesting was projected to affect 93,490 km^2 of forest cover. The Cascades was the only level III ecoregion where the overall change was projected to be greater than 20 percent (fig. 6.1); however, cutting was still projected to occur at relatively high rates in the East Cascades—Slopes and Foothills, Klamath Mountains, Northern Rockies, and North Cascades. In contrast to the economically oriented scenarios, the forested area in this scenario was projected to decrease by only 140 km^2 (from 546,560 km^2 in 2005), while agricultural lands were projected to decrease by 50 km^2 (from 16,700 km^2 in 2005) (fig. 6.5). Furthermore, the B1 scenario is the only one that indicated a projected increase in wetlands; in 2005, wetlands accounted for 3,660 km^2 and in 2050 they were projected to account for 3,750 km^2. Similar to the A2 scenario, developed areas were projected to increase by 1,940 km^2 and were concentrated around the city of Spokane, Washington, in the Northern Rockies. Figure 6.6 shows a comparison of projected LULC changes resulting from forest harvesting activities near Crater Lake, Oregon, in the Cascades and East Cascades—Slopes and Foothills.

6.3.2.2. Marine West Coast Forest

The Marine West Coast Forest level II ecoregion includes the Coast Range, Puget Lowland, and Willamette Valley level III ecoregions. The ecoregion consists of a highly dynamic, heterogeneous landscape with regionally unique LULC. The conifer-covered, rolling hills of the sparsely populated Coast Range give way to the low-lying, agriculture-dominated Willamette Valley to the east and the intensively developed Puget Lowland in the north. The three subregional economies are distinct from each other and contribute to marked differences in projected LULC change. Forestry and forest products are major drivers of the region's economy, along with agriculture, information technology, manufacturing, construction, and service industries (Sleeter, Soulard, and others, 2012). Although timber harvesting is common throughout the ecoregion, privately owned forests in the Coast Range and along the periphery of the Willamette Valley are the most heavily logged. Much less cutting has occurred on public lands since the Federal enactment of species protection through the Northwest Forest Plan (U.S. Department of Agriculture and U.S. Department of the Interior, 1994). According to the USGS Land Cover Trends data (Sleeter, Soulard, and others, 2012), forest cutting in the past three decades was the highest ranking LULC change and affected over 16 percent of the total land area. Urbanization was also an important LULC transition with large areas of forest and agriculture converted to urban land in the Puget Lowland and Willamette Valley, respectively. Overall, the Marine West Coast Forest ecoregion experienced the highest rates of late-20^{th}-century LULC change in the Western United States. The drivers of LULC change included regional and global timber demand, market competition, population expansion, conversion of forested lands to agricultural lands, and environmental protection (Daniels, 2005).

The projected LULC change was greatest in the Marine West Coast Forest in comparison with the other four ecoregions in the Western United States; 20 percent or more of the ecoregion was projected to experience LULC change in all of the scenarios. Forest harvesting was projected to be greatest in each of the three scenarios with the majority of harvesting occurring in the Coast Range. The extent of developed lands was projected to increase in all of the scenarios, with most new development occurring in the Puget Lowland and successively smaller amounts occurring in the Willamette Valley and Coast Range. Agricultural land was projected to increase in the A1B and A2 scenarios and decline in the B1 scenario. Figure 6.7 shows the baseline ecosystem composition and the projected net change for each ecosystem in each scenario studied for this assessment.

In the A1B scenario, anthropogenic land-use demand was projected to increase almost a full percent of the land area (to 25.6 percent) while natural land covers were projected to decline (to 74.4 percent) from the baseline conditions. The projected forest-related LULC change was the greatest of any of the scenarios, with nearly 31,000 km^2 of the forested part of the ecoregion harvested between 2005 and 2050 (table 6.3) and over 2,500 km^2 cleared for development. More than 81 percent of all cutting was projected to occur on private lands, whereas the Coast Range included more than half of the modeled clearcut land. Overall, forests were projected to decline by 3,760 km^2 (from 64,600 km^2 in 2005). By 2050, developed lands were projected to increase by 79 percent (3,510 km^2) from 4,720 km^2 in 2005. The Puget Lowland was projected to grow the most (64 percent of all new developed lands) followed by the Willamette Valley (27 percent of all new developed lands). In the Puget Lowland, 67 percent of all new developed land was projected to be converted from forested land. Another notable change was the projected addition of 560 km^2 of new hay/pasture land (from 7,900 km^2 in 2005), mostly in the Coast Range as cleared forests were converted to agricultural land.

In the A2 scenario, more than 27,500 km^2 of forests was projected to be harvested by 2050. In this scenario, nearly 22 percent of all trees harvested came from public lands (both national forests and other public forests; table 6.3), which was the greatest percentage of any scenario. In the Coast Range, nearly 25 percent of all forest cutting was projected to occur in public forests, the highest percentage for any scenario.

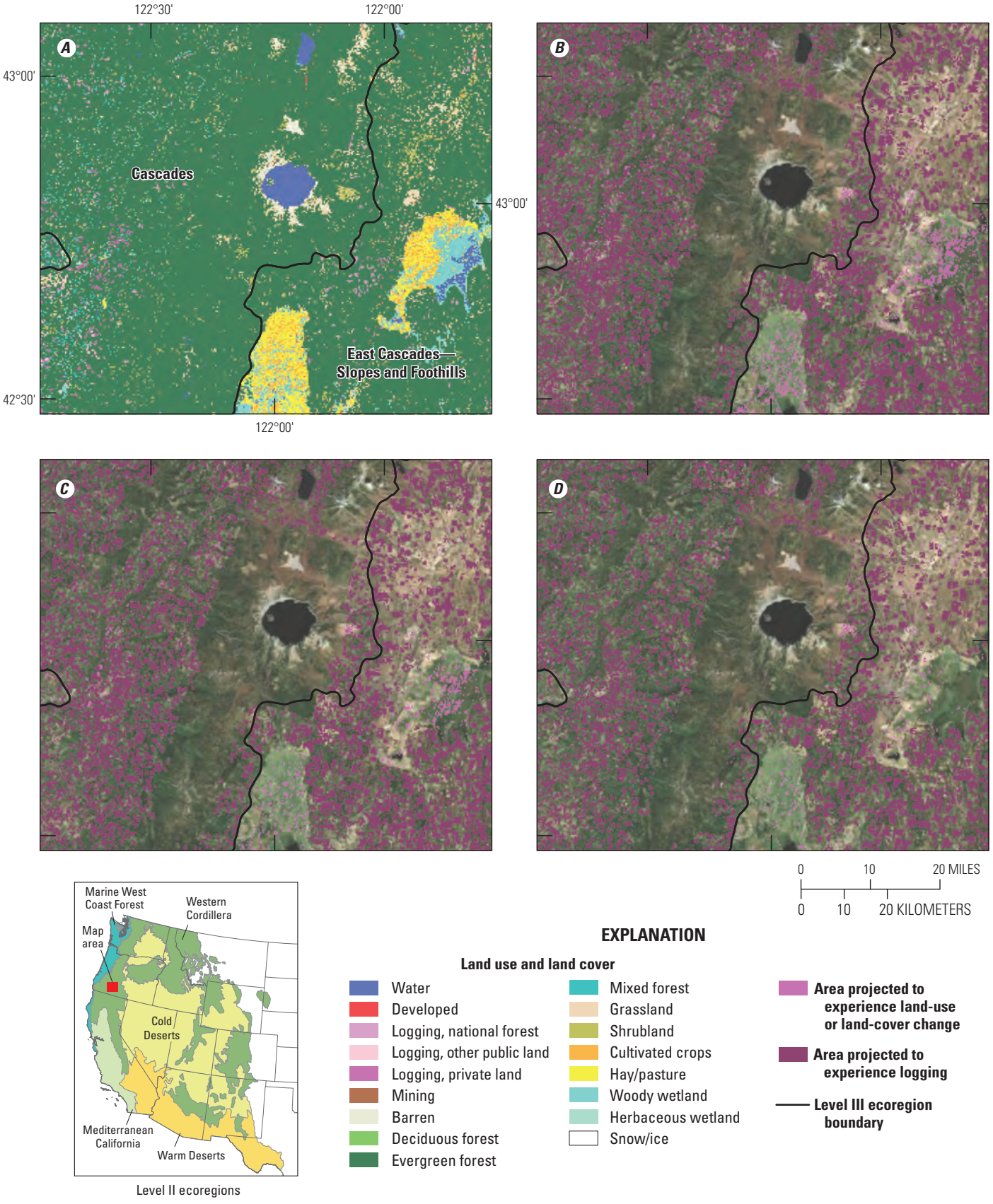

Figure 6.6. Maps showing land use and land cover (LULC) in 2005 and a comparison of the projected LULC changes in the A1B, A2, and B1 scenarios in 2050 for the area around Crater Lake, Oregon, in the Western Cordillera ecoregion. Changes were projected to be the result of either land-use change or forest clearcutting. *A*, LULC in 2005. *B*, Projected LULC change in the A1B scenario. *C*, Projected LULC change in the A2 scenario. *D*, Projected LULC change in the B1 scenario. Crater Lake is located in the center of the image.

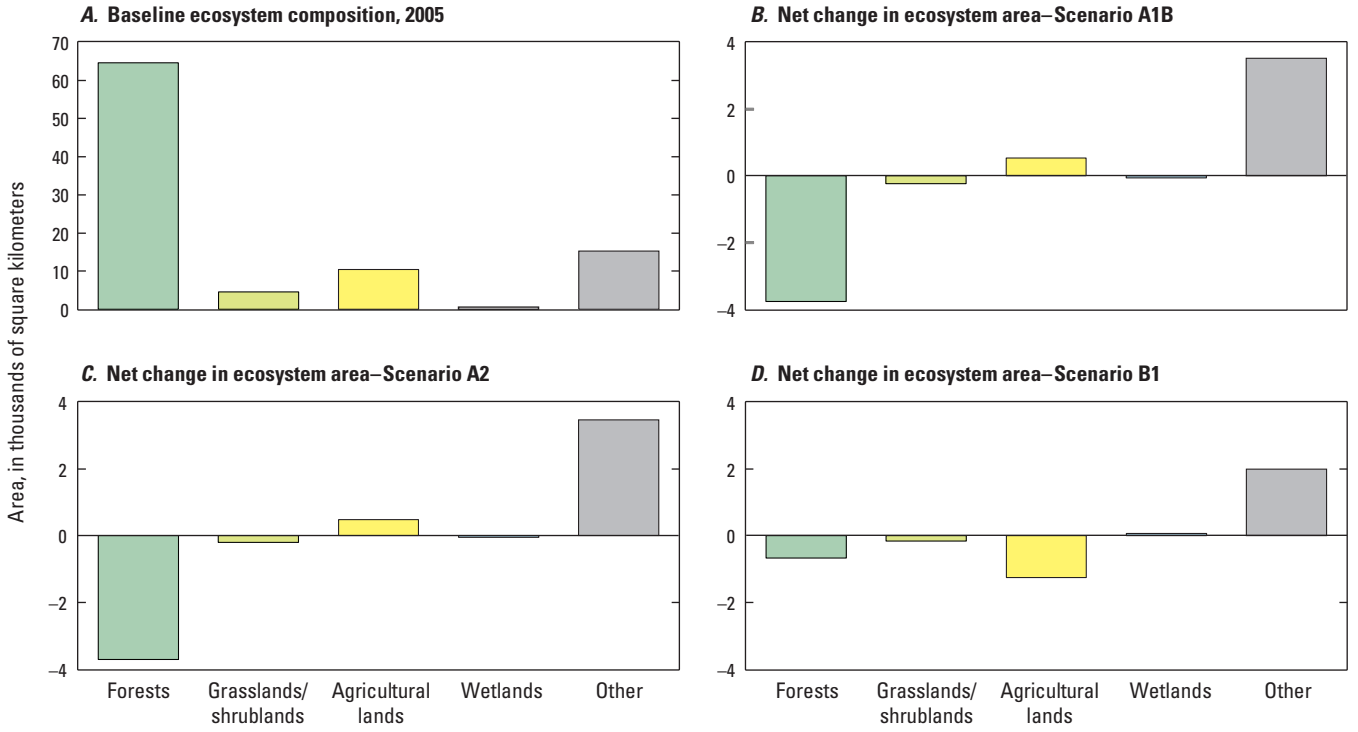

Figure 6.7. Charts showing the baseline composition of and projected net change in major ecosystems between 2005 and 2050 in the Marine West Coast Forest ecoregion, for the final year of the baseline period and for each scenario. *A*, The percent of land area assigned to each of the major ecosystems at the end of the baseline period (2005). *B*, The projected net land-use- and land-cover-change, in percent, between 2005 and 2050 for scenario A1B. *C*, The projected net land-use- and land-cover-change, in percent, between 2005 and 2050 for scenario A2. *D*, The projected net land-use- and land-cover-change, in percent, between 2005 and 2050 for scenario B1. Forests that had been harvested (logged) were included within the forest ecosystem totals. The "other" ecosystem includes developed land, mined land, barren land, and water. The large projected net changes in the "other" class were primarily attributed to the projected increases in developed land.

New developed land was projected to expand by 3,450 km^2 to 8,160 km^2 by 2050, which was an increase of 77 percent over 2005 levels. More than 500 km^2 of natural land cover (forest, wetlands, and grasslands/shrublands) was projected to be converted to agricultural land. Agricultural land was projected to increase by 5 percent, from 10,400 km^2 in 2005 to 10,900 km^2 in 2050; cultivated cropland was projected to remain relatively stable at 2,500 km^2, whereas hay/pasture was projected to increase from 7,900 km^2 to 8,410 km^2. In the Willamette Valley, agricultural land was projected to remain relatively stable, whereas in the Coast Range ecoregion, a large resource base and low demand for urban land use was projected to result in both cultivated cropland and hay/pasture land increasing by 40 km^2 and 680 km^2, respectively. By 2050, natural land cover was projected to account for 74.9 percent of all land area, while anthropogenic LULC was projected to account for 25.1 percent.

The projected LULC change was lowest under the B1 scenario. Overall, the projected forest harvest levels were the lowest of the three scenarios with roughly 23,300 km^2 of forest cutting projected to occur between 2005 and 2050, which is 25 percent less than the area projected in scenario A1B. The strong environmental regulation of public land was projected to lead to a higher proportion of forest cutting occurring in privately owned forests compared to the A1B and A2 scenarios. By 2050, nearly 80 percent of all land in the Marine West Coast Forest was projected to be natural land cover (from 75.2 percent in 2005), the highest proportion of any scenario. Developed land use was projected to expand, albeit at a slower rate than in the economically oriented scenarios. Only 2,030 km^2 of new developed lands was projected to be added by 2050 (from 4,720 km^2 in 2005), with the majority of the land conversions coming from agricultural lands and hay/pasture lands. Agricultural land was projected to decline by 12 percent with projected losses of nearly 340 km^2 of cultivated crops and 900 km^2 of hay/pasture lands; nearly 60 percent of the projected loss in agricultural land was in the Willamette Valley ecoregion. Figure 6.8 shows a comparison between projections for the A1B, A2, and B1 scenarios.

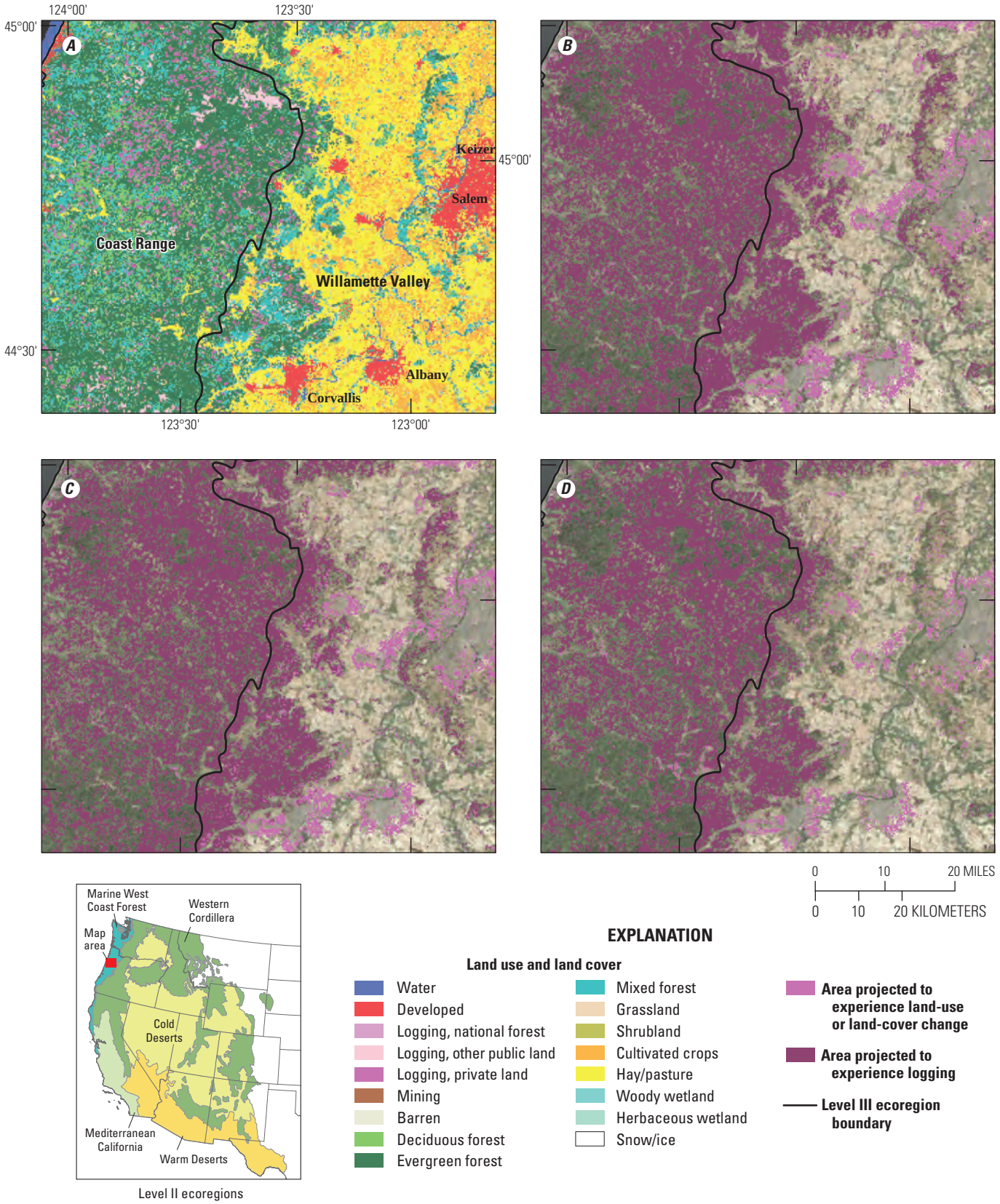

Figure 6.8. Maps showing land use and land cover (LULC) in 2005 and a comparison of projected LULC changes in the A1B, A2, and B1 scenarios in 2050 for an area near Salem, Oregon, in the Marine West Coast Forest ecoregion. Changes were projected to be the result of either land-use change or forest clearcutting. *A*, LULC in 2005. *B*, Projected LULC change in the A1B scenario. *C*, Projected LULC change in the A2 scenario. *D*, Projected LULC change in the B1 scenario.

6.3.2.3. Cold Deserts

The Cold Deserts level II ecoregion includes the following level III ecoregions: Columbia Plateau, Snake River Plain, Northern Basin and Range, Central Basin and Range, Wyoming Basin, Colorado Plateaus, and Arizona-New Mexico Plateau. The ecoregion is characterized by low rainfall and large temperature contrasts between winter and summer. This arid region has a variety of landforms, including a series of basins and mountain ranges, broad plateaus, and valleys. Rare perennial streams typically originate in the bordering mountainous ecoregions. The few small perennial streams that originate in the higher mountain ranges within the Cold Deserts commonly disappear before they reach the lower elevations, which contributes to the aridity. Natural landscapes dominate, with about three-fourths of the region covered by natural grasslands and shrublands. Agricultural land is the most common anthropogenic land use where irrigation is possible from groundwater or from the Snake or Columbia Rivers. Urbanization is sparse and dispersed because of the vast open space, limited access to water, and poor proximity to goods and services. Salt Lake City, Utah; and the Reno and Carson City, Nevada, corridor are the two most notable developed areas. Data from the USGS Land Cover Trends project indicated that only 3 percent of the Cold Deserts experienced a change in land use or land cover between 1973 and 2000 (Sleeter, Soulard, and others, 2012). Historically, the largest conversion was an increase of 6,000 km^2 in agricultural lands from grasslands/shrublands. Over 50 percent of this change occurred in the Columbia Plateau. In general, LULC change was geographically highly variable and ranged from 9.2 percent in the Columbia Plateau to 1.2 percent in the Arizona-New Mexico Plateau.

In the A1B scenario, the projected LULC change between 2005 and 2050 was characterized by agricultural expansion coupled with a moderate increase in developed lands (fig. 6.9).

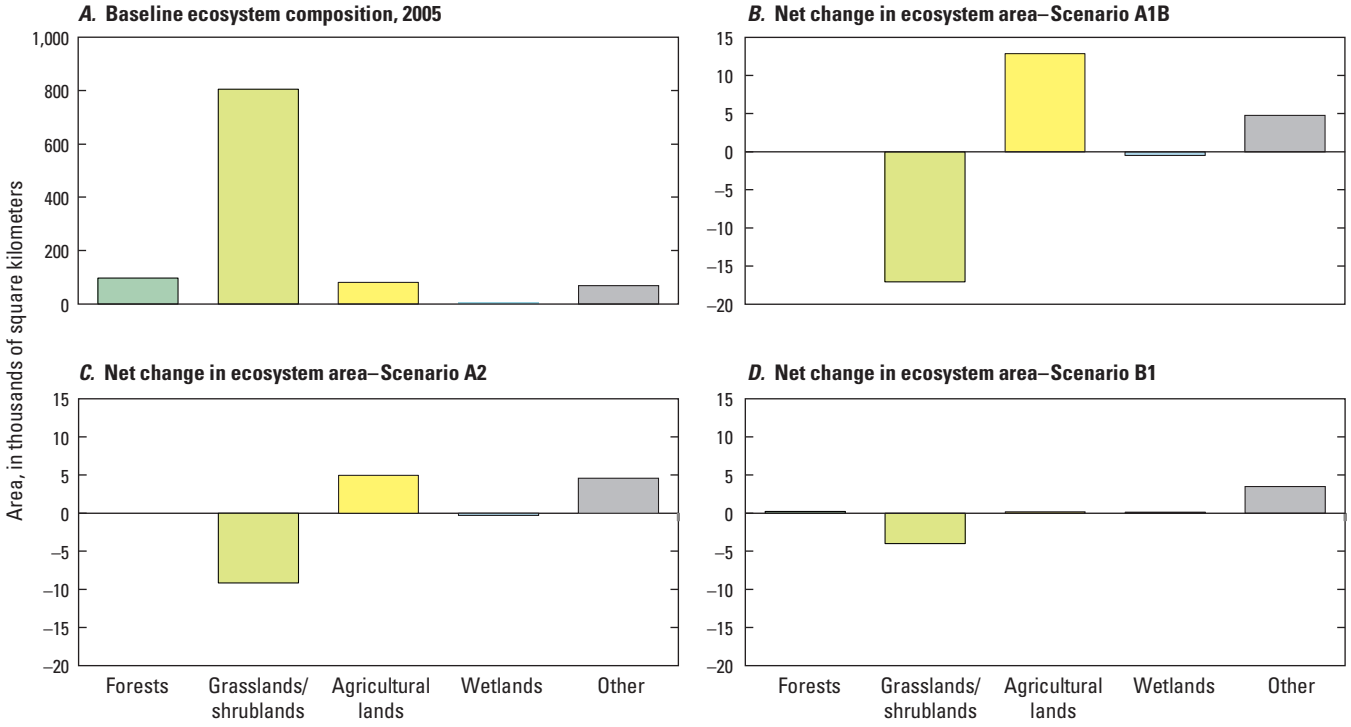

Figure 6.9. Charts showing the baseline composition of and projected net change in major ecosystems between 2005 and 2050 in the Cold Deserts ecoregion for the final year of the baseline period and for each scenario. *A*, The percent of land area assigned to each of the major ecosystems at the end of the baseline period (2005). *B*, The projected net land-use- and land-cover-change, in percent, between 2005 and 2050 for scenario A1B. *C*, The projected net land-use- and land-cover-change, in percent, between 2005 and 2050 for scenario A2. *D*, The projected net land-use- and land-cover-change, in percent, between 2005 and 2050 for scenario B1. Forests that had been harvested (logged) were included within the forest ecosystem totals. The "other" ecosystem includes developed lands, mined lands, barren lands, and water. The large projected net changes in the "other" class were primarily attributed to projected increases in developed lands.

Agricultural lands were projected to increase by 16 percent, from 81,190 km^2 in 2005 to 94,040 km^2 in 2050. The most common projected conversion was from grasslands/shrublands to agricultural lands. Approximately 80 percent of this conversion was projected to occur in the Columbia Plateau and Snake River Plain. The increase in agricultural land was driven by the projected increase of cultivated cropland (11,400 km^2) and a small projected increase in hay/pasture land (1,450 km^2). Developed land was projected to expand by 4,440 km^2 (from 6,240 km^2 in 2005). About 50 percent of the new developed land was projected to be located in the Central Basin and Range, where the urban areas associated with Salt Lake City, Utah; and Reno, Nevada, are located. Collectively, the projected expansion of agricultural and developed lands contributed to over 17,100 km^2 in grassland/shrubland losses by 2050, a 2 percent decline from the baseline areal extent. Figure 6.10 shows a comparison of agricultural growth and grassland/shrubland loss between the three scenarios.

In the A2 scenario, the projected expansions of agricultural and new developed lands were common themes, although less pronounced than in the A1B scenario. Agricultural lands were projected to increase from 81,190 km^2 in 2005 to 86,160 km^2 in 2050, while grasslands/shrublands were projected to decrease by 9,160 km^2 (from 804,700 km^2 in 2005). A total of 6,690 km^2 of grasslands/shrublands was projected to be converted to cultivated cropland between 2005 and 2050, which accounted for the largest amount of LULC change in the A2 scenario for the projected time period; however, 2,800 km^2 of cultivated cropland and hay/pasture was projected to be converted to new developed lands, thus offsetting the projected increases in agricultural land. Developed lands were projected to expand by 4,370 km^2 (from 6,240 km^2 in 2005), which is a rate similar to that projected in the A1B scenario. Collectively, the expansion of agricultural and developed lands resulted in the projected decline of grasslands/shrublands by 1 percent, from 804,660 km^2 in 2005 to 795,500 km^2 in 2050.

The projected LULC change was smallest under the B1 scenario. Between 2005 and 2050, agricultural land was projected to increase by less than 1 percent, by only 190 km^2 (from 81,190 km^2 in 2005). Cultivated crops were projected to expand by 270 km^2 (from 51,870 km^2 in 2005), while hay/pasture land was projected to decline by 80 km^2 (from 29,330 km^2 in 2005). Developed land was projected to increase by 3,620 km^2 (from 6,240 km^2 in 2005), primarily in the Central Basin and Range (by 1,700 km^2) and the Columbia Plateau (by 600 km^2). The projected loss of grasslands/shrublands to anthropogenic land use totaled 3,980 km^2 by 2050 (from 804,660 km^2 in 2005). Wetlands were projected to remain relatively stable with a small increase of 110 km^2 (from 4,640 km^2 in 2005) because of the projected reduction in demand for agricultural and developed land in this scenario.

6.3.2.4. Warm Deserts

The Warm Deserts level II ecoregion includes four level III ecoregions: Mojave Basin and Range, Sonoran Basin and Range, Madrean Archipelago, and Chihuahuan Deserts. The ecoregion is characterized by the subtropical continental Mojave, Sonoran, and Chihuahuan Deserts and the Sky Islands (mountains surrounded by lowlands of a drastically different environment in the Madrean Archipelago ecoregion). The basin-and-range terrain has typically north-to-south-trending mountains separated by broad basins, and these valleys are bordered by sloping alluvial fans. The region is also characterized by extreme aridity and extremely high air and soil temperatures. Winter snow is rare. Compared to the Cold Deserts to the north, most of the annual precipitation in these deserts falls during the summer months, contributing to a diversity of plants and animals. Desert scrub consisting of creosote bush and white bursage is common in the Mojave Desert and western and central Sonoran Desert. In the eastern Sonoran Desert, the vegetation consists of various palo verde and cacti species, and mixed scrub. The higher Chihuahuan Desert to the east consists of some desert grassland and large areas of arid shrubland dominated by creosote bush. Oaks, juniper, and pinyon woodlands occur on the higher mountains. Large parts of the Warm Deserts are Federally owned.

Urbanization was the primary projected type of LULC change in the Warm Deserts. In the A1B scenario, developed land was projected to increase by 119 percent between 2005 and 2050 with a projected increase of 6,840 km^2 of new urban-industrial areas. Nearly all of the new developed land use was projected to be converted from the grasslands/shrublands ecosystems, which were projected to decline by 2 percent, from 403,390 km^2 in 2005 to 395,350 km^2 in 2050. The projected spatial pattern of urbanization was distributed heterogeneously across the landscape, with most expansion projected to occur adjacent to the Las Vegas, Nevada, Phoenix, Arizona, and Tucson, Arizona, metropolitan areas. Urban expansion was also projected to be common along the boundary of the Mojave Basin and Range and the Southern California Mountains near the Los Angeles, California, metropolitan area. Major environmental factors (limited moisture and high temperatures) potentially limit the expansion of agricultural lands throughout the Warm Deserts; however, small areas, generally near perennial streams, potentially could support the production of cultivated crops and hay/pasture land. These areas were projected to increase by 7 percent in the A1B scenario, from 11,340 km^2 in 2005 to 12,130 km^2 in 2050. Forests and wetlands remained relatively unchanged throughout the projection period.

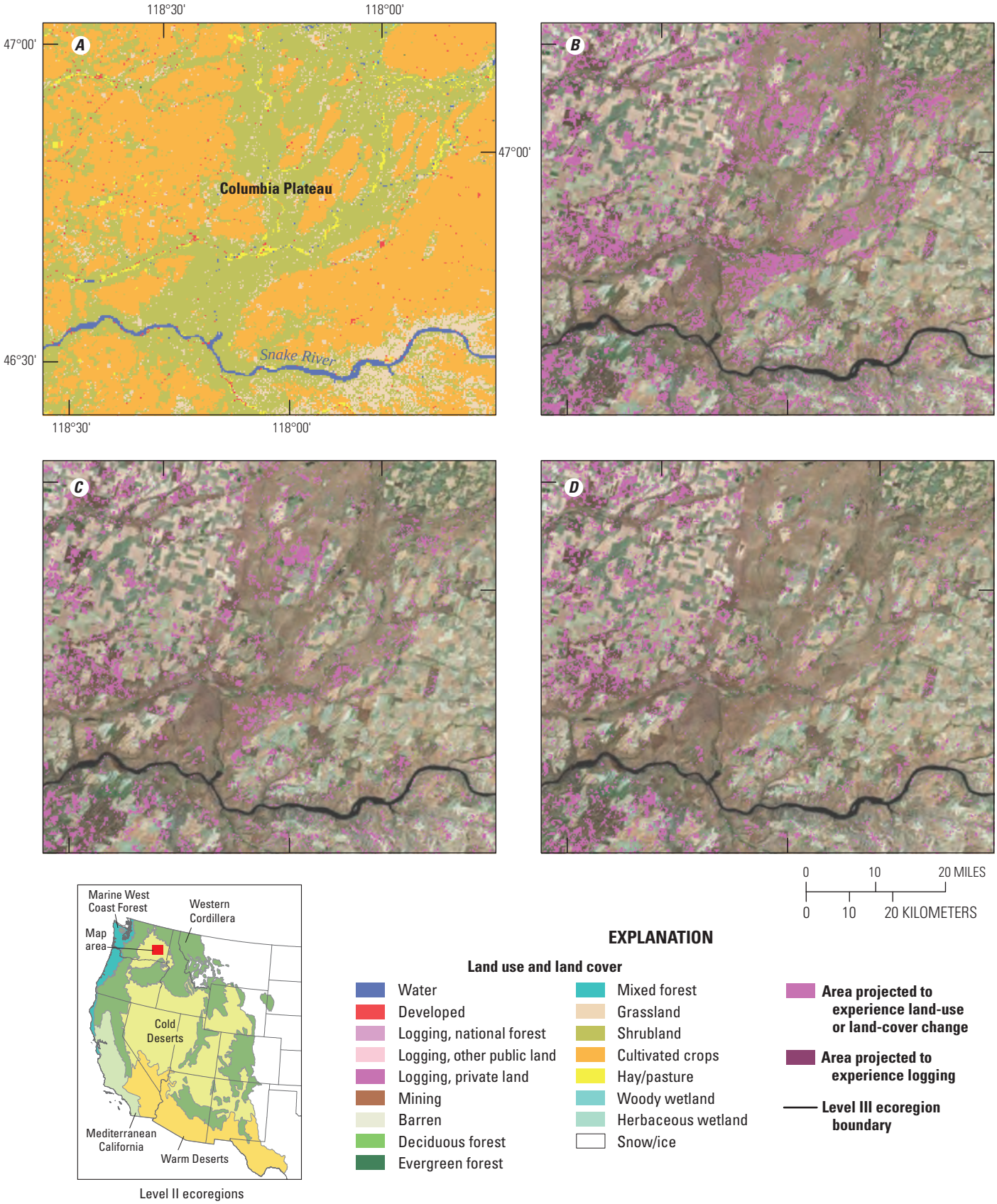

Figure 6.10. Maps showing land use and land cover (LULC) in 2005 and a comparison of the A1B, A2, and B1 scenarios in 2050 for an intensively agricultural area along the Snake River in Washington in the Cold Deserts ecoregion. Changes were projected to be the result of either land-use change or forest clearcutting. *A*, LULC in 2005. *B*, Projected LULC change in the A1B scenario. *C*, Projected LULC change in the A2 scenario. *D*, Projected LULC change in the B1 scenario.

The A2 scenario had the smallest projected increase in new developed land of all the scenarios. New urban areas were projected to increase 71 percent, from 5,750 km^2 in 2005 to 9,810 km^2 in 2050. The result is a projected 1 percent decline in grasslands/shrublands (a projected loss of 4,860 km^2). All of the other ecosystems remained relatively stable throughout the projection period (fig. 6.11). In the B1 scenario, developed land was projected to increase by 86 percent, rising to 10,710 km^2 by 2050. As in the economically oriented scenarios, the vast majority of the projected new developed land resulted from the projected conversion of grasslands/shrublands. Overall, grassland/shrublands were projected to decline by 5,340 km^2, a loss of 1 percent of their area from 2005. Forests, agricultural lands, and wetlands were projected to remain relatively stable (fig. 6.11). Figure 6.12 shows both the initial and the projected urbanization near Las Vegas, Nevada, in all three scenarios.

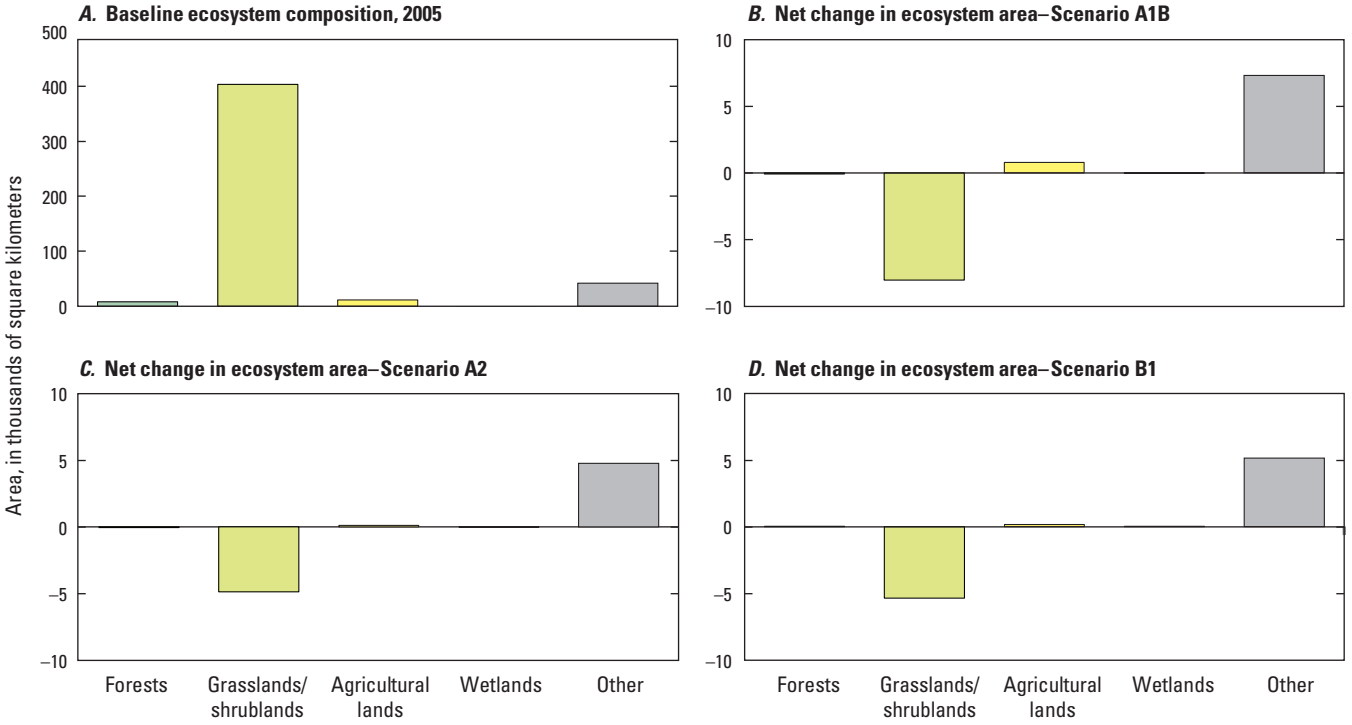

Figure 6.11. Charts showing the baseline composition of and projected net change in major ecosystems between 2005 and 2050 in the Warm Deserts ecoregion for the final year of the baseline period and for each scenario. *A*, The percent of land area assigned to each of the major ecosystems at the end of the baseline period (2005). *B*, The projected net land-use- and land-cover-change, in percent, between 2005 and 2050 for scenario A1B. *C*, The projected net land-use- and land-cover-change, in percent, between 2005 and 2050 for scenario A2. *D*, The projected net land-use- and land-cover-change, in percent, between 2005 and 2050 for scenario B1. Forests that had been harvested (logged) were included within the forest ecosystem totals. The "other" ecosystem includes developed lands, mined lands, barren lands, and water. The large projected net changes in the "other" ecosystem were primarily attributed to projected increases in developed lands.

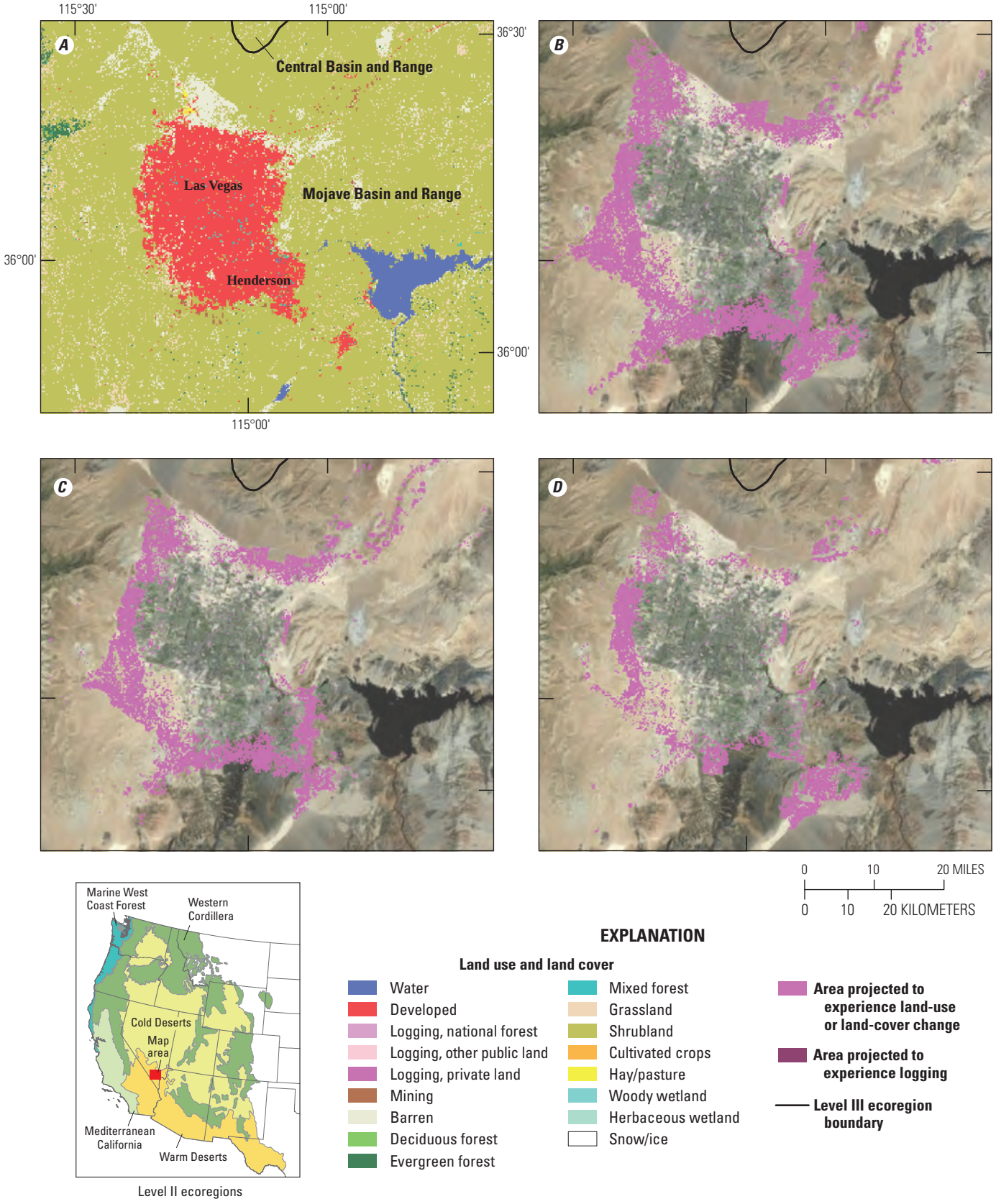

Figure 6.12. Maps showing land use and land cover (LULC) in 2005 and a comparison of the A1B, A2, and B1 scenarios in 2050 for the Las Vegas, Nevada, area in the Warm Deserts ecoregion. Changes were projected to be the result of either land-use change or forest clearcutting. *A*, LULC in 2005. *B*, Projected LULC change in the A1B scenario. *C*, Projected LULC change in the A2 scenario. *D*, Projected LULC change in the B1 scenario.

6.3.2.5. Mediterranean California

The Mediterranean California level II ecoregion includes three unique level III ecoregions in California: the Southern and Central California Chaparral and Oak Woodlands (referred to herein as "Oak Woodlands" for simplicity), the Central California Valley, and the Southern California Mountains. The ecoregion is distinguished by its warm, mild Mediterranean climate with alternating wet and dry seasons. There is great variability in annual precipitation, and extreme droughts are not uncommon. The shrubland vegetation of chaparral mixed with areas of grassland and oak savanna is prone to wildland fires. The ecoregion has several agriculturally productive valleys and contains a high population (over 30 million people) in extensive urban agglomerations. Low coastal mountain ranges and the Sierra Nevada foothills surround the broad San Joaquin and Sacramento Valleys. Higher mountain ranges are located in the southern part of the ecoregion, which includes large areas of Federally owned land. In the larger valleys, the hydrological and ecological systems have been greatly altered by widespread agriculture and some sprawling urban and suburban development. Recent historical LULC change has been characterized most visibly by rapid urbanization. The Oak Woodlands and the Central California Valley combined contain most of the population of California, which has seen a 37 percent increase in the State's developed landscape since 1973 (Sleeter and others, 2011). Demand for agricultural land has also been an important component of LULC change in the ecoregion despite remaining relatively stable in terms of total area. Agricultural land in some parts of the ecoregion expanded while others experienced losses (Sleeter and others, 2011).

Urban development was the primary type of projected LULC change in the ecoregion in all three of the scenarios. In the A1B scenario, developed land was projected to increase 89 percent, from 13,160 km^2 in 2005 to 24,820 km^2 in 2050. New developed land was projected to increase primarily in the Oak Woodlands (7,650 km^2) and the Central California Valley (3,040 km^2). The low-lying valleys of the Oak Woodlands and periphery of large urban areas in the Central California Valley were projected to be the main locations for urban expansion. Grasslands/shrublands were projected to experience the largest change of any LULC class, declining 17 percent between 2005 and 2050 (from a baseline of 74,300 km^2) while forests and wetlands were projected to remain relatively stable (fig. 6.13). Agricultural lands were projected to increase by 1,320 km^2 by 2050 (from 41,050 km^2 in 2005); however, projected changes involving agricultural lands affected a much greater area than is reflected in the net change projections alone. For example, 4,750 km^2 of agricultural land was projected to be converted to developed land, whereas only 870 km^2 of agricultural land was projected to be converted to grasslands/shrublands. Conversely, the projected increased demand for new agricultural land resulted in a projected 6,700 km^2 of grassland/shrubland converting into new cultivated croplands or hay/pasture lands.

In the A2 scenario, developed land was projected to increase by 62 percent, from 13,160 km^2 in 2005 to 21,380 km^2 in 2050. The location of new developed land was projected to be generally in the same areas as in the A1B scenario, with the vast majority in the Oak Woodlands (62 percent) and Central California Valley (33 percent). New developed land was projected to increase by approximately 450 km^2 in the Southern California Mountains. The high demand for new developed land was projected to result in a 2 percent decline in agricultural lands (from 41,050 km^2 in 2005 to 40,060 km^2 in 2050) and an 8 percent decline in grasslands/shrublands (from 74,300 km^2 in 2005 to 67,390 km^2 in 2050) (fig. 6.13). By 2050, 3,870 km^2 of grasslands/shrublands and 4,200 km^2 of agricultural land was projected to be converted to new developed land; however, like the A1B scenario, the projected net change masked overall projected rates of LULC change; 3,600 km^2 of grasslands/shrublands were projected to be converted into agricultural land, whereas 530 km^2 of agriculture was projected to be converted into grasslands/shrublands. Forests and wetlands remained relatively stable (fig. 6.13).

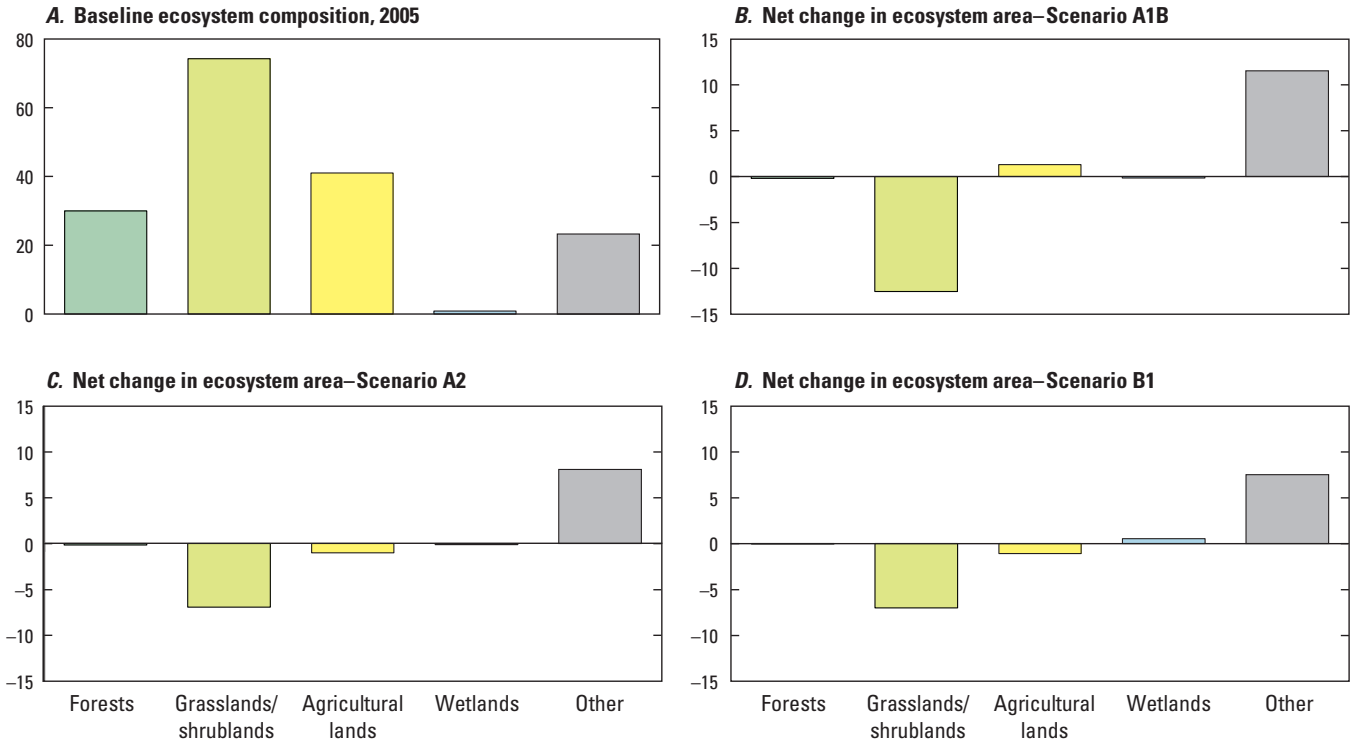

Figure 6.13. Charts showing the baseline composition of and projected net change in major ecosystems between 2005 and 2050 in the Mediterranean California ecoregion for the final year of the baseline period and for each scenario. *A*, The percent of land area assigned to each of the major ecosystems at the end of the baseline period (2005). *B*, The projected net land-use- and land-cover-change, in percent, between 2005 and 2050 for scenario A1B. *C*, The projected net land-use- and land-cover-change, in percent, between 2005 and 2050 for scenario A2. *D*, The projected net land-use- and land-cover-change, in percent, between 2005 and 2050 for scenario B1. Forests that had been harvested (logged) were included within the forest ecosystem totals. The "other" ecosystem includes developed lands, mining lands, barren lands, and water. The large projected net changes in the "other" ecosystem were primarily attributed to projected increases in developed lands.

Despite dramatically different storylines, by 2050 the B1 scenario was projected to follow trends in LULC change that were similar to those in the A2 scenario. Developed land was projected to increase by 57 percent (7,500 km^2), with most of the expansion projected to occur in the Oak Woodlands and Central California Valley. Nearly 4,940 km^2 of grasslands/shrublands were projected to be converted to developed lands, whereas 2,500 km^2 of agricultural land was projected to be converted to developed land. By 2050, agricultural land was projected to decline by 3 percent, from 41,050 km^2 to 39,980 km^2. Also similar to the A2 scenario was the projected 9 percent decline in grasslands/shrublands needed to meet the projected demand for new developed land and agricultural land. Forests remained relatively unchanged at approximately 29,950 km^2. The greatest divergence from the economically oriented scenarios was the projected trend in wetlands. The strengthening of environmental protection in the B1 scenario resulted in a projected increase in wetlands of 62 percent, from approximately 910 km^2 to 1,470 km^2. Figure 6.14 shows both the initial LULC and the projected modeling results for each scenario for an area near Sacramento, California, in the Central California Valley.

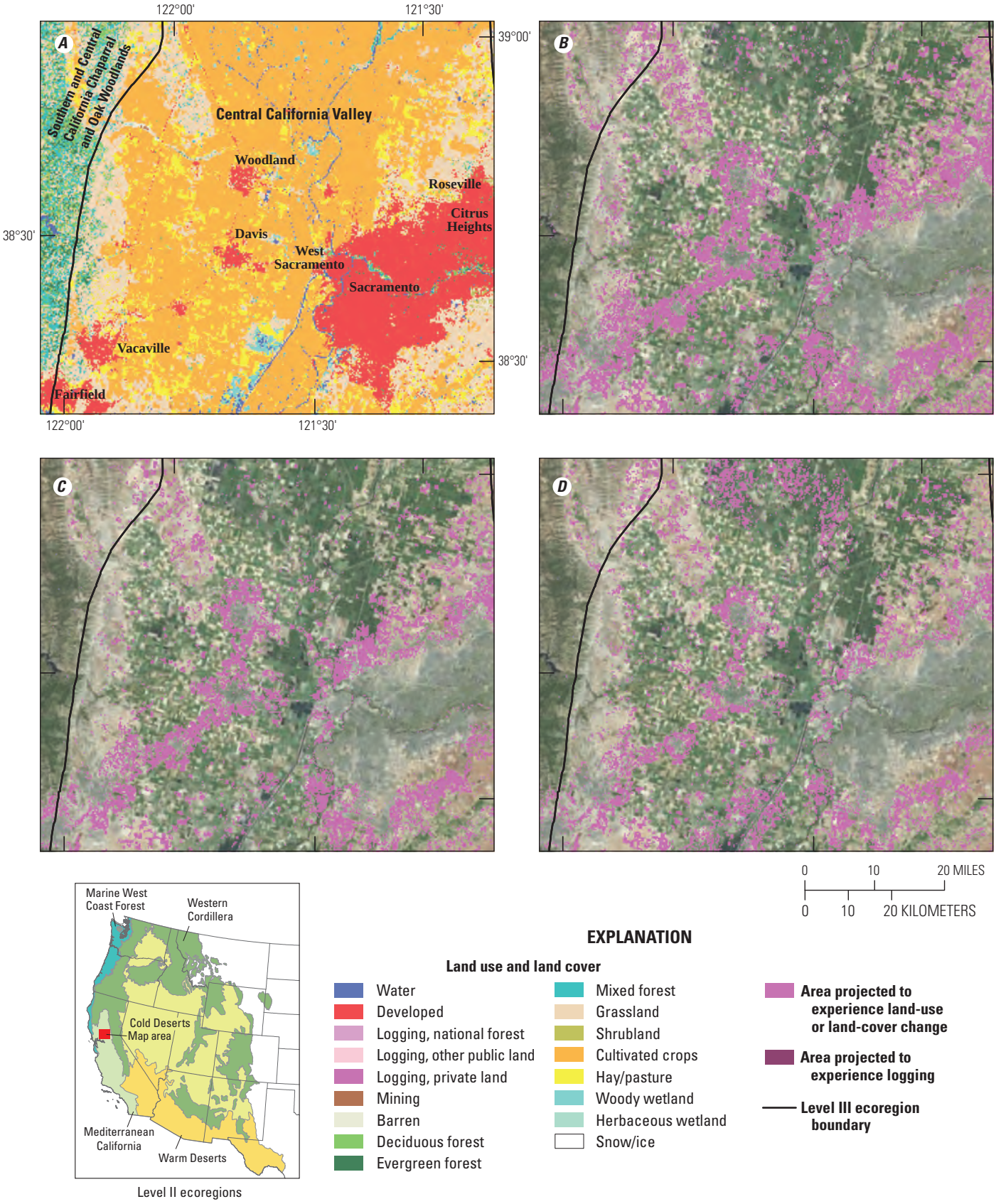

Figure 6.14. Maps showing land use and land cover (LULC) in 2005 and a comparison of the A1B, A2, and B1 scenarios in 2050 for an area near Sacramento, California, in the Mediterranean California ecoregion. *A*, LULC in 2005. *B*, Projected LULC change in the A1B scenario. *C*, Projected LULC change in the A2 scenario. *D*, Projected LULC change in the B1 scenario. Changes were projected to be the result of either land-use change or forest clearcutting.

6.4. Validation and Uncertainty

A formal validation of the projected LULC changes is impossible because there is no reference data for a future time frame. Chapter 2 provides a summary of validation concerns for the LULC modeling they applied to the baseline period; however, the same quantity and allocation disagreement measures discussed in chapter 2 can be used to examine issues of uncertainty in the projected period of 2006 to 2050, and more specifically, to examine the sources of the differences between modeled scenarios (Pontius and Millones, 2012; Sohl, Sleeter, Zhu, and others, 2012). In this context, a quantity disagreement measure can be used to examine the differences in projected LULC proportions between scenarios, and an allocation disagreement measure can be used to examine differences in how the projected LULC changes are spatially allocated between scenarios.

In this assessment, the proportions of the projected LULC change in the scenarios themselves were used to frame overall uncertainties regarding future LULC proportions. Given that the FORE–SCE model can duplicate scenario-prescribed LULC proportions, there were no uncertainty issues related to the ability to accurately map the quantity of LULC change. Quantity disagreement was thus used to examine differences in the prescribed proportions of LULC change from the scenarios themselves. The spatial modeling component of the FORE–SCE model introduced allocation disagreement between scenarios in that the spatial pattern of change differed between scenarios even if the prescribed scenario LULC proportions were similar. An application of quantity and allocation disagreement measures to each scenario pair allowed for a determination of whether the differences between scenarios were because of the scenario LULC prescriptions themselves or were a result of the spatial modeling and the placement of LULC change.

The proportion of quantity disagreement and allocation disagreement varied by scenario pair (fig. 6.15). Total disagreement was lowest between the A2-B1 scenario pair, and higher but similar for the A1B-A2 and A1B-B1 pairs. Despite that similarity, quantity disagreement made up a much higher percentage of the total disagreement in the A1B-B1 scenario pair. In all of the scenario pairs, allocation disagreement made up a significantly higher proportion of the total disagreement than did quantity disagreement, which indicated that on a per-pixel basis, the differences between the spatially explicit scenarios were due more to the FORE–SCE spatial allocation model than to quantitative differences in the prescribed amounts of LULC change from the scenarios. These differences were expected, given the relatively low amount of LULC change projected to occur in the Western United States; however, the scenario-specific parameterization of the FORE–SCE model was a contributing factor. For example, assumptions were made that urban development will be more compact in the B1 scenario than in the two other scenarios, and the FORE–SCE model was parameterized accordingly for the individual scenarios. The parameterization of the spatial model thus affected the spatial allocation of change, and, as a result, the proportion of disagreement due to allocation. It is impossible to determine how much of the allocation disagreement is due to the random nature of the placement of LULC change versus the difference in model parameterization between scenarios. Overall, it is clear that the A1B and B1 scenarios were most dissimilar when accounting for the quantified scenarios, as that scenario pair exhibited the highest overall quantity disagreement.

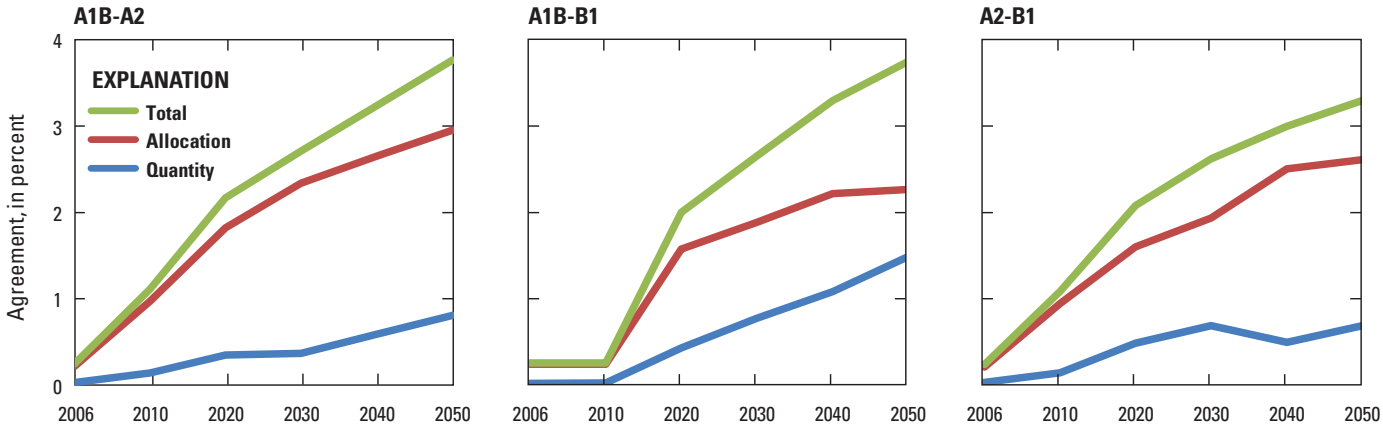

Figure 6.15. Graphs showing the quantity and allocation disagreement by scenario pair from 2006 to 2050. The total disagreement between scenario pairs is similar for A1B-A2, and A1B-B1 and smaller for A2-B1. Allocation disagreement makes up a higher proportion of total disagreement than does quantity disagreement for all scenario comparisons.

Chapter 7. Climate Projections Used for the Assessment of the Western United States

By Anne Wein[1], Todd J. Hawbaker[2], Richard A. Champion[1], Jamie L. Ratliff[1], Benjamin M. Sleeter[1], and Zhiliang Zhu[3]

7.1. Highlights

- Models of projected climate change were used in this assessment to further interpret the effects of climate change on the potential for carbon sequestration and greenhouse-gas (GHG) emissions in terrestrial ecosystems in the ecoregions of the Western United States. Climate-change data were used to support two modeling exercises: future potential wildland-fire emissions (chapter 8 of this report) and future potential carbon storage and sequestration (chapter 9 of this report).
- Climate-change data were represented in three general circulation models (GCMs) for each of three scenarios (A1B, A2, B1). The models of wildland fires and the biogeochemical modeling of carbon and GHGs used different sources of downscaling for the same GCMs because of the tasks' unique requirements. The projected patterns of precipitation differed between the two sources, particularly in mountainous areas.
- The models indicated a projected seasonal increase in mean temperature throughout the Western United States. Warming was projected to be most prevalent in summer and fall and in the eastern part of the Western United States.
- The projected warming was greater in scenarios A1B and A2; the MIROC 3.2-medres model projected the most warming and the CSIRO–Mk3.0 model projected the least. The projected increases in seasonal temperature extremes (minimums and maximums) generally followed patterns of projected increases in mean temperature.
- The projected precipitation patterns were highly variable among the GCMs, scenarios, seasons, and within the level II ecoregions, which necessitated the analyses of variabilities within each ecoregion.
- The variability in temperature and precipitation changes of the GCMs made the ranges of climate change for each scenario less distinct.

7.2. Introduction

Climate-change projections are required for modeling future potential ecosystem properties and processes. This chapter characterizes the baseline climate data and the projected climate-change data from general circulation models (GCMs); these data were used in this assessment for the wildland-fire-emission modeling discussed in chapter 8 and for the terrestrial ecosystem carbon-storage and GHG-flux modeling discussed in chapter 9. The relation between this chapter and other chapters of this report is shown in figure 1.2 of chapter 1 of this report, where climate data is featured in the "input data" and "climate projections" boxes of the diagram.

The term "climate change" refers to the changes in daily and weekly weather over months, seasons, centuries, and millennia. The climate affects the carbon cycle in terrestrial and aquatic systems through biogeochemical processes and natural disturbances (such as wildland fires), and also influences where land-use and land-cover (LULC) changes occur. This assessment sought to answer two questions related to the effects of climate change on carbon sequestration and GHG fluxes: (1) What are the projected potential changes to the critical climate variables within the ecoregions of the Western United States, and (2) What are the uncertainties for the climate-change projections in each of the ecoregions?

The climate-change data described here, along with the projected LULC scenarios (chapter 6) were aligned with the Intergovernmental Panel on Climate Change's Special Report on Emission Scenarios (IPCC–SRES; Nakicenovic and others, 2000). Although multiple scenarios (A1B, A2, and B1) provided the emission projections, the assessment used outputs from the GCMs, which were forced by the scenarios to capture the uncertainties of the analyses. The three GCMs used in this study are The Third Generation Coupled Global Climate Model of the Canadian Centre for Climate Modelling and Analysis (CCCma CGCM 3.1), Australia's Commonwealth Scientific and Industrial Research Organisation Mark 3.0 (CSIRO–Mk3.0) model, and the Model for Interdisciplinary Research on Climate version 3.2, medium resolution (MIROC 3.2-medres). The selection of GCMs represents a range of projected climate change that was constrained by the availability of suitably downscaled versions and resources to simulate multiple effects of climate change.

[1]U.S. Geological Survey, Menlo Park, Calif.

[2]U.S. Geological Survey, Denver, Colo.

[3]U.S. Geological Survey, Reston, Va.

The GCMs are mathematical representations of atmospheric, oceanic, cryospheric, and land-surface processes that express how those processes interact and respond to changes in GHG concentrations (Randall and others, 2007; U.S. Climate Change Science Program (CCSP), 2008). The GCMs subdivide the world into volumetric pixels (voxels) representing the layers of the atmosphere, land, and ocean at regularly spaced locations. The GCM outputs may include hourly, daily, and monthly estimates of temperature, precipitation, air pressure, wind, cloud cover, soil moisture, snow, humidity, or short- and long-wave fluxes of solar radiation. According to McAvaney and others (2001), projected surface-air temperatures generally have less uncertainty than projected precipitation, whereas projected cloud cover and humidity have the greatest uncertainty. Each GCM made different assumptions about global energy budgets; therefore, no single GCM projection was considered to be valid on its own and multiple models complement each other (Pierce and others, 2009). The components of this assessment that relied on GCM outputs incorporated data from multiple GCMs to help characterize uncertainties in climate projections.

The GCM outputs generally were produced at a coarse spatial resolution on the order of 1° to 3°, and spatial downscaling was performed to produce the resolution required for regional analyses. Fowler and others (2007) observed that, in general, downscaled temperature variables were more consistent with the original data than downscaled precipitation variables; downscaled winter climate variables were more consistent with the original data than downscaled summer climate variables; and downscaled wetter climate variables were more consistent with the original data than downscaled drier climate variables. These temperature and precipitation observations were not confirmed in a separate study for the Western United States (Pierce and others, 2009). Temperature and precipitation were the most common variables used in this assessment when the influence of climate change on carbon cycling was simulated. Other climate-related variables, such as humidity, were then derived from temperature and precipitation. Therefore, the discussion of potential climate change focuses on temperature and precipitation variables.

Climate and weather input data were required in order to model both wildland fires (chapters 3 and 8) and biogeochemical processes of carbon and GHG fluxes (chapters 5 and 9); however, two sources of downscaled climate and weather data were used for the same GCMs because of the unique requirements of the respective models.

The wildland-fire analyses (chapters 3 and 8) required daily weather data, including temperature, precipitation, relative humidity, and wind speeds for both the baseline and future time periods. The daily weather data were originally measured at weather stations, but were interpolated to 1/8° spatial resolution (approximately 12 km) for the conterminous United States (Maurer and others, 2002). These data span the years 1950 to 2010 and include minimum and maximum daily temperature and daily precipitation. The afternoon wind speeds and directions were taken from the 1/3° (approximately 32-km resolution) North American Regional Reanalysis data (Mesinger and others, 2006) and were joined to the daily temperature and precipitation data assembled by Maurer and others (2002). To model projected future wildland fires and emissions, the data from the three GCMs and the three climate-change scenarios were corrected for biases and downscaled to the baseline weather data (Maurer and others, 2002, 2007). Figures 7.1 and 7.2 show the baseline (1970–1999) mean daily temperature (in degrees Celsius, °C) and total precipitation (in centimeters) by season in both map and graph formats, which are based on data from Maurer and others (2002).

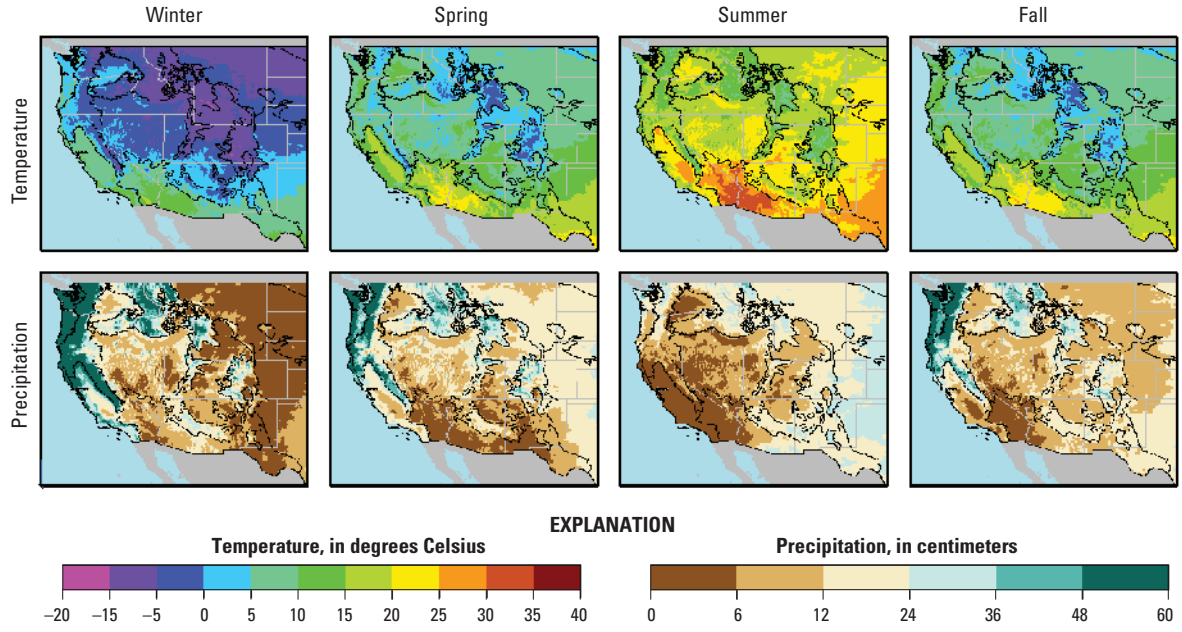

Figure 7.1. Maps showing the baseline (1970–1999) seasonal mean daily temperature (in degrees Celsius, °C) and total precipitation (in centimeters) by season. Data were from Maurer and others (2002). Winter included December, January, and February; spring included March, April, and May; summer included June, July, and August; and fall included September, October, and November.

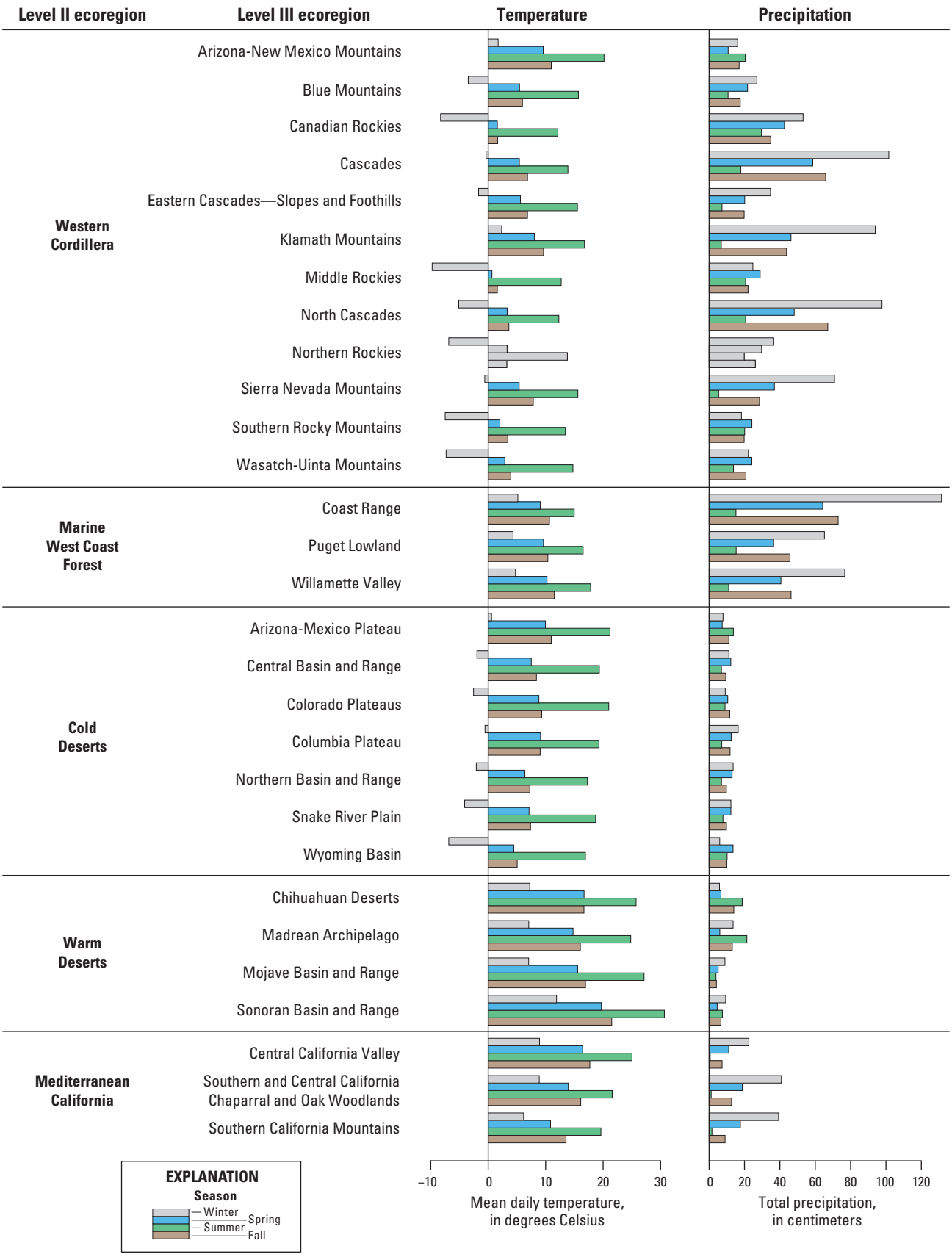

Figure 7.2. Chart showing the baseline summaries of mean daily temperature (in degrees Celsius, °C) and total precipitation (in centimeters) by season and grouped by both level II and level III ecoregions. Data were from Maurer and others (2002).

The biogeochemical modeling framework (chapter 9 of this report) required climate data that characterized the monthly mean of daily minimum and maximum temperatures and the monthly precipitation. For both the model testing period (that is, model spin up) from 1992 to 2000 and the baseline time period (2001–2005), these data were derived from the PRISM climate dataset (Daly and others, 2000; PRISM Climate Group, 2012) at 4-km spatial resolution. The projected monthly mean of daily minimum and maximum temperatures and the projected monthly precipitation were provided by the three GCMs under all three scenarios (Joyce and others, 2011). Change factors were calculated at the original resolution of the GCMs relative to the 1961 to 1990 normals, which were then spatially downscaled using ANUSPLIN software (Hutchinson, 2010) and added to (for temperatures) or multiplied by (for precipitation) the historical normals to produce the future climate projections at 1/12° resolution (approximately 10 km).

7.3. Climate Patterns

Visualizations of seasonal baseline climate patterns and potential future changes are presented in figure 7.3 for each GCM and each climate-change scenario used in the assessment. Descriptions are provided to the extent possible for within-ecoregion variations by using the level III ecoregion names (EPA, 1999); please refer to figure 1.1 of chapter 1 of this report for the geographic locations of the level II and III ecoregions. The seasonal aggregation of results reduced the information about monthly variations while preserving information aligned with the seasonal carbon cycles of winter carbon sources and summer carbon sinks (Miller, 2008). The climate variables included the temperature and precipitation variables used in the disturbance and terrestrial biogeochemical components: mean daily temperature, monthly minimum and maximum temperatures, and total precipitation.

7.3.1. Baseline Climate Patterns of the Western United States

Assessments of climate change are usually made relative to a baseline period that provides benchmark climate summaries. The choice of baseline periods is somewhat arbitrary, but for climate summaries, a 30-year period is desirable. For this general overview of potential long-term climate changes, the baseline period was the recent and relatively stable (climatically) period of 1970 to 1999.

The modeled baseline data indicated that the baseline mean daily temperatures and total precipitation had high spatial and seasonal variability across the Western United States (figs. 7.1 and 7.2). Summer temperatures were most extreme in the Warm Deserts level II ecoregion, where mean daily summer temperatures were as high as 31°C in the Sonoran Basin and Range level III ecoregion. In contrast, the Western Cordillera level II ecoregion tended to include the coldest winter temperatures, with mean daily temperatures reaching as low as −10°C in the Middle Rockies level III ecoregion and −7°C in the Southern Rockies and Wasatch-Uinta Mountains level III ecoregions. The Wyoming Basin level III ecoregion in the Cold Deserts level II ecoregion had the greatest range of seasonal temperatures, with a 24°C difference between summer and winter. In other level II ecoregions, such as the Marine West Coast Forest and Mediterranean California, the seasonal temperature variability was relatively low and temperatures remained above freezing for most of the year.

The Marine West Coast Forest level II ecoregion received extreme precipitation, up to an average of 1,841 millimeters per year (mm/yr). At the other extreme, the annual precipitation in the Warm Deserts and Cold Deserts level II ecoregions averaged only 268 and 313 mm/yr, respectively. For most of the level II ecoregions in the Western United States, the majority of the precipitation fell primarily during the winter, with the spring and fall receiving lesser amounts. Summer tended to be the driest season in most areas except in the Warm Deserts level II ecoregion.

7.3.2. Projected Climate Patterns of the Western United States

The climate projections for 2040 to 2069 were compared with the baseline data from 1960 to 1999 in order to capture gross patterns of climate change. The variability in climate-change projections appeared to be greater among the GCMs than among the three IPCC–SRES scenarios. The maps in figure 7.3 show the projected changes in mean daily temperatures and mean total precipitation, by season, scenario, and GCM. The graphs in figure 7.4 show the projected changes in mean daily temperature and precipitation, by season for each ecoregion. The maps and graphs were based on data from Maurer and others (2007). All of the GCMs projected climate warming throughout the entire region. The projected warming was most pronounced in fall and summer; however, in the northern and central Columbia Plateau and Northern Basin and Range (of the Cold Deserts) and the Blue Mountains and Northern Rockies (of the Western Cordillera), the greater projected increases in mean temperature occurred in the winter and were associated mostly with projected increases in the mean winter minimum temperatures rather than projected increases in the mean winter maximum temperatures. The least amount of projected temperature change occurred in the spring for all ecoregions, with the exceptions of (1) the Warm Deserts and (2) the Arizona-New Mexico Mountains in the southernmost part of the Western Cordillera ecoregion, where the least amount of temperature change occurred in the winter.

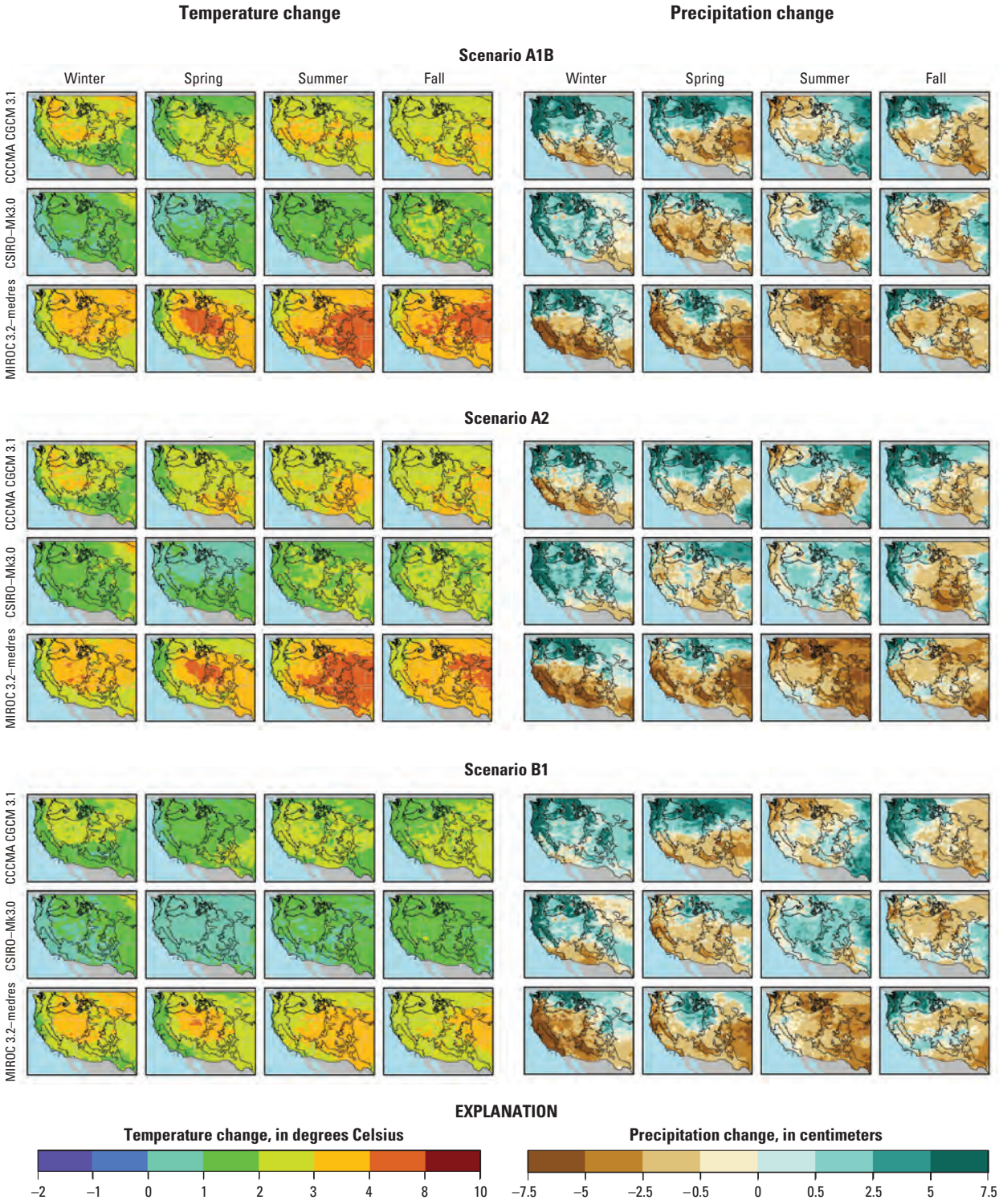

Figure 7.3. Maps showing the projected changes in mean daily temperature (in degrees Celsius, °C) and total precipitation (in centimeters) by season, calculated using the difference in mean values from 2040 to 2069 and from 1970 to 1999. Data were from Maurer and others (2007).

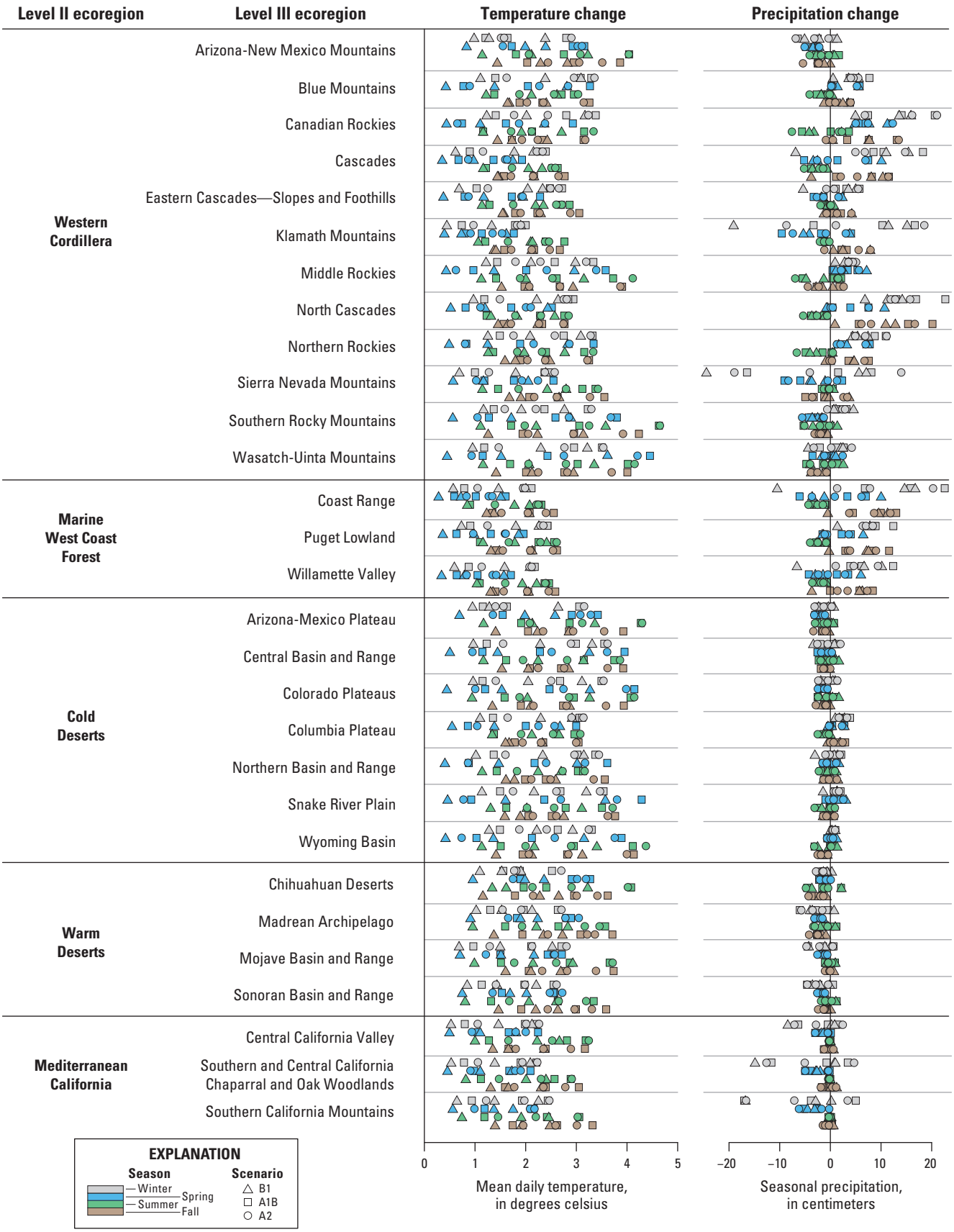

Figure 7.4. Chart showing summaries of the projected seasonal changes in mean daily temperature (in degrees Celsius, °C) and total precipitation (in centimeters) by season and grouped by both level II and III ecoregions for all general circulation models and scenarios. Squares represent the A1B scenario, circles represent the A2 scenario, and triangles represent the B1 scenario. Data were from Maurer and other (2007).

Overall, seasonal warming was projected to be greatest under the A1B and A2 scenarios and least under the B1 scenario. There was variability in the projected temperature changes among the GCMs. The greatest projected increases in mean temperature were from the MIROC 3.2-medres model for the A1B and A2 scenarios in the eastern parts of the Western United States. Specifically, the projected seasonal mean temperature exceeded 4°C during the nonwinter seasons in the Middle Rockies, Wasatch-Uinta Mountains, Southern Rockies, and Arizona-New Mexico Mountains in the eastern Western Cordillera ecoregion; the Wyoming Basin, Colorado Plateaus, and Arizona-New Mexico Plateau in the Cold Deserts ecoregion; and the Chihuahuan Deserts in the Warm Deserts ecoregion. Similarly, the greatest projected increases in mean seasonal maximum temperatures of 4°C to 6°C occurred in these same ecoregions during nonwinter months, particularly in the summer. In contrast, the CSIRO–Mk3.0 model projected the smallest temperature increases. In particular, the projected change in mean spring temperature from the CSIRO–Mk3.0 model for the B1 scenario was less than 0.5°C in the Marine West Coast Forest ecoregion and parts of adjacent regions and in the nearby Eastern Cascades—Slopes and Foothills in the Western Cordillera ecoregion.

Across all of the climate-change scenarios and GCMs, the variability in the projected warming (as measured by the standard deviation) was greatest in the eastern ecoregions of the Western United States and corresponded largely with those ecoregions where relatively large increases in mean and maximum temperatures were projected and least in the western ecoregions located in California and western Oregon and Washington.

The fire-disturbance-modeling data source presented distinct precipitation change patterns in geographical areas of the Western United States. Table 7.1 summarizes these patterns of mean change from all the scenarios and GCMs in terms of level II and level III ecoregions. In this dataset, only the Marine West Coast Forest and Mediterranean California level II ecoregions had a consistent projected seasonal precipitation change pattern across GCMs and scenarios. The projected precipitation patterns varied geographically within the other level II ecoregions. Overall, the projected increases in mean seasonal precipitation occurred in the northern and western portions of the Western United States, especially in the winter, spring, and fall; however, projected summer precipitation tended to decrease in these areas. In the southern and eastern portions of the Western United States, precipitation was projected to decrease during most seasons. In regions where mean seasonal precipitation was projected to decrease, the reductions were most prevalent during the spring and winter (in the west) and during the fall (in the east).

The greatest precipitation reductions were from the MIROC 3.2-medres model. The projected reductions occurred mostly in winter, but also in the spring across all climate-change scenarios in the Mediterranean California ecoregion and in the Sierra Nevada Mountains in the Western Cordillera ecoregion. The projected decreases in mean seasonal precipitation ranged from 7 to 24.5 cm, with the greatest projected decrease occurring in the Sierra Nevada Mountains. Across all of the GCMs, the greater projected precipitation decreases and lesser projected precipitation increases were associated with the B1 scenario. Conversely, the greatest projected seasonal precipitation increases of 10 to 22 cm were associated most often with the A1B and A2 scenarios and by the CCCma CGCM 3.1 model in the winter and fall in the Marine West Coast Forest and in the level III ecoregions within the northern part of the Western Cordillera. The smallest precipitation changes were projected to occur in the central Cold Deserts and in the adjacent Mojave Basin and Range in the Warm Deserts. In relative terms, however, the Warm Deserts and adjacent level III ecoregions were projected to be most affected by proportionate decreases in precipitation across all seasons, scenarios, and GCMs. Decreases in the mean winter and spring precipitation of more than 40 percent were projected by the MIROC 3.2-medres model in these ecoregions. Conversely, the noncoastal ecoregions to the north were projected to receive relatively more precipitation (increases of more than 20 percent in nonsummer months) across all scenarios and GCMs (in particular, the CCCma CGCM3.1 model).

In contrast to the projected mean temperature change, the projected mean seasonal precipitation changes from the two climate data sources diverged in some regions with both negative and positive change. An examination of the terrestrial biogeochemical climate-data source revealed some differences in the climate-change patterns that were mostly explainable in terms of the level II ecoregions. In particular, the mean seasonal precipitation was projected to decrease in all seasons, notably spring and winter, in all of the Western Cordillera level III ecoregions (except for the Arizona-New Mexico Mountains), the Coast Range of the Marine West Coast Forest, and the Northern Basin and Range of the Cold Deserts. Where the projected increases in mean winter precipitation were observed above in table 7.1, projected decreases in winter precipitation prevailed, with the greatest projected decreases in mean winter precipitation occurring in the Canadian Rockies, Sierra Nevada Mountains, and Klamath Mountains, which presented a disagreement with the wildland-fire climate projections of up to 27 cm of mean winter precipitation change. Conversely, for the Southern and Central California Chapparral and Oak Woodlands and the Central California Valley level III ecoregions within the Mediterranean California ecoregion, the reductions in average winter precipitation in the wildland-fire disturbance climate dataset contrasted with increases in average winter precipitation in the terrestrial biogeochemical climate datasets.

Table 7.1. Projected changes in precipitation patterns derived from averaging the results from all the scenarios and general circulation models.

[Data from Maurer and others (2007)]

Projected change in precipitation pattern	Affected level II ecoregions	Affected level III ecoregions
Increases in winter, spring, and fall	Marine West Coast Forest	All.
	Western Cordillera	Cascades, North Cascades, Blue Mountains, Northern Rockies, Canadian Rockies.
	Cold Deserts	Columbia Plateau.
Increases in winter and fall	Western Cordillera	Klamath Mountains, East Cascades—Slope and Foothills.
Increases in winter and spring	Western Cordillera	Middle Rockies.
	Cold Deserts	Wyoming Basin.
Increases in winter	Western Cordillera	Wasatch-Uinta Mountains, Southern Rockies.
	Cold Deserts	Northern Basin and Range.
Decreases in all seasons; greatest decrease in winter and spring	Mediterranean California	All.
	Western Cordillera	Sierra Nevada Mountains.
	Warm Deserts	Mojave Basin and Range, Sonoran Basin and Range.
Decreases in all seasons; greatest decrease in fall and spring	Cold Deserts	Central Basin and Range, Colorado Plateaus, Arizona-New Mexico Plateau.
Decreases in all seasons; greatest decrease in fall, spring, and winter	Western Cordillera	Arizona-New Mexico Mountains.
	Warm Deserts	Madrean Archipelago, Chihuahuan Deserts.

Similarly, the terrestrial biogeochemical climate-change data projected greater precipitation increases, including positive summer precipitation change, in the Puget Lowland and Willamette Valley when using the terrestrial biogeochemical climate-change data compared with the climate-change data related to wildland-fire disturbances. Finally, the terrestrial biogeochemical climate projections indicated less of a decrease in the mean winter precipitation and increases in the mean fall precipitation in the Southern California Mountains and Madrean Archipelago level III ecoregions. Otherwise, mostly in the Warm and Cold Deserts, the projected changes in precipitation patterns in the biochemical climate data were comparable to those described for the wildland-fire-disturbance data.

In addition, proportional seasonal precipitation changes differed between climate data sources. In the biogeochemical model's climate data source, the A2 and A1B scenarios and the MIROC 3.2-medres and CCCma CGCM3.1 models indicated a projected precipitation decrease of approximately 40 percent in the Canadian Rockies during the winter, in the Southern Rockies and Arizona-New Mexico Mountains in the spring, and in the Madrean Archipelago in winter and spring. The B1 and A1B scenarios and mostly the CSIRO–Mk3.0 model indicated a projected seasonal mean precipitation increase of more than 30 percent in the Warm Deserts and Mediterranean California in all seasons except spring, and in the Central Basin and Range and Colorado Plateaus of the Cold Deserts during the summer.

7.4. Summary and Discussion of Caveats Using the Climate Data

Climate data was integral to this assessment and for scenario evaluation. The use of projected future climate-change data, however, contributed to uncertainties in the assessment results. The following caveats should be considered:

- The wildland-fire modeling (chapter 8) and biogeochemical modeling (chapter 9) relied heavily on weather and climate data to characterize baseline conditions and estimate future potential changes, but several different climate and weather datasets were used to complete the simulations. The baseline wildland-fire-disturbance data consistently indicated a wetter baseline climate than did the biogeochemical baseline data; however, the discrepancies that occurred in the projected changes of precipitation patterns, in mountainous areas in particular, were attributable to differences in the downscaled climate projections. In mountainous areas, the interpolation of precipitation patterns have been more challenging because of the orographic effects of the topography (Daly and others, 1993).

- Although future LULC allocation algorithms can incorporate climate-change data to allow for adaptation (Mu and others, 2012), the dynamic interactions between climate and LULC change is currently an unsolved problem (Mendelsohn and Dinar, 2009). For example, the IMAGE 2.2 model was the first to incorporate the consequences of the IPCC–SRES emissions scenarios on the carbon cycle in combination with the dynamically modeled LULC-change maps, but the biogeophysical effects of LULC change were not accounted for in that simple climate model (Sitch, 2005). On the other hand, although the LULC-change scenarios developed for this assessment (chapter 6) did not directly incorporate GCM data, an indirect effect of climate change on the viability and, therefore, resolved demand for future LULC is inherent in the use of the IMAGE 2.2 global model (Image Team, 2001) results. The IMAGE 2.2 model was developed on the basis of an alternative GCM (Hadley Centre Coupled Model 2, HadCM2; Johns and others, 1997). The projected LULC allocations have been further complicated by the projected seasonal changes in precipitation and snowmelt and the implications for irrigation (for example, Vano and others, 2010). This assessment assumes that agricultural irrigation practices were static despite changes in precipitation patterns.

- The assessment of carbon cycling in inland aquatic ecosystems (chapter 10) was for the baseline time period only; projections were not made for future carbon fluxes. The incorporation of climate change into the aquatic system components would require water-discharge projections from downscaled climate predictions and the application of flow-generation models, such as the Precipitation-Runoff Modeling System (PRMS, Leavesley and others, 1983).

- In addition to the documented uncertainties in the GCM outputs, the challenges of using GCMs for modeling effects of climate change in biogeochemical and wildland-fire models included the number of GCM datasets to use in the model runs. In their study of the Western United States, Pierce and others (2009) emphasized the importance of having ensembles of climate model runs with enough realizations to reduce the effects of the natural internal climate variability; they determined that a projected mean derived from a multimodel ensemble was superior to a projected mean derived from just one individual model because of the cancellation of offsetting errors and they advised that five models may be sufficient to derive an appropriate projected mean. There are practical and computational limitations, however, to using multiple GCMs; therefore, only three were used for this assessment.

- The projected potential changes in seasonal temperatures and precipitation were characterized in this chapter to provide a general understanding of when and where climate shifts may occur. Other relevant carbon-cycling models, such as the Palmer Drought Severity Index (PDSI), were not calculated. The wildland-fire projections, however, relied heavily on fuel-moistures data for live and dead biomass, which are a function of temperature, relative humidity, precipitation, and the delayed change in moisture conditions.

This page intentionally left blank.

Chapter 8. Projected Future Wildland Fires and Emissions for the Western United States

By Todd J. Hawbaker[1] and Zhiliang Zhu[2]

8.1. Highlights

- Wildland-fire occurrence and greenhouse-gas emissions increased in the Western United States under all of the climate-change scenarios considered in this assessment.
- The projected median amount of area burned annually from 2041 to 2050 was 31 to 66 percent greater than the median amount of area burned annually during the baseline years from 2001 to 2008 (12,136 km^2, reported in chapter 3). The median annual emissions were projected to increase 28 to 56 percent from the baseline median annual emissions, which were approximately 41.0 $TgCO_{2\text{-}eq}$/yr (11.2 TgC/yr) (reported in chapter 3).
- Extreme fire years are projected to become more extreme. The 95th percentile of the amount of area burned annually was projected to increase 79 to 95 percent from the baseline conditions of 2001 to 2008 (23,261 km^2, reported in chapter 3), and the 95th percentile of annual wildland-fire emissions was projected to increase 73 to 150 percent from the baseline 95th percentile estimate, which was approximately 65.0 $TgCO_{2\text{-}eq}$ (17.7 TgC/yr) (reported in chapter 3).

8.2. Introduction

An assessment of the area burned by, the severity of, and the emissions from wildland fires during the baseline period (2001 to 2008) for the Western United States is presented in chapter 3 of this report; this chapter focuses on the projected future extent and severity of, and emissions from wildland fires for the period 2041 to 2050. Modeling of future wildland-fire characteristics required input from the baseline wildland-fire assessment (chapter 3) and projected future climate changes (chapter 7). The wildland-fire projections described in this chapter were provided as input into the modeling of projected future terrestrial carbon storage and greenhouse-gas fluxes described in chapter 9. The relations between this chapter and others are depicted in figure 1.2 of chapter 1 of this report.

Wildland-fire regimes are a function of the interactions between vegetation, land use, and, ultimately, the climate (Swetnam and Betancourt, 1990; Gedalof and others, 2005; Westerling and others, 2006; Falk and others, 2007). A changing climate may result in changes in wildland-fire regimes, including their occurrence, severity, and frequency. Hessl (2011) outlined the primary pathways through which climate change may alter wildland-fire regimes, including (1) altered fuel conditions, such as a change in fuel moisture; (2) altered fuel loads; and (3) changes in ignitions. The effects of climate change on wildland-fires in the Western United States are expected to be significant and result in changes in weather patterns that would alter (1) ignition patterns, (2) wildland-fire behavior, and (3) to a lesser extent, the distribution of vegetation. No single study, however, has addressed all three types of changes simultaneously at the scale required by this assessment (Flannigan and others, 2009).

Potential shifts in weather patterns and wildland-fire behavior, as indicated by variables such as the Keetch-Byram Drought Index (Y. Liu and others, 2010), the seasonal severity rating computed by Flannigan and others (2000), and an energy-release component (ERC) (T.J. Brown and others, 2004), are influenced by climate change and could increase the duration of the wildland-fire season and the severity of conditions under which fires may burn. Climate-driven changes in ignition patterns are not as well understood, but lightning ignitions were projected to increase as much as 44 percent across the United States under a scenario where the atmospheric carbon-dioxide concentration was doubled (Price and Rind, 1994). Regional changes may be greater; for

[1]U.S. Geological Survey, Denver, Colo.

[2]U.S. Geological Survey, Reston, Va.

instance, Westerling and Bryant (2008) examined wildland-fire risk (the probability of a >200-hectare (ha) fire) in California, Nevada, and parts of neighboring States. They compared the observed risk from 1961 to 1990 with the projected risk for 2070 to 2099 using a logistic regression under the A2 and B1 climate-change scenarios (Nakicenovic and others, 2000) with data from the Geophysical Fluid Dynamics Laboratory (GFDL; Delworth and others, 2006) model and the Parallel Climate Model (PCM; Washington and others, 2000) general circulation models (GCMs). The results indicated a projected increase in wildland-fire risk that ranged from 12 to 40 percent for the entire region and ranged from 15 to 90 percent for California alone; the results also indicated that there was substantial spatial variability among the GCMs and scenarios where the changes in risk occurred.

Projections of the extent of the burned area under climate-change scenarios have been made using climate data, sometimes with derived wildland-fire-behavior indices, at national and regional scales. The aforementioned Price and Rind (1994) study of climate change and fires ignited by lightning also suggested that a 44 percent increase in lightning ignitions may result in a 78 percent increase in the extent of the burned area across the conterminous United States. Bachelet and others (2003) suggested a 4 to 31 percent increase in the extent of the burned area by 2100, and Lenihan and others (2008) suggested a 9 to 15 percent increase in the extent of the burned area by 2100 on the basis of simulations made with the MC1 Dynamic General Vegetation Model (DGVM) model (Bachelet and others, 2001) under various climate-change scenarios for the conterminous United States. Multiple regional analyses also suggested that the extent of the burned area is likely to increase under the climate-change scenarios. Littell and others (2010) projected the annual area burned within ecosections defined by Bailey (1995) in Washington State under the A1B climate-change scenario and data from the Third Generation Coupled Global Climate Model of the Canadian Centre for Climate Modelling and Analysis (CCCma CGCM3.1; Flato and Boer, 2001) and the Hadley Centre for Climate Prediction and Research Couple Model 3 (HadCM3; Gordon and others, 2000); their results suggested that the annual extent of area burned may more than double by the 2040s and triple by the 2080s. Interannual variability also increased and the probability of having an extreme fire year (defined as a year in which the area burned is greater than the 95th percentile of the long-term distribution of total areas burned) increased from 0.05 to 0.48 by the 2080s. A study by Rogers and others (2011) yielded similar results for area burned and also demonstrated that burn severity was projected to increase in the Pacific Northwest. Litschert and others (2012) used an approach that was similar to Littell and others (2010) in the Southern Rocky Mountains and fit models to project the percent of area burned each year under the A2 and B1 climate-change scenarios using data from the HadCM3 model and the Max Planck Institute for Meteorology's European Centre for Medium-Range Weather Forecasts—Hamburg 5 (ECHAM5; Roeckner and others, 2003) model; their projections suggested that the median annual area burned may increase up to 500 percent between 1970 and 2006 and between 2010 and 2070. These studies demonstrated that the extent of the area affected by wildland fires in the Western United States was projected to increase under a range of climate-change scenarios and GCMs; however, the studies do not provide the necessary information to estimate changes in wildland-fire emissions.

Few studies have addressed how wildland-fire emissions might change with the projected increases in the extent of burned areas under climate-change scenarios for the conterminous United States, but there has been an extensive amount of work completed for boreal regions (Flannigan and others, 2005; Balshi, McGuire, Duffy, Flanigan, Kicklighter, and Melillo, 2009). Most of the existing estimates demonstrated that emissions usually changed in proportion to the amount of area burned (Spracklen and others, 2009), unless disturbances or climate change caused substantial shifts in vegetation. For instance, work by Spracklen and others (2009) used climate-change projections from the Goddard Institute for Space Studies (GISS; Russell and others, 2000) GCM under a scenario in which the concentration of carbon dioxide was doubled ($2 \times CO^2$); the simulation indicated a projected increase in mean annual area burned of 50 percent and a projected near doubling of carbonaceous aerosol emissions by 2050 across the Western United States, with the majority of the change projected to occur in the Pacific Northwest and Rocky Mountain regions. An earlier study by Bachelet and others (2004) used the MC1 DGVM model (Bachelet and others, 2001) to simulate past (1905–1995) and future (1996–2100) carbon stocks and fluxes with climate data from the HadCM2Sul (Johns and others 1997) and the CCCma CGCM1 (Flato and others, 2000) models; their results showed that biomass consumed by wildland fires steadily increased from 110 teragrams of carbon per year (TgC/yr) to 180 TgC/yr in the Western United States (specifically, Arizona, California, western Colorado, western New Mexico, Nevada, western Texas, and Utah) and from 100 TgC/yr to 160 TgC/yr in the Northwestern United States (specifically, Oregon, Washington, Idaho, and western Montana). A more recent study by Lenihan and others (2008) using the MC1 DVGM model suggested that carbon stocks in the Western United States are projected to remain stable, largely because projected increases in primary productivity would result in the storage of additional carbon, which would outweigh the carbon losses from the projected increase in wildland fires.

In spite of the large amount of research linking wildland fires to climate change, there is no existing framework that fully incorporates the mechanisms through which climate change will influence wildland-fire occurrence, behavior, and effects (Flannigan and others, 2009; Hessl, 2011); therefore, a model was developed for this assessment to simulate the influence of climate change on patterns of wildland-fire ignitions, spread, and emissions. This simulation model was calibrated using historical fire, weather, and climate data and

then used to generate projections under the climate-change scenarios. The simulations were designed to address the following questions: (1) What are the potential changes in wildland-fire occurrence and emissions for the Western United States under climate change? (2) How do the potential changes vary among ecoregions and climate-change scenarios? This chapter focuses primarily on the results of the wildland-fire simulations, although wildland-fire scars for both the baseline and projection periods were also used in the analysis of projected future carbon storage and greenhouse-gas fluxes of terrestrial ecosystems (chapter 9).

8.3. Input Data and Methods

The studies described above generally indicated that the area affected by large wildland fires and their emissions was a function of both ignition patterns and fire behavior, primarily spread; both were largely influenced by weather conditions, fuels, and topography (Cary and others, 2009) and, in some regions, ignitions were influenced by human activity (Cardille and others, 2001; Syphard and others, 2007). Projecting the potential changes in wildland-fire patterns, therefore, required an understanding and accurate characterization of the drivers that created the observed, past patterns of ignitions, spread, and emissions (Keane and others, 2003; Flannigan and others, 2009; Hessl, 2011). Accordingly, the wildland-fire modeling approach used for this assessment incorporated three primary components: wildland-fire ignitions, spread, and effects (fig. 8.1). The parameters for the ignition and spread components were selected through a calibration process using the baseline observed data and then used to simulate future potential wildfires. The datasets and methods used by the various wildland-fire modeling components are described in the following sections.

The wildland-fire models were applied to each level III ecoregion in the Western United States. Some ecoregions that had similar fire regimes and were adjacent to each other were grouped to improve the data-processing efficiency. The following level III ecoregions were grouped together to form one region each: (1) the Cascades, North Cascades, and East Cascades—Slope and Foothills; (2) the Northern Rockies and Canadian Rockies; and (3) the Southern and Central California Chaparral and Oak Woodlands and the Southern California Mountains. In a few other level III ecoregions (the Puget Lowland, Willamette Valley, and Central California Valley), there were too few wildland fires to analyze.

After simulations were completed for the level III ecoregions, the results were aggregated to each level II ecoregion and to the entire Western United States for reporting. The simulated number of wildland fires, area burned, and emissions were summarized by climate-change scenario for each decade as the 50th and 95th percentiles, which represented typical and extreme fire years, respectively. Additionally, the relative change between the baseline decade (2001–2010) and the future decade (2041–2050) is reported.

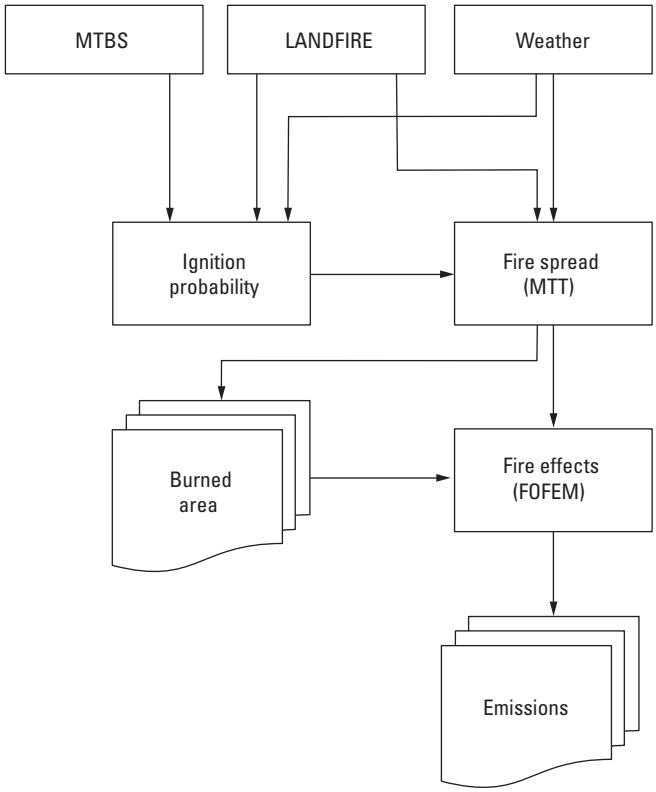

Figure 8.1. Flowchart showing the components of the disturbance model, which was used for generating projections of future potential wildland-fire ignitions, burned area, and emissions. FOFEM, First Order Fire Effects Model; LANDFIRE, Landscape Fire and Resource Management Planning Tools project; MTBS, Monitoring Trends in Burn Severity project; MTT, minimum travel time.

8.3.1. Wildland-Fire Data

The locations of wildland-fire scars were taken from the Monitoring Trends in Burn Severity data (MTBS; Eidenshink and others, 2007) to calibrate the ignition and spread components of the wildland-fire modeling system. The MTBS data described fires that occurred from 1984 to 2008 and that were greater than 404 ha (1,000 acres) and 202 ha (500 acres) in the Western and Eastern United States, respectively. The MTBS data did not include small fires but captured the majority of the area burned because they included the largest fires, which contributed most to total area burned (Strauss and others, 1989; Stocks and others, 2002). Each wildland fire detailed in the MTBS database was identified in State or Federal fire records, and its burn scar and severity were manually mapped using pre- and post-fire Landsat scenes. Because of the MTBS methodology, there was a high degree of confidence in the spatial and temporal accuracy of the wildland-fire data, whereas other wildland-fire databases had known problems, including duplicate records and erroneous locations (T.J. Brown and others, 2002), which would require laborious error checking before use.

8.3.2. Weather and Climate Data

The assessment methodology required daily weather data, including temperature, precipitation, relative humidity, and wind speeds, for both the baseline and future time periods. For the baseline time period, gridded daily weather data for the conterminous United States with 1/8° spatial resolution (approximately 12 km) were used (Maurer and others, 2002). These data, which span the period from 1950 to 2010, were interpolated from weather stations and included the minimum and maximum daily temperature and daily precipitation. The data on afternoon wind speed and direction from the 1/3° (approximately 32 km) North American Regional Reanalysis (Mesinger and others, 2006) were joined to the 1/8° daily temperature and precipitation data.

In order to simulate the effects of the climate-change scenarios on wildland-fire occurrence and emissions, downscaled monthly climate data provided by the World Climate Research Programme's (WCRP's) Coupled Model Intercomparison Project phase 3 (CMIP3) multimodel dataset were used. The CMIP3 data were corrected for bias and spatially downscaled to match the 1/8°-resolution baseline weather data (Maurer and others, 2007). For this analysis, the downscaled data from the CCCma CGCM 3.1 (Flato and Boer, 2001), Australia's Commonwealth Scientific and Industrial Research Organisation Mark 3.0 (CSIRO–Mk3.0; Gordon and others, 2002) model, and the Model for Interdisciplinary Research on Climate version 3.2, medium resolution (MIROC 3.2-medres; Hasumi and Emori, 2004) for each of the A1B, A2, and B1 climate-change scenarios were downloaded from the Bias Corrected and Downscaled WCRP CMIP3 Climate Projections archive (Maurer and others, 2007; Lawrence Livermore National Laboratory, 2012). The GCMs and scenarios were selected on the basis of their ability to capture past climate patterns (Balshi, McGuire, Duffy, Flanigan, Walsh, and Melillo, 2009). Additionally, the range of variability among the projections generally bracketed the extremes of temperature and precipitation projections for the conterminous United States (Gonzalez, Neilson, and others, 2010). Climate-change summaries for temperature and precipitation are provided in chapter 7 of this report.

The downscaled climate data only provided monthly temperature and precipitation values, so a temporal disaggregation algorithm (Wood and others, 2002) was implemented to produce the daily values necessary for wildland-fire simulations. This algorithm randomly rearranged year-long sequences of the baseline weather data for each future year and then adjusted the disaggregated daily values of temperature and precipitation so that their monthly means matched the values provided by the monthly climate forecasts. Using this methodology, 3 replicate weather sequences were generated for each GCM and climate-change scenario combination for a total of 27 simulation runs. The number of GCMs used and replicate runs was somewhat arbitrary but limited by computing power and processing times.

For both the baseline and future climate change scenarios, additional processing steps were taken to produce the live and dead fuel moisture variables required for simulating wildland-fire spread and behavior. First, the Mountain Climate Simulator (MT–CLIM) algorithms (Glassy and Running, 1994) were used to calculate relative humidity based on minimum and afternoon daily temperatures (Kimball and others, 1997). Once humidity was estimated, the National Fire Danger Rating System (NFDRS) algorithms were used to estimate daily values for live and dead fuel moistures, as well as wildland-fire behavior indices such as the energy release component (ERC) (Deeming and others, 1977; Bradshaw and others, 1983; Burgan, 1988). The NFDRS algorithms required information about the beginning of both spring ("green-up") and fall ("brown-down") to estimate live fuel moistures. To generate green-up and brown-down dates, a methodology was implemented that determined the dates of seasonal changes based on the daily photoperiod, minimum temperature, and the vapor-pressure deficit (Jolly and others, 2005).

8.3.3. Fuels and Topography

In addition to daily weather sequences, the methodology relied on the LANDFIRE vegetation, fuels, and topography data (Rollins, 2009). These data included information about existing vegetation, fire-behavior fuel models, and tree canopy fuels (cover, height, base height, and bulk density), as well as the elevation, slope, and aspect of the terrain. To calculate emissions from wildland fires, the LANDFIRE fuel-loading model data layer (FLM; Lutes and others, 2009) was also used. Vegetation and fuels were held static throughout the simulations and were not altered by simulated disturbances and other types of land-use and land-cover (LULC) change. All raster data were aggregated to 250-m resolution in order to improve the processing efficiency using a nearest-neighbor rule. The nearest-neighbor aggregation was desirable because it preserved the proportion of vegetative-cover types within the study area, whereas other aggregation methods were more likely to result in common vegetative-cover types being overrepresented and uncommon vegetative-cover types being underrepresented.

8.3.4. Model Components

8.3.4.1. Ignitions

General linear models (GLMs) with a binary response were constructed to predict daily ignition probabilities within each 1/8° weather grid cell. From the data described above, a suite of potential predictor variables was compiled that included daily weather statistics (minimum and maximum temperature and energy release component), monthly weather summaries (temperature and precipitation), seasonal weather summaries (temperature and precipitation), as well as regional summaries of temperature and precipitation, both

at monthly and seasonal time steps. Also included within the 1/8° weather grid cells as potential predictors in the GLM modeling were the proportions of land area classified as public or urban, as well as existing vegetation type groups from the LANDFIRE database.

Most observations (grid cells with daily weather data) had no data on ignitions; therefore, a subsample was selected using a case-control sampling design. Any observation with precipitation greater than 0.25 cm was removed. All observations with ignition data were retained along with a randomly selected set of observations without ignition data. The number of observations without ignition data was 10 times the number of observations with ignition data. The choice of design was somewhat arbitrary, but justified because the predictive performance of models using case-control sampling designs has been shown to increase with the ratio of cases to controls (Hastie and others, 2009). The intercept of the GLM was adjusted using equation 1 to account for unequal proportions of cases (ignitions) and controls (non-ignitions) in the sample compared with the population (Preisler and others, 2004; Hastie and others, 2009).

$$\log\left(\frac{non\text{-}ignitions_{sample}}{non\text{-}ignitions_{population}}\right)-\log\left(\frac{ignitions_{sample}}{ignitions_{population}}\right) \quad (1)$$

To build the GLMs, an initial set of predictor variables was selected using forward stepwise regression, including only variables with p-values ≤0.05 and limiting the number of predictors to 1/10 the number of wildland-fire observations. Each GLM was then evaluated and modified as needed to ensure that the selected predictor variables accurately described weather and climate conditions known to affect wildland-fire occurrence in a given ecoregion. The overall performance of the final GLM was judged using the area under the curve (AUC) of a receiver-operator characteristic plot (Hanley and McNeil, 1982). The AUC measured the probability of correctly classifying a random pair of fire and non-fire observations; an AUC value of 0.5 indicated that the model predictions were equivalent to a random guess and an AUC value of 1.0 indicated perfect predictions. AUC values above 0.8 were generally considered to be good.

8.3.4.2. Spread

During the simulations, the MTT algorithm (Finney, 2002) was used to simulate the spread of wildland fires after ignition. The MTT algorithm has been used extensively for local and national-scale simulations of burn probability (Calkin and others, 2011; Finney and others, 2011). In addition to an ignition location, the MTT algorithm relied on fuels (surface and canopy), topography (elevation, slope, and aspect), weather (wind speed and direction), and live and dead fuel moistures data. The MTT algorithm also required a specified number of days and minutes per day that a wildland fire can spread. The outputs produced by the MTT algorithm included the arrival time (duration of the wildland fire since ignition) of every pixel representing burned area, as well as wildland-fire-behavior metrics such as fireline intensity and crown-fire activity.

8.3.4.3. Emissions

To calculate emissions, the First Order Fire Effects Model (FOFEM; Reinhardt and others, 1997; Reinhardt and Keane, 2009) was applied to each pixel that indicated burned area in the simulated wildland fires. The FOFEM used fuel loads along with fuel moistures to estimate the amount of forest litter and downed deadwood that was consumed (Albini and others, 1995; Albini and Reinhardt, 1995, 1997). The consumption of duff (decaying forest litter), trees, plants, and shrubs was estimated as a function of the region, season, fuel moistures, and fuel loads. The emissions of carbon monoxide (CO), carbon dioxide (CO_2), and methane (CH_4) were then calculated on the basis of the amount of fuel consumed, the organic content of the fuel, and how efficiently it burned.

The FOFEM also required estimates about the proportion of the tree canopy affected by crown fires. In the simulated wildland fires, burn severity estimates were used to quantify the proportion of canopy fuels consumed; the burn-severity categories (low, medium, and high) were assigned randomly on the basis of their observed frequencies in LANDFIRE's existing vegetation groups. When calculating emissions with the FOFEM, 20-, 60-, and 100-percent canopy consumption was assumed for low, moderate, and high burn severity, respectively, on the basis of published literature (Spracklen and others, 2009; Zhu and others, 2010).

To simplify the reporting of results, the emission estimates were summarized for all carbon-containing constituents to carbon dioxide equivalent ($CO_{2\text{-}eq}$) using equation 2.

$$CO_{2-eq} = CO_2 + (2.33 \times CO) + (21.0 \times CH_4) \quad (2)$$

8.3.4.4. Calibration

A number of calibration simulations were required to determine the appropriate number of days and minutes per day to allow wildland fires to spread using the MTT algorithm. The initial values for the minimum and maximum number of days to allow the spread and minutes of spread per day were selected on the basis of values derived from Federal fire records. Nine replicate simulations were run using the baseline weather data (1984–2008). After the simulations were complete, a 2-sided t-test was used to determine if there was a significant difference in the annual average area burned between the simulated fires and observed fires in the MTBS data. If the differences were significant, the number of days of fire spread and the minutes of spread per day were altered and the calibration process was repeated until the p-value of the t-test was less than 0.05, indicating that the calibration simulations reproduced the baseline fire patterns.

8.3.4.5. Simulations of Future Fires

After calibration, future potential wildland-fire ignitions, spread, and emissions were generated for three replicate simulations for each of the climate-change scenarios and GCMs, starting in 2001 and ending in 2050. The replicate simulations were run to help quantify uncertainty because of the stochastic nature of the models; more replicate simulations would have been ideal, but processing times limited the number of replicates to three. The results of each simulation were summarized in terms of area burned and amount of carbon emissions per year.

8.4. Results

General linear models were fit to each level III ecoregion and used to generate daily ignition probabilities in the simulations. In general, the model fits were quite good with the AUC values averaging 0.90 and ranging from 0.80 to 0.93. The best model fits were in the level III ecoregions within the Cold Deserts and the worst model fit was for the Mediterranean California ecoregion. Most models included the ERC as a predictor (which captured day-to-day variability in fuel moistures) and monthly and seasonal weather summaries (which captured seasonal and year-to-year variability). Most ecoregions also included at least one vegetation predictor. Developed land (which included high- and low-density urban areas, golf courses, urban parks, and highways) typically was not included, except in the Wyoming Basin and Mediterranean California ecoregions.

Calibration simulations were run for each level III ecoregion to ensure that the patterns of wildland-fire occurrence from 1984 to 2008 could be reproduced. For all of the ecoregions, there was no significant difference in the average annual burned area between the calibration simulation and the observed values from the MTBS database, assuming that differences were not significant when a p-value of 0.05 or greater was calculated using a 2-sided t-test that assumed unequal variance. After the calibration process, the simulated wildland fires were allowed to spread 240 minutes/day, and the burn durations ranged from 1 to 21 days, depending on the ecoregion.

Across all of the climate-change scenarios, the simulations resulted in a projected increase in wildland-fire ignitions, area burned, and emissions between the first and last decades (2001–2010 and 2041–2050; fig. 8.2 and table 8.1). In typical years (50th percentile), the number of ignitions was projected to increase 39 to 70 percent. The greatest projected increases in ignitions were observed under the A2 (70 percent) and A1B (58 percent) scenarios and the smallest projected increase was observed under the B1 (39 percent) scenario. The area burned was projected to increase, ranging from a 31 percent increase in the B1 scenario to a 66 percent increase in each of the A1B and A2 scenarios. Wildland-fire emissions followed similar patterns, with projected increases of 56 percent, 54 percent, and 28 percent under the A1B, A2, and B1 scenarios, respectively. The simulated changes in ignitions, area burned, and emissions were greater in extreme fire years (95th percentiles), and across the Western United States, ignitions were projected to increase between 62 and 74 percent, area burned was projected to increase between 79 and 95 percent, and emissions were projected to increase between 73 and 150 percent (fig. 8.2 and table 8.1). The rate of change was generally nonlinear and the greatest increases in ignitions, area burned, and emissions were projected to occur in from 2031 to 2040 and from 2041 to 2050.

Projected increases in ignitions, area burned, and emissions were simulated for all three climate-change scenarios in the Western Cordillera ecoregion (fig. 8.3 and table 8.2). The number of ignitions per year was projected to increase between 21 and 38 percent in typical fire years, and between 39 and 99 percent in extreme fire years. The changes in the extent of area burned were more variable but generally were projected to increase in typical fire years under the A1B (34 percent) and A2 (55 percent) scenarios, but decrease slightly under the B1 (−5 percent) scenario. The extent of the area burned in extreme years was projected to change at much greater rates than typical fire years, up to 167 percent under the A2 scenario. Emissions were projected to increase in both typical (15–64 percent) and extreme (28–188 percent) fire years. The projected increases were greatest for the A2

Table 8.1. Projected relative change (increases) in the 50th and 95th percentiles for wildland-fire ignitions, area burned, and emissions between the first and last decades (2001–2010 and 2041–2050), by climate-change scenario, for the Western United States.

[Climate-change scenarios are from the Intergovernmental Panel on Climate Change Special Report on Emissions Scenarios (Nakicenovic and others, 2000)]

Climate-change scenario	Percentile	Relative change (percent)		
		Ignitions	Area burned	Emissions
A1B	50th	58	66	56
	95th	74	95	73
A2	50th	70	66	54
	95th	62	84	150
B1	50th	39	31	28
	95th	73	79	118

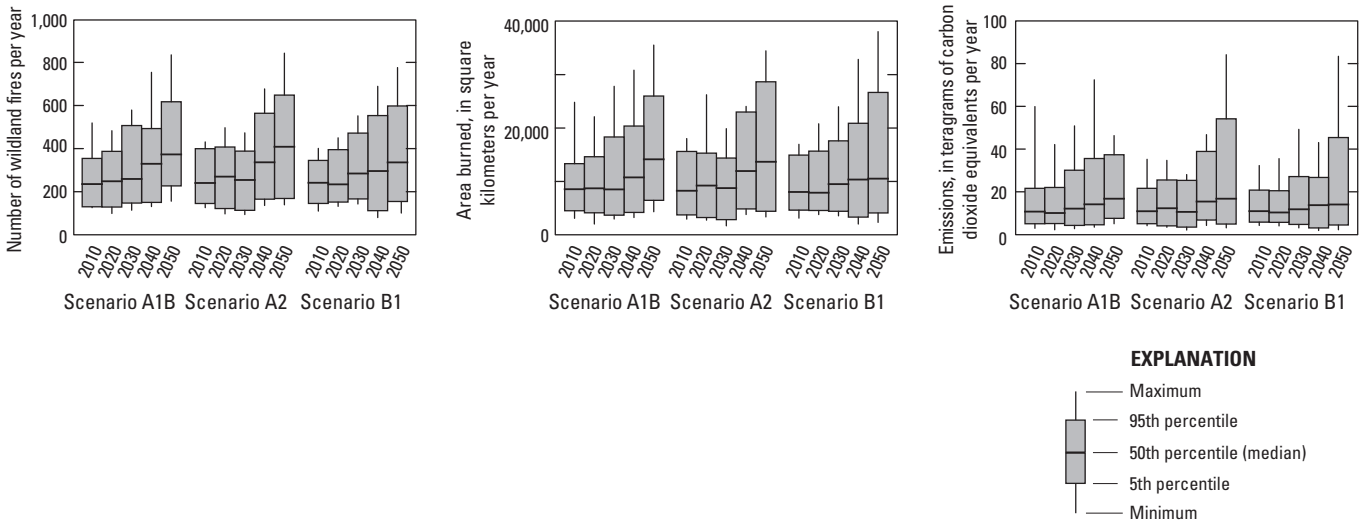

Figure 8.2. Graphs showing summaries of projected wildland-fire ignitions, area burned, and emissions for the Western United States for each decade between 2001 and 2050. The X-axis labels indicate the last year in the decade; for example, "2010" corresponds to the decade from 2001 to 2010. Scenarios are from the Intergovernmental Panel on Climate Change Special Report on Emissions Scenarios (Nakicenovic and others, 2000).

scenario but were also high for the B1 scenario. The projected changes under the A1B scenario tended to be smaller than under the other two scenarios, in part because fewer ignitions were projected to occur and a smaller area was projected to burn during the 2041 to 2050 decade under the A1B scenario.

Of the five level II ecoregions, the least amount of wildland-fire activity was observed in the Marine West Coast Forest and the simulated changes in wildland-fire occurrence and emissions were minimal (fig. 8.3 and table 8.2). The projected number of ignitions did not change in both typical and extreme years, except under extreme years in the A2 scenario, where ignitions actually declined. The projected extent of area burned and emissions were less stable, and there were no clear patterns in the projected changes (fig. 8.3), sometimes increasing (A1B and B1 scenarios) and other times decreasing (A2 scenario, extreme years).

In the baseline analysis (chapter 3 of this report), there was substantial wildland-fire activity in the Cold Deserts ecoregion. The simulations of future wildland fires projected a substantial increase in wildland-fire activity across all three climate-change scenarios (fig. 8.3 and table 8.2). The projected increases in wildland-fire ignitions ranged from 39 to 85 percent and from 72 to 103 percent for typical and extreme fire years, respectively. These projected increases in ignitions resulted in (1) projected increases in burned area of 34 to 95 percent in typical fire years and 58 to 101 percent for extreme fire years and (2) projected increases in emissions of 44 to 87 percent in typical years and 88 to 129 percent in extreme years. The projected changes in burned area and emissions were generally greatest under the A1B and A2 scenarios.

In the Warm Deserts ecoregion, ignitions were projected to increase by 5 to 64 percent (typical years) and 19 to 133 percent (extreme years), the area burned was projected to increase by 1 to 80 percent (typical years) and 22 to 155 percent (extreme years), and emissions were projected to increase by 3 to 69 percent (typical years) and –12 to 98 percent (extreme years) (fig. 8.3 and table 8.2). The projected changes in ignitions, area burned, and emissions were consistently high under the A1B climate-change scenario for both typical and extreme fire years, respectively. Under the B1 scenario, wildland-fire activity was limited in the decade between 2001 and 2010, and the changes relative to that decade were large. The changes projected under the A2 scenario were minimal, but ignitions, area burned, and emissions tended to be greater in all decades under the A2 scenario than they were under both the A1B and B1 scenarios.

In the Mediterranean California ecoregion, wildland fire ignitions, area burned, and emissions were projected to increase under all three climate-change scenarios (fig. 8.3 and table 8.2), but the differences between typical and extreme fire years were less pronounced than in other ecoregions. The projected number of wildland-fire ignitions for the decade between 2041 and 2050 was 36 to 62 percent greater than in the decade between 2001 and 2010 in typical years and 43 to 67 percent greater in extreme years. The projected increase in the number of ignitions resulted in a projected increase in burned area of 47 to 86 percent in typical years and 48 to 61 percent in extreme years. Emissions were projected to increase up to 80 percent in typical fire years and up to 55 percent in extreme years.

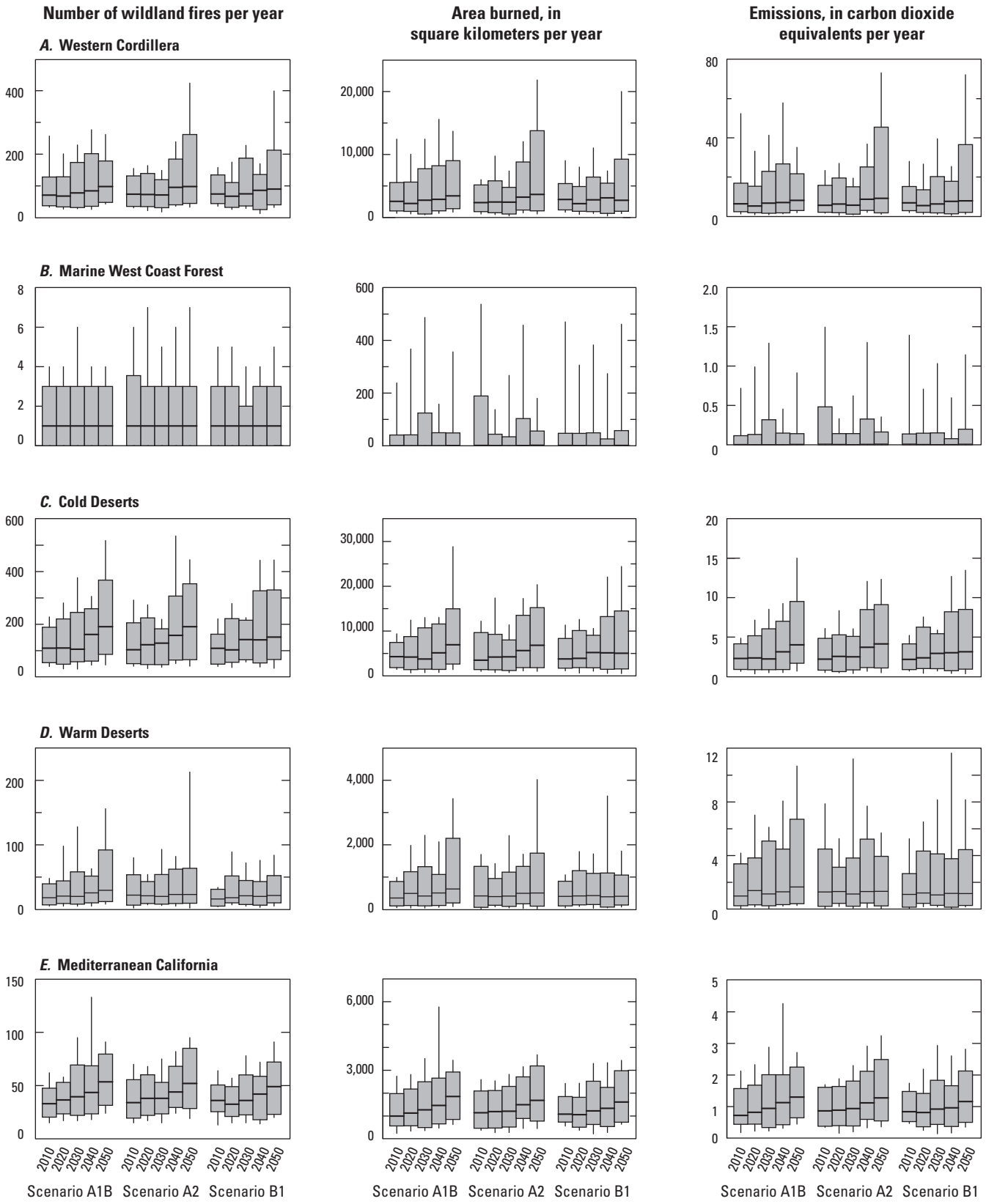

Figure 8.3. Graphs showing summaries of projected wildland-fire ignitions, area burned, and emissions by level II ecoregion, for each decade between 2001 and 2050. The X-axis labels indicate the last year in the decade; for example, "2010" corresponds to the decade from 2001 to 2010. Scenarios are from the Intergovernmental Panel on Climate Change Special Report on Emissions Scenarios (Nakicenovic and others, 2000). See figure 8.2 for an explanation of the bars.

Table 8.2. Relative projected changes in the 50th and 95th percentiles for wildland-fire ignitions, area burned, and emissions per year between the 2001-to-2010 decade and the 2041-to-2050 decade, by scenario and level II ecoregion.

[Climate-change scenarios from the Intergovernmental Panel on Climate Change Special Report on Emissions Scenarios (Nakicenovic and others, 2000)]

Climate-change scenario	Percentile	Level II ecoregion (percent)				
		Western Cordillera	Marine West Coast Forest	Cold Deserts	Warm Deserts	Mediterranean California
			Ignitions			
A1B	50th	38	0	74	64	62
	95th	39	0	95	133	67
A2	50th	32	0	85	5	53
	95th	99	−15	72	19	53
B1	50th	21	0	39	34	36
	95th	58	0	103	68	43
			Area burned			
A1B	50th	34	53	62	80	86
	95th	63	19	101	155	48
A2	50th	55	29	95	22	47
	95th	167	−70	58	31	52
B1	50th	−5	0	34	1	49
	95th	72	22	74	22	61
			Emissions			
A1B	50th	28	42	75	69	80
	95th	28	22	129	98	43
A2	50th	64	13	87	3	48
	95th	188	−66	88	−12	55
B1	50th	15	−12	44	6	38
	95th	141	44	105	68	44

8.5. Discussion

Wildland-fire ignitions and area burned were projected to increase across all the climate-change scenarios for the Western United States as a whole and in almost all of the climate-change scenarios in each of the five ecoregions in the Western United States. Emissions were also projected to increase, but the pattern was more variable, possibly because the projected increase in the area burned may have resulted in relatively more light fuels (grass and shrub) and less heavy fuels (coniferous forest) being consumed. The projected increases in emissions were greater in extreme fire years (73–150 percent) than in typical fire years (28–56 percent). Given that the baseline wildland-fire emissions were roughly equivalent to 11.6 (7.9–87.0) percent of the mean sequestered carbon in terrestrial ecosystems (chapter 3), future efforts to increase carbon storage in ecosystems may be challenged by the potential carbon losses due to the projected climate-driven increases in wildland-fire occurrence.

The projected changes in wildland-fire patterns in the Western Cordillera ecoregion were most likely a result of the projected increases in temperatures during most of the seasons and the projected decreases in precipitation during the spring and summer, the seasons in which wildland fires are most common. In terms of the entire Western United States, the Western Cordillera ecoregion accounted for a large proportion of the baseline area burned and the majority of wildland-fire emissions (chapter 3). The results of the simulations made for this assessment indicate that wildland-fire ignitions, area burned, emissions, and associated management challenges, will likely increase in the future compared to other regions in the nation.

In the Marine West Coast Forest, wildland-fire activity has been historically infrequent and minimal changes were projected under the climate-change scenarios modeled in this assessment. The climate-change projections indicated a warming trend in this ecoregion; however, this ecoregion was also projected to have the greatest increase in precipitation under all of the climate-change scenarios among all the ecoregions of the Western United States, especially during the winter, spring, and fall. Because of the lag effects in fuel moistures, these projected changes could limit and even reduce wildland-fire activity. Because vegetation in this region historically has been highly productive, the wildland fires were extensive and severe when they occurred during droughts. This phenomenon most likely produced the highly variable projected trends in wildland-fire activity in the simulations.

The climate-change projections were variable for the Cold Deserts. As with most of the ecoregions in the Western United States, the temperatures were projected to increase. Drying patterns were projected in the southern and western portions of the ecoregion, especially in the spring, but increased precipitation in the summer was projected in the northern parts of the ecoregion. The exception was the simulation by the MIROC 3.2-medres model, which largely projected a drier climate across the entire ecoregion. These projected climate changes resulted in consistent projected increases in wildland-fire ignitions, area burned, and emissions, regardless of the climate-change scenario.

The Warm Deserts ecoregion was projected to have a consistently drier climate than the other ecoregions for most seasons under all scenarios, except under the B1 scenario during the summer (when projected by the CSIRO–Mk3.0 model) and winter (when projected by the CCCma CGCM3.1 model). Higher summer and fall temperatures were also projected. Wildland-fire activity and emissions were projected to increase under the A1B and A2 scenarios, although they were projected to be somewhat reduced under the B1 scenario. Similarly, the projected warmer temperatures (especially in the summer and fall) and drier spring and fall seasons in the Mediterranean California ecoregion corresponded to the projected increases in wildfire ignitions, area burned, and emissions.

The projected increases in fire activity that were simulated in the Cold Desert, Warm Deserts, and Mediterranean California ecoregions for this assessment were likely to be conservative estimates because vegetation types and fuel loads were static throughout the 50-year simulation period. There were strong and positive correlations between wildland-fire activity and the presence of invasive species after fire in all three ecoregions. These correlations suggest that as wildland-fire frequency increases, native ecosystems may be at risk of invasion by exotic grasses, which in turn may further increase the likelihood of wildland fires by providing fuel under some climate conditions (D'Antonio and Vitousek, 1992; Brooks and others, 2004; Keeley, 2006; Brooks and Chambers, 2011). The results of the wildland-fire simulations produced for this assessment may have been amplified if those feedback relations had been included.

The methods used here to simulate wildland fires were quite different than those used in most of the previously published studies that examined the effects of climate change on wildland-fire occurrence. Previous studies did not explicitly simulate the wildland-fire ignition locations, spread, or the effects on ecosystems; instead, they projected the probability that a grid cell contained a wildland-fire ignition (Westerling and Bryant, 2008) or the proportion of an ecoregion that burned (Littell and others, 2010; Litschert and others, 2012). The one exception is the recent paper by Westerling and others (2011), which projected wildland-fire ignition locations and size separately but did not explicitly simulate ignition locations and spread on the landscape. In spite of the differences in the methods used in this assessment, the results presented here were somewhat similar to past studies in that all of them projected an increase in the area burned in the near future; however, this assessment projected a smaller, more conservative increase in area burned than did the previously published estimates.

8.6. Limitations and Uncertainties

The MTBS database does not typically include wildland fires less than 404 ha (1,000 acres) in size in the Western United States, and because the simulation models used for this assessment were calibrated using the MTBS data, they were not influenced by smaller fires. Smaller fires are not likely to change the baseline results by much, but there is the possibility that ignitions which historically resulted in a small burned area and emissions could grow into large fires under different climate conditions. Thus, for this assessment, the simulated changes in wildland-fire occurrence and emissions may yield conservative estimates.

Throughout the wildland-fire simulations, vegetation and fuels remained static, which introduced some limitations into the assessment. Because of succession and disturbances, the composition and structure of forest vegetation may change substantially over the 50-year time span used in this assessment (Cooper, 1960; Aplet and others, 1988; Moore and others, 2004). These changes were often projected to result in altered surface and canopy fuels that determined potential wildland-fire behavior and emissions. Disturbances were especially important to consider because they were projected to reduce fuel loads and effectively act as fire breaks for future wildland fires. By holding vegetation and fuels static, the interactions among wildland fire and LULC change were oversimplified, which are limitations that are shared

by many broad-scale studies of projected climate change and wildland fires. Vegetation dynamics have often been ignored in climate-change projections in part because of the difficulty of parameterizing the successional trajectories of each individual ecosystem type and the lack of information about how ecosystems may shift across the landscape under climate change. The influence that vegetation dynamics might have had on the results of this assessment is uncertain. In spite of the projected increases in wildland-fire ignitions and area burned simulated for this assessment, the extent of the area burned each year was projected to be quite small relative to the extent of area that could potentially burn in an ecoregion. Thus, in the Western United States, it is unlikely that the amount and arrangement of burnable vegetation on the landscape will limit wildland fires. Shifts in vegetation, however, might affect the type of vegetation and the amount of fuel available to burn; thus, past wildland fires might alter the fuels, behavior, and emissions of future wildland fires (Bachelet and others, 2001, 2003). Incorporating vegetation dynamics into the ecosystem-disturbance model component is a priority task for future carbon assessments (Running, 2008; Goetz and others, 2012).

There was a large amount of variability in wildland-fire ignitions, area burned, and emissions in the simulations under the three climate-change scenarios. For each of the 3 GCMs, 3 replicate simulations were run, resulting in 9 simulations for each climate-change scenario, or 27 simulations total. It is uncertain whether those simulations fully characterized the variability in the simulated changes. Ideally, more simulations for different GCMs would have been incorporated to better characterize the variability, but practical limitations on computing resources and processing times effectively restricted the number of simulations that were run in this assessment. As a test in this study, additional GCMs were used in simulations for the Southern Rockies level III ecoregion with a greater number of replicates. The results suggested that the general projected patterns reported here will not change substantially.

8.7. Management Implications

Wildland-fire emissions produce greenhouse gases that may contribute to and accelerate climate change (Crutzen and Andreae, 1990; Andreae and Merlet, 2001) and may alter the structure and function of ecosystems (Bachelet and others, 2003; Lenihan and others, 2008). Fire-management strategies may need to be reassessed to determine whether and how best to counteract the projected increases in wildland-fire area burned and greenhouse-gas emissions, especially because managing wildland fires to reduce greenhouse-gas emissions might be at odds with other fire-management objectives, such as maintaining the historical range of variability in ecosystem disturbance regimes (McKenzie and others, 2004; Fule, 2008).

In certain cases, increased fire suppression efforts might be appropriate. Past simulation studies suggested that fire suppression in some ecosystems in the Western United States may increase carbon stocks by as much as 10 percent because of the unchecked woody encroachment and increased vegetation growth rates (Lenihan and others, 2008). In ecosystems where wildland-fire frequency has increased beyond the historical range of variability because of the influence of human development (Syphard and others, 2007) and invasive species (Brooks and others, 2004; Keeley, 2006), increased fire suppression might be a management strategy that meets the multiple goals of reducing greenhouse-gas emissions while maintaining ecosystem dynamics. The potential success of increasing wildland-fire suppression efforts remains unknown, however; fire suppression and containment efforts may become more difficult as the results of this assessment suggested that fires in both typical and extreme fire years were projected to be more severe in the future.

In other ecosystems, especially the dry forests in the Western United States, years of wildland-fire suppression have led to increased fuel loads and more severe fires, and increasing the suppression efforts in these areas may lead to additional undesirable effects (Stephens, 1998; Keane and others, 2002; Agee, 2003; Stephens and Ruth, 2005). These same ecosystems have been the targets of restoration efforts designed to reduce fuel loads and fire severity to historical conditions (Agee and Skinner, 2005; Reinhardt and others, 2008), and fuel treatments have been shown to benefit both ecosystem restoration and efforts to reduce greenhouse-gas emissions (Stephens and others, 2009; Reinhardt and Holsinger, 2010; Wiedinmyer and Hurteau, 2010; North and Hurteau, 2011). In forests at higher elevations, where the effects of suppression have not substantially altered fire regimes, the usefulness of fuel treatments to reduce wildland-fire severity and greenhouse-gas emissions is questionable (Schoennagel and others, 2004; Sibold and others, 2006; Mitchell and others, 2009). Some authors, however, have indicated that a more active management approach should be considered in forests at higher elevations in order to encourage ecosystem migration under changing climates and wildland-fire regimes (Hansen and others, 2001; Fule, 2008).

Uncertainty about the short- and long-term advantages and disadvantages of wildland-fire management and fuel treatments is high even without considering climate change, but may increase when climate change is considered. Additional analyses would be required to assess the effects of various management scenarios. Even though wildland-fire emissions in the Western United States are greater than in other parts of the country, they are still relatively small when compared to fossil-fuel emissions, and it is questionable whether any strategy designed to reduce wildland-fire emissions will have a measureable effect at a national scale.

This page intentionally left blank.

Chapter 9. Projected Future Carbon Storage and Greenhouse-Gas Fluxes of Terrestrial Ecosystems in the Western United States

By Shuguang Liu[1], Yiping Wu[2], Claudia J. Young[3], Devendra Dahal[4], Jeremy M. Werner[1], Jinxun Liu[4], Zhengpeng Li[5], Zhengxi Tan[2], Gail L. Schmidt[4], Jennifer Oeding[4], Terry L. Sohl[1], Todd J. Hawbaker[6], and Benjamin M. Sleeter[7]

9.1. Highlights

- On the basis of the land-use and land-cover (LULC) scenarios, climate-change projections, and biogeochemical models used in this assessment, the total carbon stored in the ecosystems of the Western United States in 2050 was projected to range from 13,743 to 19,407 TgC, an increase of 1,325 to 3,947 TgC from the mean baseline conditions (2001–2005; chapter 5 of this report). The amount of projected future potential carbon stored was highly variable among multiple model runs, ecoregions, and ecosystems.
  - The Western Cordillera ecoregion was projected to store the most carbon, accounting for 60 percent of the projected total stored carbon in Western United States, followed by the Cold Deserts (18 percent of the total), Marine West Coast Forest (10 percent), Mediterranean California (8 percent), and Warm Deserts (4 percent) ecoregions.
  - Among the different ecosystems, forests were projected to store the most carbon, accounting for 70 percent of the projected total carbon stored in the Western United States, followed by grasslands/shrublands (23 percent of the total), agricultural lands (6 percent), and other lands (1 percent).
  - About 80 percent of the projected total carbon storage was evenly distributed in aboveground live biomass and soil organic carbon in the top 20 centimeters of the soil layer, with the remaining 20 percent stored in dead biomass (forest litter and dead, woody debris).
- Between 2006 and 2050, and depending on the LULC scenarios, climate projections, and biogeochemical models used in this assessment, the mean annual net carbon flux was projected to range between −113.9 and 2.9 TgC/yr for the Western United States. (Negative values denote a carbon sink.) Compared to the baseline net carbon flux estimates (−162.9 to −13.6 TgC/yr; chapter 5 of this report), the future carbon-sequestration rates in the Western United States were projected to decline by 16.5 to 49 TgC/yr.
  - The Western Cordillera ecoregion was projected to be the largest carbon sink, accounting for 65 percent of the total carbon sequestered in the Western United States, followed by the Mediterranean California (17 percent of the total), the Cold Deserts (11 percent), and the Marine West Coast Forest (7 percent) ecoregions. The Warm Deserts ecoregion was projected to be either a minor carbon source or carbon neutral.
  - All of the major ecosystems modeled in the assessment were projected to gain more carbon than lose it to the atmosphere. The carbon uptake in forests was projected to account for 73 percent of the projected total sink, followed by agricultural lands (13 percent of the total), grasslands/shrublands (11 percent), wetlands (1 percent), and other lands (2 percent).
  - Of the total projected carbon sink, about 50 percent was projected to accumulate in live biomass, 44 percent was projected to accumulate in soil organic carbon, and the remaining 5 percent was projected to accumulate in dead biomass.

[1]U.S. Geological Survey, Sioux Falls, S.D.

[2]Artic Slope Regional Corporation Research and Technology Solutions, Sioux Falls, S.D.

[3]ERT, Inc., Sioux Falls, S.D.

[4]Stinger Ghaffarian Technologies, Inc., Sioux Falls, S.D.

[5]University of Maryland, College Park, Md.

[6]U.S. Geological Survey, Denver, Colo.

[7]U.S. Geological Survey, Menlo Park, Calif.

- The Western United States was projected to be a weak sink for methane (−3.1 to −2.8 $TgCO_{2\text{-}eq}$/yr) and a weak source for nitrous oxide (1.6 to 1.7 $TgCO_{2\text{-}eq}$/yr); these results were similar to the baseline estimates (chapter 5 of this report). When combined with the projected net carbon fluxes (−113.9 to 2.9 TgC/yr, or −417.9 to 10.9 $TgCO_{2\text{-}eq}$/yr), the net total flux of these three greenhouse gases was projected to be −419 to 10 $TgCO_{2\text{-}eq}$/yr by 2050.

9.2. Introduction

The results of the terrestrial carbon storage and flux modeling for the baseline years (2001–2005) were introduced in chapter 5 of this report. This chapter presents the methods and results of assessing the projected amounts of carbon stored in terrestrial ecosystems and projected greenhouse-gas (GHG) fluxes. The task of modeling future carbon storage and flux projections is linked with land-use and land-cover (LULC) mapping and modeling (chapter 2), future LULC scenarios (chapter 6), future climate-change projections (chapter 7), and the projected future extent and severity of wildland fires (chapter 8). The relations between this chapter and the other chapters are depicted in figure 1.2 of chapter 1 of this report. The definitions of the ecosystems used in this assessment are found table 2.1 of chapter 2 of this report.

The atmospheric concentrations of the major GHGs—carbon dioxide (CO_2,), methane (CH_4,), and nitrous oxide (N_2O)—increased by 36, 148, and 18 percent, respectively, from 1750 (the pre-industrial era) to 2006, mainly because of increased human activities (Intergovernmental Panel on Climate Change, 2007). According to the most recent inventory provided by the U.S. Environmental Protection Agency (EPA, 2012), GHG emissions in the United States increased at an average rate of 0.5 percent per year since 1990, and the total emissions for the United States were 6,821.8 teragrams of carbon dioxide equivalent ($TgCO_{2\text{-}eq}$) in 2010, which was an increase of 213.5 $TgCO_{2\text{-}eq}$ (or 3 percent) over the 2009 level. This increase, as reported in EPA (2012), was principally attributed to an increase in energy consumption across all economic sectors and an increased demand for electricity induced by a warming period (especially warmer summers during this period in the United States).

Studies that used both atmospheric and ground-based methods agreed on the presence of a carbon sink in the conterminous United States (Houghton and others, 1999; Pacala and others, 2007; Pan, Birdsey, and others, 2011). A global carbon sink of approximately 2 to 6 petagrams of carbon per year (PgC/yr) was estimated for 1990 through 2100, and the variability of the sink depended on the emissions scenarios that were used in the studies (Levy and others, 2004). Projections of future carbon sources and sinks in the United States were highly variable (Bachelet and others, 2001, 2003; Hurtt and others, 2002). Hurtt and others (2002) suggested that a significant reduction in the sink may be possible during the 21st century and that the carbon sink in the United States would decline from 0.33 PgC/yr in the 1980s to 0.21 PgC/yr by 2050 to 0.13 PgC/yr by 2100. This modeled decline was based on the premise that the ecosystem recovery process that had been primarily responsible for the contemporary carbon sink in the United States would slow down over the 21st century. For temperate forests in the United States, recent studies yielded uncertain results. Heath and Birdsey (1993) estimated a smaller carbon sink during a projected period between 1987 and 2050 (average of 60 teragrams of carbon per year, or TgC/yr) than during the period between 1952 and1987 (average of 250 TgC/yr). On the basis of forest inventory data, Pan, Birdsey, and others (2011) determined that the United States' forests were a stronger carbon sink during the 2000s (94 grams of carbon per square meter per year, or gC/m^2/yr) than during the 1990s (72 gC/m^2/yr). According to Hurtt and others (2002), the existing carbon sink in the United States could become a source under the scenario of a failed wildland-fire-suppression effort, resulting in a loss of 20 PgC to the atmosphere during the 21st century. Smithwick and others (2002) suggested that the carbon-sequestration potential of the Pacific Northwest region could be much higher than the current rates. The National Forest Carbon Inventory Scenarios for the Pacific Southwest Region (California) indicated that the national forests may become a carbon source in the mid-21st century due to wildfire, disease, and other disturbances (Goines and Nechodom, 2009; U.S. Department of Agriculture (USDA) Forest Service, 2012a).

The purpose of this chapter is to report the estimated projections of carbon sequestration and GHG emissions reduction in the Western United States from 2006 to 2050. The input data and methods used in this chapter followed an overall assessment methodology (Zhu and others, 2010), which included climate-change projections; LULC-change projections; simulations of wildland-fire extent, severity, and emissions; and biogeochemical modeling of carbon dynamics and GHG fluxes.

9.3. Input Data and Methods

For the biogeochemical component of this assessment, the General Ensemble Biogeochemical Modeling System (GEMS) (S. Liu and others, 2012; S. Liu, 2009; chapter 5 of this report) was used to simulate the carbon sources and sinks and GHG fluxes in the Western United States. The modeling framework incorporated several biogeochemical models: the CENTURY model (Metherell and others, 1993), the Erosion-Deposition-Carbon Model (EDCM; S. Liu and others, 2003), and a spreadsheet model (Zhu and others, 2010). The input and output data layers used with these models were described in S. Liu and others (2009, 2011; chapters 4 and 5 of this

report). Examples of some of the specific input data are shown in figure 9.1 below. The GEMS was calibrated and validated extensively using net primary productivity data derived from the Moderate Resolution Imaging Spectroradiometer (MODIS NPP) and U.S. Department of Agriculture (USDA) grain yield information (chapter 5 of this report).

In order to explore the carbon dynamics and GHG emissions under a wide range of projected future conditions, 21 GEMS model runs were performed for the future projections. These runs were as follows:

- Three spreadsheet model runs. Each run represented carbon dynamics and GHG fluxes under an LULC scenario that was developed in accordance with storylines A1B, A2, or B1 from the Intergovernmental Panel on Climate Change Special Report on Emissions Scenarios (IPCC–SRES; Nakicenovic and others, 2000; chapter 6 of this report). The spreadsheet model did not simulate the effects of climate change.
- Nine EDCM simulations. Each simulation was a unique combination of an LULC-change scenario corresponding to an IPCC–SRES storyline and a climate-change projection by a general circulation model (GCM). In this assessment, three IPCC–SRES scenarios (A1B, A2, and B1) were used (Sleeter, Sohl, Bouchard, and others, 2012) along with climate-change projections by three GCMs: Model for Interdisciplinary Research on Climate 3.2 medium resolution (MIROC 3.2–medres), Australia's Commonwealth Scientific and Industrial Research Organisation Mark 3.0 (CSIRO–Mk3.0), and The Third Generation Coupled Global Climate Model of the Canadian Centre for Climate Modelling and Analysis (CCCma CGCM3.1) (Joyce and others, 2011).
- Nine CENTURY model simulations. The setups for the CENTURY model runs were the same as for the EDCM.

As with the baseline model runs, a sampling strategy was used to improve overall modeling efficiency. The spreadsheet-model simulations were performed for all ecosystems at 250-m resolution; however, a 1 percent systematic sampling rate was used to accelerate the CENTURY model and and EDCM simulations for the Western United States. As noted in chapter 5 of this report, this sampling procedure was representative of the whole population (all pixels).

For the rest of the modeling process, the modeling architecture, initialization, and execution were the same as for the baseline years (chapter 5 of this report). Therefore, the rest of this chapter focuses on the methods and results that were relevant to the future projections. The key concepts and terminology used in this chapter, including net carbon flux, net primary production (NPP), net ecosystem production (NEP), and net ecosystem carbon balance (NECB), follow conventions used in the literature, as described in chapter 1 of this report.

9.4. Results and Discussion

9.4.1. Projected Carbon Stocks in 2050

Annual maps of total carbon stock in ecosystems from 2006 to 2050 were generated for the Western United States on the basis of the 21 simulation model runs described previously. As a result, there were 21 carbon stock maps for each year from 2006 to 2050. Figure 9.2 represents an average of the 21 annual maps and shows the spatial distribution of the average total amount of carbon (carbon in biomass plus SOC in the top 20 cm of the soil layer) stored in ecosystems in the Western United States in 2050 (the final year of the scenario period) and the standard deviation around the mean value for the 21 simulation model runs. The spatial pattern of stored carbon in 2050 was in general agreement with that of 2005 (chapter 5 of this report).

The projected minimum and maximum amounts of stored carbon from the 21 simulation model runs are provided in table 9.1, by carbon pool, ecosystem, and ecoregion in the Western United States for 2050. The overall total carbon stored in all five ecoregions was projected to range from approximately 13,743 to 19,406 TgC, compared to 12,418 to 15,460 TgC in 2005. Among the ecoregions, the Western Cordillera was projected to have the most carbon stored by 2050, accounting for 60 percent of the total carbon stored in the Western United States, followed by the Cold Deserts (18 percent of the total), Marine West Coast Forest (10 percent), Mediterranean California (8 percent), and Warm Deserts (4 percent) ecoregions. Among the different ecosystems, forests were projected to store the most carbon (70 percent) in the Western United States, followed by grasslands/shrublands (23 percent of the total), agricultural lands (6 percent), and other lands (1 percent). About 80 percent of the total carbon stored was projected to be equally allocated to the live biomass and SOC pools and the remaining 20 percent was projected to be stored in dead biomass (such as forest litter and dead, woody debris). The projected allocation was similar to the pattern of total carbon stored in the same pools in 2005 (chapter 5 of this report).

The projected average future carbon density (carbon stored per unit of area) of the ecosystems varied substantially across ecoregions (fig. 9.2*A* and table 9.1); ranging from high to low, they were forests (15.2 kilograms of carbon per square meter, or kgC/m^2), wetlands (9.0 kgC/m^2), agricultural lands (5.4 kgC/m^2), grasslands/shrublands (2.4 kgC/m^2), and other lands (0.6 kgC/m^2). Geographically, the projected average future carbon density in forests alone was distributed in the Marine West Coast Forest (24.7 kgC/m^2), Mediterranean California (20.7 kgC/m^2), Western Cordillera (15.4 kgC/m^2), Cold Deserts (7.9 kgC/m^2), and Warm Deserts (5.9 kgC/m^2) ecoregions. Similarly, the highest and lowest carbon densities for grasslands/shrublands were projected to be found in the Marine West Coast Forest (9.7 kgC/m^2) and the Warm Deserts (1.5 kgC/m^2). The projected carbon stored in 2050 is briefly described by ecoregion, below.

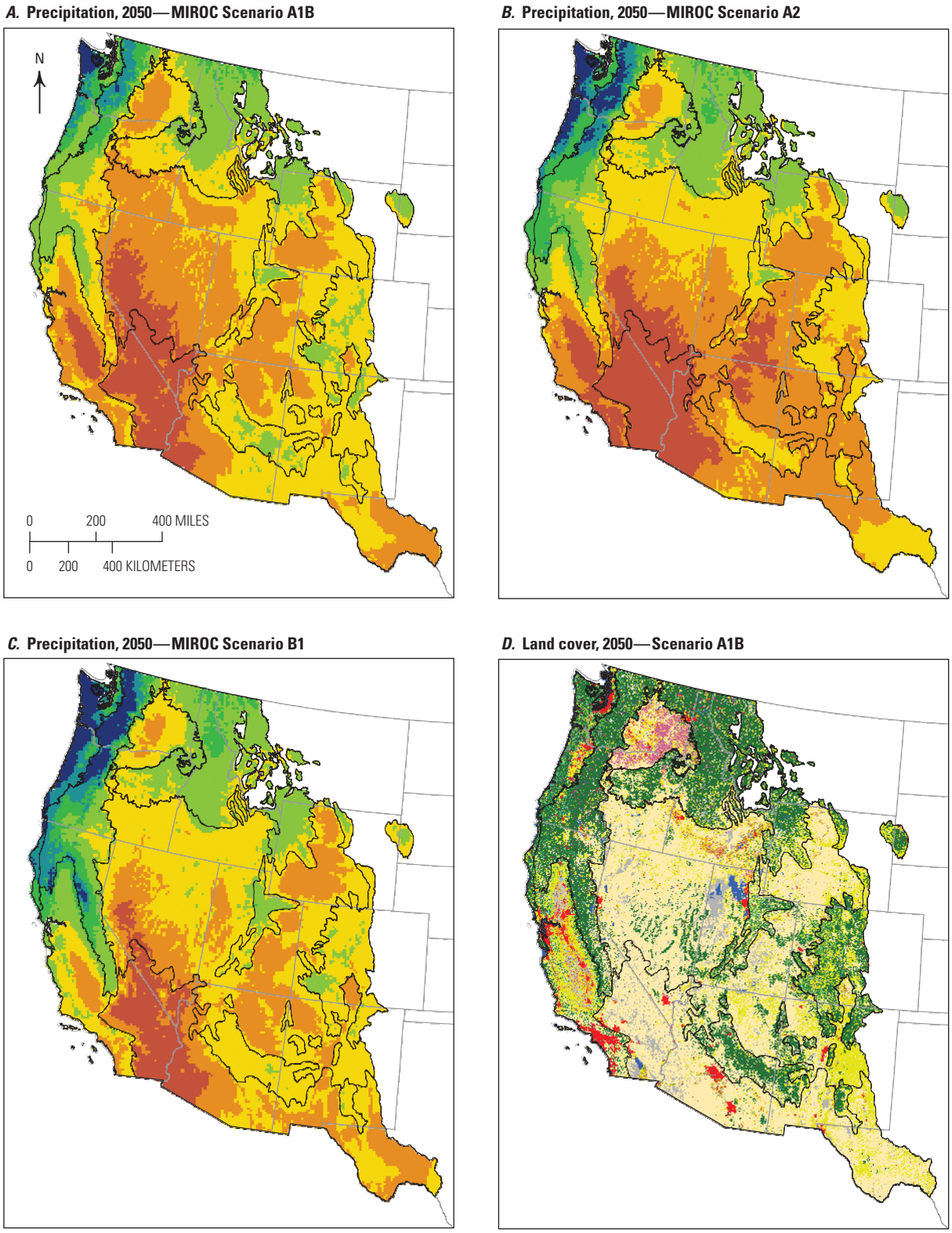

Figure 9.1. Maps showing projected total annual precipitation under the three IPCC–SRES scenarios and projected land cover under the A1B scenario in 2050. *A*, Projected total annual precipitation under the A1B scenario in 2050. *B*, Projected total annual precipitation under the A2 scenario in 2050. *C*, Projected total annual precipitation under the B1 scenario in 2050. *D*, Projected land use and land cover (LULC) map under the A1B scenario in 2050 in 2050. The precipitation data were projected by the MIROC 3.2–medres general circulation model (Joyce and others, 2011). The projected LULC change was from chapter 6 of this report with downscaling of agriculture to crop types by Schmidt and others (2011). IPCC–SRES, Intergovernmental Panel on Climate Change Special Report on Emissions Scenarios (Nakicenovic and others, 2000); MIROC 3.2–medres, Model for Interdisciplinary Research on Climate 3.2 medium resolution.

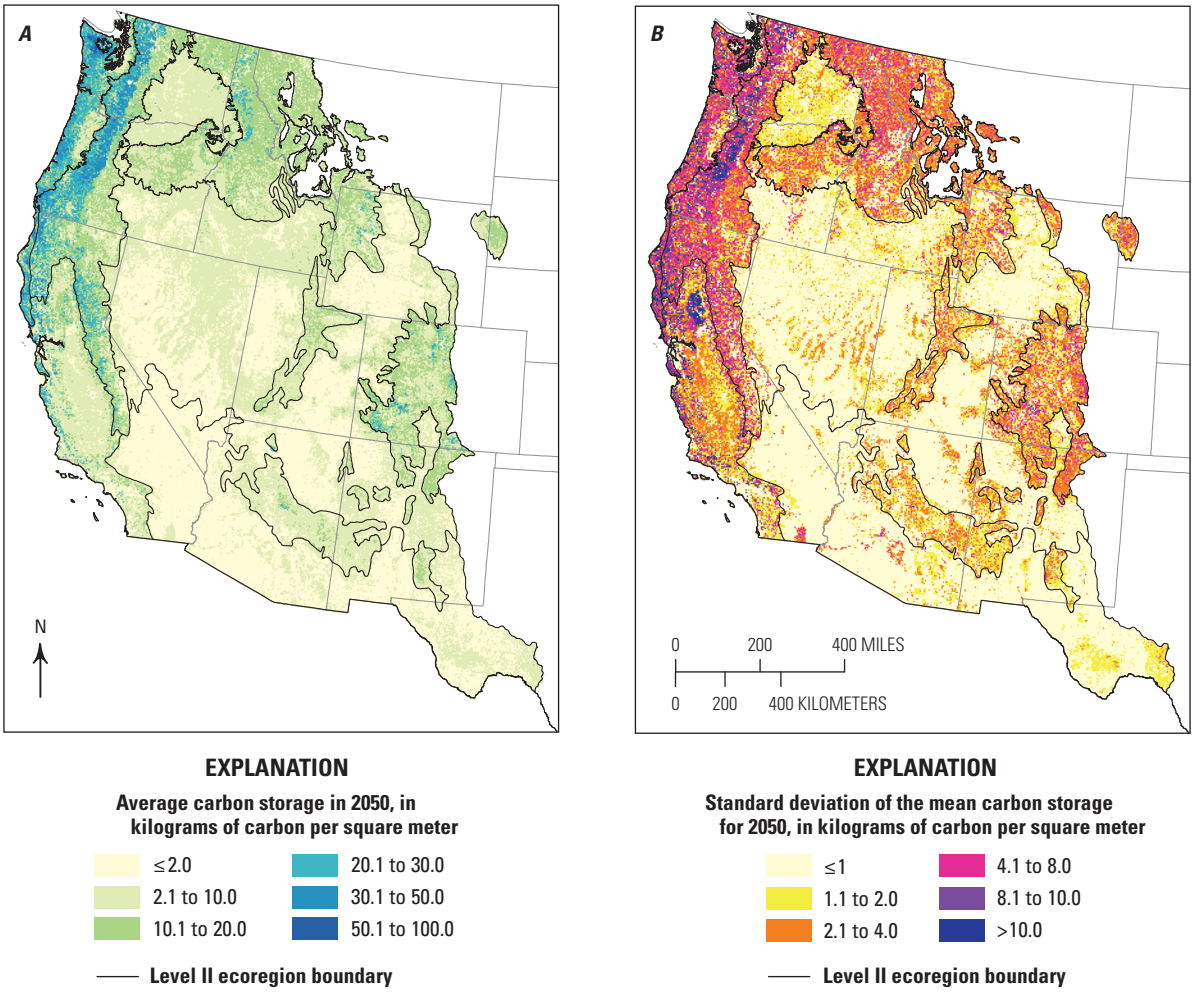

Figure 9.2. Maps showing the projected mean carbon stored and the standard deviation in 2050. *A*, Projected mean carbon stored in 2050 derived from 21 simulation model runs using three biogeochemical models (spreadsheet model, CENTURY model, and EDCM) under three IPCC–SRES scenarios (A1B, A2, and B1) and three general circulation models (MIROC 3.2–medres, CSIRO–MK3.0, and CCCma CGCM). *B*, The projected standard deviation around the mean of the 21 simulation model runs. CCCma CGCM3.1, The Third Generation Coupled Global Climate Model of the Canadian Centre for Climate Modelling and Analysis; CSIRO–Mk3.0, Australia's Commonwealth Scientific and Industrial Research Organisation Mark 3.0; EDCM, Erosion-Deposition-Carbon Model; IPCC–SRES, Intergovernmental Panel on Climate Change Special Report on Emissions Scenarios (Nakicenovic and others, 2000); MIROC 3.2–medres, Model for Interdisciplinary Research on Climate 3.2 medium resolution.

9.4.1.1. Western Cordillera

The total carbon stored in the Western Cordillera ecoregion (the largest of the five ecoregions) was projected to range between approximately 8,703 and 10,670 TgC in 2050 (table 9.1). Live biomass, SOC, and deadmass were projected to store an average of 46, 32, and 22 percent of the total carbon, respectively. Among the different ecosystems, forests were projected to store the most carbon (average of 87 percent of the total) followed by grasslands/shrublands (12 percent). The carbon stored in agricultural lands, wetlands, and other lands (combined) was projected to be only 1 percent of the total carbon. The projected allocation of carbon varied substantially between the three pools (live biomass, soil organic carbon, and dead biomass) across ecosystems. Live biomass was projected to account for 51 percent of the total carbon stored in forests, which was more than the projected sum of the other two pools. In contrast, soil organic carbon was projected to be the dominant storage pool in 2050, holding 76, 86, 64, and 90 percent for grasslands/shrublands, agricultural lands, wetlands, and other lands, respectively.

9.4.1.2. Marine West Coast Forest

The estimated carbon stored in the Marine West Coast Forest in 2050 was projected to range from approximately 1,513 to 1,908 TgC (table 9.1). Live biomass and soil organic carbon were projected to contain 48 and 33 percent, respectively, of this total amount which was similar to the projected allocation pattern in the Western Cordillera. Among the different ecosystems, forests were projected to store the most carbon (91 percent of the projected total carbon), followed by agricultural lands (4.5 percent), and grasslands/shrublands (2.5 percent). The total carbon projected to be stored in wetlands and other lands accounted for only 2.4 percent of the projected total carbon stored in this ecoregion. The live biomass carbon pool was projected to contain the most carbon in both forests and wetlands, accounting for 52 and 46 percent of their totals, respectively, whereas the soil organic carbon pool was projected to be the largest for other ecosystems accounting for 75, 87, and 78 percent of the total carbon stored in grasslands/shrublands, agricultural lands, and other lands, respectively.

9.4.1.3. Cold Deserts

The estimated carbon stored in the Cold Deserts ecoregion was projected to range from approximately 2,260 to 4,060 TgC in 2050 (table 9.1). In contrast to the Western Cordillera and Marine West Coast Forest ecoregions, soil organic carbon was projected to be the primary carbon pool (accounting for 61 percent of the projected total amount of carbon), followed by live biomass (20 percent). Unlike the Western Cordillera and Marine West Coast Forest, grasslands/shrublands were projected to serve as the primary carbon storage pool (58 percent), followed by forests (26 percent) and agricultural lands (13.7 percent). The total percentage of carbon stored in wetlands and other lands was projected to be about 2 percent. Like the Western Cordillera and the Marine West Coast Forest ecoregions, live biomass was projected to serve as the major carbon pool in forests (52 percent of the total forests), but for the other ecosystems, most carbon was projected to be stored in the soil organic carbon pool, ranging from 69 percent (for grasslands/shrublands) to 98 percent (for other lands). The difference in the projected carbon allocation among ecosystems in the Cold Deserts ecoregion compared with that of the Western Cordillera and Marine West Coast Forest was most likely caused by the different projected land-cover fractions. The Cold Deserts ecoregion was projected to be dominated by grasslands and shrublands, and the Western Cordillera and Marine West Coast Forest ecoregions were projected to be dominated by forests.

9.4.1.4. Warm Deserts

The Warm Deserts ecoregion stored the least amount of carbon in 2005 (chapter 5 of this report). By 2050, this ecoregion was projected to still store the least amount of carbon of all the ecoregions, with projected estimates ranging from approximately 465 to 1,177 TgC from all simulation runs (table 9.1). The projected allocation of carbon across the various ecosystems in the Warm Deserts was similar to that of the the Cold Deserts because of the similarities in ecosystem composition and processes. Like the Cold Deserts ecoregion (although much smaller in extent), soil organic carbon was projected to be the primary carbon pool by storing 63 percent of the total carbon, and live biomass was projected to store only 23 percent. Grasslands/shrublands were projected to store the most carbon (84 percent of the total), followed by agricultural lands (7.3 percent) and forests (6.9 percent). Live biomass was projected to account for 58 percent of the total carbon stock in forests, and soil organic carbon was projected to be the primary pool in grasslands/shrublands (64 percent), agricultural lands (82 percent), wetlands (41 percent), and others lands (97 percent).

9.4.1.5. Mediterranean California

For the Mediterranean California ecoregion, the total carbon stored in 2050 was projected to range from 801.5 to 1,591.2 TgC (table 9.1). Soil organic carbon was projected to be the primary carbon pool (storing 49 percent of the total carbon) and live biomass was projected to store 33 percent. The majority of the stored carbon was projected to be in forests (48.5 percent of the total) across all scenarios, followed by grasslands/shrublands (26 percent) agricultural lands (22 percent), and other lands (less than 1 percent). As with other ecoregions, live biomass was projected to be the primary

Table 9.1. Minimum and maximum projections of carbon stored in in the Western United States in 2050, based on 21 simulation model runs, by ecosystem and ecoregion.

[Only soil organic carbon (SOC) in the top 20 cm of the soil layer was calculated. Numbers may not sum due to rounding. km^2, square kilometers; max, maximum; min, minimum; TgC, teragrams of carbon or 10^{12} grams of carbon]

Ecoregion	Ecosystem	Area (km^2)	Live biomass (TgC)		Soil organic carbon (TgC)		Dead biomass (TgC)		Total (TgC)	
			Min	Max	Min	Max	Min	Max	Min	Max
Western Cordillera	Forests	545,522	3,980.7	4,649.6	1,592.7	2,577.4	1,696.6	2,353.1	7,874.3	9,002.6
	Grasslands/shrublands	274,643	72.3	146.9	616.4	1,023.8	0.0	277.8	731.0	1,446.5
	Agricultural lands	18,338	0.2	4.3	64.1	97.8	0.0	20.8	66.7	119.6
	Wetlands	3,531	6.5	8.3	12.2	32.1	2.4	8.6	24.4	47.7
	Other lands	30,234	0.2	2.2	5.5	53.9	0.0	2.6	7.3	54.1
	Total	872,268	4,060.0	4,811.4	2,290.9	3,785.1	1,699.0	2,662.9	8,703.6	10,670.4
Marine West Coast Forest	Forests	61,889	699.6	953.9	375.7	508.9	249.5	367.0	1,411.2	1,710.9
	Grasslands/shrublands	4,347	1.6	6.4	18.0	36.0	0.0	7.9	19.5	47.2
	Agricultural lands	10,342	0.3	4.7	56.2	74.2	0.0	14.6	57.9	89.6
	Wetlands	575	3.6	5.2	3.1	5.4	0.6	1.7	7.3	12.3
	Other lands	18,259	0.0	5.8	10.4	48.0	0.0	7.3	16.9	48.0
	Total	95,411	705.1	976.0	463.3	672.6	250.1	398.5	1,512.9	1,907.9
Cold Deserts	Forests	97,202	332.9	501.6	159.9	290.9	114.9	234.8	674.6	987.4
	Grasslands/shrublands	794,594	208.8	370.0	962.9	1,625.8	0.0	540.4	1,321.5	2,458.3
	Agricultural lands	87,191	0.1	17.4	221.6	421.9	0.0	87.6	235.8	509.8
	Wetlands	4,401	2.3	5.2	13.2	34.5	2.0	8.0	21.5	45.3
	Other lands	72,666	0.0	1.1	6.7	59.5	0.0	0.3	6.8	59.5
	Total	1,056,055	544.1	895.3	1,364.3	2,432.6	116.9	871.0	2,260.2	4,060.3
Warm Deserts	Forests	8,045	21.0	34.1	6.7	15.6	6.5	21.5	38.1	62.7
	Grasslands/shrublands	397,311	91.0	191.6	276.9	598.0	0.0	210.3	411.1	991.8
	Agricultural lands	11,700	0.0	2.4	10.8	78.6	0.0	15.4	12.9	95.7
	Wetlands	322	0.3	0.5	0.3	2.0	0.1	2.1	0.9	4.6
	Other lands	47,907	0.0	0.7	2.0	22.3	0.0	0.3	2.1	22.3
	Total	465,285	112.2	229.5	296.6	716.4	6.6	249.6	465.0	1,177.0
Mediterr-anean California	Forests	29,830	361.0	405.6	56.5	158.5	119.5	128.4	557.9	686.4
	Grasslands/shrublands	65,480	23.5	43.0	103.2	296.6	0.0	81.9	126.7	414.0
	Agricultural lands	40,799	0.0	8.1	88.8	341.2	0.0	65.0	96.3	413.9
	Wetlands	1,019	0.6	1.9	4.0	18.2	0.5	4.5	5.6	22.6
	Other lands	32,327	0.0	2.8	14.7	54.4	0.0	0.6	15.0	54.4
	Total	169,455	385.2	461.4	267.2	868.9	119.9	280.4	801.5	1,591.2
Western United States (total)	Forests	742,488	5,395.2	6,544.9	2,191.5	3,551.4	2,187.0	3,104.8	10,556.0	12,449.9
	Grasslands/shrublands	1,536,375	397.2	758.0	1,977.4	3,580.0	0.0	1,118.3	2,609.8	5,357.8
	Agricultural lands	168,371	0.7	37.0	441.4	1,013.7	0.0	203.4	469.6	1,228.5
	Wetlands	9,847	13.3	21.2	32.7	92.3	5.5	24.8	59.6	132.4
	Other lands	201,393	0.2	12.5	39.2	238.1	0.0	11.1	48.2	238.3
	Total	2,658,474	5,806.7	7,373.5	4,682.2	8,475.5	2,192.5	4,462.4	13,743.2	19,406.8

carbon pool for forests, accounting for 61 percent of the total carbon stored in forests, whereas in other ecosystems, most carbon was projected to be stored in the soil organic carbon pool, ranging from 73 percent in grassslands/shrublands to 95 percent in other lands.

9.4.2. Projected Future Net Ecosystem Carbon Fluxes Between 2006 and 2050

The projected future annual net carbon fluxes (or net ecosystem carbon balance (NECB)) between 2006 and 2050 were calculated as the difference in carbon stock between two consecutive years. A mean annual NECB was derived by averaging all 21 simulation model runs from 2006 to 2050. The standard deviation of the 21 model runs over the simulation time period was also calculated. The resulting models are depicted by the two maps shown in figure 9.3. Figure 9.3*A* indicates that the projected high levels of carbon sequestration (negative NECB, shown by green hues on the map) were strongly associated with the presence of forest ecosystems and that simulated disturbances, such as clearcutting in the Pacific Northwest, were projected to be responsible for a large number of carbon-release hot spots (positive NECB, indicated by red hues on the map). Carbon sequestration was also projected to occur in the agricultural lands of the Central California Valley and the Columbia Plateau level III ecoregions. The mean annual NECB was projected to be minimal in the majority of arid lands of the Western United States. The standard deviation map was spatially similar to the pattern of the mean annual NECB, and the spread was projected to be generally greater in areas with higher mean annual NECB value or higher carbon sequestration.

The projected minimum and maximum mean annual NECB values—from the 21 simulations and averaged annually between 2006 and 2050—are provided in table 9.2 by carbon pool, ecosystem, and ecoregion in the Western United States. The mean annual NECB values listed in this table represent the projected net carbon gain or loss after harvesting (timber and grain harvest) and wildland-fire emissions. The mean annual NECB estimates were projected to vary between −113.9 and 2.9 TgC/yr in the Western United States, which generally agrees with a projected increase in future carbon gains that has been documented elsewhere (Bachelet and others, 2001; J.E. Smith and Heath, 2008).

As shown in table 9.2, the mean annual NECB in the ecoregions of the Western United States was projected to be highly variable. Although the Western Cordillera ecoregion was projected to maintain the greatest carbon sink in the Western United States (accounting for 65 percent of the total mean annual NECB), other ecoregions were projected either to have smaller shares of the total mean annual NECB or to fluctuate between the carbon sink and source. Indeed, this was the case for the entire Western United States, with the overall mean NECB from the 21 model runs projected to vary between −113.9 and 2.9 TgC/yr. When compared with the estimated range of the mean annual NECB during the baseline years (−162.9 to −13.6; see chapter 5 of this report), the projected future mean annual NECB for the entire assessment region was down by 16.5 to 49 TgC/yr. Among all ecosystems, forests were projected to remain strong terrestrial carbon sinks, accounting for approximately 73 percent of the projected total mean NECB. The other ecosystems also were projected to have the potential to sequester carbon, but the interannual variability between carbon sinks or sources was projected to be high. On average, about 50 percent of the total carbon was projected to accumulate in live biomass, 44 percent in soil organic carbon, and the remaining 5 percent in dead biomass (forest litter and dead, woody debris). Wetlands were projected to have the highest mean annual NECB per unit of area (−57 $gC/m^2/yr$), compared with forests (−50 $gC/m^2/yr$), agricultural lands (−40 $gC/m^2/yr$), grasslands/shrublands (−3.9 $gC/m^2/yr$), and other lands (−3.5 $gC/m^2/yr$). The projected carbon sequestration rate per unit of area by forests in the Western United States was lower than the estimate of 75 $gC/m^2/yr$ for 2007 by D.P. Turner, Gockede, and others (2011). The simulated carbon-sequestration rate in agricultural lands was higher than the estimate of 19 $gC/m^2/yr$ by Kroodsma and Field (2006). Detailed descriptions for each ecoregion are given below.

9.4.2.1. Western Cordillera

In the Western Cordillera ecoregion, the projected mean annual NECB between 2006 to 2050 ranged from −61.9 to −6.7 TgC/yr (table 9.2). Among the different ecosystems, forests were projected to gain −27.9 TgC/yr (86 percent of the total), averaged across all model runs, followed by grasslands/shrublands with 3.9 TgC/yr (11 percent of the total), and the sum of the rest of the ecosystems at −0.9 TgC/yr (2.8 percent of the total).

9.4.2.2. Marine West Coast Forest

The projected mean annual NECB in the Marine West Coast Forest ecoregion between 2006 to 2050 ranged from −9.5 TgC/yr (a sink) to 1.8 TgC/yr (a source) (table 9.2), depending on which LULC scenarios, climate-change projections, or biogeochemical models were used. The projected mean annual NECB for forests in this ecoregion was –2.4 TgC/yr (or 73 percent of the total) across all model runs, followed by grasslands/shrublands (–0.3 TgC/yr) and agricultural lands (–0.2 TgC/yr). Wetlands and other lands were projected to account for −0.4 TgC/yr, or 12 percent of the total mean annual NECB.

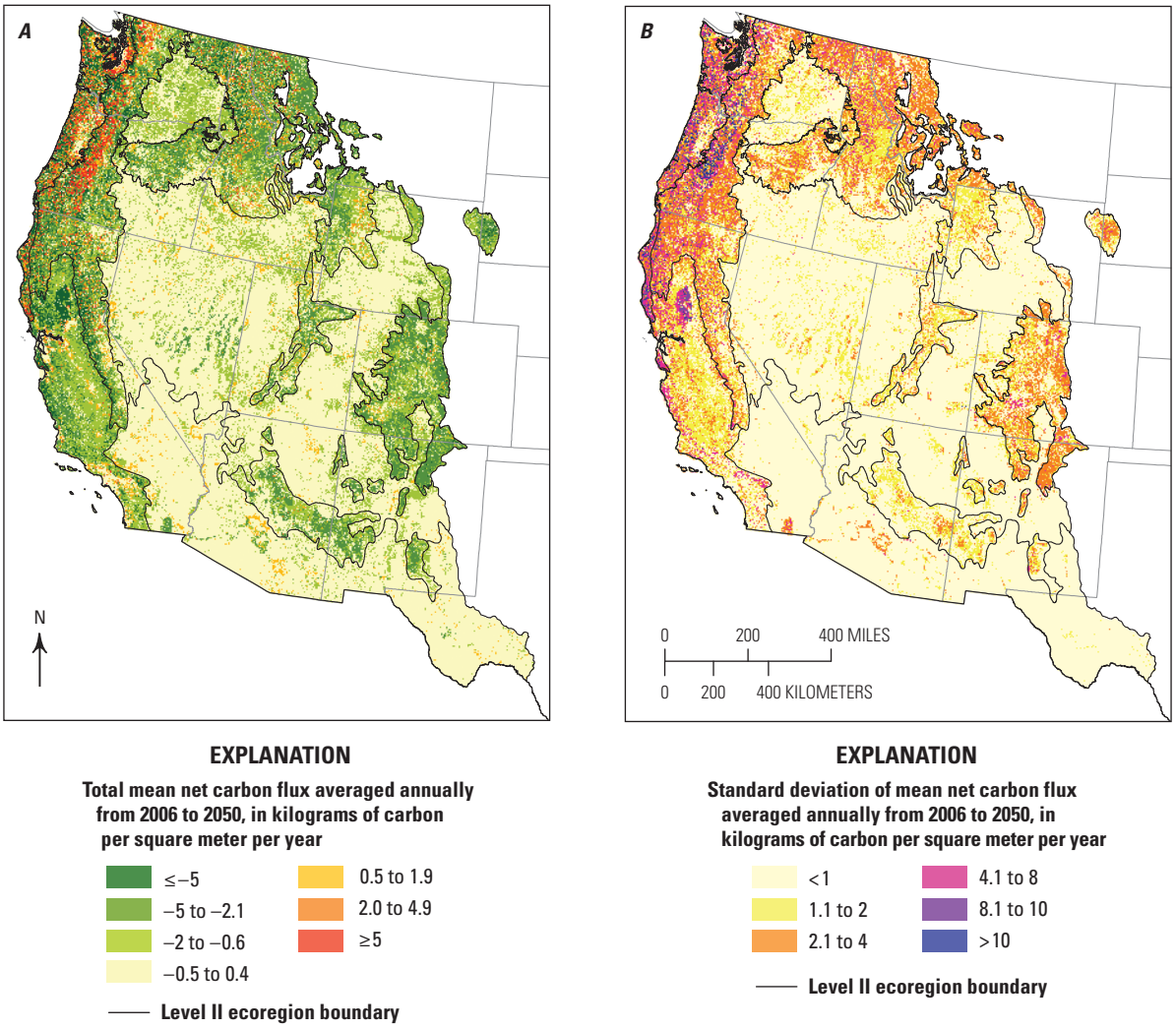

Figure 9.3. Maps showing the projected mean annual net ecosystem carbon balance (NECB), averaged annually from 2006 to 2050, and the standard deviation. *A*, Projected mean annual NECB derived from 21 simulation model runs using three biogeochemical models (spreadsheet model, CENTURY model, and EDCM), three IPCC–SRES scenarios (A1B, A2, and B1) and three general circulation models (MIROC 3.2–medres, CSIRO–MK3.0, and CCCma CGCM). Negative mean annual NECB values indicate projected carbon sinks or carbon gains by terrestrial ecosystems, and positive values denote projected carbon losses. *B*, The projected standard deviation around the mean of the 21 simulation model runs between 2006 and 2050. CCCma CGCM3.1, The Third Generation Coupled Global Climate Model of the Canadian Centre for Climate Modelling and Analysis; CSIRO–Mk3.0, Australia's Commonwealth Scientific and Industrial Research Organisation Mark 3.0; EDCM, Erosion-Deposition-Carbon Model; IPCC–SRES, Intergovernmental Panel on Climate Change Special Report on Emissions Scenarios (Nakicenovic and others, 2000); MIROC 3.2–medres, Model for Interdisciplinary Research on Climate 3.2 medium resolution.

Table 9.2. The projected minimum and maximum mean net ecosystem carbon balance (NECB) values simulated in 21 model runs and averaged between 2006 and 2050, by ecoregion and ecosystem in the Western United States.

[Negative NECB values indicate carbon uptake or sequestration by ecosystems. Only soil organic carbon (SOC) in the top 20 cm of the soil layer was calculated. Numbers may not sum due to rounding. km^2, square kilometers; max, maximum; min, minimum; TgC, teragrams of carbon or 10^{12} grams of carbon]

Ecoregion	Ecosystem	Area (km^2)	Carbon net flux (TgC/yr)							
			Live biomass		Soil organic carbon		Dead biomass		Total	
			Min	Max	Min	Max	Min	Max	Min	Max
Western Cordillera	Forests	545,522	−28.6	−6.5	−15.3	0.1	−8.4	4.5	−52.3	−7.0
	Grasslands/shrublands	274,643	−0.7	0.5	−6.8	0.3	−1.2	0.0	−7.9	0.3
	Agricultural lands	18,338	0.0	0.0	−0.7	0.0	−0.3	0.0	−1.0	0.0
	Wetlands	3,531	−0.1	0.0	−0.3	0.0	−0.1	0.0	−0.4	0.0
	Other lands	30,234	0.0	0.0	−0.2	0.1	0.0	0.0	−0.2	0.0
	Total	872,268	−29.5	−6.0	−23.4	0.6	−10.0	4.5	−61.9	−6.7
Marine West Coast Forest	Forests	61,889	−5.0	0.9	−2.1	0.5	−1.0	0.3	−8.1	1.8
	Grasslands/shrublands	4,347	−0.1	0.0	−0.3	0.0	0.0	0.0	−0.4	0.0
	Agricultural lands	10,342	−0.1	0.0	−0.3	0.2	−0.2	0.0	−0.5	0.2
	Wetlands	575	−0.1	0.0	0.0	0.0	0.0	0.0	−0.1	0.0
	Other lands	18,259	−0.1	0.0	−0.4	−0.1	−0.1	0.0	−0.5	−0.1
	Total	95,411	−5.3	0.9	−3.1	0.6	−1.3	0.3	−9.5	1.8
Cold Deserts	Forests	97,202	−4.6	−0.9	−1.7	0.6	−1.4	0.8	−7.7	−0.8
	Grasslands/shrublands	794,594	−0.7	3.3	−9.7	0.7	−0.5	3.8	−8.7	4.5
	Agricultural lands	87,191	−0.1	0.0	−3.7	0.0	−1.0	0.0	−4.7	0.0
	Wetlands	4,401	0.0	0.0	−0.3	0.0	−0.1	0.0	−0.4	0.0
	Other lands	72,666	0.0	0.0	−0.2	0.1	0.0	0.0	−0.2	0.1
	Total	1,056,055	−5.4	2.4	−15.7	1.5	−2.9	4.6	−21.8	3.8
Warm Deserts	Forests	8,045	−0.3	0.0	−0.1	0.0	−0.1	0.1	−0.5	0.0
	Grasslands/shrublands	397,311	0.0	2.3	−4.0	0.6	−0.1	2.5	−3.9	5.4
	Agricultural lands	11,700	0.0	0.0	−1.2	0.0	−0.2	0.0	−1.3	0.0
	Wetlands	322	0.0	0.0	0.0	0.0	0.0	0.0	−0.1	0.0
	Other lands	47,907	0.0	0.0	−0.1	0.1	0.0	0.0	−0.1	0.0
	Total	465,285	−0.3	2.3	−5.4	0.7	−0.4	2.6	−5.9	5.4
Mediterranean California	Forests	29,830	−3.4	−1.8	−1.6	0.0	−0.8	−0.1	−5.8	−2.0
	Grasslands/shrublands	65,480	−0.3	0.1	−2.6	0.5	−0.4	0.0	−3.0	0.6
	Agricultural lands	40,799	0.0	0.0	−4.3	0.1	−0.7	0.0	−5.0	0.1
	Wetlands	1,019	0.0	0.0	−0.3	0.0	−0.1	0.0	−0.3	0.0
	Other lands	32,327	−0.1	0.0	−0.5	−0.1	0.0	0.0	−0.5	−0.2
	Total	169,455	−3.9	−1.7	−9.3	0.5	−2.0	0.0	−14.7	−1.4
Western United States (total)	Forests	742,488	−42.0	−8.2	−20.9	1.3	−11.7	5.7	−74.4	−8.0
	Grasslands/shrublands	1,536,375	−1.7	6.1	−23.3	2.1	−2.3	6.3	−23.9	10.8
	Agricultural lands	168,371	−0.3	0.0	−10.3	0.3	−2.3	0.0	−12.6	0.3
	Wetlands	9,847	−0.2	−0.1	−1.0	0.1	−0.2	0.0	−1.4	0.0
	Other lands	201,393	−0.2	0.0	−1.5	0.0	−0.2	0.0	−1.5	−0.1
	Total	2,658,474	−44.4	−2.1	−57.0	3.9	−16.7	12.0	−113.9	2.9

9.4.2.3. Cold Deserts

The projected mean annual NECB in the Cold Deserts ecoregion between 2006 to 2050 ranged from −21.8 to 3.8 TgC/yr (table 9.2) across all model runs. The projected variability was represented by both forests and agricultural lands, each with 45 percent of the total mean annual NECB.

9.4.2.4. Warm Deserts

The projected mean annual NECB in the Warm Deserts ecoregion between 2006 to 2050 ranged from −5.9 to 5.4 TgC/yr (table 9.2). Among all the ecoregions, this ecoregion was projected to be the only carbon source, with a mean carbon emission of 0.3 TgC/yr. The dominant ecosystem in the ecoregion, grasslands/shrublands, was projected to contribute about 1 TgC/yr in emissions, whereas forests and agricultural lands combined were projected to account for −0.7 TgC/yr.

9.4.2.5. Mediterranean California

The projected mean annual NECB in the Mediterranean California ecoregion between 2006 and 2050 ranged from −14.7 to −1.4 TgC/yr, of which forests were projected to accumulate the most carbon (−3.7 TgC/yr or 42 percent of the total), followed by agricultural lands (−2.8 TgC/yr) and grasslands/shrublands (−1.9 TgC/yr). Wetlands and other lands were each projected to accumulate about –0.1 TgC/yr, or 1 percent of the total mean annual NECB in this region.

9.4.3. Variability in the Projected Mean Carbon Stock and Mean Net Ecosystem Carbon Balance

As noted previously, 21 simulation model runs were conducted. The objective was to project a range of estimates for the amount of carbon stored and the NECB in order to assess the future carbon storage and sequestration capacities in the region. The variability in the ranges of the resulting estimates represents a major portion of the uncertainty in the assessment results. Table 9.3 compares the projected estimates of mean carbon stocks in 2050 and the mean annual NECB from 2006 to 2050. The data were derived by averaging all of the combinations of the 21 model runs for each ecosystem, for each of the five ecoregions, and for the entire Western United States. A variability value was also calculated as a percent measure for each of the three subsets of the model runs by dividing the range of the minimum and maximum estimates of the subset by their mean, and multiplying by 100.

Among the three biogeochemical models, the EDCM and the spreadsheet model performed similarly, whereas the CENTURY model consistently led to a higher projected estimate of stored carbon than the other two. The models performed differently across ecoregions with the smallest discrepancy found in the Marine West Coast Forest (6 percent variability across three models) and the highest in the Warm Deserts (58 percent). For the projected mean annual NECB estimates, the CENTURY model almost always yielded the highest estimates, followed by the EDCM, and the spreadsheet model (table 9.3). The variability among the models in projecting the mean annual NECB was very high, ranging from 129 percent in the Cold Deserts to 258 percent in the Warm Deserts, suggesting that future effort should be directed to investigating the causes of the divergence of the models and reducing the models' uncertainties.

The variability in the projected carbon stock estimates among the three LULC scenarios was small, ranging from 1 to 9 percent across the ecoregions (table 9.3). The variability of in the projected mean annual NECB under these scenarios was relatively higher than that of the carbon stock, ranging from 4 percent in the Mediterranean California to 200 percent in the Warm Deserts. The higher variability of the projected mean annual NECB across scenarios in some ecoregions did not necessarily indicate that there was a big difference among the results of the scenario modeling. The high variability may have been simply related to the low projected mean annual NECB estimates in the arid regions and how the percent variability was defined. Overall, the projected estimates of carbon stock and mean annual NECB were not significantly affected by the GCMs (table 9.3), with variability ranging from 0.4 to 25 percent for projected carbon stocks and from 3 to 1,139 percent for the projected mean annual NECB. Again, the large relative variability was associated with the low projected mean annual NECB. The projected mean annual NECB varied from −62.2 TgC/yr under the CSIRO–Mk3.0 model to −51.2 TgC/yr under the MIROC 3.2–medres model.

9.4.4. Projected Future Greenhouse-Gas Fluxes from 2006 to 2050

For this assessment, carbon dioxide (CO_2) fluxes were simulated by the EDCM and the CENTURY model as part of the carbon flux assessment described in the previous section of this chapter, whereas methane (CH_4) and nitrous oxide (N_2O) fluxes were simulated separately by the spreadsheet model. To calculate the global warming potential (GWP) in carbon dioxide equivalent ($CO_{2\text{-eq}}$), a factor of 21 was used for methane and of 310 for nitrous oxide (EPA, 2003). The uptake of GWP indicates that GHG fluxes into ecosystems were greater than fluxes out of ecosystems. The projected minimum and maximum mean annual fluxes and their total GWP for 2006 to 2050 are listed by ecoregion and ecosystem in table 9.4. Note that these flux estimates did not include the wildland-fire emission estimates presented in chapter 8 of this report and that the climate-change projections (using GCMs) were not considered in modeling the methane and nitrous oxide fluxes.

Table 9.3. Comparison of projected mean carbon stocks in 2050 and projected mean annual net ecosystem carbon balance from 2006 to 2050, and their percent variability, derived from combinations of three biogeochemical models, three land-use and land-change scenarios, and three general circulation models for each of the five ecoregions and for the entire Western United States.

[EDCM, Erosion-Deposition-Carbon Model; NA, not applicable; NECB, net ecosystem carbon balance; TgC, teragrams of carbon; TgC/yr, teragrams of carbon per year]

	Projected mean carbon stock in 2050 (TgC)						Projected mean annual NECB from 2006 to 2050 (TgC/yr)					
	Western Cordillera	Marine West Coast Forest	Cold Deserts	Warm Deserts	Mediterranean California	Western United States (total)	Western Cordillera	Marine West Coast Forest	Cold Deserts	Warm Deserts	Mediterranean California	Western United States (total)
Biogeochemical models												
CENTURY	10,302.1	1,744.7	3,402.7	898.6	1,495.0	17,843.1	−54.1	−6.0	−7.7	0.3	−12.8	−80.3
EDCM	9,217.6	1,637.5	2,583.1	510.6	1,186.2	15,135.1	−18.9	−1.7	−5.3	0.4	−7.2	−32.8
Spreadsheet	8,874.0	1,653.3	2,429.1	586.7	849.6	14,392.7	−9.7	−0.5	−1.5	−0.1	−1.9	−13.6
Variability	15	6	35	58	55	22	161	204	129	258	148	158
Land-use and land-change scenarios												
A1B	9,540.0	1,631.1	2,909.8	678.8	1,261.1	16,020.8	−30.6	−2.2	−5.8	0.5	−8.6	−46.7
A2	9,615.1	1,648.1	2,902.2	681.0	1,273.6	16,120.1	−32.3	−2.5	−5.6	0.4	−8.9	−48.9
B1	9,744.8	1,777.9	2,925.1	703.5	1,276.7	16,428.0	−35.2	−5.4	−6.1	−0.1	−9.0	−55.7
Variability	2	9	1	4	1	3	14	97	9	200	4	18
General circulation models												
CCCma CGCM	9,772.1	1,699.2	2,979.3	682.0	1,342.7	16,475.2	−36.8	−4.0	−6.2	0.8	−10.0	−56.2
CSIRO–Mk3,0	9,775.0	1,682.7	3,138.2	802.2	1,345.6	16,743.7	−36.8	−3.7	−9.8	−1.8	−10.1	−62.2
MIROC 3.2–medres	9,732.5	1,691.5	2,861.2	629.6	1,333.6	16,248.4	−35.9	−3.9	−3.6	2.0	−9.8	−51.2
Variability	0	1	9	25	1	3	3	10	94	1,139	3	19
All combinations												
Minimum	9,062.1	1,580.6	2,468.4	479.2	1,172.2	NA	−60.9	−8.6	−18.4	−5.8	−13.3	NA
Maximum	10,606.9	1,862.0	3,882.4	1,169.5	1,520.5	NA	−15.5	−0.4	0.5	4.1	−6.9	NA
Overall variability	16	17	47	98	26	NA	−124	−212	−290	2,937	−64	NA

The Western United States was generally projected to incur low levels of methane and nitrous oxide fluxes annually over the projection period of 2006 to 2050, which was similar to the baseline years of 1992 to 2005. As presented in chapter 5, the baseline estimates for methane and nitrous oxide ranged from −3.1 to −2.9 $TgCO_{2\text{-}eq}$/yr and from 1.7 to 1.7 $TgCO_{2\text{-}eq}$/yr, respectively, for the two gases. In comparison, the projected future methane and nitrous oxide fluxes, in comparison, ranged from −3.1 to −2.8 and from 1.63 to 1.68 $TgCO_{2\text{-}eq}$/yr, respectively, which indicates virtually no change over the two periods of the assessment. When combined with the projected net carbon dioxide fluxes for 2006 to 2050, which ranged from −418 to 11 $TgCO_{2\text{-}eq}$/yr, the total resulting GWP for the Western United States was projected to range from −419 to 9.8 $TgCO_{2\text{-}eq}$/yr. The details of methane and nitrous oxide fluxes by ecoregion are described below.

9.4.4.1. Western Cordillera

The mean annual GWP of the Western Cordillera ecoregion between 2006 and 2050 was projected to range from −227.9 to −25.1 $TgCO_{2\text{-}eq}$/yr (table 9.4). The mean methane uptake in this ecoregion was projected to be −1.3 $TgCO_{2\text{-}eq}$/yr with the highest contribution from forests (−0.89 $TgCO_{2\text{-}eq}$/yr) and grasslands/shrublands (−0.81 $TgCO_{2\text{-}eq}$/yr). The rate of methane emissions in wetlands was projected to be 0.40 $TgCO_{2\text{-}eq}$/yr. The mean annual emission of nitrous oxide was projected to be 0.58 $TgCO_{2\text{-}eq}$/yr, of which forests and grasslands/shrublands contributed 52 percent and 40 percent, respectively.

9.4.4.2. Marine West Coast Forest

The mean annual GWP of the Marine West Coast Forest ecoregion between 2006 and 2050 was projected to range from −34.42 to 7.11 $TgCO_{2\text{-}eq}$/yr (table 9.4), depending on the model runs. Most of the uptake was due to the projected future carbon sequestration in the region, which was estimated to sequester the most carbon among all ecoregions on a per-unit-area basis. The methane and nitrous-oxide fluxes were projected to continue to remain emission-neutral.

9.4.4.3. Cold Deserts

The mean annual GWP of the Cold Deserts ecoregion between 2006 and 2050 was projected to range from −81.89 to 12.23 $TgCO_{2\text{-}eq}$/yr (table 9.4). The mean methane uptake was projected to be about −2 $TgCO_{2\text{-}eq}$/yr with contributions from grassslands/shrublands (−2.77 $TgCO_{2\text{-}eq}$/yr), forests (−0.42 $TgCO_{2\text{-}eq}$/yr), and agricultural lands (−0.06 $TgCO_{2\text{-}eq}$/yr). Wetlands and other lands were projected to emit about 1.2 $TgCO_{2\text{-}eq}$/yr of methane. The mean emission of nitrous oxide was 0.40 $TgCO_{2\text{-}eq}$/yr, of which grasslands/shrublands and agricultural lands contributed about 47 percent and 34 percent, respectively.

9.4.4.4. Warm Deserts

The mean annual GWP of the Warm Deserts ecoregion between 2006 and 2050 was projected to range from −22.32 to 19.5 $TgCO_{2\text{-}eq}$/yr (table 9.4). The methane and nitrous oxide fluxes were projected to remain emission-neutral.

9.4.4.5. Mediterranean California

The mean annual GWP of the Mediterranean California ecoregion between 2006 and 2050 was projected to range from −53.68 to −3.88 $TgCO_{2\text{-}eq}$/yr (an overall sink; table 9.4). In a separate study, the major GHG fluxes in forests of the State of California in recent years (2000–2006) were estimated to be −10.7 $TgCO_{2\text{-}eq}$/yr (California Environmental Protection Agency Air Resources Board, 2009). The projected mean annual emissions of methane and nitrous oxide remained low compared to the carbon sink in the ecoregion. Forests and grasslands/shrublands were projected to sequester methane (−0.25 $TgCO_{2\text{-}eq}$/yr), but not enough to offset methane emissions of 1.2 $TgCO_{2\text{-}eq}$/yr from agricultural lands, wetlands, and other lands. The projected mean annual emission of nitrous oxide was 0.18 $TgCO_{2\text{-}eq}$/yr, of which agricultural lands and grasslands/shrublands contributed about 48 percent and 38 percent, respectively.

9.4.4.6. Mean Annual Global Warming Potential of Ecosystems

Among the ecosystems in the Western United States, grasslands/shrublands were projected to play a primary role in the uptake of methane and release of nitrous-oxide with a combined mean annual flux rate of −4.0 to −3.8 $TgCO_{2\text{-}eq}$/yr for the two gases, followed by forests (−1.25 to −1.21 $TgCO_{2\text{-}eq}$/yr). Wetlands were projected to have the highest methane emissions with a mean annual rate of 1.43 to 1.75 $TgCO_{2\text{-}eq}$/yr. Grasslands/shrublands, which were projected to cover about 59 percent of the Western United States, were projected to contribute the most nitrous oxide emissions (53 percent of the total). Agricultural lands, which were projected to cover only 6 percent of the Western United States, were projected to emit 16 percent of the total nitrous oxide.

Figure 9.4 shows the projected GHG fluxes in the Western United States from 2006 to 2050, by LULC scenario. The projected carbon dioxide fluxes indicated more interannual variability than either the projected methane or nitrous oxide fluxes because the carbon dioxide projections included climate-change projections and the projected fluxes of the other two GHGs did not. The projected fluxes of methane ranged from 2.8 to 3 $TgCO_{2\text{-}eq}$/yr and diverged among the three IPCC_SRES scenarios, with an increasing trend (less than 0.004 $TgCO_{2\text{-}eq}$/yr) under the B1 scenario and slightly decreasing trends under the A1B and A2 scenarios. The projected nitrous-oxide emissions indicated minimal variability over time, with a projected mean annual flux of 1.7 $TgCO_{2\text{-}eq}$/yr in the Western United States.

Table 9.4. The projected minimum and maximum of the mean annual carbon dioxide, methane, and nitrous oxide fluxes and their total global warming potential (GWP), averaged from 2006 to 2050, by ecoregions and ecosystems.

[Projected fluxes of methane and nitrous oxide were estimated by the spreadsheet model, and projected flux of carbon dioxide was estimated from the spreadsheet model, CENTURY model, and EDCM. $TgCO_{2\text{-}eq}$, teragrams of carbon dioxide equivalent per year]

Ecoregion	Ecosystem	Area (km^2)	Carbon dioxide ($TgCO_{2\text{-}eq}$/yr)		Methane ($TgCO_{2\text{-}eq}$/yr)		Nitrous oxide ($TgCO_{2\text{-}eq}$/yr)		Global warming potential ($TgCO_{2\text{-}eq}$/yr)	
			Min	Max	Min	Max	Min	Max	Min	Max
Western Cordillera	Forests	−191.9	−25.9	−0.89	−0.88	0.3	0.31	−192.49	−26.47	−7.0
	Grasslands/shrublands	−29.1	1.2	−0.82	−0.81	0.23	0.24	−29.69	0.63	0.3
	Agricultural lands	−3.8	0.1	−0.01	−0.01	0.02	0.02	−3.79	0.11	0.0
	Wetlands	−1.5	0	0.37	0.42	0	0	−1.13	0.42	0.0
	Other lands	−0.8	0.1	0.03	0.03	0.01	0.01	−0.76	0.14	0.0
	Total	−227.2	−24.4	−1.29	−1.26	0.58	0.58	−227.91	−25.08	−6.7
Marine West Coast Forest	Forests	−29.5	6.5	−0.22	−0.2	0.03	0.03	−29.69	6.33	1.8
	Grasslands/shrublands	−1.3	0.1	−0.01	0	0	0	−1.31	0.1	0.0
	Agricultural lands	−1.8	0.7	−0.01	0	0.01	0.01	−1.8	0.71	0.2
	Wetlands	−0.4	−0.1	0.12	0.15	0	0	−0.28	0.05	0.0
	Other lands	−1.7	−0.5	0.42	0.42	0.02	0.02	−1.26	−0.06	−0.1
	Total	−34.8	6.7	0.32	0.34	0.06	0.07	−34.42	7.11	1.8
Cold Deserts	Forests	−28.4	−2.9	−0.42	−0.42	0.06	0.06	−28.76	−3.26	−0.8
	Grasslands/shrublands	−32.1	16.4	−2.8	−2.74	0.18	0.19	−34.72	13.85	4.5
	Agricultural lands	−17.4	−0.1	−0.07	−0.06	0.13	0.16	−17.34	0	0.0
	Wetlands	−1.4	0.1	0.74	0.87	0	0	−0.66	0.97	0.0
	Other lands	−0.9	0.3	0.41	0.41	0.02	0.02	−0.47	0.73	0.1
	Total	−80.2	13.8	−2.08	−1.99	0.39	0.42	−81.89	12.23	3.8
Warm Deserts	Forests	−1.9	0.1	−0.02	−0.02	0	0	−1.92	0.08	0.0
	Grasslands/shrublands	−14.4	19.7	−1.03	−1.01	0.37	0.38	−15.06	19.07	5.4
	Agricultural lands	−4.9	0	−0.01	−0.01	0.02	0.02	−4.89	0.01	0.0
	Wetlands	−0.3	0	0.07	0.07	0	0	−0.23	0.07	0.0
	Other lands	−0.4	0.2	0.05	0.05	0.02	0.02	−0.33	0.27	0.0
	Total	−21.8	20	−0.94	−0.92	0.42	0.42	−22.32	19.5	5.4
Mediterranean California	Forests	−21.3	−7.2	−0.11	−0.11	0.02	0.02	−21.39	−7.29	−2.0
	Grasslands/shrublands	−10.9	2.2	−0.16	−0.13	0.06	0.07	−11	2.14	0.6
	Agricultural lands	−18.4	0.4	0.79	0.86	0.08	0.1	−17.53	1.36	0.1
	Wetlands	−1.3	0	0.13	0.24	0	0	−1.17	0.24	0.0
	Other lands	−1.9	−0.6	0.23	0.24	0.01	0.01	−1.66	−0.35	−0.2
	Total	−53.8	−5.1	0.94	1.03	0.18	0.19	−52.68	−3.88	−1.4
Western United States (total)	Forests	−273.1	−29.3	−1.66	−1.63	0.41	0.42	−274.35	−30.51	−8.0
	Grasslands/shrublands	−87.8	39.6	−4.82	−4.7	0.84	0.88	−91.78	35.78	10.8
	Agricultural lands	−46.4	1.1	0.69	0.77	0.26	0.31	−45.45	2.18	0.3
	Wetlands	−5	0	1.43	1.75	0	0	−3.57	1.75	0.0
	Other lands	−5.6	−0.5	1.14	1.15	0.08	0.08	−4.38	0.73	−0.1
	Total	−417.9	10.9	−3.05	−2.8	1.63	1.68	−419.32	9.78	2.9

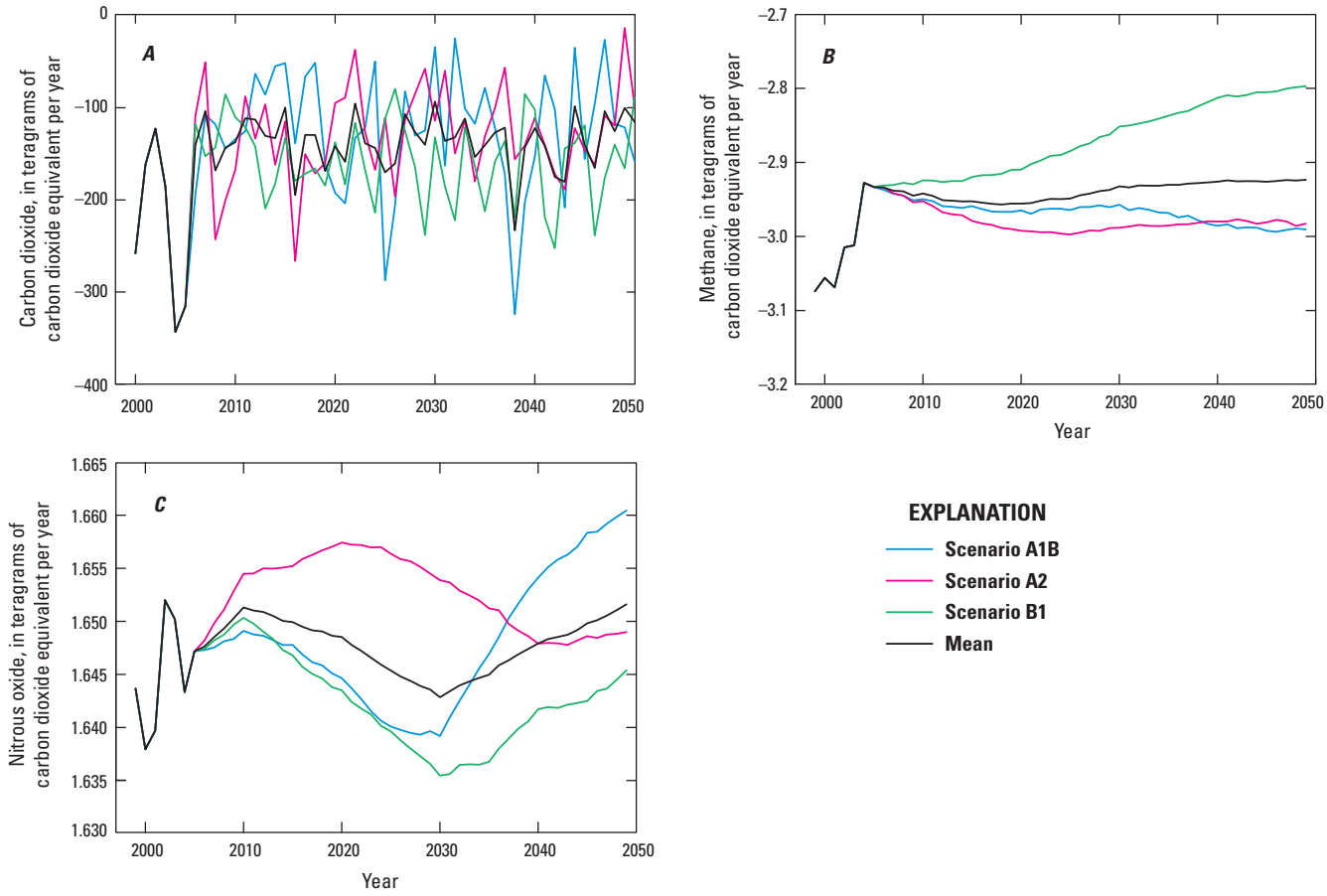

Figure 9.4. Graphs showing the baseline and projected temporal changes in global warming potential (GWP) of carbon dioxide, methane, and nitrous oxide fluxes from 2006 to 2050. *A*, Carbon dioxide. *B*, Methane, *C*, Nitrous oxide. $TgCO_{2\text{-}eq}$/yr, teragrams of carbon dioxide equivalent per year.

9.5. Summary

Using multiple biogeochemical models on the GEMS platform, projected LULC change data, and climate-change scenarios, the projected dynamics of carbon stocks, net ecosystem carbon balance, and GHG fluxes during the period from 2006 to 2050 were assessed. The results indicated that the total carbon stored in the ecoregions of the Western United States was projected to reach from 13,743 to 19,406 TgC by 2050, with the variability resulting from using different biogeochemical models, the LULC scenarios, and climate-change projections. About 80 percent of the total carbon stored would be equally allocated to the live biomass and soil organic carbon pools, and the rest would be allocated to the dead biomass pool (such as forest litter and dead, woody debris). The Western Cordillera ecoregion was projected to store the most carbon by 2050 (59 percent of the total) in the Western United States, and the Warm Deserts ecoregion was projected to store the least (4 percent). Forests were projected to have the highest carbon density with average stocks of 15.3 kgC/m^2, followed by wetlands (9.0 kgC/m^2), agricultural lands (5.4 kgC/m^2), grasslands/shrublands (2.4 kgC/m^2), and other lands (0.6 kgC/m^2).

The projected mean annual NECB varied from −113.9 to 2.9 TgC/yr as the result of the 21 simulation model runs, with approximately 50 percent of the total carbon accumulated in live biomass, 44 percent in soil organic carbon, and the remaining 5 percent in dead biomass. Compared to the baseline net carbon flux estimates for 2001 to 2005 (−162.9 to −13.6 TgC/yr, chapter 5 of this report), the projected future carbon-sequestration rates in the Western United States indicated a decline of 16.5 to 49 TgC/yr by 2050 (the end of the projection period). The Western Cordillera ecoregion was projected to be the largest carbon sink, sequestering 65 percent of the total stored carbon in the Western United States, whereas the Warm Deserts ecoregion was projected to be a small carbon source, emitting 0.2 TgC/yr. Wetlands and forests were projected to have relatively strong mean per-unit-of-area carbon-sequestration rates (−57 $gC/m^2/yr$ and −50 $gC/m^2/yr$, respectively), followed by agricultural lands (−40 $gC/m^2/yr$), other lands (−3.9 $gC/m^2/yr$), and grasslands/shrublands (−3.5 $gC/m^2/yr$). The projected NECB and per-unit-of-area flux estimates varied spatially among ecoregions and ecosystems, and they varied temporally over the projection period, which indicated that each of the ecosystems could be a carbon sink or source for a given ecoregion, driven by LULC, climate, land management, and wildland-fire disturbance conditions.

The projected mean annual fluxes of methane and nitrous oxide were shown to be largely low to neutral, continuing the trend from the baseline period. The Western United States was projected to take up methane at a mean annual rate of −3.1 to −2.8 $TgCO_{2\text{-}eq}/yr$. The annual average nitrous oxide emission was projected to range from 1.63 to 1.68 $TgCO_{2\text{-}eq}/yr$. Given that the mean annual net flux of carbon dioxide in the Western United States was projected to range from −417.9 to 10.9 $TgCO_{2\text{-}eq}/yr$, the total combined GWP for the Western United States was projected to range from −419.3 to 9.8 $TgCO_{2\text{-}eq}/yr$. Although forests and grasslands/shrublands were projected to be a sink for methane, with an average sequestration rate ranging from −1.7 to −4.8 $TgCO_{2\text{-}eq}/yr$, the other ecosystems (agricultural lands, wetlands, and other lands) acted as a methane source, with wetlands emitting the most methane (1.6 $TgCO_{2\text{-}eq}/yr$).

Chapter 10. Baseline Carbon Sequestration, Transport, and Emission From Inland Aquatic Ecosystems in the Western United States

By Sarah M. Stackpoole[1], David Butman[2], David W. Clow[1], Cory P. McDonald[3], Edward G. Stets[4], and Robert G. Striegl[4]

10.1. Highlights

- There was considerable variability in the estimated aquatic carbon fluxes among the five ecoregions in the Western United States, most likely because of differences in precipitation, levels of organic matter inputs, lithology, and topography.
- Inland aquatic ecosystems in the Western United States were both sources and sinks of carbon. Riverine and lacustrine systems were sources of carbon dioxide to the atmosphere, but lacustrine systems also buried carbon in sediments. Total aquatic carbon flux rates were estimated for all five ecoregions in the Western United States using empirical data from 1920 to 2011. The carbon dioxide efflux from lacustrine and riverine systems (combined) was estimated to be 28.1 teragrams of carbon per year (TgC/yr) (confidence interval from 16.8 to 48.7 TgC/yr). The dissolved inorganic and total organic carbon export from riverine systems was estimated to be 7.2 TgC/yr (confidence interval from 5.5 to 8.9 TgC/yr). The carbon burial in sediments of lacustrine systems was estimated to be −2.1 TgC/yr (confidence interval from −1.1 to −3.2 TgC/yr).
- The total aquatic yields (flux rates normalized by land area) for all five western ecoregions were estimated using empirical data from 1920 to 2011. The carbon dioxide efflux yield from riverine systems was estimated to be 14.0 grams of carbon per square meters per year ($gC/m^2/yr$; confidence interval from 6.0 to 17.1 $gC/m^2/yr$) and from lacustrine systems was estimated to be 0.5 $gC/m^2/yr$ (confidence interval from 0.0 to 1.0 $gC/m^2/yr$). The dissolved inorganic and total organic carbon export yield from riverine systems was estimated to be 3.4 $gC/m^2/yr$ (confidence interval from 2.6 to 4.2 $gC/m^2/yr$). The carbon burial yield in sediments of lacustrine systems was estimated to be −1.2 $gC/m^2/yr$ (confidence interval from −0.6 to −1.8 $gC/m^2/yr$).

10.2. Introduction

The aquatic ecosystems discussed in this chapter include streams, rivers, perennial ponds, lakes, and impoundments. Despite the small portion of the land surface area that they cover, lacustrine systems (perennial ponds, lakes, and impoundments) and riverine systems (rivers and streams) can play a major role in the regional and continental-scale carbon budgets (Dean and Gorham, 1998; Cole and others, 2007; Battin and others, 2008). These ecosystems are constantly exchanging carbon with the terrestrial and atmospheric environments, so they can be active sites for transport, transformation, and storage of carbon (Cole and others, 2007; Striegl and others, 2007; Tranvik and others, 2009).

Many processes affect the overall magnitude of fluxes in aquatic ecosystems and determine whether the system is a source or a sink of carbon. Estuarine and lacustrine systems can be sinks of carbon derived from both autochthonous sources (formed at the site of deposition) and allochthonous sources (formed outside of the site of deposition), and riverine systems can transport carbon from upland terrestrial systems to the ocean. Riverine and lacustrine systems, however, can also be supersaturated in carbon dioxide and, therefore, can be sources of carbon to the atmosphere (Kling and others, 1991; Cole and others, 1994, 2007; Aufkenkampe and others, 2011). Some important drivers of carbon fluxes in aquatic ecosystems include (1) timing and magnitude of precipitation and flow, (2) autochthonous and allochthonous carbon production, and (3) physical parameters such as topographic slope, air and water temperature, and seasonality (Michmerhuizen and others, 1996; Tranvik and others, 2009; Einola and others, 2011).

[1]U.S. Geological Survey, Denver, Colo.

[2]U.S. Geological Survey, New Haven, Conn.

[3]Wisconsin Department of Natural Resources, Madison, Wis.

[4]U.S. Geological Survey, Boulder, Colo.

Due to a shortage of empirical data and the lack of a coupled terrestrial and aquatic modeling framework, carbon fluxes and burial rates in the inland aquatic ecosystems of the Western United States were assessed separately from those of the terrestrial processes (chapters 5 and 9), as depicted in figure 1.2 of chapter 1 of this report. This chapter provides baseline estimates of carbon fluxes from inland aquatic systems that were calculated using empirical data spanning a time period from 1920 to 2011. More specifically, this chapter will provide estimates of (1) coastal export and within-ecoregion transport of both dissolved inorganic carbon (DIC) and total organic carbon (TOC) in riverine systems, (2) gaseous carbon emissions in the form of carbon dioxide from lacustrine and riverine systems, and (3) carbon burial rates in sediments of lacustrine systems. In contrast, the following chapter (chapter 11) supplies both baseline and projected changes in TOC fluxes from 1992 to 2050 to coastal areas and assesses the effect of nutrients and land cover on carbon burial rates in coastal estuaries, which are transition zones between the riverine and the oceanic systems.

The baseline estimates of carbon fluxes in inland aquatic ecosystems presented in this chapter benefited from two strengths in the methodology: (1) the estimated values were all based on large, spatially consistent datasets of water chemistry, flow, and sedimentation rates, and (2) the models made use of updated national hydrographic datasets in the conterminous United States, which improved the accuracy of these broad-scale fluxes. The value of computing these estimates is that it is possible to compare the relative magnitude of all fluxes across ecoregions, where changes in physiography and land-use associated with each ecoregion can have a large effect on carbon storage, transport, and loss to the atmosphere. Additionally, these baseline estimates can be used in an integrated analysis (chapter 12) to estimate an overall regional carbon budget that encompasses all of the ecosystems in the Western United States.

10.3. Input Data and Methods

10.3.1. Lateral Carbon Transport in Riverine Systems

Lateral carbon fluxes in riverine systems included carbon derived from terrestrial ecosystems (forests, wetlands, agricultural lands), groundwater, and in-stream production (photosynthesis) minus the losses from sedimentation and carbon dioxide efflux to the atmosphere. Water-quality data were obtained from the National Water Information Service (NWIS) Web site (U.S. Geological Survey, 2012d). The dissolved inorganic carbon (DIC) concentration was estimated from pH, temperature, and either filtered or unfiltered alkalinity. The estimated total organic carbon (TOC) concentration was taken directly from water-quality data or was calculated as the sum of dissolved and particulate organic carbon (Stets and Striegl, 2012).

Carbon fluxes (in kilograms per day, kg/day) were estimated from water-quality and daily streamflow data using the U.S. Geological Survey's (USGS's) Load Estimator Model (LOADEST; Runkel and others, 2004). LOADEST is a multiple-regression Adjusted Maximum Likelihood Estimation (AMLE) model which uses measured DIC or TOC concentration values to calibrate a regression between constituent load, streamflow, seasonality, and time (equation 1).

$$\ln LOAD = a_0 + a_1 \ln Q + a_2 \ln Q^2 + a_3 \sin\left(2\prod dtime\right) + a_4 \cos\left(2\prod dtime\right) + a_5 dtime + a_6 dtime^2 + \varepsilon \quad (1)$$

where

$\ln LOAD$ was the natural log of the constituent load (kg/d),

Q was the discharge,

$dtime$ was time in decimal years, $a_0, a_1, \ldots a_n$ were regression coefficients, and

ε was an independent and normally distributed error.

The model calibration required at least 12 paired water-quality and daily streamflow values. The input data were log-transformed to avoid bias and centered to avoid multicollinearity. The models that were used to estimate loads for individual USGS stations varied in terms of coefficients and estimates of log load (equation 1), and the program was set to permit LOADEST to select the best of nine models based on Akaike's Information Criterion (Runkel and others, 2004). The estimated loads and their standard errors were used to develop 95-percent confidence intervals for various time periods. The model's performance was examined by reviewing its output, such as the AMLE's coefficient of determination (R^2) values and residuals (model error).

Two different datasets were used to estimate lateral TOC and DIC transport in riverine systems: the Coastal Export Dataset and the Ecoregional Comparison Dataset. The Coastal Export Dataset included data on NWIS sites located just upstream from the point where a river meets the coast or a national border. The coastal export of carbon was important to include in this assessment because the significant amounts of carbon transferred from terrestrial systems by rivers and delivered to coastal areas can help balance the overall regional or continental-scale carbon budgets (Schlesinger and Melack, 1981).

The Colorado River and the Rio Grande deliver carbon to the Gulf of California and western Gulf of Mexico, respectively. Carbon is delivered to the coastal Pacific Ocean from watersheds in California, Oregon, and Washington. The largest watershed is that of the Columbia River. In addition, several large endorheic basins (basins that do not drain to the ocean) exist in the Western United States, the largest of which is the Great Basin. Endorheic basins may contain streams and, although there is lateral carbon movement within them, they do not reach the ocean; therefore, the carbon from those streams was not included in estimates of lateral carbon flux to the coastal ocean. The total exorheic drainage area (basins that do drain to the ocean) in the Western United States was 1.66 million square kilometers (km^2). The Coastal Export Dataset included TOC and DIC export estimates from 36 sites in the Western United States (fig. 10.1*A*).

The carbon export to the ocean was estimated by summing the mean observed carbon export from individual sites and then correcting for the drainage area that was not represented by the watersheds included in the database (Stets and Striegl, 2012). The total carbon export estimate (Total E_C) was calculated using equation 2:

$$\text{Total } E_C = E_{C(IN)} \times \left(A_{TOT} / A_{IN}\right) \quad (2)$$

where

$E_{C(IN)}$ was the carbon export estimated from sites included in the database,

A_{TOT} was the total exorheic drainage area, and

A_{IN} was the total drainage for which lateral flux estimates could be made.

This correction assumed an equivalent areal carbon yield from the remaining (unmeasured) exorheic drainage area. This estimate was performed separately for the Colorado River, Rio Grande, and for basins draining to the coastal Pacific Ocean**.**

Fluxes calculated from streamgages located near coastal waters were assigned to an associated coastal receiving waters' region; however, some rivers within one receiving waters' region often crossed ecoregional boundaries, so they were not necessarily instructive about differences in carbon fluxes among the ecoregions. Because a primary goal of this assessment was to explore ecoregional variability in carbon storage and fluxes across all of the Western United States, a second dataset (the Ecoregional Comparison Dataset) was created to include drainage basins contained entirely within single ecoregions in order to characterize lateral carbon flux. This dataset also included fluxes that were estimated from streamgages located upstream from coastal areas. This dataset included DIC estimates from 333 sites and TOC estimates from 94 sites (fig. 10.1*B*). These estimates were derived from smaller drainage basins ranging in size from 1.1 to 16,000 km^2 and draining a total area of 327,902 km^2.

The methods used for uncertainty analysis were applied in a similar manner for results from both the Coastal Export and Ecoregional Comparison Datasets. Daily carbon fluxes (kg/d) were summed by ecoregion for each representative station's flux within either dataset. Then, daily fluxes were converted to annual fluxes (kilograms per year, kg/yr), and 95-percent confidence intervals were calculated from associated standard errors. Each flux value was connected to a USGS streamgage station, which had an associated drainage area (km^2). The drainage areas for fluxes included in a particular receiving waters' region or ecoregion were summed. The total DIC and TOC yields for an ecoregion (in grams of carbon per square meter per year, $gC/m^2/yr$) were calculated by dividing the summed ecoregional annual fluxes by the summed drainage areas. All of the ecoregion boundaries used in this chapter are consistent with those presented in chapter 1 and are slightly modified from the U.S. Environmental Protection Agency's (EPA's) level II ecoregions (EPA, 1999).

10.3.2. Carbon Dioxide Efflux From Riverine Systems

Three values were required to measure the gas fluxes from aquatic systems: (1) the concentration of dissolved carbon dioxide, (2) the gas transfer velocity (k), and (3) the surface area of the water body. The vertical efflux of carbon dioxide from riverine systems in the Western United States was modeled according to established methods (Butman and Raymond, 2011) and as outlined in equation 3:

$$CO_2 \text{ Flux} = \left(CO_{2\text{-water}} - CO_{2\text{-air}}\right) * kCO_2 * SA \quad (3)$$

where

CO_2 Flux was the total net emission of carbon dioxide from riverine systems of the Western United States (in teragrams of carbon per year, TgC/yr),

$CO_{2\text{-water}}$ was the riverine carbon dioxide concentration (in moles per liter, moles/L),

$CO_{2\text{-air}}$ was the carbon dioxide concentration in the atmosphere (in moles/L),

kCO_2 was the gas transfer velocity of carbon dioxide across the air-water interface (in meters per second, m/s), and

SA was the riverine surface area (in square meters, m^2).

The total flux was estimated by summing all of the mean annual fluxes for a stream order (Strahler, 1952) within an ecoregion.

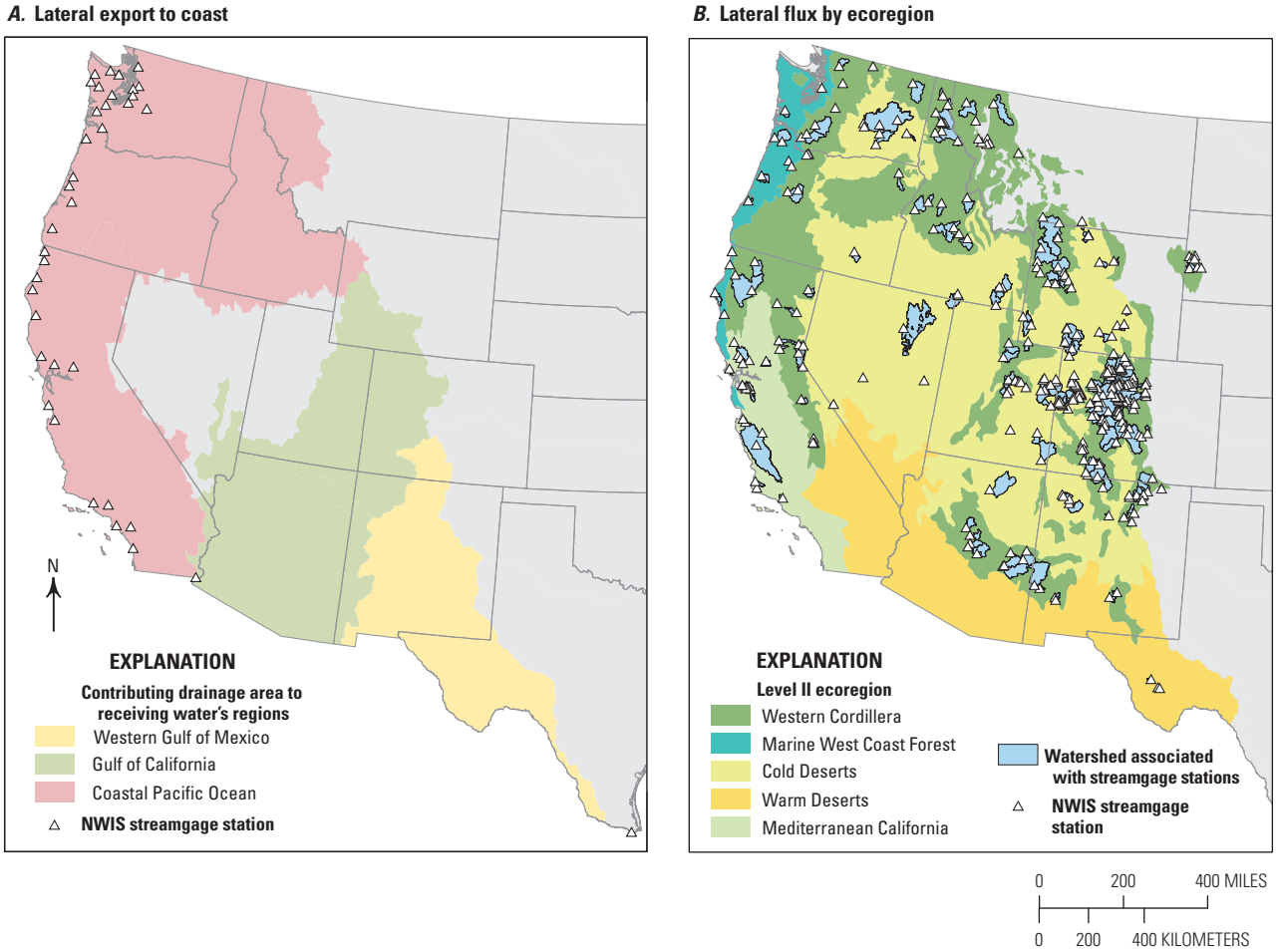

Figure 10.1. Maps showing the locations of the National Water Information System (NWIS) streamgage stations and associated drainage areas. *A*, Stations included in the Coastal Export Dataset. *B*, Stations included in the Ecoregional Comparison Dataset.

The dissolved carbon dioxide concentrations ($CO_{2\text{-water}}$) were estimated from riverine alkalinity data available through NWIS using the CO2SYS program[5] (van Heuven and others, 2009). CO2SYS linked parameters such as temperature, pH, and alkalinity to estimate the dissolved carbon dioxide concentrations by incorporating disassociation constants for carbonic acid (H_2CO_3) into its values. Disassociation constants are mathematical values that describe the tendency of a large molecule such as carbonic acid (H_2CO_3) to disassociate into smaller molecules such as bicarbonate (HCO_3^-), carbonate (CO_3^{2-}), and carbon dioxide (CO_2) in an aqueous environment. The disassociation constants used in the CO2SYS equations for this assessment were from Millero (1979).

Water-chemistry data were collected from the late 1920s through 2011, and daily measurements of pH paired with temperature and alkalinity measurements were used to estimate dissolved carbon dioxide. For the five ecoregions in the Western United States, 1,545 USGS streamgaging-station locations had an adequate chemistry record, and their data were used for the carbon dioxide efflux estimate (fig. 10.2*B*). A minimum of 12 sampling dates was required for inclusion in this analysis. A total of 101,852 daily chemical measurements was identified. The concentration of carbon dioxide in the atmosphere ($CO_{2\text{-air}}$) was assumed to be constant at 390 ppm for all of the ecoregions in the Western United States in equation 3.

The gas transfer velocity (kCO_2), which is the rate of exchange of carbon dioxide across the air-water interface, was based on the physical parameters of stream slope and water velocity (Melching and Flores, 1999; Raymond and others, 2012). The average slope was derived from the NHDPlus datasets (Horizon Systems Corporation, 2005) for each stream order within each ecoregion in the Western United States. The average stream velocity estimates were based on hydraulic geometry parameters for each stream order. The stream discharge (volume of water per unit of time, in cubic

[5] Mathworks, Inc., Natick, Mass.

meters per second, m^3/s) was dependent on the width (m) and depth (m) of the stream channel as well as the velocity of the water moving within the stream (meters per second, m/s) (Leopold and Maddock, 1953; Park, 1977). The stream surface area (SA) in square meters (m^2) was calculated as the product of the average width and total length of the stream by stream order.

Error propagation and uncertainty analyses were performed for each component of equation 3. A bootstrapping technique outlined in Efron and Tibshirani (1993) and Butman and Raymond (2011) was used to estimate error. Bootstrap with replacement ($\alpha = 0.05$) was run for 1,000 iterations to calculate 95-percent confidence intervals for the concentrations of pCO_2 for each stream order within an ecoregion. Similarly, bootstrap with replacement was used to estimate confidence intervals associated with the hydraulic geometry coefficients derived from the measurements of stream width and velocity, which were subsequently used to estimate both the stream surface area and gas transfer velocity (R Development Core Team, 2008). The overall bias associated with the estimates of pCO_2 remained low and had a negligible effect on the error associated with the use of the mean value for each stream order. Similarly, the effect of bootstrapping the hydraulic geometry parameters produced minimal bias.

A Monte Carlo simulation was performed for each stream-order estimate of the total flux (TgC/yr) from riverine surfaces (equation 3). The 5^{th} to 95^{th} confidence intervals derived from the bootstrapping discussed above were used to constrain the Monte Carlo simulation for each parameter of equation 3. The total flux calculation was replicated 1,000 times. This approach was considered to be conservative as it allowed for the same probability of all combinations of each parameter in the total flux equation to be selected for each stream order and may have overestimated the error associated with the riverine efflux.

All of the estimates for the total carbon flux within an ecoregion were presented with the 5th and 95th confidence intervals derived from the Monte Carlo simulation. By using this conservative approach, the range of estimates generally had a high bias because of a slight positive skew in the distribution of pCO_2 concentration within a stream order and ecoregion. The mean concentrations were chosen over the median values because the broader spatial representation was better approximated by incorporating mean values in the Western United States. All of the estimates derived from the Monte Carlo simulation were adjusted to account for monthly temperatures below freezing because it was assumed that riverine efflux did not occur when monthly temperatures averaged below 0°C. This adjustment reduced the estimated efflux measurements for the Western Cordillera and the Cold Deserts ecoregions by 25 percent and 19 percent, respectively.

10.3.3. Carbon Dioxide Efflux From Lacustrine Systems

Water-chemistry data were obtained from the EPA's 2007 National Lakes Assessment (NLA; EPA, 2009a). The NLA used a probability-based survey design to select lakes and reservoirs that met the following criteria: (1) greater than 4 hectares (ha) in area, with a minimum of 0.1 ha of open water; (2) at least 1 m deep; and (3) not classified or described as treatment or disposal ponds, or as brackish-water or ephemeral bodies (EPA, 2009a). Of the 68,223 lakes and reservoirs in the conterminous United States, 1,028 met those criteria. Of those, 252 were located in the Western United States; their locations are shown in figure 10.2*C*.

Sampling took place during the summer of 2007; 50 percent of the samples were obtained between July 12 and August 23, and nearly all (99 percent) were obtained between June 1 and September 30. Twenty-two lakes were sampled twice, and these replicates helped to increase the sample data accuracy. For the lakes that were sampled twice, the data were averaged. The data were assigned to one of the five ecoregions in the Western United States. The number of lakes ranged from 12 to 166 per ecoregion, or one lake for every 38,700 to 2,300 km^2 of total area (including both land and water).

Various biological, physical, and chemical indicators were measured during the NLA (EPA, 2009a), and only a subset of water-chemistry and physical data was used in this assessment: acid-neutralizing capacity (ANC, assumed to be equal to alkalinity), pH, temperature, and dissolved organic carbon (DOC). The final working dataset represented 260 observations from 245 sites.

The estimated carbon dioxide flux from lacustrine systems was calculated using the general equation 3. The estimated dissolved carbon dioxide (CO_{2water}) was computed using the equilibrium geochemical model PHREEQC (Parkhurst and Appelo, 1999). This model is similar to CO2SYS in that parameters such as water, temperature, pH, and alkalinity were used to estimate carbon dioxide concentrations.

The gas transfer velocity (k) for lacustrine systems is largely a function of windspeed (m/s) Cole and Caraco (1998). The estimated mean summer (June to September) wind speeds for each ecoregion were determined from the National Aeronautics and Space Administration's (NASA's) surface meteorology and solar energy data (NASA, 2012; Cory P. McDonald, USGS, unpub. data, 2012). The surface areas of lakes and reservoirs were tabulated for each ecoregion, as in McDonald and others (2012).

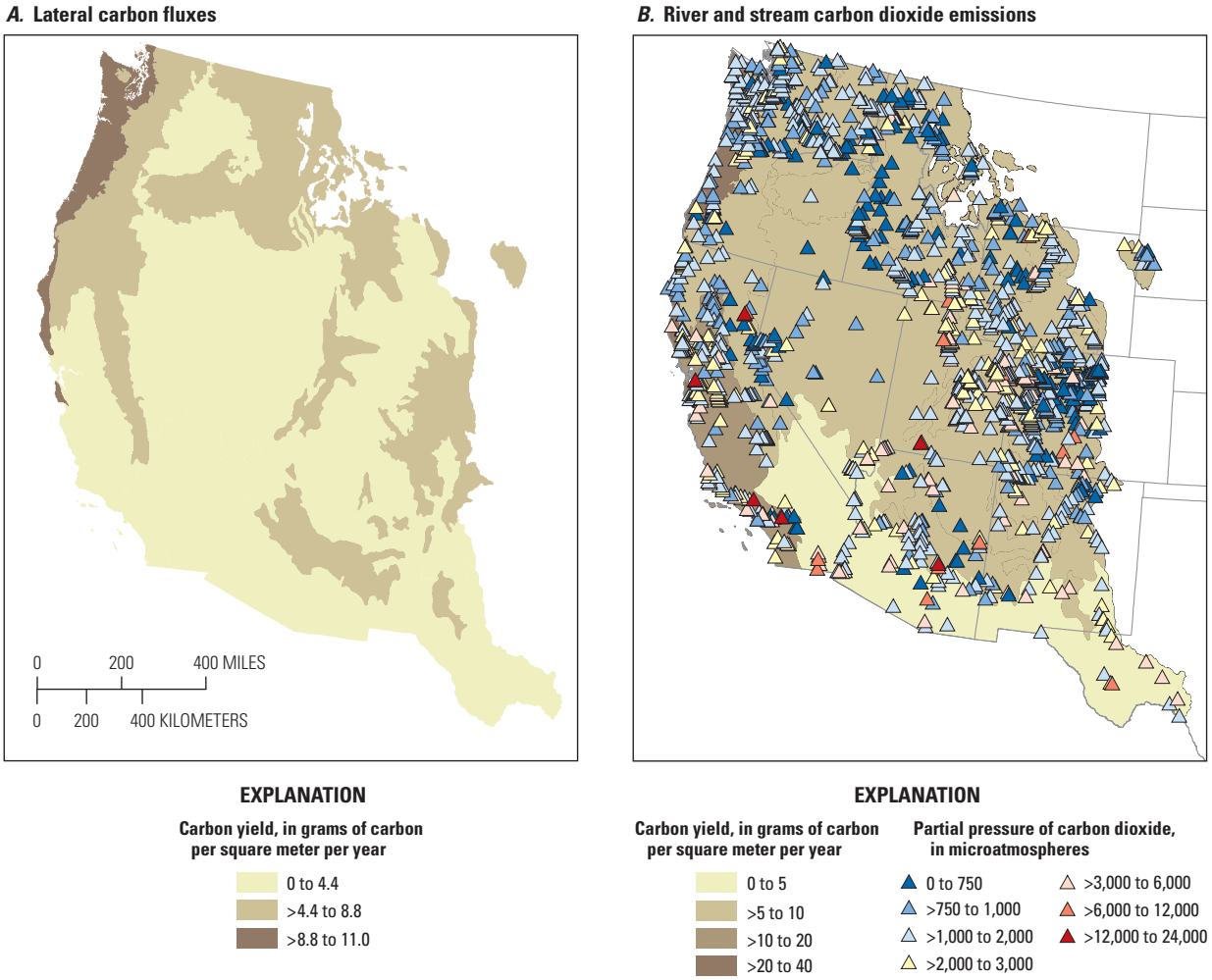

Figure 10.2. Maps showing the estimated relative magnitude of carbon yields, in grams of carbon per square meter per year ($gC/m^2/yr$). *A*, Lateral carbon fluxes in riverine systems. *B,* Carbon dioxide emissions from riverine systems. *C*, Carbon dioxide emissions from lacustrine systems. *D*, Carbon burial rates in lacustrine systems. Parts *B* to *D* show locations of calibrated sample data, and parts *B* and *C* also indicate the estimated relative magnitude of the partial pressure of carbon dioxide (pCO_2) concentrations at the sampling locations.

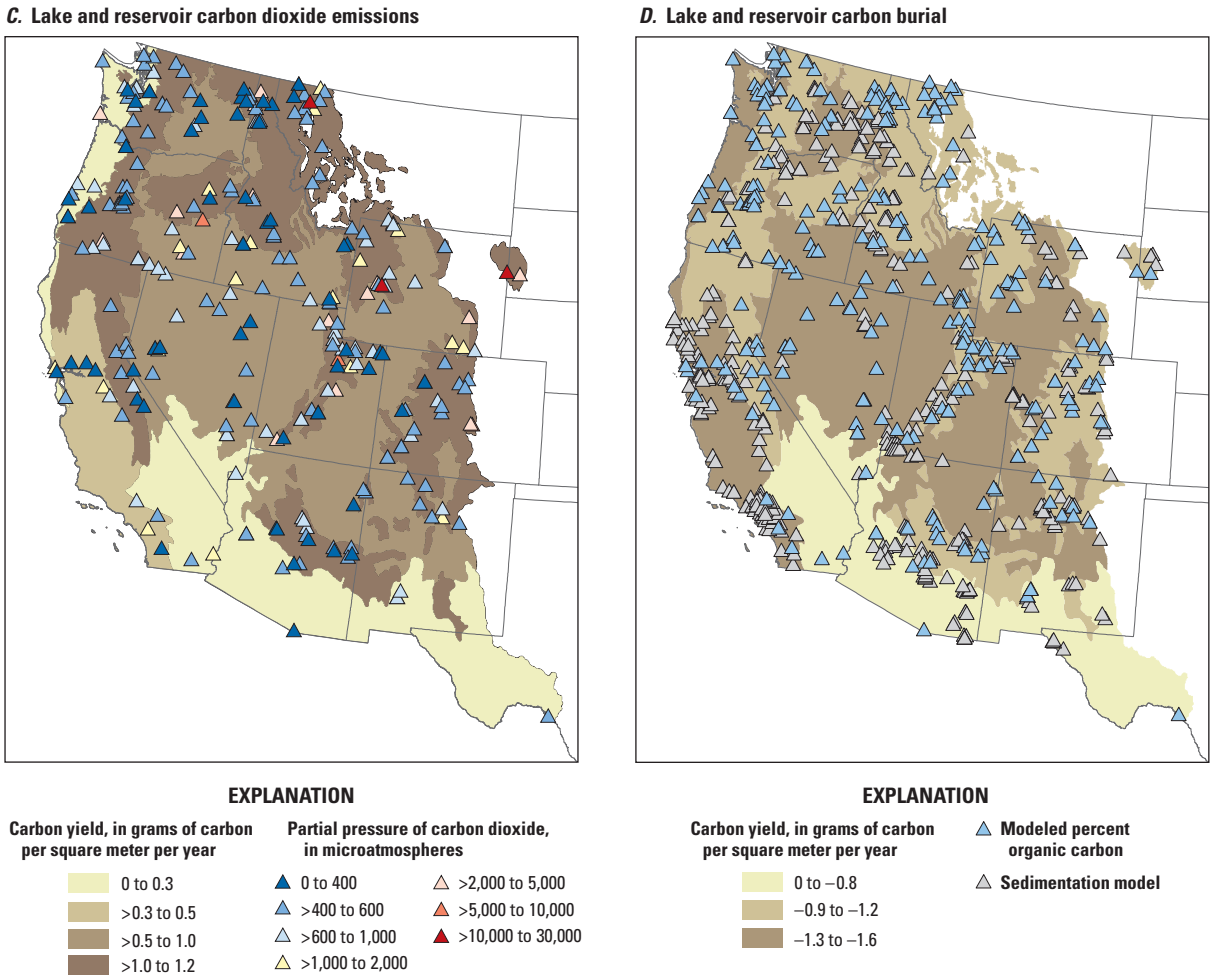

Figure 10.2.—Continued

Many of the parameters involved in these calculations violated normality assumptions; therefore, nonparametric confidence intervals (95 percent) were determined on 1 million ordinary bootstrap replicates. The confidence intervals for the estimated fluxes were determined by propagation of uncertainty, except for the total values (for example, the sum of the regional estimates). In those cases, the confidence intervals were assumed to be additive (uncertainty was not propagated) because potential errors in the regional estimates were likely to be systematic. For the two ecoregions with extended periods of below-freezing air temperatures (the Western Cordillera and the Cold Deserts), the lower confidence interval was adjusted by assuming that carbon dioxide only degasses (at the estimated rate) during the ice-free season. This approach was conservative because carbon dioxide stored under ice is released when the ice melts.

10.3.4. Carbon Burial in Lacustrine Systems

Carbon burial in lacustrine systems is a function of sedimentation rates, carbon concentrations in lacustrine sediments, and the areal extent of lacustrine systems:

$$C_{burial} = SedRt * C_{conc} * SA_{WB} * 10^{-12} \quad (4)$$

where

C_{burial} was the carbon burial rate (in TgC/yr),

SedRt was the sedimentation rate (in $gC/m^2/yr$),

C_{conc} was the concentration of carbon in sediments (in percent by dry weight),

SA_{WB} was the surface area of the water body (in m^2), and

10^{-12} was a conversion factor to convert from grams to teragrams.

Data on sedimentation rates and on carbon concentrations in sediments were sparse, necessitating an empirical approach that relied on existing data to build geostatistical models, which were then used to estimate carbon burial rates. The input data included (1) sedimentation rates derived from a national database (for reservoirs) and peer-reviewed literature (for lakes) and (2) carbon concentrations obtained from measurements on sediment samples collected as part of a national-scale synoptic survey on the water quality of lacustrine systems.

The areal extents of lacustrine systems were derived from the high-resolution (1:24,000) USGS National Hydrography Dataset (NHD; USGS, 2012c). Both sedimentation rates in lakes and carbon concentrations in lake sediments are usually different from those in reservoirs (Mulholland and Elwood, 1982; Dean and Gorham, 1998); thus, the water bodies were separated into lake and reservoir classes. Water bodies were classified as reservoirs if they met any of the following criteria: (1) the water body was tagged as a reservoir in the NHD, (2) the water body name included the word "reservoir" in it, or (3) the water body was included in the National Inventory of Dams database (U.S. Army Corps of Engineers, 2012). Water bodies that were not classified as reservoirs were assumed to be lakes. A comparison with ground-based observations on the 697 lakes that were visited during the 2007 NLA (EPA, 2009a) indicated that this classification scheme was correct 80 percent of the time; however, misclassification rates might have been higher for small water bodies (≤4 ha), such as farm ponds, which were not sampled during the NLA.

The best available national dataset of reservoir sedimentation rates was the Reservoir Sedimentation Database (RESSED; Advisory Committee on Water Information, Subcommittee on Sedimentation, 2012), which included sedimentation-rate data on over 1,800 georeferenced reservoirs in the United States (Mixon and others, 2008; Ackerman and others, 2009). The sedimentation rates in the RESSED database were estimated from repeat bathymetric surveys and were expressed in acre feet per year to facilitate the estimation of storage losses. On the basis of the hypothesis that sedimentation rates were related to land use, topography, soils, and vegetation characteristics in the area surrounding the reservoirs, a GIS analysis was performed to quantify these characteristics for each hydrologic unit (represented by a 12-digit hydrologic unit code, or HUC; U.S. Department of Agriculture, Natural Resources Conservation Service, 2012) adjacent to each reservoir. The sedimentation rates in the RESSED database strongly correlated with the net contributing area (coefficient of determination, $R^2 = 0.94$). The values for the net contributing area, however, were not available for most reservoirs in the United States; therefore, a reservoir's surface area, which should scale with the net contributing area, was used as a surrogate for the net contributing area.

The RESSED dataset was split evenly into calibration and validation datasets, and a stepwise multiple-linear-regression (MLR) analysis was performed on the calibration data, where the sedimentation rate was the dependent variable and the land-use and basin characteristics were explanatory variables. The explanatory variable that explained the most variance in the sedimentation rate entered the model first. The variances explained by the remaining explanatory variables were recalculated, and the variable that explained the next greatest amount of variance entered the model next. This iterative process was repeated until no additional variables showed statistically significant correlations to sedimentation rates, using a p-value ≤0.1. The multicollinearity among explanatory variables was evaluated using the variance inflation factor ($1/1–R^2$) (Hair and others, 2005), which had a threshold for exclusion of 0.2. The resulting MLR equation was used to estimate the sedimentation rates for all of the reservoirs in the NHD. The standard error of the equation was used to calculate uncertainty with 95-percent confidence intervals for the predicted sedimentation rates for sites in the validation dataset.

A national dataset of lake sedimentation rates does not exist; therefore, sedimentation rates were estimated on the basis of data in peer-reviewed literature. Lake sedimentation rates have been calculated for over 80 lakes around the world using ^{210}Pb and ^{137}Cs isotope dating techniques on sediment cores; in most studies, multiple cores were collected from each lake. A review of peer-reviewed literature identified data for sites in North America, Europe, Africa, Asia, New Zealand, and Antarctica. The data were compiled and a statistical analysis was performed to characterize a probability distribution function (pdf) of lake sedimentation rates. A sedimentation rate was assigned to each lake in the NHD using random sampling with replacement. This procedure was repeated 100 times, drawing a new value from the statistical distribution each time, in order to obtain 100 possible sedimentation-rate values. Each of these values was used to calculate a carbon burial rate using equation 4, providing a range of carbon burial estimates for each lake in the NHD. Uncertainty at the 95-percent confidence level was calculated as 2×F-pseudosigma, which is a nonparametric equivalent to the standard deviation when sample data have a normal distribution.

Carbon concentrations were measured on sediment samples collected from 697 water bodies during the 2007 NLA (EPA, 2009a). The data were split into calibration and validation datasets, and a stepwise MLR analysis was performed using the same methods and explanatory variables as in the reservoir sedimentation-rate analysis. The resulting equation was used to estimate carbon concentrations in lake and reservoir sediments in unsampled water bodies across the Western United States. Uncertainty and model performance were evaluated as in the reservoir sedimentation-rate analysis.

10.4. Results

10.4.1. Lateral Carbon Transport in Riverine Systems

The total carbon export from exorheic basins, calculated using the Coastal Export Dataset, was estimated to be 7.2 (ranging from 5.5 to 8.9) TgC/yr (table 10.1), with more than 75 percent of the export occurring as DIC. The carbon exported to the western Gulf of Mexico and the Gulf of California was a small proportion of this total, estimated at approximately 0.1 TgC/yr (table 10.1); the remainder, an estimated 7.1 TgC/yr, was exported to the coastal Pacific Ocean (table 10.1). The Columbia River exported the highest carbon load in this region at an estimated 3.1 TgC/yr. The Klamath River, which had the next highest load, carried approximately one-tenth the carbon load of the Columbia River at an estimated 0.32 TgC/yr.

Table 10.1. Estimated carbon exports, carbon yields (fluxes normalized to watershed areas), and percentages of the total export as dissolved inorganic carbon organized by the three main receiving waters' regions in the Western United States.

[Sites represent U.S. Geological Survey streamgaging stations for which data were available to calculate estimated carbon fluxes from exorheic basins. The 95-percent confidence intervals for the yields and exports are given in the parentheses. The estimated total exports and yields were calculated by summing the dissolved inorganic carbon (DIC) and total organic carbon (TOC). gC/m^2/yr, grams of carbon per square meter per year; TgC/yr, teragrams of carbon per year]

Receiving water's region	Number of sites	Estimated total export (95-percent confidence interval) (TgC/yr)	Estimated total yield (95-percent confidence interval) (gC/m^2/yr)	Estimated flux as dissolved inorganic carbon (percent of total export)
Coastal Pacific Ocean	35	7.10 (5.42, 8.78)	6.29 (5.90, 6.68)	77
Western Gulf of Mexico[1]	1	0.020 (0.011, 0.028)	0.06 (0.05, 0.07)	79
Gulf of California[2]	1	0.076 (0.074, 0.079)	0.12 (0.10, 0.13)	93
All regions	37	7.20 (5.52, 8.88)	3.38 (2.59, 4.17)	77

[1] Rio Grande, partially drains the South-Central Semi-Arid Prairies ecoregion of the Great Plains region.

[2] Colorado River.

The estimated carbon yields and fluxes, calculated using the Ecoregional Comparison Dataset, were highest in the Marine West Coast Forest ecoregion and lowest in the Warm Deserts ecoregion (table 10.2; fig. 10.2*A*). The Marine West Coast Forest ecoregion had a relatively high estimated total carbon yield, but the estimated total export was low because of the ecoregion's small area, which is approximately 10 times smaller than the Western Cordillera ecoregion. Conversely, the Cold Deserts had a relatively high estimated export value because of its extensive land surface area, which is the largest in the Western United States at 1,055,715 km^2. The estimated dissolved inorganic carbon was between 65 and 75 percent of the estimated total carbon export from all regions.

Much of the variability in ecoregional estimates can be explained by differences in the mean runoff and in mean DIC and TOC concentrations. There was substantial variability in the mean runoff among the ecoregions (ranging from an estimated 14 to 1,259 millimeters per year, or mm/yr). The greatest mean runoff was estimated in the Marine West Coast Forest and the Western Cordillera ecoregions and the smallest amount was in the Warm Deserts ecoregion. For each of the ecoregions, the estimated mean DIC concentrations were higher than the estimated mean TOC concentrations, but the estimated mean DIC concentrations in the Cold Deserts ecoregion (62.4 milligrams per liter, or mg/L) were nearly eight times higher than the estimated mean DIC concentrations in the Marine West Coast Forest ecoregion (8.7 mg/L).

10.4.2. Carbon Dioxide Efflux From Riverine Systems

The estimated mean concentration of dissolved carbon dioxide in riverine systems across the Western United States exceeded atmospheric concentrations, indicating that these ecosystems were sources of carbon to the atmosphere. The estimated mean pCO_2 concentration was greatest in the Warm Deserts at 2,391 microatmospheres (µatm; 6.1 times greater than the atmospheric concentrations of carbon dioxide) and smallest in the Western Cordillera at 1,357 µatm (3.4 times greater than the atmospheric concentrations of carbon dioxide). The estimated mean pCO_2 for all five ecoregions combined was 1,893 µatm (3.4 times greater than the atmospheric concentrations of carbon dioxide) (fig. 10.2*C*).

Stream surface areas ranged from 365 km^2 in the Mediterranean California ecoregion to 2,336 km^2 in the Western Cordillera (table 10.3), which was from 0.22 to 0.27 percent of the total area of the ecoregion, respectively. Although its total area was small, the percentage of area covered by riverine systems in the Marine West Coast Forest was the highest of all the ecoregions at 0.73 percent. The total stream surface area for the Western United States region was 6,076 km^2, which was 0.23 percent of the region's area.

Table 10.2. Estimated carbon fluxes, yields (fluxes normalized to watershed areas), and percentages of total flux as dissolved inorganic carbon from riverine systems in the Western United States.

[Sites represent U.S. Geological Survey streamgaging stations in both endorheic and exorheic basins for which data were available to calculate estimated dissolved inorganic carbon (DIC) and total organic carbon (TOC) fluxes, respectively. The 95-percent confidence intervals for the yields and exports are presented in parentheses. The estimated total fluxes and yields were calculated by summing the estimated DIC and TOC. An asterisk (*) indicates DIC values only. $gC/m^2/yr$, grams of carbon per square meter per year; NA, not available; TgC/yr, teragrams of carbon per year]

Ecoregion	Number of sites (DIC fluxes, TOC fluxes)	Estimated total flux (95-percent confidence interval) (TgC/yr)	Estimated total yield (95-percent confidence interval) ($gC/m^2/yr$)	Estimated flux as dissoved inorganic carbon (percent of total flux)
Western Cordillera	224, 61	4.57 (4.15, 5.09)	5.23 (4.76, 5.83)	74
Marine West Coast Forest	11, 6	0.9 (0.68, 0.1.38)	11.0 (7.97, 16.24)	66
Cold Deserts	72, 23	2.41 (2.00, 2.9)	2.29 (1.9, 2.75)	80
Warm Deserts	3, NA	1.00 (0.85, 1.18)*	2.17 (1.83, 2.55)*	NA
Mediterranean California	23, 4	0.43 (0.25, 0.86)	2.61 (1.54, 5.20)	75
Western United States (total)	333, 94	9.35 (7.93, 11.41)	3.64 (3.18, 4.33)	

Table 10.3. Estimated vertical effluxes and yields of carbon dioxide from riverine systems in the five ecoregions of the Western United States.

[Sites are U.S. Geological Survey streamgaging stations for which data were available to calculate the estimated pCO_2. Errors associated with both the total flux and areal flux estimates are presented in parentheses and represent the 5th and 95th percentiles derived from Monte Carlo simulation. Estimated carbon yields were calculated by dividing the estimated total flux by the ecoregion area. $gC/m^2/yr$, grams of carbon per square meter per year; km^2, square kilometers; TgC/yr, teragrams of carbon per year]

Ecoregion	Number of sites	Stream area (km^2)	Estimated total flux (5th and 95th percentiles) (TgC/yr)	Estimated total yield (5th and 95th percentiles) ($gC/m^2/yr$)
Western Cordillera	518	2,336	11.76 (7.3, 21.0)	9.87 (8.4, 24.1)
Marine West Coast Forest	151	619	4.04 (2.0, 7.37)	35.72 (23.7, 86.5)
Cold Deserts	607	2,305	6.15 (4.1, 9.1)	7.16 (3.9, 8.7)
Warm Deserts	107	451	1.53 (0.8, 2.9)	3.57 (1.8, 6.1)
Mediterranean California	162	365	2.65 (1.5, 5.0)	17.1 (8.8, 30.5)
Western United States (total)	1,545	6,076	26.13 (15.7, 45.4)	14.03 (6.0, 17.1)

The estimated total riverine vertical carbon efflux for the Western United States was converted to carbon dioxide equivalent, which produced a value of 95.6 teragrams of carbon dioxide equivalent per year ($TgCO_{2\text{-}eq}/yr$; confidence interval from 57.0 to 166.3 $TgCO_{2\text{-}eq}/yr$). The estimated carbon efflux ranged from a high of 43.1 $TgCO_{2\text{-}eq}/yr$ (confidence interval from 26.7 to 77.0 $TgCO_{2\text{-}eq}/yr$) in the Western Cordillera to a low of 5.5 $TgCO_{2\text{-}eq}/yr$ (confidence interval from 2.9 to 10.6 $TgCO_{2\text{-}eq}/yr$) in the Warm Deserts (table 10.3). The estimated riverine efflux for the Western United States on a per-unit-of-area basis was 14.0 $gC/m^2/yr$ (confidence interval from 7.2 to 20.63 $gC/m^2/yr$); on an ecoregional basis, the estimated efflux ranged from 3.6 $gC/m^2/yr$ (confidence interval from 1.8 to 6.1 $gC/m^2/yr$) in the Warm Deserts to 35.7 $gC/m^2/yr$ (confidence interval from 23.7 to 86.6 $gC/m^2/yr$) in the Marine West Coast Forest.

10.4.3. Carbon Dioxide Efflux from Lacustrine Systems

The estimated mean concentration of pCO_2 in lacustrine systems of the Western United States was 733 µatm (fig. 10.2*C*), which was greater than the atmospheric concentrations for all of the ecoregions; this estimated mean pCO_2 indicated that the lakes generally were sources of carbon to the atmosphere. The estimated mean pCO_2 was greatest in the Western Cordillera at 1,036 µatm (2.7 times greater than the atmospheric concentration of carbon) and smallest in the Marine West Coast Forest at 599 µatm (1.5 times greater than the atmospheric concentration of carbon).

The estimated flux of carbon dioxide across the air-water interface was primarily determined by the gradient between the dissolved and atmospheric concentrations of carbon. The greatest flux was estimated for the Western Cordillera at 106 $gC/m^2/yr$ (or 389 $gCO_{2\text{-}eq}/m^2/yr$), and the smallest flux was estimated for the Marine West Coast Forest at 36.5 $gC/m^2/yr$ (or 134 $gCO_{2\text{-}eq}/m^2/yr$). These fluxes were given as the mass flow per unit of area of the water surface. The estimated mean flux across the air-water interface for all of the ecoregions was 58 grams of carbon per square meter per day ($gC/m^2/d$), or 219 grams of carbon dioxide equivalent per square meter per day ($gCO_{2\text{-}eq}/m^2/d$). The estimated gas transfer velocity was less variable than the estimated pCO_2 among all of the ecoregions—smallest in Western Cordillera (0.93 meters per day, or m/d) and greatest in the Warm Deserts (1.22 m/d).

The ecoregional estimates of total annual carbon dioxide efflux from lacustrine systems (table 10.4) ranged from 0.02 TgC/yr in the Marine West Coast Forest to 1.0 TgC/yr in the Western Cordillera, or from 0.1 to 3.6 $TgCO_{2\text{-}eq}/yr$, respectively. The total carbon dioxide efflux from the Western United States was estimated to be 2.1 TgC/yr (95-percent confidence interval of 1.1 to 3.3 TgC/yr), or 7.6 $TgCO_{2\text{-}eq}/yr$. The estimated ecoregional efflux values were directly related to the surface area of the lacustrine systems (table 10.4), which varied among the ecoregions, partially because of differences in regional morphology and climate but mainly because of differences in the size of the ecoregions.

Table 10.4. Estimated vertical flux of carbon dioxide from lacustrine systems in the five ecoregions of the Western United States.

[Sites are from the 2007 National Lakes Assessment (EPA, 2009a). The data from the 2007 NLA were used in the calculation of pCO_2. Errors associated with both the estimated total flux and yield are presented in parentheses. They represent the bootstrapped 5th and 95th confidence intervals. Estimated carbon yields were calculated by dividing the estimated total flux by the ecoregion area. gC/m^2/yr, grams of carbon per square meter per year; km^2, square kilometers; TgC/yr, teragrams of carbon per year]

Ecoregion	Number of sites	Lake and reservoir area (km^2)	Estimated total flux (5th and 95th confidence intervals) (TgC/yr)	Estimated total yield (5th and 95th confidence intervals) (gC/m^2/yr)
Western Cordillera	137	9,410	0.99 (0.63, 1.28)	1.15 (0.73, 1.49)
Marine West Coast Forest	18	689	0.02 (0.00, 0.08)	0.29 (–0.01, 1.00)
Cold Deserts	68	13,500	0.88 (0.43, 1.54)	0.84 (0.41, 1.47)
Warm Deserts	10	2,630	0.12 (0.06, 0.17)	0.25 (0.14, 0.37)
Mediterranean California	12	1910	0.07 (0.00, 0.16)	0.46 (0.00, 1.02)
Western United States (total)	245	28,139	2.08 (1.13, 3.25)	0.80 (0.43, 1.24)

In order to facilitate a direct comparison between lake and reservoir gas fluxes, lateral carbon transport, carbon burial, and terrestrial processes, the estimated carbon dioxide flux values were normalized to the total land surface area in each ecoregion to provide the carbon yield (table 10.4, fig. 10.2*C*). The estimated carbon yields ranged from 0.3 gC/m^2/yr in the Warm Deserts ecoregion to 1.1 gC/m^2/yr in the Western Cordillera ecoregon. The estimated mean carbon yield (expressed as carbon dioxide efflux per unit of area) from lacustrine systems in the Western United States was 0.6 gC/m^2/yr.

10.4.4. Carbon Burial in Lacustrine Systems

The estimated total annual carbon burial rate in lacustrine systems of the Western United States was −2.42 TgC/yr and varied substantially among ecoregions (table 10.5; fig. 10.2*D*). The Western Cordillera ecoregion had the highest estimated carbon burial rate of −1.14 TgC/yr (confidence interval from –1.71 to –0.57), and the Marine West Coast Forest ecoregion had the lowest estimated carbon burial rate of −0.10 TgC/yr (confidence interval from –0.15 to –0.05). The estimated carbon yield in lacustrine systems, normalized by ecoregion area, was −1.2 gC/m^2/yr (confidence interval from –1.8 to −0.6 gC/m^2/yr). The estimated yields ranged from −0.4 gC/m^2/yr (confidence interval from −0.8 to −0.3 gC/m^2/yr) in the Warm Deserts ecoregion to −1.3 gC/m^2/yr (confidence interval from −2.0 to −0.7 gC/m^2/yr) in the Marine West Coast Forest ecoregion.

The estimated sedimentation rates in reservoirs in the Western United States ranged from 8,622 to 10,068 gC/m^2/yr (TgC/yr normalized to the area of the water body). The lowest estimated rates were in the Warm Deserts ecoregion, and the highest estimated rates were in the Western Cordillera and Cold Deserts ecoregions. The estimated sedimentation rates for lakes compiled from the literature followed an exponential distribution, with an abundance of lakes having low rates and relatively few having high rates. The estimated mean mass sedimentation rates in the lakes were much lower than those in reservoirs, with the mean lake sedimentation rate estimated to be 2,488 gC/m^2/yr.

The carbon concentrations in lacustrine sediments varied substantially among the ecoregions of the Western United States. Sediment concentrations were highest in the Marine West Coast Forest ecoregion (11.4 percent) and relatively low in the Warm Deserts ecoregion (5.0 percent). The specific carbon burial rates (rates normalized to the area of a water body) indicated the intensity of carbon cycling in lacustrine systems. The estimated specific carbon burial rates (per unit of area) were highest in the Marine West Coast Forest at −147 gC/m^2/yr (confidence interval from –222 to –72) and lowest in the Warm Deserts at −84 gC/m^2/yr (confidence interval from –126 to –42).

Overall, the estimated specific carbon burial rates were strongly correlated with the estimated amounts of soil organic carbon (SOC, in gC/m^2) near the water bodies; the R^2 value between estimated carbon burial rates in reservoirs and estimated SOC was 0.96 (p-value=0.01), and the R^2 value between estimated carbon burial rates in lakes and estimated SOC was 0.99 (p-value=<0.001). These results

Table 10.5. Estimated carbon burial rates in lacustrine sediments in the five ecoregions of the Western United States.

[Sites are from the 2007 National Lakes Assessment dataset (EPA, 2009a), which was used to estimate carbon concentrations in sediment. The 95-percent confidence intervals associated with the estimated total fluxes and yields are presented in parentheses. Estimated carbon yields were calculated by dividing the estimated total flux divided by the ecoregion area. $gC/m^2/yr$, grams of carbon per square meter per year; TgC/yr, teragrams of carbon per year]

Ecoregion	Number of sites	Estimated total flux (95-percent confidence interval) (TgC/yr)	Estimated total yield (95-percent confidence interval) ($gC/m^2/yr$)
Western Cordillera	71	−1.14 (−1.82, −0.57)	−1.1 (−1.8, −0.6)
Marine West Coast Forest	10	−0.10 (−0.15, −0.05)	−1.3 (−2.0, −0.7)
Cold Deserts	46	−0.74 (−1.07, −0.36)	−1.3 (−2.0, −0.7)
Warm Deserts	7	−0.20 (−0.26, −0.09)	−0.4 (−0.8, −0.3)
Mediterranean California	4	−0.24 (−0.35, −0.12)	−1.3 (−2.0, −0.7)
Western United States (total)	138	−2.42 (−3.65, −1.22)	−1.2 (−1.8, −0.6)

indicate strong connections between SOC, lacustrine sediment carbon concentrations, and carbon burial rates in lacustrine systems. Of the five ecoregions in the Western United States, the Marine West Coast Forest had the highest estimated SOC (1,824 gC/m^2) and the highest estimated specific carbon burial rates (−147 $gC/m^2/yr$). The Warm Deserts had the lowest estimated SOC (246 gC/m^2) and lowest estimated specific carbon burial rates (−84 $gC/m^2/yr$). In reservoirs, the estimated specific carbon burial rates were positively correlated to the prevalence of forests in nearby areas ($R^2=0.79$, p-value = 0.04); in lakes, the specific carbon burial rates were more strongly associated with wetlands ($R^2=0.78$, p-value = 0.05).

10.5. Discussion

10.5.1. Coastal Export, Lateral Transport, and Carbon Dioxide Efflux From Riverine Systems

The coastal export values represented the estimated amount of carbon that exited the terrestrial landscape and was delivered to the coast. This carbon could potentially have been stored in the ocean or could have contributed to coastal ocean ecosystem processing. The Gulf of California and western Gulf of Mexico, both located adjacent to the drier regions of the Western United States, received waters from one dominant watershed, either the Colorado River or Rio Grande, respectively. The Pacific Northwest, however, experienced much higher precipitation, and many more river basins (about 30) delivered carbon to the receiving waters of the Pacific Ocean; in fact, the highest proportion of land area represented as riverine systems (0.73 percent) was found in the Marine West Coast Forest ecoregion, which was more than double the surface area represented by riverine systems in the other remaining ecoregions. One of the defining characteristics of the Marine West Coast Forest was the high rate of precipitation, and higher annual precipitation increased the transfer of carbon, in either organic or inorganic forms, from the terrestrial environment to streams and rivers (Omernik and Bailey, 1997).

Riverine systems in the Marine West Coast Forest delivered more carbon at a higher estimated rate per unit of area than either the Rio Grande or the Colorado River. Despite the geographic prominence of large river basins, such as the Colorado River and the Rio Grande, the large annual runoff in the Marine West Coast Forest caused this ecoregion to dominate carbon delivery such that even much smaller rivers with coastal endpoints in this ecoregion were important sources of carbon export to coastal areas. These rivers included (1) the Eel River in Scotia, California (drainage = 8,031 km^2), (2) the Elder River near Branscomb, California (drainage = 17 km^2), and (3) the Queets River near Clearwater, Washington (drainage = 1,148 km^2). The Rio Grande, despite its large drainage size, had an annual runoff of only 1 mm/yr compared with annual runoff exceeding 3,000 mm/yr just from several rivers in coastal Washington.

The coastal carbon yields were defined as the amounts of carbon remaining after balancing the inputs and outputs within a watershed, which ranged in area between about 20 and 650,000 km^2. Many of the larger watersheds crossed ecoregional boundaries; for example, the Snake River's headwaters are in the Western Cordillera, but its flow path traverses the Cold Deserts twice before reaching the mainstem portion of the Columbia River, which ultimately meets

the Pacific Ocean in the Marine West Coast Forest. The headwaters of many of the larger rivers (such as the Rogue, Klamath, and Sacramento Rivers) that contribute to coastal fluxes in the Mediterranean California and Marine West Coast Forest ecoregions are located in the uplands of the Western Cordillera ecoregion. This spatial mismatch is important to consider in terms of ecoregional carbon budgets because rivers are not passive transporters of material, and much of the carbon from the headwater source may be transformed or lost before it reaches the ocean.

In order to estimate meaningful ecoregional lateral flux values, the Ecoregional Comparison Dataset included data only from watersheds that fell entirely within the ecoregional boundaries. The benefit of this approach was that the entire watershed, and therefore both the riverine carbon sources and sinks, were defined by the ecoregion's unique characteristics. By using this approach, the differences in flux based on climate, vegetation, and topography could be more easily discerned. This approach skewed the dataset toward smaller watersheds and rivers, but the larger watersheds of the Western United States—in particular, the Columbia River, the Colorado River, and the Rio Grande—were represented in the coastal export section well.

Both the estimated coastal export and ecoregional lateral-flux values demonstrated that runoff or precipitation was a major driver in the variability of both DIC and TOC yields (Amiotte-Suchet and Probst, 1995; Raymond and Oh, 2007; Hartmann, 2009). The two sets of results also highlighted the dominant role of DIC in total carbon export to the coast, as DIC was between 77 to 93 percent of all carbon exports and was between 65 and 80 percent of ecoregional lateral fluxes. In contrast, recent global carbon studies have suggested that the global TOC and DIC export was nearly equal (Meybeck, 1982; Amiotte-Suchet and Probst, 1995). The higher proportion of DIC in the Western United States reported in this study may have had several causes: (1) a large portion of the ecoregions were in dry and arid environments, so there was little contribution of organic matter to overall fluxes; (2) the presence of easily weathered carbonate bedrock contributed unusually high amounts of DIC to the streams; and (3) the high temperatures and the prevalence of dams and reservoirs increased the residence time of water within the streams, which encouraged the organic matter to be mineralized to DIC. In general, DIC was a smaller proportion of total carbon fluxes estimated from the Ecoregional Comparison Dataset than from the Coastal Export Dataset (tables 10.1 and 10.2). The in-stream processing of organic matter may have allowed DIC to become more prominent in the coastal export values.

The concentrations of riverine DIC were especially high in the Cold Deserts ecoregion relative to the other ecoregions, which could have been caused by lithology (Amiotte-Suchet and Probst, 1995; Hartmann, 2009; Moosdorf and others, 2011). For example, there is a large carbonate-rock aquifer that extends throughout the eastern part of the Great Basin, which includes much of the Cold Deserts (Harrill and Prudic, 1998). Chemical weathering and physical erosion releases carbon into rivers, and alkalinity for rivers overlying carbonate rocks can be nearly 20 times higher than for rivers overlying igneous or metamorphic rocks (Amiotte-Suchet and others, 2003).

Considering the variability of the DIC concentrations among the five ecoregions, variation in the estimated pCO_2 values in riverine systems was expected. The contact with groundwater in these carbonate systems (in particular, in the Cold Deserts, as indicated above) could have affected the DIC concentrations, which resulted in higher estimated in-stream pCO_2 concentrations. Additionally, the carbon dioxide efflux from streams and rivers was probably supported by carbon dioxide inputs either directly from the terrestrial environment or through mineralization of terrestrially derived organic matter. It should be noted that for each ecoregion, the estimated total carbon dioxide efflux from riverine systems was always higher than the estimated total lateral flux of DIC; that is, the amount of carbon dioxide being emitted from a stream was higher than the amount of dissolved inorganic carbon material in a stream. For now, the best explanations for this apparent imbalance are that (1) uncertainty in the estimated carbon dioxide fluxes inadvertently resulted in the higher values (field validation may provide more accurate measurements) and (2) the estimates were not fully integrated with terrestrial ecosystem models (further integration may help account for additional sources of carbon to riverine systems).

Additional variables other than lithology and terrestrially derived carbon dioxide are probably needed to explain the variation in dissolved carbon dioxide in streams and rivers across the ecoregions in the Western United States. In general, water sources at high elevations originate from snowmelt. A study by Wickland and others (2001) indicated that runoff from snowmelt, if originating from the surface of the snowpack, was in close equilibrium with the atmosphere; however, throughout the year, the sources of dissolved carbon dioxide at high elevations shifted from snowmelt runoff to water that was in contact with the carbon dioxide produced from soil respiration, thus causing the mean annual carbon dioxide concentration to remain well above atmospheric levels. In the Warm Deserts, where the estimated concentrations of pCO_2 were highest, groundwater may have contributed a significant proportion of dissolved carbon dioxide or carbonates to the estimated total riverine carbon flux.

The very high estimated per-unit-of-area fluxes of carbon from the Marine Western Coast Forest were again indicative of the relatively high estimated pCO_2 concentrations and a diverse landscape along the Coast Range. Estimated gas transfer velocities ranged from 3.2 to 54 m/d, and estimated dissolved carbon dioxide ranged from 3,214 µatm in first-order drainage systems down to 824 µatm at the terminus of the large rivers at the coast. The combination of high carbon

concentrations, high gas transfer velocities, and high stream surface area in a relatively small ecoregion resulted in the very high estimated per-unit-of-area flux estimate. The error analysis for the carbon dioxide flux in streams and rivers of the Marine West Coast Forest suggested an uncertainty in the estimate of up to 33 percent, which should be acknowledged when interpreting the reported values. In general, the very high estimated carbon dioxide flux from streams and rivers in the Western Cordillera was both a function of the steep terrain and relatively fast velocities associated with the Western Cordillera and Gila Mountains (in the Warm Deserts ecoregion). The estimated gas transfer velocities ranged from 10 to 80 m/d and most likely drove the high estimated gaseous flux.

10.5.2. Carbon Dioxide Efflux From and Carbon Burial in Lacustrine Systems

There was significant variability in the number and type of water bodies in each ecoregion. The Western Cordillera contained a balanced mix of natural and artificial lakes or reservoirs (50 percent of each), and the Marine West Coast Forest and Cold Deserts contained fewer natural water bodies (23 percent and 15 percent, respectively). The Warm Deserts and Mediterranean California included only artificial water bodies. The variability in the origin of the water body (natural or artificial) did not appear to be related to the variability in carbon dioxide efflux, however, because carbon dioxide efflux from lacustrine systems was greatest in the Western Cordillera and lowest in the Marine West Coast Forest, the two ecoregions with the most natural water bodies.

The estimated dissolved carbon dioxide in lacustrine systems was in excess of atmospheric concentrations; the excess dissolved carbon dioxide must ultimately have been derived from external inputs of either organic or inorganic carbon. A greater portion of the carbon dioxide in the lacustrine systems of the Western Cordillera appears to have originated from terrestrial organic carbon inputs relative to the other ecoregions. Water bodies in more arid regions (such as the Cold Deserts, Warm Deserts, and Mediterranean California) all exhibited relatively high estimated mean alkalinities (3,200, 2,700, and 2,000 microequivalents per liter, or μeq/L, respectively), suggesting that a large amount of inorganic carbon was delivered to the lacustrine systems from their watersheds. The estimated mean DIC concentrations determined from lateral fluxes in the ecoregional riverine systems supported this hypothesis. For example, the estimated mean riverine DIC concentrations in the Cold Deserts and Mediterranean California were relatively high (62.4 and 44.9 mg/L, respectively) compared to those in the Western Cordillera and Marine West Coast Forest (19.8 and 8.7 mg/L, respectively). Such hydrologic inputs of inorganic carbon have been demonstrated to contribute to dissolved carbon dioxide in some systems (Striegl and Michmerhuizen, 1998; Stets and others, 2009).

The mean alkalinity was lower in the Western Cordillera (1,100 μeq/L) despite the fact that the estimated pCO_2 was greatest in this region, which suggests that a greater fraction of the dissolved carbon dioxide was not derived from riverine inputs, but from the products of in-lake processing of terrestrial organic carbon. The extent to which organic carbon inputs drove carbon dioxide fluxes from lacustrine systems in the Marine West Coast Forest was not clear because both alkalinity (estimated mean = 500 μeq/L) and estimated mean pCO_2 were low. It should be noted that the estimated carbon burial rate (expressed on a watershed-area basis) was highest in the Marine West Coast Forest at 119 ± 60 $gC/m^2/yr$. In contrast, the comparable estimated carbon dioxide efflux from this same ecoregion was lower than any other ecoregion at 37 $gC/m^2/yr$. Additionally, this ecoregion had a high estimated riverine pCO_2 yield, implying that there was a considerable amount of carbon emitted from the stream environment per unit of area, which may be a factor in the low alkalinities of the downstream lacustrine systems.

The differences in the estimated total annual carbon burial in lacustrine systems among the five ecoregions reflected variations in the estimated specific carbon burial rates, which were controlled by (1) soil organic carbon (SOC), (2) vegetation, and (3) sedimentation rates. The estimated specific carbon burial rates were strongly correlated with the estimated amounts of SOC (gC/m^2) near the water bodies. Of the five ecoregions in the Western United States, the Marine West Coast Forest had the largest estimated amount of SOC (gC/m^2) and the highest estimated specific carbon burial rates. The Warm Deserts had the smallest estimated amount of SOC (gC/m^2) and lowest specific carbon burial rates. Regarding vegetation, the estimated specific carbon burial rates for reservoirs were positively correlated to the prevalence of forests in nearby areas; for lakes, the estimated carbon burial rates were more strongly associated with wetlands. Both types of vegetation (forests and wetlands) contributed to the accumulation of carbon in soils near the water bodies. Soil erosion in forested areas contributed allochthonous carbon, which is particularly important in reservoirs (St. Louis and others, 2000; Tranvik and others, 2009). Because wetlands are areas of active carbon cycling (Bridgham and others, 2006), they may contribute particulate and dissolved carbon to lakes. Finally, estimated sedimentation rates, particularly in reservoirs, were strongly related to the reservoir's area; larger reservoirs had higher estimated sediment accumulation rates.

10.5.3. Limitations and Uncertainties

The lateral flux values determined from the Ecoregional Comparison Dataset (table 10.2) represented only smaller watersheds, with boundaries that lay entirely within ecoregional boundaries. This bias was balanced by also providing estimates of larger western watersheds in the Western United States that drain to the Pacific coast in the Coastal Export Dataset. There was a paucity of data, however, for the smaller watersheds, and the values presented in table 10.2 represented only 0.05 to 25 percent of the total ecoregional area. Because of the limited dataset and the large extrapolation of these values, they should be interpreted with caution.

In this assessment, the estimated carbon dioxide efflux rates from riverine systems dominated the estimated aquatic carbon fluxes. Validation data to support fluxes of this magnitude do not currently exist; however, recent research measuring oxygen transfer rates suggests that gas transfer velocities in the upper reaches of the Colorado River can range from 9 m/d in the larger main channels up to 338 m/d in rapids (Hall and others, 2012). It is important to note that the model to estimate gas transfer velocity of carbon dioxide outlined in Raymond and others (2012) and used for this assessment was developed from a dataset that did not include any measurements from steep-slope or high-altitude locations, and as such, the application of this model in highly diverse riverine landscapes must be done with appropriate caution.

The contribution of organic acids to the calculation of total alkalinity could have caused an overestimation of the dissolved pCO_2 concentrations (Tischenko and others, 2006; Hunt and others, 2011). In typical naturally occurring fresh water, the only major contributor to noncarbonate alkalinity is organic acid, primarily humic and fulvic acids (Lozovik, 2005). The concentration of free organic ions was estimated for the lakes included in the 2007 NLA (EPA, 2009a) using the empirical relations of Oliver and others (1983). The estimated organic anion concentration for each lake or reservoir was subtracted from the measured alkalinity prior to performing an analysis of pCO_2; however, an appropriate correction algorithm has not been developed for the dataset used for the flux calculation in riverine systems because of the limited locations of paired dissolved organic carbon and alkalinity measurements within the USGS's NWIS database. Because the current methodology for estimating alkalinity in riverine systems does not account for organic acids, some of the existing estimate of riverine fluxes may be high. Uncertainties in the estimates may be reduced by accounting for noncarbonate alkalinity (organic acids) when deriving pCO_2 concentration from total alkalinity measurements.

The stream and river surface-area estimates for each ecoregion ranged from 0.2 to 0.73 percent of the total area, and they are consistent with other published values (Downing and others, 2009; Aufdenkampe others, 2011); however, the accuracy of stream and river surface area estimates may improve by using remote-sensing techniques to further constrain the hydraulic geometry parameters that are appropriate at the ecoregion scale (Striegl and others, in press). Specifically, there is a need to constrain the surface areas of first-order stream systems (headwaters areas) that may be poorly characterized within the NHDPlus dataset. Regional efforts to physically map first-order stream-surface areas in combination with scaling laws would reduce uncertainties.

The location of USGS streamgaging stations, which were used in calculating the hydraulic geometry coefficients, introduced a bias because the stations were placed in a location that was best suited for accurate discharge measurements (Leopold and Maddock, 1953; Park, 1977). Therefore these station locations most likely do not represent the entire range of variability in the relationships among stream depth, width, and velocity that exists along the flowpaths of rivers in the Western United States. The results from the Monte Carlo simulation suggested levels of uncertainty approaching 50 percent for the Western Cordillera and about 30 percent for each of the four other ecoregions. In addition, the current application of bootstrapping and simulation was considered very conservative; however, as suggested above, without extensive efforts in field validation for both the gas transfer velocity and dissolved carbon dioxide concentration in small stream environments, the model estimates reported in this assessment represent the most comprehensive to date.

Using the available data, it was not possible to accurately model the impact of seasonality on estimated mean carbon dioxide efflux from lacustrine systems. In dimictic lakes (lakes that experience ice cover and mix completely in the spring and fall), carbon dioxide concentrations build up under ice cover and in the hypolimnion (bottom waters) during stratification as a result of heterotrophic respiration and are degassed rapidly during mixing (Michmerhuizen and others, 1996; Riera and others, 1999). Because the available data for the assessment were collected from surface waters only during the summer, this aspect of the seasonal pCO_2 dynamics was not included in the estimates, which most likely affected the results from the Western Cordillera and the Cold Deserts ecoregions, where lakes are at high elevations and mean air temperatures are below freezing for approximately 100 days each year. The Marine West Coast Forest, the Warm Deserts, and Mediterranean California ecoregions do not, on average, experience sustained below-freezing temperatures, but monomictic lakes (lakes that vertically mix once a year) potentially also experience one large degassing event per year.

10.6. Summary and Conclusions

There was great variability in estimated carbon fluxes among the aquatic ecosystems of the five ecoregions in the Western United States, most likely because of differences in (1) precipitation, (2) organic matter production, (3) lithology, and (4) physical characteristics of watersheds such as stream width and slope. The estimated total riverine carbon dioxide efflux in the Western United States was high (26.1 TgC/yr) relative to other aquatic ecosystems. Considering the additional estimated total carbon dioxide efflux from lacustrine systems (2.1 TgC/yr) and riverine export to coastal areas (7.2 TgC/yr), the sum of these losses totaled 35.4 TgC/yr. This loss was offset by an estimated total carbon burial rate of –2.4 TgC/yr in lacustrine systems.

Even though the extent of aquatic ecosystem fluxes presented in this chapter was extensive, it was not exhaustive. For example, it was not known how much carbon was produced by photosynthesis, lost by respiration, or buried in riverine systems; therefore, it was not possible to present a complete aquatic carbon budget for the Western United States, and the full impact of aquatic carbon fluxes on a terrestrial carbon budget could not be determined. The sum of losses from aquatic ecosystems listed above was equivalent to about 25 percent of the net ecosystem production (NEP) obtained by the terrestrial ecosystem component of this report (chapter 12). This value must be interpreted with caution; because the terrestrial and aquatic modeling systems were decoupled, it was not clear how much of the carbon dioxide efflux from riverine and lacustrine systems was already captured in a terrestrial carbon dioxide efflux value. This comparison does, however, indicate that the linkage between terrestrial and aquatic ecosystems is critically important to fully understand the role natural ecosystems play in greenhouse-gas storage and cycling. The relationship between aquatic and terrestrial ecosystem fluxes will be further explored in chapter 12.

This page intentionally left blank.

Chapter 11. Terrestrial Fluxes of Sediments and Nutrients to Pacific Coastal Waters and Their Effects on Coastal Carbon Storage Rates

By Brian A. Bergamaschi[1], Richard A. Smith[2], Michael J. Sauer[1], and Jhih-Shyang Shih[3]

11.1. Highlights

- Riverborne fluxes of total organic carbon, total nitrogen, and total suspended sediment to the Pacific coastal waters of the Western United States under baseline (1992) conditions were estimated at 1.60, 0.40, and 66.78 Tg/yr, respectively. The projected (2050) future fluxes of these same constituents under a regionally downscaled land-use and land-cover (LULC) scenario aligned with the Intergovernmental Panel on Climate Change's (IPCC's) A2 scenario were 1.62, 0.50, and 63.78 Tg/yr, respectively, which indicated a projected change of –1.4 percent, +27.7 percent, and −4.5 percent, respectively.
- The southern California region exhibited the largest projected proportional changes in flux values under the IPCC A2 scenario compared with the baseline conditions, largely due to projected changes in population and urban development.
- For the Pacific coastal waters of the Western United States, the projected nitrogen fluxes were particularly elevated under the IPCC A2 scenario conditions compared with the baseline conditions, suggesting a possible increase in the frequency and duration of coastal and estuarine hypoxia events and harmful algal blooms.
- The projected carbon storage in coastal environments (those supported by terrestrial processes) represented a significant sink for carbon compared with terrestrial biomass carbon sinks; also, the projected carbon storage was sensitive to changes in land use and population. The estimated rate of carbon storage in Pacific coastal waters was 2.02 TgC/yr under baseline conditions. The projections of land use and population changes through 2050 under the IPCC A2 scenario had a small effect on projected coastal carbon storage processes, reducing carbon storage rates to 1.93 TgC/yr, a –4.4 percent change over baseline conditions.
- The results of this modeling exercise indicate that the projected size of the carbon sink associated with terrestrial exports is substantial and sensitive to anthropogenic activity. Thus, future evaluations of how land-use policy and management actions may alter carbon storage may benefit from an evaluation of the effects of prospective alterations in terrestrial processes on coastal carbon storage rates.

11.2. Introduction

This chapter assesses the effect of terrestrial processes on carbon storage rates in the Pacific coastal waters of the Western United States as part of the larger assessment of carbon stocks, carbon sequestration, and greenhouse-gas (GHG) fluxes in ecosystems of the Western United States. In order to model the baseline (1992) and projected (2050) fluxes of total organic carbon (TOC), total nitrogen (TN), and total suspended sediment (TSS) to the coastal waters, the results of LULC mapping and modeling described in chapter 2 and models of future land-use and land cover (LULC) change scenarios were required. The results of the baseline and future potential carbon fluxes and burial in the Pacific coastal waters presented in this chapter were used in an integrated analysis (chapter 12) to assemble a regional estimate of the baseline and projected amounts of carbon stored in ecosystems of the Western United States. The relation between this chapter and the other chapters is depicted in figure 1.2 of chapter 1 of this report.

[1]U.S. Geological Survey, Sacramento, Calif.

[2]U.S. Geological Survey, Reston, Va.

[3]Resources for the Future, Washington, D.C.

Globally, coastal ocean processes account for the removal of an estimated 1.1 petagrams of carbon per year (PgC/yr) from the atmosphere through the processes driving the production of carbon by phytoplankton and the burial of organic carbon in sediments (Hedges and Keil, 1995; Sarmiento and Gruber, 2002; Muller-Karger and others, 2005; Hales and others, 2006; Dunne and others, 2007). This carbon sink is greater than the terrestrial biomass carbon sink (Sarmiento and Gruber, 2002) and is also susceptible to disruption by anthropogenic activities in terrestrial systems. In particular, changes to the supply of sediments and nutrients to coastal oceans can alter the magnitude of this carbon sink; ample evidence exists that they already have been significantly altered by anthropogenic activity (Syvitski and others, 2005; Boyer and others, 2006).

The inputs of sediment and nutrients from the terrestrial environment to the coastal waters exert significant control on the carbon storage processes in the marine coastal systems. Although the vast majority of carbon buried in coastal sediments or exported to the deep ocean has a marine provenance (Blair and others, 2004; Burdige, 2005), the fluxes of nutrients from the continents support coastal phytoplankton production and sediment fluxes aid the transport of this material from the photic zone to the deep ocean and bury it outside of the zone of oxygen penetration, where mineralization rates are dramatically reduced. Thus, to quantify the anthropogenic effects on the carbon storage rates in coastal environments, it is necessary to quantify the fluxes of TOC, TN, and TSS exported from terrestrial environments to coastal oceans, all of which have been demonstrably affected by anthropogenic activity (U.S. Climate Change Science Program, 2007).

The properties of the watersheds that drain into the Pacific coastal waters and the physical attributes of the adjacent continental shelf affect the rate of carbon storage that occurs under current conditions and how it may be altered in the future. Globally, large river deltas are responsible for much of the coastal carbon burial because of their high productivity and rapid sediment accumulation rates (Blair and others, 2004; Syvitski, 2011); however, because of the relatively steep bathymetry just offshore of the Western United States, there are few accreting delta systems associated with large river mouths. For example, the relatively steep bathymetry prevents the formation of a distinct accreting delta for the fourth largest river in the United States, the Columbia River. Instead, sediment from the Columbia River is deposited in deeper waters, relatively far from the mouth (Gross and Nelson, 1966; Sternberg, 1986). The Western United States possesses additional physiographic characteristics, however, that do act to increase the storage of carbon. Discharge into the Pacific coastal waters is dominated by small, mountainous rivers, which carry high loads of sediment and nutrients. These rivers tend to be short, draining watershed areas with high relief, and their mouths typically discharge near the coast rather than into an estuary (Milliman and Syvitski, 1992; Wheatcroft and others, 2010). Globally, the sediment discharge from small, mountainous river systems accounts for nearly half the coastal sediment that buries carbon (Milliman and Syvitski, 1992; Leithold and others, 2005; Wheatcroft and others, 2010).

The amount of sediment and nutrients delivered to coastal oceans has changed considerably over the past several decades, significantly altering patterns of coastal carbon burial (Leithold and others, 2005; Syvitski and others, 2005; Mayorga and others, 2010). Increasing population and changes in land use are expected to accelerate these changes (Harrison and others, 2005; Syvitski and others, 2005; Mayorga and others, 2010). Although much of the discharge into Pacific coastal waters is from small, mountainous rivers, both the Columbia and Sacramento Rivers (the two largest rivers in the Western United States) drain areas of intensive agriculture and carry elevated nutrient loads to coastal waters, thus promoting higher phytoplankton production (Hales and others, 2008). The riverborne supply of these external nutrients to Pacific coastal waters is important because phytoplankton production supported by the externally supplied nutrients contributes to the potential net removal of carbon from the atmosphere.

The estimates of carbon storage rates in the Pacific coastal waters can be complicated by a decoupling in the timing of sediment and nutrient supply. The burial of the phytoplankton biomass in the coastal sediments requires coherence between inputs of nutrients and inputs of sediments—phytoplankton production must occur near the time of the episodic delivery of the sediments (Wheatcroft and others, 2010). Although nutrients supporting phytoplankton production in Pacific coastal waters are largely supplied by the summer upwelling of nutrient-rich, deep-ocean water, the nutrient supply by rivers is also significant, particularly in Oregon and Washington (Hales and others, 2008). Any increases or decreases in the nutrient supply by rivers will affect the potential productivity in the adjacent coastal area. Changes in nutrient supply can be caused by changes in population, river discharge, agricultural practices, reforestation, and many other similar land-use- or climate-related variables (Billen and Garnier, 2007). Under the projected future conditions, an increase in nutrients associated with the sediment contained in discharge waters could have the potential to improve the efficiency of carbon transport and burial.

This coastal assessment focused exclusively on characterizing the potential magnitude of processes in the coastal marine system that have been, and potentially could be, affected by changing land use and population (fig. 2.1). The focus was only on the terrestrial sources of nutrients and sediments that influence marine carbon storage rates and not on marine processes such as the upwelling of oceanic nutrients, which also significantly contribute to primary productivity and total carbon storage rates in coastal waters. To accomplish this task, the fluxes of total organic carbon (TOC), total nitrogen (TN, organic and inorganic), and total suspended sediment (TSS) to coastal waters were estimated on the basis of current and projected land use using a model that was calibrated using long-term water quality and stream

discharge data. The baseline and projected amounts of carbon that were buried were estimated according to established models of oceanographic processes (Armstrong and others, 2002; Dunne and others, 2007).

The geographic extent of the assessment was from the northern to the southern borders of the Western United States and included all of the watersheds that drain this region into the adjacent coastal waters (herein referred to as the "Pacific coastal waters"). The coastal waters of the Gulf of California, which receives the discharge of the Colorado River, were not included because other sources of discharge into those coastal waters extended beyond the geographic boundary of the conterminous United States. The assessment considered only processes affected by the terrestrial supply of nutrients and sediments to coastal waters. These processes extended from the coast into the deep ocean with no western boundary because carbon exported into the deep ocean was presumed to be sequestered (Sarmiento and Gruber, 2002, Hales and others, 2006).

The riverine delivery of carbon, nutrients, and sediment to coastal waters can be estimated from routine monitoring data, provided that the records cover a sufficient length of time and include accurate streamflow measurements (Cohn and others, 1992). Determining the sources of the transported material is much more difficult, however, especially in the case of large rivers with heterogeneous basin characteristics. Isotopic methods have been developed to distinguish specific classes of sources of nutrients (for example, atmospheric or sewage effluent) with good success, but require specialized analytical procedures and have not been used historically in broad-scale, long-term monitoring programs (Kendall and McDonnell, 1998). There has been considerable progress in the past two decades: (1) development of statistical modeling approaches, which can be used to identify the sources of constituents; (2) continuing development of geographic information systems (GIS) technology; and (3) availability of spatial data on basin characteristics (Peters, 1984; R.A. Smith and others, 1997; Goolsby and others, 1999). The use of the SPARROW model (a "spatially referenced regression on watershed attributes" water-quality model; R.A. Smith and others, 1997) for regional interpretations of contaminant sources is now a routine part of the U.S. Geological Survey's water-quality assessment activities (Preston and others, 2011).

11.3. Input Data and Methods

The modeling approach used here divides the analysis of Pacific coastal waters into three components: (1) the supply of TOC, TN, and TSS from terrestrial systems to the coastal ocean, (2) phytoplankton production supported by terrestrial nutrients, and (3) storage rates of carbon in coastal sediments or deep ocean waters. The first model component assesses the TOC, TN, and TSS supply from rivers to the coastal ocean under baseline (1992) and projected (2050) conditions.

A hybrid statistical-mechanical modeling approach was used to calculate the fluxes of TOC, TN, and TSS from rivers to the coastal waters. The SPARROW model (R.A. Smith and others, 1997; Schwarz and others, 2006) consists of process-based mass-transport components for water flow paths, in-stream processing, and mass-balance constraints on model inputs, losses, and outputs (Schwarz and others, 2006). Modeled estimates of TSS, TN, and TOC fluxes were produced for each coastal or inland hydrologic unit (by 12-digit hydrologic unit code; U.S. Department of Agriculture, Natural Resources Conservation Service, 2012) that produced runoff to the western coast of the United States. Both the baseline LULC and LULC projections by the "forecasting scenarios of land cover change" (FORE–SCE) model, as described in chapter 2 of this report, were included in the SPARROW modeling process. Estimates of TOC that were developed using a different modeling approach (presented in chapter 10 of this report) agree with those presented here. The SPARROW model, however, permits assessment using the future potential land use and population conditions in 2050, which are presented in chapter 2.

For surface-water monitoring stations that had sufficient data on discharge and water quality, parameters were estimated by spatially correlating the stream data with georeferenced data on the constituent sources (for example, atmospheric deposition, fertilizers, human and animal wastes) and delivery factors (for example, precipitation, topography, vegetation, soils, and water routing). Parameter estimation ensured that the calibrated model would not be more complex than can be supported by the data.

SPARROW models describe mass transport in watersheds as three sequential processes: (1) source supply, (2) land-to-water transport, and (3) channel-network transport (R.A. Smith and others, 1997). Data describing these processes are developed on a stream reach and associated catchment basis. There are approximately 13,000 reaches or catchments in the Western United States assessment area and 63,000 reaches or catchments in the national-scale data set, which were used to calibrate the models. Table 11.1 provides information on the TOC, TN, and TSS models used here to quantify the flux of material to coastal waters. More detailed information is available from the references provided in the table.

The source variables (table 11.1) were of particular importance because they served as the basis for translating the projected LULC changes under the A2 scenario (from the Intergovernmental Panel on Climate Change's Special Report on Emissions Scenarios, IPCC–SRES; Nakicenovic and others, 2001) into changes in coastal delivery of TOC, TN, and TSS from the baseline period to 2050. The IPCC–SRES scenarios are discussed in more detail in chapter 6 of this report. Table 11.2 summarizes the correspondence between the LULC classes and the SPARROW model's source categories. An underlying assumption made in modeling the future changes in coastal flux was that the rate of the source supply will change in proportion to the LULC changes in each

Table 11.1. Variables used in the SPARROW models of total organic carbon, total nitrogen, and total suspended sediment fluxes, and their sources.

[SPARROW, "spatially referenced regressions of watershed attributes" water-quality model]

Model	Number of sites	Coefficient of determination (R^2)	Source variables	Reference
Total organic carbon (TOC)	1,125	0.928	Cultivated land, pasture, deciduous forest, evergreen forest, mixed forest, rangeland, urban land, wetlands, in-stream photosynthesis	Shih and others (2010)
Total nitrogen (TN)	425	0.933	1990 population, atmospheric total nitrogen deposition, corn or soybean fertilizer, alfalfa fertilizer, wheat fertilizer, other crop fertilizer, farm animal waste, forest, barren land, shrubland	Alexander and others (2008)
Total suspended sediment (TSS)	1,828	0.711	Urban area, forest, crop and pasture land, Federal land, other marginal land, channel storage and erosion	Schwarz (2008)

Table 11.2. Assumed correspondences between the SPARROW model's source categories and the land-use and land-cover classes used in this assessment.

[See chapter 2 of this report for definitions of the LULC classes. LULC, land use and land cover; NA, not applicable; SPARROW, "spatially referenced regressions of watershed attributes" water-quality model]

Total organic carbon (TOC) model		Total nitrogen (TN) model		Total suspended sediment (TSS) model	
Model source	Land use and land cover class	Model source	Land use and land cover class	Model source	Land use and land cover class
Cultivated land	Agriculture	Human population	Developed land	Developed land	Developed land
Pasture	Hay/pasture	Atmospheric nitrate (NO_3) deposition	Developed land	Forested land	Deciduous, evergreen, mixed forests
Deciduous forest	Deciduous forest	Fertilizer nitrogen applied to agriculture	Agriculture	Federally managed land	Barren land, grassland and shrubland
Evergreen forest	Evergreen forest	Nitrogen content of farm animal waste	Grassland and shrubland	Crop and pasture land	Agriculture
Mixed forest	Mixed forest	Forest	Deciduous, evergreen, mixed forests	Other land	Barren land, grassland, and shrubland
Rangeland	Grassland and shrubland	Barren land	Barren land	Stream channels	No LULC correspondence; assumed to be constant
Developed land	Developed land	Shrubland	Shrubland	NA	NA
Wetlands	Herbaceous and woody wetland	NA	NA	NA	NA
In-stream photosynthesis	No LULC correspondence; assumed to be constant	NA	NA	NA	NA

model's catchment. The A2 scenario was selected because it is consistent with this assumption in one important aspect: it projects that population growth by 2050 (+48 percent) may be nearly matched by an increase in area classified as developed land (+46 percent). Thus, for example, the change in the value of the population variable in the TN model within each catchment was approximated by the projected change in the developed land area presented in chapter 6 of this report. The A2 scenario also assumed that environmental sustainability remains approximately constant, which is reflected in the LULC and SPARROW modeling (Sohl, Sleeter, and Zhu, 2012; also see chapter 6 of this report). Thus, for example, the per-acre fertilizer application rates and point and nonpoint pollution-control efficiencies are assumed to remain constant.

The 90-percent confidence intervals for the coastal flux estimates in table 11.3 were developed through a "bootstrap" procedure in which 200 equally likely estimates for each entry in the table were randomly generated on the basis of the error characteristics of the model determined during calibration. The width of the confidence intervals surrounding the 1992 and 2050 flux estimates included both coefficient error and residual (that is, model specification) error (Schwarz and others, 2006). It was assumed that the residual errors of the flux estimates for individual coastal rivers within each region reflected idiosyncrasies of the river watersheds. The estimated errors surrounding the "percent-change" estimates for each coastal river, however, were assumed to be caused only by coefficient error on the basis of the further assumption that the idiosyncrasies of a given river can be assumed to be the same in 1992 and 2050. Thus, the confidence intervals for the percent-change estimates were smaller than those for the separate 1992 and 2050 flux estimates.

The effects of climate change have not been specifically modeled because there is no known consensus regarding their effects on nutrients or biota in the coastal ocean. Although the effects of climate change may alter TOC, TN, and TSS fluxes in the future, LULC is expected to be the main driver of the variability in these parameters between 1992 and 2050, suggesting that uncertainty in the model is controlled by LULC. The A2 scenario was chosen to represent the projected changes in coastal carbon sequestration stemming from LULC. The use of the A2 scenarios limits the SPARROW model's runtime and represented a worst-case scenario for population increase and anthropogenic emissions with continued regional fragmentation in economic growth and technology. In contrast to the other IPCC–SRES scenarios (A1B and B1), environmental protection and sustainability were not considered to be important in A2.

Table 11.3. Estimates of total organic carbon, total nitrogen, and total suspended sediment fluxes to the Pacific coastal waters of the conterminous United States (with 90-percent confidence intervals) and the total carbon burial rate under baseline (1992) and projected (2050) conditions.

[A2 scenario selected from Intergovernmental Panel on Climate Change's Special Report on Emissions Scenarios (Nakicenovic and others, 2001). Numbers may not sum precisely due to rounding. Tg/yr, teragrams per year; TgC/yr, teragrams of carbon per year]

Variables	Region	1992 baseline estimate (90-percent confidence interval)	2050 projected estimate under A2 scenario (90-percent confidence interval)	Percent change (90-percent confidence interval)
Total organic carbon flux (TgC/yr)	Southern California	0.04 (0.01 to 0.08)	0.04 (0.02 to 0.10)	18.2 (17.95 to 18.45)
	Northern California	0.32 (0.13 to 0.71)	0.33 (0.13 to 0.73)	2.5 (2.43 to 2.57)
	Oregon and Washington	1.24 (0.49 to 2.97)	1.25 (0.49 to 2.99)	0.6 (0.56 to 0.64)
	Total	1.60 (0.63 to 3.77)	1.62 (0.64 to 3.82)	1.4 (1.34 to 1.46)
Total nitrogen flux (Tg/yr)	Southern California	0.04 (0.01 to 0.10)	0.05 (0.03 to 0.13)	31.7 (31.52 to 31.88)
	Northern California	0.06 (0.02 to 0.15)	0.08 (0.13 to 0.19)	34.7 (34.18 to 35.22)
	Oregon and Washington	0.29 (0.09 to 0.72)	0.37 (0.12 to 0.93)	25.7 (24.88 to 26.52)
	Total	0.40 (0.13 to 0.96)	0.50 (0.17 to 1.24)	27.7 (27.00 to 28.40)
Total suspended sediment flux (Tg/yr)	Southern California	6.27 (0.22 to 19.88)	7.69 (0.27 to 24.28)	22.7 (22.20 to 23.20)
	Northern California	19.75 (0.69 to 55.44)	19.31 (0.65 to 54.39)	−2.2 (−2.68 to −1.72)
	Oregon and Washington	40.76 (0.65 to 111.5)	36.78 (0.53 to 99.24)	−9.8 (−10.37 to −9.23)
	Total	66.78 (1.55 to 187.8)	63.78 (1.45 to 178.9)	−4.5 (−4.91 to −4.09)
Total carbon burial rate (TgC/yr)	Southern California	0.12 (0.01 to 0.39)	0.16 (0.01 to 0.52)	33.5 (33.8 to 35.2)
	Northern California	0.65 (0.29 to 1.87)	0.67 (0.06 to 1.93)	3.6 (2.9 to 4.5)
	Oregon and Washington	1.25 (0.03 to 3.51)	1.1 (0.03 to 3.05)	−12.1 (−11.8 to −13.2)
	Total	2.02 (0.06 to 5.78)	1.93 (0.09 to 5.50)	−4.4 (−4.7 to −4.2)

Sediment and carbon transport from the surface ocean into the deep ocean and carbon burial in sediments were modeled using the methods presented by Dunne and others (2007). This approach modeled the transport of terrestrial and marine, photosynthetically derived carbon to the sediment surface in coastal waters or to the deep ocean using an empirical modeling approach. The same approach was used to model sedimentation to the pycnocline. A hypsographic valuation of the bathymetric properties of the sediment deposition zones was determined by using a GIS and the NOAA bathymetric database. The burial of organic carbon in sediments was modeled as a function of the sediment deposition rate (Berger, 1989, Dunne and others, 2007) with no net deposition assumed above 10 meters because of wave- or event-driven resuspension of sediment. Sediment in the water column above 10 m depth was presumed to be transported to deeper regions with a 50 percent loss in carbon by mass and no dissolution of terrestrial sediments during transit (Armstrong and others, 2002). Carbon buried in sediments below the depth of oxygen penetration or transported to the deep ocean below the level of the pycnocline was considered to be "stored" for the purpose of this assessment, as this carbon has mean turnover times of hundreds to thousands of years (Hedges and Keil, 1995). The 90-percent confidence intervals for the coastal carbon accumulation shown in table 11.3 were developed using the confidence intervals from the flux estimates and assumed no additional error in the coastal model. Note that the modeling effort did not include an evaluation of silica, iron, and other micronutrient fluxes or of the coastal phytoplankton production that such fluxes may affect.

11.4. Results

11.4.1. Flux of Organic Carbon, Nitrogen, and Suspended Sediment to Coastal Waters

The model estimates of TOC, TN, and TSS fluxes to the Pacific coastal waters under baseline and projected (2050) conditions and based on the IPCC–SRES scenario A2 are presented in tables 11.3 and 11.4. Estimates are presented for each of the three physiographic provinces in the region: southern California (northern boundary at latitude 37°), northern California (to the Oregon State line), and the Pacific Northwest, which includes the States of Oregon and Washington.

11.4.1.1. Total Organic Carbon

The total baseline flux of TOC to the Pacific coastal waters for the three regions was estimated to be approximately 1.6 TgC/yr (tables 10.3, 10.4; fig. 11.1*A*–*C*). About 78 percent of the total flux was delivered to coastal waters of Oregon and Washington, reflecting the interaction of a large coastal drainage area, high streamflows, and extensive forest cover in the region (table 11.4; fig. 11.1*C*). By contrast, a much lower estimated baseline TOC flux (2 percent of total) was delivered from the smaller and drier Southern California region, largely from urban sources. The estimated baseline TOC flux from the Northern California region (especially that draining to San Francisco Bay) reflects a combination of urban and agricultural sources (table 11.4; fig. 11.1*C*). The model estimates of TOC yield to the coastline after in-stream losses are subtracted are shown in figure 11.1*B*. Regardless of the TOC source, the catchments with the highest coastal yield are typically located either near the coast or near large rivers, which tended to have low in-stream loss rates (Alexander and others, 2000). It should be noted that the preponderance of evidence suggests that terrestrial organic carbon borne by rivers into the coastal ocean is largely remineralized, and little is stored (Hedges and others, 1997; Blair and others, 2004; Burdige, 2005).

The estimated projected changes in TOC flux to the coastal waters from the 1992 to 2050 (tables 11.3, 11.4; fig. 11.1*D*–*G*) were relatively small in the two northern regions, but the estimated projected change was greater (more than 18 percent) in the Southern California region, where population and urban development were projected to increase dramatically by mid-century. The near absence of change in total TOC flux from Oregon and Washington (0.8 percent) over the period masked the occurrence of more substantial but opposing trends in the region: a decreasing flux from the loss of forest and forested wetlands versus an increasing flux from population growth.

11.4.1.2. Total Nitrogen

The SPARROW model estimated a baseline total TN flux of 0.395 Tg/yr (tables 11.3, 11.4; fig. 11.2*A*–*C*). As with TOC, approximately three quarters of the estimated TN flux entered the Pacific coastal waters from the large, wet parts of Oregon and Washington, where forest cover and atmospheric deposition together supplied about 63 percent of the regional flux (table 11.4). Farther south, in the northern and southern California regions, TN was mainly from urban sources (table 11.4).

The estimated TN flux from all three coastal regions was projected to greatly increase (table 11.4), mainly because of the importance of urban and atmospheric sources of nitrogen (and, to a lesser extent, agricultural sources in the northern California region). Under the A2 scenario, the U.S. population was projected to increase to 417 million by 2050, and nationwide agricultural production was projected to increase substantially in order to meet elevated worldwide demand. The estimated TN flux from all three regions was projected to increase more than 25 percent, with increases in the northern California region alone projected to be a third more than the baseline estimate (table 11.3; fig. 11.2*D*–*G*).

Table 11.4. Estimates of total organic carbon, total nitrogen, and total suspended sediment fluxes to the Pacific coastal waters of the conterminous United States by source of the fluxes, under baseline (1992) and projected (2050) conditions.

[Numbers may not sum precisely due to rounding. Gg/yr, gigagrams per year; GgC/yr, gigagrams of carbon per year]

Source	Southern California			Northern California			Oregon and Washington		
	1992	2050	Change	1992	2050	Change	1992	2050	Change
Total organic carbon (GgC/yr)									
Cultivated land	3.38	2.64	−0.74	24.24	23.67	−0.57	71.43	74.67	3.24
Deciduous forest	0.33	0.33	−0.01	5.87	5.85	−0.02	26.74	27.12	0.38
Evergreen forest	5.52	5.46	−0.06	96.16	95.00	−1.16	387.83	375.65	−12.18
Mixed forest	2.94	2.91	−0.03	25.34	25.79	0.45	72.10	68.79	−3.31
Urban land	17.53	25.01	7.49	19.74	31.73	12.00	31.35	54.97	23.62
Wetlands	0.67	0.51	−0.16	24.04	21.47	−2.56	57.86	53.19	−4.67
In-stream photosynthesis	5.33	5.33	0.00	126.17	126.17	0.00	593.73	593.73	0.00
Total	35.71	42.19	6.49	321.55	329.68	8.13	1,241.1	1,248.1	7.07
Total nitrogen (Gg/yr)									
Population	37.39	50.76	13.36	26.55	42.11	15.56	22.27	38.97	16.70
Atmospheric deposition	0.37	0.72	0.36	5.82	11.53	5.71	65.02	128.71	63.69
Corn and soybean	0.03	0.02	−0.01	1.02	1.01	−0.02	4.97	5.06	0.09
Alfalfa	0.04	0.03	−0.01	1.43	1.47	0.04	6.87	7.19	0.33
Wheat	0.03	0.03	0.00	0.57	0.56	−0.01	8.49	8.62	0.13
Other crops	2.33	1.69	−0.64	5.91	6.08	0.17	26.40	27.70	1.30
Farm animal waste	0.20	0.17	−0.03	3.58	3.22	−0.36	15.27	14.76	−0.51
Forest	0.29	0.28	0.00	13.40	13.27	−0.13	120.76	118.43	−2.33
Barren land	0.04	0.04	0.00	0.40	0.36	−0.04	15.85	12.29	−3.56
Shrubland	0.30	0.27	−0.03	1.47	1.44	−0.03	8.17	7.85	−0.32
Total	41.02	54.01	13.00	60.15	81.04	20.89	294.06	369.57	75.51
Total sediment supply (Gg/yr)									
Urban	1,646.68	3,094.10	1,447.40	4,020.00	6,598.27	2,578.08	4,105.60	5,076.30	970.67
Forest	36.05	35.65	−0.40	576.30	573.32	−3.01	963.74	945.16	−18.58
Federal land	2,715.14	2,800.60	85.48	7,231.00	4,995.05	−2,235.84	12,033.00	8,237.03	−3,796.00
Crop and pasture land	240.03	240.85	0.82	999.40	1,042.56	43.14	2,541.20	2,878.60	337.36
Grassland, shrubland, barren land	1,260.02	1,149.60	−110.45	3,968.00	3,143.52	−823.93	3,056.40	1,581.30	−1,475.10
Channel storage or erosion	367.61	367.61	0.00	2,956.00	2,956.70	0.00	18,063.00	18,063.00	0.00
Total	6,265.50	7,688.40	1,422.80	19,751.00	19,309.40	−441.56	40,763.00	36,781.30	−3,981.70

11.4.1.3. Total Suspended Sediment

The total baseline TSS flux to the three Pacific coastal regions averaged 66.8 Tg/yr (tables 11.3, 11.4; fig. 11.3*A*–*C*). Again, there was a pronounced increasing gradient in flux from south to north, with Oregon and Washington coastal waters receiving more than half of the total (61 percent). The important sources of transported sediment in the three regions (table 11.4; see also table 11.2) included urban runoff, but also soil loss from several types of sparsely vegetated land cover types, including rangeland, shrubland, grassland, and barren land, much of which is Federally owned. Of note, however, is that the major source of sediment in Oregon and Washington was stored and eroded sediment from stream channels in the region, as was estimated in SPARROW's TSS model calibration (Schwarz, 2008).

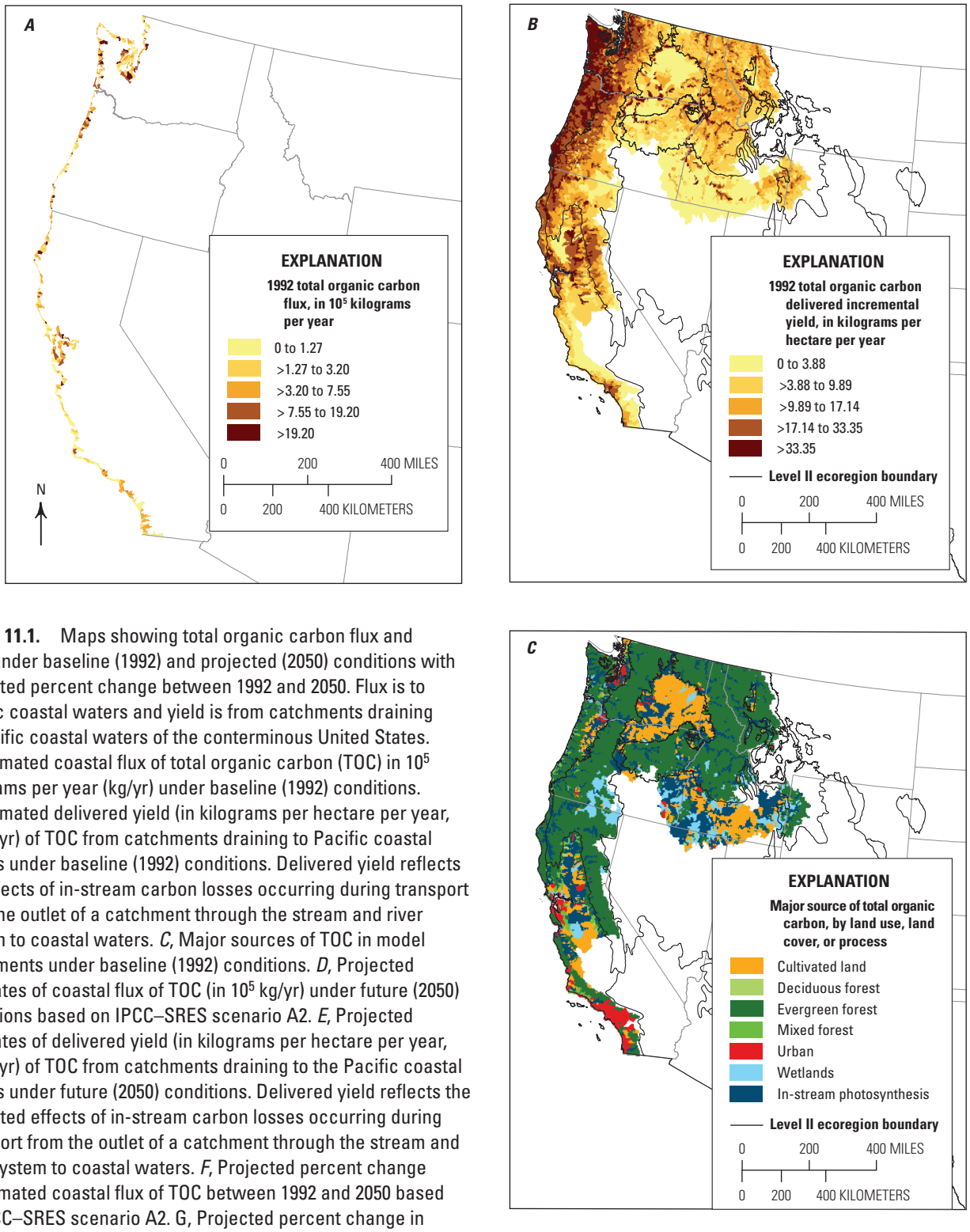

Figure 11.1. Maps showing total organic carbon flux and yield under baseline (1992) and projected (2050) conditions with projected percent change between 1992 and 2050. Flux is to Pacific coastal waters and yield is from catchments draining to Pacific coastal waters of the conterminous United States. *A*, Estimated coastal flux of total organic carbon (TOC) in 10^5 kilograms per year (kg/yr) under baseline (1992) conditions. *B*, Estimated delivered yield (in kilograms per hectare per year, kg/ha/yr) of TOC from catchments draining to Pacific coastal waters under baseline (1992) conditions. Delivered yield reflects the effects of in-stream carbon losses occurring during transport from the outlet of a catchment through the stream and river system to coastal waters. *C*, Major sources of TOC in model catchments under baseline (1992) conditions. *D*, Projected estimates of coastal flux of TOC (in 10^5 kg/yr) under future (2050) conditions based on IPCC–SRES scenario A2. *E*, Projected estimates of delivered yield (in kilograms per hectare per year, kg/ha/yr) of TOC from catchments draining to the Pacific coastal waters under future (2050) conditions. Delivered yield reflects the projected effects of in-stream carbon losses occurring during transport from the outlet of a catchment through the stream and river system to coastal waters. *F*, Projected percent change in estimated coastal flux of TOC between 1992 and 2050 based on IPCC–SRES scenario A2. G, Projected percent change in yield of TOC from catchments between 1992 and 2050 based on IPCC–SRES scenario A2. IPCC–SRES, Intergovernmental Panel on Climate Change Special Report on Emissions Scenarios (Nakicenovic and others, 2000).

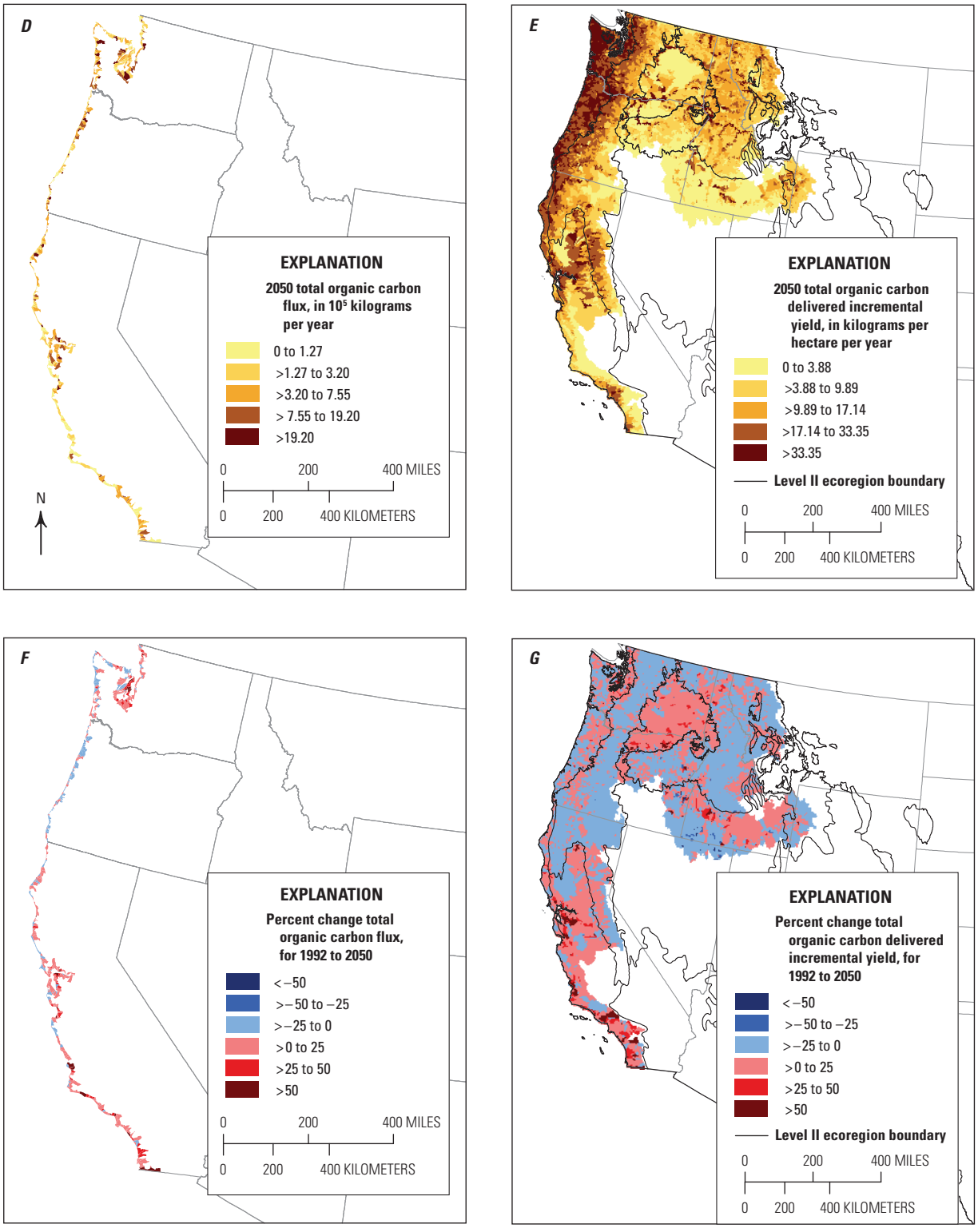

Figure 11.1.—Continued

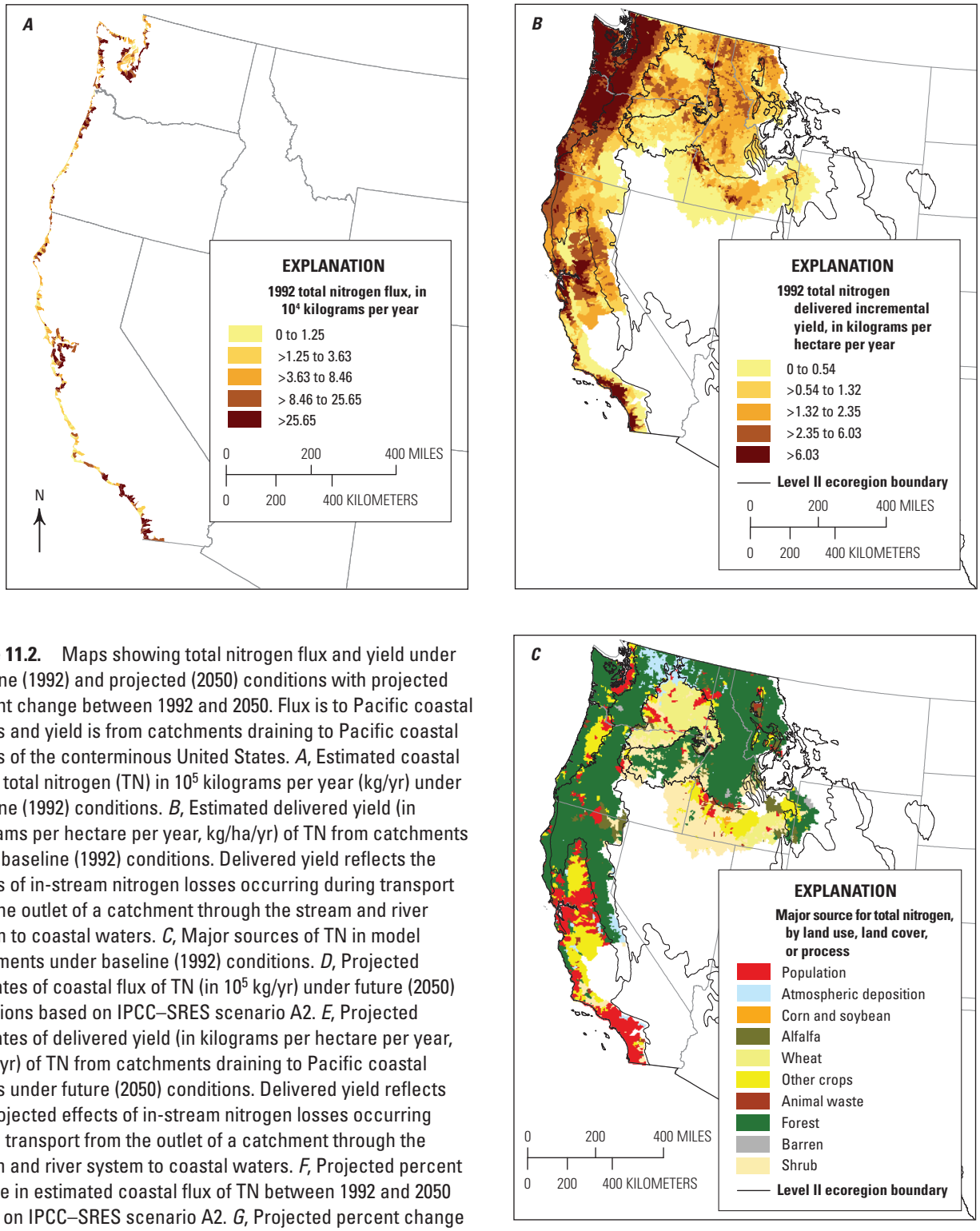

Figure 11.2. Maps showing total nitrogen flux and yield under baseline (1992) and projected (2050) conditions with projected percent change between 1992 and 2050. Flux is to Pacific coastal waters and yield is from catchments draining to Pacific coastal waters of the conterminous United States. *A*, Estimated coastal flux of total nitrogen (TN) in 10^5 kilograms per year (kg/yr) under baseline (1992) conditions. *B*, Estimated delivered yield (in kilograms per hectare per year, kg/ha/yr) of TN from catchments under baseline (1992) conditions. Delivered yield reflects the effects of in-stream nitrogen losses occurring during transport from the outlet of a catchment through the stream and river system to coastal waters. *C*, Major sources of TN in model catchments under baseline (1992) conditions. *D*, Projected estimates of coastal flux of TN (in 10^5 kg/yr) under future (2050) conditions based on IPCC–SRES scenario A2. *E*, Projected estimates of delivered yield (in kilograms per hectare per year, kg/ha/yr) of TN from catchments draining to Pacific coastal waters under future (2050) conditions. Delivered yield reflects the projected effects of in-stream nitrogen losses occurring during transport from the outlet of a catchment through the stream and river system to coastal waters. *F*, Projected percent change in estimated coastal flux of TN between 1992 and 2050 based on IPCC–SRES scenario A2. *G*, Projected percent change in yield of TN from catchments between 1992 and 2050 based on IPCC–SRES scenario A2. IPCC–SRES, Intergovernmental Panel on Climate Change Special Report on Emissions Scenarios (Nakicenovic and others, 2000).

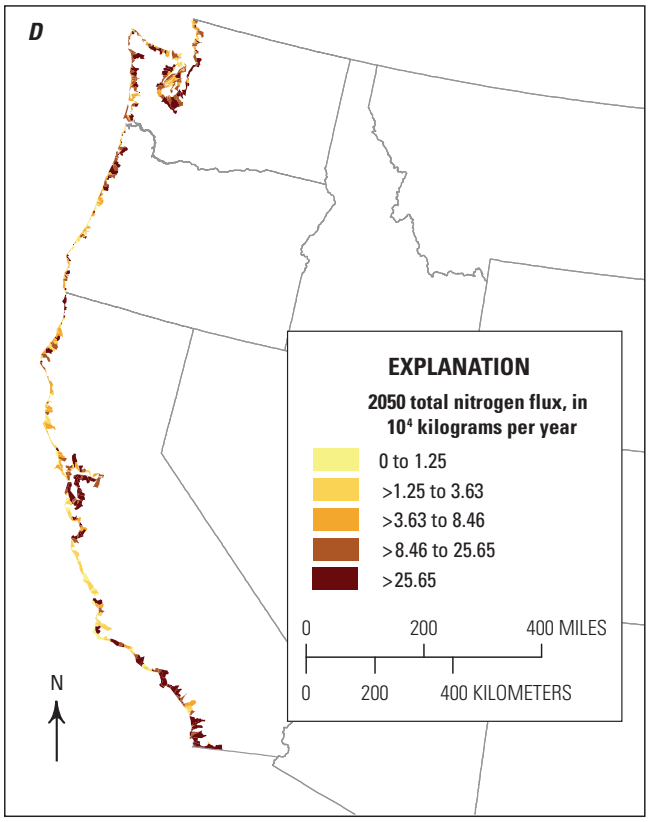

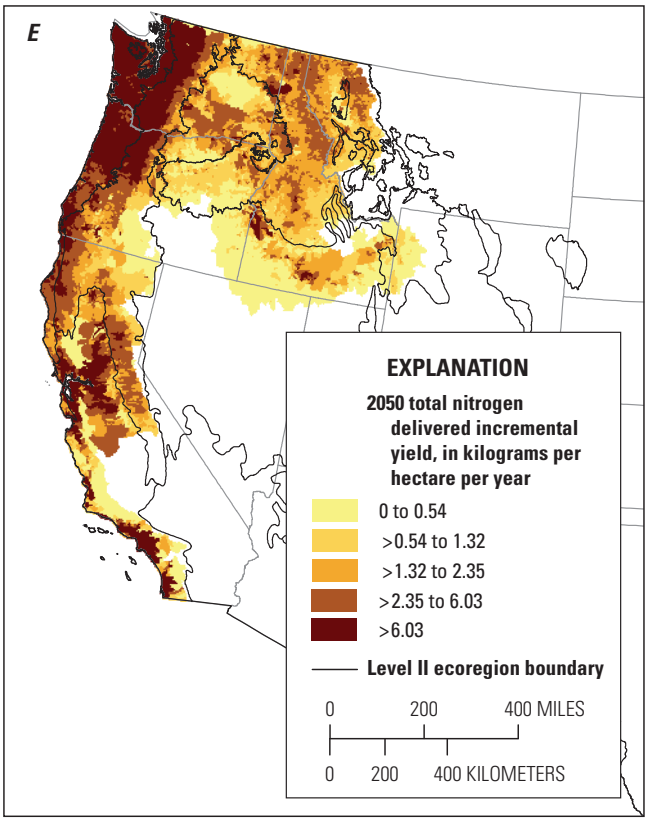

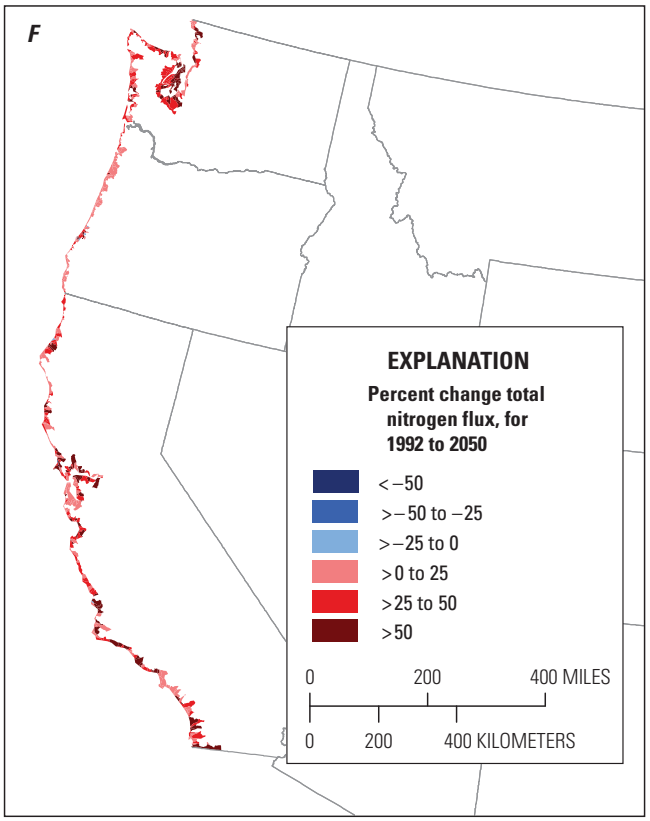

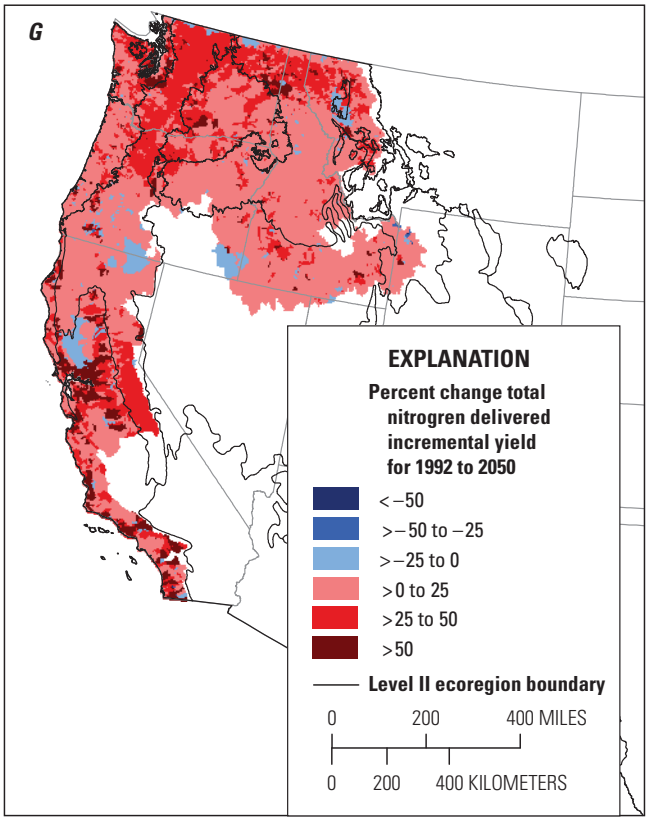

Figure 11.2.—Continued

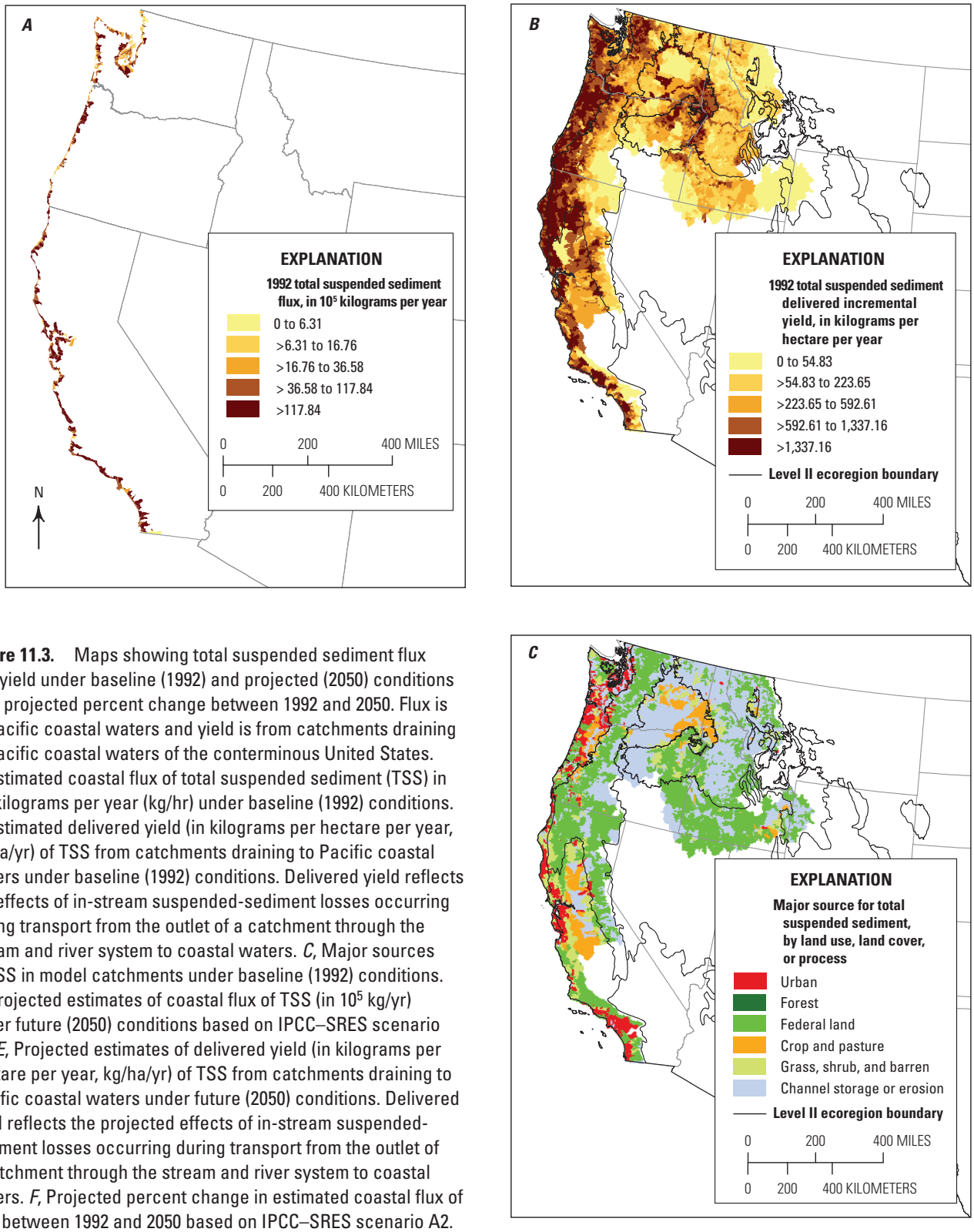

Figure 11.3. Maps showing total suspended sediment flux and yield under baseline (1992) and projected (2050) conditions with projected percent change between 1992 and 2050. Flux is to Pacific coastal waters and yield is from catchments draining to Pacific coastal waters of the conterminous United States. *A*, Estimated coastal flux of total suspended sediment (TSS) in 10^5 kilograms per year (kg/hr) under baseline (1992) conditions. *B*, Estimated delivered yield (in kilograms per hectare per year, kg/ha/yr) of TSS from catchments draining to Pacific coastal waters under baseline (1992) conditions. Delivered yield reflects the effects of in-stream suspended-sediment losses occurring during transport from the outlet of a catchment through the stream and river system to coastal waters. *C*, Major sources of TSS in model catchments under baseline (1992) conditions. *D*, Projected estimates of coastal flux of TSS (in 10^5 kg/yr) under future (2050) conditions based on IPCC–SRES scenario A2. *E*, Projected estimates of delivered yield (in kilograms per hectare per year, kg/ha/yr) of TSS from catchments draining to Pacific coastal waters under future (2050) conditions. Delivered yield reflects the projected effects of in-stream suspended-sediment losses occurring during transport from the outlet of a catchment through the stream and river system to coastal waters. *F*, Projected percent change in estimated coastal flux of TSS between 1992 and 2050 based on IPCC–SRES scenario A2. G, Projected percent change in yield of TSS from catchments between 1992 and 2050 based on IPCC–SRES scenario A2. IPCC–SRES, Intergovernmental Panel on Climate Change Special Report on Emissions Scenarios (Nakicenovic and others, 2000).

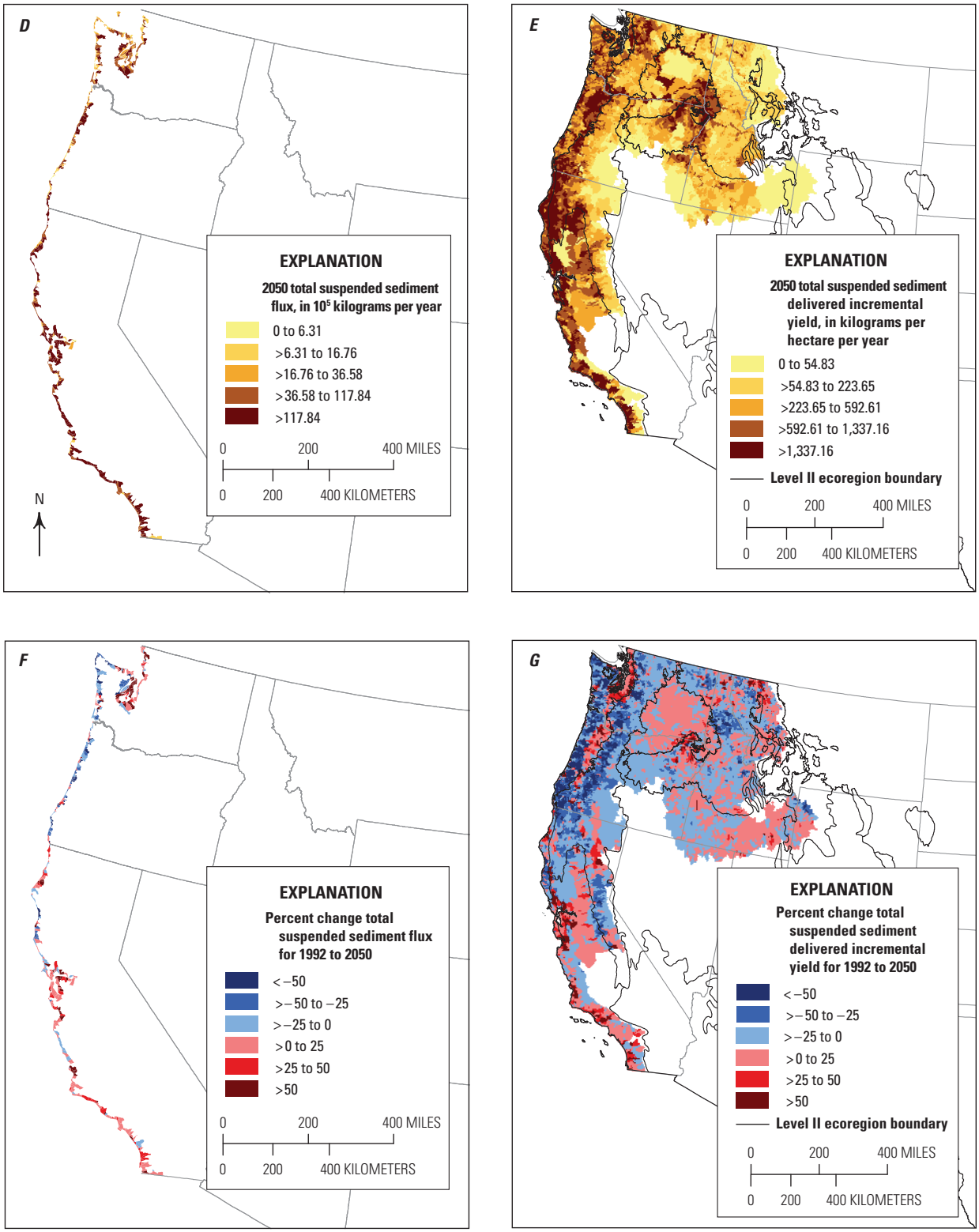

Figure 11.3.—Continued

The projected future regional changes in TSS flux to the Pacific coastal waters were mixed and included a substantial increase (23 percent) in the southern California region and decreases of 10 and 2 percent, respectively, in Oregon and Washington and in the northern California region (tables 11.3, 11.4; fig. 11.3*D*–*G*). The reasons for the projected changes in TSS flux vary. The large projected increase in the southern California region stemmed from projections of continued urban development, and the moderate projected decrease in Oregon and Washington stemmed largely from the projected development of marginal lands (table 11.4).

11.4.2. Carbon Processes in Coastal Waters

The baseline rate of coastal carbon storage due only to terrestrial processes in Pacific coastal waters was estimated to be 0.12 TgC/yr for the southern California region, 0.65 TgC/yr for the northern California region, and 1.25 TgC/yr, for Oregon and Washington (table 11.3). For all three regions combined, the baseline rate of total carbon storage due only to terrestrial processes was 2.0 TgC/yr (table 11.3). From 1992 to 2050, the total baseline carbon storage due only to terrestrial processes in Pacific coastal waters was roughly 100 TgC. The results suggest that under baseline conditions, approximately 82 percent of this carbon was stored at water depths less than 100 m. Between water depths of 50 and 100 m, relatively little carbon storage was due to burial in sediments (17 percent), whereas between 0 and 50 m, a moderate amount of carbon storage was due to burial in sediments (70 percent). Approximately 18 percent of the total carbon stored was in water depths below 100 m. These estimates were generally in agreement with previous estimates of sediment and carbon transport to Pacific coastal waters (Sternberg, 1986; Hales and others, 2006).

Most of the current and projected carbon storage in Pacific coastal waters occurred in regions of high nutrient and sediment load, with an estimated 62 percent of the modeled baseline carbon storage occurring in the coastal waters of Oregon and Washington (table 11.3). The Columbia River alone discharged 27.9 TgC/yr of sediment, resulting in a model-estimated rate of coastal carbon storage of 0.9 TgC/yr or 46 percent of the total carbon stored in Pacific coastal waters. The San Francisco Bay region also contributed significant nutrient and sediment fluxes and accumulated significant carbon, according to the model; however, much of this production and storage likely occurred within the San Francisco Bay, which was not modeled separately.

The changes in sediment and nutrient loadings to Pacific coastal waters under the projected land-use and population changes envisioned in the IPCC–SRES A2 scenario resulted in a change in the estimated projections of carbon that was transported and buried in the deep ocean. Under the A2 scenario in 2050, the rate of carbon storage in Pacific coastal waters was projected to increase by 33 percent in the southern California region and by 4 percent in the northern California region (table 11.3). In Oregon and Washington, however, where most of carbon storage presently occurs, the model projected a 12 percent decline in the rate of carbon storage. Taken together, the cumulative effect of projected land-use change by 2050 under the A2 scenario was a decrease in the projected rates of carbon storage in Pacific coastal waters by 4 percent overall. This decrease corresponded to a projected decrease in the total carbon storage to 112 TgC over the 58 years between 1992 and 2050, for a net difference of 3 percent.

The nutrient fluxes that support phytoplankton production Pacific coastal waters are largely supplied by seasonal upwelling (Kudela and others, 2006; Hales and others, 2008). Nevertheless, higher rates of annual phytoplankton production have been observed close to rivers (Kudela and others, 2006; Hales and others, 2008), and the model results indicated the total nitrogen supply to Pacific coastal waters may support up to 15 percent of the total production under baseline conditions (G.C. Anderson, 1964; Kudela and others, 2006). The projected cumulative changes to the rate of carbon storage in Pacific coastal waters that were due to a projected increase in nutrient exports by 2050 under the A2 scenario were relatively minor in comparison to the changes due to sediment flux; even though the projected increase in total nitrogen flux due to land-use and population change was in the range of 28 percent, there was less than a 3 percent projected increase in the total nutrients available to support phytoplankton production.

11.5. Discussion

The results indicate that the rate of carbon storage in the Pacific coastal waters that resulted directly from terrestrial processes contributed significantly to the carbon balance of the Western United States under both baseline and projected future conditions. The rate of modeled carbon storage that was due to terrestrial fluxes accounted for half to two thirds of the total estimated carbon storage in the same region (3 to 4 TgC/yr) (Hales and others, 2008). The rate of modeled carbon storage due to terrestrial fluxes is comparable to the estimated 1.2 TgC/yr rate in inland reservoirs (chapter 10), but much lower than the estimated 86 TgC/yr rate in terrestrial ecosystems (chapter 5).

The majority of terrestrial contribution to coastal carbon storage occurred in the coastal waters of Oregon and Washington under both the baseline and projected future conditions because of the large discharge of nutrients and sediments from the rivers located in that region. Sediment discharge and carbon storage was also high in the vicinity of the Eel River in the northern California region and near San Francisco Bay, but much lower in the southern California region.

The majority of the coastal carbon sequestration related to terrestrial processes resulted from the transport of TOC below the level of the pycnocline rather than burial in sediments. Of the total carbon stored, the model results suggested that approximately 70 percent was directly transported to the deep ocean and approximately 30 percent was buried in coastal sediments. For the amount buried in sediments, the model results indicated that approximately 70 percent was buried at depths less than 50 m, approximately 15 percent was buried between 50 m and 100 m depth, and the remainder (approximately 15 percent) was buried in the deep ocean. The decreased burial in the deeper zones was because of the lower sediment flux in this region and the deeper water column. These results agree with Dunne and others (2007), who suggested that previous ocean models of carbon storage rates did not account for the appreciable carbon storage that occurs in shallow coastal sediments.

The projected increase in sediment flux in the southern California region (23 percent from the baseline flux) corresponded with a projected increase in carbon storage rates in coastal waters, but the projected overall decline in sediment flux in the other regions resulted in an overall decrease in the projected coastal carbon storage rates for the region. The increase in carbon storage rates in southern California was driven by the elevated modeled fluxes from small, mountainous rivers in southern California which respond more sensitively to land-use and population changes than larger river systems, such as those in northern California and the Pacific Northwest.

Small, mountainous rivers were important generally to coastal carbon storage processes despite their relatively small watershed areas because of their large sediment loads (Milliman and Syvitski, 1992; Blair and others, 2004). For example, in 1992, the modeled sediment discharge from the Columbia River was 28 Tg/yr, while the discharge from small, mountainous rivers was 21 Tg/yr for the same year. Small, mountainous rivers, therefore, contributed 75 percent of the sediment discharge of the fourth largest river in the United States. These results indicated that small, mountainous rivers should be included in estimates of terrestrial and ocean carbon balances and that focusing only on large river systems may significantly underestimate fluxes and coastal carbon storage. The model results suggest that under the land-use projections of scenario A2 in 2050, rates of carbon storage due to small, mountainous rivers was projected to decrease by 12 percent; however, and perhaps more importantly, nutrient discharges for these rivers were projected to increase by 26 percent.

The concomitant increase in sediment and nutrients in small, mountainous rivers has the potential to increase carbon storage rates beyond that which was estimated by the model because the projected increase in nutrients may stimulate additional phytoplankton production at the same time and location that sediment fluxes are projected to increase (Wheatcroft and others, 2010). Normally, phytoplankton production is elevated in the summer due to the upwelling of nutrient-rich waters, while sediment flux peaks in winter with peak river discharge (Wheatcroft and others, 2010). The projected coincidence of phytoplankton production and sediment concentration is expected to accelerate the transport of phytoplankton carbon from the surface ocean to the deep ocean (Armstrong and others, 2009) and, therefore, increase carbon burial efficiency.

The projected increases in nutrient fluxes that would result from land-use and population changes under the A2 storyline in 2050 may have additional effects that were not captured by the model. Depending on future water-quality regulations and the form of the nutrients, the additional nutrients may (1) exacerbate hypoxia that has been periodically observed at the mouth of the Columbia and elsewhere on the Pacific Coast or (2) stimulate the production of harmful algal blooms (Glibert, 2010). Despite the obvious deleterious effects on water quality, broader areas of hypoxia in surface or bottom water will likely increase the rates of carbon storage in these regions (Bergamaschi and others, 1997).

This page intentionally left blank.

Chapter 12. Toward an Integrated Assessment of Baseline and Projected Future Carbon Storage and Greenhouse-Gas Fluxes in Ecosystems of the Western United States—Further Analyses and Observations

By Shuguang Liu[1], Zhiliang Zhu[2], Terry L. Sohl[1], Todd J. Hawbaker[3], Benjamin M. Sleeter[4], Sarah M. Stackpoole[3], and Richard A. Smith[2]

12.1. Highlights

- The sum of the estimated mean net fluxes of carbon from terrestrial and aquatic pools was approximately −91.0 teragrams of carbon per year (TgC/yr) in the Western United States from 2001 to 2005. Terrestrial ecosystems sequestered 95 percent of the total carbon sequestered in the region. This rate of the total ecosystem carbon sequestration is equivalent to 4.9 percent of the total greenhouse-gas emissions from the United States in 2010.
- Compared with the baseline net ecosystem carbon balance (NECB) estimates for terrestrial ecosystems, which ranged from −162.9 to −13.6 TgC/yr, the projected future potential NECB for terrestrial ecosystems in the Western United States ranged from −113.9 to 2.9 TgC/yr, representing a potentially significant decline by as much as 30 to 121 percent (or from 16.5 to 49 TgC/yr). This projected decrease was estimated by considering land-use- and land-cover- (LULC-) change scenarios and general circulation models, incorporating simulated wildland-fire disturbances, and using biogeochemical models.
- The estimated baseline wildland-fire emissions were equivalent to 11 to 12 percent of the estimated rate of sequestration by terrestrial ecosystems in the Western United States. Because wildland-fire emissions were projected to increase and sequestration by terrestrial ecosystems was projected to decline under future climate conditions, the projected wildland-fire emissions could potentially be equivalent to 27 to 43 percent of the projected sequestration by terrestrial ecosystems. The carbon stored in arid and semiarid regions of the Western United States was especially vulnerable to wildland-fire emissions under both the baseline and projected future conditions.

12.2. Introduction

This assessment was a multidisciplinary effort to study carbon stocks, carbon sequestration, and greenhouse-gas (GHG) fluxes in terrestrial and aquatic ecosystems in the context of major controlling processes such as land-use and land-cover (LULC) changes, climate changes, and wildland-fire occurrences. All of the major ecosystems were included in the assessment in a spatially and temporally explicit fashion, thus allowing for opportunities to analyze relations between input and output data, parameters and estimates, drivers and results, and geographies and time horizons. Specifically, there are four objectives for this chapter:

1. Examine the baseline carbon stocks, sequestration, and fluxes that were estimated from the different assessment components (chapters 2, 3, 5, 10, and 11) in order to provide a heuristic view of the carbon cycle and budget in the Western United States.
2. Compare similarities and differences between the estimated baseline and projected terrestrial net carbon fluxes and greenhouse-gas (GHG) fluxes. Because projections were not available for inland aquatic ecosystems, the comparison does not include processes related to them.
3. Synoptically examine the impacts of LULC change, disturbances, and climate change on carbon stocks and sequestration across the Western United States.
4. Discuss and summarize the major accomplishments and limitations of this assessment.

[1]U.S. Geological Survey, Sioux Falls, S.D.

[2]U.S. Geological Survey, Reston, Va.

[3]U.S. Geological Survey, Denver, Colo.

[4]U.S. Geological Survey, Menlo Park, Calif.

12.3. Observations and Examinations

12.3.1. Carbon Cycle and Budget in Terrestrial and Aquatic Systems During the Baseline Period

The estimated baseline (2001–2005) carbon stocks and changes in carbon stocks (fluxes) of the pools that were studied in the Western United States and were calculated during this assessment are shown in figure 12.1. The diagram depicts the results from the previous chapters. For simplicity, the estimated carbon stocks in all terrestrial ecosystems were lumped together in this diagram within two carbon pools: one for biomass carbon and the other for soil organic carbon (chapter 5 of this report). The emissions from wildland-fire combustions represented average conditions between 2001 and 2008 (chapter 3 of this report). Aquatic fluxes and sequestration (chapters 10 and 11) were based on input data representing average conditions from the 1970s to 2012.

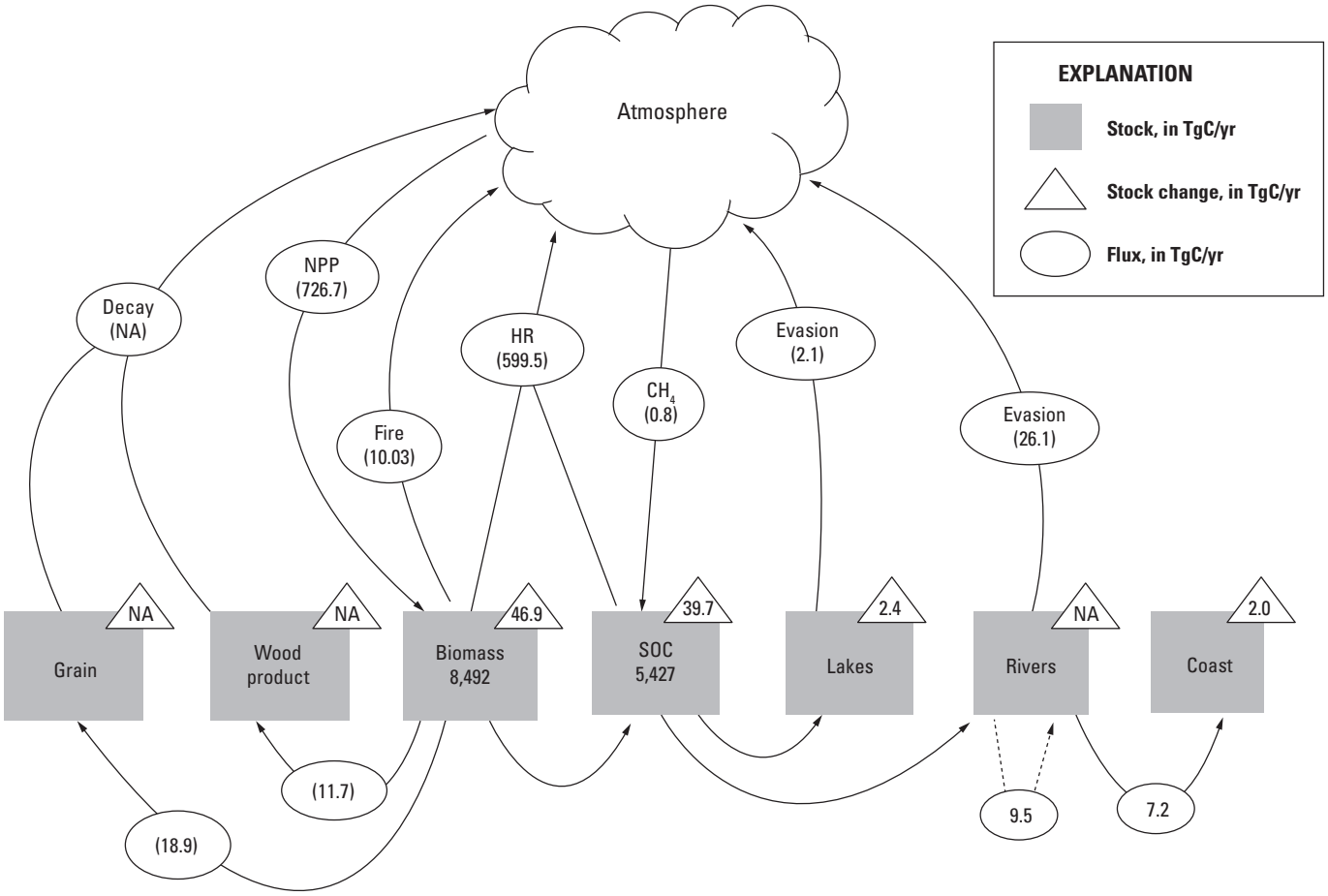

Figure 12.1. Flow diagram showing average carbon stocks and fluxes and changes in average carbon stock for primary carbon pools in the Western United States during the baseline period (2001–2005). Not all carbon stocks and fluxes are included in this diagram; only those stocks and fluxes that were examined in the assessment are shown. Changes in carbon storage rates in lacustrine systems (lakes and reservoirs) and in coastal waters (by burial in sediment) were included, but the carbon stocks in these ecosystems were not included. In quantifying the changes in average carbon stocks of soils and biomass, carbon combustion by fire and transfer to products by harvesting were considered but not their export to the aquatic ecosystems. There was no coupling between the estimates of carbon stocks in the terrestrial and aquatic systems. Positive carbon stock change indicates a carbon storage increase, and therefore represents carbon sequestration. The dotted arrow under the "Rivers" box indicates the lateral flux of carbon within the streams and rivers. NA, not applicable, due to either a lack of input data or the choice of methods; NPP, net primary production of terrestrial ecosystems; HR, heterotrophic respiration of terrestrial ecosystems; SOC, soil organic carbon; TgC/yr, teragrams of carbon per year.

As noted in chapter 1 of this report and above, the baseline years varied for different components of the overall carbon cycle because of the varying availability of input data. As a result, figure 12.1 should be interpreted as a composite representation of contemporary carbon-cycle processes in the region. The common time period for all the components was from 2001 to 2005, which is the nominal baseline period for this assessment (chapter 1 of this report).

On average, the terrestrial ecosystems (forests, agricultural lands, grasslands/shrublands, wetlands, and other lands) in the five ecoregions of the Western United States stored a total of 13,919 TgC during the baseline period (2001–2005). Carbon in biomass pools (such as live and dead vegetative materials aboveground and belowground, except for those removed from agricultural fields and forests) accounted for 8,492 TgC (61 percent) of the total, and the rest was stored in the top 20 cm of the soil layer. Carbon stored in other pools (such as grain and wood products removed from the landscape) was not estimated in this assessment, although its influx was calculated. The regional NECB was estimated to be −91.0 TgC/yr in the Western United States. This estimate represented the sum of carbon removed from the atmosphere and sequestered in terrestrial pools and in sediments in lakes, reservoirs, and coastal waters in this region. Of the total NECB in the region, the terrestrial ecosystems were responsible for an average of −86.6 TgC/yr (95 percent of the total NECB), including −46.9 TgC/yr and −39.7 TgC/yr in biomass and soils, respectively (fig. 12.1). The average amount of carbon sequestered annually in the Western United States during the baseline period was equivalent to about 4.9 percent of the fossil-fuel emissions in the United States in 2010 (EPA, 2012).

Among the various types of flux, the largest were the net primary production (NPP) and heterotrophic respiration of the terrestrial ecosystems. About 12 percent of the annual NPP was sequestered in biomass and soils. The amount of carbon removed by timber harvesting (only clearcut areas were considered) from the landscape was 11.7 TgC/yr, which was similar in magnitude to the carbon emissions from wildland fires (10.0 TgC/yr). The amount of carbon removed by harvesting grain from agricultural lands was 18.9 TgC/yr, which is a large amount considering that agricultural land was not the dominant land-cover type in the Western United States. The amount of carbon removed by timber harvesting was largely underestimated compared with estimates in other studies (Hudiburg and others, 2011; D.P. Turner, Ritts, and others, 2011) and in the U.S. Department of Agriculture's timber statistics reports (USDA, 2011a). The underestimation was likely caused by the omission of partial forest cutting in the assessment, which was due to the absence of geospatial data layers describing the location, extent, and intensity of partial forest cutting with adequate spatial and temporal resolution.

Although carbon fluxes related to timber and grain harvesting were estimated, no life-cycle analysis was conducted to evaluate the long-term decomposition rates of the harvests. Also not included in this assessment were carbon fluxes related to forest thinning, forest defoliation and mortality from insects, and rangeland grazing. As documented in chapter 4 of this report, these land-management concerns and natural disturbances, which are highly relevant to the carbon cycle in the Western United States, were not supported with sufficient input data. As a result, their exclusion introduced uncertainty in the assessment.

Inland aquatic ecosystems in the Western United States represented only a small portion of the total area (1.5 percent), but they played an important role in determining the fate of a large portion of the total carbon flux in the region. The total flux (lateral and efflux) of inland aquatic ecosystems at 37.7 TgC/yr was previously unaccounted for and is regionally significant (such as in the Marine West Coast Forest ecoregion). Several processes related to the carbon cycle of the inland and coastal aquatic systems were not included in the study: the effluxes of carbon dioxide from the Pacific coastal waters, lateral transport of carbon by soil erosion and deposition, and the interactions of carbon between terrestrial and aquatic ecosystems.

The export of carbon by riverine systems into the Pacific coastal waters was estimated to be 7.2 TgC/yr. Only a small amount of the carbon exported by riverine system was estimated to be stored in the Pacific coastal waters, but terrestrial processes (such as primary production by different terrestrial ecosystems) were directly involved in storing approximately 2.0 TgC/yr.

12.3.2. Comparing Baseline and Projected Future Estimates of Net Ecosystem Carbon Balance

The minimum and maximum estimates of the mean terrestrial net ecosystem carbon balance are listed in table 12.1 for both baseline (2001–2005) and projected future (2006–2050) conditions. The negative NECB values indicate carbon sequestration in terrestrial ecosystems, and positive values suggest carbon loss from ecosystems (partially by lateral transport of terrestrial ecosystems, such as grain and timber harvesting).

Table 12.1. Minimum and maximum estimates of mean net ecosystem carbon balance under baseline (2001–2005) and projected future (2006–2050) conditions for all major ecosystems for the Western United States.

[Negative net ecosystem carbon balance (NECB) values indicate carbon sequestration in terrestrial ecosystems and positive values indicate carbon loss. Minimum mean and maximum mean represent the annual means of the minimum and maximum NECB among the 21 General Ensemble Modeling System (GEMS) simulations over the baseline and projection periods under various biogeochemical models, land-use- and land-cover-change scenarios, and climates projected by general circulation models (see chapters 5 and 9 of this report). For the column indicating the difference between the baseline and projected NECB, negative values indicate a decrease in NECB from baseline to future projections, and positive values indicate an increase. TgC/yr, teragrams of carbon per year]

Ecoregion	Ecosystem	Baseline NECB (TgC/yr)		Projected NECB (TgC/yr)		Difference between baseline and projected NECB (TgC/yr)	
		Minimum mean	Maximum mean	Minimum mean	Maximum mean	Minimum mean	Maximum mean
Western Cordillera	Forests	−70.3	−19.6	−52.3	−7.0	−18.0	−12.6
	Grasslands/shrublands	−14.6	0.2	−7.9	0.3	−6.7	−0.1
	Agricultural lands	−0.4	0.0	−1.0	0.0	0.6	0.0
	Wetlands	−0.7	−0.1	−0.4	0.0	−0.3	−0.1
	Other lands	−0.2	0.4	−0.2	0.0	0.0	0.4
	Total	−86.2	−19.1	−61.8	−6.7	−24.4	−12.4
Marine West Coast Forest	Forests	−6.0	−1.3	−8.1	1.8	2.1	−3.1
	Grasslands/shrublands	−0.7	0.0	−0.4	0.0	−0.3	0.0
	Agricultural lands	0.0	0.1	−0.5	0.2	0.5	−0.1
	Wetlands	0.0	0.0	−0.1	0.0	0.1	0.0
	Other lands	−0.2	0.2	−0.5	−0.1	0.3	0.3
	Total	−6.9	−1.0	−9.6	1.9	2.7	−2.9
Cold Deserts	Forests	−7.8	1.5	−7.7	−0.8	−0.1	2.3
	Grasslands/shrublands	−20.9	3.8	−8.7	4.5	−12.2	−0.7
	Agricultural lands	−3.0	0.0	−4.7	0.0	1.7	0.0
	Wetlands	−0.6	0.0	−0.4	0.0	−0.2	0.0
	Other lands	−0.3	0.4	−0.2	0.1	−0.1	0.3
	Total	−32.6	5.7	−21.7	3.8	−10.9	1.9
Warm Deserts	Forests	−0.6	0.2	−0.5	0.0	−0.1	0.2
	Grasslands/shrublands	−16.1	2.7	−3.9	5.4	−12.2	−2.7
	Agricultural lands	−1.8	0.0	−1.3	0.0	−0.5	0.0
	Wetlands	0.0	0.0	−0.1	0.0	0.1	0.0
	Other lands	−0.1	0.0	−0.1	0.0	0.0	0.0
	Total	−18.6	2.9	−5.9	5.4	−12.7	−2.5
Mediterranean California	Forests	−6.1	−2.6	−5.8	−2.0	−0.3	−0.6
	Grasslands/shrublands	−6.4	0.3	−3.0	0.6	−3.4	−0.3
	Agricultural lands	−5.6	0.2	−5.0	0.1	−0.6	0.1
	Wetlands	−0.1	0.1	−0.3	0.0	0.2	0.1
	Other lands	−0.4	−0.1	−0.5	−0.2	0.1	0.1
	Total	−18.6	−2.1	−14.6	−1.5	−4.0	−0.6
Western United States (total)	Forests	−90.8	−21.8	−74.4	−8.0	−16.4	−13.8
	Grasslands/shrublands	−58.7	7.0	−23.9	10.8	−34.8	−3.8
	Agricultural lands	−10.8	0.3	−12.5	0.3	1.7	0.0
	Wetlands	−1.4	0.0	−1.3	0.0	−0.1	0.0
	Other lands	−1.2	0.9	−1.5	−0.2	0.3	1.1
	Total	−162.9	−13.6	−113.6	2.9	−49.3	−16.5

During the baseline period, the NECB of the terrestrial ecosystems in the Western United States was estimated to range from −162.9 to −13.6 TgC/yr, with a mean value of −86.6 TgC/yr. In comparison, the projected future range of the NECB was estimated to range from −113.6 to 2.9 TgC/yr. The comparison in table 12.1 indicates a projected decline in future potential sequestration ranging from 16.5 to 49.3 TgC/yr, which represents an estimated 30 to 121 percent decrease in the potential of those ecosystems to sequester carbon.

The projected decline in the NECB was highly variable among ecoregions and ecosystems. Forests were estimated to be the largest carbon sink during the baseline period with a mean rate of −53.9 TgC/yr, which accounted for 62 percent of the total NECB in the Western United States; however, this sink was projected to decrease by 13.8 to 16.4 TgC/yr by 2050. This result correlates with previous studies which hypothesized that the aging of forest ecosystems in the United States may result in weakened carbon sequestration by forests over time (Hurtt and others, 2002; Pan, Chen, and others, 2011; D.P. Turner, Ritts, and others, 2011). Grasslands/shrublands were estimated to be the second largest carbon sink during the baseline period because of their extensive coverage of part of the Western United States; however, this estimated sink was projected to have the largest decrease in the NECB, with losses ranging from 34.8 to 3.8 TgC/yr by 2050. In general, the NECB in the rest of the ecosystems in the Western United States was projected to remain relatively stable between the baseline and projected time periods.

Table 12.2 shows the differences between the baseline estimated mean annual NECB (table 5.4 of chapter 5) and the projected mean annual NECB by biogeochemical model, climate-change scenario, and general circulation model (table 9.2 of chapter 9) for each ecoregion and for the Western United States as a whole. Among the three biogeochemical models, the CENTURY model projected the largest decrease for the Western United States as a whole, followed by the spreadsheet model and the Erosion-Deposition-Carbon Model (EDCM). The EDCM projected an increase in the NECB in the Cold and Warm Deserts ecoregions, whereas the CENTURY model projected a decrease of about 20 percent and the spreadsheet model projected a similar trend. All three biogeochemical models projected that the NECB for the Marine West Coast Forest would remain relatively flat.

Table 12.2. Differences between the baseline and projected net ecosystem carbon balance for each ecoregion, categorized by biogeochemical model, land-use- and land-cover-change scenario, and general circulation model.

[CCCma CGCM3.1, Canadian Centre for Climate Modelling and Analysis's Coupled Global Climate Model version 3.1; CSIRO-Mk3.0, Commonwealth Scientific and Industrial Research Organization Mark 3.0; EDCM, Erosion-Deposition-Carbon Model; GCM, general circulation model; MIROC 3.2-medres, Model for Interdisciplinary Research on Climate (version 3.2, medium resolution); TgC/yr, teragrams of carbon per year]

Model or scenario	Western Cordillera (TgC/yr)	Marine West Coast Forest (TgC/yr)	Cold Deserts (TgC/yr)	Warm Deserts (TgC/yr)	Mediterranean California (TgC/yr)	Western United States (TgC/yr)
CENTURY biogeochemical model	−31.2	−0.2	−22.4	−18.7	−5.3	−77.7
EDCM biogeochemical model	−5.7	−0.3	7.3	2.3	−6.0	−2.4
Spreadsheet biogeochemical model	−10.0	−1.7	−0.4	−0.1	−0.5	−12.7
A1B scenario	−19.3	−1.6	−6.6	−7.2	−5.1	−39.8
A2 scenario	−17.6	−1.3	−6.8	−7.2	−4.8	−37.6
B1 scenario	−14.8	1.6	−6.3	−6.7	−4.7	−30.9
CCCma CGCM3.1 GCM	−18.2	−0.1	−7.8	−8.7	−5.6	−40.3
CSIRO–Mk3.0 GCM	−18.1	−0.4	−4.3	−6.0	−5.5	−34.4
MIROC 3.2–medres GCM	−19.0	−0.2	−10.5	−9.9	−5.8	−45.3

The differences between the baseline and projected carbon fluxes under the three scenarios chosen from the Intergovernmental Panel on Climate Change's Special Report on Emissions Scenarios (IPCC–SRES; Nakicenovic and others, 2000) were relatively consistent, varying from −39.8 TgC/yr (A1B scenario) to −30.9 TgC/yr (B1 scenario) for the entire Western United States, and this consistency can also be seen across all the ecoregions. The climate projections affected the magnitude of carbon-flux change as well. The most significant decline of −45.3 TgC/yr was projected under the Model for Interdisciplinary Research on Climate (version 3.2, medium resolution; MIROC 3.2-medres), and the smallest decline (−34.4 TgC/yr) was projected under the Commonwealth Scientific and Industrial Research Organization Mark 3.0 (CSIRO–Mk3.0) model. The largest differences in carbon flux under the different GCMs were manifested in the Cold and Warm Deserts, which were the most climate-sensitive ecoregions in the Western United States.

12.3.3. Preliminary Observations of Land-Use and Land-Cover Change, Disturbances, and Climate Change

12.3.3.1. Land-Use and Land-Cover Change

The effects of estimated LULC change on carbon sequestration were observed by examining the net change in area and the net change in the amount of carbon stored (NECB) within three major ecosystems in the Western United States (forests, grasslands/shrublands, and agricultural lands). Each 5-year time period was plotted for each of the three scenarios (fig. 12.2). Although figure 12.2 may be useful for examining some effects of LULC change, interpretations should be made with these caveats:

- The changes in carbon storage depicted in figure 12.2 were all-inclusive and represented not only the effects of net LULC change, but also the effects of other driving forces such as climate change and location-specific LULC transitions.
- Gross LULC change (LULC transitions both to and from a given LULC class) may have led to a change in carbon storage, even if there was no net change in area, because of the geographic differences in carbon storage within the same land cover. The effects of gross LULC change on carbon could be investigated in the future.
- Changes in carbon storage in each LULC category did not necessarily indicate carbon sequestration from or release to the atmosphere. The changes may have simply indicated the reassignment of carbon storage from one LULC type to another following a LULC transition. For example, if an area of marginal agricultural land (with an assumed amount of carbon storage of 3,000 gC/m^2) transitions to grassland (with an assumed amount of carbon storage of 3,030 gC/m^2), it could incur a net carbon gain of 30 $gC/m^2/yr$. The change in carbon storage would be indicated as a loss of 3,000 gC/m^2 for the agricultural land and a gain of 3,030 gC/m^2 for the grassland one year after the transition.

Among the three scenarios, the rate of carbon sequestration was projected to decline precipitously over time under the A1B and A2 scenarios, while remaining relatively stable under the B1 scenario after an initial drop (fig. 12.2). An exploration of the exact causes and their relative contributions to the trends was not conducted for this report; however, the following observations were made:

- Despite either positive or negative changes in individual ecosystems, carbon storage in all ecosystems increased consistently in the Western United States throughout the projected time period, but the rate of increase declined under the A1B and A2 scenario (fig. 12.2). This result suggested a complex relation between LULC change and the net change in carbon storage that likely involved the effects of other factors. For example, the large amount of carbon sequestered in some forests may have been dictated by their relatively young age (Pan, Chen, and others, 2011), which was the result of forest-management policies that were created in the first half of the 20th century (Houghton and others, 1999; D.P. Turner, Ritts, and others, 2011). As the forests matured and aged, their sequestration capacity may have been in an overall decline.
- The projected increase in carbon storage in agricultural lands may have been largely driven by the modeled increase in biomass production capacity over time on the basis of assumptions made in the model about improvements in genetic engineering, cultivation, and management practices (S. Liu and others, 2003). On the other hand, changes in carbon storage and sequestration by grasslands/shrublands were projected to follow changes in the ecosystem's land area with a time lag.

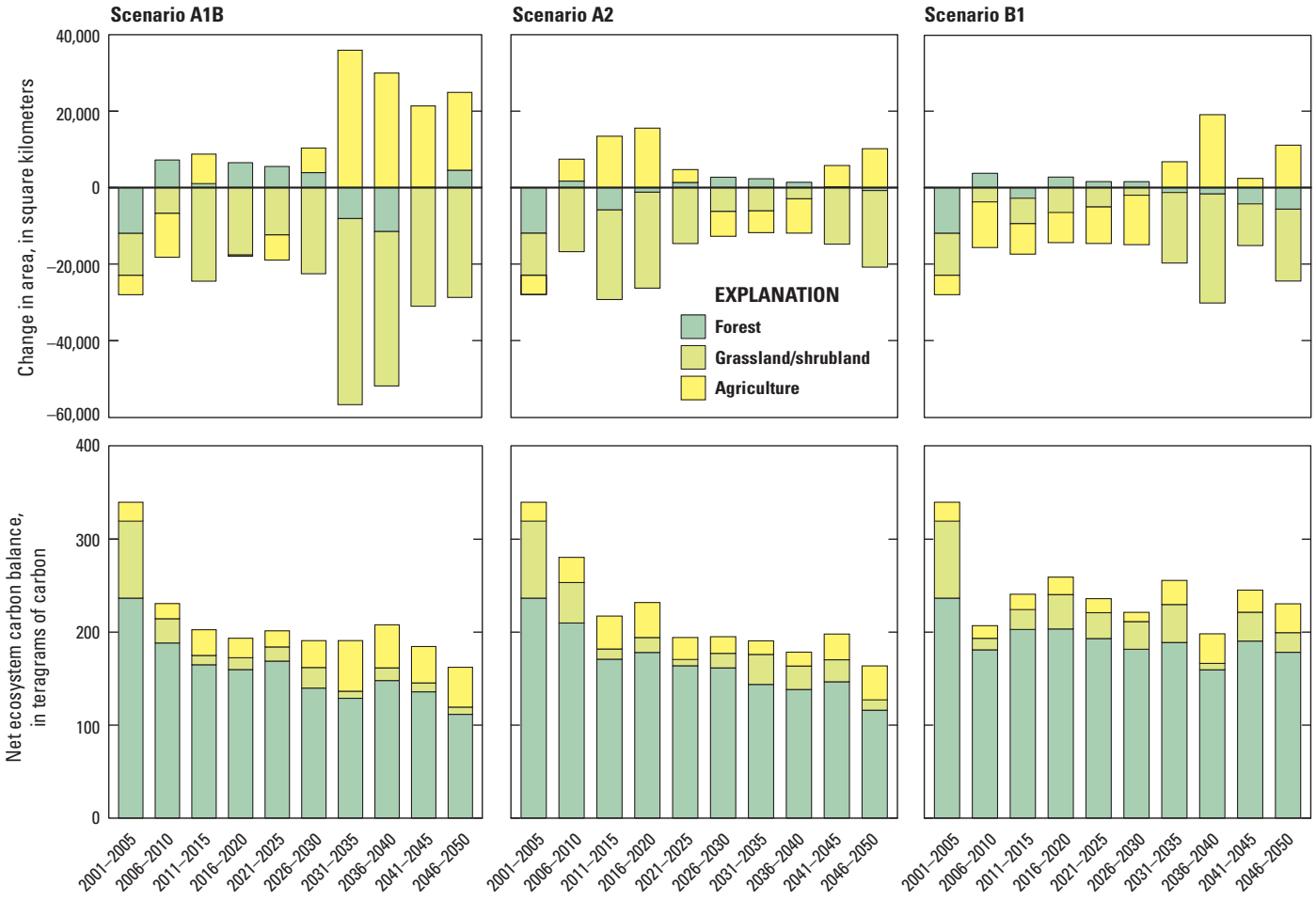

Figure 12.2. Charts showing comparisons of net change in the area of major land-use and land-cover classes and net ecosystem carbon balance (NECB), by 5-year intervals in the Western United States from the baseline (2001–2005) through the projected (2006–2050) time periods.

12.3.3.2. Land Management and Disturbances

Across the Western United States, forest cutting was projected to increase from the baseline under the A1B and A2 scenarios, but was projected to decline from the baseline under the B1 scenario (chapter 6 of this report). These projections were used to simulate the amount of timber harvested (fig. 12.3). The projections of reduced forest cutting under the B1 scenario, which effectively increased the rotation length of harvesting, largely explained the differences in carbon sequestration between the B1 scenario and the other two IPCC–SRES scenarios (fig. 12.3). For example, under the B1 scenario, the projected increase in carbon by forests was more pronounced and sustained than under the other scenarios in the Marine West Coast Forest and Western Cordillera ecoregions, where most forest cutting was expected to take place. The annual differences in carbon sequestration by forest cutting among all three IPCC scenarios were as great as 3 TgC/yr in the Marine West Coast Forest and 7.5 TgC/yr in the Western Cordillera. The results agreed well with past observations that changes in forest harvesting regimes have a large effect on carbon sequestration (Cohen and others, 1996; Houghton and others, 1999; D.P. Turner, Ritts, and others, 2011).

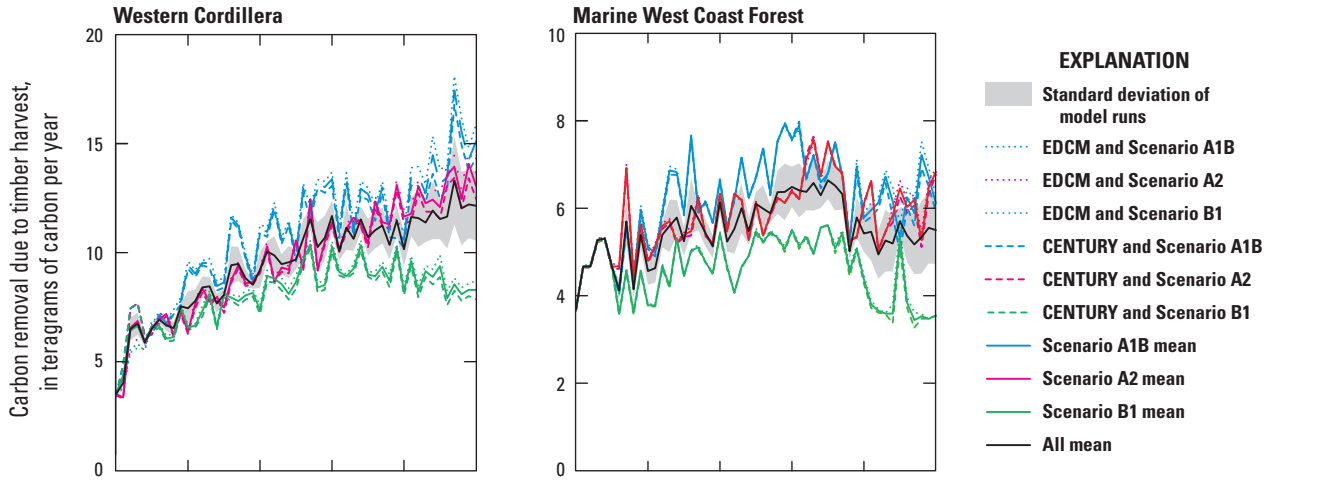

Figure 12.3. Graphs showing carbon removal from the Western Cordillera and Marine West Coast Forest ecoregions during the baseline (2001–2005) and projected (2006–2050) time periods as the result of forest harvesting activities, simulated under the three selected climate-change scenarios and two of the biogeochemical models. The other ecoregions studied in the assessment were estimated to have smaller amounts of carbon removal because they had limited forest coverage; the results from those ecoregions are not presented here. Scenarios are from the Intergovernmental Panel on Climate Change's Special Report on Emissions Scenarios (Nakicenovic and others, 2000). EDCM, Erosion-Deposition-Carbon Model; TgC/yr, teragrams of carbon per year.

Across the Western United States, the median area burned annually by wildland fires was 12,136 km^2 during the baseline time period (2001–2008), but the interannual variability in burned area was large; specifically, 23,261 km^2 burned during extreme years, defined as the 95th percentile of the area burned annually. Wildland fires emitted a median of 41.0 $TgCO_{2\text{-}eq}$/yr and emitted 65.0 $TgCO_{2\text{-}eq}$/yr in extreme years. Median and extreme wildfire emissions were approximately 0.07 percent and 0.13 percent, respectively, of the total carbon stock (14,182 TgC) in the Western United States from 2001 to 2008.

Both the area burned by wildland fires and GHG emissions were projected to increase in the Western United States under all three of the climate-change scenarios considered in this assessment (chapter 8 of this report). The projected median of the area burned annually increased 31 to 66 percent relative to the baseline conditions (average of 2001 to 2008, which was 12,136 km^2) and the projected median annual emissions increased 28 to 56 percent from a baseline median of 41.0 $TgCO_{2\text{-}eq}$/yr. These increases resulted in the median of the area burned annually ranging between 15,900 and 20,100 km^2 and emissions ranging between 52.5 and 64.0 $TgCO_{2\text{-}eq}$ in the decade between 2041 and 2050. Thus, a typical (median) fire year in the future could be rather similar to an extreme (95th percentile) fire year in the baseline period. Extreme fire years were projected to become even more extreme; the 95th percentile of the area burned annually increased 79 to 95 percent from baseline conditions (2001–2008), from 23,261 km^2/yr to between 41,600 and 45,400 km^2/yr. The emissions in extreme fire years increased 73 to 150 percent to between 112 and 163 $TgCO_{2\text{-}eq}$/yr relative to the 65.0 $TgCO_{2\text{-}eq}$/yr during the baseline period.

The relative amount of carbon stocks lost in each ecosystem for each year through wildland-fire emissions was projected to increase. The future potential carbon stocks in the decade between 2041 and 2050 were projected to be 16,492 TgC across the Western United States. Carbon losses through emissions in a typical fire year in the same decade were projected to range between 0.08 and 0.09 percent of the potential carbon stock, which is a 0.01 to 0.02 percent increase from the baseline time period; in an extreme fire year during the same decade, carbon losses were projected to range between 0.19 and 0.27 percent of the potential carbon stock (table 12.3). The patterns of change in carbon stocks across the Western United States were generally consistent within the ecoregions, except for the Marine West Coast Forest, where little change in wildland-fire occurrences and emissions was projected, and in Cold Deserts, where the projected changes in emissions relative to carbon stocks were small. Over the same time period, the rate of carbon sequestration was projected to decrease by 45 to 58 percent across the Western United States. Even though carbon stocks were projected to increase over time, carbon sequestration rates were projected to ultimately decrease, partially because of the projected increase in wildland-fire emissions.

Table 12.3. Estimated wildland-fire emissions relative to total ecosystem carbon stocks during typical and extreme fire years for the baseline (2001–2008) and future (2041–2050) time periods.

Ecoregion	Typical fire years (in percent)			Extreme fire years (in percent)		
	Baseline	Future projected low	Future projected high	Baseline	Future projected low	Future projected high
Western Cordillera	0.100	0.090	0.130	0.180	0.200	0.440
Marine West Coast Forest	0.010	0.010	0.010	0.010	0.000	0.010
Cold Deserts	0.040	0.050	0.070	0.070	0.120	0.150
Warm Deserts	0.090	0.100	0.160	0.230	0.200	0.460
Mediterranean California	0.060	0.050	0.070	0.110	0.110	0.120
Western United States	0.070	0.080	0.090	0.130	0.190	0.270

12.3.3.3. Effects of Climate Change

Globally, increased carbon dioxide and climate change may cause change in the terrestrial ecosystem carbon cycle (Birdsey and others, 1993). Levy and others (2004) noted that the global carbon sink for 1990 through 2100 may range between 2 and 6 PgC/yr because of different fossil-fuel-emissions scenarios (Levy and others, 2004). According to Fung and others (2005), the terrestrial carbon sink may decrease globally in the coming decades and the amount could vary, depending on emissions scenarios. In the United States, the carbon sink could continue but could weaken over the 21st century (Hurtt and others, 2002). The following observations were made on the potential effects of climate change:

- The grasslands/shrublands ecosystem in the Western United States was sensitive to climate change and variability. The temporal variability of carbon stock change (sources or sinks) in the Cold Deserts and Warm Deserts ecoregions, as examples, were high and did not follow the corresponding temporal variability of the change in the extent of the grasslands/shrublands ecosystem (fig. 12.2). Flux-tower observations at the site-specific and regional scales have shown strong interannual variability in carbon-storage changes in the grasslands/shrublands ecosystem in this region (Scott and others, 2011; Xiao and others, 2011).
- All of the GCMs consistently projected future warming trends in all ecoregions, but the degree of warming varied by GCM and ecoregion (chapter 7 of this report). The projected changes in precipitation were highly variable. Figure 12.4 compares the density functions of relative change of precipitation during two time periods: 2001 to 2010 and 2041 to 2050. All of the GCMs projected extensive changes at the pixel level as indicated by the spread and shift of the density functions from $x = 0$ (which indicates no change). As an example, in the Cold Deserts ecoregion, where the carbon balance in the grasslands/shrublands ecosystem changed from a sink to a source under the A1B and A2 IPCC–SRES scenarios, two out of three GCMs suggested a 5 to 20 percent decrease in precipitation under all three IPCC–SRES scenarios (fig. 12.4).
- The GCMs projected a high degree of spatial variability in climate change even within ecoregions, as indicated by the spreading of the density curves of temperature and precipitation changes. In order to understand the effects of climate change at the ecoregion level, the spatial variability of climate change needed to be considered. For example, for the Marine West Coast Forest ecoregion, all of the GCMs projected, on average, small increases in precipitation under the A1B and A2 scenarios and small decreases under the B1 scenario; however, the patterns of carbon-storage change across scenarios in forests did not correlate to projected precipitation increases or decreases in the ecoregion. Future efforts to analyze the effects of climate may be aided by considering the spatial variability of those effects.

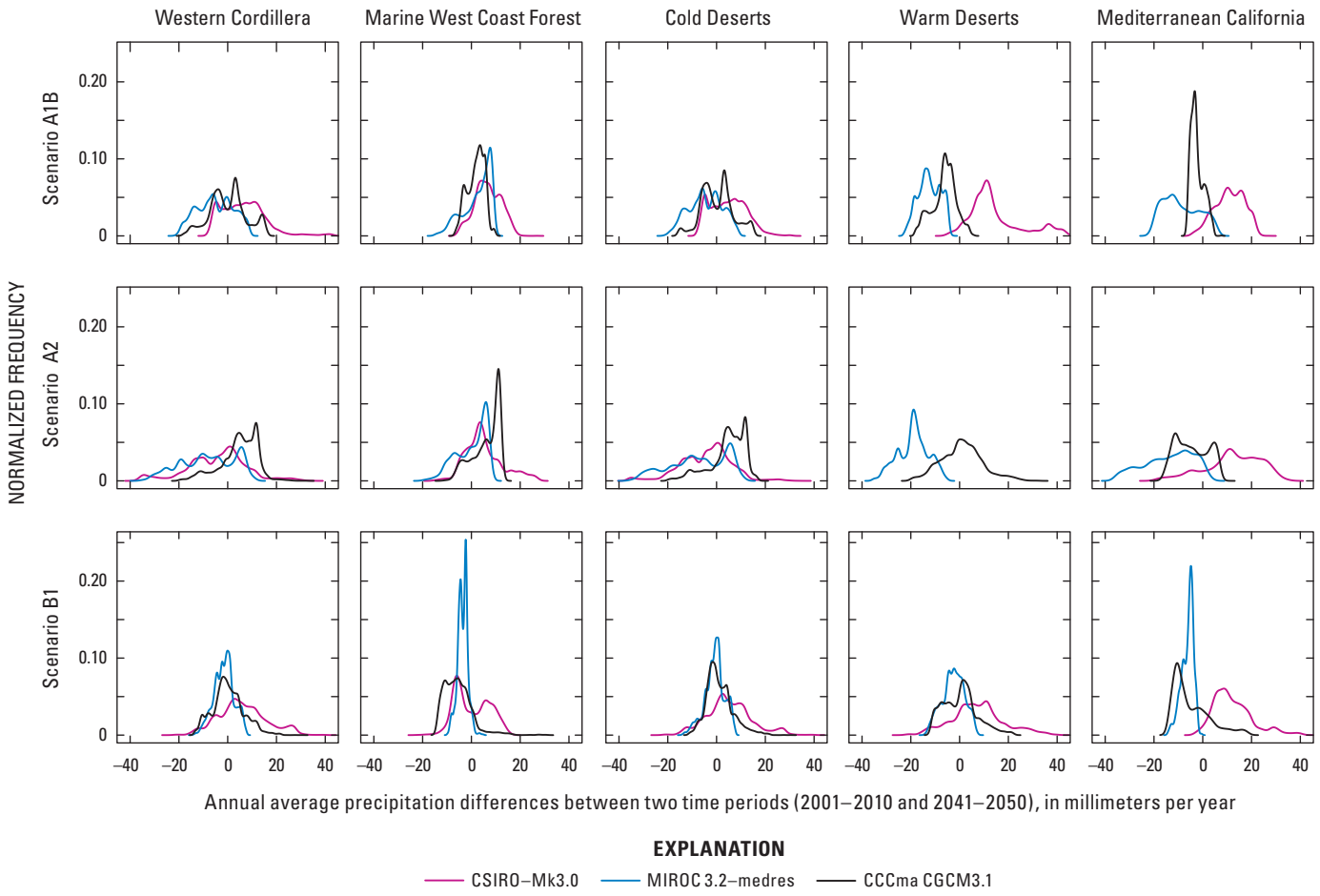

Figure 12.4. Graphs showing the distribution of annual average precipitation differences between the two time periods: 2001 to 2010 and 2041 to 2050. These averages were derived from the three general circulation models (CCCma CGCM3.1, CSIRO–Mk3.0, MIROC 3.2 medres) under three IPCC–SRES scenarios (A1B, A2, B1) for five ecoregions in the Western United States. The vertical axis shows the relative frequency and the integral (or area under each curve) equals 1. CCCma CGCM3.1, Canadian Centre for Climate Modelling and Analysis's Coupled Global Climate Model version 3.1; CSIRO–Mk3.0, Commonwealth Scientific and Industrial Research Organisation Mark 3.0 model; IPCC–SRES, Intergovernmental Panel of Climate Change's Special Report on Emissions Scenarios (Nakicenovic and others, 2000); MIROC 3.2–medres, Model for Interdisciplinary Research on Climate version 3.2, medium resolution.

12.4. Gaps, Uncertainties, and Limitations

This report covered broad and comprehensive topics designed to fulfill the requirements of the Energy Independence and Security Act of 2007 (described in chapter 1 of this report; U.S. Congress, 2007). The results, data products, and publications (including this report) were designed to assist the scientific community, land managers, and policy stakeholders in a variety of applications. Gaps in the assessment remain, however. There were both natural and anthropogenic ecosystem processes that were not explored and critical relations and feedback loops not yet analyzed and reported. The following gaps contributed to uncertainties in the results of this assessment and could be considered for future investigations.

- Major land-management activities in the Western United States (see chapter 4 of this report for more information) were not fully addressed. Two of the most important land-management activities in the Western United States, forest thinning and rangeland grazing, were not included in the assessment and their effects on carbon and GHG fluxes were not analyzed.
- Although emissions from wildland-fire combustions and effects on carbon dynamics over time were estimated using the best available data and models, an analysis of the long-term effects on net ecosystem production, including decomposition and regeneration of forests, was not included in the report.
- The estimated mean baseline carbon stock of 13,921 TgC (ranging from 12,418 to 15,460 TgC) for the Western United States reflected only terrestrial ecosystems. Baseline and projected estimates of carbon stocks were not made for the aquatic ecosystems. The estimates for the aquatic ecosystems focused only on carbon fluxes.
- Carbon sequestration estimates for both the baseline and the projected time periods were based on three future scenarios, which reflected the combined effects of LULC change, available land-management activities, wildland fires, and climate change (for future projections only). An understanding of the specific contributions by each of these controlling processes would require model runs using experimental designs. Instead, for this report, only preliminary analyses of possible individual effects were provided.

For all of the major technical processes in this assessment, practical efforts were made to validate baseline estimates and evaluate uncertainties in both the baseline and projected results. The validation steps and uncertainty in the results have been documented in this report. Uncertainties were quantified based on traditional statistical methods to account for the spread of multiple model runs. The actual spread of uncertainties in the results, as well as contributions from specific sources (including input data, model structure and parameterization, shortfalls in land-management activities and natural disturbances (as noted above), and connections or coupling between technical components of the assessment methodology) were not statistically quantified. Additional observations concerning uncertainties were made:

- The LULC changes and wildland-fire disturbances were modeled and estimates were made separately. The estimates were calculated for each pixel, but these estimates were not integrated; therefore, it is possible that a forest pixel that was modeled to be burned would still have a chance of being harvested at the same time or within a few years of the wildland-fire occurrence. Nevertheless, over the scale of an ecoregion, the integration of LULC with wildland-fire models and estimates is unlikely to be a major source of uncertainty.
- Aquatic and terrestrial methods were not coupled such that the aquatic methods used direct input from terrestrial models (for example, erosion and deposition) in order to estimate the effects and fate of terrestrial exports. Thus, it is uncertain how much of the aquatic carbon fluxes came from terrestrial sources. In addition, the possibility of overlaps in counting the surface areas between aquatic features (such as streams and rivers) and terrestrial ecosystems (such as wetlands) could lead a small portion of carbon fluxes to be counted twice.
- Ultimately, for projected future potential carbon storage and fluxes, it is the use of various input data layers (including the LULC-change and climate-change scenarios within the three IPCC–SRES storylines) and biogeochemical models that dictated the overall spread of the uncertainties in the assessment results. Uncertainties from these models and data layers were undoubtedly large, and future effort should emphasize the quantification and attribution of uncertainty in estimating carbon sequestration over large areas.

In using this report, as well as publications and data products generated for the assessment, caution should be exercised by considering the above-noted constraints and uncertainties together with the major findings and unique aspects of the assessment. In addition, this assessment was conducted in the framework of the five ecoregions, which were used to parameterize the assessment models. The results were therefore presented at the ecoregional scale. Therefore, although this assessment's spatial-data products were delivered at a 250-m-pixel resolution, the scale of the ecoregions is the most appropriate scale for applying the results of this assessment to further activities.

This page intentionally left blank.

References Cited

[Note: Some entries require a subscription for access.]

Ackerman, K.V., Mixon, D.M., Sundquist, E.T., Stallard, R.F., Schwarz, G.E., and Stewart, D.W., 2009, RESIS–II; An updated version of the original reservoir sedimentation survey information system (RESIS) database: U.S. Geological Survey Data Series 434, 22 p., database, accessed July 11, 2012, at http://pubs.usgs.gov/ds/ds434/.

Agee, J.K., 1993, Fire ecology of Pacific Northwest forests: Washington, D.C., Island Press, 505 p.

Agee, J.K., 2003, Historical range of variability in eastern Cascades forests, Washington, USA: Landscape Ecology, v. 18, no. 8, p. 725–740, doi:10.1023/B:LAND.0000014474.49803.f9.

Agee, J.K., and Skinner, C.N., 2005, Basic principles of forest fuel reduction treatments: Forest Ecology and Management, v. 211, no. 1–2, p. 83–96, doi:10.1016/j.foreco.2005.01.034.

Albini, F.A., Brown, J.K., Reinhardt, E.D., and Ottmar, R.D., 1995, Calibration of a large fuel burnout model: International Journal of Wildland Fire, v. 5, no. 3, p. 173–192, doi:10.1071/WF9950173.

Albini, F.A., and Reinhardt, E.D., 1995, Model ignition and burning rate of large woody natural fuels: International Journal of Wildland Fire, v. 5, no. 2, p. 81–91, doi:10.1071/WF9950081.

Albini, F.A., and Reinhardt, E.D., 1997, Improved calibration of a large fuel burnout model: International Journal of Wildland Fire, v. 7, no. 1, p. 21–28, doi:10.1071/WF9970021.

Alcamo, Joseph, Leemans, Rik, and Kreileman, Eric, eds., 1998, Global change scenarios of the 21st century; Results from the IMAGE 2.1 model: [Tarrytown, N.Y.,] Pergamon, 296 p.

Alexander, R.B., Smith, R.A., and Schwarz, G.E., 2000, Effect of stream channel size on the delivery of nitrogen to the Gulf of Mexico: Nature, v. 403, p. 758–761, doi:10.1038/35001562.

Alexander, R.B., Smith, R.A., Schwarz, G.E., Boyer, E.W., Nolan, J.V., and Brakebill, J.W., 2008, Differences in phosphorus and nitrogen delivery to the Gulf of Mexico from the Mississippi River basin: Environmental Science and Technology, v. 42, no. 3, p. 822–830, doi:10.1021/es0716103.

Alluvione, Francisco, Halvorson, A.D., and Del Grosso, S.J., 2009, Nitrogen, tillage, and crop rotation effects on carbon dioxide and methane fluxes from irrigated cropping systems: Journal of Environmental Quality, v. 38, no. 5, p. 2023–2033, doi:10.2134/jeq2008.0517.

Amiotte-Suchet, P.A., and Probst, J.L., 1995, A global model for present-day atmospheric/soil CO_2 consumption by chemical erosion of continental rocks (GEM–CO_2): Tellus B: Chemical and Physical Meteorology, v. 47, p. 273–280, doi:10.1034/j.1600-0889.47.issue1.23.x

Amiotte Suchet, Philippe, Probst, Jean-Luc, and Ludwig, Wolfgang, 2003, Worldwide distribution of continental rock lithology; Implications for the atmospheric/soil CO_2 uptake by continental weathering and alkalinity river transport to the oceans: Global Biogeochemical Cycles, v. 17, no. 2, 1038, 14 p., doi:10.1029/2002GB001891.

Anderson, G.C., 1964, The seasonal and geographic distribution of primary productivity off the Washington and Oregon coasts: Limnology and Oceanography, v. 9, no. 3, p. 284–292. (Also available at http://wap.aslo.org/lo/toc/vol_9/issue_3/0284.pdf.)

Andreae, M.O., and Merlet, P., 2001, Emission of trace gases and aerosols from biomass burning: Global Biogeochemical Cycles, v. 15, no. 4, p. 955–966, doi:10.1029/2000GB001382.

Aplet, G.H., Laven, R.D., and Smith F.W., 1988, Patterns of community dynamics in Colorado Engelmann spruce subalpine fir forests: Ecology, v. 69, no. 2, p. 312–319.

Armstrong, R.A., Lee, Cindy, Hedges, J.I., Honjo, Susumu, and Wakeham, S.G., 2002, A new, mechanistic model for organic carbon fluxes in the ocean based on the quantitative association of POC with ballast minerals: Deep Sea Research Part II: Topical Studies in Oceanography, v. 49, no. 1–3, p. 219–236, doi:10.1016/S0967-0645(01)00101-1.

Armstrong, R.A., Peterson, M.L., Lee, Cindy, and Wakeham, S.G., 2009, Settling velocity spectra and the ballast ratio hypothesis: Deep Sea Research Part II: Topical Studies in Oceanography, v. 56, no. 18, p. 1470–1478, doi:10.1016/j.dsr2.2008.11.032.

Asner, G.P., Archer, Steve, Hughes, R.F., Ansley, R.J., and Wessman, C.A., 2003, Net changes in regional woody vegetation cover and carbon storage in Texas Drylands, 1937–1999: Global Change Biology, v. 9, no. 3, p. 316–335, doi:10.1046/j.1365-2486.2003.00594.x.

Aufdenkampe, A.K., Mayorga, Emilio, Raymond, P.A., Melack, J.M., Doney, S.C., Alin, S.R., Aalto, R.E., and Yoo, Kyungsoo, 2011, Riverine coupling of biogeochemical cycles between land, oceans, and atmosphere: Frontiers in Ecology and the Environment, v. 9, no. 1, p. 53–60, doi:10.1890/100014.

Bachelet, Dominique, Neilson, R.P., Hickler, Thomas, Drapek, R.J., Lenihan, J.M., Sykes, M.T., Smith, Benjamin, Sitch, Stephen, and Thonicke, Kirsten, 2003, Simulating past and future dynamics of natural ecosystems in the United States: Global Biogeochemical Cycles, v. 17, no. 2, 1045, 21 p., doi:10.1029/2001GB001508.

Bachelet, Dominique, Neilson, R.P., Lenihan, J.M., and Drapek, R.J., 2001, Climate change effects on vegetation distribution and carbon budget in the United States: Ecosystems, v. 4, no. 3, p. 164–185, doi:10.1007/s10021–001–0002-7.

Bachelet, Dominique, Neilson, R.P., Lenihan, J.M., and Drapek, R.J., 2004, Regional differences in the carbon source-sink potential of natural vegetation in the U.S.A.: Environmental Management, v. 33, supplement 1, p. S23–S43, doi:10.1007/s00267-003-9115-4.

Bailey, R.G., comp., 1995, Description of the ecoregions of the United States: U.S. Department of Agriculture, Forest Service, Miscellaneous Publication Number 1391, 77 p. (Also available at http://www.fs.fed.us/land/ecosysmgmt/.)

Balshi, M.S., McGuire, A.D., Duffy, P., Flannigan, M., Kicklighter, D.W., and Melillo, J., 2009, Vulnerability of carbon storage in North American boreal forests to wildfires during the 21st century: Global Change Biology, v. 15, no. 6, p. 1491–1510, doi:10.1111/j.1365-2486.2009.01877.x.

Balshi, M.S., McGuire, A.D., Duffy, Paul, Flannigan, Mike, Walsh, John, and Melillo, Jerry, 2009, Assessing the response of area burned to changing climate in western boreal North America using a Multivariate Adaptive Regression Splines (MARS) approach: Global Change Biology, v. 15, no. 3, p. 578–600, doi:10.1111/j.1365-2486.2008.01679.x.

Barger, N.N., Archer, S.R., Campbell, J.L., Huang, Choying, Morton, J.A., and Knapp, A.K., 2011, Woody plant proliferation in North American drylands; A synthesis of impacts on ecosystem carbon balance: Journal of Geophysical Research—Biogeosciences, v. 116, 17 p., doi:10.1029/2010JG001506.

Battin, T.J., Kaplan, L.A., Findlay, Stuart, Hopkinson, C.S., Marti, Eugenia, Packman, A.I., Newbold, J.D., and Sabater, Francesc, 2008, Biophysical controls on organic carbon fluxes in fluvial networks: Nature Geoscience, v. 1, p. 95–100, doi:10.1038/ngeo101.

Benke, A.C., and Cushing, C.E., 2005, Rivers of North America: Burlington, Mass., Elsevier Academic Press, 1,144 p.

Bergamaschi, B.A., Tsamakis, Elizabeth, Keil, R.G., Eglinton, T.I., Montlucon, D.B., and Hedges, J.I., 1997, The effect of grain size and surface area on organic matter, lignin and carbohydrate concentration, and molecular compositions in Peru Margin sediments: Geochimica et Cosmochimica Acta, v. 61, no. 6, p. 1247–1260, doi:10.1016/S0016-7037(96)00394-8.

Berger, W.H., 1989, Global maps of ocean productivity, *in* Berger, W.H., Smetacek, V.S., and Wefer, Gerold, eds., Productivity of the ocean; present and past; Report of the Dahlem Workshop on Productivity of the Ocean, Present and Past, Berlin, 1988 April 24–29: New York, N.Y., John Wiley, p. 429–455.

Beuter, J.H., Johnson, K.N., and Scheurman, H.L., 1976, Timber for Oregon's tomorrow; an analysis of reasonably possible occurrences: Oregon State University, School of Forestry, Forest Research Laboratory Research Bulletin 19, 111 p. (Also available at http://ir.library.oregonstate.edu/xmlui/bitstream/handle/1957/9382/Tim_For_Ore_Tom.pdf.)

Billen, Gilles, and Garnier, Josette, 2007, River basin nutrient delivery to the coastal sea; Assessing its potential to sustain new production of non-siliceous algae: Marine Chemistry, v. 106, no. 1–2, p. 148–160, doi:10.1016/j.marchem.2006.12.017.

Birdsey, R.A., Plantinga, A.J., and Heath, L.S., 1993, Past and prospective carbon storage in United States forests: Forest Ecology and Management, v. 58, no. 1–2, p. 33–40, doi:10.1016/0378-1127(93)90129-B.

Blair, N.E., Leithold, E.L., and Aller, R.C., 2004, From bedrock to burial; the evolution of particulate organic carbon across coupled watershed-continental margin systems: Marine Chemistry, v. 92, no. 1–4, p. 141–156, doi:10.1016/j.marchem.2004.06.023.

Boyer, E.W., Howarth, R.W., Galloway, J.N., Dentener, F.J., Green, P.A., and Vörösmarty, C.J., 2006, Riverine nitrogen export from the continents to the coasts: Global Biogeochemical Cycles, v. 20, 9 p., doi:10.1029/2005GB002537.

Bradley, B.A., Houghton, R.A., Mustard, J.F., and Hamburg, S.P., 2006, Invasive grass reduces aboveground carbon stocks in shrublands of the Western US: Global Change Biology, v. 12, no. 10, p. 1815–1822, doi:10.1111/j.1365-2486.2006.01232.x.

Bradshaw, L.S., Deeming, J.E., Burgan, R.E., and Cohen, J.D., comps., 1983, The 1978 National Fire-Danger Rating System; technical documentation: Ogden, Utah, U.S. Forest Service Intermountain Forest and Range Experiment Station, General Technical Report GTR INT–169, 44 p. (Also available at http://www.treesearch.fs.fed.us/pubs/29615.)

Brevik, E.C., and Homburg, J.A., 2004, A 5000 year record of carbon sequestration from a coastal lagoon and wetland complex, Southern California, USA: CATENA, v. 57, no. 3, p. 221–232, doi:10.1016/j.catena.2003.12.001.

Bridgham, S.D., Megonigal, J.P., Keller, J.K., Bliss, N.B., and Trettin, C., 2006, The carbon balance of North American wetlands: Wetlands, v. 26, p. 889–916.

Brooks, M.L., and Chambers, J.C., 2011, Resistance to invasion and resilience to fire in desert shrublands of North America: Rangeland Ecology & Management, v. 64, no. 5, p. 431–438, doi:10.2111/REM-D-09-00165.1.

Brooks, M.L., D'Antonio, C.M., Richardson, D.M., Grace, J.B., Keeley, J.E., DiTomaso, J.M., Hobbs, R.J., Pellant, Mike, and Pyke, David, 2004, Effects of invasive alien plants on fire regimes: Bioscience, v. 54, no. 7, p. 677–688, doi:10.1641/0006-3568(2004)054[0677:EOIAPO]2.0.CO;2.

Brown, Sandra, Pearson, Timothy, Dushku, Aaron, Kadyzewski, John, and Qi, Ye, 2004, Baseline greenhouse gas emissions for forest, range, and agricultural lands in California: California Energy Commission, Public Interest Energy Research Final Project Report 500–04–069F, 80 p., accessed July 11, 2012, at http://www.energy.ca.gov/pier/project_reports/500-04-069.html. [Prepared by Winrock International, Ecosystem Services Unit, Arlington, Va., under contract 100–98–001.]

Brown, T.J., Hall, B.L., Mohrle, C.R., and Reinbold, H.J., 2002, Coarse assessment of Federal wildland fire occurrence data; Report for the National Wildfire Coordinating Group: Desert Research Institute Program for Climate, Ecosystem and Fire Applications (CEFA) Report 02–04, 31 p. (Also available at http://cefa.dri.edu/Publications/fireoccurrencereport.pdf.)

Brown, T.J., Hall, B.L., and Westerling, A.L., 2004, The impact of twenty-first century climate change on wildland fire danger in the western United States; An applications perspective: Climatic Change, v. 62, no. 1–3, p. 365–388, doi:10.1023/B:CLIM.0000013680.07783.de.

Burdige, D.J., 2005, Burial of terrestrial organic matter in marine sediments; A re-assessment: Global Biogeochemical Cycles, v. 19, 7 p., doi:10.1029/2004GB002368.

Burgan, R.E., 1988, 1988 revisions to the 1978 National Fire-Danger Rating System: U.S. Forest Service, Southeastern Forest Experiment Station, Research Paper SE–273, 39 p. (Also available at http://www.treesearch.fs.fed.us/pubs/593.)

Butman, David, and Raymond, P.A., 2011, Significant efflux of carbon dioxide from streams and rivers in the United States: Nature Geoscience, v. 4, p. 839–842, doi:10.1038/ngeo1294.

California Department of Forestry and Fire Protection, 2010, California's forests and rangelands; 2010 Assessment: Sacramento, Calif., California Department of Forestry and Fire Protection Web site accessed August 4, 2012, at http://frap.fire.ca.gov/assessment2010.html.

California Environmental Protection Agency, Air Resources Board, 2009, Forest and rangelands methods, *excerpted as a separate document from* California's 1990–2004 greenhouse gas emissions inventory and 1990 emissions level: Sacramento, Calif., California Environmental Protection Agency, Air Resources Board, 21 p. (Available at http://www.arb.ca.gov/cc/inventory/doc/methods_v1/tsd_excerpt_forests.pdf.)

Calkin, D.E., Thompson, M.P., Finney, M.A., and Hyde, K.D., 2011, A real-time risk assessment tool supporting wildland fire decisionmaking: Journal of Forestry, v. 109, no. 5, p. 274–280.

Campbell, John, Donato, Dan, Azuma, David, and Law, Beverly, 2007, Pyrogenic carbon emission from a large wildfire in Oregon, United States: Journal of Geophysical Research, v. 112, 11 p., doi:10.1029/2007JG000451.

Canadian Forest Service, 2012, Climate change scenario data: Canadian Forest Service database accessed May 31, 2012, at http://cfs.nrcan.gc.ca/projects/3/5.

Cardille, J.A., Ventura, S.J., and Turner, M.G., 2001, Environmental and social factors influencing wildfires in the Upper Midwest, United States: Ecological Applications, v. 11, no. 1, p. 111–127.

Cary, G.J., Flannigan, M.D., Keane, R.E., Bradstock, R.A., Davies, I.D., Lenihan, J.M., Li, Chao, Logan, K.A., and Parsons, R.A., 2009, Relative importance of fuel management, ignition management and weather for area burned; Evidence from five landscape-fire-succession models: International Journal of Wildland Fire, v. 18, no. 2, p. 147–156.

Chapin, F.S., Woodwell, G.M., Randerson, J.T., Rastetter, E.B., Lovett, G.M., Baldocchi, D.D., Clark, D.A., Harmon, M.E., Schimel, D.S., Valentini, R., Wirth, C., Aber, J.D., Cole, J.J., Goulden, M.L., Harden, J.W., Heimann, M., Howarth, R.W., Matson, P.A., McGuire, A.D., Melillo, J.M., Mooney, H.A., Neff, J.C., Houghton, R.A., Pace, M.L., Ryan, M.G., Running, S.W., Sala, O.E., Schlesinger, W.H., and Schulze, E.-D., 2006, Reconciling carbon-cycle concepts, terminology, and methods: Ecosystems, v. 9, p. 1041–1050, doi:10.1007/s10021-005-0105-7.

Chmura, G.L., Anisfeld, S.C., Cahoon, D.R., and Lynch, J.C., 2003, Global carbon sequestration in tidal, saline wetland soils: Global Biogeochemical Cycles, v. 17, no. 4, 12 p. (Available at http://www.agu.org/pubs/crossref/2003/2002GB001917.shtml.)

Claggett, P.R., Jantz, C.A., Goetz, S.J., and Bisland, Carin, 2004, Assessing development pressure in the Chesapeake Bay watershed; An evaluation of two land-use change models: Environmental Monitoring and Assessment, v. 94, p. 129–146.

Cleary, M.B., Pendall, Elise, and Ewers, B.E., 2010, Aboveground and belowground carbon pools after fire in mountain big sagebrush steppe: Rangeland Ecology & Management, v. 63, no. 2, p. 187–196.

Cleland, D.T., Crow, T.R., Saunders, S.C., Dickmann, D.I., Maclean, A.L., Jordan, J.K., Watson, R.L., Sloan, A.M., and Brosofske, K.D., 2004, Characterizing historical and modern fire regimes in Michigan (USA); A landscape ecosystem approach: Landscape Ecology, v. 19, no. 3, p. 311–325.

Cohen, W.B., Harmon, M.E., Wallin, D.O., and Fiorella, Maria, 1996, Two decades of carbon flux from forests of the Pacific Northwest: BioScience, v. 46, no. 11, p. 836–844. (Also available at http://www.jstor.org/stable/1312969.)

Cohn, T.A., Caulder, D.L., Gilroy, E.J., Zynjuk, L.D., and Summers, R.M., 1992, The validity of a simple statistical model for estimating fluvial constituent loads; An empirical study involving nutrient loads entering Chesapeake Bay: Water Resources Research, v. 28, no. 9, p. 2353–2363.

Cole, J.J., and Caraco, N.F., 1998, Atmospheric exchange of carbon dioxide in a low-wind oligotrophic lake measured by the addition of SF_6: Limnology and Oceanography, v. 43, no. 4, p. 647–656.

Cole, J.J., and Caraco, N.F., Kling, G.W., and Kratz, T.K., 1994, Carbon dioxide supersaturation in the surface waters of lakes: Science, v. 265, p. 1568–1570.

Cole, J.J., Prairie, Y.T., Caraco, N.F., McDowell, W.H., Tranvik, L.J., Striegl, R.G., Duarte, C.M., Kortelainen, P., Downing, J.A., Middelburg, J.J., and Melack, J., 2007, Plumbing the global carbon cycle; Integrating inland waters into the terrestrial carbon budget: Ecosystems, v. 10, no. 1, p. 172–185, doi:10.1007/s10021-006-9013-8.

Collins, B.M., Stephens, S.L., Roller, G.B., and Battles, J.J., 2011, Simulating fire and forest dynamics for a landscape fuel treatment project in the Sierra Nevada: Forest Science, v. 57, no. 2, p. 77–88.

Commission for Environmental Cooperation, 2006, Ecological regions of North America; Level I–II: Montreal, Quebec, Canada, Commission for Environmental Cooperation, scale 1:10,000,000. (Also available online at http://www.epa.gov/wed/pages/ecoregions/na_eco.htm.)

Conservation Technology Information Center, 2012, Crop residue management (CRM) survey data: Conservation Technology Information Center dataset, accessed May 31, 2012, at http://www.ctic.purdue.edu/CRM/crm_search.

Cooper, C.F., 1960, Changes in vegetation, structure, and growth of southwestern pine forests since white settlement: Ecological Monographs, v. 30, no. 2, p. 129–164.

Cotrim Da Cunha, Leticia, Buitenhuis, E.T., Le Quéré, Corrine, Giraud, Xavier, and Ludwig, Wolfgang, 2007, Potential impact of changes in river nutrient supply on global ocean biogeochemistry: Global Biogeochemical Cycles, v. 21, 15 p., doi:10.1029/2006GB002718.

Crumpacker, D.W., 1984, Regional riparian research and a multi-university approach to the special problem of livestock grazing in the Rocky Mountains and Great Plains, *in* Warner, R.E., and Hendrix, K.M., eds., California riparian systems—ecology, conservation, and productive management: Berkeley, Calif., University of California Press, p. 413–422.

Crutzen, P.J., and Andreae, M.O., 1990, Biomass burning in the tropics; Impact on atmospheric chemistry and biogeochemical cycles: Science, v. 250, no. 4988, p. 1669–1678.

Daly, Christopher, Neilson, R.P., and Phillips, D.L., 1993, A statistical-topographic model for mapping climatological precipitation over mountainous terrain: Journal of Applied Meteorology, v. 33, p. 140–58. (Also available at http://www.prism.oregonstate.edu/pub/prism/docs/jappclim94-modeling_mountain_precip-daly.pdf.)

Daly, C., Taylor, G.H., Gibson, W.P., Parzybok, T.W., Johnson, G.L., and Pasteris, P.A., 2000, High-quality spatial climate data sets for the United States and beyond: Transactions of the American Society of Agricultural and Biological Engineers, v. 43, no. 6, p. 1957–1962.

Daniels, J.M., 2005, The rise and fall of the Pacific Northwest log export market: U.S. Department of Agriculture, Forest Service, Pacific Northwest Research Station, General Technical Report PNW–GTR–624, 88 p. (Also available at http://www.fs.fed.us/pnw/pubs/pnw_gtr624.pdf.)

D'Antonio, C.M., and Vitousek, P.M., 1992, Biological invasions by exotic grasses, the grass/fire cycle, and global change: Annual Review of Ecology and Systematics, v. 23, no. 1, p. 63–87.

Dean, W.E., and, Gorham, E., 1998, Magnitude and significance of carbon burial in lakes, reservoirs, and peatlands: Geology, v. 26, p. 535–538.

Deeming, J.E., Burgan, R.E., and Cohen, J.D., 1977, The national fire-danger rating system—1978: U.S. Department of Agriculture, Forest Service, Intermountain Forest and Range Experiment Station, General Technical Report INT–39, 66 p.

Delworth, T.L., Broccoli, A.J., Rosati, Anthony, Stouffer, R.J., Balaji, V., Beesley, J.A., Cooke, W.F., Dixon, K.W., Dunne, John, Dunne, K.A., Durachta, J.W., Findell, K.L., Ginoux, Paul, Gnanadesikan, Anand, Gordon, C.T., Griffies, S.M., Gudgel, Rich, Harrison, M.J., Held, I.M., Hemler, R.S., Horowitz, L.W., Klein, S.A., Knutson, T.R., Kushner, P.J., Langenhorst, A.R., Lee, Hyun-Chul, Lin, Shian-Jiann, Lu, Jian, Malyshev, S.L., Milly, P.C.D., Ramaswamy, V., Russell, Joellen, Schwarzkopf, M.D., Shevliakova, Elena, Sirutis, J.J., Spelman, M.J., Stern, W.F., Winton, Michael, Wittenberg, A.T., Wyman, Bruce, Zeng, Fanrong, and Zhang, Rong, 2006, GFDL's CM2 Global Coupled Climate Models; Part I—Formulation and simulation characteristics: Journal of Climate, v. 19, no. 5, 643–674, doi:10.1175/JCLI3629.1.

Derner, J.D., and Schuman, G.E., 2007, Carbon sequestration and rangelands; A synthesis of land management and precipitation effects: Journal of Soil and Water Conservation, v. 62, no. 2, p. 77–85.

Donnegan, Joseph, Campbell, Sally, and Azuma, Dave, eds., 2008, Oregon's forest resources, 2001–2005; five-year Forest Inventory and Analysis report: U.S. Forest Service, Pacific Northwest Research Station General Technical Report PNW–GTR–765. 186 p. (Also available at http://www.fs.fed.us/pnw/publications/gtr765/.)

Downing, J.A., Duarte, C.M., and Gene, E.L., 2009, Abundance and size distribution of lakes, ponds and impoundments, *in* Likens, G.F., Encyclopedia of inland waters: Oxford, Academic Press, p. 469–478.

Duan, Q.Y., Sorooshian, S., and Gupta, V., 1992, Effective and efficient global optimization for conceptual rainfall-runoff models: Water Resources Research, v. 28, no. 4, p. 1015–1031.

Dunne, J.P., Sarmiento, J.L., and Gnanadesikan, Anand, 2007, A synthesis of global particle export from the surface ocean and cycling through the ocean interior and on the seafloor: Global Biogeochemical Cycles, v. 21, no. 4, 16 p., doi:10.1029/2006GB002907.

Efron, Bradley, and Tibshirani, R.J., 1993, An introduction to the bootstrap: New York, Chapman & Hall, 456 p.

Eidenshink, Jeff, Schwind, Brian, Brewer, Ken, Zhu, Zhi-Liang, Quayle, Brad, and Howard, Stephen, 2007, A project for monitoring trends in burn severity: Fire Ecology, v. 3, no. 1, p. 3–21, doi:10.4996/fireecology.0301003.

Einola, E., Rantakari, M., Kankaala, P., Kortelainen, P., Ojala, A., Pajunen, H., Makela, S., and Arvola, L., 2011, Carbon pools and fluxes in a chain of five boreal lakes; A dry and wet year comparison: Journal of Geophysical Research—Biogeosciences, v. 116, 13 p.

Falk, D.A., Miller, Carol, McKenzie, Donald, and Black, A.E., 2007, Cross-scale analysis of fire regimes: Ecosystems, v. 10, p. 810–823.

Fellin, D.G., and Dewey, J.E., 1992, Western spruce budworm: U.S. Department of Agriculture, Forest Service, Forest Insect & Disease Leaflet 53, 10 p. (Also available at http://www.na.fs.fed.us/spfo/pubs/fidls/westbw/fidl-wbw.htm.)

Finney, M.A., 2001, Design of regular landscape fuel treatment patterns for modifying fire growth and behavior: Forest Science, v. 47, no. 2, p. 219–228.

Finney, M.A., 2002, Fire growth using minimum travel time methods: Canadian Journal of Forest Research, v. 32, no. 8, p. 1420–1424, doi:10.1139/x02-068.

Finney, M.A., 2007, A computational method for optimising fuel treatment locations: International Journal of Wildland Fire, v. 16, no. 6, p. 702–711.

Finney, M.A., McHugh, C.W., Grenfell, I.C., Riley, K.L., and Short, K.C., 2011, A simulation of probabilistic wildfire risk components for the continental United States: Stochastic Environmental Research and Risk Assessment, v. 25, no. 7, p. 973–1000.

Finney, M.A., Seli, R.C., McHugh, C.W., Ager, A.A., Bahro, Bernhard, and Agee, J.K., 2007, Simulation of long-term landscape-level fuel treatment effects on large wildfires: International Journal of Wildland Fire, v. 16, no. 6, p. 712–727.

Flannigan, M.D., Krawchuk, M.A., de Groot, W.J., Wotton, B.M., and Gowman, L.M., 2009, Implications of changing climate for global wildland fire: International Journal of Wildland Fire, v. 18, no. 5, p. 483–507.

Flannigan, M.D., Logan, K.A., Amiro, B.D., Skinner, W.R., and Stocks, B.J., 2005, Future area burned in Canada: Climatic Change, v. 72, no. 1–2, p. 1–16.

Flannigan, M.D., Stocks, B.J., and Wotton, B.M., 2000, Climate change and forest fires: Science of the Total Environment, v. 262, no. 3, p. 221–229.

Flato, G.M., and Boer, G.J., 2001, Warming asymmetry in climate change simulations: Geophysical Research Letters, v. 28, no. 1, p. 195–198. (Also available at http://www.agu.org/journals/gl/v028/i001/2000GL012121/.)

Flato, G.M., Boer, G.J., Lee, W.G., McFarlane, N.A., Ramsden, D., Reader, M.C., and Weaver, A.J., 2000, The Canadian Centre for Climate Modelling and Analysis Global Coupled Model and its climate: Climate Dynamics, v. 16, no. 6, p. 451–467, doi:10.1007/s003820050339.

Fleischner, T.L., 1994, Ecological costs of livestock grazing in western North America: Conservation Biology, v. 8, no. 3, p. 629–644, doi:10.1046/j.1523-1739.1994.08030629.x.

Follett, R.F., 2001, Soil management concepts and carbon sequestration in cropland soils: Soil and Tillage Research, v. 61, no. 1, p. 77–92.

Follett, R.F., 2010, Symposium—Soil carbon sequestration and greenhouse gas mitigation: Soil Science Society of America Journal, v. 74, p. 345–346, doi:10.2136/sssaj2009.cseqghgsymp.intro.

Fowler, H.J., Blenkinsop, S., and Tebaldi, C., 2007, Linking climate change modeling to impacts studies; Recent advances in downscaling techniques for hydrological modelling: International Journal of Climatology, v. 27, no. 12, p. 1547–1578.

French, N.H.F., de Groot, W.J., Jenkins, L.K., Rogers, B.M., Alvarado, Ernesto, Amiro, Brian, de Jong, Bernardus, Goetz, Scott, Hoy, Elizabeth, Hyer, Edward, Keane, Robert, Law, B.E., McKenzie, Donald, McNulty, S.G., Ottmar, Roger, Perez-Salicrup, D.R., Randerson, James, Robertson, K.M., and Turetsky, Merritt, 2011, Model comparisons for estimating carbon emissions from North American wildland fire: Journal of Geophysical Research—Biogeosciences, v. 116, 21 p., doi:10.1029/2010JG001469.

Fule, P.Z., 2008, Does it make sense to restore wildland fire in changing climate?: Restoration Ecology, v. 16, no. 4, p. 526–531.

Fung, I.Y., Doney, S.C., Lindsay, Keith, and John, Jasmin, 2005, Evolution of carbon sinks in a changing climate: Proceedings of the National Academy of Sciences of the United States of America, v. 102, no. 32, p. 11,201–11,206, doi:10.1073/pnas.0504949102.

Gedalof, Z., Peterson, D.L., and Mantua, N.J., 2005, Atmospheric, climatic, and ecological controls on extreme wildfire years in the northwestern United States: Ecological Applications, v. 15, no. 1, p. 154–174.

Giglio, Louis, Descloitres, Jacques, Justice, C.O., and Kaufman, Y.J., 2003, An enhanced contextual fire detection algorithm for MODIS: Remote Sensing of Environment, v. 87, no. 2–3, p. 273–282, doi:10.1016/S0034-4257(03)00184-6.

Giglio, L., Randerson, J.T., van der Werf, G.R., Kasibhatla, P.S., Collatz, G.J., Morton, D.C., and DeFries, R.S., 2010, Assessing variability and long-term trends in burned area by merging multiple satellite fire products: Biogeosciences, v. 7, no. 3, p. 1171–1186.

Glassy, J.M., and Running, S.W., 1994, Validating diurnal climatology logic of the MT–CLIM model across a climatic gradient in Oregon: Ecological Applications, v. 4, no. 2, p. 248–257.

Gleason, R.A., Tangen, B.A., Browne, B.A., and Euliss, N.H., Jr., 2009, Greenhouse gas flux from cropland and restored wetlands in the Prairie Pothole Region: Soil Biology and Biochemistry, v. 41, no. 12, p. 2501–2507, doi:10.1016/j.soilbio.2009.09.008.

Glibert, P.M., 2010, Long-term changes in nutrient loading and stoichiometry and their relationships with changes in the food web and dominant pelagic fish species in the San Francisco Estuary, California: Reviews in Fisheries Science, v. 18, p. 211–232.

Goetz, S.J., Bond-Lamberty, B., Law, B.E., Hicke, J.A., Huang, C., Houghton, R.A., McNulty, S., O'Halloran, T., Harmon, M., Meddens, A.J.H., Pfeifer, E.M., Mildrexler, D., and Kasischke, E.S., 2012, Observations and assessment of forest carbon dynamics following disturbance in North America: Journal of Geophysical Research—Biogeosciences, v. 117, doi:10.1029/2011JG001733.

Goines, B., and Nechodom, M., 2009, National forest carbon inventory scenarios for the Pacific Southwest Region (California), Region 5 Climate Change Interdisciplinary Team: Albany, Calif., U.S. Department of Agriculture, Forest Service, Region 5 Climate Change Interdisciplinary Team report, 85 p.

Gonzalez, Patrick, Neilson, R.P., Lenihan, J.M., and Drapek, R.J., 2010, Global patterns in the vulnerability of ecosystems to vegetation shifts due to climate change: Global Ecology and Biogeography, v. 19, no. 6, p. 755–768.

Goolsby, D.A., Battaglin, W.A., Lawrence, G.B., Artz, R.S., Aulenbach, B.T., Hooper, R.P., Keeney, D.R., and Stensland, G.J., 1999, Flux and sources of nutrients in the Mississippi-Atchafalaya River Basin; Topic 3 report for the integrated assessment on hypoxia in the Gulf of Mexico: Washington, D.C., National Oceanic and Atmospheric Administration, National Ocean Service, Coastal Ocean Program, Decision Analysis Series No. 17, 150 p.

Gordon, C., Cooper, C., Senior, C.A., Banks, H.T., Gregory, J.M., Johns, T.C., Mitchell, J.F.B., and Wood, R.A., 2000, The simulation of SST, sea ice extents and ocean heat transports in a version of the Hadley Centre coupled model without flux adjustments: Climate Dynamics, v. 16, no. 2–3, p. 147–168, doi:10.1007/s003820050010.

Goward, S.N., Masek, J.G., Cohen, Warren, Moisen, Gretchen, Collatz, G.J., Healey, Sean, Houghton, R.A., Huang, Chengquan, Kennedy, Robert, Law, Beverly, Powell, Scott, Turner, David, and Wulder, M.A., 2008, Forest disturbance and North American carbon flux: Eos, Transactions American Geophysical Union, v. 89, no. 11, doi:10.1029/2008EO110001.

Gross, M.G., and Nelson, J.L., 1966, Sediment movement on the continental shelf near Washington and Oregon: Science, v. 154, p. 879–885.

Hair, J.F., Black, W.C., Babin, Barry, Anderson, R.E., and Tatham, R.L., 2005, Multivariate data analysis (6th ed.): Upper Saddle River, N.J., Prentice Hall, 928 p.

Hales, Burke, Cai, W.-J., Mitchell, B.G., Sabine, C.L., and Schofield, Oscar, eds., 2008, North American Continental Margins; A Synthesis and Planning Workshop; Report of the North American Continental Margins Working Group for the U.S. Carbon Cycle Scientific Steering Group and Interagency Working Group: Washington, D.C., U.S. Carbon Cycle Science Program, 115 p.

Hales, Burke, Karp-Boss, Lee, Perlin, Alexander, and Wheeler, P.A., 2006, Oxygen production and carbon sequestration in an upwelling coastal margin: Global Biogeochemical Cycles, v. 20, no. 3, 15 p., doi:10.1215/21573689-1572535.

Hanley, J.A., and McNeil, B.J., 1982, The meaning and use of the area under a receiver operating characteristic (ROC) curve: Radiology, v. 143, no. 1, p. 29–36.

Hansen, A.J., Neilson, R.P., Dale, V.H., Flather, C.H., Iverson, L.R., Currie, D.J., Shafer, Sarah, Cook, Rosamonde, and Bartlein, P.J., 2001, Global change in forests; Responses of species, communities, and biomes: Bioscience, v. 51, no. 9, p. 765–779.

Harrill, J.R., and Prudic, D.E., 1998, Aquifer aystems in the Great Basin region of Nevada, Utah, and adjacent states—Summary Report: U.S. Geological Survey Professional Paper 1409–A, 75 p. (Also available at http://pubs.er.usgs.gov/publication/pp1409A#.)

Harrison, J.A., Seitzinger, S.P., Bouwman, A.F., Caraco, N.F., Beusen, A.H.W., and Vörösmarty, C.J., 2005, Dissolved inorganic phosphorus export to the coastal zone; Results from a spatially explicit, global model: Global Biogeochemical Cycles, v. 19, no. 4, 15 p.

Hartmann, J., 2009, Bicarbonate-fluxes and CO_2-consumption by chemical weathering on the Japanese Archipelago—Application of a multi-lithological model framework: Chemical Geology, v. 265, no. 3–4, p. 237–271.

Hastie, Trevor, Tibshirani, Robert, and Friedman, Jerome, 2009, The elements of statistical learning; Data mining, inference, and prediction (2d ed.): New York, N.Y., Springer, 746 p.

Hayes, D.J., Turner, D.P., Stinson, Graham, McGuire, A.D., Wei, Yaxing, West, T.O., Heath, L.S., de Jong, Bernardus, McConkey, B.G., Birdsey, R.A., Kurz, W.A., Jacobson, A.R., Huntzinger, D.N., Pan, Yude, Post, W.M., and Cook, R.B., 2012, Reconciling estimates of the contemporary North American carbon balance among terrestrial biosphere models, atmospheric inversions, and a new approach for estimating net ecosystem exchange from inventory-based data: Global Change Biology, v. 18, no. 4, p. 1281–1289, doi:10.1111/j.1365-2486.2011.02627.x

Heath, L.S., and Birdsey, R.A., 1993, Carbon trends of productive temperate forests of the conterminous United States: Water, Air, & Soil Pollution, v. 70, no. 1–4, p. 279–293, doi:10.1007/BF01105002.

Heath, L.S., Smith, J.E., Woodall, C.W., Azuma, D.L., and Waddell, K.L., 2011, Carbon stocks on forestland of the United States with emphasis on USDA Forest Service ownership: Ecosphere, v. 2, no. 1, 21 p., doi:10.1890/ES10-00126.1.

Hedges, J.I., and Keil, R.G., 1995, Sedimentary organic-matter preservation—An assessment and speculative synthesis: Marine Chemistry, v. 49, p. 81–115.

Hedges, J.I., Keil, R.G., and Benner, R., 1997, What happens to terrestrial organic matter in the ocean?: Organic Geochemistry, v. 27, no. 5, p. 195–212.

Hessl, A.E., 2011, Pathways for climate change effects on fire; Models, data, and uncertainties: Progress in Physical Geography, v. 35, no. 3, p. 393–407.

Hicke, J.A., Jenkins, J.C., Ojima, D.S., and Ducey, Mark, 2007, Spatial patterns of forest characteristics in the western United States derived from inventories: Ecological Applications, v. 17, no. 8, p. 2387–2402, doi:10.1890/06-1951.1.

Homer, Collin, Dewitz, Jon, Fry, Joyce, Coan, Michael, Hossain, Nazmul, Larson, Charles, Herold, Nate, McKerrow, Alexa, Van Driel, J.N., and Wickham, James, 2007, Completion of the 2001 National Land Cover Database for the conterminous United States: Photogrammetric Engineering and Remote Sensing, v. 73, no. 4, p. 337–341. (Also available at http://www.asprs.org/a/publications/pers/2007journal/april/highlight.pdf.)

Horizon Systems Corporation, 2005, NHDPlus, version 2: Herndon, Va., Horizon Systems Corporation Web page accessed October 1, 2012, at http://www.horizon-systems.com/nhdplus/.

Houghton, R.A., Hackler, J.L., and Lawrence, K.T., 1999, The U.S. carbon budget; Contributions from land-use change: Science, v. 285, no. 5427, p. 574–578, doi:10.1126/science.285.5427.574.

Huang, Chengquan, Goward, S.N., Masek, J.G., Thomas, Nancy, Zhu, Zhiliang, and Vogelmann, J.E., 2010, An automated approach for reconstructing recent forest disturbance history using dense Landsat time series stacks: Remote Sensing of Environment, v. 114, no. 1, p. 183–198, doi:10.1016/j.rse.2009.08.17.

Huang, Cho-ying, Asner, G.P., Barger, N.N., Neff, J.C., and Floyd, M.L., 2010, Regional aboveground live carbon losses due to drought-induced tree dieback in piñon-juniper ecosystems: Remote Sensing of Environment, v. 114, no. 7, p. 1471–1479, doi:10.1016/j.rse.2010.02.003.

Hudiburg, Tara, Law, Beverly, Turner, D.P., Campbell, John, Donato, Dan, and Duane, Maureen, 2009, Carbon dynamics of Oregon and northern California forests and potential land-based carbon storage: Ecological Applications, v. 19, p. 163–180, doi:10.1890/07-2006.1.

Hudiburg, T.W., Law, B.E., Wirth, Christian, and Luyssaert, Sebastiaan, 2011, Regional carbon dioxide implications of forest bioenergy production: Nature Climate Change, v. 1, no. 8, p. 419–423.

Hunt, C.W., Salisbury, J.E., and Vandemark, D., 2011, Contribution of non-carbonate anions to total alkalinity and overestimation of pCO_2 in New England and New Brunswick rivers: Biogeosciences, v. 8, p. 3069–3076, doi:10.5194/bg-8-3069-2011.

Huntzinger, D.N., Post, W.M., Wei ,Y., Michalak, A.M., West, T.O., Jacobson, A.R., Baker, I.T., Chen, J.M., Davis, K.J., Hayes, D.J., Hoffman, F.M., Jain, A.K., Liu, S., McGuire, A.D., Neilson, R.P., Potter, Chris, Poulter, B., Price, David, Raczka, B.M., Tian, H.Q., Thornton, P., Tomelleri, E., Viovy, N., Xiaos, J., Yuant, W., Zengu, N., Zhaov, M., and Cook, R., 2012, North American Carbon Project (NACP) regional interim synthesis; terrestrial biospheric model intercomparison: Ecological Modelling, v. 232, p. 144–157, 10.1016/j.ecolmodel.2012.02.004.

Hurteau, M.D., and Brooks, M.L., 2011, Short- and long-term effects of fire on carbon in US dry temperate forest systems: Bioscience, v. 61, no. 2, p. 139–146.

Hurtt, G.C., Pacala, S.W., Moorcroft, P.R., Caspersen, J., Shevliakova, E., Houghton, R.A., and Moore, B., III, 2002, Projecting the future of the U.S. carbon sink: Proceedings of the National Academy of Sciences of the United States of America, v. 99, no. 3, doi:10.1073/pnas.012249999.

Hutchinson, M.F., 2010, ANUSPLIN Version 4.0: Australian National University, Fenner School of Environment & Society. (Available at http://fennerschool.anu.edu.au/publications/software/anusplin.php.)

IMAGE Team, 2001, The IMAGE 2.2 implementation of the SRES scenarios; a comprehensive analysis of emissions, climate change and impacts in the 21st century: Bilthoven, The Netherlands, National Institute of Public Health and the Environment, RIVM CD–ROM Publication 481508018.

Intergovernmental Panel on Climate Change, 2007, Climate change 2007 [Fourth assessment report (AR4) of the IPCC]: Cambridge, United Kingdom, Cambridge University Press, The AR4 synthesis report and 3 v. (The physical science basis, by Working Group I; Impacts, adaptation, and vulnerability, by Working Group II; Mitigation of climate change, by Working Group III), accessed November 14, 2011, at http://www.ipcc.ch/publications_and_data/publications_and_data_reports.htm.

Jackson, R.B., Jobbágy, E.G., Avissar, Roni, Roy, S.B., Barrett, D.J., Cook, C.W., Farley, K.A., le Maitre, D.C., McCarl, B.A., and Murray, B.C., 2005, Trading water for carbon with biological sequestration: Science, v. 310, no. 5756, p. 1944–1947.

Johns, T.C., Carnell, R.E., Crossley, J.F., Gregory, J.M., Mitchell, J.F.B., Senior, C.A., Tett, S.F.B., and Wood, R.A., 1997, The second Hadley Center coupled ocean-atmosphere GCM; Model description, spinup and validation: Climate Dynamics, v. 13, no. 2, p. 103–134, doi:10.1007/s003820050155.

Jolly, W.M., Nemani, Ramakrishna, and Running, S.W., 2005, A generalized, bioclimatic index to predict foliar phenology in response to climate: Global Change Biology, v. 11, no. 4, p. 619–632.

Joyce, L.A., Price, D.T., McKenney, D.W., Siltanen, R.M., Papadopol, Pia, Lawrence, Kevin, and Coulson, D.P., 2011, High resolution interpolation of climate scenarios for the conterminous USA and Alaska derived from general circulation model simulations: Fort Collins, Colo., U.S. Department of Agriculture, Forest Service, Rocky Mountain Research Station General Technical Report RMRS–GTR–263, 87 p.

Kashian, D.M., Romme, W.H., Tinker, D., Turner, M.G., and Ryan, M.G., in press, Post-fire changes in forest carbon storage over a 300-year chronosequence of Pinus contorta-dominated forests: Ecological Monographs (pre-press version accessed November 14, 2012), doi:10.1890/11-1454.1.

Kashian, D.M., Romme, W.H., Tinker, D.B., Turner, M.G., and Ryan, M.G., 2006, Carbon storage on landscapes with stand-replacing fires: BioScience, v. 56, no. 7, p. 598–606, doi:10.1641/0006-3568(2006)56[598:CSOLWS]2.0.CO;2.

Keane, R.E., Cary, G.J., and Parsons, Russell, 2003, Using simulation to map fire regimes; An evaluation of approaches, strategies, and limitations: International Journal of Wildland Fire, v. 12, no. 3–4, p. 309–322.

Keane, R.E., Ryan, K.C., Veblen, T.T., Allen, C.D., Logan, J.A., and Hawkes, Brad, 2002, Cascading effects of fire exclusion in Rocky Mountain ecosystems; A literature review: Fort Collins, Colo., U.S. Department of Agriculture, Forest Service, Rocky Mountain Research Station General Technical Report RMRS–GTR–91, 24 p.

Keeley, J.E., 2006, Fire management impacts on invasive plants in the western United States: Conservation Biology, v. 20, no. 2, p. 375–384.

Keeley, J.E., Fotheringham, C.J., and Morais, M., 1999, Reexamining fire suppression impacts on brushland fire regimes: Science, v. 284, no. 5421, p. 1829–1832.

Kellndorfer, Josef, Walker, Wayne, Pierce, Leland, Dobson, Craig, Fites, Jo Ann, Hunsaker, Carolyn, Vona, John, and Clutter, Michael, 2004, Vegetation height estimation from Shuttle Radar Topography Mission and National Elevation Datasets: Remote Sensing of Environment, v. 93, no. 3, p. 339–358, doi:10.1016/j.rse.2004.07.017.

Kendall, Carol, and McDonnell, J.J., 1998, Isotope tracers in catchment hydrology: Amsterdam, Elsevier, 870 p.

Kessavalou, Anabayan, Mosier, A.R., Doran, J.W., Drijber, R.A., Lyon, D.J., and Heinemeyer, O., 1998, Fluxes of carbon dioxide, nitrous oxide, and methane in grass sod and winter wheat-fallow tillage management: Journal of Environmental Quality, v. 27, no. 5, p. 1094–1104.

Kimball, J.S., Running, S.W., and Nemani, R., 1997, An improved method for estimating surface humidity from daily minimum temperature: Agricultural and Forest Meteorology, v. 85, no. 1–2, p. 87–98, doi:10.1016/S0168-1923(96)02366-0.

Kling, G.W., Kipphut, G.W., and Miller, M.C., 1991, Arctic lakes and streams as gas conduits to the atmosphere—Implications for tundra carbon budgets: Science, v. 251, p. 298–301.

Korontzi, Stefania, McCarty, Jessica, Loboda, Tatiana, Kumar, Suresh, and Justice, Chris, 2006, Global distribution of agricultural fires in croplands from 3 years of Moderate Resolution Imaging Spectroradiometer (MODIS) data: Global Biogeochemical Cycles, v. 20, no. 2, 15 p., doi:10.1029/2005GB002529.

Kroodsma, D.A., and Field, C.B., 2006, Carbon sequestration in California agriculture, 1980–2000: Ecological Applications, v. 16, no. 5, p. 1975–1985, doi:10.1890/1051-0761(2006)016[1975:CSICA]2.0.CO;2.

Kudela, R.M., Cochlan, W.P., Peterson, T.D., and Trick, C.G., 2006, Impacts on phytoplankton biomass and productivity in the Pacific Northwest during the warm ocean conditions of 2005: Geophysical Research Letters, v. 33, 6 p., doi:10.1029/2006GL026772.

Lal, R., 2004, Carbon sequestration in dryland ecosystems: Environmental Management, v. 33, no. 4, p. 528–544.

Lal, R., Kimble, J.M., Follett, R.F., and Cole, C.V., 1998, The potential of U.S. cropland to sequester carbon and mitigate the greenhouse effect: Boca Raton, Fla., CRC Press, 144 p.

Larkin, N.K., O'Neill, S.M., Solomon, Robert, Raffuse, Sean, Strand, Tara, Sullivan, D.C., Krull, Candace, Rorig, Miriam, Peterson, Janice, and Ferguson, S.A., 2009, The BlueSky smoke modeling framework: International Journal of Wildland Fire, v. 18, no. 8, p. 906–920.

Law, B.E., Turner, D., Campbell, J., Sun, O.J., Van Tuyl, S., Ritts, W.D., and Cohen, W.B., 2004, Disturbance and climate effects on carbon stocks and fluxes across Western Oregon USA: Global Change Biology, v. 10, no. 9, p. 1429–1444.

Leavesley, G.H., Lichty, R.W., Troutman, B.M., and Saindon, L.G., 1983, Precipitation-runoff modeling system; user's manual: U.S. Geological Survey Water-Resources Investigations Report 83–4238, 207 p.

Leithold, E.L., Perkey, D.W., Blair, N.E., and Creamer, T.N., 2005, Sedimentation and carbon burial on the northern California continental shelf; the signatures of land-use change: Continental Shelf Research, v. 25, no. 3, p. 349–371.

Lenihan, J.M., Bachelet, Dominique, Neilson, R.P., and Drapek, Raymond, 2008, Simulated response of conterminous United States ecosystems to climate change at different levels of fire suppression, CO_2 emission rate, and growth response to CO_2: Global and Planetary Change, v. 64, no. 1–2, p. 16–25.

Lentz, R.D., and Lehrsch, G.A., 2010, Nutrients in runoff from a furrow-irrigated field after incorporating inorganic fertilizer or manure: Journal of Environmental Quality, v. 39, no. 4, p. 1402–1415, doi:10.2134/jeq2009.0374.

Leopold, L.B., and Maddock, Thomas, Jr., 1953, The hydraulic geometry of stream channels and some physiographic implications: U.S. Geological Survey Professional Paper 252, 57 p. (Also available at http://pubs.usgs.gov/pp/0252/report.pdf.)

Lettenmaier, D.P., Major, D., Poff, L., and Running, S., 2008, Water resources, *in* The effects of climate change on agriculture, land resources, water resources, and biodiversity in the United States; a report by the U.S. Climate Change Science Program and the Subcommittee on Global Change Research: U.S. Climate Change Science Program Synthesis and Assessment Product 4.3, p. 121–150. (Also available at http://www.climatescience.gov/Library/sap/sap4-3/final-report/sap4-3-final-water.pdf.)

Levy, P.E., Cannell, M.G.R., and Friend, A.D., 2004, Modelling the impact of future changes in climate, CO_2 concentration and land use on natural ecosystems and the terrestrial carbon sink: Global Environmental Change, v. 14, no. 1, p. 21–30, doi:10.1016/j.gloenvcha.2003.10.005.

Liebig, M.A., Tanaka, D.L., and Gross, J.R., 2010, Fallow effects on soil carbon and greenhouse gas flux in central North Dakota: Soil Science Society of America Journal, v. 74, no. 2, p. 358–365, doi:10.2136/sssaj2008.0368.

Litschert, S.E., Brown, T.C., and Theobald, D.M., 2012, Historic and future extent of wildfires in the Southern Rockies Ecoregion, USA: Forest Ecology and Management, v. 269, p. 124–133.

Littell, J.S., McKenzie, Donald, Peterson, D.L., and Westerling, A.L., 2009, Climate and wildfire area burned in western U.S. ecoprovinces, 1916–2003: Ecological Applications, v. 19, no. 4, p. 1003–1021.

Littell, J.S., Oneil, E.E., McKenzie, Donald, Hicke, J.A., Lutz, J.A., Norheim, R.A., and Elsner, M.M., 2010, Forest ecosystems, disturbance, and climatic change in Washington State, USA: Climatic Change, v. 102, no. 1–2, p. 129–158, doi:10.1007/s10584-010-9858-x.

Liu, Jinxun, Vogelmann, J.E., Zhu, Zhiliang, Key, C.H., Sleeter, B.M., Price, D.T., Chen, J.M., Cochrane, M.A., Eidenshink, J.C., Howard, S.M., Bliss, N.B., Jiang, Hong, 2011, Estimating California ecosystem carbon change using process model and land cover disturbance data: 1951–2000: Ecological Modelling, v. 222, p. 2333–2341.

Liu, Shuguang, 2009, Quantifying the spatial details of carbon sequestration potential and performance, *in* McPherson, B.J., and Sundquist, E.T., eds., Carbon sequestration and its role in the global carbon cycle: American Geophysical Union Monograph 183, p. 117–128, doi:10.1029/2006GM000524.

Liu, Shuguang, Bliss, Norman, Sundquist, Eric, and Huntington, T.G., 2003, Modeling carbon dynamics in vegetation and soil under the impact of soil erosion and deposition: Global Biogeochemical Cycles, v. 17, no. 2, p. 1074, doi:10.1029/2002GB002010.

Liu, Shuguang, Bond-Lamberty, Ben, Hicke, J.A., Vargas, Rodrigo, Zhao, Shuqing, Chen, Jing, Edburg, S.L., Hu, Yueming, Liu, Jinxun, McGuire, A.D., Xiao, Jingfeng, Keane, Robert, Yuan, Wenping, Tang, Jianwu, Luo, Yiqi, Potter, Christopher, and Oeding, Jennifer, 2011, Simulating the impacts of disturbances on forest carbon cycling in North America; processes, data, models, and challenges: Journal of Geophysical Research, v. 116, G00K08, 22 p., doi:10.1029/2010JG001585.

Liu, S., Kaire, M., Wood, E., Diallo, O., and Tieszen, L.L., 2004, Impacts of land use and climate change on carbon dynamics in south-central Senegal: Journal of Arid Environments, v. 59, p. 583.

Liu, Shuguang, Liu, Jinxun, and Loveland, T.R., 2004, Spatial-temporal carbon sequestration under land use and land cover change, *in* Proceedings of the 12th International Conference on Geoinformatics—Geospatial Information Research; Bridging the Pacific and Atlantic: University of Gävle, Sweden, June 7–9, 2004: Gavle, Sweden, Gävle University Press, p. 525–532. (Also available at http://fromto.hig.se/~bjg/geoinformatics/files/p525.pdf).

Liu, Shuguang, Loveland, T.R., and Kurtz, R.M., 2004, Contemporary carbon dynamics in terrestrial ecosystems in the southeastern plains of the United States: Environmental Management, v. 33, supplement 1, p. S442–S456, doi:10.1007/s00267-003-9152-z.

Liu, Shuguang, Tan, Zhengxi, Chen, Mingshi, Liu, Jinxun, Wein, Anne, Li, Zhengpeng, Huang, Shengli, Oeding, Jennifer, Young, Claudia, Verma, S.B., Suyker, A.E., Faulkner, Stephen, and McCarty, G.W., 2012, The General Ensemble Biochemical Modeling System (GEMS) and its applications to agricultural systems in the United States, *in* Liebig, M.A., Franzluebbers, A.J., and Follett, R.F., eds., Managing agricultural greenhouse gases—Coordinated agricultural research through GRACEnet to address our changing climate: London, United Kingdom, Academic Press, p. 309–323.

Liu, Y., 2004, Variability of wildland fire emissions across the contiguous United States: Atmospheric Environment, v. 38, no. 21, p. 3489–3499.

Liu, Yongqiang, Stanturf, John, and Goodrick, Scott, 2010, Trends in global wildfire potential in a changing climate: Forest Ecology and Management, v. 259, no. 4, p. 685–697.

Loveland, T.R., Sohl, T.L., Stehman, S.V., Gallant, A.L., Sayler, K.L., and Napton, D.E., 2002, A strategy for estimating the rates of recent United States land-cover changes: Photogrammetric Engineering and Remote Sensing, v. 68, p. 1091–1099.

Lozovik, P.A., 2005, Contribution of organic acid anions to the alkalinity of natural humic water: Journal of Analytical Chemistry, v. 60, no. 11, p. 1000–1004.

Lutes, D.C., Keane, R.E., and Caratti, J.F., 2009, A surface fuel classification for estimating fire effects: International Journal of Wildland Fire, v. 18, no. 7, p. 802–814.

MacDonald, James, Ribaudo, Marc, Livingston, Michael, Beckman, Jayson, and Huang, Wen-yuan, 2009, Manure use for fertilizer and for energy; Report to Congress: USDA Economic Research Service Administrative Publication AP–037, 53 p. (Also available at http://www.ers.usda.gov/publications/ap-administrative-publication/ap-037.aspx.)

Man, Gary, comp., 2010, Major forest insect and disease conditions in the United States—2009 update: U.S. Department of Agriculture, Forest Service, General Technical Report FS–952, 28 p. (Also available at http://www.fs.fed.us/foresthealth/publications/ConditionsReport_2009.pdf.)

Maurer, E.P., Brekke, L., Pruitt, T., and Duffy, P.B., 2007, Fine-resolution climate projections enhance regional climate change impact studies: Eos, v. 88, no. 47, p. 504.

Maurer, E.P., Wood, A.W., Adam, J.C., Lettenmaier, D.P., and Nijssen, B., 2002, A long-term hydrologically based dataset of land surface fluxes and states for the conterminous United States: Journal of Climate, v. 15, no. 22, p. 3237–3251, doi:10.1175/1520-0442(2002)015<3237:ALTHBD>2.0.CO;2.

Mayorga, Emilio, Seitzinger, S.P., Harrison, J.A., Dumont, Egon, Beusen, A.H.W., Bouwman, A.F., Fekete, B.M., Kroeze, Carolien, and Van Drecht, Gerard, 2010, Global nutrient export from WaterSheds 2 (NEWS 2); Model development and implementation: Environmental Modelling & Software, v. 25, p. 837–853, doi:10.1016/j.envsoft.2010.01.007.

McAvaney, B.J., Covey, C., Joussaume, S., Kattsov, V., Kitoh, A., Ogana, W., Pitman, A.J., Weaver, A.J., Wood, R.A., and Zhao, Z.-C., 2001, Model evaluation, chap. 8 *in* Houghton, J.T., Ding, Y., Griggs, D.J., Noguer, M., van der Linden, P.J., Dai, X., Maskell, K., and Johnson, C.A., eds., Climate Change 2001—The scientific basis, Contribution of Working Group I to the Third Assessment Report of the Intergovernmental Panel on Climate Change: Cambridge, U.K., Cambridge University Press, 881 p. (Also available at http://www.grida.no/publications/other/ipcc%5Ftar/?src=/climate/ipcc_tar/wg1/index.htm.)

McCauley, S., and Goetz, S.J., 2004, Mapping residential density patterns using multi-temporal Landsat data and a decision-tree classifier: International Journal of Remote Sensing, v. 25, no. 6, p. 1077–1094.

McDonald, C.P., Rover, J.A., Stets, E.G., and Striegl, R.G., 2012, The regional abundance and size distribution of lakes and reservoirs in the United States and implications for estimates of global lake extent: Limnology and Oceanography, v. 57, no. 2, p. 597–606.

McKenzie, D., Gedalof, Z., Peterson, D.L., and Mote, P., 2004, Climatic change, wildfire, and conservation: Conservation Biology, v. 18, no. 4, p. 890.

McKinley, D.C., Ryan, M.G., Birdsey, R.A., Giardina, C.P., Harmon, M.E., Heath, L.S., Houghton, R.A., Jackson, R.B., Morrison, J.F., Murray, B.C., Pataki, D.E., and Skog, K.E., 2011, A synthesis of current knowledge on forests and carbon storage in the United States: Ecological Applications, v. 21, no. 6, p. 1902–1924.

Meigs, G.W., Donato, D.C., Campbell, J.L., Martin, J.G., and Law, B.E., 2009, Forest fire impacts on carbon uptake, storage, and emission; The role of burn severity in the Eastern Cascades, Oregon: Ecosystems, v. 12, 22 p., doi:10.1007/s10021-009-9285-x.

Melack, J.M., Dozier, Jeff, Goldman, C.R., Greenland, David, Milner, A.M., and Caiman, R.J., 1997, Effects of climate change on inland water of the Pacific Coastal Mountains and Western Great Basin of North America: Hydrological Processes, v. 11, no. 8, p. 971–992, doi:10.1002/(SICI)1099-1085(19970630)11:8%3C971::AID-HYP514%3E3.0.CO;2-Y.

Melching, C.S., and Flores, H.E., 1999, Reaeration equations derived from U.S. Geological Survey database: Journal of Environmental Engineering, v. 125, no. 5, p. 407–414.

Mendelsohn, Robert, and Dinar, Ariel, 2009, Land use and climate change interactions: Annual Review of Resource Economics, v. 1, p. 309–332.

Mensing, Scott, Livingston, Stephanie, and Barker, Pat, 2006, Long-term fire history in Great Basin sagebrush reconstructed from macroscopic charcoal in spring sediments, Newark Valley, Nevada: Western North American Naturalist, v. 66, no. 1, p. 64–77, doi:10.3398/1527-0904(2006)66[64:LFHIGB]2.0.CO;2.

Mesinger, Fedor, DiMego, Geoff, Kalnay, Eugenia, Mitchell, Kenneth, Shafran, P.C., Ebisuzaki, Wesley, Jović, Dušan, Woollen, Jack, Rogers, Eric, Berbery, E.H., Ek, M.B., Fan, Yun, Grumbine, Robert, Higgins, Wayne, Li, Hong, Lin, Ying, Manikin, Geoff, Parrish, David, and Shi, Wei, 2006, North American regional reanalysis: Bulletin of the American Meteorological Society, v. 87, no. 3, p. 343–360, doi:10.1175/BAMS-87-3-343.

Metherell, A.K., Harding, L.A., Cole, C.V., and Parton, W.J., 1993, CENTURY soil organic matter model environment, technical documentation, Agroecosystem Version 4.0: U.S. Department of Agriculture, Agricultural Research Service, Great Plains System Research Unit Technical Report 4, available at http://www.nrel.colostate.edu/projects/century/MANUAL/html_manual/man96.html. (Accessed October 23, 2012.)

Meybeck, Michel, 1982, Carbon, nitrogen, and phosphorous transport by world rivers: American Journal of Science, v. 282, p. 401–450.

Michigan Tech Research Institute, 2012, Wildland Fire Emissions Information System: Michigan Tech Research Institute database, accessed August 3, 2012, at http://wfeis.mtri.org/.

Michmerhuizen, C.M., Striegl, R.G., and McDonald, M.E., 1996, Potential methane emission from north-temperate lakes following ice melt: Limnology and Oceanography, v. 41, no. 5, p. 985–991.

Miller, J.B., 2008, Carbon cycle; Sources, sinks and seasons: Nature, v. 451, p. 26–27, doi:10.1038/451026a.

Millero, F.J., 1979, Thermodynamics of the carbonate system in seawater: Geochimica et Cosmochimica Acta, v. 43, p. 1651–1661, doi:10.1016/0016-7037(79)90184-4.

Milliman, J.D., and Syvitski, J.P.M., 1992, Geomorphic tectonic control of sediment discharge to the ocean—The importance of small mountainous rivers: Journal of Geology, v. 100, p. 525–544.

Mitchell, S.R., Harmon, M.E., and O'Connell, K.E.B., 2009, Forest fuel reduction alters fire severity and long-term carbon storage in three Pacific Northwest ecosystems: Ecological Applications, v. 19, no. 3, p. 643–655.

Mixon, D.M., Kinner, D.A., Stallard, R.F., and Syvitski, J.P.M., 2008, Geolocation of man-made reservoirs across terrains of varying complexity using GIS: Computers & Geosciences, v. 34, no. 10, p. 1184–1197, doi:10.1016/j.cageo.2008.02.015.

Moore, M.M., Huffman, D.W., Fule, P.Z., Covington, W.W., and Crouse, J.E., 2004, Comparison of historical and contemporary forest structure and composition on permanent plots in southwestern ponderosa pine forests: Forest Science, v. 50, no. 2, p. 162–176.

Moosdorf, Nils, Hartmann, Jens, Lauerwald, Ronny, Hagedorn, Benjamin, and Kempe, Stephan, 2011, Atmospheric CO_2 consumption by chemical weathering in North America: Geochimica et Cosmochimica Acta, v. 75, no. 24, p. 7829–7854, doi:10.1016/j.gca.2011.10.007.

Moritz, M.A., Moody, T.J., Krawchuk, M.A., Hughes, Mimi, and Hall, Alex, 2010, Spatial variation in extreme winds predicts large wildfire locations in chaparral ecosystems: Geophysical Research Letters, v. 37, no. 4, 5 p., doi:10.1029/2009GL041735.

Mosier, A.R., Parton, W.J., Valentine, D.W., Ojima, D.S., Schime, D.S., and Heinemeyer, O., 1997, CH_4 and N_2O fluxes in the Colorado shortgrass steppe; 2. Long-term impact of land use change: Global Biogeochemical Cycles, v. 11, no. 1, p. 29–42, doi:10.1029/96GB03612.

Mu, J.E., McCarl, B.A., and Wein, A.M., 2012, Adaptation to climate change; Changes in farmland use and stocking rate in the U.S.: Mitigation and Adaptation Strategies for Global Change, 18 p., doi:10.1007/s11027-012-9384-4.

Mulholland, P.J., and Elwood, J.W., 1982, The role of lake and reservoir sediments as sinks in the perturbed global carbon cycle: Tellus, v. 34, no. 5, p. 490–499.

Muller-Karger, F.E., Varela, Ramon, Thunell, Robert, Luerssen, Remy, Hu, Chuanmin, and Walsh, J.J., 2005, The importance of continental margins in the global carbon cycle: Geophysical Research Letters, v. 32, no. 1, p. 1–4, doi:10.1029/2004GL021346.

Nakicenovic, Nebojsa, Alcamo, Joseph, Davis, Gerald, de Vries, Bert, Fenhann, Joergen, Gaffin, Stuart, Gregory, Kenneth, Grübler, Arnulf, Jung, T.Y., Kram, Tom, La Rovere, E.L., Michaelis, Laurie, Mori, Shunsuke, Morita, Tsuneyuki, Pepper, William, Pitcher, Hugh, Price, Lynn, Riahi, Keywan, Roehrl, Alexander, Rogner, H.-H., Sankovski, Alexei, Schlesinger, Michael, Shukla, Priyararshi, Smith, Steven, Swart, Robert, van Rooijen, Sascha, Victor, Nadejda, and Dadi, Zhou, 2000, Special report on emissions scenarios; A special report of Working Group III of the Intergovernmental Panel on Climate Change [IPCC]: Cambridge, United Kingdom, Cambridge University Press, 599 p., at http://www.grida.no/publications/other/ipcc%5Fsr/?src=/climate/ipcc/emission/index.htm. (Accessed November 15, 2011.)

National Interagency Fire Center, 2012, National Interagency Fire Center: National Interagency Fire Center Web page accessed August 4, 2012, at http://www.nifc.gov/fireInfo/fireInfo_statistics.html.

Nelson, M.D., and Vissage, John, 2005, Mapping forest inventory and analysis forest land use—Timberland, reserved forest land, and other forest land, *in* McRoberts, R.E., Reams, G.A., Van Deusen, P.C., and McWilliams, W.H., eds., Proceedings of the seventh annual forestry and analysis symposium: U.S. Department of Agriculture, Forest Service General Technical Report WO–77, p. 185–191. (Also available at http://nrs.fs.fed.us/pubs/gtr/gtr_wo077/gtr_wo077_185.pdf.)

North, M.P., and Hurteau, M.D., 2011, High-severity wildfire effects on carbon stocks and emissions in fuels treated and untreated forest: Forest Ecology and Management, v. 261, no. 6, p. 1115–1120, doi:10.1016/j.foreco.2010.12.039.

Oak Ridge National Laboratory Distributed Active Archive Center, 2012, Global Fire Emissions Database: Oak Ridge National Laboratory Distributed Active Archive Center database accessed August 9, 2012, at http://daac.ornl.gov/VEGETATION/guides/global_fire_emissions_v2.1.html.

Ogle, S.M., Breidt, F.J., and Paustian, Keith, 2005, Agricultural management impacts on soil organic carbon storage under moist and dry climatic conditions of temperate and tropical regions: Biogeochemistry, v. 72, no. 1, p. 87–121 doi:10.1007/s10533-004-0360-2.

Olander, L.P., Cooley, D.M., and Galik, C.S., 2012, The potential role for management of U.S. public lands in greenhouse gas mitigation and climate policy: Environmental Management, v. 49, no. 3, p. 523–533, doi:10.1007/s00267-011-9806-1.

Oliver, B.G., Thurman, E.M., and Malcolm, R.L., 1983, The contribution of humic substances to the acidity of colored natural waters: Geochimica et Cosmochimica Acta, v. 47, no. 11, p. 2031–2035, doi:10.1016/0016-7037(83)90218-1.

Omernik, J.M., and Bailey, R.G., 1997, Distinguishing between watersheds and ecoregions: Journal of the American Water Resources Association, v. 33, no. 5, p. 935–949, doi: 10.1111/j.1752-1688.1997.tb04115.x.

Orme, A.R., ed., 2002, Physical geography of North America: Oxford, U.K., Oxford University Press, 551 p.

Ottmar, R.D., Prichard, S.J., Vihnanek, R.E., and Sandberg, D.V., 2008, Modification and validation of fuel consumption models for shrub and forested lands in the Southwest, Pacific Northwest, Rockies, Midwest, Southeast and Alaska: U.S. Department of Agriculture, Forest Service, Fire and Environmental Applications Team, Pacific Northwest Research Station, Pacific Wildland Fire Sciences Laboratory, Final Report, JFSP Project 98–1–9–06, 97 p., available at http://www.firescience.gov/projects/98-1-9-06/project/98-1-9-06_final_report.pdf.

Ottmar, R.D., Sandberg, D.V., Riccardi, C.L., and Prichard, S.J., 2007, An overview of the Fuel Characteristic Classification System—Quantifying, classifying, and creating fuelbeds for resource planning: Canadian Journal of Forest Research, v. 37, no. 12, p. 2383–2393, doi:10.1139/X07-077.

Pacala, S.W., Hurtt, G.C., Baker, D., Peylin, P., Houghton, R.A., Birdsey, R.A., Heath, L., Sundquist, E.T., Stallard, R.F., Ciais, P., Moorcroft, P., Caspersen, J.P., Shevliakova, E., Moore, B., Kohlmaier, G., Holland, E., Gloor, M., Harmon, M.E., Fan, S.-M., Sarmiento, J.L., Goodale, C.L., Schimel, D., and Field, C.B., 2001, Consistent land- and atmosphere-based U.S. carbon sink estimates: Science, v. 292, no. 5525, p. 2316–2320, doi:10.1126/science.1057320.

Pacala, S., Birdsey, R.A., Bridgham, S.D., Conant, R.T., Davis, K., Hales, B., Houghton, R.A., Jenkins, J.C., Johnston, M., Marland, G., and Paustian, K., 2007, The North American carbon budget past and present, *in* King, A.W., Dilling, Lisa, Zimmerman, G.P., Fairman, D.M., Houghton, R.A., Marland, Gregg, Rose, A.Z., and Wilbanks, T.J., eds., The First State of the Carbon Cycle Report (SOCCR); The North American carbon budget and implications for the global carbon cycle; A report by the U.S. Climate Change Science Program and the Subcommittee on Global Change Research: U.S Climate Change Science Program Synthesis and Assessment Product 2.2, p. 29–36. (Also available at http://www.climatescience.gov/Library/sap/sap2-2/final-report/sap2-2-final-chapter3.pdf.)

Pan, Yude, Birdsey, R.A., Fang, Jingyun, Houghton, Richard, Kauppi, P.E., Kurz, W.A., Phillips, O.L., Shvidenko, Anatoly, Lewis, S.L., Canadell, J.G., Ciais, Philippe, Jackson, R.B., Pacala, S.W., McGuire, A.D., Piao, Shilong, Rautiainen, Aapo, Sitch, Stephen, and Hayes, Daniel, 2011, A large and persistent carbon sink in the world's forests: Science, v. 333, no. 6045, p. 988–993, doi:10.1126/science.1201609.

Pan, Y., Chen, J.M., Birdsey, R., McCullough, K., He, L., and Deng, F., 2011, Age structure and disturbance legacy of North American forests: Biogeosciences, v. 8, no. 3, p. 715–732, doi:10.5194/bg-8-715-2011.

Park, C.C., 1977, World-wide variations in hydraulic geometry exponents of stream channels; An analysis and some observations: Journal of Hydrology, v. 33, no. 1–2, p. 133–146.

Parkhurst, D.L., and Appelo, C.A.J., 1999, User's guide to PHREEQC (Version 2); A computer program for speciation, batch-reaction, one-dimensional transport, and inverse geochemical calculations: U.S. Geological Survey Water-Resources Investigations Report 99–4259, 312 p.

Parton, W.J., Ojima, D.S., and Schimel, D.S., 1994, Environmental change in grasslands; Assessment using models: Climate Change, v. 28, no. 1–2, p. 111.

Parton, W.J., Schimel, D.S., Cole, C.V., and Ojima, D.S., 1987, Analysis of factors controlling soil organic matter levels in Great Plains grasslands: Soil Science Society of America Journal, v. 51, no. 5, p. 1173–1179, doi:10.2136/sssaj1987.03615995005100050015x.

Parton, W.J., Scurlock, J.M.O., Ojima, D.S., Gilmanov, T.G., Scholes, R.J., Schimel, D.S., Kirchner, T., Menaut, J.-C., Seastedt, T., Garcia Moya, E., Kamnalrut, Apinan, and Kinyamario, J.I., 1993, Observations and modeling of biomass and soil organic matter dynamics for the grassland biome worldwide: Global Biogeochemical Cycles, v. 7, no. 4, p. 785–809, doi:10.1029/93GB02042.

Pervez, M.S., and Brown, J.F., 2010, Mapping irrigated lands at 250-m scale by merging MODIS data and national agricultural statistics: Remote Sensing, v. 2, no. 10, p. 2388–2412, doi:10.3390/rs2102388.

Peters, N.E., 1984, Evaluation of environmental factors affecting yields of major dissolved ions of streams in the United States: U.S. Geological Survey Water-Supply Paper 2228, p. 39.

Pfeifer, E.M., Hicke, J.A., and Meddens, A.J.H., 2011, Observations and modeling of aboveground tree carbon stocks and fluxes following a bark beetle outbreak in the western United States: Global Change Biology, v. 17, no. 1, p. 339–350, doi:10.1111/j.1365-2486.2010.02226.x.

Piao, Shilong, Fang, Jingyun, Ciais, Philippe, Peylin, Philippe, Huang, Yao, Sitch, Stephen, and Wang, Tao, 2009, The carbon balance of terrestrial ecosystems in China: Nature, v. 458, p. 1009–1013, doi:10.1038/nature07944.

Pierce, D.W., Barnett, T.P., Santer, B.D., and Gleckler, P.J., 2009, Selecting global climate models for regional climate change studies: Proceedings of the National Academy of Science, v. 106, no. 21, p. 8441–8446. (Also available at http://www.pnas.org/content/106/21/8441.abstract; supporting information at www.pnas.org/cgi/content/full/0900094106/DCSupplemental.)

Poffenbarger, H.J., Needelman, B.A., and Megonigal, J.P., 2011, Salinity influence on methane emissions from tidal marshes: Wetlands, v. 31, no. 5, p. 831–842, doi:10.1007/s13157-011-0197-0.

Pontius, R.G., Jr., and Millones, Marco, 2012, Death to Kappa; Birth of quantity disagreement and allocation disagreement for accuracy assessment: International Journal of Remote Sensing, v. 32, no. 15, p. 4407–4429, doi:10.1080/01431161.2011.552923.

Potter, Christopher, Klooster, Steven, Genovese, Vanessa, Hiatt, Cyrus, Boriah, Shyam, Kumar, Vipin, Mithal, Varun, and Garg, Ashish, 2012, Terrestrial ecosystem carbon fluxes predicted from MODIS satellite data and large-scale disturbance modeling: International Journal of Geosciences, v. 3, no. 3, p. 469–479, doi:10.4236/ijg.2012.33050.

Potter, C.S., Randerson, J.T., Field, C.B., Matson, P.A., Vitousek, P.M., Mooney, H.A., and Klooster, S.A., 1993, Terrestrial ecosystem production—A process model based on global satellite and surface data: Global Biogeochemical Cycles, v. 7, no. 4, p. 811–841, doi:10.1029/93GB02725.

Preisler, H.K., Brillinger, D.R., Burgan, R.E., and Benoit, J.W., 2004, Probability based models for estimation of wildfire risk: International Journal of Wildland Fire, v. 13, no. 2, p. 133–142.

Preston, S.D., Alexander, R.B., and Wolock, D.M., 2011, SPARROW modeling to understand water-quality conditions in major regions of the United States—A featured collection introduction: Journal of the American Water Resources Association, v. 47, no. 5, p. 887–890, doi:10.1111/j.1752-1688.2011.00585.x.

Price, C., and Rind, D., 1994, The impact of a $2\times CO_2$ climate on lightning-caused fires: Journal of Climate, v. 7, no. 10, p. 1484–1494.

PRISM Climate Group, 2012, PRISM data: PRISM Climate Group dataset accessed October 23, 2012, at http://www.prism.oregonstate.edu/.

Protected Areas Database of the United States (PAD–US) Partnership, 2009, A map for the future—Creating the next generation of protected area inventories in the United States: Protected Areas Database of the United States Partnership, 20 p., at http://www.protectedlands.net/images/PADUS_FinalJuly2009LowRes.pdf. (Accessed June 18, 2010.)

R Development Core Team, 2008, R—A language and environment for statistical computing: Vienna, Austria, R Foundation for Statistical Computing.

Raffa, K.F., Aukema, B.H., Bentz, B.J., Carroll, A.L., Hicke, J.A., Turner, M.G., and Romme, W.H., 2008, Cross-scale drivers of natural disturbances prone to anthropogenic amplification—The dynamics of bark beetle eruptions: BioScience, v. 58, no. 6, p. 501–517, doi:10.1641/B580607.

Randall, D.A., Wood, R.A., Bony, S., Colman, R., Fichefet, T., Fyfe, J., Kattsov, V., Pitman, A., Shukla, J., Srinivasan, J., Stouffer, R.J., Sumi, A., and Taylor, K.E., 2007, Chapter 8—Climate models and their evaluation, *in* Solomon, S., Qin, D., Manning, M., Chen, Z., Marquis, M., Averyt, K.B., Tignor, M., and Miller, H.L., eds., Climate change 2007—The physical science basis, Contribution of Working Group I to the Fourth Assessment Report of the Intergovernmental Panel on Climate Change: Cambridge, U.K., Cambridge University Press, 996 p. (Also available at http://www.ipcc.ch/publications_and_data/publications_ipcc_fourth_assessment_report_wg1_report_the_physical_science_basis.htm.)

Raymond, P.A., and Oh, N.-H., 2007, An empirical study of climatic controls on riverine C export from three major U.S. watersheds: Global Biogeochemical Cycles, v. 21, 9 p., doi:10.1029/2006GB002783.

Raymond, P.A., Zappa, C.J., Butman, David, Bott, T.L., Potter, Jody, Mulholland, Patrick, Laursen, A.E., McDowell, W.H., and Newbold, Denis, 2012, Scaling the gas transfer velocity and hydraulic geometry in streams and small rivers: Limnology and Oceanography—Fluids and Environments, v. 2, p. 41–53, doi:10.1215/21573689-1597669.

Reinhardt, Elizabeth, and Holsinger, Lisa, 2010, Effects of fuel treatments on carbon-disturbance relationships in forests of the northern Rocky Mountains: Forest Ecology and Management, v. 259, no. 8, p. 1427–1435.

Reinhardt, Elizabeth, and Keane, R.E., 2009, FOFEM: The First-Order Fire Effects Model Adapts to the 21st Century: Joint Science Program, Fire Science Brief, 6 p. (Also available at http://www.firescience.gov/projects/98-1-8-03/supdocs/98-1-8-03_fsbrief62-final.pdf.)

Reinhardt, E.D., Keane, R.E., and Brown, J.K., 1997, First Order Fire Effect Model; FOFEM 4.0 user's guide: Ogden, Utah, U.S. Forest Service Intermountain Research Station General Technical Report INT–GTR–344, 65 p. (Also available at http://www.fs.fed.us/rm/pubs_int/int_gtr344.pdf.)

Reinhardt, E.D., Keane, R.E., Calkin, D.E., and Cohen, J.D., 2008, Objectives and considerations for wildland fuel treatment in forested ecosystems of the interior western United States: Forest Ecology and Management, v. 256, no. 12, p. 1997–2006.

Riera, J.L., Schindler, J.E., and Kratz, T.K., 1999, Seasonal dynamics of carbon dioxide and methane in two clear-water lakes and two bog lakes in northern Wisconsin, U.S.A.: Canadian Journal of Fisheries and Aquatic Sciences, v. 56, no. 2, p. 265–274.

Robards, T.A., 2010, Current forest and woodland carbon storage and flux in California—An estimate for the 2010 Statewide Assessment: Sacramento, Calif., California Department of Forestry and Fire Protection, 11 p., at http://www.bof.fire.ca.gov/board_committees/policy_committee/current_projects/current_projects/carbon_white_paper_-_final.pdf. (Accessed October 23, 2012.)

Roeckner, E., Baumi, G., Bonaventura, L., Brokopf, R., Esch, M., Giorgetta, M., Hagemann, S., Kirchner, I., Kornblueh, L., Manzini, E., Rhodin, A., Schlese, U., Schulzweida, U., and Tompkins, A., 2003, The atmospheric general circulation model ECHAM5; part I, Model description: Max Planck Institute for Meteorology Report 349, 127 p. (Also available at http://www.mpimet.mpg.de/fileadmin/publikationen/Reports/max_scirep_349.pdf.)

Rogers, B.M., Neilson, R.P., Drapek, Ray, Lenihan, J.M., Wells, J.R., Bachelet, Dominique, and Law, B.E., 2011, Impacts of climate change on fire regimes and carbon stocks of the U.S. Pacific Northwest: Journal of Geophysical Research, v. 116, 13 p., doi:10.1029/2011jg001695.)

Rollins, M.G., 2009, LANDFIRE; A nationally consistent vegetation, wildland fire, and fuel assessment: International Journal of Wildland Fire, v. 18, no. 3, p. 235–249, doi:10.1071/WF08088.

Rollins, M.G., Swetnam, T.W., and Morgan, Penelope, 2001, Evaluating a century of fire patterns in two Rocky Mountain wilderness areas using digital fire atlases: Canadian Journal of Forest Research, v. 31, no. 12, p. 2107–2123, doi:10.1139/cjfr-31-12-2107.

Roy, D.P., Lewis, P.E., and Justice, C.O., 2002, Burned area mapping using multi-temporal moderate spatial resolution data—A bi-directional reflectance model-based expectation approach: Remote Sensing of Environment, v. 83, no. 1–2, p. 263–286.

Runkel, R.L., Crawford, C.G., and Cohn, T.A., 2004, Load Estimator (LOADEST); A FORTRAN program for estimating constituent loads in streams and rivers: U.S. Geological Survey Techniques and Methods, Book 4, Chapter A5, 69 p., accessed November 14, 2011, at http://pubs.usgs.gov/tm/2005/tm4A5/.

Running, S.W., 2008, Ecosystem disturbance, carbon, and climate: Science, v. 321, no. 5889, p. 652–653, doi:10.1126/science.1159607.

Russell, G.L., Miller, J.R., Rind, David, Ruedy, R.A., Schmidt, G.A., and Sheth, Sukeshi, 2000, Comparison of model and observed regional temperature changes during the past 40 years: Journal of Geophysical Research—Atmospheres, v. 105, no. D11, p. 14,891–14,898. (Also available at http://www.agu.org/journals/jd/v105/iD11/2000JD900156/.)

Ruyle, George, and Ogden, Phil, 1993, What is an A.U.M.?, *in* Gum, Russell, Ruyle, George, and Rice, Richard, eds., Arizona Ranchers' Management Guide: Tucson, Ariz., Arizona Cooperative Extension, 4 p.

Sainju, U.M., Jabro, J.D., and Stevens, W.B., 2008, Soil carbon dioxide emission and carbon content as affected by irrigation, tillage, cropping system, and nitrogen fertilization: Journal of Environmental Quality, v. 37, no. 1, p. 98–106, doi:10.2134/jeq2006.0392.

Sarmiento, J.L., and Gruber, Nicolas, 2002, Sinks for anthropogenic carbon: Physics Today, v. 55, no. 8, p. 30–36, doi:10.1063/1.1510279.

Schlesinger, W.H., and Melack, J.M., 1981, Transport of organic carbon in the world's rivers: Tellus, v. 33, no. 2, p. 172–187, doi:10.1111/j.2153-3490.1981.tb01742.x.

Schmidt, G.L., Liu, Shuguang, and Oeding, Jennifer, 2011, Derived crop management data for the LandCarbon Project: U.S. Geological Survey Open-File Report 2011–1303, 15 p., available only at http://pubs.usgs.gov/of/2011/1303/.

Schoennagel, Tania, Veblen, T.T., and Romme, W.H., 2004, The interaction of fire, fuels, and climate across rocky mountain forests: Bioscience, v. 54, no. 7, p. 661–676.

Schuman, G.E., Ingram, L.J., Stahl, P.D., Derner, J.D., Vance, G.F., and Morgan, J.A, 2009, Influence of management on soil organic carbon dynamics in northern mixed-grass rangeland, *in* Lal, Rattan, and Follett, R.F., eds., Soil carbon sequestration and the greenhouse effect: Madison, Wis., Soil Science Society of America Special Publication 57, p. 169–180.

Schwalm, C.R., Williams, C.A., Schaefer, Kevin, Anderson, Ryan, Arain, M.A., Baker, Ian, Barr, Alan, Black, T.A., Chen, Guangsheng, Chen, J.M., Ciais, Philippe, Davis, K.J., Desai, Ankur, Dietze, Michael, Dragoni, Danilo, Fischer, M.L., Flanagan, L.B., Grant, Robert, Gu, Lianhong, Hollinger, David, Izaurralde, R.C., Kucharik, Chris, Lafleur, Peter, Law, B.E., Li, Longhui, Li, Zhengpeng, Liu, Shuguang, Lokupitiya, Erandathie, Luo, Yiqi, Ma, Siyan, Margolis, Hank, Matamala, Roser, McCaughey, Harry, Monson, R.K., Oechel, W.C., Peng, Changhui, Poulter, Benjamin, Price, D.T., Riciutto, D.M., Riley, William, Sahoo, A.K., Sprintsin, Michael, Sun, Jianfeng, Tian, Hanqin, Tonitto, Christina, Verbeeck, Hans, Verma, Shashi, 2010, A model-data intercomparison of CO_2 exchange across North America; Results from the North American Carbon Program site synthesis: Journal of Geophysical Research, v. 115, 22 p., doi:10.1029/2009JG001229.

Schwarz, G.E., 2008, A preliminary SPARROW model of suspended sediment for the conterminous United States: U.S. Geological Survey Open-File Report 2008–1205, 12 p., available only online at http://pubs.usgs.gov/of/2008/1205/ofr2008-1205.pdf.

Schwarz, G.E., Hoos, A.B., Alexander, R.B., and Smith, R.A., 2006, The SPARROW surface water-quality model—Theory, application, and user documentation: U.S. Geological Survey Techniques and Methods Report 6–A3, available only at http://pubs.usgs.gov/tm/2006/tm6b3/.

Scott, R.L., Hamerlynck, E.P., Jenerette, G.D., Moran, M.S., and Barron-Gafford, G.A., 2010, Carbon dioxide exchange in a semidesert grassland through drought-induced vegetation change: Journal of Geophysical Research, v. 115, 12 p., doi:10.1029/2010JG001348.

Seiler, Wolfgang, and Crutzen, P.J., 1980, Estimates of gross and net fluxes of carbon between the biosphere and the atmosphere from biomass burning: Climatic Change, v. 2, no. 3, p. 207–247.

Shih, J.-S., Alexander, R.B., Smith, R.A., Boyer, E.W., Schwarz, G.E., and Chung, Susie, 2010, An initial SPARROW model of land use and in-stream controls on total organic carbon in streams of the conterminous United States: U.S. Geological Survey Open-File Report 2010–1276, 22 p., available only at http://pubs.usgs.gov/of/2010/1276.

Sibold, J.S., Veblen, T.T., and González, M.E., 2006, Spatial and temporal variation in historic fire regimes in subalpine forests across the Colorado Front Range in Rocky Mountain National Park, Colorado, USA: Journal of Biogeography, v. 33, no. 4, p. 631–647.

Sitch, Stephen, Brovkin, Victor, von Bloh, Werner, van Vuuren, Detlef, Eickhout, Bas, and Ganopolski, Andrey, 2005, Impacts of future land cover changes on atmospheric CO_2 and climate: Global Biogeochemical Cycles, v. 19, 15 p., doi:10.1029/2004GB002311.

Sleeter, B.M., Sohl, T.L., Bouchard, M.A., Reker, R.R., Soulard, C.E., Acevedo, William, Griffith, G.E., Sleeter, R.R., Auch, R.F., Sayler, K.L., Prisley, Stephen, and Zhu, Zhiliang, 2012, Scenarios of land use and land cover change in the conterminous United States; Utilizing the Special Report on Emission Scenarios at ecoregional scales: Global Environmental Change, v. 22, no. 4, p. 896–914, doi:10.1016/j.gloenvcha.2012.03.008.

Sleeter, B.M., Soulard, C.E., Wilson, T.S., and Sorenson, D.G., 2012, Land-cover trends in the Western United States—1973 to 2000, *in* Sleeter, B.M., Wilson, T.S., and Acevedo, W., eds., Status and trends of land change in the Western United States—1973 to 2000: U.S. Geological Survey Professional Paper 1794–A, p. 3–29.

Sleeter, B.M., Wilson, T.S., and Acevedo, W., eds., 2012, Status and trends of land change in the Western United States—1973 to 2000: U.S. Geological Survey Professional Paper 1794–A, 324 p.

Sleeter, B.M., Wilson, T.S., Soulard, C.E., and Liu, Jinxun, 2011, Estimation of late twentieth century landscape change in California: Environmental Monitoring and Assessment, v. 173, no. 1, p. 251–266, doi:10.1007/s10661-010-1385-8.

Smith, J.E., and Heath, L.S., 2008, Carbon stocks and stock changes in U.S. forests; and Appendix C, *in* U.S. Agriculture and Forestry Greenhouse Gas Inventory; 1990–2005: Washington, D.C., U.S. Department of Agriculture, Office of the Chief Economist, Technical Bulletin 1921, p. 65–80, p. C-1–C-7.

Smith, R.A., Schwarz, G.E., and Alexander, R.B., 1997, Regional interpretation of water-quality monitoring data: Water Resources Research, v. 33, no. 12, p. 2781–2798.

Smith, W.B., and Darr, David, 2004, U.S. forest resource facts and historical trends: U.S. Department of Agriculture, Forest Service FS–801, 37 p. (Also available at http://www.fia.fs.fed.us/library/briefings-summaries-overviews/docs/2002_ForestStats_%20FS801.pdf.)

Smithwick, E.A.H., Harmon, M.E., Remillard, S.M., Acker, S.A., Franklin, J.F., 2002, Potential upper bounds of carbon stores in forests of the Pacific Northwest: Ecological Applications, v. 12, no. 5, p. 1303–1317.

Smithwick, E.A.H., Ryan, M.G., Kashian, D.M., Romme, W.H., Tinker, D.B., and Turner, M.G., 2009, Modeling the effects of fire and climate change on carbon and nitrogen storage in lodgepole pine (*Pinus contorta*) stands: Global Change Biology, v. 15, no. 3, p. 535–548.

Soetaert, Karline, and Petzoldt, Thomas, 2010, Inverse modelling, sensitivity and Monte Carlo analysis in R using package FME: Journal of Statistical Software, v. 33, no. 3, 28 p.

Sohl, Terry, and Sayler, Kristi, 2008, Using the FORE-SCE model to project land-cover change in the southeastern United States: Ecological Modelling, v. 219, nos. 1–2, p. 49–65, doi:10.1016/j.ecolmodel.2008.08.003.

Sohl, T.L., Sleeter, B.M., Zhu, Zhiliang, Sayler, K.L., Bennett, Stacie, Bouchard, Michelle, Reker, Ryan, Hawbaker, Todd, Wein, Anne, Liu, Shuguang, Kanengieter, Ronald, and Acevedo, William, 2012, A land-use and land-cover modeling strategy for the assessment of carbon stocks and fluxes: Applied Geography, v. 34, p. 111–124, doi:10.1016/j.apgeog.2011.10.019.

Sohl, T.L., Sleeter, B.M., Sayler, K.L., Bouchard, M.A., Reker, R.R., Bennett, S.L., Sleeter, R.L., Kanengieter, R.L., and Zhu, Zhiliang, 2012, Spatially explicit land-use and land-cover scenarios for the Great Plains of the United States: Agriculture, Ecosystems & Environment, v. 153, p. 1–15, doi:10.1016/j.agee.2012.02.019.

Spracklen, D.V., Mickley, L.J., Logan, J.A., Hudman, R.C., Yevich, R., Flannigan, M.D., and Westerling, A.L., 2009, Impacts of climate change from 2000 to 2050 on wildfire activity and carbonaceous aerosol concentrations in the western United States: Journal of Geophysical Research–Atmospheres, v. 114, 17 p., doi:10.1029/2008JD010966.

St. Louis, V.L., Kelly, C.A., Duchemin, E., Rudd, J.W.M., and Rosenberg, D.M., 2000, Reservoir surfaces as sources of greenhouse gases to the atmosphere; A global estimate: BioScience, v. 50, no. 9, p. 766–774.

Stehman, S.V., Wickham, J.D., Smith, J.H., and Yang, L., 2003, Thematic accuracy of the 1992 national land-cover data for the eastern United States—Statistical methodology and regional results: Remote Sensing of Environment, v. 86, no. 4, p. 500–516, doi:10.1016/S0034-4257(03)00128-7.

Stephens, S.L., 1998, Evaluation of the effects of silvicultural and fuels treatments on potential fire behaviour in Sierra Nevada mixed-conifer forests: Forest Ecology and Management, v. 105, no. 1–3, p. 21, doi:10.1016/S0378-1127(97)00293-4.

Stephens, S.L., Moghaddas, J.J., Hartsough, B.R., Moghaddas, E.E.Y., and Clinton, N.E., 2009, Fuel treatment effects on stand-level carbon pools, treatment-related emissions, and fire risk in a Sierra Nevada mixed-conifer forest: Canadian Journal of Forest Research, v. 39, no. 8, p. 1538–1547, doi:10.1139/X09-081.

Stephens, S.L., and Ruth, L.W., 2005, Federal forest-fire policy in the United States: Ecological Applications, v. 15, no. 2, p. 532–542.

Sternberg, R.W., 1986, Transport and accumulation of river-derived sediment on the Washington continental shelf, USA: Journal of the Geological Society, v. 143, no. 6, p. 945–956.

Stets, E.G., and Striegl, R.G., 2012, Carbon export by rivers draining the conterminous United States: Inland Waters, v. 2, no. 4, p. 177–184, doi:10.5268/IW-2.4.510.

Stets, E.G., Striegl, R.G., Aiken, G.R., Rosenberry, D.O., and Winter, T.C., 2009, Hydrologic support of carbon dioxide flux revealed by whole-lake carbon budgets: Journal of Geophysical Research, v. 114, p. 1–14, doi:10.1029/2008JG000783.

Stewart, I.T., Cayan, D.R., and Dettinger, M.D., 2004, Changes in snowmelt runoff timing in western North America under a ‘business as usual’ climate change scenario: Climatic Change, v. 62, p. 217–232.

Stocks, B.J., Mason, J.A., Todd, J.B., Bosch, E.M., Wotton, B.M., Amiro, B.D., Flannigan, M.D., Hirsch, K.G., Logan, K.A., Martell, D.L., and Skinner, W.R., 2002, Large forest fires in Canada, 1959–1997: Journal of Geophysical Research–Atmospheres, v. 108, 12 p., doi:10.1029/2001JD000484.

Strahler, A.N., 1952, Dynamic basis of geomorphology: Geological Society of America Bulletin, v. 63, no. 9, p. 923–938.

Strauss, D., Bednar, L., and Mees, R., 1989, Do one percent of forest fires cause ninety-nine percent of the damage?: Forest Science, v. 35, no. 2, p. 319–328.

Strengers, Bart, Leemans, Rik, Eickhout, Bas, de Vries, Bert, and Bouwman, Lex, 2004, The land-use projections and resulting emissions in the IPCC SRES scenarios as simulated by the IMAGE 2.2 model: GeoJournal, v. 61, no. 4, p. 381–393, doi:10.1007/s10708-004-5054-8.

Striegl, R.G., Dornblaser, M.M., Aiken, G.R., Wickland, K.P., and Raymond, P.A., 2007, Carbon export and cycling by the Yukon, Tanana, and Porcupine Rivers, Alaska, 2001–2005: Water Resources Research, v. 43, no. 2, W02411, 9 p., doi:10.1029/2006WR005201.

Striegl, R.G., Dornblaser, M.M., McDonald, C.P., Rover, J., and Stets, E.G., in press, Carbon dioxide and methane emissions from the Yukon River system: Global Biogeochemical Cycles (prepress article accessed October 16, 2012), doi:10.1029/2012GB004306.

Striegl, R.G., and Michmerhuizen, C.M., 1998, Hydrologic influence on methane and carbon dioxide dynamics at two north-central Minnesota lakes: Limnology and Oceanography, v. 43, no. 7, p. 1519–1529.

Sundquist, E.T., Ackerman, K.V., Bliss, N.B., Kellndorfer, J.M., Reeves, M.C., and Rollins, M.G., 2009, Rapid assessment of U.S. forest and soil organic carbon storage and forest biomass carbon sequestration capacity: U.S. Geological Survey Open-File Report 2009–1283, 15 p., available only at http://pubs.usgs.gov/of/2009/1283/.

Swetnam, T., and Betancourt, J.L., 1990, Fire-southern oscillation relations in the southwestern United States: Science, v. 249, no. 4972, p. 1017–1020.

Syphard, A.D., Radeloff, V.C., Keeley, J.E., Hawbaker, T.J., Clayton, M.K., Stewart, S.I., and Hammer, R.B., 2007, Human influence on California fire regimes: Ecological Applications, v. 17, no. 5, p. 1388–1402.

Syvitski, J.P., Vörösmarty, C.J., Kettner, A.J., and Green, P., 2005, Impact of humans on the flux of terrestrial sediment to the global coastal ocean: Science, v. 308, p. 376–380.

Syvitski, J.P.M., 2011, Global sediment fluxes to the Earth's coastal ocean: Applied Geochemistry: v. 26, p. S373–S374, doi:10.1016/j.apgeochem.2011.03.064.

Tang, J., Bolstad, P.V., and Martin, J.G., 2009, Soil carbon fluxes and stocks in a Great Lakes forest chronosequence: Global Change Biology, v. 15, no. 1, p. 145–155, doi:10.1111/j.1365-2486.2008.01741.x.

Tishchenko, P.Y., Wallmann, K., Vasilevskaya, N.A., Volkova, T.I., Zvalinskii, V.I., Khodorenko, N.D., and Shkirnikova, E.M., 2006, The contribution of organic matter to the alkaline reserve of natural waters: Oceanology, v. 46, p. 192–199, doi:10.1134/S0001437006020068.

Tranvik, L.J., Downing, J.A., Cotner, J.B., Loiselle, S.A., Striegl, R.G., Ballatore, T.J., Dillon, Peter, Finlay, Kerri, Fortino, Kenneth, Knoll, L.B., Kortelainen, P.L., Kutser, Tiit, Larsen, Soren, Laurion, Isabelle, Leech, D.M., McCallister, S.L., McKnight, D.M., Melack, J.M., Overholt, Erin, Porter, J.A., Prairie, Yves, Renwick, W.H., Roland, Fabio, Sherman, B.S., Schindler, D.W., Sobek, Sebastian, Tremblay, Alain, Vanni, M.J., Verschoor, A.M., von Wachenfeldt, Eddie, and Weyhenmeyer, G.A., 2009, Lakes and reservoirs as regulators of carbon cycling and climate: Limnology and Oceanography, v. 54, no. 6, part 2, p. 2298–2314. (Also available at http://www.aslo.org/lo/toc/vol_54/issue_6_part_2/2298.pdf.)

Tulbure, M.G., Wimberly, M.C., Roy, D.P., and Henebry, G.M., 2011, Spatial and temporal heterogeneity of agricultural fires in the central United States in relation to land cover and land use: Landscape Ecology, v. 26, no. 2, p. 211–224, doi:10.1007/s10980-010-9548-0.

Turner, D.P., Göckede, M., Law, B.E., Ritts, W.D., Cohen, W.B., Yang, Z., Hudiburg, T., Kennedy, R., and Duane, M., 2011, Multiple constraint analysis of regional land-surface carbon flux: Tellus B, v. 63, no. 2, p. 207–221, doi:10.1111/j.1600-0889.2011.00525.x.

Turner, D.P., Ritts, W.D., Yang, Zhiqiang, Kennedy, R.E., Cohen, W.B., Duane, M.V., Thornton, P.E., and Law, B.E., 2011, Decadal trends in net ecosystem production and net ecosystem carbon balance for a regional socioecological system: Forest Ecology and Management, v. 262, no. 7, p. 1318–1325, doi:10.1016/j.foreco.2011.06.034.

Turner, M.G., Baker, W.L., Peterson, C.J., and Peet, R.K., 1998, Factors influencing succession; Lessons from large, infrequent natural disturbances: Ecosystems, v. 1, no. 6, p. 511.

U.S. Army Corps of Engineers, 2012, National Inventory of Dams: U.S. Army Corps of Engineers Web site accessed June 22, 2012, at http://geo.usace.army.mil/pgis/f?p=397:12.

U.S. Census Bureau, 2012, TIGER, TIGER/Line and TIGER-related products: U.S. Census Bureau Web page accessed August 5, 2012, at http://www.census.gov/geo/www/tiger/.

U.S. Climate Change Science Program, 2007, The first state of the carbon cycle report (SOCCR)—The North American carbon budget and implications for the global carbon cycle (King, A.W., Dilling, Lisa, Zimmerman, G.P., Fairman, D.M., Houghton, R.A., Marland, Gregg, Rose, A.Z., and Wilbanks, T.J., eds.): National Oceanic and Atmospheric Administration, National Climatic Data Center, 242 p., accessed October 23, 2012, at http://www.climatescience.gov/Library/sap/sap2-2/final-report/default.htm

U.S. Congress, 2007, Energy Independence and Security Act of 2007—Public Law 110–140: U.S. Congress, 311 p., available at http://frwebgate.access.gpo.gov/cgi-bin/getdoc.cgi?dbname=110_cong_public_laws&docid=f:publ140.110.pdf.

U.S. Department of Agriculture, 2008, U.S. agriculture and forestry greenhouse gas inventory; 1990–2005: U.S. Department of Agriculture, Office of the Chief Economist, Technical Bulletin 1921, 161 p., at http://www.usda.gov/oce/climate_change/AFGGInventory1990_2005.htm

U.S. Department of Agriculture, 2011, USDA agriculture and forestry greenhouse gas inventory; 1990–2008: U.S. Department of Agriculture, Office of the Chief Economist, Climate Change Program Office Technical Bulletin 1930, 162 p. (Also available at http://www.usda.gov/oce/climate_change/AFGGInventory1990_2008.htm.)

U.S. Department of Agriculture, Economic Research Service, 2011a, ARMS farm financial and crop production practices; tailored reports: U.S. Department of Agriculture, Economic Research Service database, accessed August 16, 2011, at http://www.ers.usda.gov/Data/ARMS/app.

U.S. Department of Agriculture, Economic Research Service, 2011b, Fertilizer use and price: U.S. Department of Agriculture, Economic Research Service database, accessed August 16, 2011, at http://www.ers.usda.gov/Data/FertilizerUse.

U.S. Department of Agriculture, Forest Service, 2011, Timber products output studies: U.S. Department of Agriculture, Forest Service Web page accessed August 29, 2012, at http://www.fia.fs.fed.us/program-features/tpo.

U.S. Department of Agriculture, Forest Service, 2012a, Carbon inventory assessment: U.S. Department of Agriculture, Forest Service Web page accessed September 25, 2012, at http://www.fs.usda.gov/detail/r5/landmanagement/?cid=stelprdb5289572.

U.S. Department of Agriculture, Forest Service, 2012b, Forest inventory and analysis national program: U.S. Department of Agriculture, Forest Service Web site accessed November 25, 2012, at http://www.fia.fs.fed.us/tools-data.

U.S. Department of Agriculture, Forest Service, 2012c, FS Geodata Clearinghouse—Forest biomass across the lower 48 States and Alaska data: Department of Agriculture, Forest Service database accessed September 5, 2012, at http://fsgeodata.fs.fed.us/rastergateway/biomass/.

U.S. Department of Agriculture, Forest Service, 2012d, Fuels Characterization Classification System: U.S. Department of Agriculture, Forest Service Web site accessed August 12, 2012, at http://www.fs.fed.us/pnw/fera/fccs/applications.shtml.

U.S. Department of Agriculture, National Agricultural Statistics Service, 2011, Quick Stats: U.S. Department of Agriculture, National Agricultural Statistics Service database, accessed September 5, 2012, at http://www.nass.usda.gov/Quick_Stats/.

U.S. Department of Agriculture, Natural Resources Conservation Service, 2009, Soil Survey Geographic (SSURGO) Database: U.S. Department of Agriculture, Natural Resources Conservations Service database accessed August 14, 2012, at http://soildatamart.nrcs.usda.gov/.

U.S. Department of Agriculture, Natural Resources Conservation Service, 2012, Watershed Boundary Dataset: U.S. Department of Agriculture, Natural Resources Conservation Service Web site accessed October 3, 2012, at http://www.nrcs.usda.gov/wps/portal/nrcs/main/national/water/watersheds/dataset.

U.S. Department of Agriculture and U.S. Department of the Interior, 1994, Record of decision for amendments to Forest Service and Bureau of Land Management planning documents within the range of the northern spotted owl: Portland, Ore., U.S. Bureau of Land Management, 78 p. (Also available at http://www.blm.gov/or/plans/nwfpnepa/FSEIS-1994/newroda.pdf.)

U.S. Department of the Interior, 2012, Federal Wildland Fire Occurrence Data: U.S. Department of the Interior database accessed August 12, 2012, at http://wildfire.cr.usgs.gov/firehistory/data.html.

U.S. Environmental Protection Agency, 1999, Level III ecoregions of the continental United States: Corvallis, Ore., U.S. Environmental Protection Agency, National Health and Environmental Effects Research Laboratory, scale 1:7,500,000.

U.S. Environmental Protection Agency, 2003, International analysis of methane and nitrous oxide abatement opportunities; Report to Energy Modeling Forum, Working Group 21: Washington, D.C., U.S. Environmental Protection Agency, 9 p., available at http://www.epa.gov/methane/pdfs/methodologych4.pdf. (Accessed September 25, 2012.)

U.S. Environmental Protection Agency, 2009, National lakes assessment—A collaborative survey of the nation's lakes: Washington, D.C., U.S. Environmental Protection Agency, Office of Water and Office of Research and Development, EPA 841–R–09–001, 103 p., available at http://www.epa.gov/owow/LAKES/lakessurvey/pdf/nla_report_low_res.pdf. (Accessed October 23, 2012.)

U.S. Environmental Protection Agency, 2012, Inventory of U.S. greenhouse gas emissions and sinks; 1990–2010: Washington, D.C., U.S. Environmental Protection Agency, Office of Atmospheric Programs, Report EPA 430–R–12–001, 481 p., accessed October 23, 2012, at http://epa.gov/climatechange/emissions/usinventoryreport.html.

U.S. Geological Survey, 2010, Moderate Resolution Imaging Spectroradiometer (MODIS) Irrigated Agriculture Dataset for the United States (MIrAD-US): U.S. Geological Survey Web page accessed August 4, 2012, at http://earlywarning.usgs.gov/USirrigation/.

U.S. Geological Survey, 2012a, Land cover trends data: U.S. Geological Survey, Land Cover Trends, dataset accessed May 31, 2012, at http://landcovertrends.usgs.gov.

U.S. Geological Survey, 2012b, National Elevation Dataset: U.S. Geological Survey database accessed August 5, 2012, at http://ned.usgs.gov/.

U.S. Geological Survey, 2012c, National Hydrography Dataset: U.S. Geological Survey database accessed August 6, 2012, at http://nhd.usgs.gov/.

U.S. Geological Survey, 2012d, National Water Information Service: U.S. Geological Survey Web site accessed October 1, 2012, at http://waterdata.usgs.gov/nwis.

United Nations Framework Convention on Climate Change, 1997, Kyoto Protocol to United Nations Framework Convention on Climate Change: Bonn, Germany, United Nations Framework Convention on Climate Change, 21 p. (Also available at http://unfccc.int/key_documents/kyoto_protocol/items/6445.php.)

Van Auken, O.W., 2000, Shrub invasions of North American semiarid grasslands: Annual Review of Ecology and Systematics, v. 31, p. 197–215, doi:10.1146/annurev.ecolsys.31.1.197.

van Heuven, S., Pierrot, D., Lewis, E., and Wallace, D.W.R., 2009, MATLAB program developed for CO_2 system calculations: Oak Ridge, Tenn., U.S. Department of Energy, Oak Ridge National Laboratory, Carbon Dioxide Information Analysis Center, ORNL/CDIAC-105b.

van Vuuren, D.P., Lucas, P.L., and Hilderink, Henk, 2007, Downscaling drivers of global environmental change scenarios; Enabling use of the IPCC–SRES scenarios at the national and grid level: Global Environmental Change, v. 17, no. 1, p. 114–130, doi:doi.org/10.1016/j.gloenvcha.2006.04.004.

van Vuuren, D.P., Smith, S.J., and Riahi, Keywan, 2010, Downscaling socioeconomic and emissions scenarios for global environmental change research; a review: Climate Change, v. 1, no. 3, p. 393–404.

van der Werf, G.R., Randerson, J.T., Giglio, L., Collatz, G.J., Mu, M., Kasibhatla, P.S., Morton, D.C., DeFries, R.S., Jin, Y., and van Leeuwen, T.T., 2010, Global fire emissions and the contribution of deforestation, savanna, forest, agricultural, and peat fires (1997–2009): Atmospheric Chemistry and Physics, v. 10, no. 23, p. 11,707–11,735, doi:10.5194/acp-10-11707-2010.

Vano, J.A., Scott, M.J., Voisin, Nathalie, Stöckle, C.O., Hamlet, A.F., Mickelson, K.E.B., Elsner, M.M., and Lettenmaier, D.P., 2010, Climate change impacts on water management and irrigated agriculture in the Yakima River Basin, Washington, USA: Climatic Change, v. 102, no. 1–2, p. 287–317, doi:10.1007/s10584-010-9856-z.

Vogelmann, J.E., Howard, S.M., Yang, Limin, Larson, C.R., Wylie, B.K., and Van Driel, Nick, 2001, Completion of the 1990s National Land Cover Data Set for the conterminous United States: Photogrammetric Engineering and Remote Sensing, v. 67, no. 6, p. 650–652. (Also available at http://www.asprs.org/PE-RS-Journals-Past-Issues/PE-RS-Journals/PE-RS-Past-Issues/PE-RS-Journals-2001/PE-RS-June-2001.html.)

Wagner, F.H., 1978, Livestock grazing and the livestock industry, *in* Brokaw, H.P., ed., Wildlife and America: Washington, D.C., Council on Environmental Quality, p. 121–145.

Warren, D.D., 1999, Production, prices, employment, and trade in Northwest forest industries, fourth quarter 1997: Portland, Ore., U.S. Department of Agriculture, Forest Service, Pacific Northwest Research Station, Resource Bulletin RB–230 99–080, 130 p.

Washington, W.M., Weatherly, J.W., Meehl, G.A., Semtner, A.J., Jr., Bettge, T.W., Craig, A.P., Strand, W.G., Jr., Arblaster, J., Wayland, V.B., James, R., and Zhang, Y., 2000, Parallel climate model (PCM) control and transient simulations: Climate Dynamics, v. 16, no. 10–11, p. 755–774, doi:10.1007/s003820000079.

Watson, R.T., Noble, I.R., Bolin, Bert, Ravindranath, N.H., Verardo, D.J., and Dokken, D.J., eds., 2000, Land use, land-use change and forestry: Cambridge, UK, Cambridge University Press, A Special Report of the Intergovernmental Panel on Climate Change, 375 p. (Also available at http://www.ipcc.ch/ipccreports/sres/land_use/index.php?idp=0.)

Westerling, A.L., and Bryant, B.P., 2008, Climate change and wildfire in California: Climate Change, v. 87, suppl. 1, p. S231–S249, doi:10.1007/s10584-007-9363-z.

Westerling, A.L., Hidalgo, H.G., Cayan, D.R., and Swetnam, T.W., 2006, Warming and earlier spring increase western U.S. forest wildfire activity: Science, v. 313, no. 5789, p. 940–943, doi:10.1126/science.1128834.

Westerling, A.L., Turner, M.G., Smithwick, E.A.H., Romme, W.H., and Ryan. M.G., 2011, Continued warming could transform Greater Yellowstone fire regimes by mid-21st century: Proceedings of the National Academy of Sciences, v. 108, no. 32, p. 13,165–13,170, doi:10.1073/pnas.1110199108.

Wheatcroft, R.A., Goni, M.A., Hatten, J.A., Pasternack, G.B., and Warrick, J.A., 2010, The role of effective discharge in the ocean delivery of particulate organic carbon by small, mountainous river systems: Limnology and Oceanography, v. 55, no. 1, p. 161–171.

Wickham, J.D., Stehman, S.V., Smith, J.H., and Yang, L., 2004, Thematic accuracy of the 1992 National Land-Cover Data for the western United States: Remote Sensing of Environment, v. 91, no. 3–4, p. 452–468.

Wickland, K.P., Striegl, R.G., Mast, M.A., and Clow, D.W., 2001, Carbon gas exchange at a southern Rocky Mountain wetland, 1996–1998: Global Biogeochemical Cycles, v. 15, no. 2, p. 321–335.

Wiedinmyer, Christine, and Hurteau, M.D., 2010, Prescribed fire as a means of reducing forest carbon emissions in the western United States: Environmental Science and Technology, v. 44, no. 6, p. 1926–1932, doi:10.1021/es902455e.

Wiedinmyer, Christine, and Neff, J.C., 2007, Estimates of CO_2 from fires in the United States; Implications for carbon management: Carbon Balance and Management, v. 2, 12 p., doi:10.1186/1750-0680-2-10.

Williams, C.A., Collatz, G.J., Masek, Jeffrey, and Goward, S.N., 2012, Carbon consequences of forest disturbance and recovery across the conterminous United States: Global Biogeochemical Cycles, v. 26, 13 p., doi:10.1029/2010gb003947.

Wood, A.W., Maurer, E.P., Kumar, A., and Lettenmaier, D.P., 2002, Long-range experimental hydrologic forecasting for the eastern United States: Journal of Geophysical Research–Atmospheres, v. 107, 15 p., doi:10.1029/2001JD000659.

Wu, L.S., Wood, Yvonne, Jiang, P.P., Li, L.Q., Pan, G.X., Lu, J.H., Chang, A.C., and Enloe, H.A., 2008, Carbon sequestration and dynamics of two irrigated agricultural soils in California: Soil Science Society of America Journal, v. 72, no. 3, p. 808–814, doi:10.2136/sssaj2007.0074.

Wu, Yiping, and Liu, Shuguang, 2012, Automating calibration, sensitivity and uncertainty analysis of complex models using the R package Flexible Modeling Environment (FME); SWAT as an example: Environmental Modelling & Software, v. 31, p. 99–109, doi:10.1016/j.envsoft.2011.11.013.

Xian, G., Homer, C., and Fry, J., 2009, Updating the 2001 National Land Cover Database land cover classification to 2006 by using Landsat imagery change detection methods: Remote Sensing of Environment, v. 113, no. 6, p. 1133–1147.

Xiao, Jingfeng, Zhuang, Qianlai, Law B.E., Baldocchi, D.D., Chen, Jiquan, Richardson, A.D., Melillo, J.M., Davis, K.J., Hollinger, D.Y., Wharton, Sonia, Oren, Ram, Noormets, Asko, Fischer, M.L., Verma, S.B., Cook, D.R., Sun, Ge, McNulty, Steve, Wofsy, S.C., Bolstad, P.V., Burns, S.P., Curtis, P.S., Drake, B.G., Falk, Matthias, Foster, D.R., Gu, Lianhong, Hadley, J.L., Katul, G.G., Litvak, Marcy, Ma, Siyan, Martin, T.A., Matamala, Roser, Meyers, T.P., Monson, R.K., Munger, J.W., Oechel, W.C., Paw U, K.T., Schmid, H.P., Scott, R.L., Starr, Gregory, Suyker, A.E., and Torn, M.S., 2011, Assessing net ecosystem carbon exchange of U.S. terrestrial ecosystems by integrating eddy covariance flux measurements and satellite observations: Agricultural and Forest Meteorology, v. 151, no. 1 p. 60–69, doi:10.1016/j.agrformet.2010.09.002.

Zhao, Maosheng, Heinsch, F.A., Nemani, R.R., and Running, S.W., 2005, Improvements of the MODIS terrestrial gross and net primary production global data set: Remote Sensing of Environment, v. 95, no. 2, p. 164–176, doi:10.1016/j.rse.2004.12.011.

Zhu, Zhiliang, ed., Bergamaschi, Brian, Bernknopf, Richard, Clow, David, Dye, Dennis, Faulkner, Stephen, Forney, William, Gleason, Robert, Hawbaker, Todd, Liu, Jinxun, Liu, Shuguang, Prisley, Stephen, Reed, Bradley, Reeves, Matthew, Rollins, Matthew, Sleeter, Benjamin, Sohl, Terry, Stackpoole, Sarah, Stehman, Stephen, Striegl, Robert, Wein, Anne, and Zhu, Zhiliang, 2010, A method for assessing carbon stocks, carbon sequestration, and greenhouse-gas fluxes in ecosystems of the United States under present conditions and future scenarios: U.S. Geological Survey Scientific Investigations Report 2010–5233, 188 p. (Also available at http://pubs.usgs.gov/sir/2010/5233/.) (Supersedes U.S. Geological Survey Open-File Report 2010–1144.)

Zhu, Zhiliang, ed., Bouchard, Michelle, Butman, David, Hawbaker, Todd, Li, Zhengpeng, Liu, Jinxun, Liu, Shuguang, McDonald, Cory, Reker, Ryan, Sayler, Kristi, Sleeter, Benjamin, Sohl, Terry, Stackpoole, Sarah, Wein, Anne, and Zhu, Zhiliang, 2011, Baseline and projected future carbon storage and greenhouse-gas fluxes in the Great Plains region of the United States: U.S. Geological Survey Professional Paper 1787, 28 p. (Also available at http://pubs.usgs.gov/pp/1787/.)

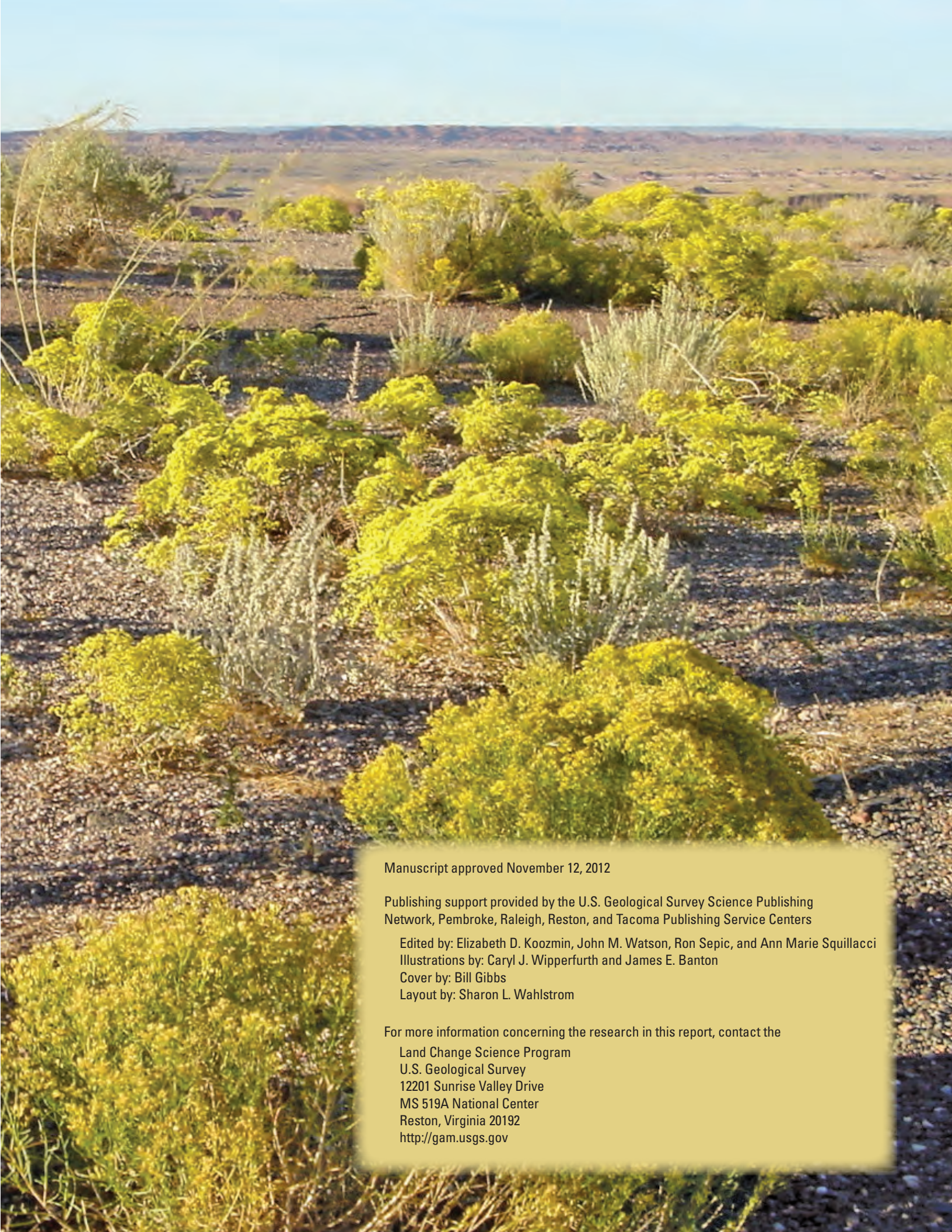

Manuscript approved November 12, 2012

Publishing support provided by the U.S. Geological Survey Science Publishing Network, Pembroke, Raleigh, Reston, and Tacoma Publishing Service Centers

Edited by: Elizabeth D. Koozmin, John M. Watson, Ron Sepic, and Ann Marie Squillacci
Illustrations by: Caryl J. Wipperfurth and James E. Banton
Cover by: Bill Gibbs
Layout by: Sharon L. Wahlstrom

For more information concerning the research in this report, contact the

Land Change Science Program
U.S. Geological Survey
12201 Sunrise Valley Drive
MS 519A National Center
Reston, Virginia 20192
http://gam.usgs.gov

USGS

Zhu and Reed, eds.— **Baseline and Projected Future Carbon Storage and Greenhouse-Gas Fluxes in Ecosystems of the Western United States**—Professional Paper 1797

ISBN 978-1-4113-3519-6